Anatomy Atlas and Interpretation of Spine Surgery

Jian-gang Shi
Wen Yuan
Jing-chuan Sun
Editors

Springer

Anatomy Atlas and Interpretation of Spine Surgery

Jian-gang Shi • Wen Yuan • Jing-chuan Sun
Editors

Anatomy Atlas and Interpretation of Spine Surgery

SSTP

Springer

Editors
Jian-gang Shi
Second Department of Spine Surgery
Changzheng Hospital
Second Military Medical University
Shanghai
China

Jing-chuan Sun
Second Department of Spine Surgery
Changzheng Hospital
Second Military Medical University
Shanghai
China

Wen Yuan
Changzheng Hospital
Second Military Medical University
Shanghai
China

ISBN 978-981-10-5905-6 ISBN 978-981-10-5906-3 (eBook)
https://doi.org/10.1007/978-981-10-5906-3

Library of Congress Control Number: 2017960333

The print edition is not for sale in China Mainland. Customers from China Mainland please order the print book from: Shanghai Scientific and Technical Publishers.

Printed on acid-free paper

This Springer imprint is published by Springer Nature
The registered company is Springer Science+Business Media Singapore Pte Ltd.
The registered company address is: 152 Beach Road, #21-01/04 Gateway East, Singapore 189721, Singapore

Foreword I for Chinese Version

Scientific and technological progress in the past 30 years has spurred significant theoretical and technical advancements in spine surgery, making it one of the important branches in the field of orthopedics. With greater understanding of spinal trauma and disease in the recent years, surgeons have gained deeper knowledge of previously unclear or incomprehensible diseases and, as a result, have developed various treatments for new diseases and opened up new areas of expertise that facilitated the early and accurate diagnosis and treatment of spinal traumas and diseases. This progress not only greatly enhanced treatment accuracy and efficacy, providing unprecedented support to clinical judgment of disease, treatment selection, and high-risk and difficult local surgical intervention, but it also helps surgeons in the prognosis of the patient's conditions. This book has introduced diagnostic and therapeutic techniques in spine surgery from various aspects. The main purpose of this book is to describe how the transition from clinical manifestation to actual lesions reveals the pathogenesis of injury and disease and the means to achieve satisfactory clinical efficacy in treatment.

Ever since the late 1950s, surgeons in China have accumulated a wealth of experience in spine surgery for over 60 years. The rapid theoretical and technical advancements in spine surgery in the past 20 years have also fostered a distinct group of professional talents who actively participated in the transmission and exchange of advanced theories and techniques in frequent academic communications at home and abroad. The field of spine surgery has already become an important field of expertise in China, and the continuous emergence of new theories and techniques has significantly improved the efficacy of clinical treatments. However, these advances were also accompanied by an increase in the incidence of surgical complications.

In response to clinical needs, *Anatomy Atlas and Interpretation of Spine Surgery* was written as a comprehensive guide to various spinal surgical techniques, which includes summaries of the authors' past experiences as well as new theories and techniques that have been recently developed. This book not only reflects the world's most recent progresses in spinal injury, degeneration, deformity, and tumor within the field of orthopedics, but it also provides the readers with an anatomical analysis of the causes of surgical complications as well as a comprehensive understanding of the pathological characteristics of spinal injuries and diseases.

In *Anatomy Atlas and Interpretation of Spine Surgery*, the various surgical techniques were described from different perspectives with detailed texts and pictures based on the author's wealth of clinical experiences as well as theoretical and technical advances around the world. The writing in this monograph is fluent, thoughtful, and rich in content and thereby serves as a great inspiration and clinical guidance to spine surgeons.

I am very happy to see that the chief editor of this book has accumulated numerous innovative theories and techniques during his time in the field of spine surgery. I believe that the publication of *Anatomy Atlas and Interpretation of Spine Surgery* will bring vast help to the readers. The authors have invested a great amount of effort on this book, and the repeated modifications, additions, and deletions have shaped it into a scientifically advanced and practical academic monograph.

With the development of new theories and techniques, the authors are still constantly exploring and summarizing the unknowns of their clinical work. It is only with continuous summarization, learning, thinking, and innovation can spine surgery continue to advance to higher levels. I, as one of the older generation of orthopedic surgeons, am pleased to see the publication of this monograph which displays the simultaneous advancements of surgical theories and techniques for the spine. I believe that with the younger generation of spine surgeons, who unremittingly collated their results and experiences in the midst of their busy clinical work, spine surgery in China will be able to advance more quickly in the near future. I sincerely hope that the readers will enjoy this monograph.

Lianshun Jia
Changzheng Hospital
Second Military Medical University
Shanghai, China
September, 2014

Foreword II for English Version

With the rapid development of modern surgery, the emergence of countless new techniques and tools continues to renew the knowledge surgeons have toward surgery. However, all the novel concepts and techniques including minimally invasive surgery, precise excision, and function-preserving/replacement surgery are built upon the foundation of a thorough understanding of clinical anatomy.

If anatomy is the invaluable treasure that nature gives to surgeons, then publication of *Anatomy Atlas and Interpretation of Spine Surgery* is the golden key that allows us to open the treasure of spine surgery. This book cleverly interweaves surgical techniques with anatomy, providing readers with numerous high-resolution intraoperative images, surgical diagrams, and cadaveric dissection that vividly restore the relevant anatomy of various spine surgical procedures from the base of the skull all the way down to the sacrum and the sacroiliac joint. They allow spine surgeons to "reconstruct" a three-dimensional anatomical view in their mind when performing the surgery.

The book's chief editor, Professor Shi Jiangang, and his team are from the world-renowned Spine Surgery Center of Changzheng Hospital, where more than 8000 spine surgeries were performed annually. The authors integrated their clinical experiences, spirit of the craftsman, diligence, and innovative thinking into bringing out the essence of spine surgery through the anatomical images, hence making this book an excellent reference for spine surgeons around the world.

This book is one of the few specialized books translated into English in the field of surgery in China. I believe that with China's increasingly close connection with the world, it is not only China's advanced engineering technology but also its advanced medical ideas and clinical experiences that will leave their marks in the world. ***Anatomy Atlas and Interpretation of Spine Surgery*** is the perfect example of this first milestone toward the global exchange of knowledge. It is a great pleasure of mine to write this preface and deliver congratulations to the publication of the English version of this book. To the spine surgeons, this book will serve as a must-have educational tool, a jewel on their bookshelves, and an indispensable asset to their career.

Yinghao Sun
Second Military Medical University
Shanghai, China
Chinese Academy of Engineering
Beijing Shi, China
May 30, 2017

Preface for English Edition

Anatomy Atlas and Interpretation of Spine Surgery has been widely recognized and highly praised by spine surgeons and readers after its first publication in China in 2015 mainly for three reasons:

1. This book highlights the anatomical key points for preventing surgical difficulties and complications, along with real anatomical images instead of tedious texts, to provide readers with more reliable information and easier understanding and mastering of the key surgical techniques. Unlike traditional anatomy atlas that contains abstract and obscure descriptions which are hard to understand, or textbook of surgery that introduces surgical approaches without fully illustrating the anatomical key points, the combination of anatomical and surgical illustrations in this book not only helps complement the shortcomings in either areas, but it also meets the needs of spine surgeons and drives innovation.
2. With the advancement of spine surgery and surgical techniques, it is important for spine surgeons to study and be more familiarized with anatomical key points in greater details. For example, in order for surgeons to shorten the learning curve and master new techniques more quickly, such as the new minimally invasive surgical techniques for the lumbar vertebrae (XLIF, OLIF, ALIF) that emerged in recent years, they will require greater and more comprehensive knowledge of the anatomy. Considering these needs, this book is customized to point out the anatomical key points for studying and mastering the new surgical techniques and to provide insights into the development of new surgical approaches.
3. Every detailed anatomical image in this book is the result of the countless hours and effort our spine surgeons and anatomy experts have spent on dissecting, taking photos, and marking the anatomical key points. It took almost 3 years of patience and perfection to complete the second edition, in which the labeled diagrams are now accompanied by the original photos so that readers cannot only identify the anatomical points accurately but they can also gain a clear visualization from the images that words simply cannot provide. This book is a first-class work that condenses the wisdom of spine surgeons and anatomy experts and a valuable tool that provides preoperative guidance, intraoperative references, and postoperative review for spine surgeons. Its innovative format and authentic contents are also the main reasons behind the praise and love from the readers.

While writing this book, we have also received many guidance and valuable advice from the academicians of the Chinese Academy of Engineering, Professor Yinghao Sun, Professor Guixing Qiu, Professor Shizhen Zhong, and numerous renowned Chinese spine experts, including Professor Lianshun Jia, Professor Shuxun Hou, Professor Yan Wang, Professor Yingze Zhang, Professor Wei Tian, Professor Yong Qiu, Professor Jianyuan Jiang, and many others. This book is the fruit of all the hard work put together by many Chinese surgeons and experts.

We sincerely hope that with the global release of this book, we will receive more guidance, opinions, and advice from leading experts worldwide to help us continuously enrich and improve this work. We also hope that this book can serve as an academic reference to international spine surgeons and contribute to the development of spine surgery worldwide.

Shanghai, China

Jiangang Shi
May 15, 2017

Preface for Chinese Edition

While compiling *Corrections on the Errors of Medical Works*, the anatomist and physician in the Qing Dynasty once said, "Writing medical works without understanding viscera and bowels is nothing different from talking nonsense by a fool; treating diseases without understanding viscera and bowels is nothing short of blind men walking in the dark." Anatomy plays an important role in the ability of a physician to perform satisfactory medical work, and the same is true for spine surgeons. With greater understanding of spine diseases, the therapeutic methods for spine diseases, including surgical concepts, approaches, and techniques, are also keeping pace with the time. The accomplishment of these improvements and their clinical application require further understanding of anatomical knowledge, which constitutes the basis for writing this book.

Based on the completed spine surgeries, the authors have summarized the clinical experience of around 30,000 cervical spine operations, and over 6000 upper cervical, thoracic, and lumbar spine operations, and has clearly demonstrated significant anatomical features by means of various types of specimens to help solve the key clinical problems encountered in surgical procedures where complications may easily occur. Each anatomical figure in this book was completed after about 2 years of preparation in accordance to the relevant surgical needs, and it allows spine surgeons to become familiarized with the spinal structures as well as the surrounding tissues so that they can perform surgeries with ease and reduce surgical complications. Therefore, this book will serve as a perfect companion for spine surgeons.

This book has condensed years of clinical experiences on spinal diseases from numerous orthopedic specialists in the Spine Surgery Department of Shanghai Changzheng Hospital, as well as the work on spine anatomy by the Anatomy Teaching and Research Office of the Second Military Medical University. What is especially valuable in the book is that the authors have the surgical technique interpretation displayed in a clear and "visible" way through the use of specimen anatomical figures.

The compilation of this book owes much to the help of numerous specialists from the Chinese Medical Doctor Association, Third Affiliated Hospital of Beijing University, General Hospital of the People's Liberation Army, Beijing Jishuitan Hospital, Huashan Hospital Affiliated to Fudan University, Ruijin Hospital Affiliated to Shanghai Jiaotong University, Southern Medical University, and Second Military Medical University. I would like to extend my deep gratitude for all the help in this regard.

This book was compiled by several authors during their spare time, amidst their onerous daily clinical work, and as a result has exhausted almost all of their rest time. Nonetheless, there may still be inadequacies in this book, and therefore readers' remarks will be much appreciated for the perfection of this book in its subsequent editions.

Shanghai, China — Wen Yuan
Shanghai, China — Jiangang Shi
June 21, 2014

Contents

List of Editors and Contributors

Editors

Jian-gang Shi, Ph.D. Second Department of Spine Surgery, Changzheng Hospital, Second Military Medical University, Shanghai, China

Jing-chuan Sun, Ph.D. Second Department of Spine Surgery, Changzheng Hospital, Second Military Medical University, Shanghai, China

Wen Yuan, Ph.D. Changzheng Hospital, Second Military Medical University, Shanghai, China

Contributors

Li-ming Chen, Ph.D. Shanghai Tongji Hospital, The Affiliated Hospital of Tongji University, Shanghai, China

De-yu Chen, Ph.D. Second Department of Spine Surgery, Changzheng Hospital, Second Military Medical University, Shanghai, China

Xiong-sheng Chen, Ph.D. Third Department of Spine Surgery, Changzheng Hospital, Second Military Medical University, Shanghai, China

Hua-jiang Chen, Ph.D. First Department of Spine Surgery, Changzheng Hospital, Second Military Medical University, Shanghai, China

Yu Chen, Ph.D. Second Department of Spine Surgery, Changzheng Hospital, Second Military Medical University, Shanghai, China

Kai Chen, Ph.D. Second Department of Spine Surgery, Changzheng Hospital, Second Military Medical University, Shanghai, China

Yong-fei Guo, Ph.D. Second Department of Spine Surgery, Changzheng Hospital, Second Military Medical University, Shanghai, China

Xiao-dan Guo, Ph.D. Department of Anatomy, Changzheng Hospital, Second Military Medical University, Shanghai, China

Ding-jun Hao, Ph.D. Xi'an Jiaotong University Medical College Red Cross Hospital, Xian, China

Lian-shun Jia, Ph.D. Department of Spine Surgery, Changzheng Hospital, Second Military Medical University, Shanghai, China

Jian-yuan Jiang, Ph.D. Department of Orthopaedics, Huashan Hospital, Fudan University, Shanghai, China

Qing-jie Kong, Ph.D. Second Department of Spine Surgery, Changzheng Hospital, Second Military Medical University, Shanghai, China

Ming Li, Ph.D. Department of Orthopaedics, Changhai Hospital, First Military Medical University, Shanghai, China

Zhong-jun Liu, Ph.D. Department of Orthopaedics, Peking University Third Hospital, Beijing, China

Tie-long Liu, Ph.D. Department of Orthopaedic Tumor, Changzheng Hospital, Second Military Medical University, Shanghai, China

Yang Liu, Ph.D. The 173th Hospital of Chinese PLA, Xinxiang, China

Xu-hua Lu, Ph.D. Fourth Department of Spine Surgery, Changzheng Hospital, Second Military Medical University, Shanghai, China

Zhuo-jing Luo, Ph.D. Department of Orthopaedics, Xijing Hospital, Fourth Military Medical University, Xian, China

Guo-hua Lv, Ph.D. Department of Orthopaedics, The Second Xiangya Hospital of Central South University, Hunan, China

Xiang-yang Ma, Ph.D. Second Department of Spine Surgery, General Hospital of Guangzhou Military Command of PLA, Guanghzou, China

Yuan Ma, Ph.D. Department of Spine Surgery, Sixth Affiliated Hospital of Xinjiang Medical University, Wulumuqi, China

Ke-ya Mao, Ph.D. Department of Spine Surgery, Chinese PLA General Hospital, Beijing, China

Jin-hao Miao, Ph.D. Second Department of Spine Surgery, Changzheng Hospital, Second Military Medical University, Shanghai, China

Bin Ni, Ph.D. Changzheng Hospital, Second Military Medical University, Shanghai, China

Lin Nie, Ph.D. Department of Spine Surgery, Qilu Hospital of Shandong University, Jinan, China

Bao-gan Peng, Ph.D. Second Department of Orthopaedics, The General Hospital of Chinese People's Armed Police Forces, Beijing, China

Qiang Qi, Ph.D. Department of Lumber Spine Surgery, Peking University Third Hospital, Beijing, China

Bang-ping Qian, Ph.D. Department of Orthopaedics, Nanjing Drum Tower Hospital, The Affiliated Hospital of Nanjing University Medical School, Nanjing, China

Yong Qiu, Ph.D. Department of Orthopaedics, Nanjing Drum Tower Hospital, The Affiliated Hospital of Nanjing University Medical School, Nanjing, China

Jian-xiong Shen, Ph.D. Department of Orthopaedics, Peking Union Medical College Hospital, Beijing, China

Wei-bin Sheng, Ph.D. Department of Orthopaedics, First Affiliated Hospital of Xinjiang Medical University, Wulumuqi, China

Guo-dong Shi, Ph.D. Second Department of Spine Surgery, Changzheng Hospital, Second Military Medical University, Shanghai, China

Yu Sun, Ph.D. Department of Cervical Spine Surgery, Peking University Third Hospital, Beijing, China

Kai-qiang Sun, Ph.D. Second Department of Spine Surgery, Changzheng Hospital, Second Military Medical University, Shanghai, China

Zheng Wang, Ph.D. Department of Spine Surgery, Chinese PLA General Hospital, Beijing, China

Xin-wei Wang, Ph.D. First Department of Spine Surgery, Changzheng Hospital, Second Military Medical University, Shanghai, China

Yuan Wang, Ph.D. Second Department of Spine Surgery, Changzheng Hospital, Second Military Medical University, Shanghai, China

Ying-jie Wang, Ph.D. Second Department of Spine Surgery, Changzheng Hospital, Second Military Medical University, Shanghai, China

De-sheng Wu, Ph.D. Department of Spine Surgery, Shanghai Dongfang Hospital, The Affiliated Hospital of Tongji University, Shanghai, China

Hong Xia, Ph.D. General Hospital of Guangzhou Military Command of PLA, Guanghzou, China

Jian-ru Xiao, Ph.D. Changzheng Hospital, Second Military Medical University, Shanghai, China

Yi Xiao, Ph.D. Department of Radiology, Changzheng Hospital, Second Military Medical University, Shanghai, China

Guo-hua Xu, Ph.D. Second Department of Spine Surgery, Changzheng Hospital, Second Military Medical University, Shanghai, China

Peng Xu, Ph.D. Second Department of Spine Surgery, Changzheng Hospital, Second Military Medical University, Shanghai, China

Xi-ming Xu, Ph.D. Second Department of Spine Surgery, Changzheng Hospital, Second Military Medical University, Shanghai, China

Tao Xu, Ph.D. The 113th Hospital of Chinese PLA, Ningbo, China

Hui-lin Yang, Ph.D. Department of Orthopaedics, The First Affiliated Hospital of Soochow University, Suzhou, China

Li-li Yang, Ph.D. Third Department of Spine Surgery, Changzheng Hospital, Second Military Medical University, Shanghai, China

Hai-song Yang, Ph.D. Second Department of Spine Surgery, Changzheng Hospital, Second Military Medical University, Shanghai, China

Xing-hai Yang, Ph.D. Department of Orthopaedic Tumor, Changzheng Hospital, Second Military Medical University, Shanghai, China

Xiao-jian Ye, Ph.D. Changzheng Hospital, Second Military Medical University, Shanghai, China

Bin-sheng Yu, Ph.D. Department of Orthopaedics, Peking University Shenzhen Hospital, Shenzhen, China

Hong-bin Yuan, Ph.D. Department of Anesthesiology, Changzheng Hospital, Second Military Medical University, Shanghai, China

Xue-song Zhang, Ph.D. Department of Spine Surgery, Chinese PLA General Hospital, Beijing, China

Jie Zhao, Ph.D. Department of Orthopaedics, Shanghai Ninth People's Hospital, Shanghai JiaoTong University School of Medicine, Shanghai, China

Zhao-min Zheng, Ph.D. Department of Spine Surgery, The First Affiliated Hospital, Sun Yat-sen University, Guangzhou, China

Xu-hui Zhou, Ph.D. Fourth Department of Spine Surgery, Changzheng Hospital, Second Military Medical University, Shanghai, China

Ze-zhang Zhu, Ph.D. Department of Orthopaedics, Nanjing Drum Tower Hospital, The Affiliated Hospital of Nanjing University Medical School, Nanjing, China

Surgical Anatomy of Upper Cervical Spine

1

Jian-gang Shi, Wen Yuan, and Jing-chuan Sun

1 Atlantoaxial Exposure by the Transoral–Transpharyngeal Approach

1.1 Overview

First reported by Kanavel in 1917, the transoral–transpharyngeal approach is the most direct surgical approach to the anterior occipitocervical area. This approach can preferably expose the anterior atlantoaxial structure and is often used for the resection of the anterior arch of the atlas and treatment of odontoid process base invagination, infection, tumor, and irreducible odontoid fractures during chronic dislocation. It is also used in the management of congenital malformation in the anterior atlantoaxial region. Since this surgical approach is limited by the mandible and oral cavity, its field of vision is relatively narrow. Its exposure generally ranges from the basilar clivus to the upper part of C3, but can be expanded toward the head by incising the soft and hard palates. The range of mandibular joint motion should be evaluated prior to surgery by physical examination and X-ray. For patients who have difficulty in opening their mouths, other surgical approaches should be considered. The advantage of the anterior approach is the absence of major vessels and nerves, and the most common complications are infection and cerebrospinal fluid leakage.

J.-g. Shi (✉) • W. Yuan • J.-c. Sun
Department of Orthopedics, Changzheng Hospital, Shanghai, China
e-mail: shijiangang616@163.com; yuanwenspine@163.com; sjchxc@foxmail.com

1.2 Position

The patient is placed in supine position. Shoulders are supported by soft pillows, and the neck is cushioned with a neck pillow in order to mildly extend the cervical spine (Fig. 1.1).

Insert the retractor systems to keep the mouth open and retract the tubes out of view (Figs. 1.2 and 1.3).

Fig. 1.1 Atlantoaxial exposure by the transoral–transpharyngeal approach

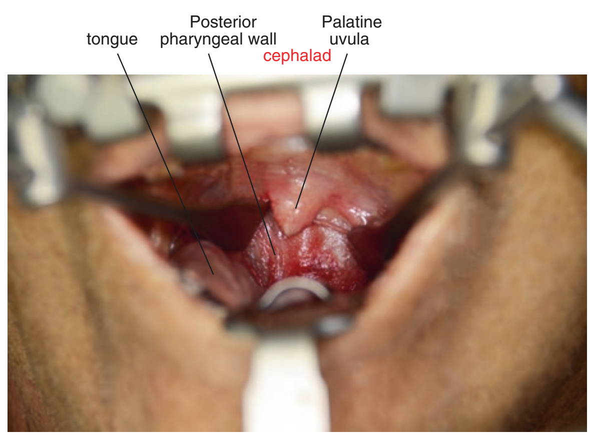

Fig. 1.2 Insertion of automatic retractor into the oropharynx to expose the posterior pharyngeal wall

J.-g. Shi et al. (eds.), *Anatomy Atlas and Interpretation of Spine Surgery*, https://doi.org/10.1007/978-981-10-5906-3_1

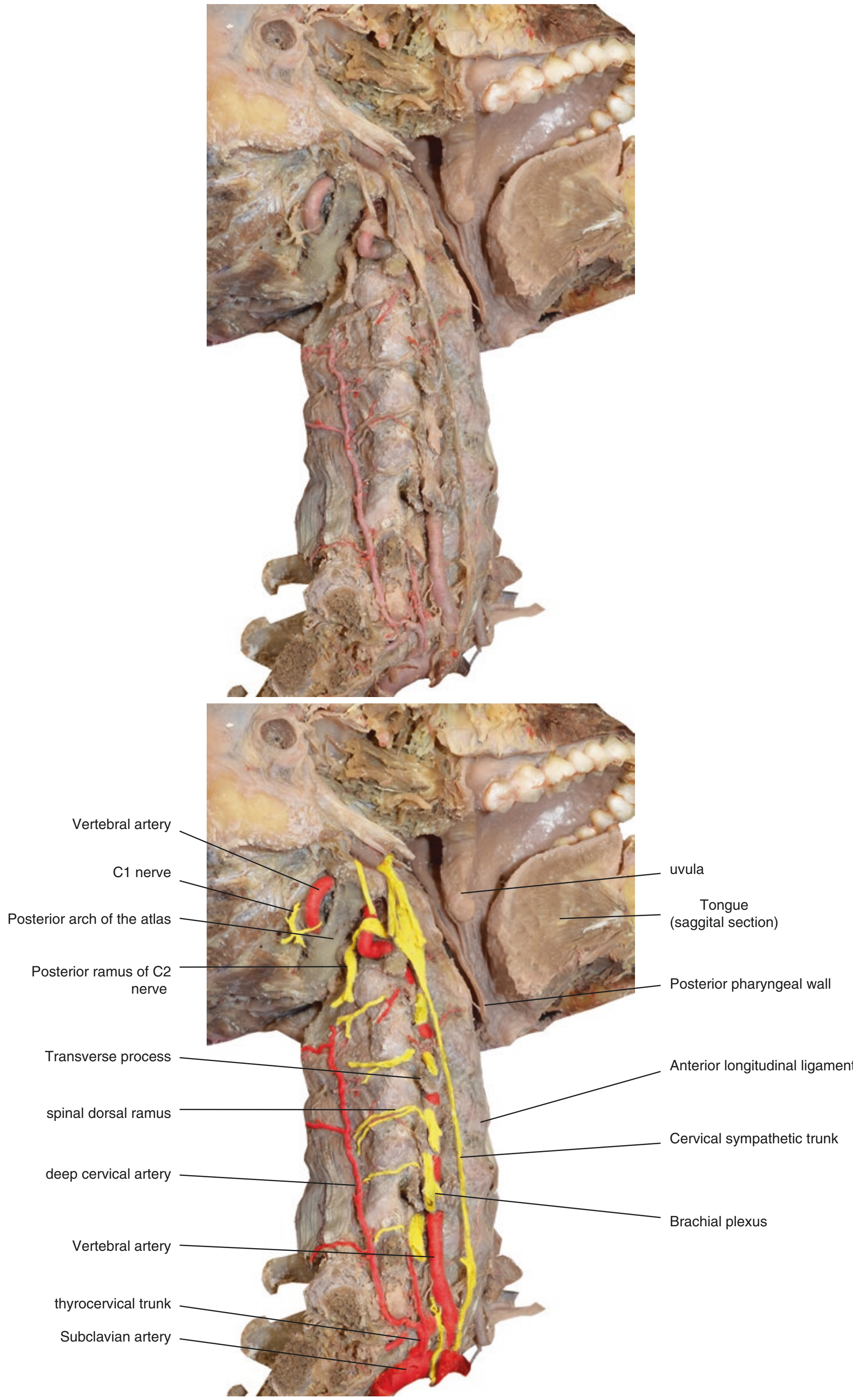

Fig. 1.3 Lateral view of the anatomic relationship between the oral cavity proper, posterior pharyngeal wall, and upper cervical spine

1.3 Exposure

Steroid should be used locally in the oropharynx to avoid the airway obstruction caused by postoperative edema. Meanwhile, the retractors should be adjusted to a suitable position in order to avoid excessive retraction and compression of the soft tissues.

Epinephrine and lidocaine are injected into the anterior tubercle of the atlas in order to reduce intraoperative bleeding and stretch the posterior pharyngeal wall soft tissues.

Make a 3 cm vertical incision in the midline of the anterior tubercle of the atlas, which can be extended to the C2 or C3 level. Incision is made through the mucosa, superior pharyngeal constrictor muscle, and pharyngobasilar fascia layer by layer until the prevertebral fascia to expose the longus colli muscle and the attachment site of anterior longitudinal ligament (Fig. 1.4).

The anterior tubercle of the atlas is off-center in cases of atlantoaxial joint dislocation. Therefore, in addition to touching the anterior tubercle, the location of the surgical incision can be confirmed by observing the position of uvula and X-ray in order to avoid the deflective incision resulting in imperfect exposure or injury of important structures.

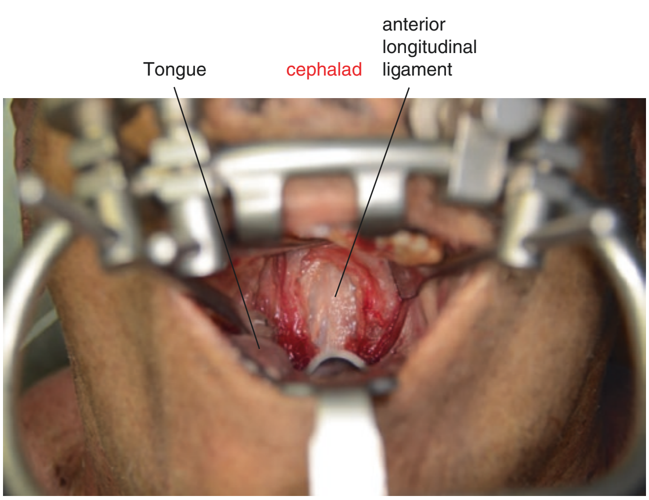

Fig. 1.4 Incision of the posterior pharyngeal wall and exposure of the prevertebral fascia

Superior pharyngeal constrictor muscle: a quadrilateral muscle that is thinner than the middle and inferior pharyngeal constrictor muscles. Stylopharyngeus and glossopharyngeal nerve are located between the base of the superior and the middle pharyngeal constrictor muscles. The retropharyngeal space is adjacent to the prevertebral muscle and prevertebral fascia and bounded by the ascending pharyngeal artery, pharyngeal venous plexus, glossopharyngeal nerve, lingual nerve, styloglossus, middle pharyngeal constrictor muscle, medial pterygoid, stylopharyngeus, and stylohyoid ligament. The superior pharyngeal constrictor muscle is innervated by the pharyngeal branch of ascending pharyngeal artery and the tonsillar branch of facial artery. Contraction of the superior pharyngeal constrictor muscle is mainly controlled by the transcranial accessory nerve and results in the contraction of the upper pharynx (Figs. 1.5 and 1.26).

Subperiosteal dissection is performed along the midline. The anterior arch of the atlas and the atlantoaxial joint are exposed by distracting the longus colli muscle laterally (Fig. 1.6).

Exposure of the atlas and axis should be maintained within 15 mm in width to protect the superior cervical ganglion from injury. Artery location should be confirmed by preoperative imaging to prevent injuries to the vertebral artery and internal carotid artery.

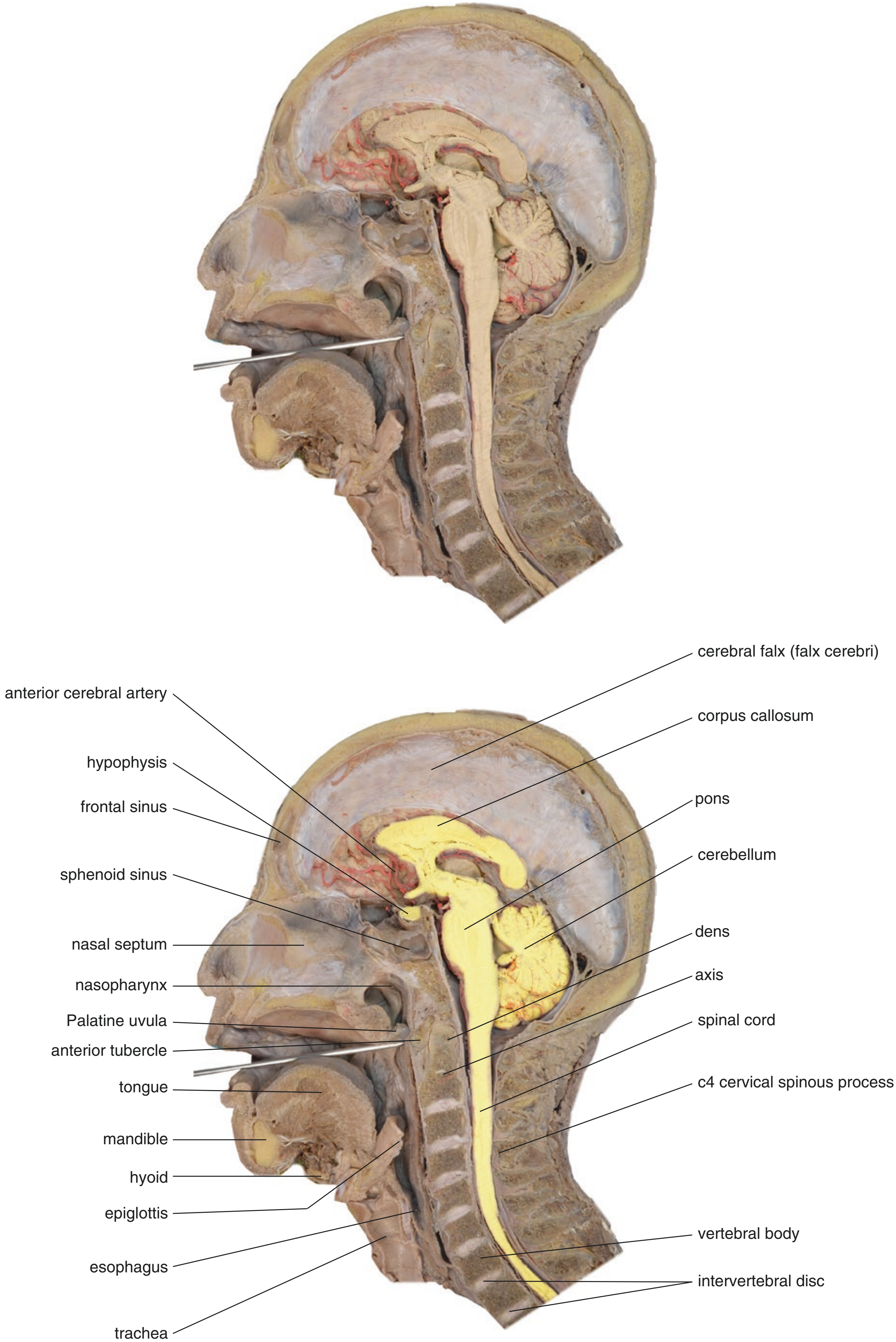

Fig. 1.5 Midsagittal section of the head and neck

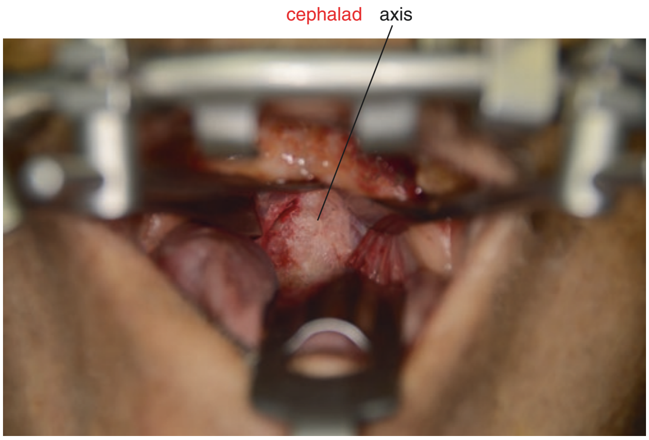

Fig. 1.6 Exposure of the axis by distracting the longus colli muscle laterally

Superior cervical ganglion (SCG): the largest of the three cervical sympathetic ganglia adjacent to C2 and C3. The SCG is sandwiched between the internal carotid artery (front) and the longus capitis muscle (back). SCG branches provide vasoconstrictor nerves for the face and neck and sudomotor nerves for the sweat glands. They also lead to orbitalis and superior tarsal muscle relaxation and pupil dilation. Some SCG branches ascend into the brain through the carotid canal along with the internal carotid artery (Fig. 1.7).

Anterior atlantooccipital membrane: a broad structure composed of densely woven fibers which connects the anterior margin of the foramen magnum to the upper border of the anterior arch of the atlas. It is laterally continuous with the articular capsules.

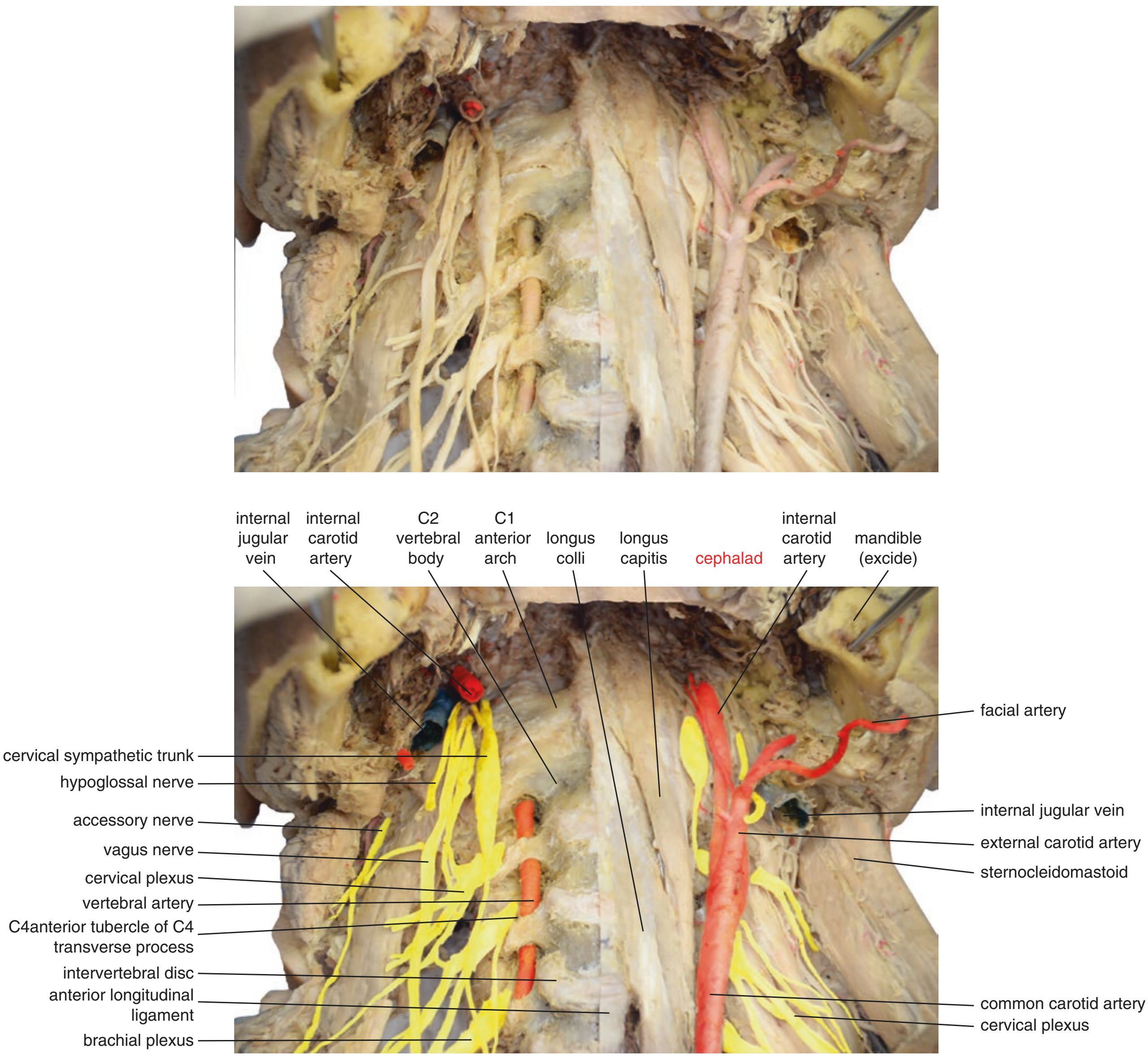

Fig. 1.7 Anterior cervical vertebral neurovascular and musculoligamentous structures

2 Anterior Atlantoaxial Exposure by Transmandibular Approach

2.1 Overview

Although exposure of the lower cervical spine is quite limited through the transoral approach, the clivus to upper cervical spine can be extensively exposed by a more complex approach involving jaw splitting. Ever since the introduction of the transmandibular approach by Martin in 1961, more surgeons have reported different approaches to anterior craniocervical junction. Wood et al. reported an expanded surgical approach involving the splitting of the soft and hard palates in addition to mandibulo glossotomy in 1980. Delgado et al. reported a case of chordoma resection from the clivus and upper cervical spine by mandibulotomy in 1981. Advantages of transmandibular approach include simultaneous exposure of the upper and lower (abdominal level) cervical spine, absence of major vessels and nerves, and avoidance of lateral retraction of important structures. However, extensive oropharyngeal swelling and infection are the main concern of postoperative management. The transmandibular approach is mainly used for the treatment of benign and malignant tumors in the ventral midline of the spinal cord, as well as congenital and posttraumatic deformities in the craniocervical junction.

2.2 Position

Patient is placed in supine position, and the head of the patient maintains traction with slight extension (Fig. 1.8).

Fig. 1.8 Anterior atlantoaxial exposure by transmandibular approach

2.3 Exposure

Mental foramen: usually located underneath the root of the second premolar tooth, at the midpoint between the superior and inferior borders of the mandible, and is about 2.5 cm lateral from the midline. The mental foramen opens backward, upward, or outward, with mental nerves and arteries passing through.

Mental nerve: terminal branch of the inferior alveolar nerve. It enters through the mental foramen into the face and innervates the skin of lower lip.

Mental artery: branches from the first segment of maxillary artery and the terminal branch of the inferior alveolar artery. It enters the face through the mandibular canal from the mental foramen and supplies blood to the muscle and skin of the mandible region.

The lower lip incision is made in the midline which should bypass the protruding mentum. The skin and subcutaneous tissue are incised along the midline to the level of hyoid bone (Figs. 1.8 and 1.9).

Subperiosteal dissection of the soft tissue should be limited within 2.5 cm from the midline in order to avoid intraoperative injuries to the mental nerve and artery.

Methylene blue shall be injected for accurate alignment of the boundary between mucosa and skin during the conclusion of the procedure in order to maximize the cosmetical realignment.

Subperiosteal dissection of both sides of the mandibular bone surface is done to fully expose the mandible body.

The bone surface should be pre-drilled before splitting the mandible to ensure accurate realignment of mandible and avoid postoperative occlusal disorder.

The mandible is split in a zigzag fashion with oscillating saw.

The posterior pharyngeal wall is exposed by pulling the tongue and hyoid bone downward with the retractors.

The tongue can be split medially when necessary.

The tongue and mandible should be retracted laterally to make a satisfactory access to the posterior pharyngeal wall.

Make sure to keep the incision in the middle when cutting through the mucosa at the base of the oral cavity to prevent injury to the salivary ducts on either sides of the lingual frenulum. Salivary duct injury may cause continuous postoperative exudation of clear saliva from the skin wounds.

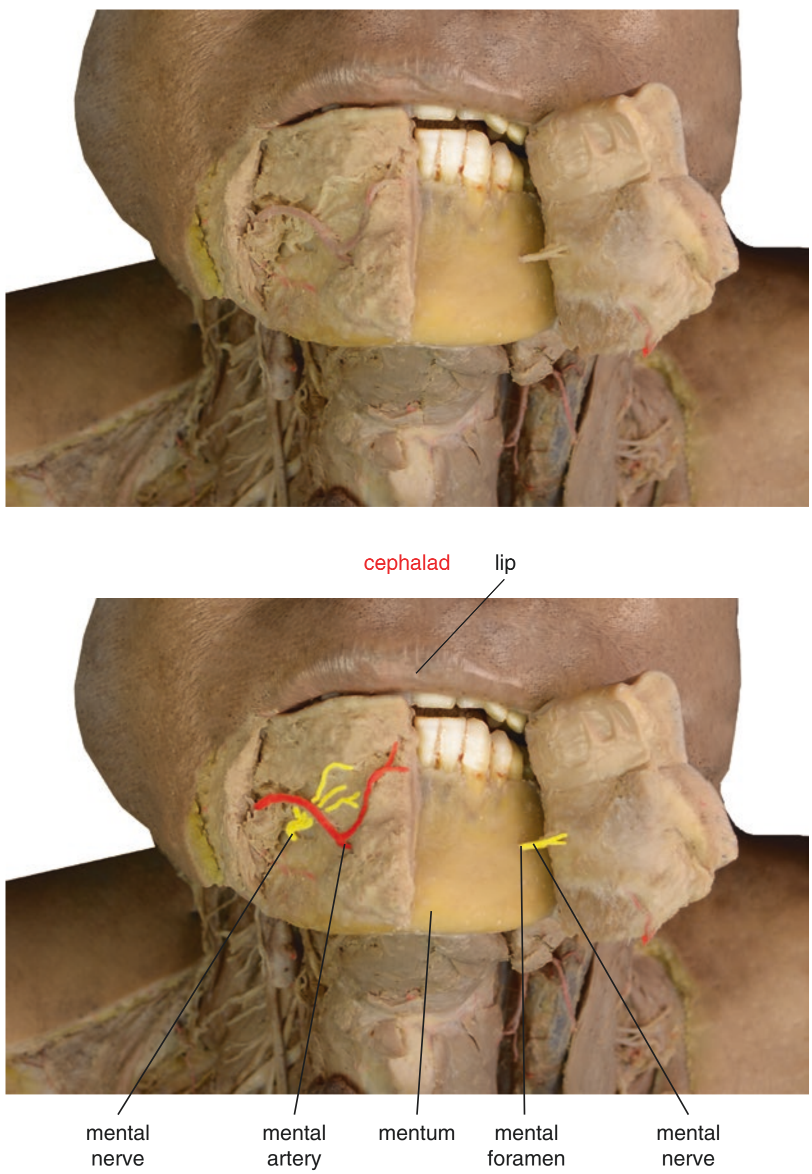

Fig. 1.9 Vessels and nerves in the mandible region

Submental artery: the largest cervical branch of the facial artery, which arises from the level of the facial artery, leaves the submandibular gland, and runs forward upon the mylohyoid muscle just below the mandible. The submental artery supplies the surrounding skin and muscles (Figs. 1.10 and 1.11).

Submandibular duct: about 5 cm in length and opens at the summit of the sublingual caruncle, which lie on the floor of the mouth on either sides of the lingual frenulum. The submandibular duct passes between the lingual and hypoglossal nerves as it runs across the hyoglossus until the anterior margin of the hyoglossus. The lingual nerve crosses laterally under the submandibular duct, and its terminal branch runs upward along the interior of the submandibular duct (Fig. 1.12).

Sublingual duct: the sublingual gland braches into 8–20 excretory ducts. Small sublingual ducts open on the summit of sublingual fold at the back of the gland. Small branches at the anterior of the gland sometimes form a major sublingual duct which opens at the sublingual fold alone or together with the submandibular gland.

Palatine uvula: a conic projection from the posterior edge of the middle of the soft palate that hangs between the oral cavity and the pharynx (Fig. 1.13).

Epiglottis: a leaf-shaped structure on the back of the tongue composed of fibroelastic cartilage. The front bottom of the epiglottis connects to the superior margin of the hyoid bone through the elastic hyoepiglottic ligament. The epiglottis is separated from the thyrohyoid membrane by adipose tissue, forming the preepiglottic space (Fig. 1.13).

Structures attached on the anterior tubercle of the atlas: the uppermost pair of muscle bundles of the longuscolli muscle converges toward the anterior tubercle of the atlas. The anterior longitudinal ligaments of the cervical spine between the two muscle bundles also end on the anterior tubercle of the atlas. Identification of the structures mentioned above during operation can help surgeons identify the position of the anterior tubercle in case of dislocation (Fig. 1.14).

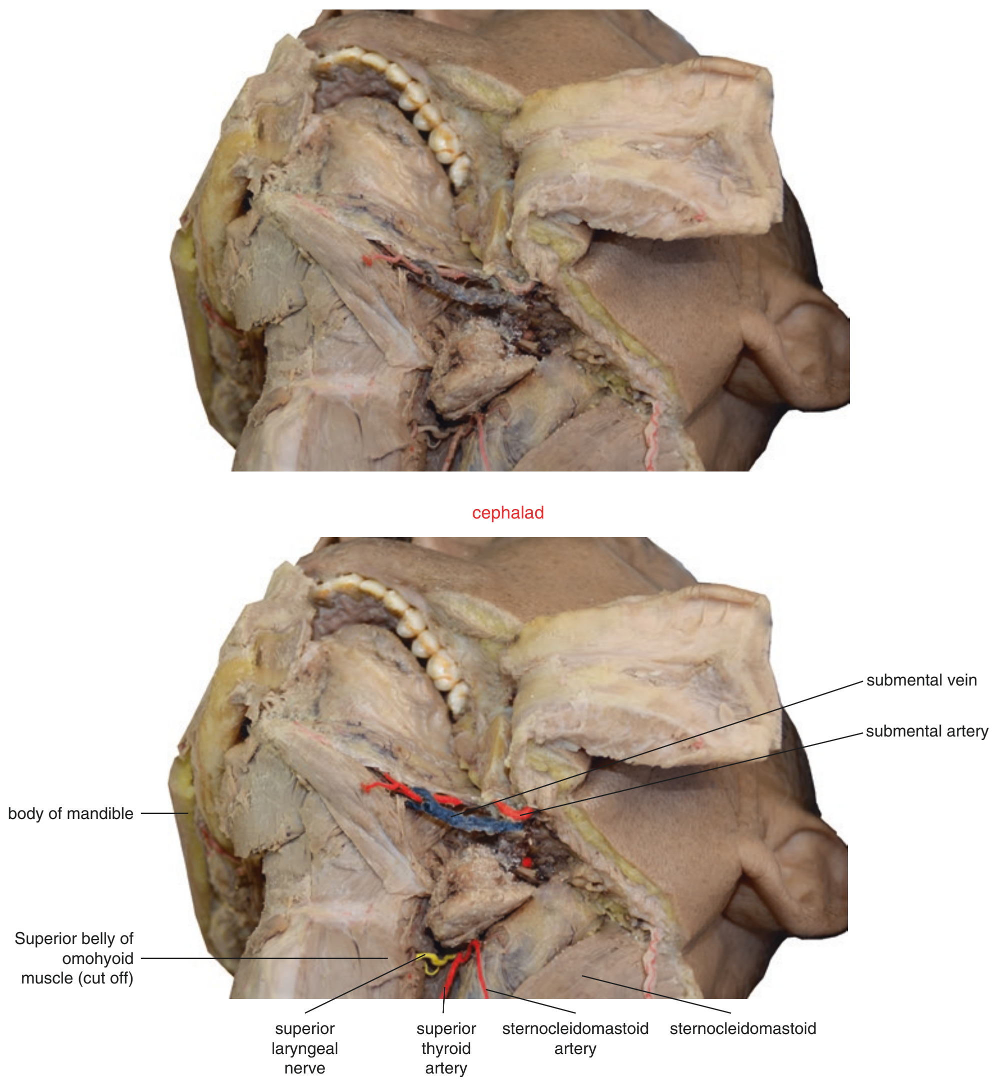

Fig. 1.10 Submental artery and vein and digastric muscles below the mandible

Fig. 1.11 Submandibular blood vessels and nerves

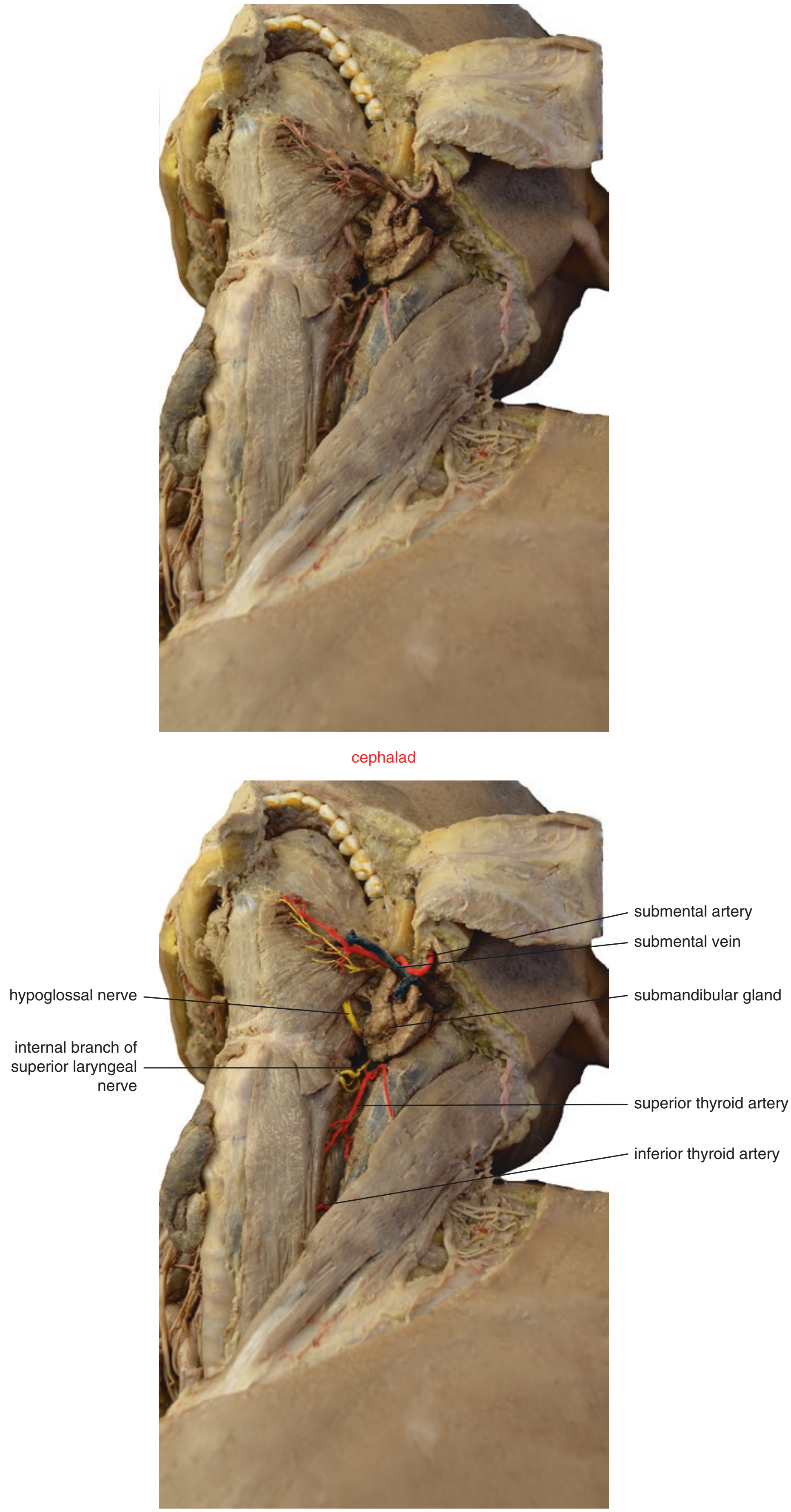

Fig. 1.12 Sublingual nerves, glands, and ducts

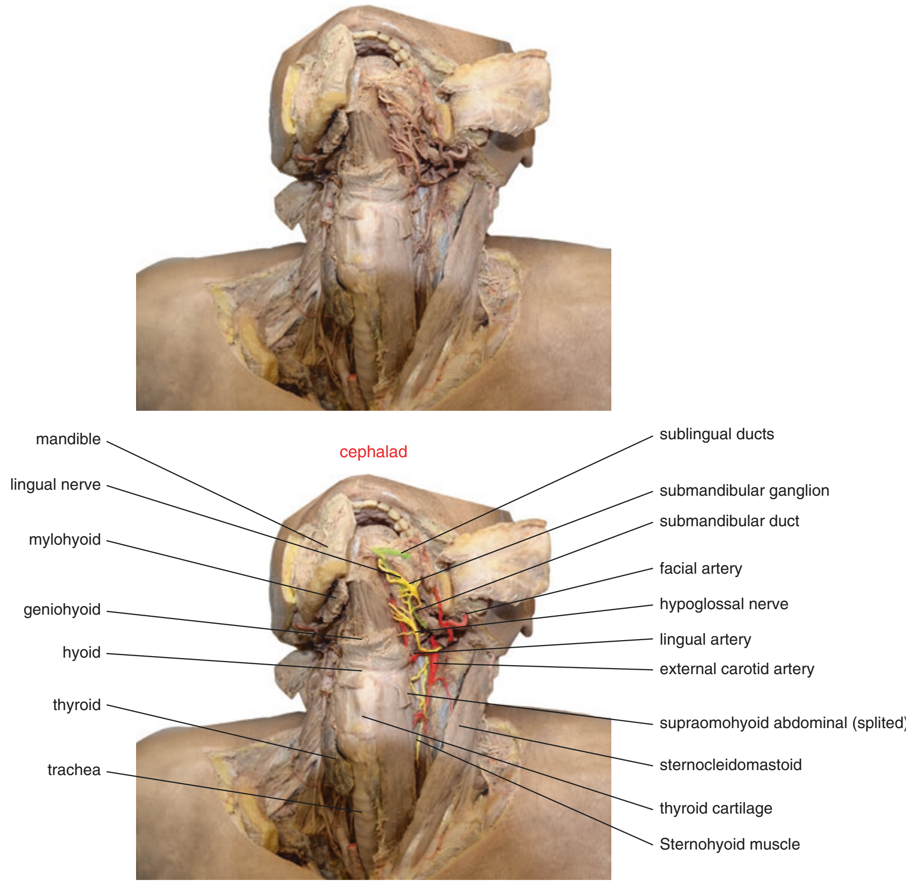

Fig. 1.13 Structure of the posterior pharyngeal wall after splitting the tongue

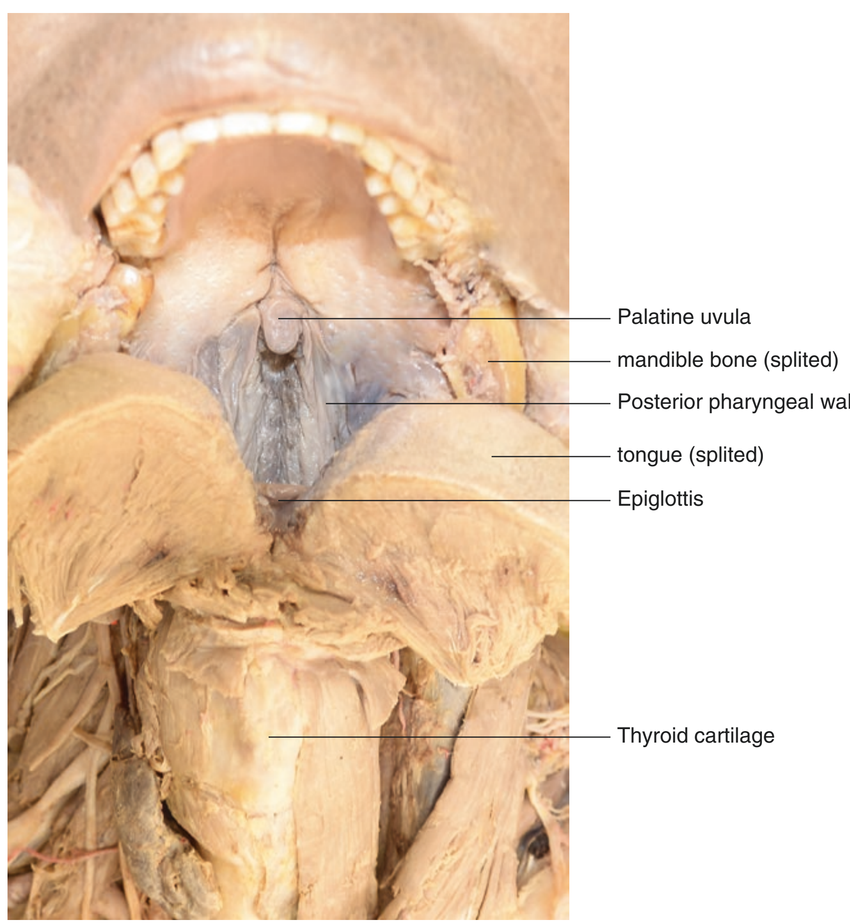

Fig. 1.14 Anterior of axis after splitting the tongue and posterior pharyngeal wall

There are various extended transoral approaches:

Median mandibulotomy without glossotomy:

The mandible is split without cutting through the skin of lower lip in this approach.

This approach only requires stealth incision of the mucosa between the lower lip and mandible before sawing open the mandible, and the superior margin of C3 is exposed after stealth peeling of the periosteum.

Median mandibulotomy without glossotomy is suitable for patients with ventral lesions in upper cervical spine accompanied with difficulty opening the mouth.

This approach leaves no scars after the operation and thus has cosmetical significance.

Transmandibular circumglossal approach:

The mandible is split, and the lateral side of the tongue is split through the sublingual muscles without cutting the tongue body.

Although this approach results in little trauma, the exposure is smaller than the former approach.

Transmandibular circumglossal approach is suitable for patients with ventral lesions in the upper and lower cervical spine and lesions that occur on one side.

The hypoglossal nerve should be isolated and protected if applying the paramedian mandibulotomy approach.

Median mandibulotomy with glossotomy:

The tongue, sublingual muscles, and mandible are split through along the midline.

This approach allows the full exposure of the posterior pharyngeal wall up to the inferior border of C5 and is suitable for dealing with patients with ventral lesions on the upper and lower cervical spine.

This approach is convenient for the treatment of vertebral lesions involving many segments of the upper and lower cervical spine.

3 Lateral Atlantoaxial Exposure and Odontoidectomy by Suprahyoid Approach

3.1 Overview

The anteromedial retropharyngeal approach to the upper cervical spine was improved by Southwick and Robinson (1975) to expose the middle and the inferior cervical spine. This approach can be applied to anterior tumor resection, debridement and atlantoaxial fixation of the upper cervical spine, as well as odontoid fixation. It can directly expose the clivus to C3 and can even be expanded to expose the middle to lower cervical spine. This approach accesses the retropharyngeal space from the medial side of the carotid sheath, which can avoid injuries to the carotid artery and basicranial nerves. However, it also has a greater chance of damaging the superior laryngeal nerve, glossopharyngeal nerve, and vertebral artery compared to lateral carotid sheath approach. The advantage of this technique is that it is completely an extramucosal approach and thereby can effectively reduce the chance of infection. The disadvantage is that it is not a direct approach and it results in long exposure and the need of tracheotomy.

3.2 Position

Patient is placed in a supine position, with the head slightly extended backward and turned to the opposite side at a 30°. A moderate head elevation provides better surgical vision and venous drainage (Figs. 1.15, 1.16, and 1.17).

General anesthesia with fiberoptic nasotracheal intubation can prevent excessive neck movement and avoid the low position mandible obstructing the surgical field in orotracheal intubation case.

Fig. 1.15 Position of lateral atlantoaxial exposure and incision by suprahyoid approach

Fig. 1.16 Position of lateral atlantoaxial exposure and incision by suprahyoid approach

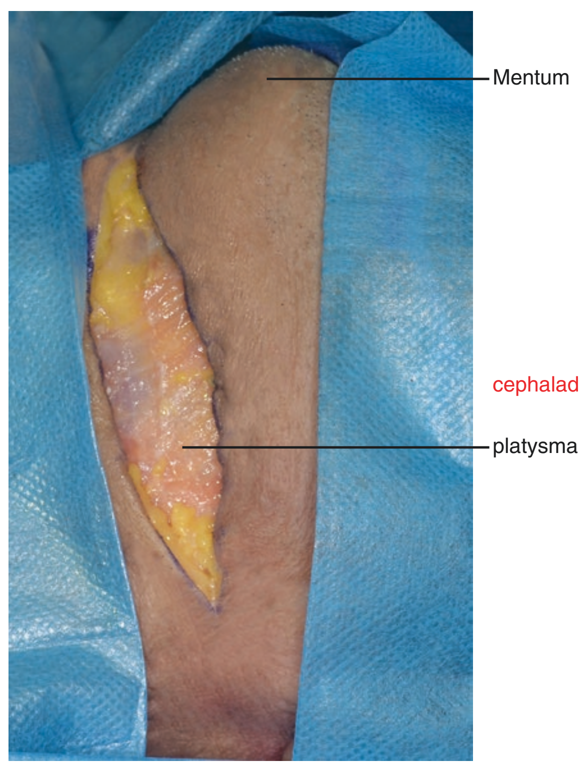

Fig. 1.17 Submandibular incision on the skin

3.3 Exposure

The incision is made parallel with 2 cm below the inferior border of the mandible. The skin incision is usually designed from hyoid bone (medial) to mastoid process (lateral).

A longitudinal incision intersecting the submandibular incision can be made to further expose the posterior end (Fig. 1.18).

Platysma is incised along the incision line.

After the superficial fascia is dissected from the platysma, the junction of the jugular vein and the retromandibular vein is coagulated with ligation or bipolar electrocautery (Fig. 1.19).

Special attention should be paid to the marginal mandibular branch of the facial nerves. Injury of this branch may lead to dropping at the corner of the mouth on the affected side (Fig. 1.20).

Fig. 1.18 Expansion of exposure by longitudinal incision along the sternocleidomastoid muscle

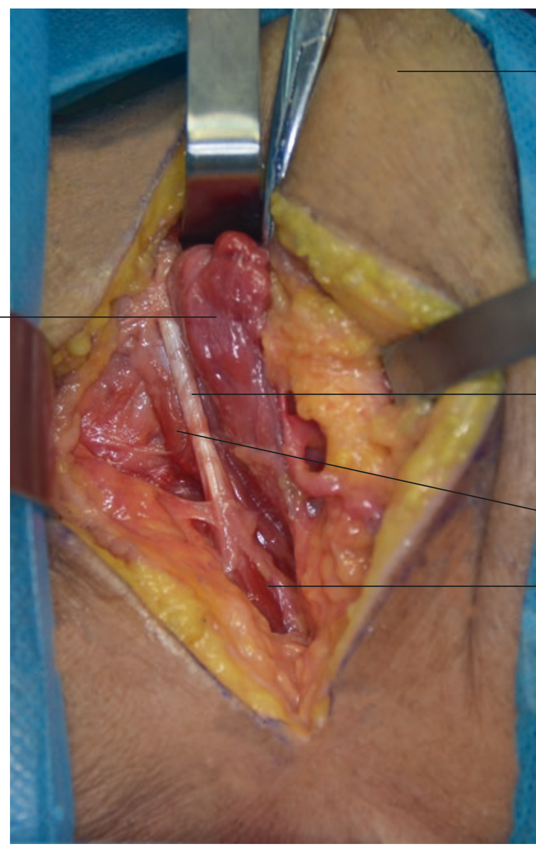

Fig. 1.19 Dissection of the superficial fascia and the platysma to expose the submandibular gland and digastric muscle

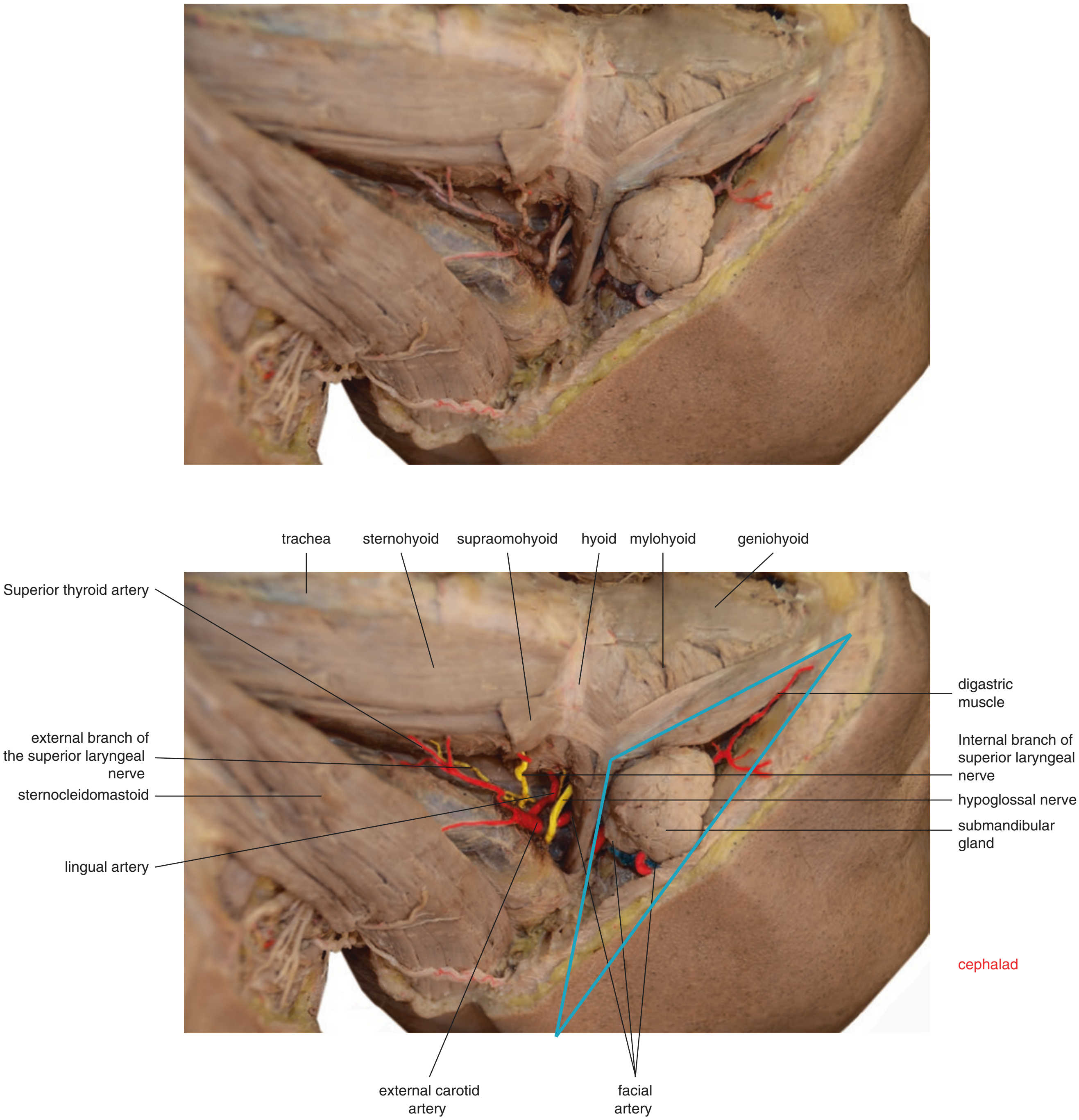

Fig. 1.20 Anatomic relation of the digastric triangle

Digastric triangle: bounded superior by a line drawn from the lower border of mandible to the mastoid process, lateral by posterior belly of the digastric and stylohyoid muscle, and medial by the anterior belly of the digastric muscle. The submandibular gland is anterior to the digastric triangle. The submental artery and facial artery are located in its superficial fascia, while the facial artery can be found in the deep fascia (Fig. 1.20).

Marginal mandibular branch of the facial nerve: usually comprised of two branches. It passes forward from the angle of mandible beneath the platysma, then runs through the superficial layer of the submandibular triangle and crosses the anterior body of mandible, and eventually passes beneath the depressor angulioris. The branch innervates the risorius and lower lip muscles and joins the mental nerve (Fig. 1.21).

Common facial vein: often runs parallel with the anterior branch of the retromandibular vein. The marginal mandibular branch of the facial nerve usually crosses above the anterior of the retromandibular vein and the anterior of the anterior facial vein (Fig. 1.21).

Lesser occipital nerve: a branch of the cervical plexus that ascends from the posterior border of the sternocleidomastoid muscle and innervates the skin above and behind the ears (Fig. 1.21).

Facial vein: collects blood from the supratrochlear vein and supraorbital vein; facial vein is one of the major veins in the face. It runs obliquely downward beside the nose, descends along the surface of the masseter muscle, crosses the body of mandible, and finally enters into the internal jugular vein.

Submandibular gland: located in the digastric triangle with the lingual nerve that runs above while the hypoglossal nerve and the lingual vein run below. The submandibular gland is supplied by the branches of the facial artery and lingual artery (Fig. 1.23).

Digastric muscle: located under the jaw, arises from the mastoid process, medial to the mentum. It consists of two muscular bellies united by an intermediate rounded tendon. The intermediate tendon is attached to the body of hyoid bone and the greater horn of hyoid bone by a fibrous loop. The posterior belly of the digastric muscle is supplied by the posterior auricular and occipital arteries, while the anterior belly is supplied by the submental artery of facial artery branch. The anterior belly is innervated by the inferior alveolar nerve of the mylohyoid muscle, and the posterior belly is innervated by the facial nerves. Contraction of the digastric muscle can lift the hyoid bone. The posterior belly plays a stronger role especially at the time of swallowing and chewing (Figs. 1.22 and 1.23).

Lingual artery: provides the blood supply to the tongue and the bottom of oral cavity. It arises from the external carotid between the superior thyroid artery and facial artery. It passes posteromedially to the hyoglossus muscle and runs forward through the deep surface of the muscle to the tip of the tongue (Fig. 1.24).

Facial artery: above the lingual artery and arises from the external carotid artery. It passes obliquely up beneath the digastric muscle and submandibular gland, arches over the interior border of the mandible, and enters into the face through the anterior border of the masseter muscle. The facial artery is remarkably tortuous in order to accommodate the swallowing movement of the pharynx, the mandible, lip, and cheeks (Fig. 1.25).

Hypoglossal nerve: main nerve that innervates the extrinsic and intrinsic muscles of the tongue. It arises from the skull and descends laterally behind the internal carotid artery, hypoglossal nerve, and vagus nerve, to the angle of mandible between the internal carotid artery and internal jugular artery. After passing the posterior belly of the digastric muscle, the hypoglossal nerve becomes superficial and crosses the internal and external carotid arteries and the lingual artery while sending out branches that supply the omohyoid, thyrohyoid, and geniohyoid muscles. The other branches converge with the descending branches of the cervical nerve to form the ansa cervicalis (Figs. 1.25 and 1.26).

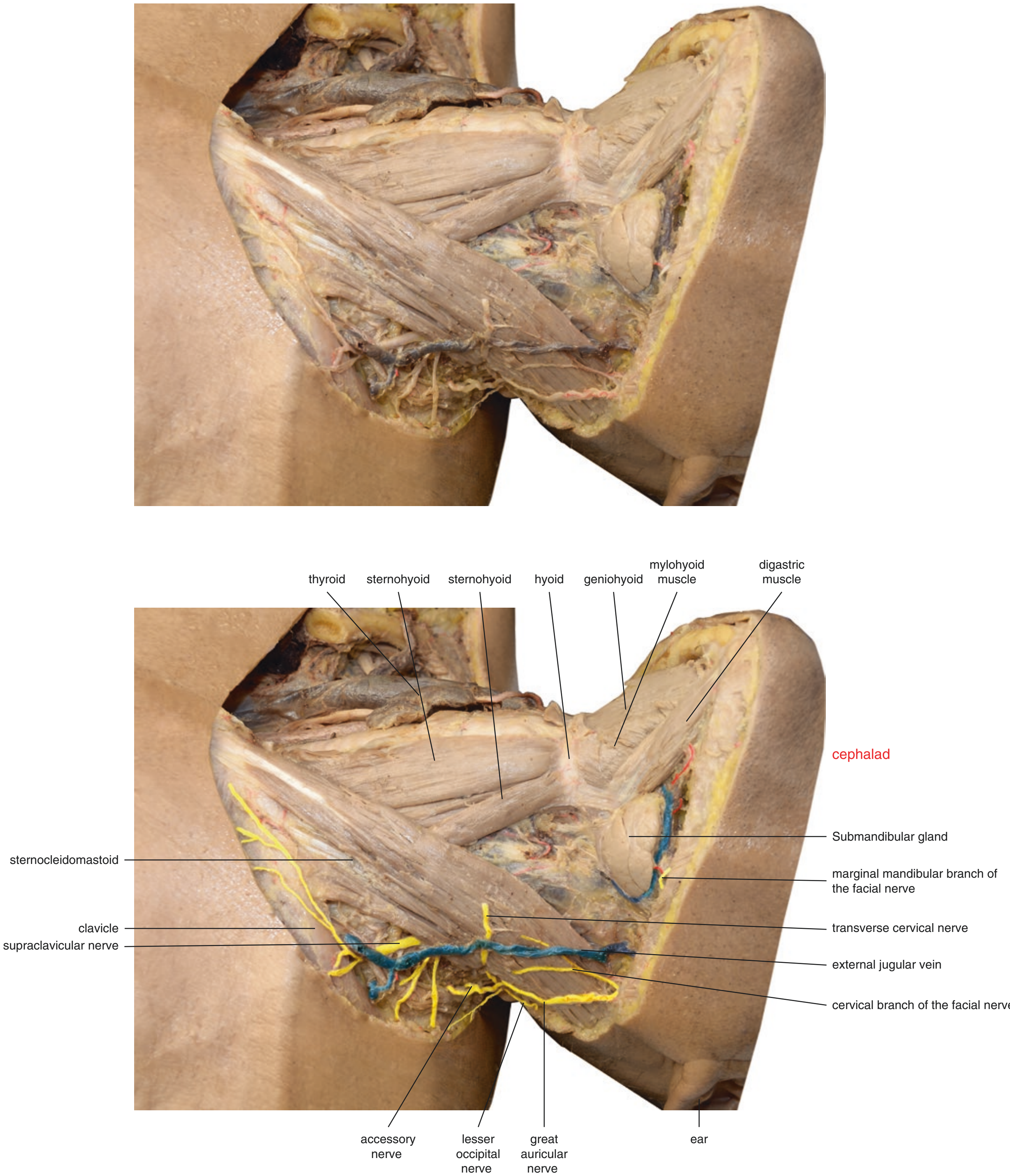

Fig. 1.21 Deep cervical structures on the left side

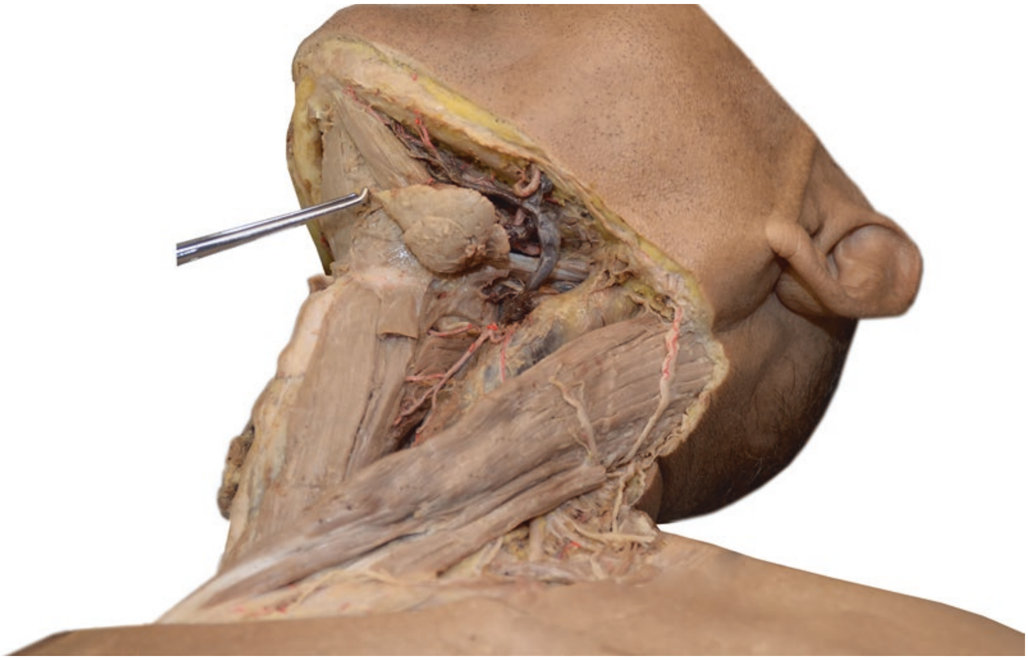

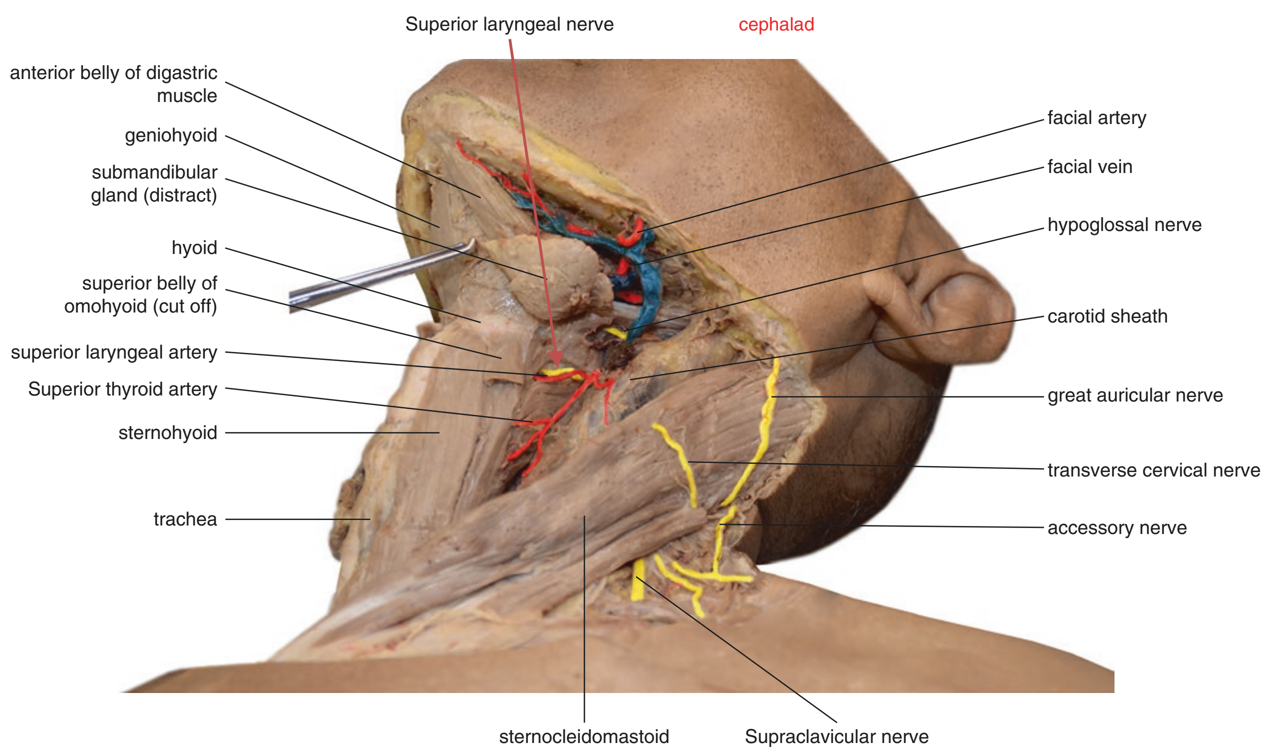

Fig. 1.22 Deep cervical structure on the left side

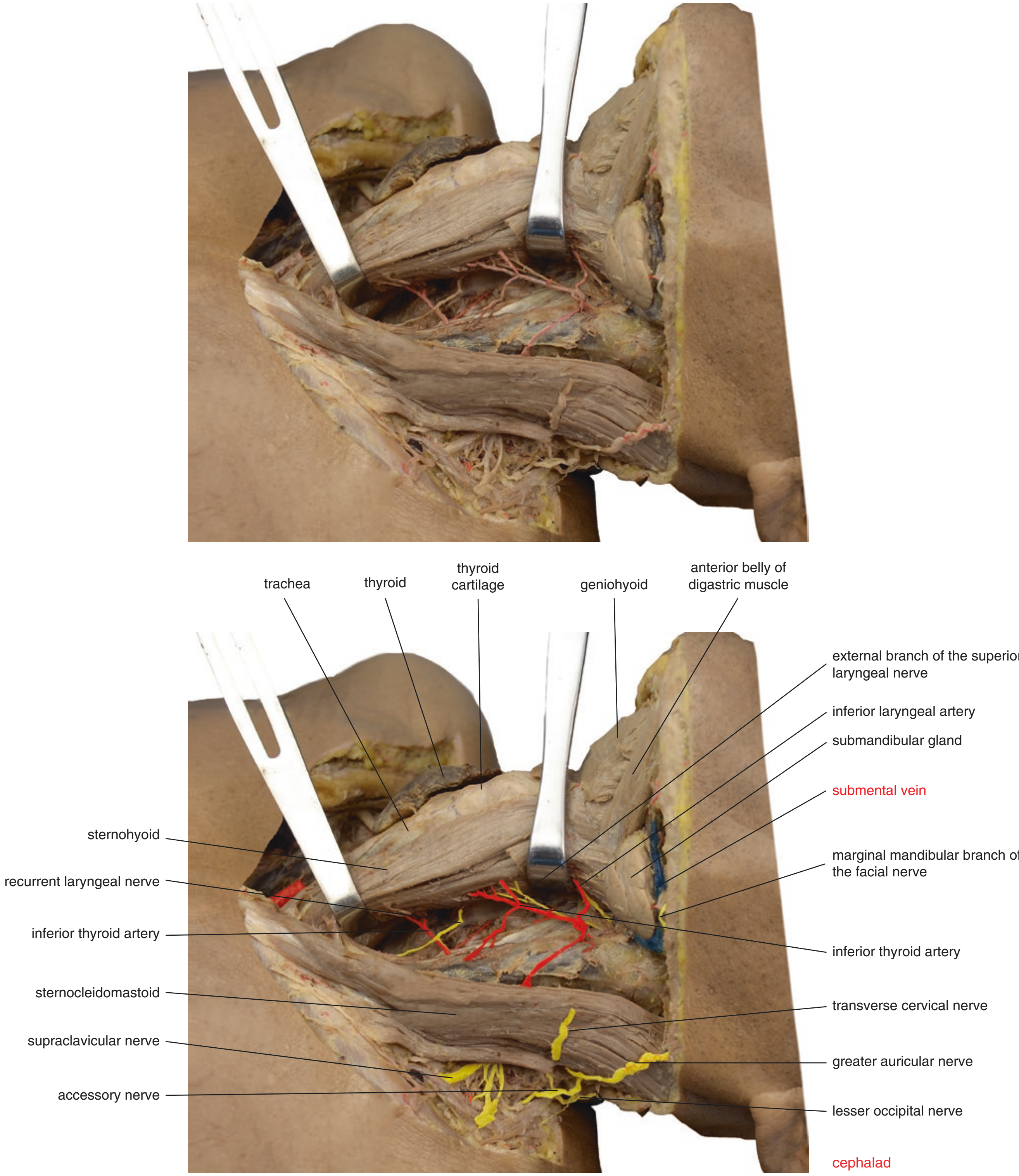

Fig. 1.23 Deep cervical structures on the left side (trachea and esophagus distracted to expose the prevertebral fascia)

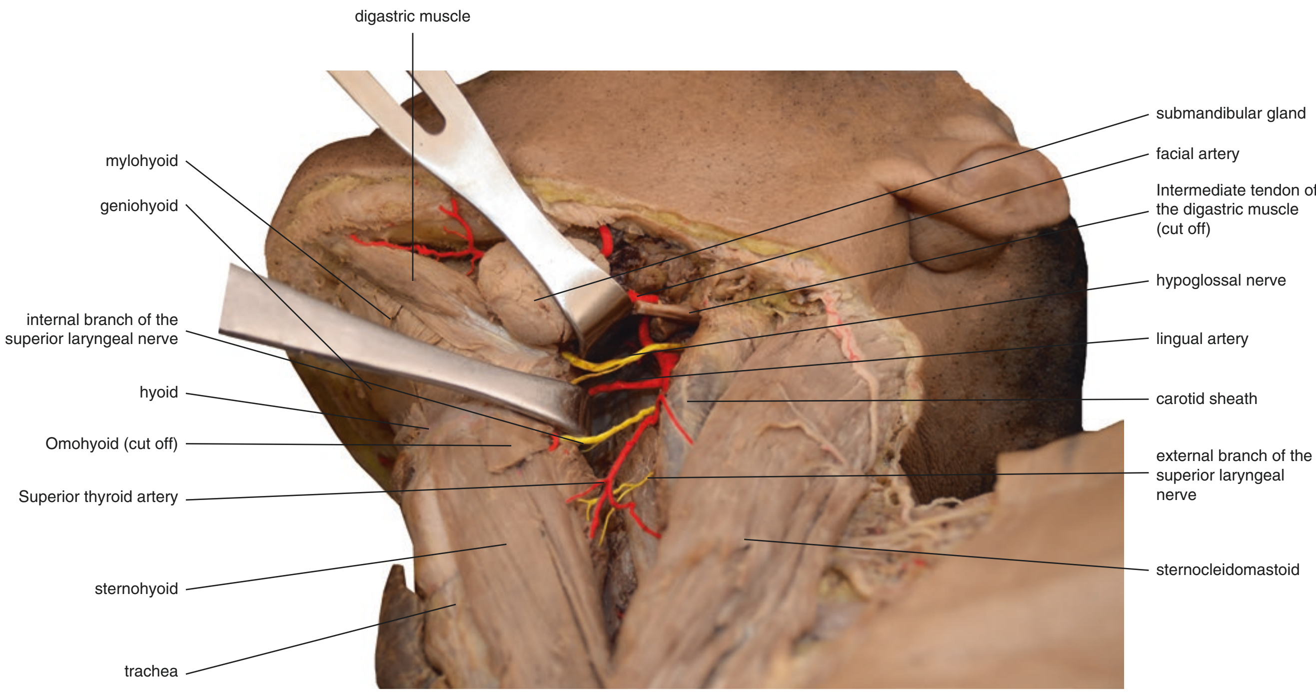

Fig. 1.24 Deep cervical structures on the left side (trachea and esophagus distracted to expose the prevertebral fascia)

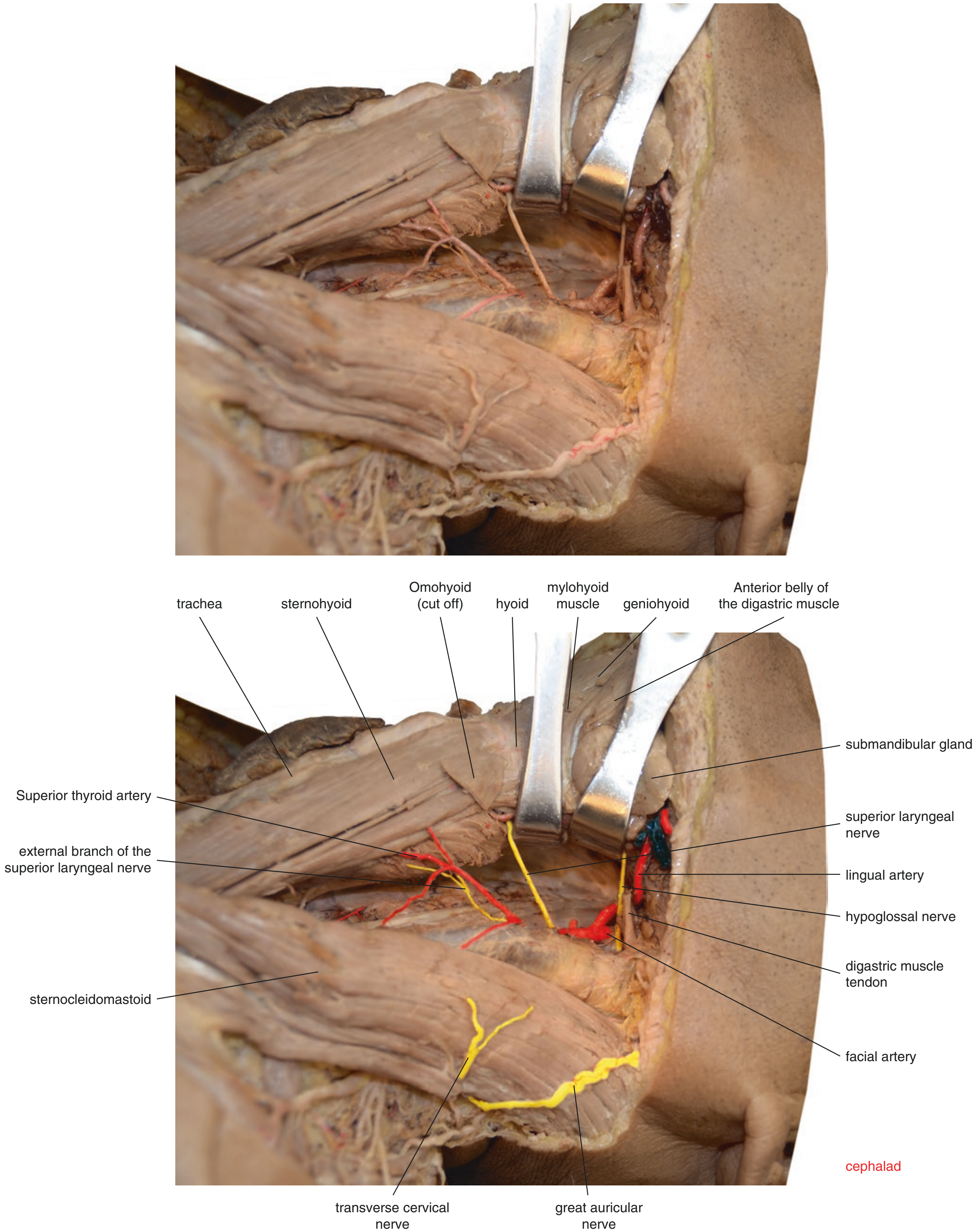

Fig. 1.25 Deep cervical structure on the left side (lingual artery resected, trachea and esophagus distracted to expose the prevertebral fascia)

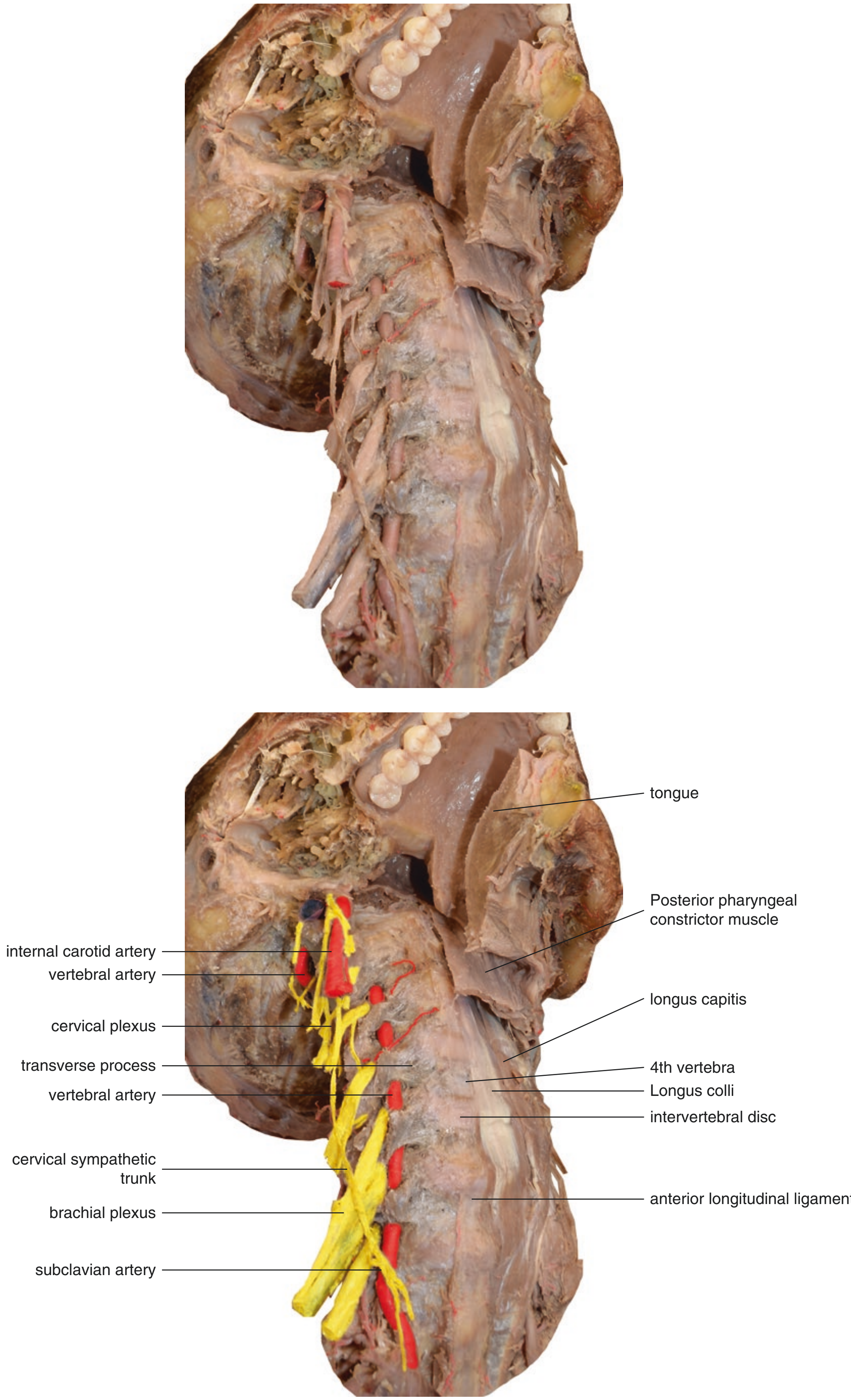

Fig. 1.26 Anterior and lateral structures of each layer of the vertebral body

Identify and ligate the facial vein that runs on the surface of the submandibular gland.

The submandibular gland is isolated upward to expose the intersection of the digastric muscle and stylohyoid muscle.

The digastric muscle and stylohyoid muscle are retracted toward the mandible to expose the fascia.

The hypoglossal nerve lies slightly inferior and beneath the digastric muscle tendon and is parallel to the direction of the tendon. The hypoglossal nerve should be protected carefully (Fig. 1.27).

Both the posterior belly of the digastric muscle and the stylohyoid muscle are within the area of operation in this approach. Surgeons should avoid pulling the lateral part of the posterior belly of digastric muscle and stylohyoid muscle with the retractor in order to prevent damage to the facial nerve.

The hypoglossal nerve is retracted downward. Bluntly dissect the deep fascia and palpate the carotid sheath on the lateral.

Retract the carotid sheath laterally and the posterior pharyngeal constrictor medially to find entrance to the retropharyngeal space. If fat pad within the retropharyngeal space is observed, then the exposure has been done correctly (Fig. 1.28).

The hypoglossal nerve is medial to the vagus nerve and the internal carotid artery near the angle of mandible. It runs inwardly in front of the lingual and facial arteries and innervates the tongue muscles.

The lingual artery and facial artery can be ligated if necessary. Otherwise they should be retained to help prevent overstretching of the hypoglossal nerve.

When the esophagus is injured during surgery, suture and repeat washout should be performed immediately. The nasogastric tube should be retained for 1 week after the surgery.

Dissector is used to clean the alar fascia and prevertebral fascia.

The longus colli muscle is longitudinally bifurcated in the midline and attached to both sides of the anterior arch of the atlas (Figs. 1.29 and 1.30).

The longus colli muscle and anterior longitudinal ligament are subperiosteal dissected toward lateral sides. This exposes the anterior atlantoaxial spine and C2 vertebra (Fig. 1.31).

In order to avoid invading the anterior atlantooccipital membrane, the incision should not exceed the cranial border of the atlas.

Subperiosteal dissection should be conducted no more than 15 mm from the atlantoaxial midline to prevent damages to the vertebral artery.

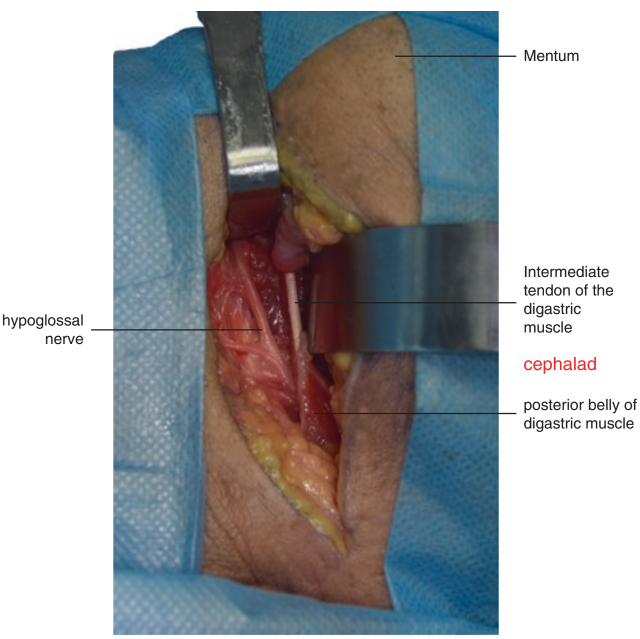

Fig. 1.27 Retraction of the digastric muscle and stylohyoid muscle toward the mandible

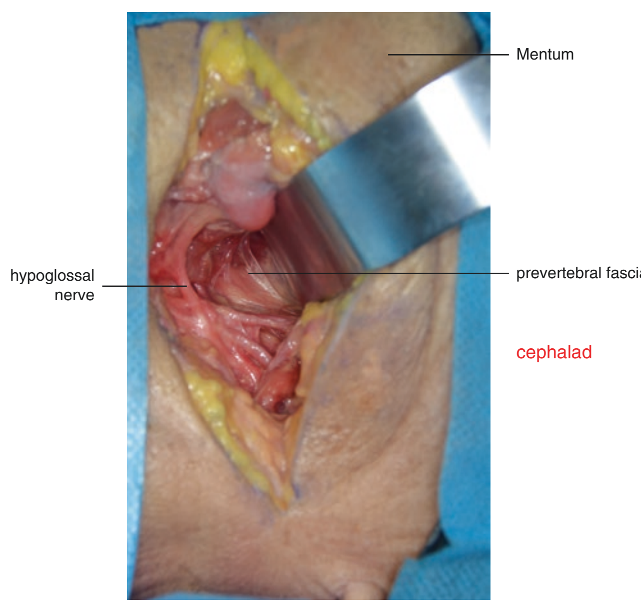

Fig. 1.28 Access through the retropharyngeal space to the prevertebral fascia

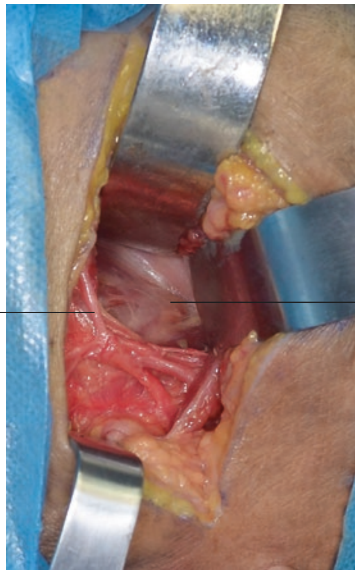

Fig. 1.29 Exposure of the anterior atlas

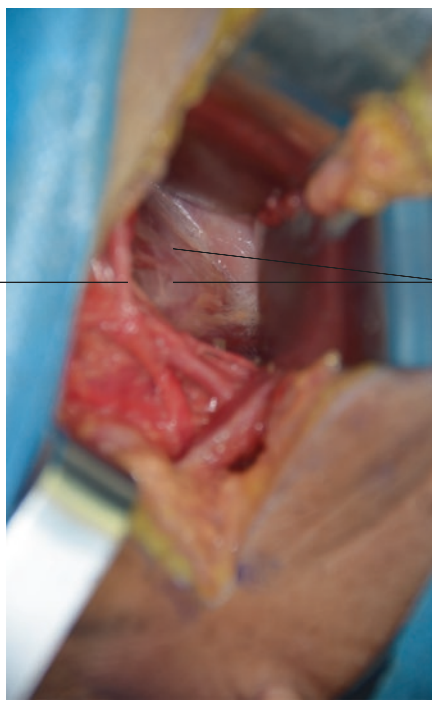

Fig. 1.30 Exposure of the anterior atlas

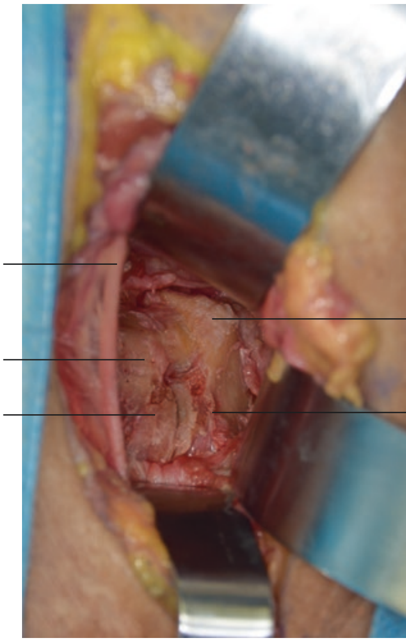

Fig. 1.31 Subperiosteal dissection of the longus colli muscle on the anterior atlantoaxial spine

3.4 Odontoidectomy

Remove the anterior tubercle of the atlas by Kerrison's rongeur to expose the odontoid process (Fig. 1.32).

Surgeon should intermittently release the retractors on the internal carotid artery in order to avoid cerebral ischemia.

Resection of the odontoid process is performed by a high-speed drill. When most of odontoid process have been resected, a diamond burring should be used for the inner cortex attached with the cruciate ligament (Fig. 1.33).

The remaining cortical bone is removed from the odontoid process and the posterior wall of the C2 vertebra using a sharp curette. The cruciate ligament is resected using a pulposus forceps to release the pressure on the tectorial membrane.

If local scar tissue is observed, it should be removed until the tectorial membrane is fully exposed.

The tectorial membrane is resected until both sides of the dural sac are bulged forward. Decompression is sufficient when active pulsation of the dural sac is observed.

Dural sac pulsation can be observed after removal of the tectorial membrane (Fig. 1.34).

Since the thinnest region of the prevertebral soft tissue of the upper cervical spine is only 5–7 mm thick. It is best to use low-profile fixation devices to avoid foreign body sensation of the pharynx after surgery.

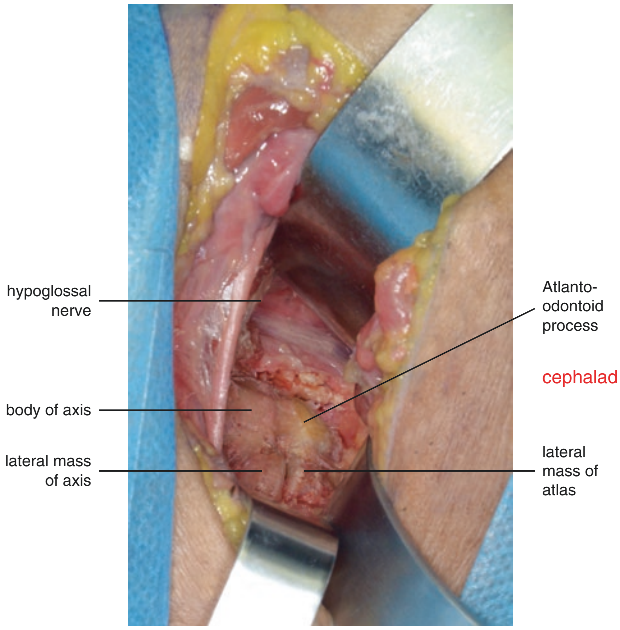

Fig. 1.32 Removal of the anterior tubercle of the atlas by Kerrison's rongeur to expose the odontoid process

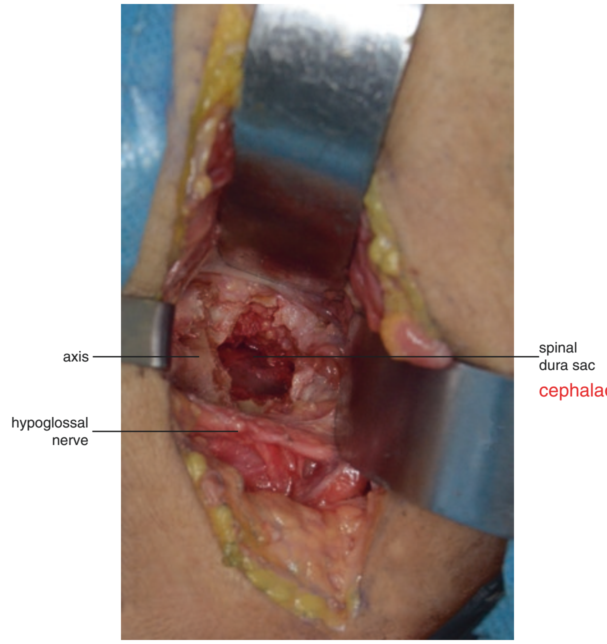

Fig. 1.34 Removal of the tectorial membrane to expose the dural sac

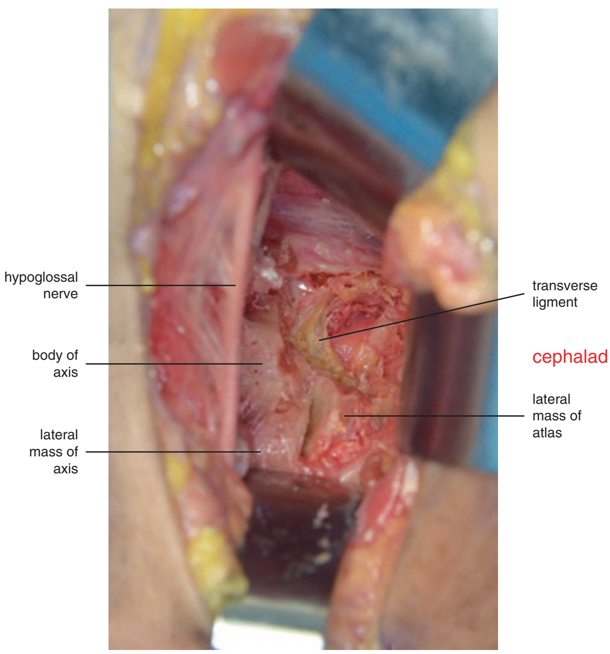

Fig. 1.33 Excision of the odontoid process with a high-speed drill

Tectorial membrane: a continuation of the posterior longitudinal ligament and a wide and strong ligament. Its superficial layer is above the foramen magnum and is attached to the skull and merges with the dural sac of skull. Its deep layer is composed of a strong central band and two side bands. The central band runs upward to the foramen magnum, and the two side bands run to the foramen magnum and merge with atlantooccipital joint capsule (Figs. 1.35 and 1.36).

Cruciate ligament of the atlas: composed of the transverse ligament and longitudinal ligament. The transverse ligament is wide and strong, about 2 cm long, with both sides arising from the axial lateral mass which arches across the back of the odontoid process and serves as an important structure for stabilizing the atlantoaxial joint. The superior border of the transverse ligament emits a tough central longitudinal ligament, which runs upward to the base of the occipital bone between the apical odontoid ligament and tectorial membrane. The bottom of the transverse ligament also emits a thin longitudinal ligament that ends at the posterior border of the axis. The transverse ligament divides the atlantoaxial canal into an anterior and a posterior section, where the anterior section consists 1/3 of the canal including the odontoid process, while the posterior section consists 2/3 of the canal including the spinal cord and its membranes (Fig. 1.37).

Alar ligament: arises from the posterolateral side of the tip of the odontoid process to the medial rough surface of the occipital condyle and is about 1 cm long. The main function of alar ligament is to restrict contralateral rotation of the atlantoaxial joint (Fig. 1.38).

Apical odontoid ligament: extends from the tip of the odontoid in the shape of a sector to the anterior margin of the foramen magnum through the alar ligaments (Figs. 1.38, 1.39, 1.40, and 1.41).

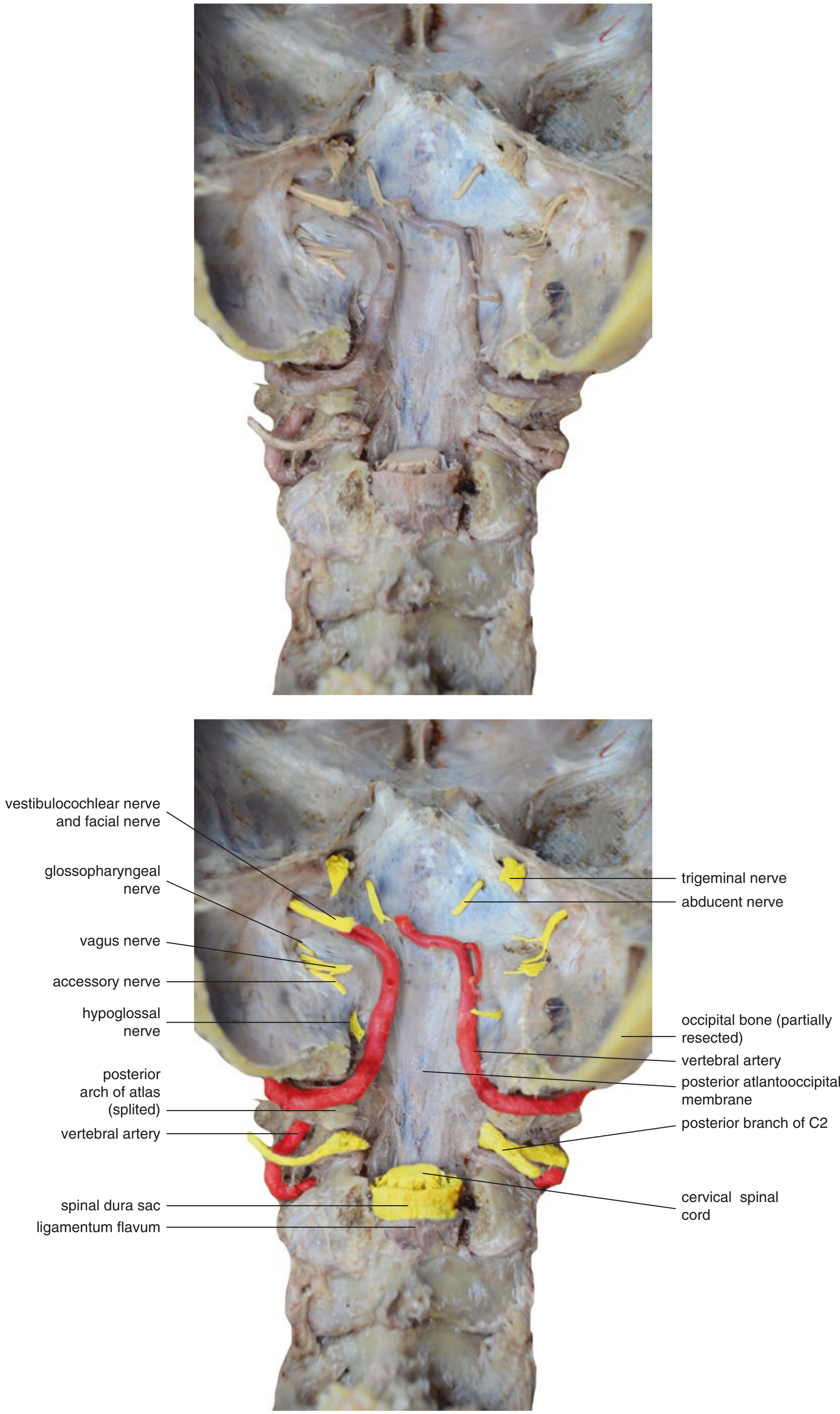

Fig. 1.35 Anterior wall structure of the upper cervical canal

Fig. 1.36 Anterior wall structure of the upper cervical canal (posterior longitudinal ligament resected)

Fig. 1.37 Cruciate ligament

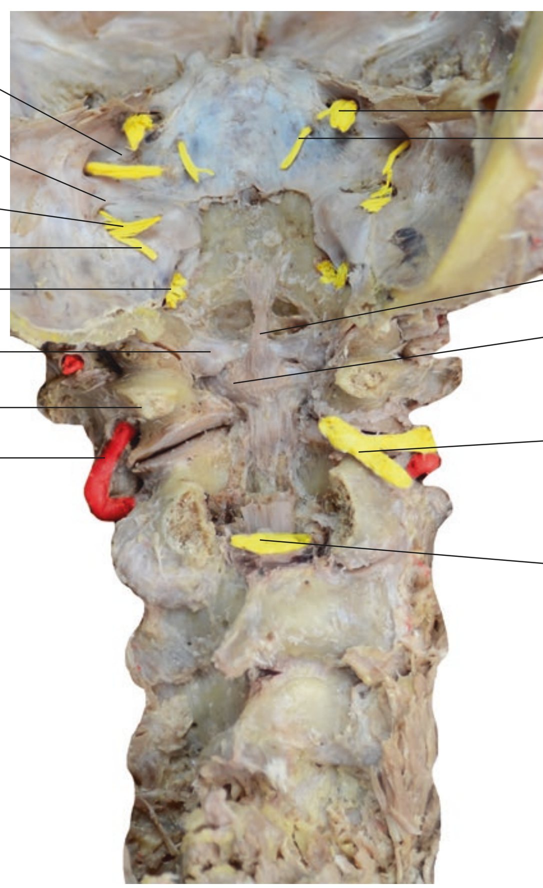

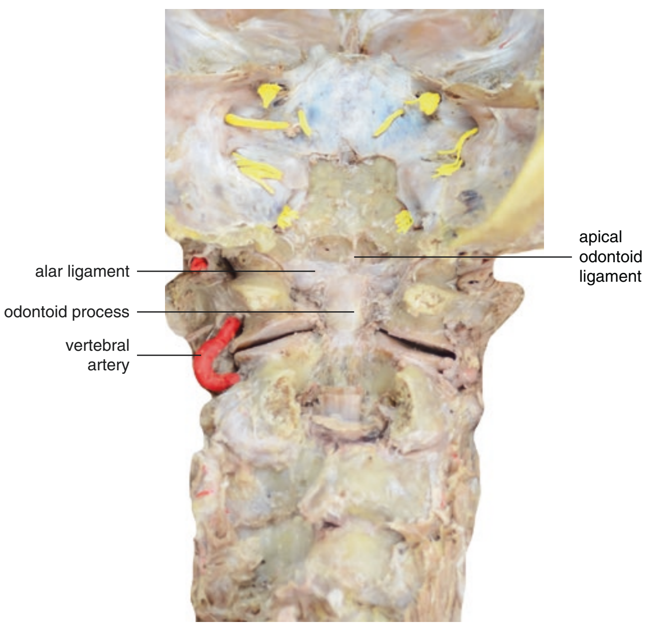

Fig. 1.38 Alar ligament and apical odontoid ligament

Fig. 1.39 Position and incision of anterior odontoid screw fixation

Fig. 1.40 Exposure and incision of the anterior odontoid screw fixation technique

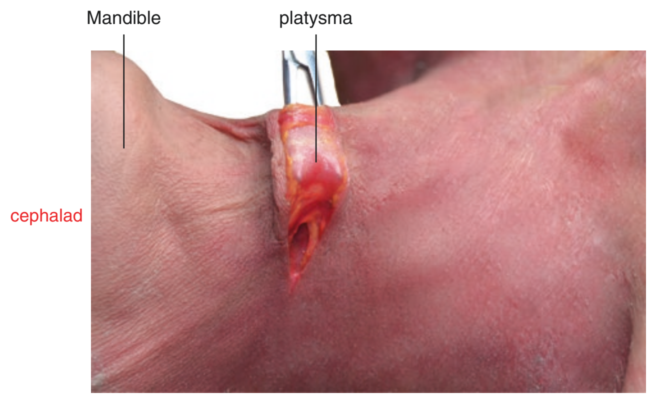

Fig. 1.41 Platysma is lifted using the hemostatic forceps

4 Anterior Odontoid Screw Fixation

4.1 Overview

The Smith–Robinson approach is the most commonly used method for exposing the middle cervical spine. It can expose the anterior of the C3–T1 vertebrae and may directly expose the intervertebral space and uncinated process in this section.

Posterior atlantoaxial fusion has always been used to treat unstable odontoid fractures. Despite the high fusion rate, the posterior fusion surgery sacrifices the vertebral movement of rotation, flexion, and extension. Bohler was the first to use odontoid screw fixation in 1981. This approach is suitable for patients with new and 3 months of nonunion odontoid fractures of the type II and type III by Anderson and D' Alonzo. However, it is necessary to ensure that the transverse ligament is not ruptured before using this technique. The advantages of this technique are preservation of the normal structure of the atlantoaxial joint, maximal retention of vertebral rotation, flexion and extension, and strong internal fixation that provides immediate stability to the fracture. Moreover, this approach is minimally invasive and has a high union rate. Anterior self-tapping partially threaded lag screw technique can not only retain the normal physiological activities of the atlantoaxial joint, but it can also firmly fix the fractured bone directly without the need of bone graft.

4.2 Position

Patient is in supine position, with padding under the shoulders. The cervical spine is extended to facilitate the trajectory of screw placement.

Open-mouth AP and lateral fluoroscopy are needed during surgery; suitable-sized gauze roll is placed into the mouth of the patient to push the tracheal incubation a side.

4.3 Exposure

Incision of the skin is made horizontally at the level of the thyroid cartilage to expose the anterior of the C4–C5 vertebra.

Since the insertion of the odontoid screw requires a greater tilt trajectory in sagittal plan, direct exposure of the C2 vertebra usually cannot achieve a satisfying trajectory for screw placement. Therefore, the C4 vertebra is exposed first, and then the inferior margin of C2 is exposed by dissecting caudally.

Isolate and resect the platysma along the skin incision.

The encountered superior thyroid artery can be protected and retracted aside and is generally not ligated (Fig. 1.42).

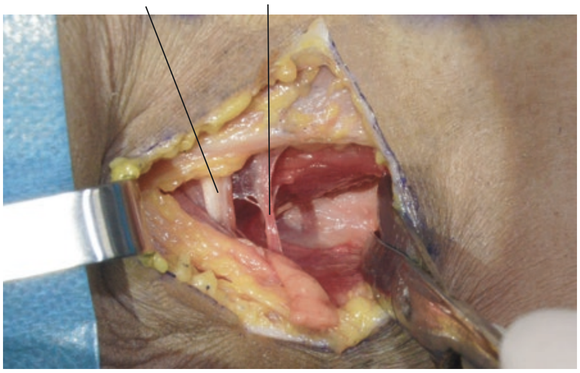

Fig. 1.42 Superior thyroid artery and digastric muscle in the surgical field

Sternocleidomastoid muscle: crosses the side of the neck obliquely and inwardly and forms a prominent body surface symbol. It is covered by skin and platysma. The external jugular vein, great auricular nerve, transverse cervical nerve, and the superficial layer of the deep cervical fascia are located on its surface. The upper sternocleidomastoid is supplied by the branches of the occipital artery and posterior auricular artery, the middle region is supplied by the branches of the superior thyroid artery, and the lower is supplied by the branches of the suprascapular artery. It is innervated by spinal segment of the accessory nerve and branches of the ventral branches of the second, third, and fourth cervical nerves (Fig. 1.43).

Superior thyroid artery: first branch of the external carotid artery, which descends from the lateral border of the thyrohyoid muscle to the thyroid lobe. The inferior pharyngeal constrictor muscle and the external branch of the superior laryngeal nerve are located on the medial side of the artery and can be easily injured during ligation (Fig. 1.44)

Superior laryngeal nerve: arises from the middle of the inferior ganglion of vagus nerve, and in its course receives a branch from the superior cervical ganglion of the sympathetic nervous system and descends along the lateral wall of the pharynx (Fig. 1.44).

Internal branch of the superior laryngeal nerve: a branch of the superior laryngeal nerve that descends to the level of the vocal fold and innervates the mucosal sensory of the larynx (Fig. 1.44).

External branch of the superior laryngeal nerve: smaller than the internal branch, which accompanies the superior thyroid artery and descends to the posterior of the sternothyroid muscle and innervates the cricothyroid muscle (Fig. 1.44).

Recurrent laryngeal nerve: the right recurrent laryngeal nerve originates from the vagus nerve trunk anterior to the subclavian artery. It loops around the artery and ascends in the tracheoesophageal groove. The nerve is closely adjacent to the inferior thyroid artery when it reaches the thyroid lobe. The left recurrent laryngeal nerve branches off from the vagus nerve inferiorly near the level of the aortic arch. It runs downward and hooks around to the aorta arch and ascends in the tracheoesophageal groove. They enter the throat through the rear of the joint composed of the inferior cornu of the thyroid cartilage and cricoid cartilage. The recurrent laryngeal nerve innervates all laryngeal muscles except the cricothyroid muscle. Its sensory fibers are distributed among the laryngeal mucosa below the vocal fold (Fig. 1.44).

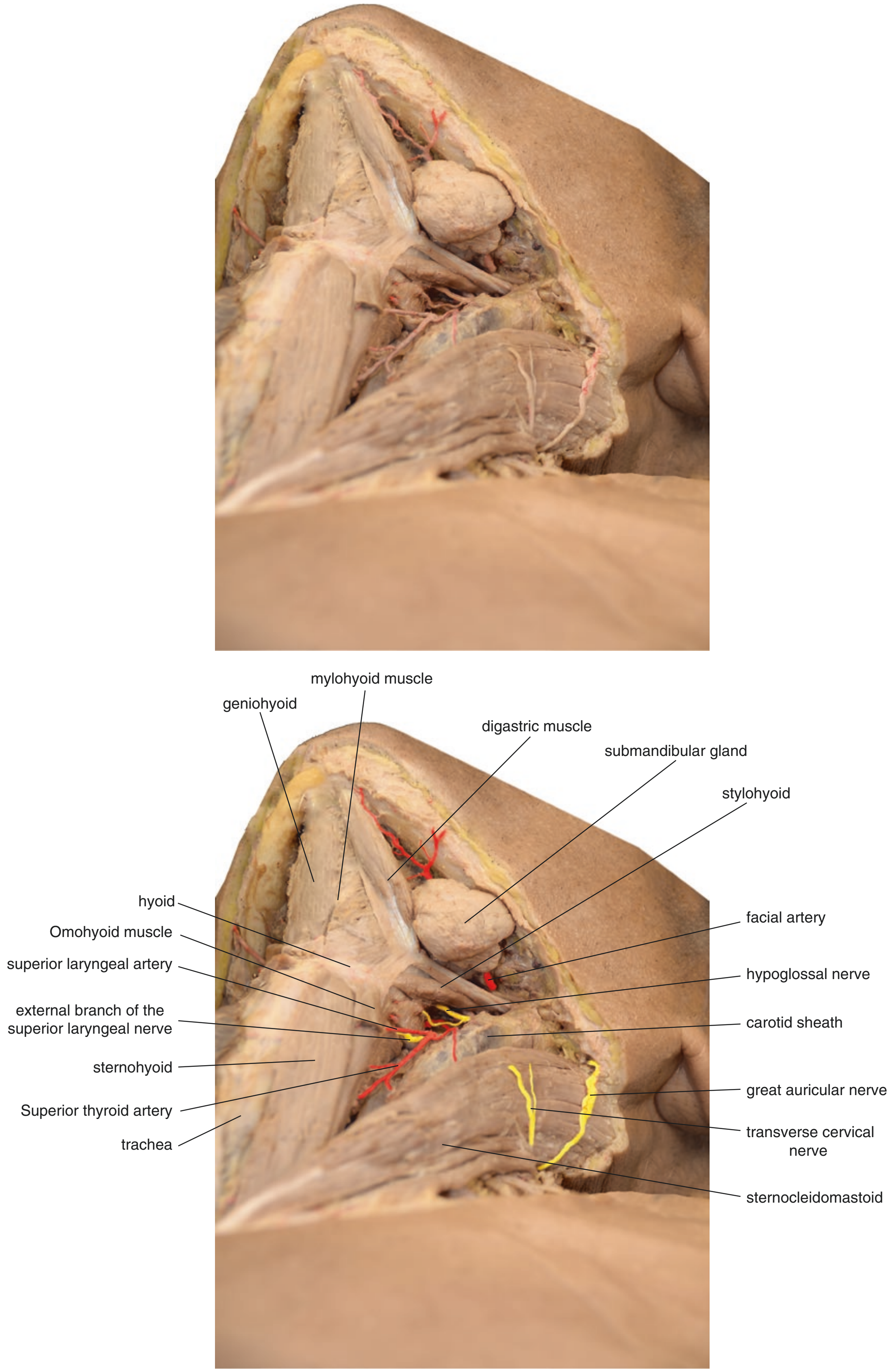

Fig. 1.43 Deep cervical structures on the left side

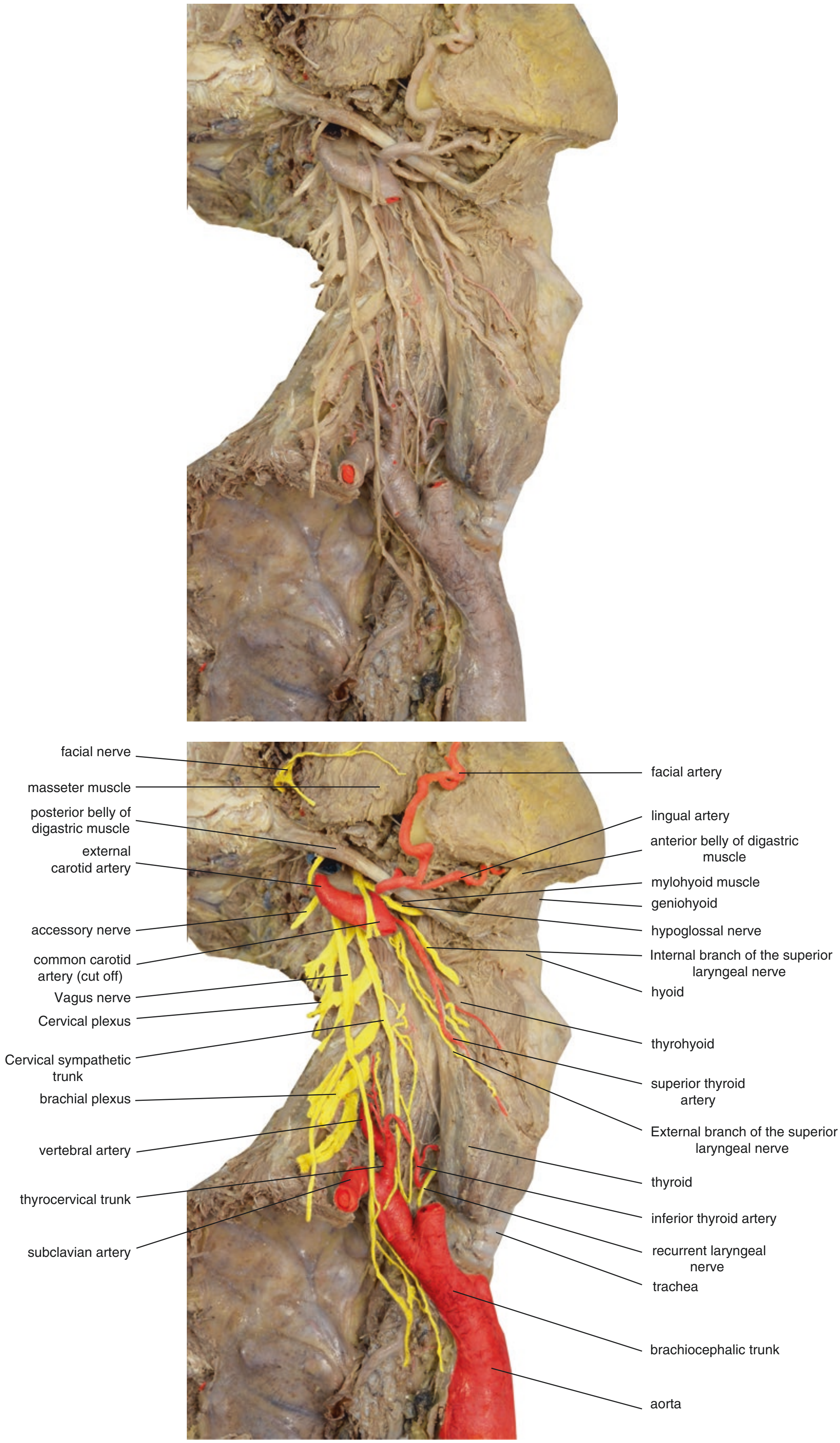

Fig. 1.44 Deep cervical neurovasculature on the right side

Expose the anterior of the C4 vertebra and bluntly dissect under the prevertebral fascia to the inferior border of the C2 (Figs. 1.45 and 1.46).

Palpate the bulge at the inferior border of the anterior axis. The C2 level is determined by lateral fluoroscopy.

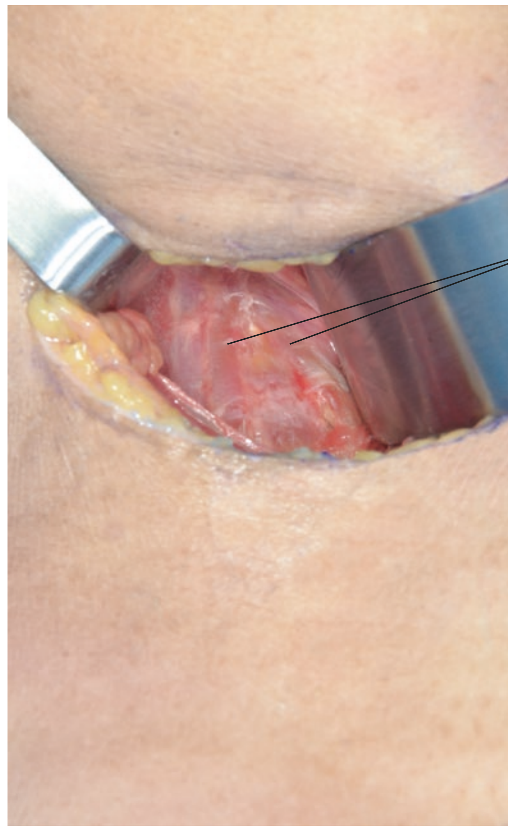

Fig. 1.45 Blunt dissection under the prevertebral fascia and pretracheal fascia to the inferior border of C2

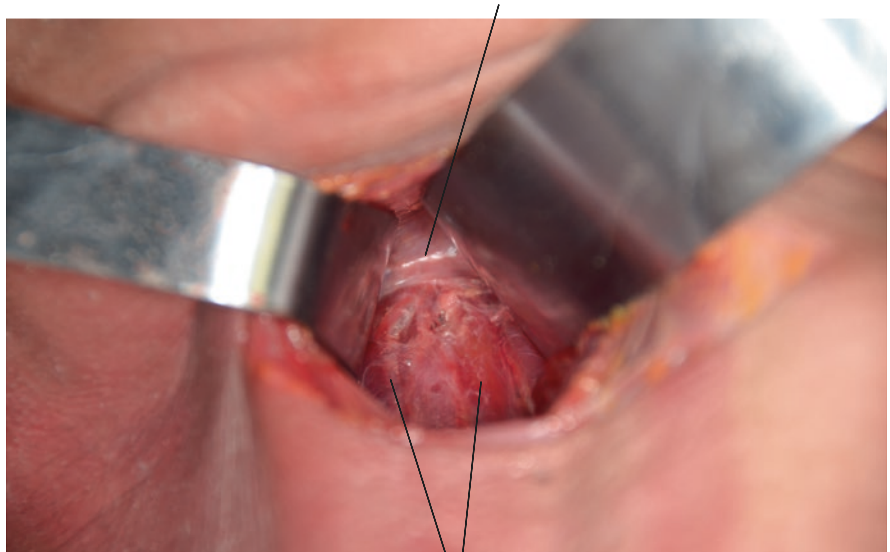

Fig. 1.46 Blunt dissection under the prevertebral fascia to the inferior border of C2

4.4 Screw Placement

The lip-shape edge of the axis is removed by rongeur. Alternatively, a groove at the inferior margin of the axis is made by high-speed drill.

Axis: slightly concave on both sides and is attached by the longus colli muscle. The lip-shape edge is attached by the anterior longitudinal ligament (Fig. 1.47).

Fix the Kirchner's wire orientator against the lower edge of the C2, and drill the Kirchner's wire into the vertebra slowly. Adjust the angle of the Kirchner's wire by verifying its position through intraoperative fluoroscopy (Fig. 1.48).

The Kirchner's wire shall be implanted into the distal part of the fracture block. The Kirchner's wire was then replaced by an adequate length AO 3.5 mm self-tapping partially threaded lag screw (Fig. 1.49).

Odontoid process: the basal part of the odontoid process and the bone cortex are rather thin; thus basilar fracture (Anderson type II) makes up 2/3 of all odontoid process fractures. The coronal diameter of the basilar part of odontoid process in asian is relatively narrow, and a 3.5 mm diameter screw can be used for fixation. (Fig. 1.50)

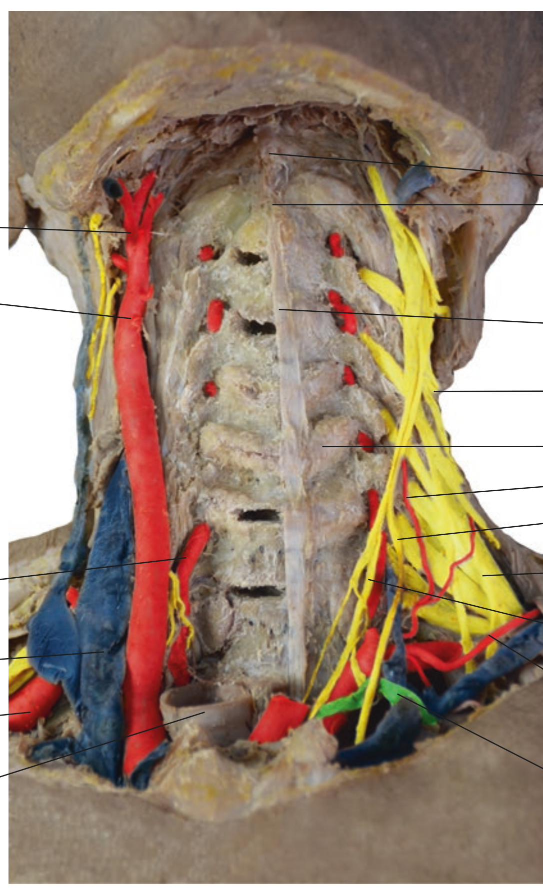

Fig. 1.47 Deep structure of the anterior cervical spine

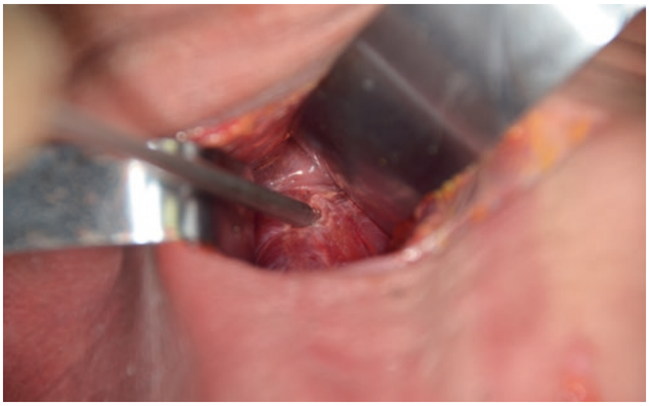

Fig. 1.48 Kirchner's wire slowly drilled into the vertebra

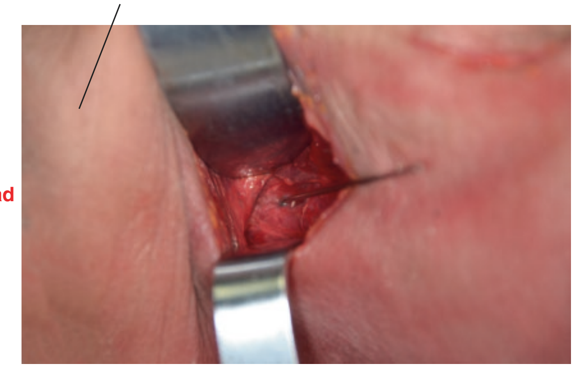

Fig. 1.49 Remove the Kirchner's wire to measure insertion depth

Fig. 1.50 Midsagittal section of the head and neck

Kirchner's wire insertion is guided by intraoperative lateral fluoroscopy. The angle between the Kirchner's wire tail and the vertical axis is approximately 15°. The tip of the Kirchner's wire is at the tip of the odontoid process (Fig. 1.51).

Kirchner's wire insertion is guided by intraoperative open-mouth fluoroscopy. The Kirchner's wire should be located in the center of the odontoid process (Fig. 1.52).

The insertion process of the screw is continuously guided by fluoroscopy to ensure that the Kirchner's wire does not enter along with the screw (Fig. 1.53).

The anterior odontoid screw fixation consists of the one-screw and two-screw techniques. The two-screw technique has a theoretically stronger anti-rotational resistance.

Since the odontoid process of asian is rather narrow, it is almost impossible to insert two screws. Therefore, a single 3.5 mm screw may be the choice.

The screw threads must cross the fracture site completely, and the screw should also extend through the posterior apical cortex of the dens fragment by a full thread turn to achieve lag compression (Fig. 1.54).

The self-tapping partially threaded lag screw is in good position after removing the Kirchner's wire as confirmed by fluoroscopy (Fig. 1.55).

The self-tapping partially threaded lag screw is in good position as confirmed by the C-arm open-mouth fluoroscopy (Fig. 1.56).

After identifying the position of odontoid screw, pull out the Kirchner's wire and make sure that the odontoid screw is embedded into the inferior margin of the axis. This small notch can reduce the irritation to the esophagus (Fig. 1.57).

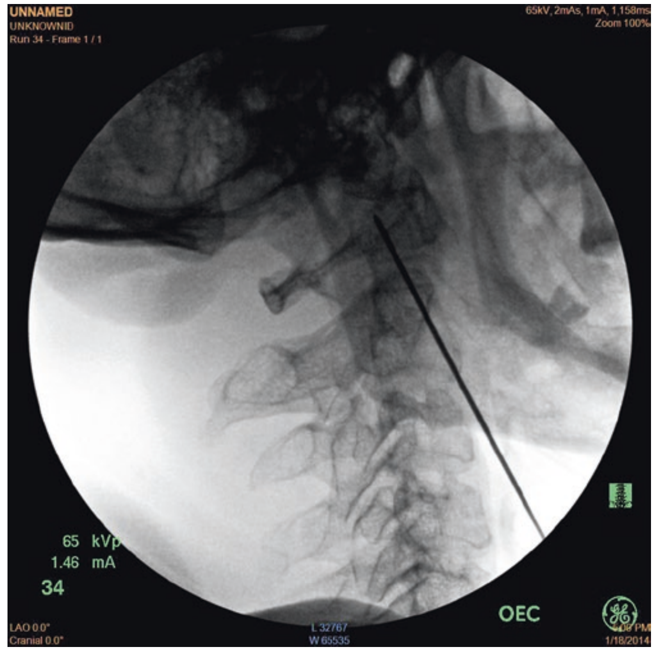

Fig. 1.51 Insertion of the Kirchner's wire under the guidance of intraoperative lateral fluoroscopic

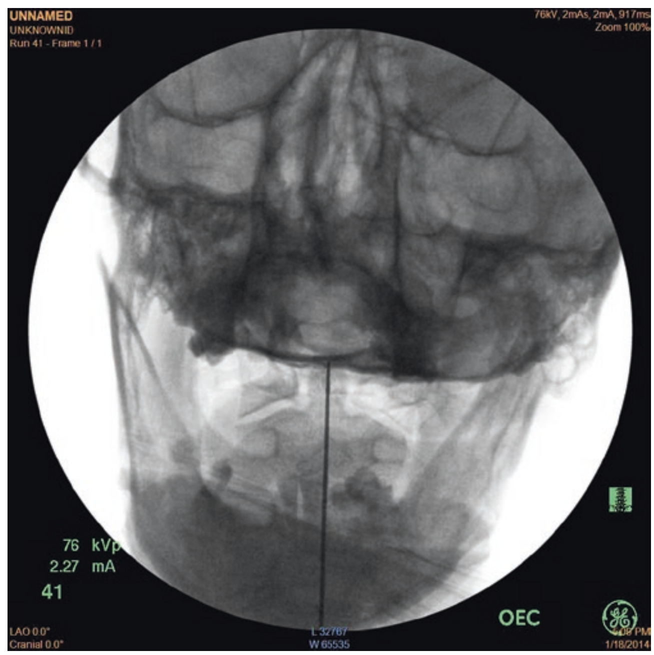

Fig. 1.52 Insertion of the Kirchner's wire under intraoperative open-mouth fluoroscopic control

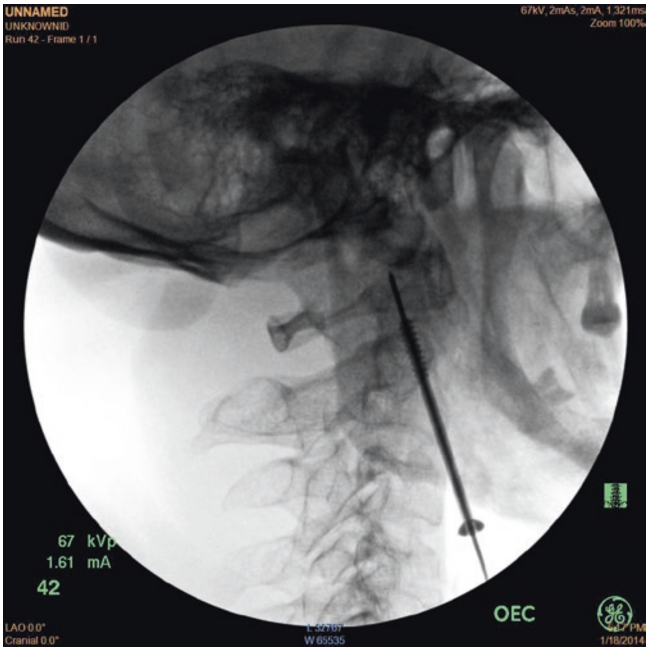

Fig. 1.53 Insertion of self-tapping partially threaded lag screw guided by fluoroscopy

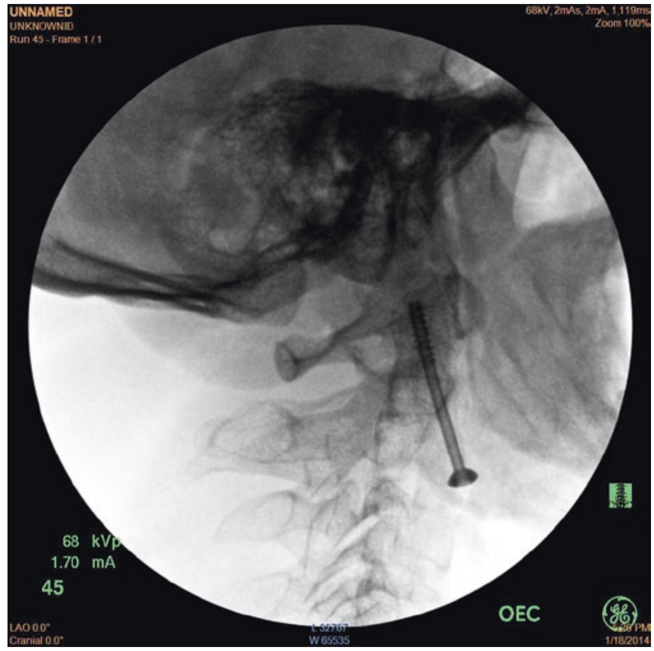

Fig. 1.55 Self-tapping partially threaded lag screw is in good position under the fluoroscopy

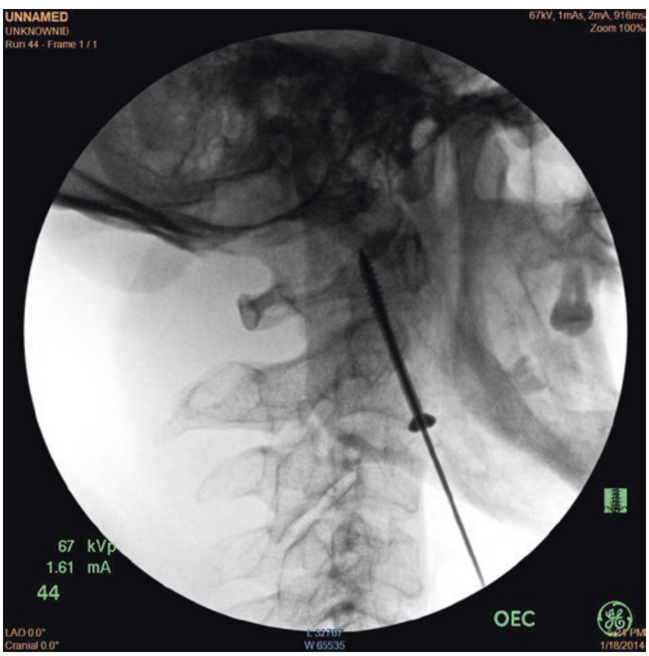

Fig. 1.54 Insertion of lag screw guided by fluoroscopy

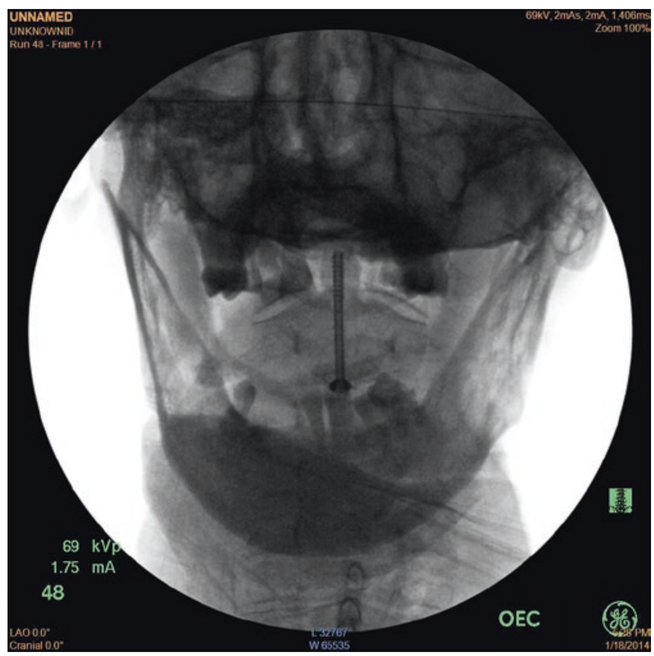

Fig. 1.56 Self-tapping partially threaded lag screw is in good position under the fluoroscopy

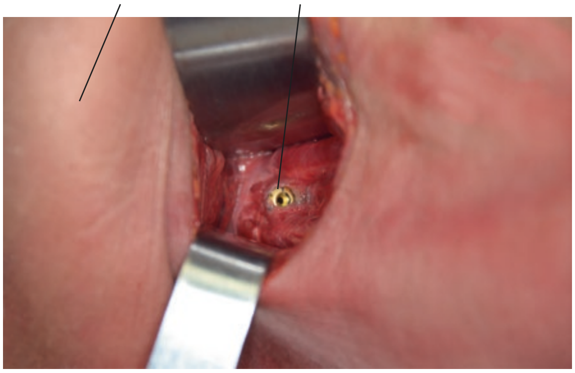

Fig. 1.57 Odontoid screw is embedded into the inferior margin of the axis after removal of the Kirchner's wire

5 Posterior Approach and Fixation Technique of Atlantoaxial and Occipitocervical Spine

5.1 Overview

The occipitocervical region is an important and complex structure connecting the head and cervical vertebra. The surgeons should be familiar with its anatomical characteristics. The posterior approach to the upper cervical spine can expose the posterior foramen magnum, posterior arch of the atlas, spinous process, lamina, and lateral mass joint.

The upper cervical fusion can be categorized into atlantoaxial fusion and occipitocervical fusion. Atlantoaxial fusion can be used to treat atlantoaxial instability while retaining the activity of the occipitocervical region. The occipitocervical fusion is performed for treating large areas of bony destruction due to rheumatoid arthritis or cancer, congenital or acquired defects of the posterior arch of the atlas, congenital atlantooccipital joint abnormalities, basilar impression, irreducible atlantoaxial dislocation, atlas fractures, and other diseases. In 1937, Cone was the first to introduced steel wires to fix the iliac bone graft for occipitocervical fusion. With the development of the lateral mass screw and pedicle screw fixation techniques for the upper cervical spine, screw-rod or screw-plate technique is widely used in occipitocervical fixation procedure.

5.2 Position

Patient is placed in a prone position, with head slightly elevated to gain a better venous drainage.

The neck shall be flexed slightly in order to facilitate intraoperative exposure.

The made-to-measure head to abdomen plaster bed (Changzheng Hospital) can be used to keep the head and neck neutral (Fig. 1.58).

5.3 Exposure

A median incision is made from the lower part of the occipital torus to the next spinous process of the fusion segment. The incision can be expanded vertically based on the need during operation (Fig. 1.59).

Skin incision in the posterior midline is made, and the fascia and nuchal ligament are dissected until the surface of the C2 spinous process.

Fig. 1.58 Position of posterior atlantoaxial approach

Fig. 1.59 Position and incision of posterior atlantoaxial approach

Palpate the bony landmark before incising the nuchal ligament to ensure that the incision is restricted on the midline. This prevents bleeding, nerve damage caused by deviation of incision.

Extend the incision to the C3 spinous process, external occipital protuberance, and posterior tubercle of the atlas.

Since the posterior arch of the atlas is difficult to be palpated, exposure can be done sequentially starting from the spinous process and lamina first, then the occipital bone and the posterior margin of the foramen magnum, and finally posterior arch of the atlas.

When exposing the posterior tubercle of the atlas, surgeon should palpate to confirm its location in order to avoid entering the spinal canal.

Subperiosteum dissection of the attached muscles along the spinous process, including rectus capitis and obliquus capitis inferior muscle. Retract them to the lateral margin of lateral mass (Fig. 1.60).

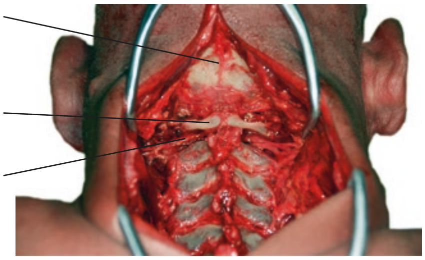

Fig. 1.60 Exposure of cervical vertebral lamina and lateral mass

Dorsal rami of the second cervical nerve: bigger than the ventral rami and all other dorsal rami of the cervical nerves. It emerges between the posterior arch of the atlas and the vertebral lamina of the axis. It is connected with the dorsal rami of the first cervical nerve and is divided into a larger medial branch and a smaller lateral branch (Fig. 1.61).

Greater occipital nerve: the medial branch of the dorsal rami of the second cervical nerve, which arises between the obliquus capitis inferior and semispinalis capitis muscles and crosses the trapezius muscle to ascend to the top of the skull, innervating the skin of the occipital region. Excessive retraction and compression of greater occipital nerve can cause pain in the occipital region (Fig. 1.61).

Occipital artery: arises from the external carotid artery, goes through the deep fascia into the scalp, and accompanies the greater occipital nerve. The bending branch runs between the skin and the occipital belly of occipitofrontal muscle, supplying blood to the skin of the occipital region and the skull periosteum (Fig. 1.61).

Suboccipital muscle: comprised of rectus capitis posterior major, rectus capitis posterior minor, obliquus capitis superior muscle, and obliquus capitis inferior muscle, which are four muscles that connect the posterior of the occipital bone and atlantoaxis. Obliquus capitis superior muscle, rectus capitis posterior major and minor mainly maintain head posture, and rectus capitis posterior major can stretch the head and turn head to the same side together with musculus obliquus capitis inferior. Rectus capitis posterior minor also has an effect on stretching the head. Obliquus capitis superior muscle can stretch the head and turn head to the same side (Figs. 1.62 and 1.63).

Rectus capitis posterior major: connects to the spinous process by a specific tendon and gradually broadens as it ascends to the lateral side of the inferior nuchal line and the occipital bone slightly below (Figs. 1.62 and 1.63).

Rectus capitis posterior minor: connects to the posterior tubercle of the atlas via a narrow tendon. It is attached to the medial side of the inferior nuchal line (Figs. 1.62 and 1.63).

Obliquus capitis superior muscle: Obliquus capitis superior muscle is connected with the transverse process of atlas by tendon fiber. Gradually broadens on the way up and ends at the occipital part between superior nuchal line and inferior nuchal line (Figs. 1.62 and 1.63).

Musculus obliquus capitis inferior: Musculus obliquus capitis inferior starts from the adjacent part between the outer part of the spinous process and upper part of lamina and ends at the inferioposterior part of transverse process of the atlas (Figs. 1.62 and 1.63)

Suboccipital triangle: It is surrounded by rectus capitis posterior minor, obliquus capitis superior muscle, and musculus obliquus capitis inferior, and its superficial entrance is covered with semispinalis muscles, and the triangle is filled with dense adipose tissues. The muscular branches of the vertebral artery and the dorsal rami of first cervical nerve go through it and enter into suboccipital muscle (Fig. 1.63).

Vertebral artery: runs through the transverse foramen of the atlas, emerges from the medial side of the rectus capitis lateralis muscle, loops backward to the posterior atlantooccipital joint, runs in the vertebral artery groove on the upper edge of posterior arch of the atlas, and enters into the posterior atlantooccipital membrane (Fig. 1.64).

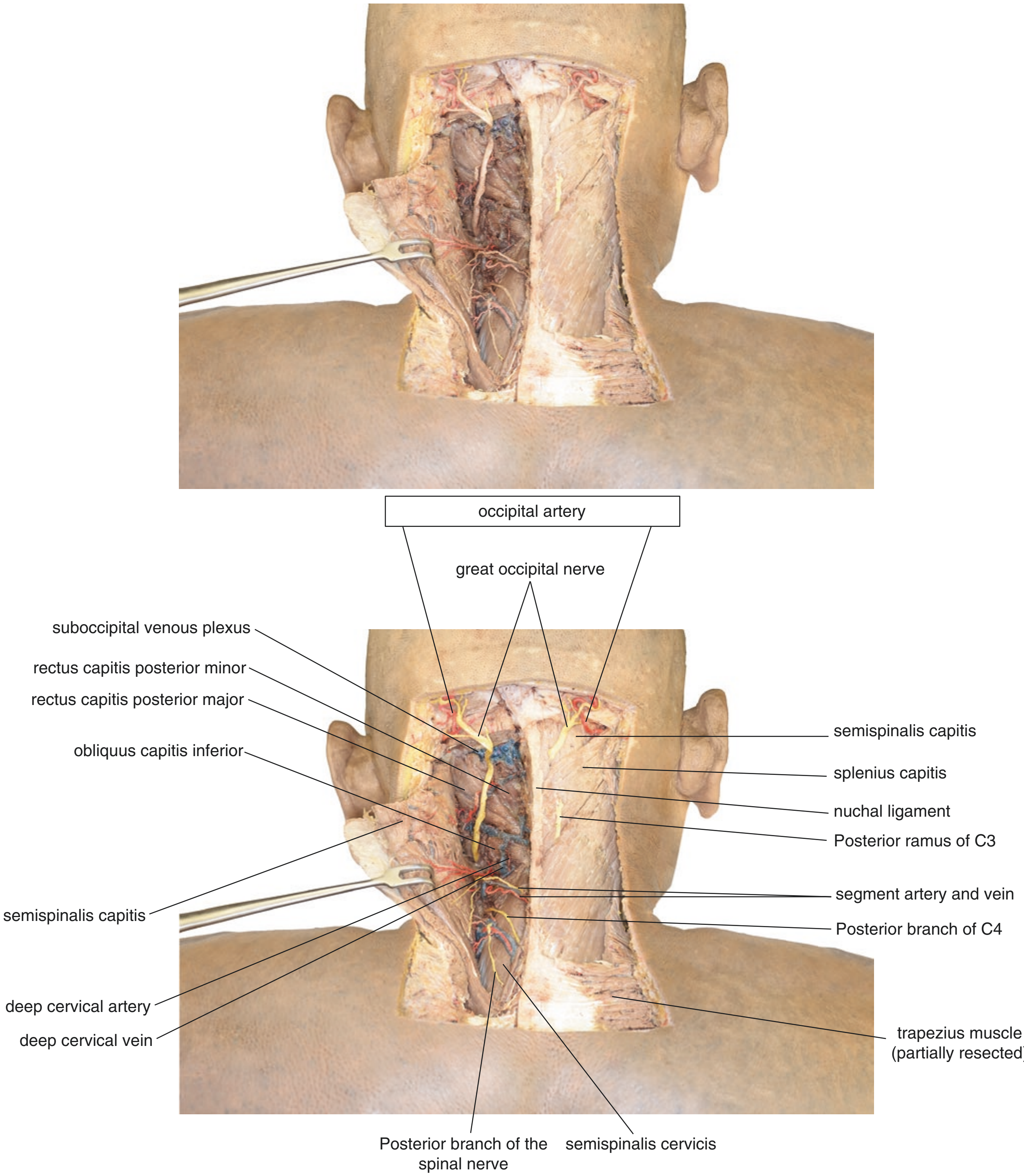

Fig. 1.61 Deep (*left*) and superficial (*right*) neurovasculature and musculature of the semispinalis capitis muscle

Fig. 1.62 Deep (*left*) and superficial (*right*) neurovasculature and musculature of the neck

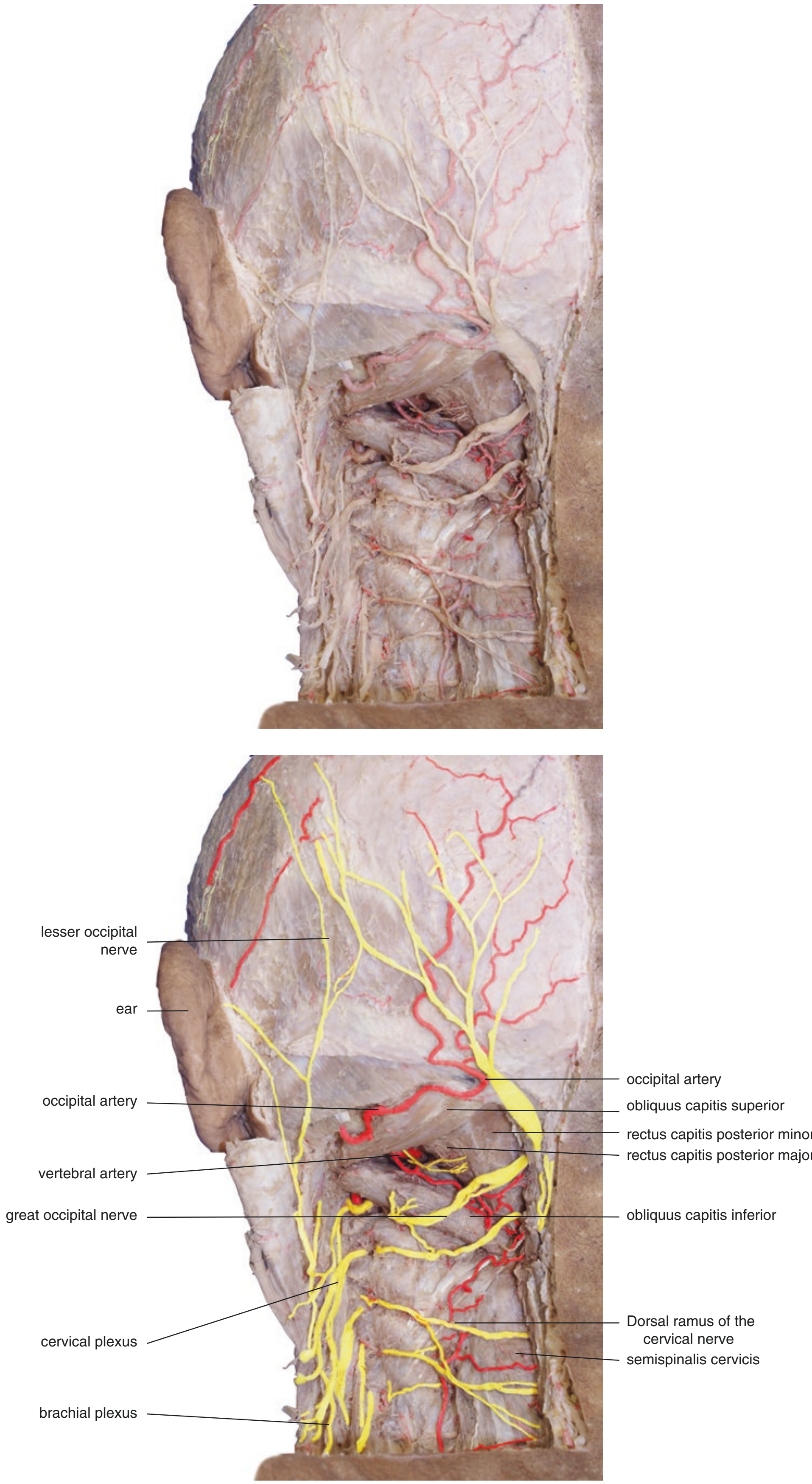

Fig. 1.63 Peripheral neurovasculature of the inferior suboccipital triangle

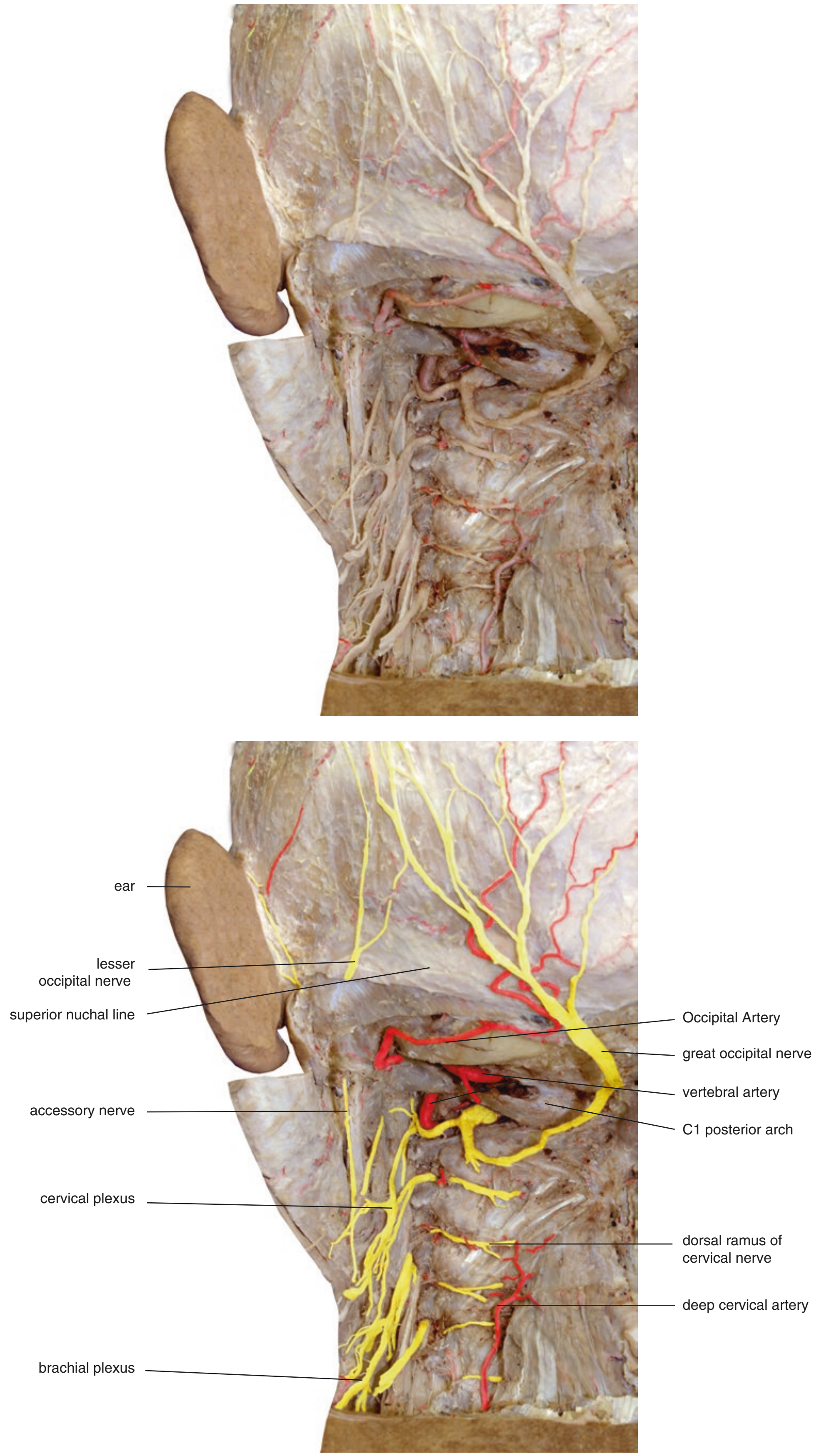

Fig. 1.64 Posterior deep cervical neurovasculature

5.4 Occipitocervical Fixation

To confirm the screw entry points of the C1, a nerve hook can be inserted into the spinal canal along the cranial margin of the C1 posterior arch to the medial surface of the pedicle of the C1 (Fig. 1.65).

In cases of sclerotic change or extremely small C1 pedicle with no medullary canal, screws cannot be placed directly. Screw entry point can be created by removing the cortex of the C1 posterior arch by rongeur or drill (Fig. 1.66).

Drill into the pedicle with a 2.5 mm depth-limited probe-guided power drill under the lateral fluoroscopy monitoring. Small pedicle can be perforated with small-sized diamond burr to make the path for the screw into the vertebral body (Figs. 1.67 and 1.68).

The sounding of the screw insertion path is performed with the pedicle sounder which finds that the path is surrounded by intact wall (Figs. 1.69 and 1.70).

Select the appropriate diameter (usually 3.0–3.5 mm) of pedicle screw, and place it into the insertion path after tapping (Fig. 1.71).

Insert the pedicle screws into the both sides of C1 and C2 (Fig. 1.72).

The pedicle screw placement of C1 and C2 is in good position under the guide of the intraoperative anteroposterior/lateral fluoroscopy (Figs. 1.73 and 1.74).

Place the low-profile occipital screws into the corresponding position of the occipital plate (Fig. 1.75).

The best occipital screw fixation position is located in midline, and the thin, squamous portion of the occiput does not allow sufficient screw purchase.

In order to avoid intracranial venous sinus injury, the screws cannot be placed upper than the superior nuchal line.

A probe is helpful for determining when the hole is bicortical. Tapping is necessary before placing the fixation screws.

Dural fearing may cause cerebrospinal fluid leakage, which is self-limited following the occipital screw placement.

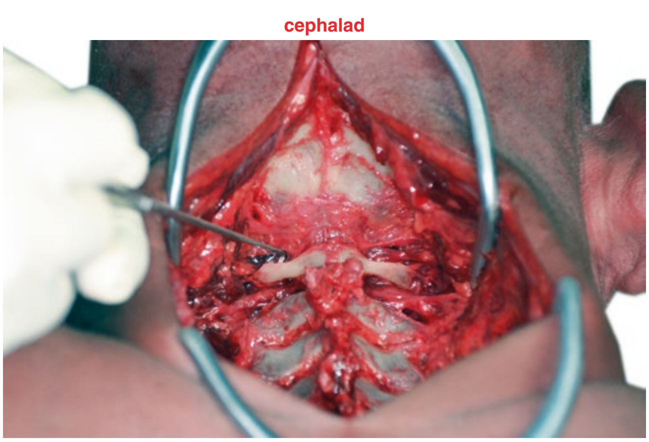

Fig. 1.65 Identify the medial margin of the pedicle (lateral mass) of the atlas by nerve hook

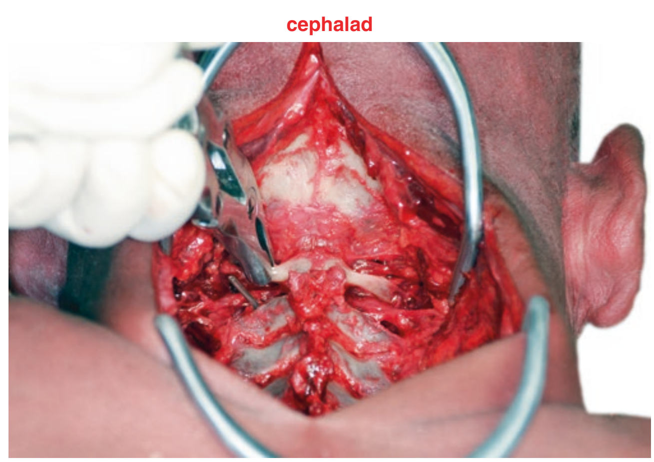

Fig. 1.66 Remove the cortex to create a screw insertion hole with the aid of rongeur or high-speed burr

cephalad

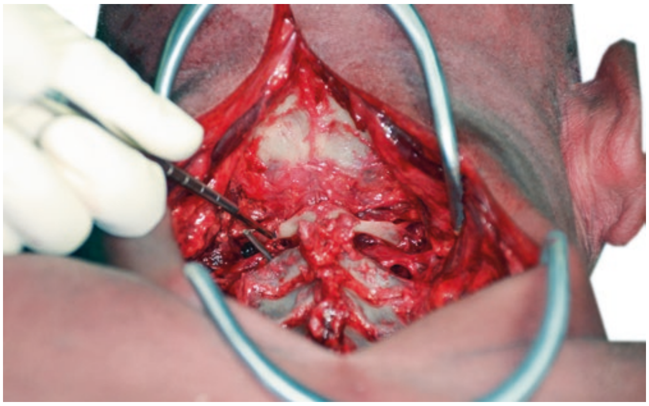

Fig. 1.67 Confirming the proper creation of screw insertion path after using pedicle sounder

cephalad

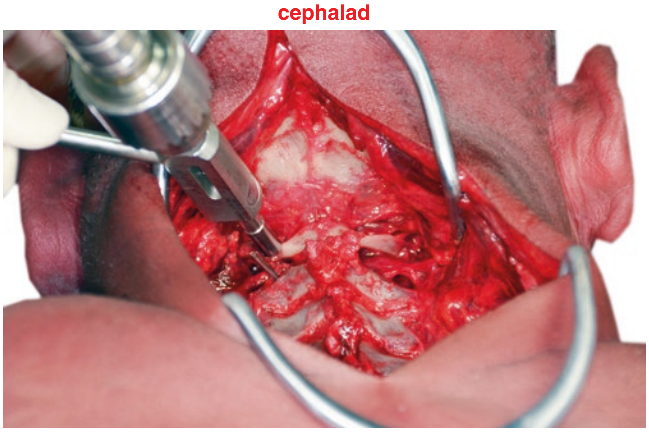

Fig. 1.68 Drill into the pedicle with a probe-guided power drill

cephalad

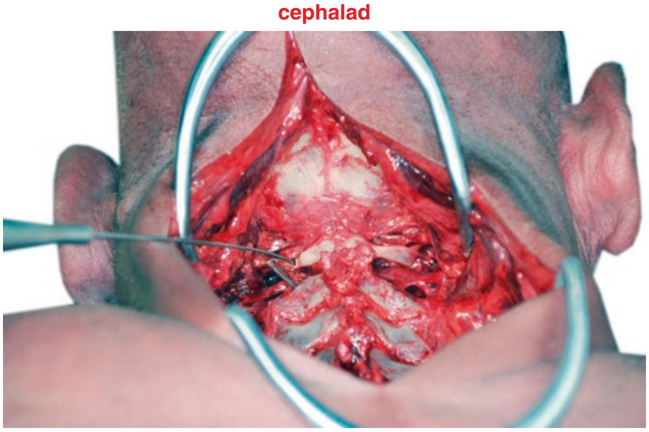

Fig. 1.69 Confirming the proper creation of screw insertion path after probing using pedicle sounder

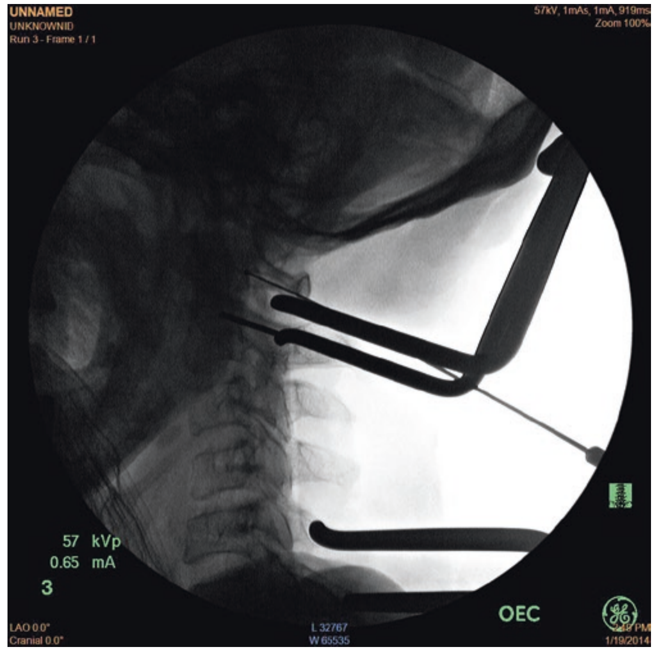

Fig. 1.70 Observation of the depth and position of the insertion path through intraoperative fluoroscopy

cephalad

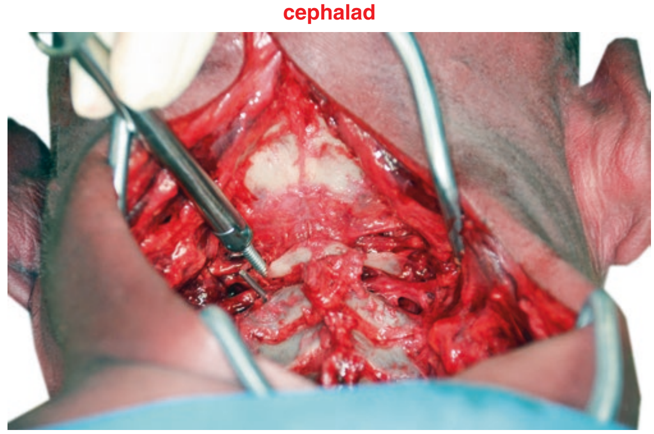

Fig. 1.71 Placement of pedicle screw

cephalad

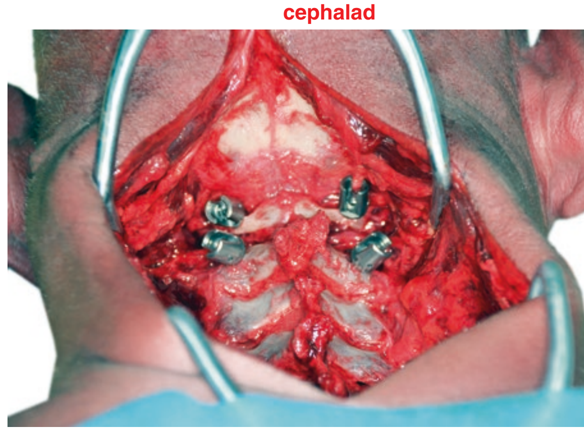

Fig. 1.72 Insertion of pedicle screws into both sides of the atlantoaxial joint

The occipitocervical connecting rod is then bent and secured (Fig. 1.76).

Bone grafting with appropriate shaped iliac bone is carried out on the occiput and laminae, and spinous processes of the levels to be fused after decortication are done to facilitate fusion.

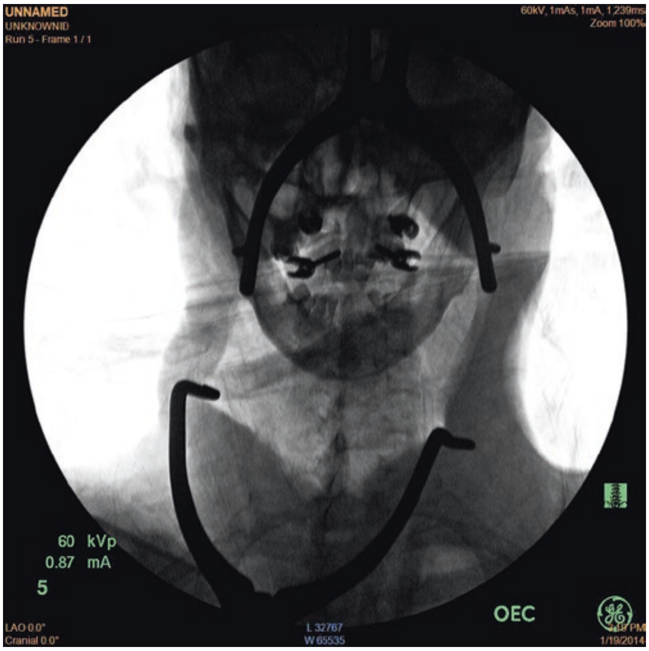

Fig. 1.73 Pedicle screw placement is in good position under the guide of the intraoperative anteroposterior fluoroscopy

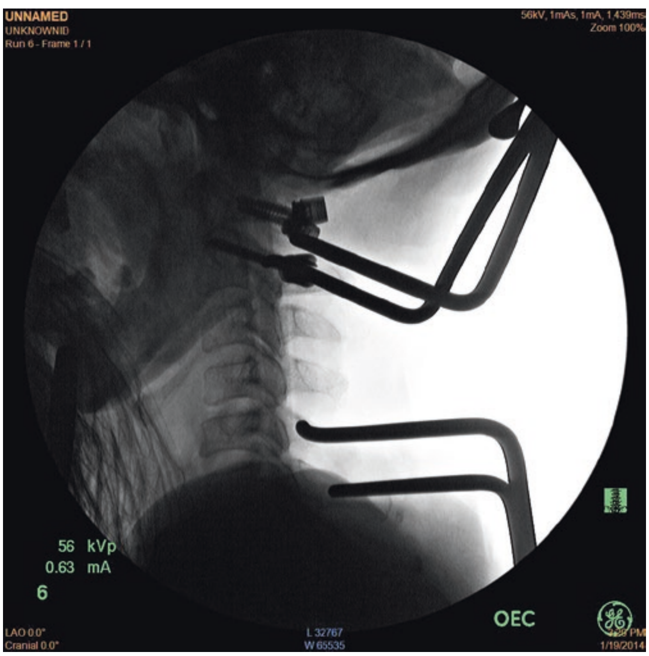

Fig. 1.74 Pedicle screw placement is in good position under the guide of the intraoperative lateral fluoroscopy

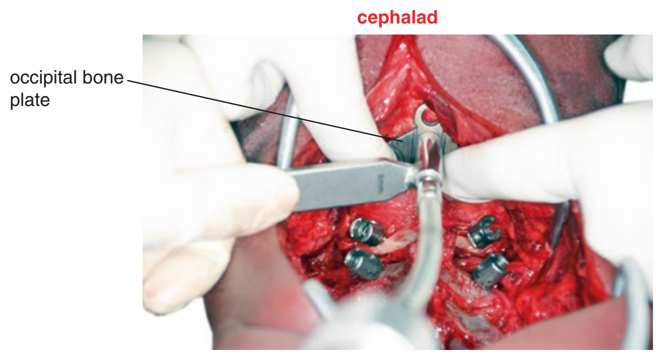

Fig. 1.75 Implantation of the occipital screws

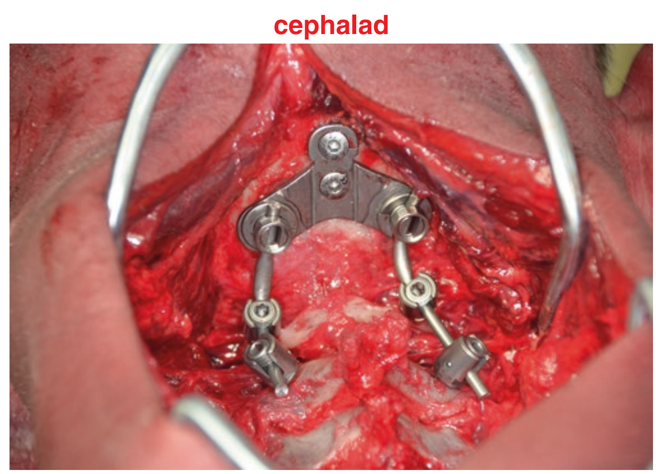

Fig. 1.76 Placement and fixation of the occipitocervical connecting rod

The occipital plate and occipital screws are in good position under the intraoperative anteroposterior/lateral fluoroscopy (Figs. 1.77 and 1.78).

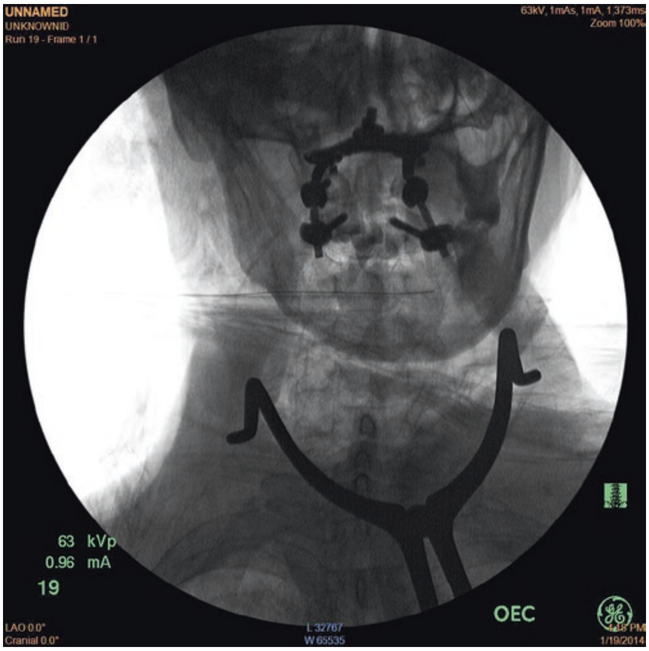

Fig. 1.77 Occipital plate and occipital screws are in good position under the intraoperative anteroposterior fluoroscopy

Fig. 1.78 Occipital plate and occipital screws are in good position under the intraoperative lateral fluoroscopy

6 Atlantoaxial Pedicle Screw and Lateral Mass Screw Placement

The C1 lateral mass screw technique was proposed by Goel and Laheri in 1994. Harms reported in 2001 that the screw-rod system of pedicle screws of C2 combined with lateral mass screw of C1 posterior pedicle screws provides better mechanical stability than traditional upper cervical spine fixation techniques including Gallie, Brooks, and Halifax interlaminar clamp. In 2002, Tan Mingsheng proposed the atlas pedicle screw technique. The risk of the injury of C2 nerve root and venous plexus is reduced with less bleeding under the Tan's technique.

6.1 Lateral Mass Screws of the Atlas and Axis

The entry point of the C1 lateral mass screws is located under the posterior arch of the C1, above the atlanto-axial joint space and on the midpoint of the axis lateral mass (Figs. 1.79 and 1.80).

The medial and lateral borders of the posterior portion of the lateral mass can be identified by a nerve hook.

Subperiosteal dissection is performed to avoid bleeding from the local epidural venous plexus.

The C2 nerve root is depressed slightly caudally to gain visualization of the screw entry point.

The coronal trajectory is angled 5–10° medially. The posterior–anterior trajectory is assessed fluoroscopically by aiming for the anterior tubercle of C1 (Fig. 1.80).

Measure the depth of the hole with a sounder. The hole is tapped first with a 3.5 tap. Screw with 3.5 mm in diameter is then placed in the hole.

Fig. 1.79 Back view of C1, C2 pedicle, and lateral mass

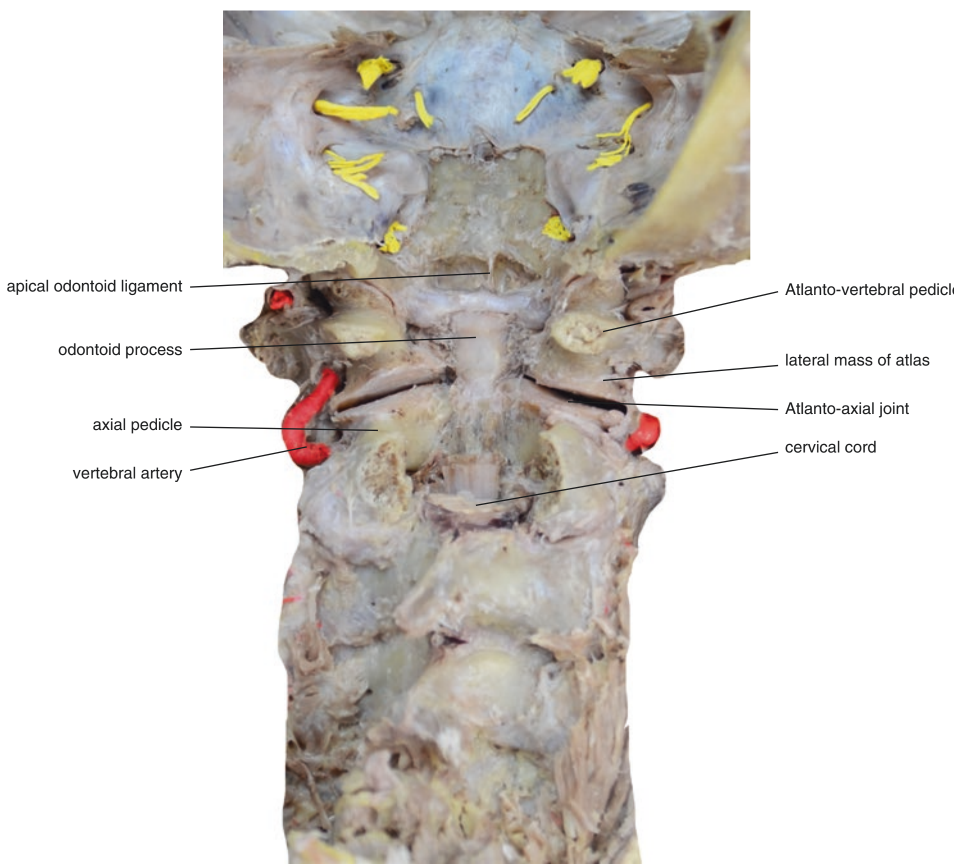

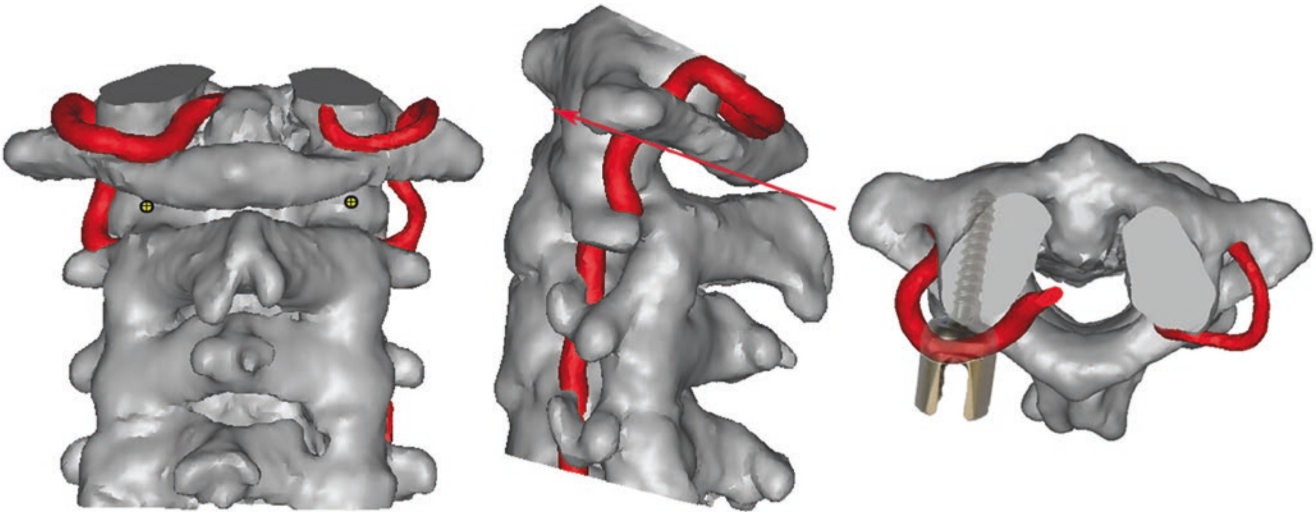

Fig. 1.80 The entry point and trajectory of C1 lateral mass screws

6.2 Pedicle Screw of the Atlas and Axis

Attention should be paid to the protection of the vertebral artery and the C2 dorsal root ganglion in the process of exposing the surgical field (Fig. 1.81 and 1.82)

There are a large number of intervertebral venous plexus in the posterior region of occipitocervical spine. When subperiosteal dissection is performed on the occipitocervical spine, excessive bleeding may be encountered. Bipolar cautery and the neurological sponges impregnated with thrombin can be used to control the hemorrhage (Fig. 1.83).

The entry point of C1 pedicle screw is located about 20 mm lateral away from the midline of posterior arch.

To confirm the screw entry points of C1, a nerve hook can be inserted into the spinal canal along the cranial margin of the C1 posterior arch to the medial surface of the pedicle of C1.

In the cases that the thickness of C1 posterior arch is less than 4 mm, the enter point of C1 pedicle screw may move to the point below the posterior arch (lateral mess screw).

The coronal trajectory is angled about 10° medially. The posterior–anterior trajectory is 5–10°.

The entry point of C2 pedicle screw is at the midpoint of lateral mass of C2 or 2–3 mm cephalad to the midpoint.

The coronal trajectory of C2 pedicle screw is angled about 15–25° medially. The posterior–anterior trajectory is 25°.

A nerve hook can be inserted into the spinal canal along the cranial margin of the C2 vertebral plate to the medial surface of the pedicle of C2 to confirm the screw entry points.

The insertion of screw is performed when the entry point and the trajectory are certified by C-arm fluoroscopy.

Insertion of 3.5 mm screw is performed after sounding and tapping of the insertion hole (Fig. 1.84).

The atlantoaxial pedicle screw is in good position checked by the intraoperative anteroposterior/lateral fluoroscopy (Figs. 1.85 and 1.86).

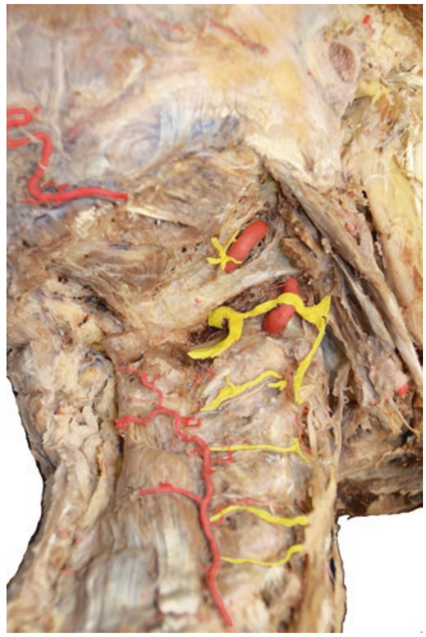

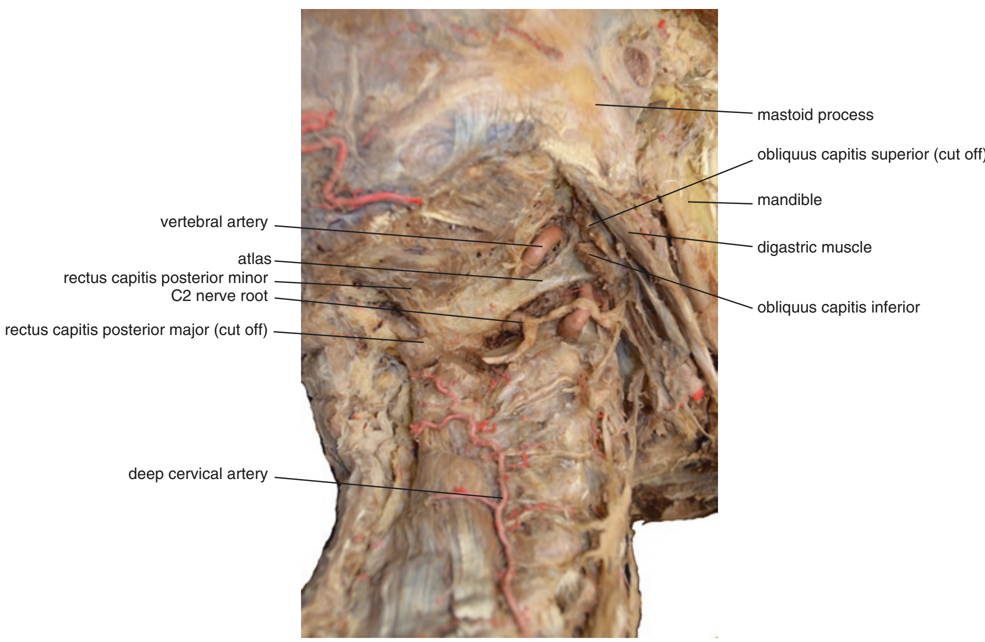

Fig. 1.81 Posterior vascular and muscle structure of occipitocervical region

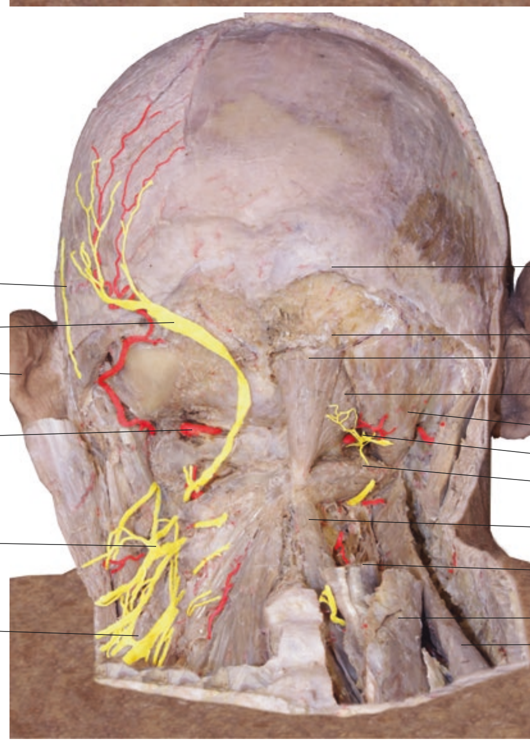

Fig. 1.82 Posterior vascular and muscle structure of occipitocervical region (attachment point mutation of rectus capitis posterior minor in this case)

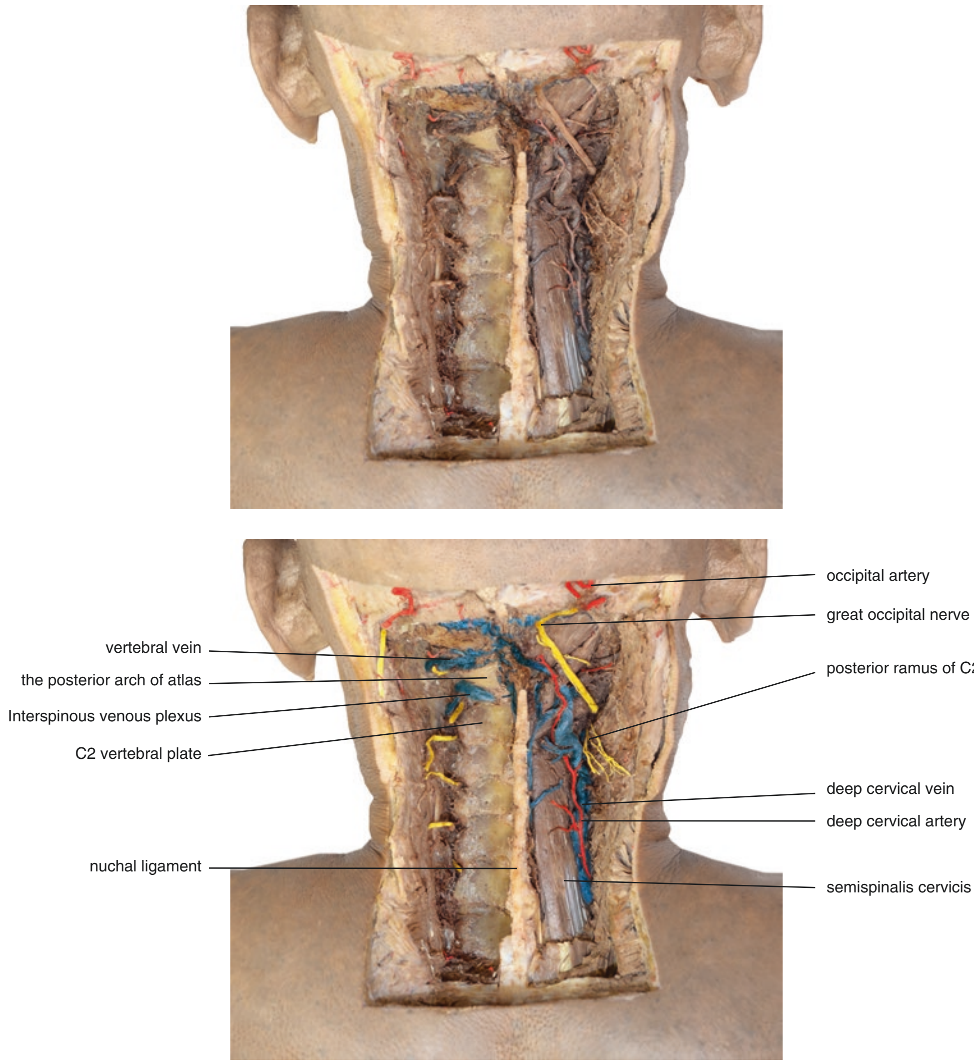

Fig. 1.83 Posterior cervical vein system

Fig. 1.84 Insertion of atlantoaxial screw

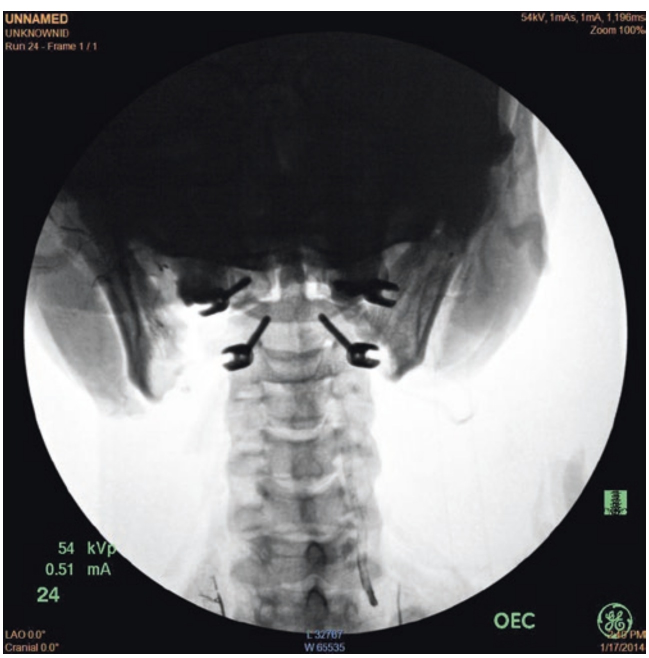

Fig. 1.85 Pedicle screw placement is in good position shown by the intraoperative anteroposterior fluoroscopy

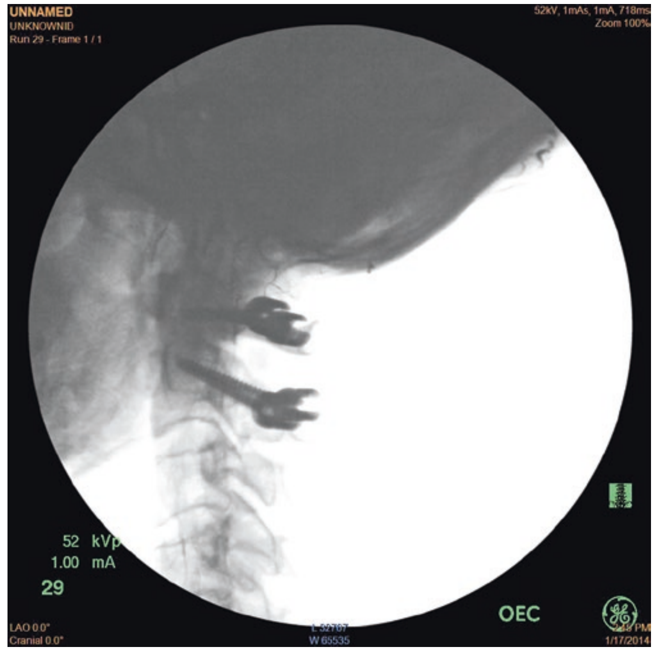

Fig. 1.86 Pedicle screw placement is in good position checked by the intraoperative lateral fluoroscopy

References

1. Yin QS, Liu JF, Xia H. The prevention of infection in atlantoaxial operations by transoral-transpharyngeal approach. Chin J Spine Spinal Cord. 2001.
2. Menezes AH, Vangilder JC. Transoral-transpharyngeal approach to the anterior craniocervical junction. Ten-year experience with 72 patients. J Neurosurg. 1988;69(6):895–903.
3. Kingdom TT, Nockels RP, Kaplan MJ. Transoral-transpharyngeal approach to the craniocervical junction. Otolaryngol Head Neck Surg. 1995;113(4):393.
4. Chen X, Liu N, Zhu F, et al. Applied anatomy of the transoral-transpharyngeal approach to the lesions of the ventral craniocervical junction. Anat Res. 2005;620(3):87–90.
5. Wang Z, Yin Q, Wang L. Applied anatomy of transoral approach to the lesion of ventral craniocervical junction. Chin J Minim Invasive Neurosurg. 2004.
6. Pásztor E. Transoral approach for epidural craniocervical pathological processes. In: Advances and technical standards in neurosurgery. Vienna: Springer; 1985. p. 125–70.
7. Kanamori Y, Miyamoto K, Hosoe H, et al. Transoral approach using the mandibular osteotomy for atlantoaxial vertical subluxation in juvenile rheumatoid arthritis associated with mandibular micrognathia. J Spinal Disord Tech. 2003;16(2):221–4.
8. Neo M, Asato R, Honda K, et al. Transmaxillary and transmandibular approach to a C1 chordoma. Spine. 2007;32(7):236–9.
9. Bertrand J, Luc B, Philippe M, et al. Anterior mandibular osteotomy for tumor extirpation: a critical evaluation. Head Neck. 2000;22(4):323–7.
10. Hiromasa K, Shin K, Seiji A, et al. Transoral anterior approach using median mandibular splitting in upper spinal tumor extirpation. Oral Surg Oral Med Oral Pathol Oral Radiol. 2012;114(5):12–6.
11. Delgado TE, Garrido E, Harwick RD. Labiomandibular, transoral approach to chordomas in the clivus and upper cervical spine. Neurosurgery. 1981;8(6):675–9.
12. Arbit E, Jr PR. Combined transoral and median labiomandibular glossotomy approach to the upper cervical spine. Neurosurgery. 1981;8(6):672–4.

13. Brookes JT, Smith RJ, Menezes AH, et al. Median labiomandibular glossotomy approach to the craniocervical region. Childs Nerv Syst. 2008;24(10):1195–201.
14. McAfee PC, Bohlman HH, Riley LH, et al. The anterior retropharyngeal approach to the upper part of the cervical spine. J Bone Joint Surg Am. 1987;69(9):1371–83.
15. Vender JR, Harrison SJ, McDonnell DE. Fusion and instrumentation at C1-3 via the high anterior cervical approach. J Neurosurg Spine. 2000;92(1):24–9.
16. Leitner Y, Shabat S, Boriani L, et al. En bloc resection of a C4 chordoma: surgical technique. Eur Spine J. 2007;16(12):2238–42.
17. Chadha M, Agarwal A, Singh AP. Craniovertebral tuberculosis: a retrospective review of 13 cases managed conservatively. Spine. 2007;32(15):1629–34.
18. Govender S, Ramnarain A, Danaviah S. Cervical spine tuberculosis in children. Clin Orthop Relat Res. 2007;460:78–85.
19. Özdemir HM, Us AK, Ögün T. The role of anterior spinal instrumentation and allograft fibula for the treatment of pott disease. Spine. 2003;28(5):474–9.
20. Anderson LD, D'Alonzo RT. Fractures of the odontoid process of the axis. J Bone Joint Surg Am. 1974;56(8):1663–74.
21. Aebi M, Etter C, Coscia M. Fractures of the odontoid process. Treatment with anterior screw fixation. Spine. 1989;14(10):1065.
22. Elsaghir H, Böhm H. Anderson type II fracture of the odontoid process: results of anterior screw fixation. J Spinal Disord. 2000;13(6):527–30.
23. Chi YL, Wang XY, Mao FM. Treatment of odontoid process fractures with anterior percutaneous screw fixation. Chin J Orthop. 2004.
24. Levine AM, Edwards CC. Traumatic lesions of the occipitoatlantoaxial complex. Clin Orthop Relat Res. 1989;239(239):53–68.
25. Grob D, Dvorak J, Panjabi M, et al. Posterior occipitocervical fusion. A preliminary report of a new technique. Spine. 1991;16(3 Suppl):S17.
26. Fourney DR, York JE, Cohen ZR, et al. Management of atlantoaxial metastases with posterior occipitocervical stabilization. J Neurosurg. 2003;98(2 Suppl):165–70.
27. Goel A, Laheri V. Plate and screw fixation for atlanto-axial subluxation. Acta Neurochir. 1994;129(1–2):47.
28. Richter M, Schmidt R, Claes L, et al. Posterior atlantoaxial fixation: biomechanical in vitro comparison of six different techniques. Spine. 2002;27(16):1724–32.
29. Magerl F, Seemann PS. Stable posterior fusion of the atlas and axis by transarticular screw fixation. In: Cervical Spine I. Vienna: Springer; 1987. p. 322–7.
30. Harms J, Melcher RP. Posterior C1–C2 fusion with polyaxial screw and rod fixation. Spine. 2001;26(22):2467.
31. Yang F, Ping YI, Tang X, et al. Posterior atlantoaxial pedicle screw fixation for atlantoaxial dislocation. Chin J Tradit Med Traumatol Orthop. 2014.
32. Goel A. C1–C2 pedicle screw fixation with rigid cantilever beam construct: case report and technical note. Neurosurgery. 2002;50(2):426.
33. Xu R, Nadaud MC, Ebraheim NA, et al. Morphology of the second cervical vertebra and the posterior projection of the C2 pedicle axis. Spine. 1995;20(3):259.
34. Howington JU, Kruse JJ, Awasthi D. Surgical anatomy of the C-2 pedicle. J Neurosurg. 2001;95(95):88–92.
35. Kelly BP, Glaser JA, Diangelo DJ. Biomechanical comparison of a novel C1 posterior locking plate with the harms technique in a C1–C2 fixation model. Spine. 2008;33(24):920–5.
36. Rocha R, Safaviabbasi S, Reis C, et al. Working area, safety zones, and angles of approach for posterior C-1 lateral mass screw placement: a quantitative anatomical and morphometric evaluation. J Neurosurg Spine. 2007;6(6):247–54.
37. Blagg SE, Don AS, Robertson PA. Anatomic determination of optimal entry point and direction for C1 lateral mass screw placement. J Spinal Disord Tech. 2009;22(4):233.

Surgical Anatomy of the Subaxial Cervical Spine

2

Jian-gang Shi, Wen Yuan, and Jing-chuan Sun

1 Anterior Cervical Spine Exposure Discectomy and Fusion

1.1 Overview

In published literatures, the Smith-Robinson approach is one of the most common methods for exposing the middle and subaxial cervical spine. It can not only expose the anterior vertebral bodies from C3 to T1, but it also directly exposes the intervertebral space and uncinated processes in this section. Indications of this approach include osteophyte resection, tumorectomy, intervertebral discectomy, and abscess drainage at the anterior and posterior of the spine.

The anterior cervical discectomy and fusion technique can be used to relieve anterior spinal pressure, stabilize the cervical spine, and restore the height of the interbody and physiological curve of the cervical spine in order to avoid cervical kyphosis. The advantages of this approach include direct decompression and minimal invasiveness. Its indications are: (1) patients who show symptomatic cervical degeneration, such as cervical instability, cervical spondylotic myelopathy, and focal or segmental ossification of the posterior longitudinal ligament, accompanied with obvious corresponding clinical symptoms. (2) Patients who show acute cervical disc herniation with obvious clinical symptoms. (3) Patients who show instable cervical spine trauma without vertebral fracture, such as dislocation or subluxation of cervical spine without vertebral fracture, and old cervical spine injury accompanied with segmental instability without vertebral fracture. Cage is most suitable for single segmental lesion, while insertion of several cages consecutively can induce secondary cervical spine deformity. Therefore, when dealing with multiple segmental cervical degeneration or disc herniations, only anterior titanium plate fixation can be used to create a stable environment for multiple segmental post-decompression bone graft fusion.

J.-g. Shi (✉) • W. Yuan • J.-c. Sun
Department of Orthopedics, Changzheng Hospital, Shanghai, China
e-mail: shijiangang616@163.com; yuanwenspine@163.com; sjchxc@foxmail.com

J.-g. Shi et al. (eds.), *Anatomy Atlas and Interpretation of Spine Surgery*, https://doi.org/10.1007/978-981-10-5906-3_2

1.2 Position

Patient is placed in a supine position, with the shoulders elevated and the head maintained in a central position and slightly extended backwards (Figs. 2.1 and 2.2).

1.3 Exposure

The position of the incision depends on the target level. There are some anatomic surface landmarks to localize skin incision.

Generally, the hyoid bone and thyroid cartilage are at the same level as C3 vertebrae C4–C5 disc, respectively, and the level of the cricoid cartilage is at the same level as C6 vertebrae. This relative relationship may differ due to individual differences, and hence the positions can be determined by preoperative imaging.

For aesthetic considerations, the natural skin creases closest to the operational level is usually chosen as the position of incision (Figs. 2.1 and 2.2).

The left or right sided approach can be chosen for the operation. In theory, exposure of spine below C5 involves the recurrent laryngeal nerve, and since the left recurrent laryngeal nerve is relatively fixed, the left approach is a more secure option for the operation.

In our institute, nearly 30,000 cases of cervical spine surgery have been performed. Although the right approach was used for most of these cases, the incidence rate of recurrent laryngeal nerve injury was very low.

In general, the anterior cervical transverse incision is made from the anterior margin of the sternocleidomastoid muscle to the anterior cervical midline. The longitudinal incision along the anterior of the sternocleidomastoid muscle can be used when exposure of more segments is required.

Fig. 2.1 Position and incision of anterior cervical spine exposure

Fig. 2.2 Position and incision of anterior cervical spine exposure

Platysma is a very thin cutaneous muscle. It arises from the investing layer of deep cervical fascia that covers the upper surface of the pectoralis major and deltoid, and its fibers cross the clavicle and move medially cranially along the side of the neck. The platysma is supplied by the submental artery and suprascapular artery, and innervated by the facial nerves, along with superficial veins and cutaneous nerves on its deep side. Contraction of platysma can tighten the neck skin, help lower the mandible, and even pull-down the corners of the mouth and lower lip during shock and surprise. When suturing the incised platysma during surgery, surgeons should make sure to align the broken ends while suturing in order to avoid post-operative scar formation (Fig. 2.3).

After incising the skin and subcutaneous tissue, isolate and incise the platysma transversely or longitudinally to expose the investing layer of deep cervical fascia (Fig. 2.4).

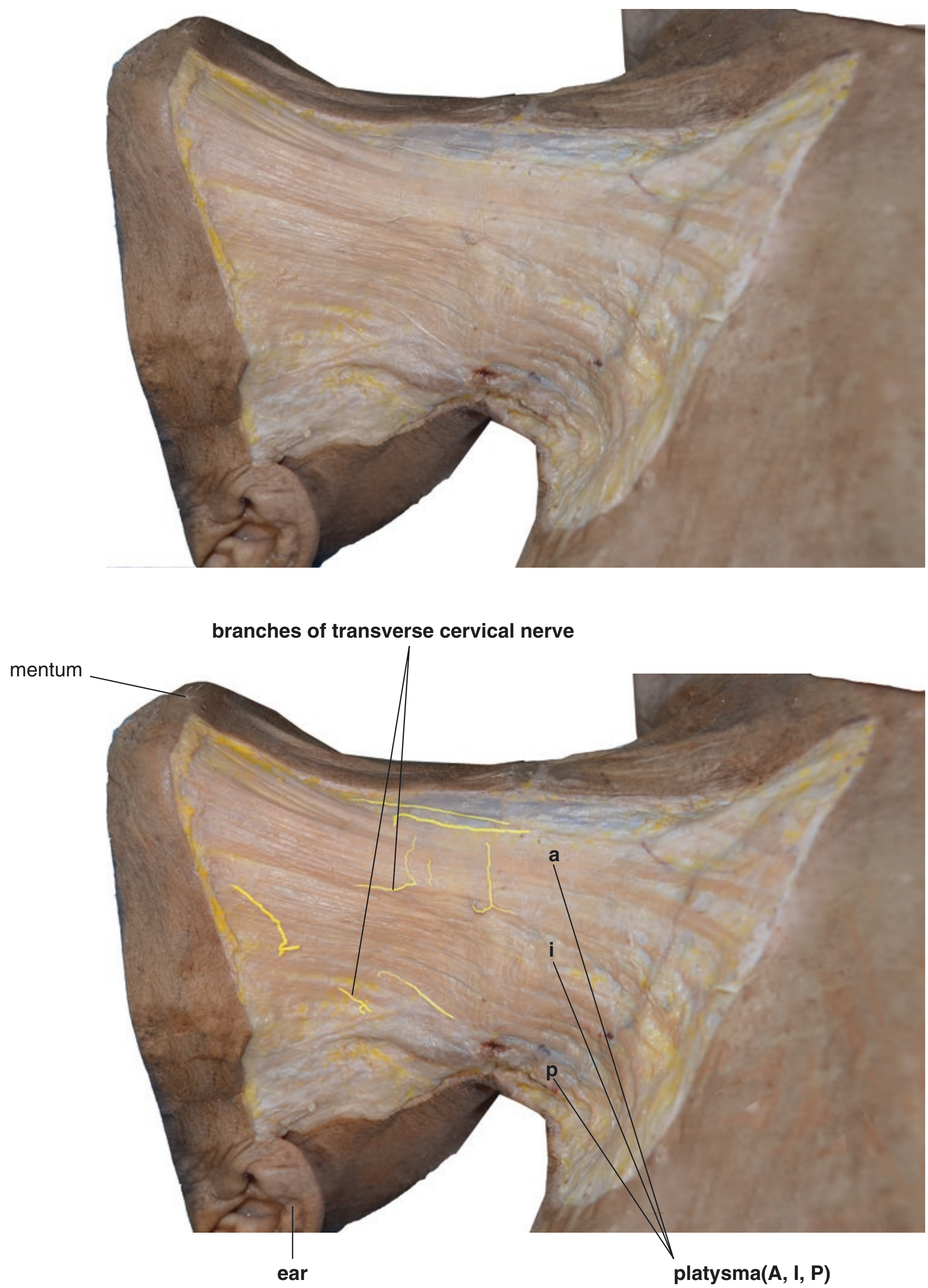

Fig. 2.3 Platysma and cutaneous nerves

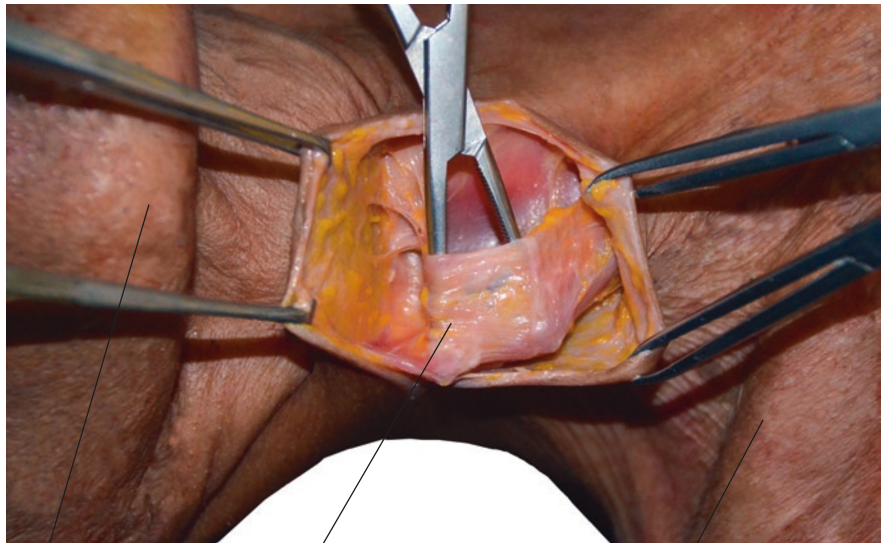

Fig. 2.4 Isolation and transverse or longitudinal incision of the platysma

During the operation, surgeons should choose a blunt dissection in the direction parallel to the platysma fibres.

The platysma of women, elders and children are thin, and the platysma of young men are thicker. Paying attention to these differences will help surgeons identify platysma during operation.

Anterior jugular vein: begins from a region of several superficial veins near the hyoid bone, and descends between the median and the anterior border of the sternocleidomastoid muscle. Communicating branches are often found between the anterior jugular vein and the internal jugular vein (Figs. 2.5 and 2.6).

Cervical branch of the facial nerve: descends from the lower part of the parotid gland and runs forward beneath the platysma to the anterior cervical region, innervating the platysma (Fig. 2.7).

Transverse cervical nerve: arises from the second and third spinal nerves, turns around the posterior border of the sternocleidomastoid muscle and runs forward beneath the external jugular vein to the anterior border of the muscle. It perforates the deep cervical fascia and provides cutaneous innervation to the skin of the anterior region of the neck (Fig. 2.7).

Blunt dissection of the fascia anterior to the sternocleidomastoid muscle (Fig. 2.8).

The omohyoid muscle can be pulled downwards for surgeries above C5, but this may damage the superior thyroid artery and superior laryngeal nerve.

The omohyoid muscle can be pulled upwards for surgeries below C6, but this may damage the inferior thyroid artery and recurrent laryngeal nerve.

In surgeries involving long cervical spine segments, the segments can be exposed respectively from above and below the omohyoid muscle. Although the omohyoid muscle is generally retained and not incised, it can be cut when necessary along with sutures at the broken ends for subsequent reconstruction.

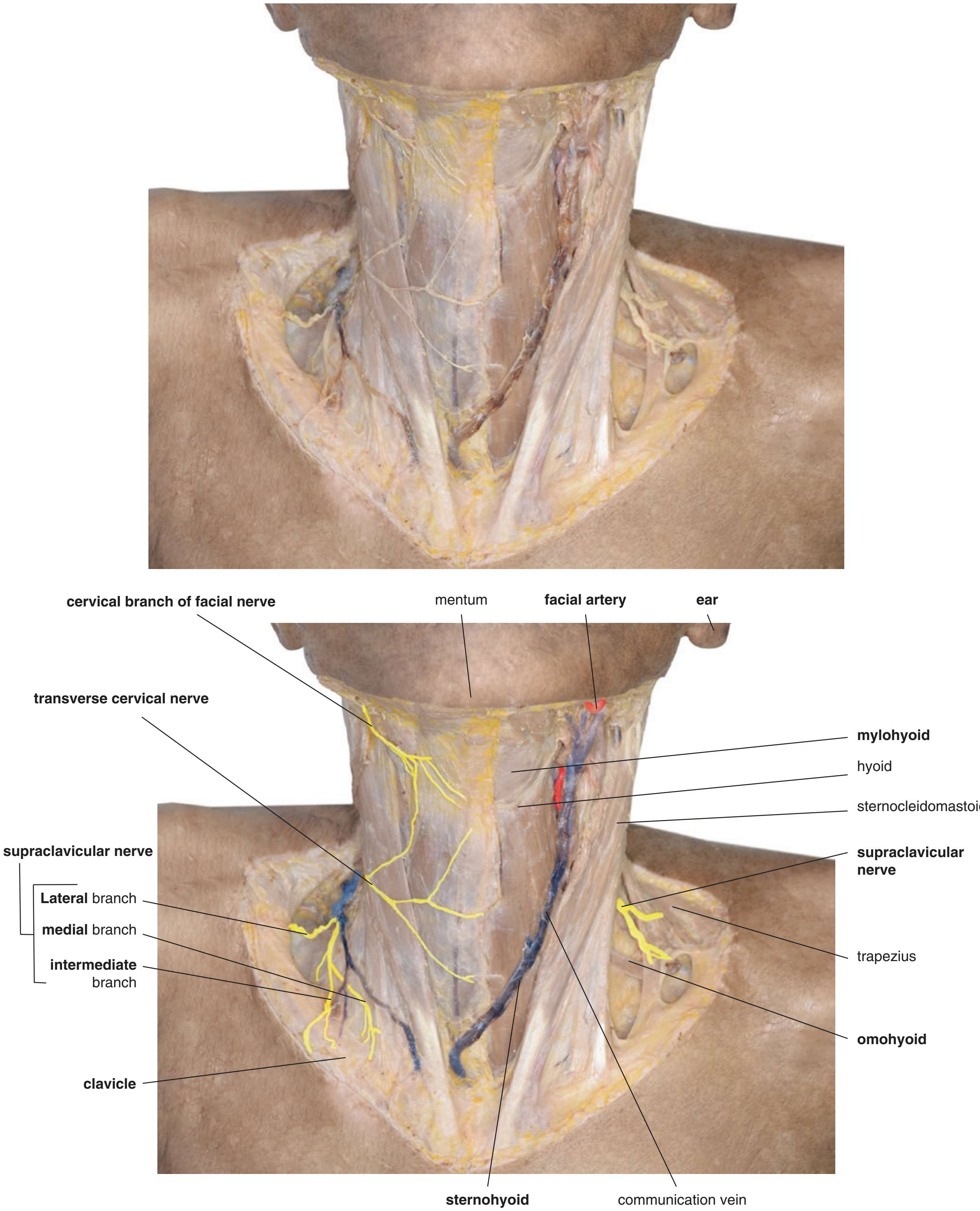

Fig. 2.5 Neurovasculature of the anterior cervical investing layer of deep cervical fascia

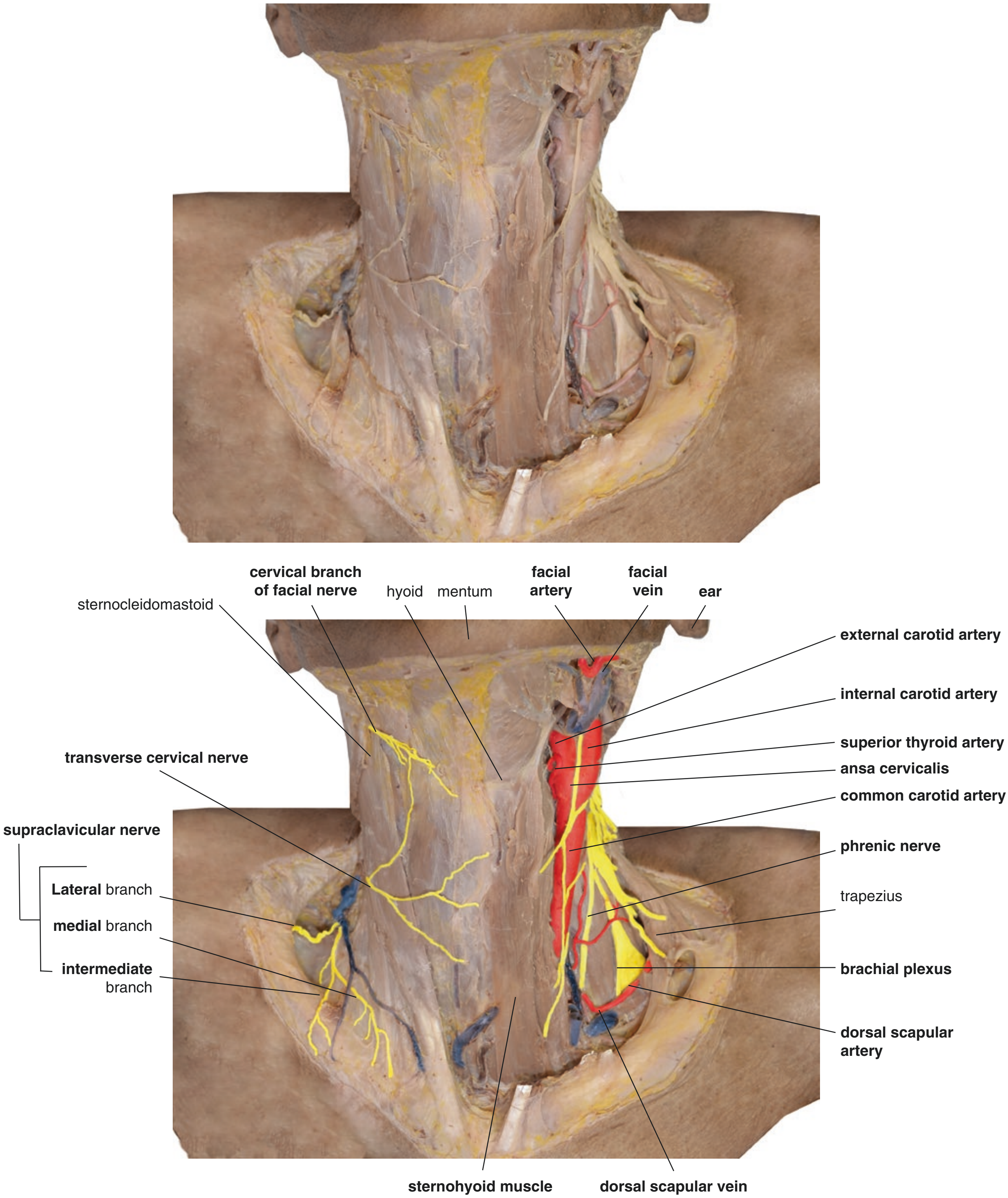

Fig. 2.6 Neurovasculature of the anterior cervical investing layer of deep cervical fascia (sternocleidomastoid muscle and carotid sheath were excised on the left)

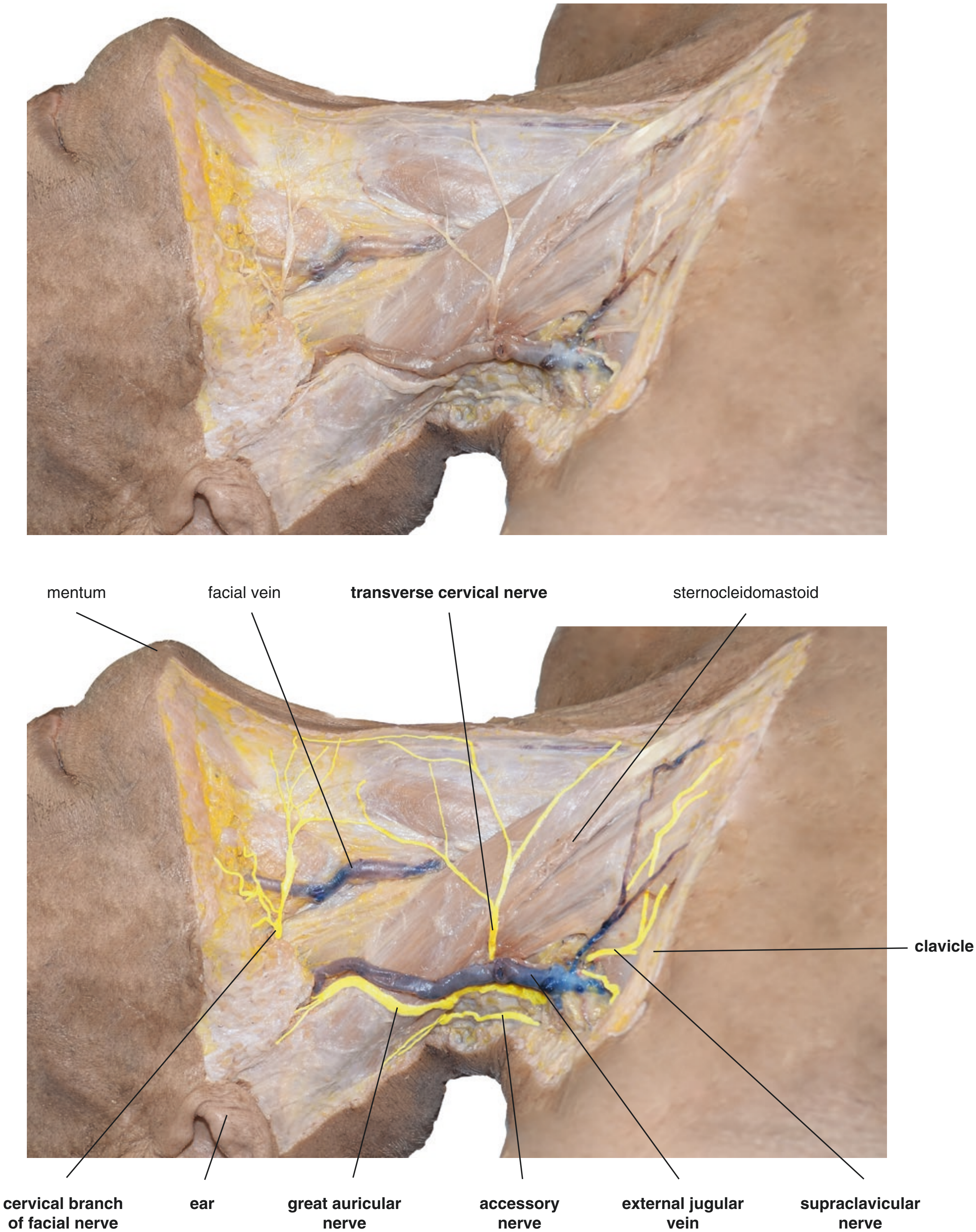

Fig. 2.7 Neurovasculature underneath the investing layer of deep cervical fascia on the right

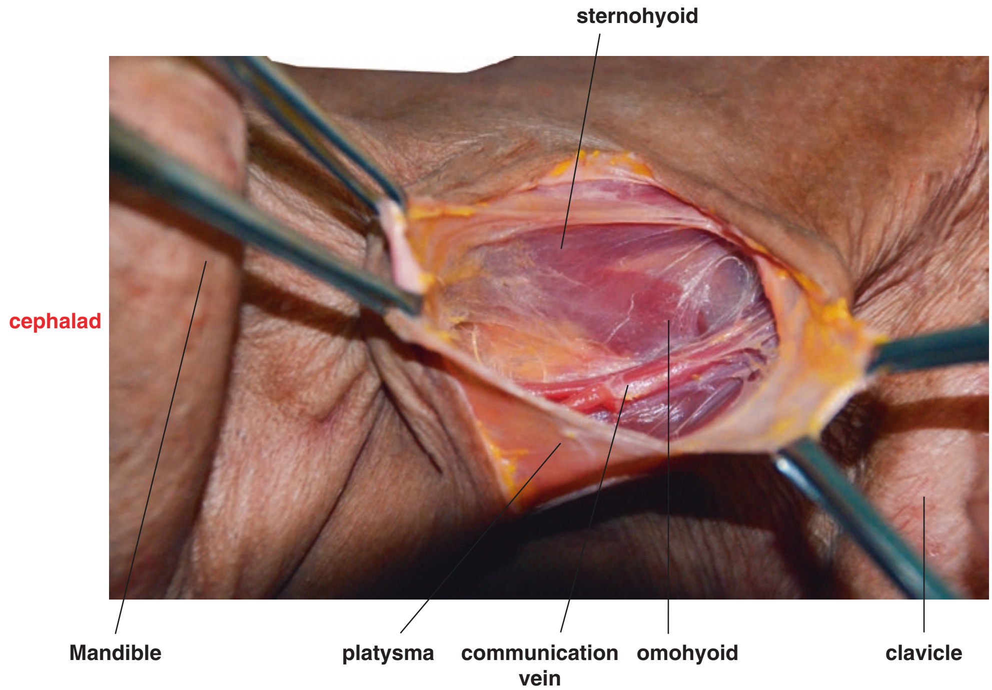

Fig. 2.8 Retract the platysma to expose the investing layer of deep cervical fascia

Omohyoid muscle: the central tendon of the muscle is sheathed by a deep fascia that arises from the clavicle and the first rib, which maintains the muscle in a bent angle. The omohyoid muscle crosses the pretracheal fascia and carotid sheath from a cranial-medial to caudal-lateral direction at the C5–C6 level. Branches of the superior thyroid artery and lingual artery supply the blood for the muscle. Its superior and inferior bellies are innervated by the branches of the superior root of ansa cervicalis (C1) and the branches of the ansa cervicalis (C1, C2 and C3). Incising the tendon of the digastric muscle can avoid damaging the innervating nerves and supply arteries of the muscle, making the digastric muscle more stable at the time of reconstruction (Fig. 2.9).

When performing blunt dissection of the investing layer of deep cervical fascia between the trachea, esophagus and carotid sheath medial to the sternocleidomastoid muscle, surgeons should palpate the carotid artery, and pull the carotid sheath outwards with fingers to avoid entering the carotid sheath (Figs. 2.10, 2.11, and 2.12).

Structural damages of the carotid artery and sheath occur mainly during dissection or placement of the retractor.

Temporal arterial pulsation should be checked while using the automatic retractor in order to avoid cerebral ischemia caused by long-term carotid artery occlusion.

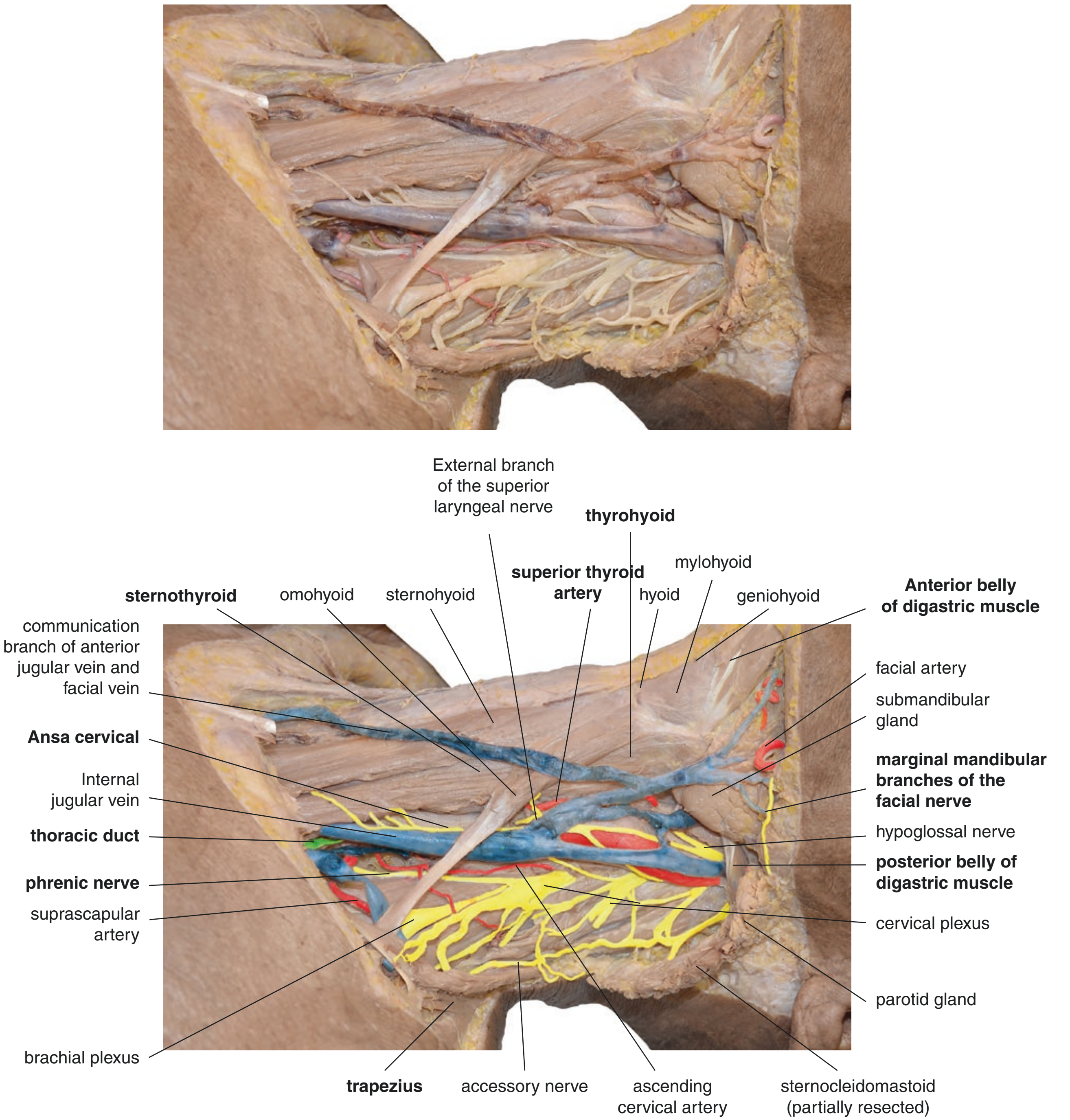

Fig. 2.9 Deep layer neurovasculature of the anterior cervical region on the left side

Thyroid retractors are commonly used instead of automatic retractor in our institute. Compression of the carotid sinus can easily lead to blood pressure fluctuations.

The superior and inferior thyroid arteries are usually not ligated to avoid injuring the superior laryngeal nerve and the recurrent laryngeal nerve. If ligation is necessary, ligation of the inferior thyroid vessels should be closed to the side of the common carotid artery, while the ligation of the superior thyroid vessels should be closed to the thyroid tissues. During ligation, surgeons must make sure that the ligated tissue only contains vessels with no nerves. Usage of bipolar electrocoagluation should be avoided as it can easily damage the nerves.

Injuries to the recurrent laryngeal nerve and the internal and external branches of the superior laryngeal nerve can result in hoarse voice, coughing and lowered tone, respectively.

Most inferior thyroid arteries originate from the thyrocervical trunk of the subclavian artery, but a few arise from the subclavian artery or vertebral artery. It passes upward along the medial side of the anterior scalene muscle to the C6 plane, and turns medially between the carotid sheath and the vertebral arteries and veins. The inferior thyroid artery divides into the superior and inferior branches when it reaches the lower border of the lateral thyroid globe, and then supplied the thyroid, parathyroid gland, trachea and esophagus (Fig. 2.13).

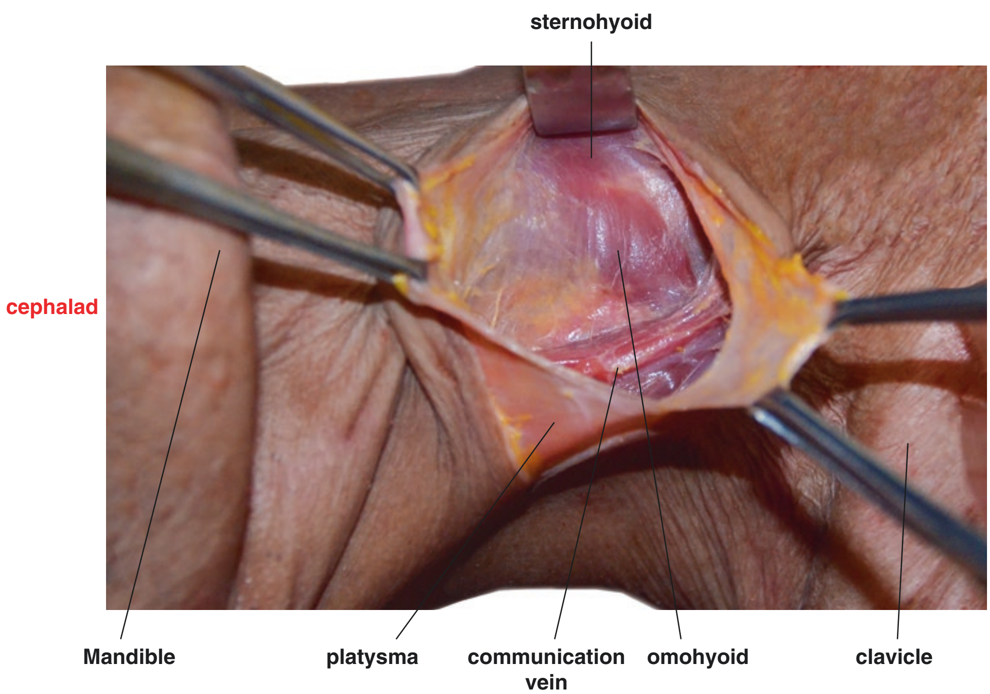

Fig. 2.10 Blunt dissection of the investing layer of deep cervical fascia between the trachea, esophagus and carotid sheath medial to the sternocleidomastoid muscle

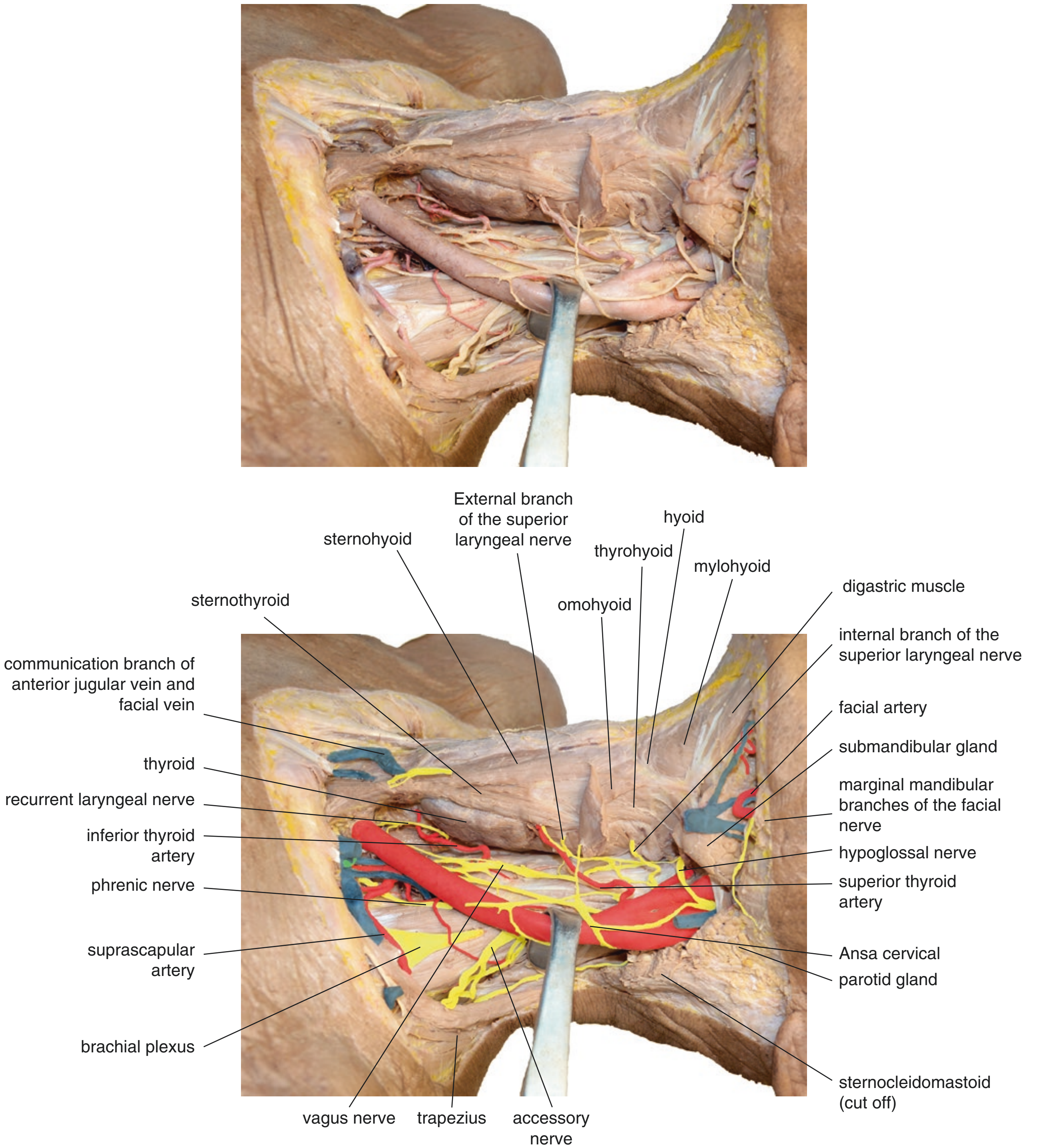

Fig. 2.11 Deep layer neurovasculature of the left anterior cervical region with the common carotid artery retracted laterally

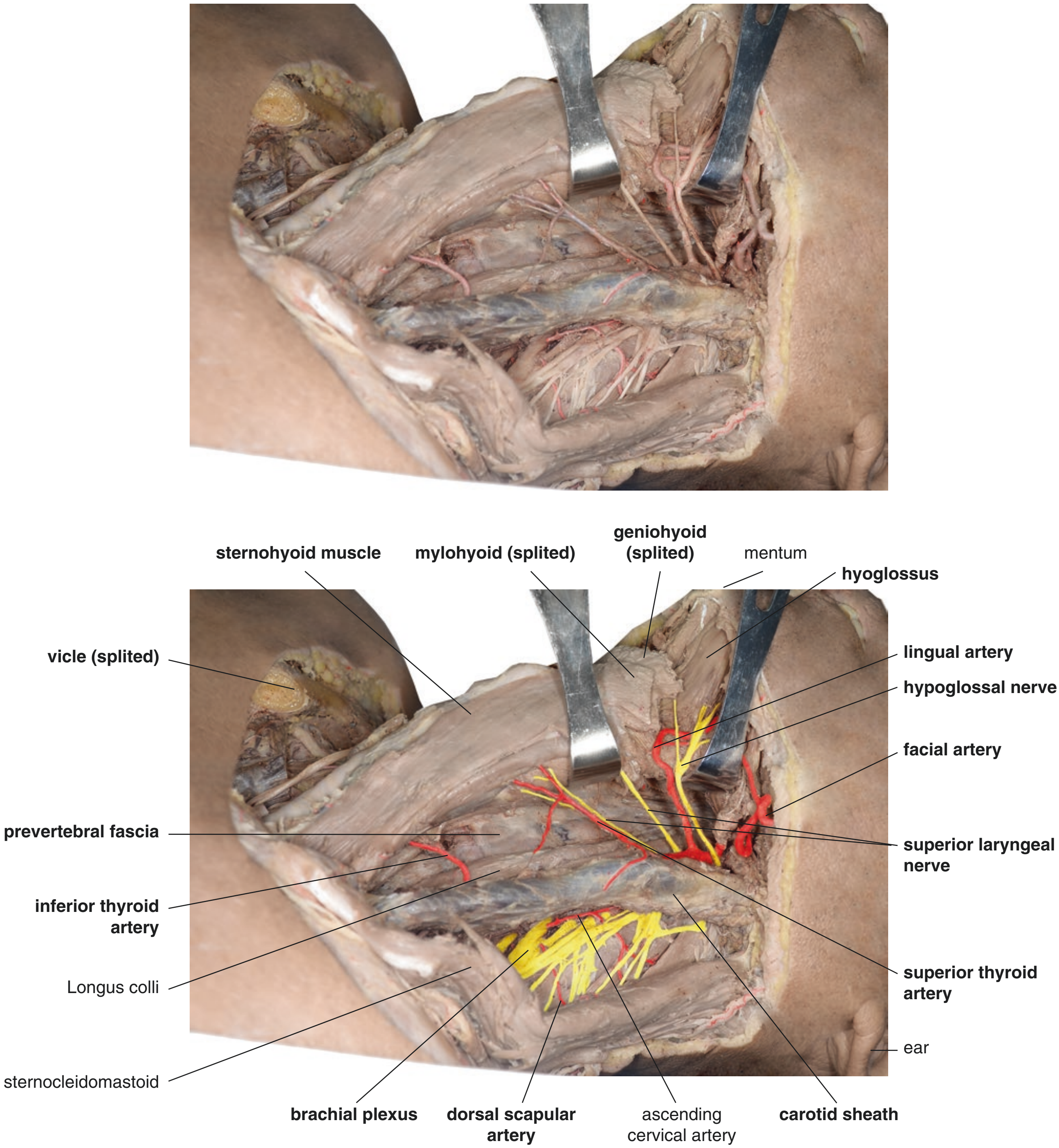

Fig. 2.12 Deep layer neurovasculature of the left anterior cervical region

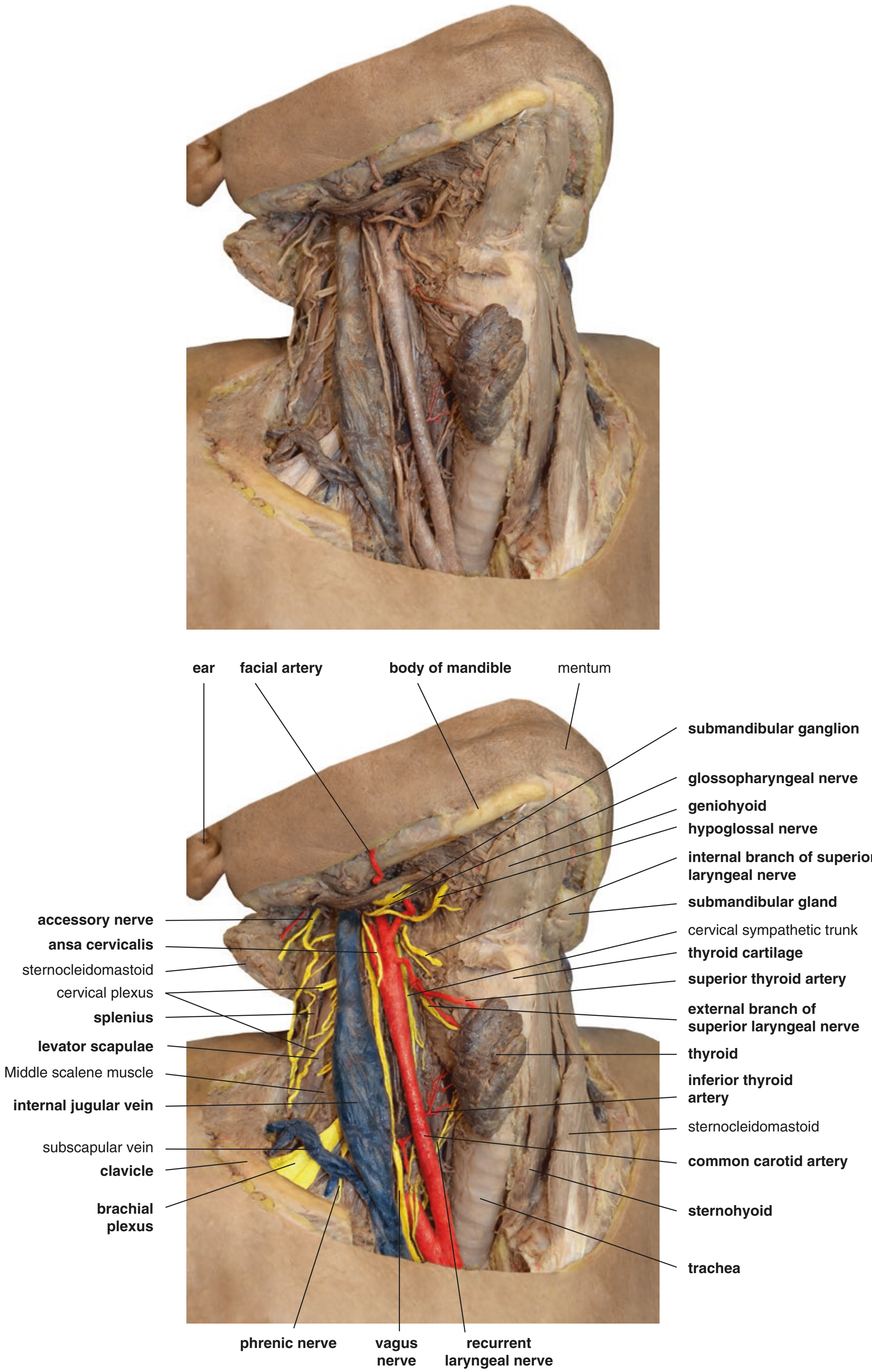

Fig. 2.13 Deep layer neurovasculature of the right anterior cervical region

The sternocleidomastoid muscle and carotid sheath are pulled towards the lateral, while the trachea and esophagus are pulled towards the midline to expose the prevertebral fascia. As shown in Fig. 2.14, the vertebrae, intervertebral disc, and longuscolli muscle are covered by the prevertebral fascia (Figs. 2.14, 2.15 and 2.16).

Injury to the vagus nerve caused by the intraoperative incision or excessive stretching of the pretracheal fascia is the main cause of postoperative dysphagia.

Anterior longitudinal ligament: a strong fibrous connective tissue that runs along the anterior of the spine. It extends from the bottom of the occipital bone to the anterior of the spine, and then continues to extend caudally to the upper sacrum (Fig. 2.15).

Longuscolli muscle: situated on the anterior surface of the vertebral column between the atlas and the third thoracic vertebra. It can be divided into three portions, a superior oblique, an inferior oblique, and a vertical, each of which starts from the tendinous bundle. While the longuscolli muscle can lead to forward neck flexion, its superior oblique portion is responsible for lateral flexion and its inferior oblique portion is responsible for contralateral rotation of the neck. In anterior cervical operation, the longuscolli muscle is often used as an anatomic landmark to determine the safety range of the decompression. However, owing to individual differences and the fact the position of the longuscolli muscle is easily affected by osteophytes during more severe degeneration of the cervical spine, surgeons should make judgments based on the patient's condition when using the muscle as a landmark (Fig. 2.15).

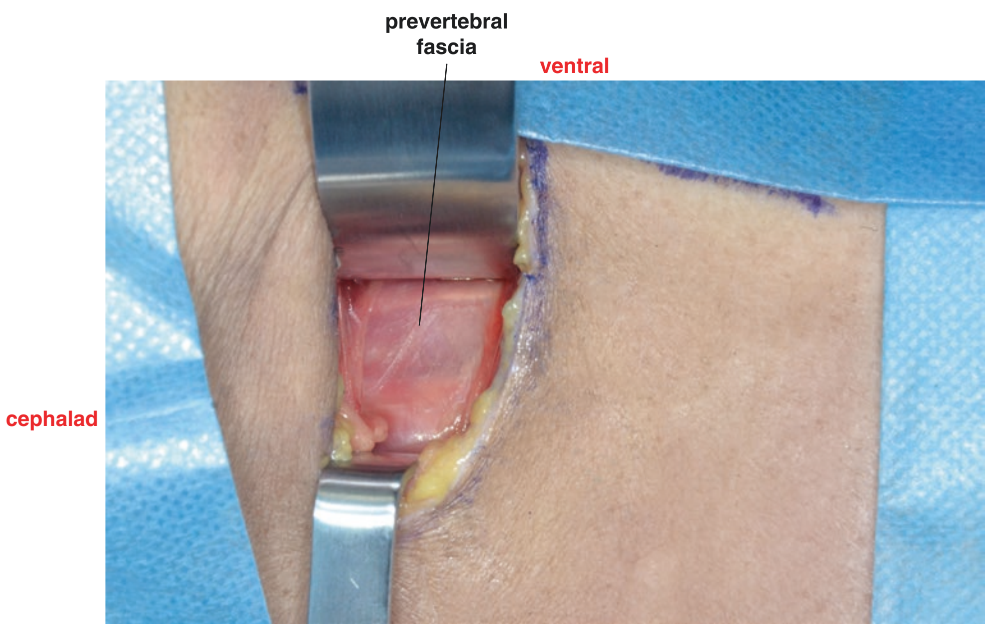

Fig. 2.14 Carotid sheath, trachea and esophagus stretched apart by retractors to expose the prevertebral fascia

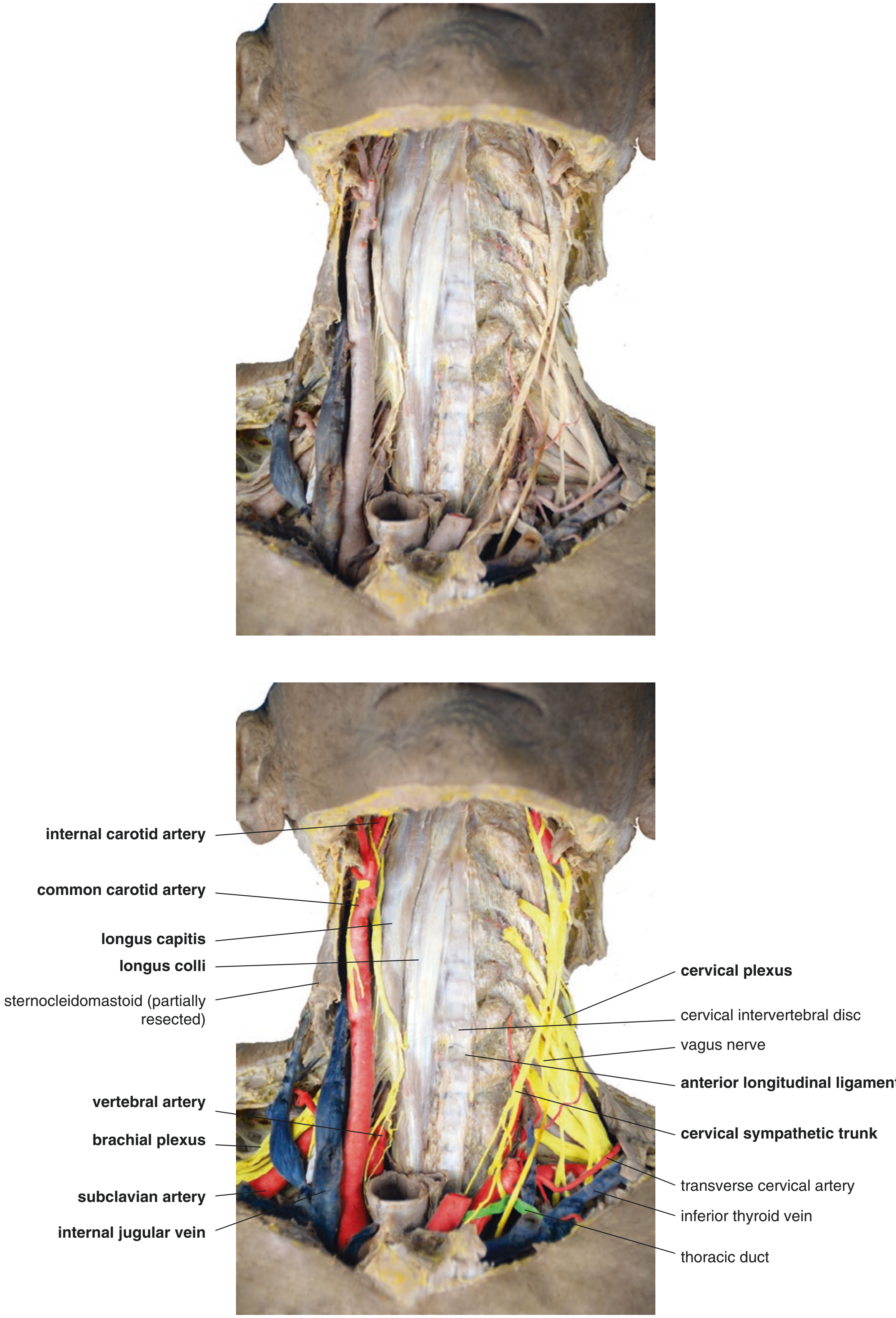

Fig. 2.15 Neurovasculature of the prevertebral fascia

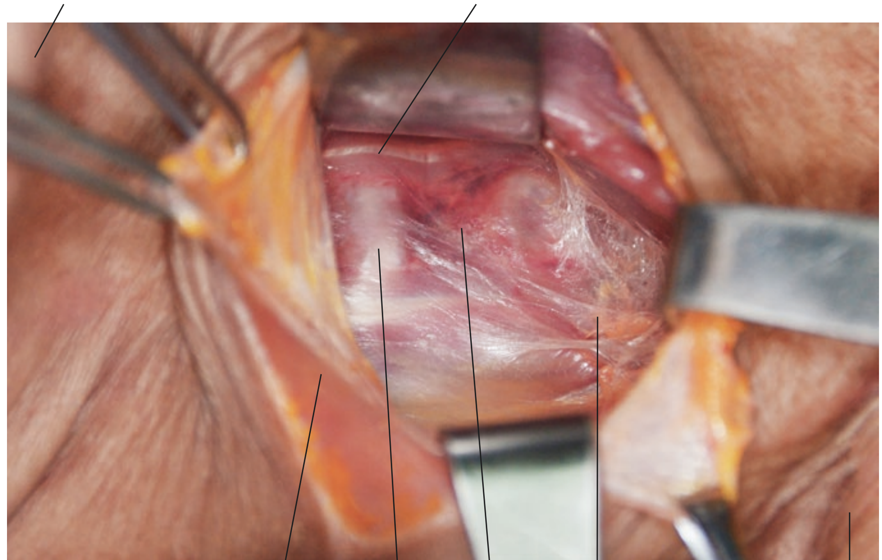

Fig. 2.16 Carotid sheath, trachea and esophagus stretched apart by retractors to expose the prevertebral fascia

The position of the esophagus should be carefully identified when incising the prevertebral fascia. If the esophagus is not completely pulled away, it may get injured during the incision of the prevertebral fascia and result in esophagostoma.

In anterior cervical revision surgery, anasogastric tube is routinely placed preoperatively in the our institute to help identify the esophagus during operation.

The prevertebral fascia is lifted by a toothed forcep and incised layer by layer. And it is further bluntly dissected longitudinally using the periosteal detacher, by which the vertebral body and intervertebral space are exposed (Fig. 2.17).

Avoid operating in the longuscolli muscle or to the outside of the lateral border of it in case of excessive bleeding. Bipolar electrocoaglution should be performed prior to discectomy to reduce bleeding.

It is important to separate the longuscolli muscle under the periosteum, otherwise the sympathetic trunk on the surface of the longuscolli muscle can be easily damaged, which causes Horner syndrome.

The width of separation should be no more than 3 mm from the medial margin when pulling the longuscolli muscle apart. Otherwise, excessive separation of longuscolli muscle may lead to iatrogenic vertebral artery injury.

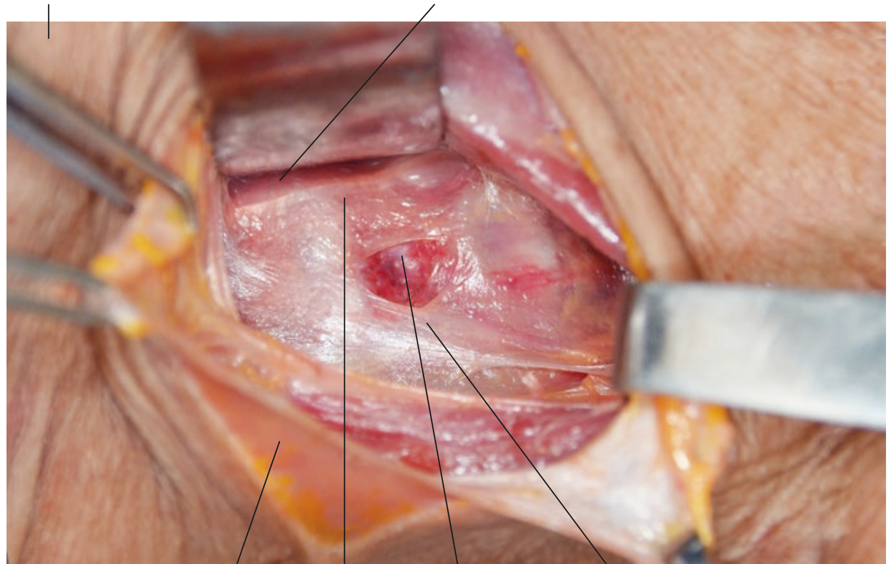

Fig. 2.17 Prevertebral fascia incised layer by layer to expose the vertebral body

1.4 Discectomy

Target segments are determined by intraoperative lateral fluoroscopy (Fig. 2.18).

The Caspar pins should be implanted into the center of the vertebral body parallel to the vertebral endplates. Disc space should be distracted gradually during decompression (Fig. 2.19).

Disc space distraction not only restores the intervertebral height, but it also stretches the thickened posterior longitudinal ligament, making discectomy safer. However, excessive dilation can induce postoperative axial pain.

For patients with traumatic spinal dislocation, disc space distraction can be a effective way to relocate the alignment in the anterior approach.

When pulling the carotid sheath to the lateral, surgeons should avoid pressing on the retractor to prevent injury of the cervical sympathetic trunk.

The anterior longitudinal ligament and the outer layer of annulus fibrosus should be incised parallel to the upper and lower endplates with a scalpel. The optimal depth is 2–4 mm, and both sides of the incision should reach as far as the uncinated process (Fig. 2.20).

If the presence of osteophytes at the anterior border of the vertebral body obstructs the direct excision of the annulus fibrosus, they should be first removed (Fig. 2.21).

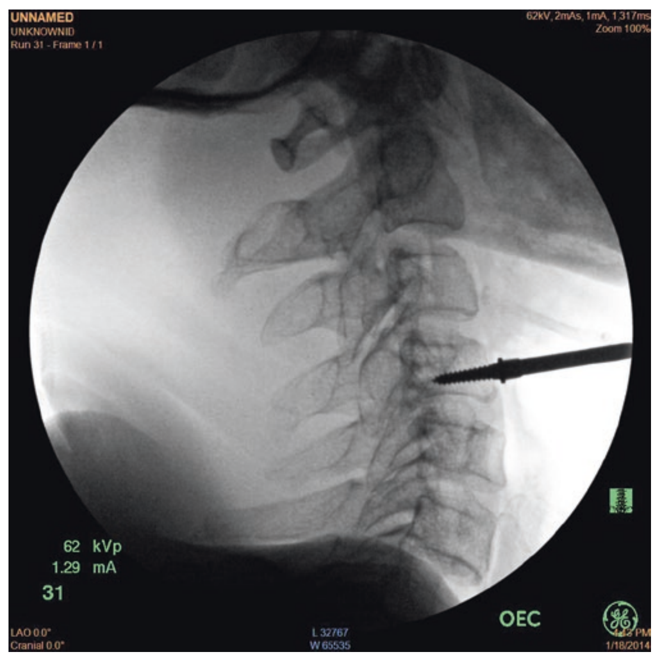

Fig. 2.18 Target segments determined by intraoperative lateral fluoroscopy

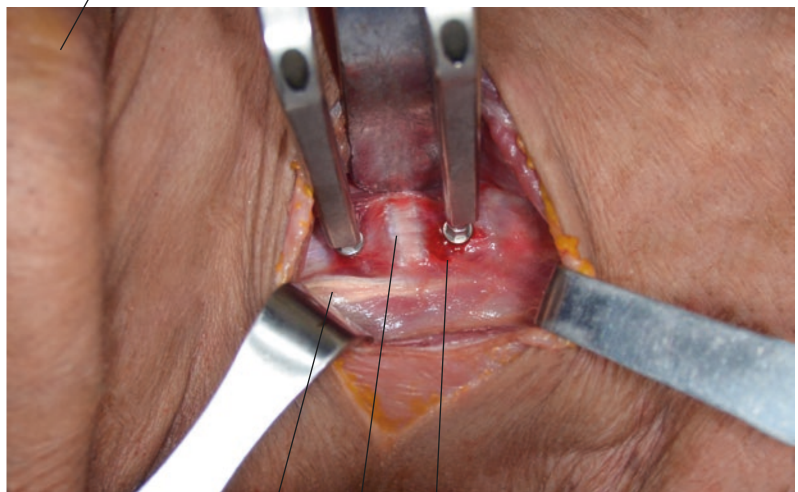

Fig. 2.19 Implantation of the Caspar retractor

Fig. 2.20 Incision and removal of the anterior longitudinal ligament and the annulus fibrosus outer layer of the intervertebral disc

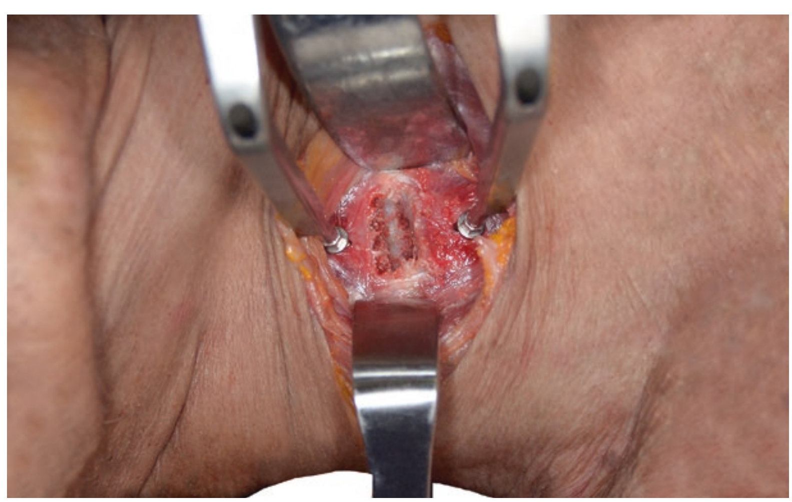

Fig. 2.21 Removal of osteophytes from the anterior border of the vertebral body

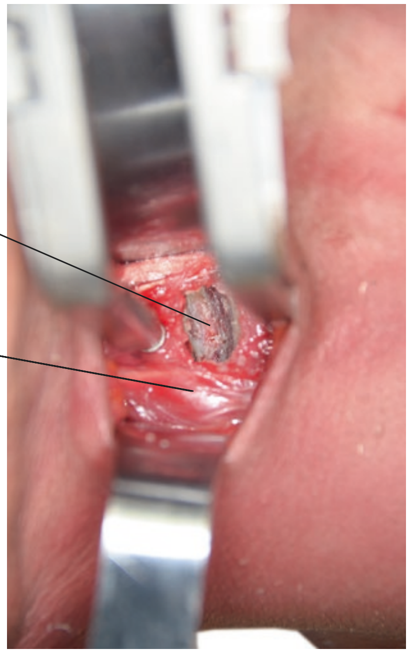

Fig. 2.22 Removal of the intervertebral disc tissue and cartilaginous endplates

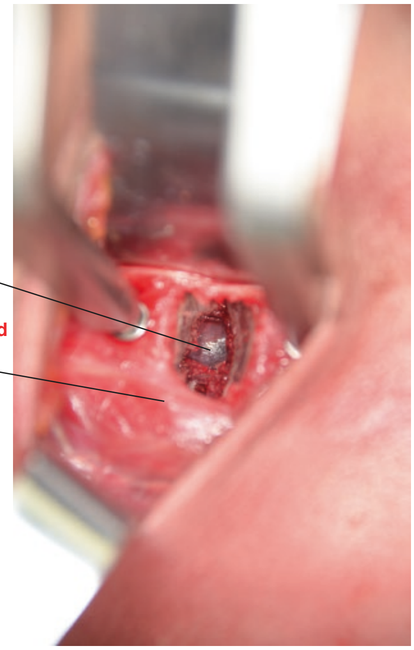

Fig. 2.23 Complete decompression of the spinal cord after resection of the posterior longitudinal ligament

The pituitary rongeur is inserted into the intervertebral space to remove the nucleus pulposus from one side to the other side (Fig. 2.22).

The nucleus pulposus should be removed slowly and the jaw of rongeur should not be opened too wide.

The depth of the forcep in the intervertebral space should be strictly monitored. If it is inserted too deep, it may lead to the injury of the spinal cord. When the forcep is near the posterior border of the vertebra, a curette should be used to remove the cartilaginous endplate (Fig. 2.21).

Curette and forcep are used to remove the osteophytes on the lateral side of the uncovertebral joint.

Curette and forcep must be used from small to large size during decompression to avoid compressing and injuring the spinal cord and nerve root.

Final examination of all direction should be done by a nerve hook showing the nerve root and spinal cord compression is fully released, all the nucleus pulposus and the protruding annulus fibrosus tissues are removed, all of which are vital for thorough decompression.

1.5 Decompression

In our institute, the posterior longitudinal ligament is routinely resected in order to achieve thorough decompression of the spinal cord.

The nerve dissector with hook is inserted through the weak part of the posterior longitudinal ligament into the anterior epidural space. The posterior longitudinal ligament can then be safely incised along the groove on the hook. The posterior longitudinal ligament is carefully removed with a Kerrison rongeur to expose the spinal dural sac (Figs. 2.23, 2.24 and 2.25).

Posterior longitudinal ligament: situated within the vertebral canal, and extends along the posterior surfaces of the bodies of the spine, from the body of the axis, where it is continuous with the membrana tectoria, to the sacrum. The fibrous border of the posterior longitudinal ligament is attached to the intervertebral disc, the transparent cartilage and the edge of the adjacent vertebra. The posterior longitudinal ligament is wide in the cevical spine and upper thoracic spine, narrow in the lower thoracic spine and lumar spine. In each segment, the posterior longitudinal ligament is wider in the intervertebral disc and relatively narrow in the vertibral body level. Its fiber is fused with the annulus fibrosus of the intervertebral disc (Figs. 2.26 and 2.27).

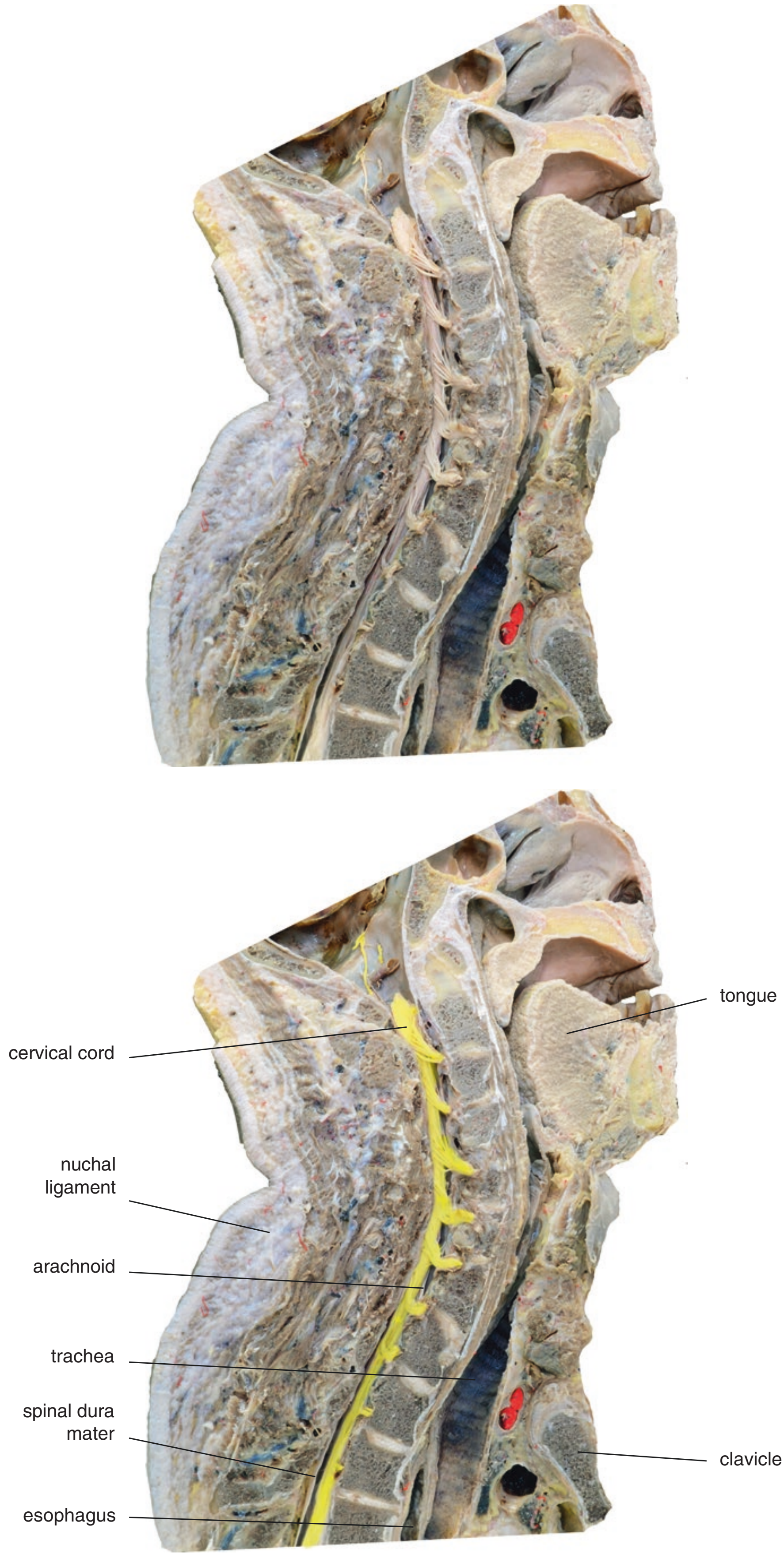

Fig. 2.24 Lateral view of the spinal cord and nerve roots

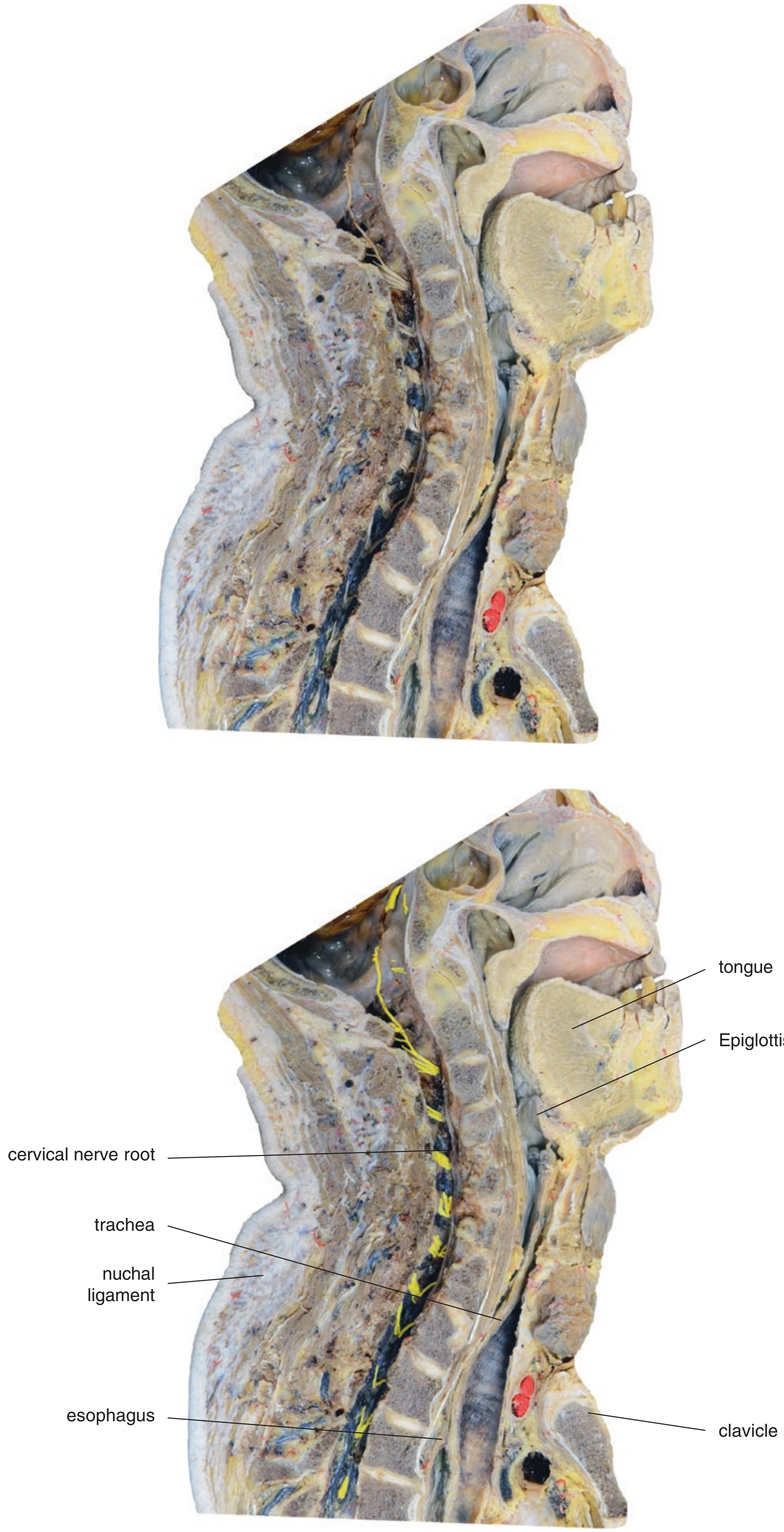

Fig. 2.25 Lateral view of the vertebral canal and nerve roots (spinal cord resected)

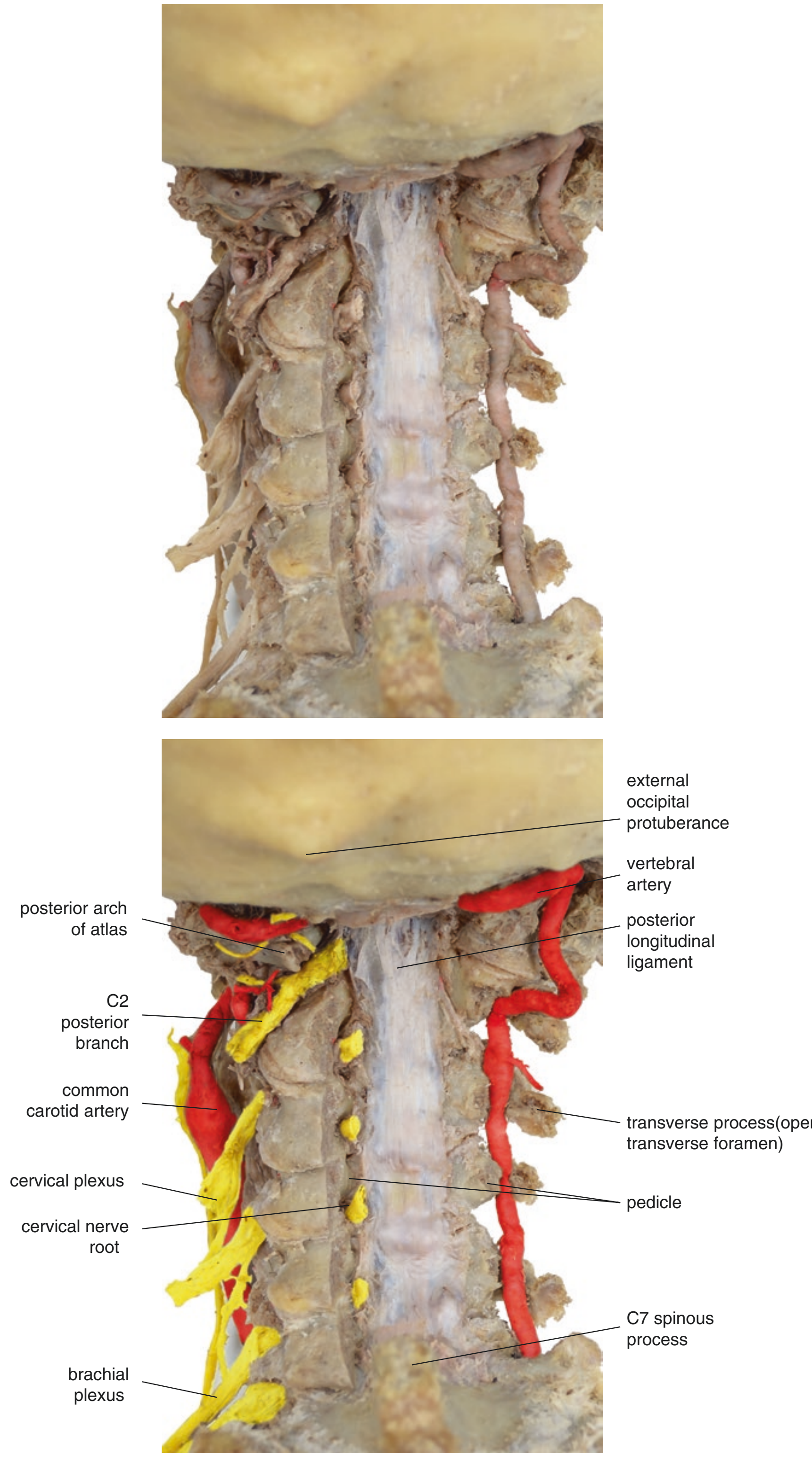

Fig. 2.26 Structures around the posterior longitudinal ligament

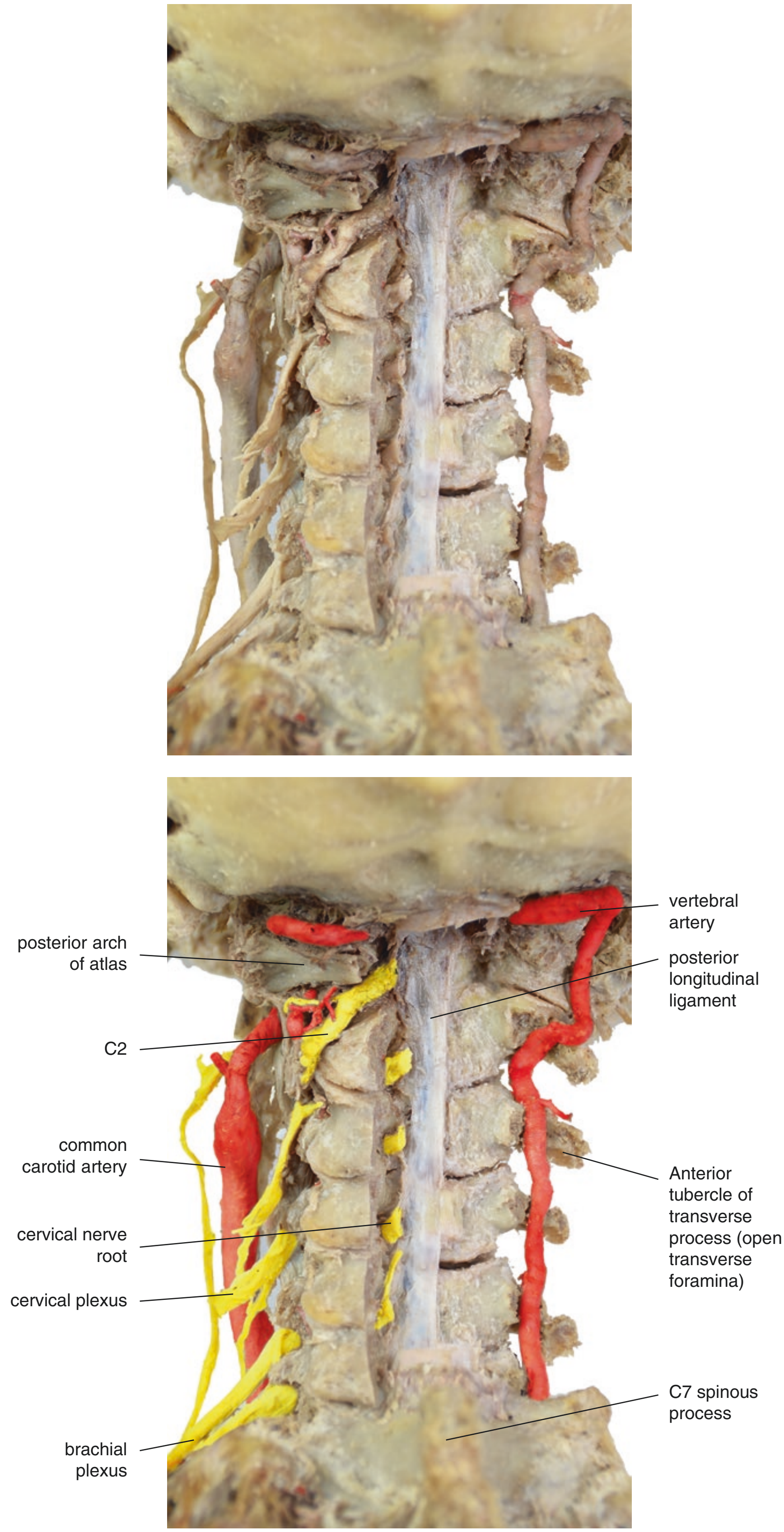

Fig. 2.27 Structures around the posterior longitudinal ligament

1.6 Fusion and Fixation

Removement of the cartilaginous endplate and the subchondral bone is done completely by curette until bleeding endplate is observed. Excessive curette usage on the endplate should be avoid to prevent graft subsidence.

Serial trial spacers are used prior to placement of the implant to find the suitable size of interbody cage.

Place the interbody cage into the treated interbody space, and release the Caspar distractor so that the interbody cage can be inserted tightly (Fig. 2.28).

The size of the anterior cervical anterior plate is selected according to the vertebral body's position. Screws are inserted after adjusting the plate's position (Fig. 2.29).

The position of the anterior cervical implant is verified under intraoperative anteroposterior lateral fluoroscopy (Figs. 2.30 and 2.31).

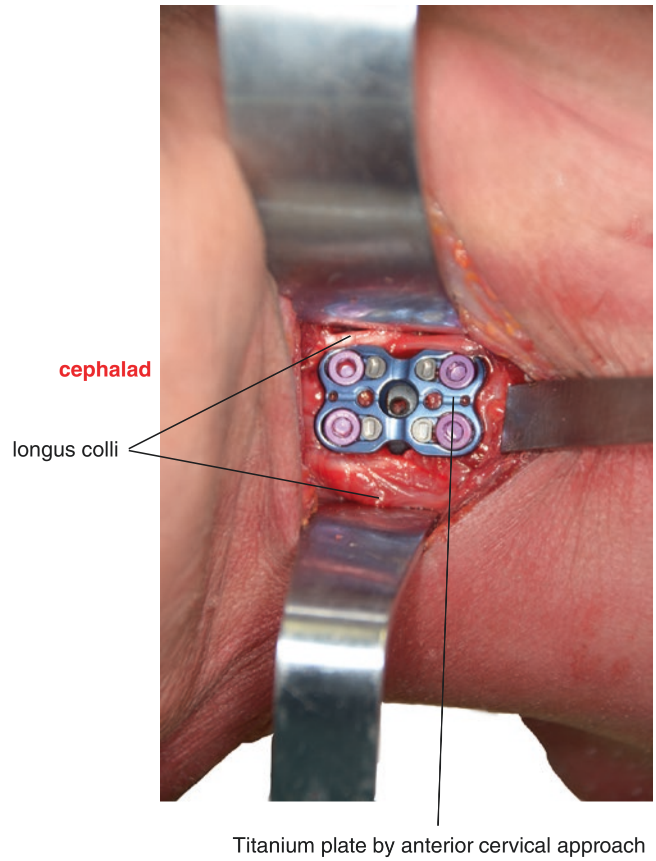

Fig. 2.29 Placement of the anterior cervical titanium plate followed by screw fixation and locking

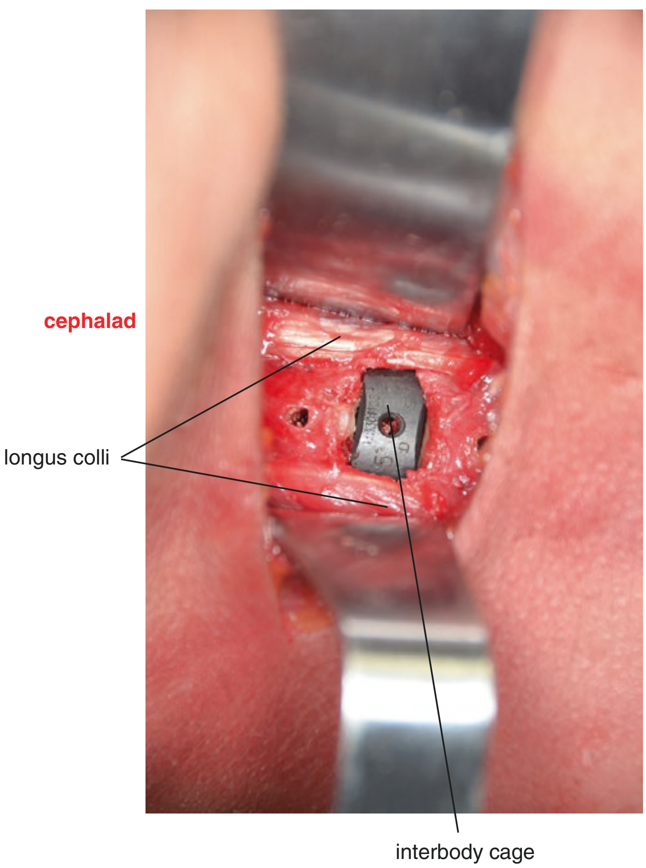

Fig. 2.28 Placement of the interbody cage

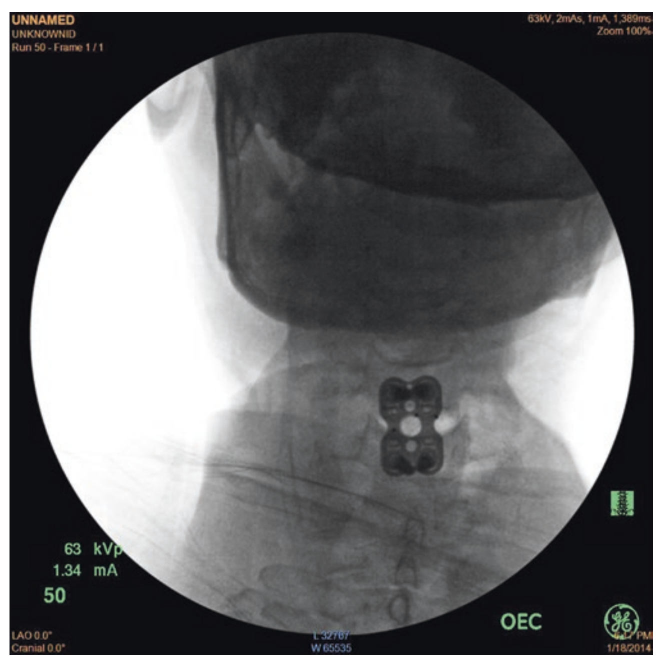

Fig. 2.30 Position of the anterior cervical implant shown by intraoperative anteroposterior fluoroscopy

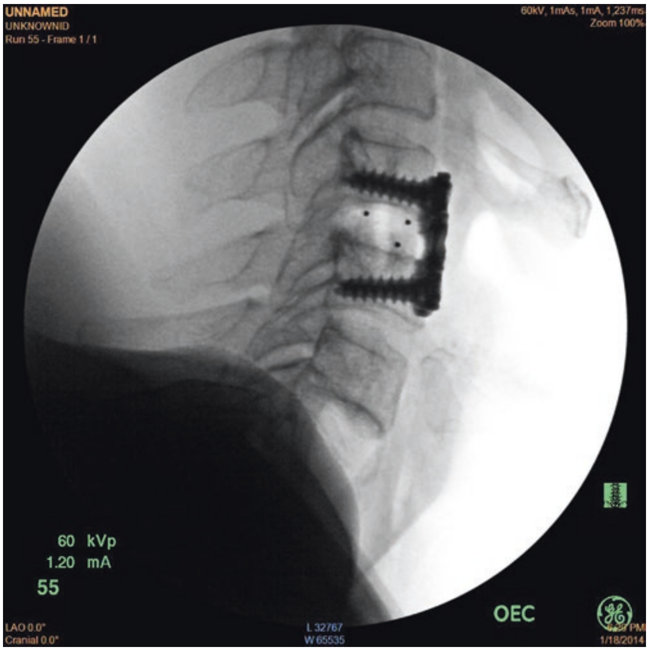

Fig. 2.31 Position of the anterior cervical implant shown by intraoperative anteroposterior fluoroscopy

2 Posterior Cervical Spine Approach, Expansive Laminoplasty and Arch Titanium Plate Fixation

2.1 Overview

The posterior approach for cervical spine approach was the mainstay of cervical vertebral laminectomy and decompression, expansive laminoplasty and multiple cervical fusion with internal fixation in the past. Cervical exposure by the posterior approach is relatively safer due to the absence of major blood vessels and organs. However, the exposure should be performed along the middle avascular zone to reduce bleeding from the friable large venous system in the posterior paraspinal muscle. In addition, stripping should be conducted under the periosteum to reduce intraoperative bleeding. Subaxial cervical spine exposure by the posterior approach can fully expose C3 to T1 spinous process, vertebral lamina, lateral mass and other posterior structures.

Expansive laminoplasty of the cervical spine was first reported by Hirabayashi in 1983. This technique, known as open-door laminoplasty, involves the combination of bicortical and unicorticalosteotomies which allows for hinging open the posterior arches. Z-plasty, and spinous process-splitting methods are also described as various laminoplasty techniques. The decompression of posterior laminoplasty must extend cephalad and caudal to the levels of compression so that the spinal cord can float posteriorly without kinking at the lamina at the rostral or caudal extent of the decompression. The complications of expansive laminoplasty including postlaminectomy kyphosis, instability, perineural adhesions, and delayed neurological decline. The advantage of this technique is its small postoperative impact on the total range of cervical motion.

2.2 Position

The patient underwent cervical laminoplasty is placed in a prone position with at three-pronged skull clamp. The operation is performed on a premade plaster bed in our institute (Fig. 2.32).

The plaster bed can stabilize the patient's cervical spine during the operation. Its reliable stability and X-ray penetrable characteristics make it popular in many hospitals in China.

Keep a moderate reverse Trendelenburg position to get a good surgical field and venous drainage. The neck should be in slightly flexion in order to facilitate intraoperative exposure.

The forehead, mandible, chest and pelvis are properly padded.

Particular attention should be paid to avoid pressure on the ocular region or the male genital.

The skin of both shoulders is retracted caudally and secured onto the operating table with long wide bandages in order to stabilize the patient and facilitate intraoperative fluoroscopy.

Fig. 2.32 Position and incision of posterior cervical laminoplasty

2.3 Exposure

The location and length of the incision are determined according to the involved segments. (Fig. 2.33)

The skin and subcutaneous tissue are dissected layer by layer to expose the deep fascia, and make sure the incision is in the midline by palpating the spinous process during the procedure.

Electrocautery is used to dissect through the ligamentum nuchae. The posterior elements of the vertebrae are exposed by subperiosteally dissect the bilateral trapezius muscle, splenius capitis muscle and the semispinalis capitis muscle (Figs. 2.34, 2.35, 2.36 and 2.37).

The supraspinous and infraspinous ligaments is preserved. The dissection is extended laterally to the facets. Care is taken to preserve the facet joint capsule.

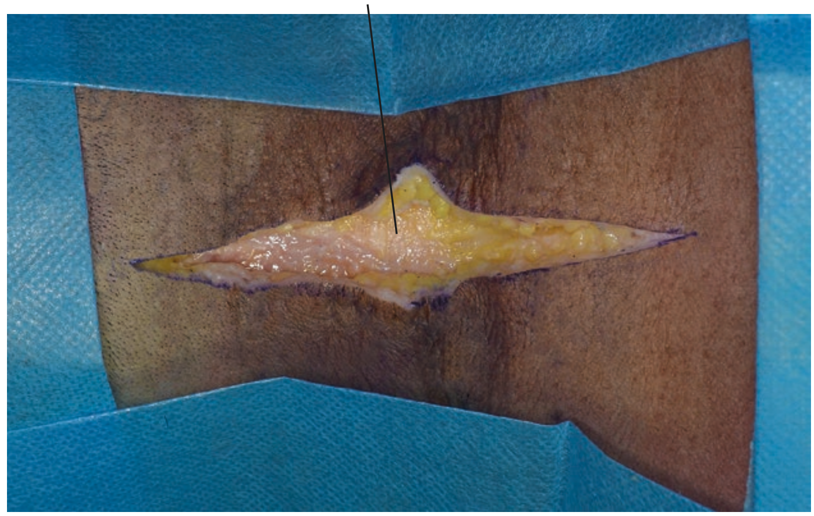

Fig. 2.33 Midline incision of the neck skin

Fig. 2.34 Incision of the deep fascia

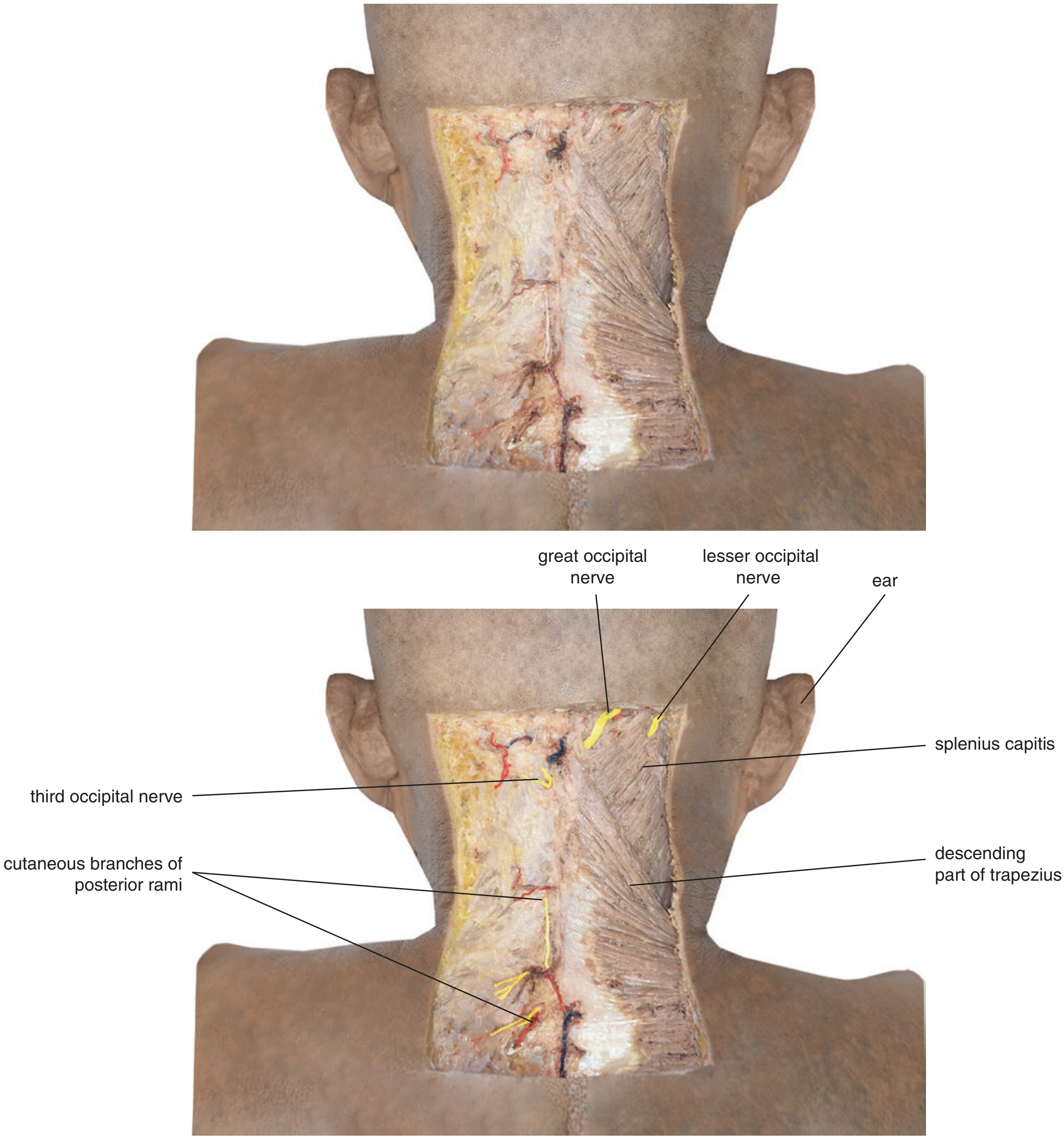

Fig. 2.35 Posterior deep cervical fascia and superficial muscles

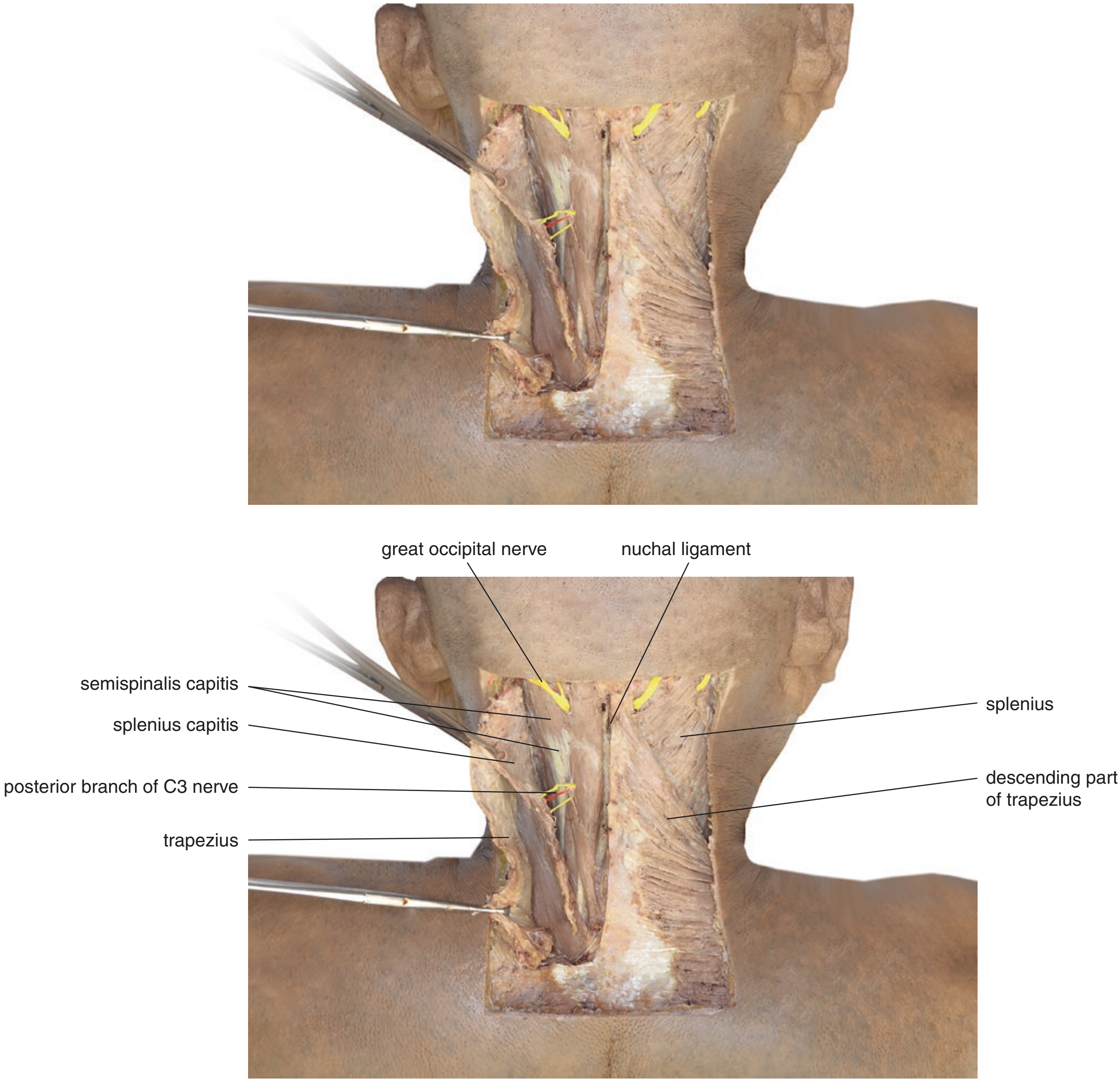

Fig. 2.36 Posterior cervical superficial and deep muscles

Fig. 2.37 Exposure of the posterior cervical spine after subperiosteal dissection of the posterior cervical muscles

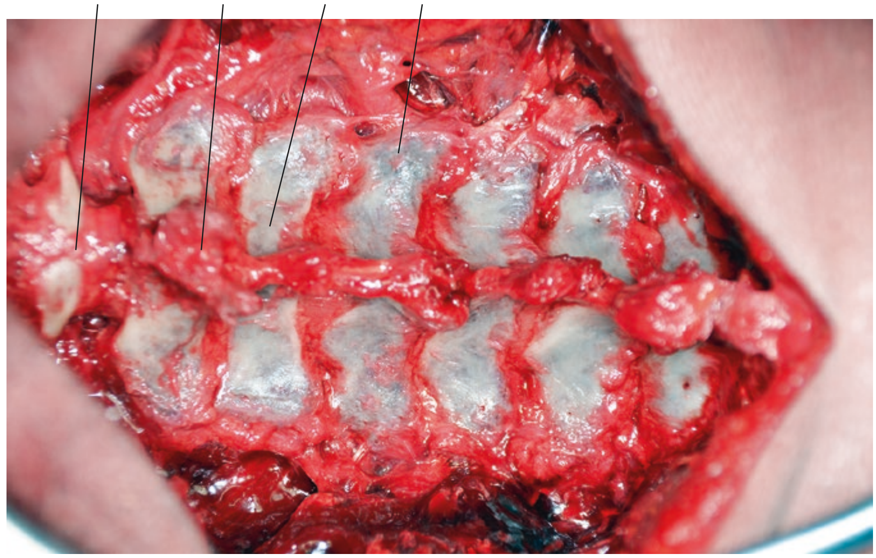

Trapezius muscle: located in the superficial layer of the posterior cervical spine. It originates from the superior nuchal line, external occipital protuberance, nuchal ligament and all of the spinous processes of the thoracic spine. The muscle fibers converge outward, stopping at 1/3 outside of the clavicle, acromion and scapular spine. The upper muscle bundle can lift the scapula and the lower muscle bundle can lower the scapula. When the scapula is fixed, muscle contraction on one side can make the neck bend to the same side and the face turn to the other side, while muscle contraction on both sides can allow the head to bend backward. The trapezius muscle is innervated by the spinal accessory nerve and the ventral rami of the third and fourth cervical nerves. The superior and the intermediate regions are mainly supplied by the superficial branch of transverse cervical artery, while the intermediate and inferior regions are supplied by the deep branch of the artery. The venous blood in the muscles mainly drains by the transverse cervical vein and the suprascapular vein (Fig. 2.35).

Nuchal ligament: a double-layer, elastic, fibrous intermuscular septum. It is continuous with the cervical supraspinous ligament and interspinous ligament, and extends from the external occipital protuberance to the C7 spinous process. The dense elastic fibrous layer on both sides of the nuchal ligament is separated by a thin lamina, and the two layers converge at the posterior free margin of the ligament. The posterior approach for cervical spine exposure often involves entry through this lamina to reduce bleeding. When nuchal ligament overload as a result of cervical instability or traumatic bleeding occurs, the ligament may calcify and ossify, which is frequently observed in the middle-lower part of the cervical spine (Fig. 2.36).

Splenius muscles: arise from the lower part of the nuchal ligament and upper part of the thoracic vertebral spinous processes, with muscle fibers that extend diagonally outward. The splenius muscles are composed of two parts: the splenius capitis muscle is in the deep part of the superior region of the sternocleidomastoid muscle which ends at the lower region of the mastoid muscle and the lateral region of the superior nuchal line; the splenius cervicis muscle is in the lateral and lower region of the splenius capitis muscle, which ends at the transverse processes of the upper three spine. Contraction of one side of the splenius muscle rotates the head to the same side, while contraction of both sides of the muscle extends the head backward. The two muscles are innervated by the lateral branches of the dorsal rami of the C2–C5 nerves (Fig. 2.36).

Longissimus capitis muscle: arises from the transverse processes of C2 to C5 and ends at the lateral border of the semispinalis capitis muscle. Its main functions are stretching the head and bending the neck to the same side. The longissimus capitis muscle is innervated by the C3 nerve, and supplied and drained by the deep cervical artery and vein, respectively (Fig. 2.36).

Semispinalis capitis muscle: arises by a series of tendons from the tips of the transverse processes of T6–T7 and C7, and from the articular processes of C4–C6. These tendons arise from the same broad muscle, which proceeds upward, and is inserted between the superior and inferior nuchal lines of the occipital bone (Fig. 2.36).

Avoid entering into the muscles during subperiosteal dissection of the posterior cervical muscles as it can easily injure the deep cervical artery and vein, and result in excessive bleeding (Fig. 2.40).

Excessive exposure to the outer margin of the lateral mass may injure the posterior rami of the cervical nerves, resulting in postoperative dysfunction of the posterior cervical muscles and skin sensation.

2.4 Laminoplasty

The ligamentum flavum between the vertebral laminas at both ends of the surgical section were removed using a Kerrison rongeur. Surgeons should beware of the depth of the rongeur inserting the spinal canal to avoid injury of the spinal cordor dural sac (Fig. 2.38).

Insert a nerve hook into the spinal canal carefully to identify the location of the medial border of the lateral mass and the hinge site and opening site for Laminoplasty (Fig. 2.39).

The opening range of the vertebral lamina should not be too wide or too narrow. A thorough decompression cannot be achieved with a narrow opening, while complete fracture of the hinge site can easily result from a wide opening, which causes difficulty on the opening and the post-opening fixation and even causes iatrogenic spinal cord compression.

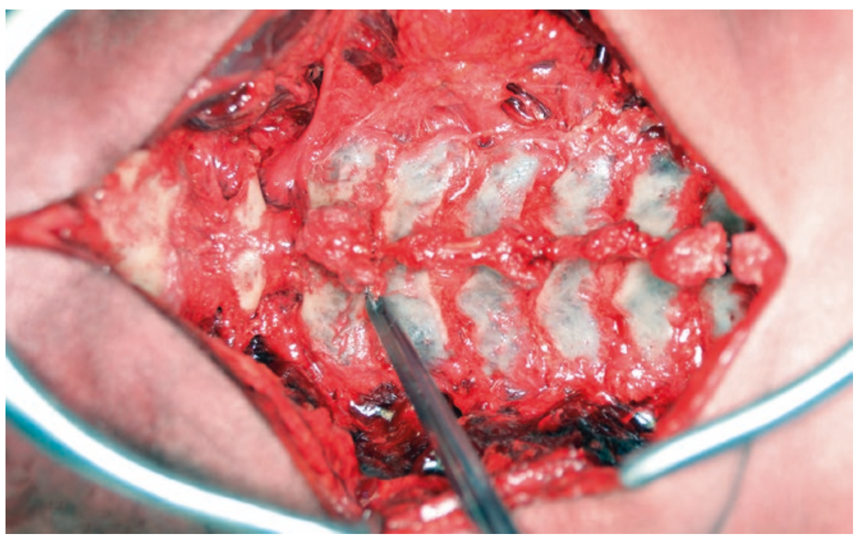

Fig. 2.38 Removal of the ligamentum flavum between the vertebral plates at both ends of the surgical section using a Kerrison rongeur

cephalad

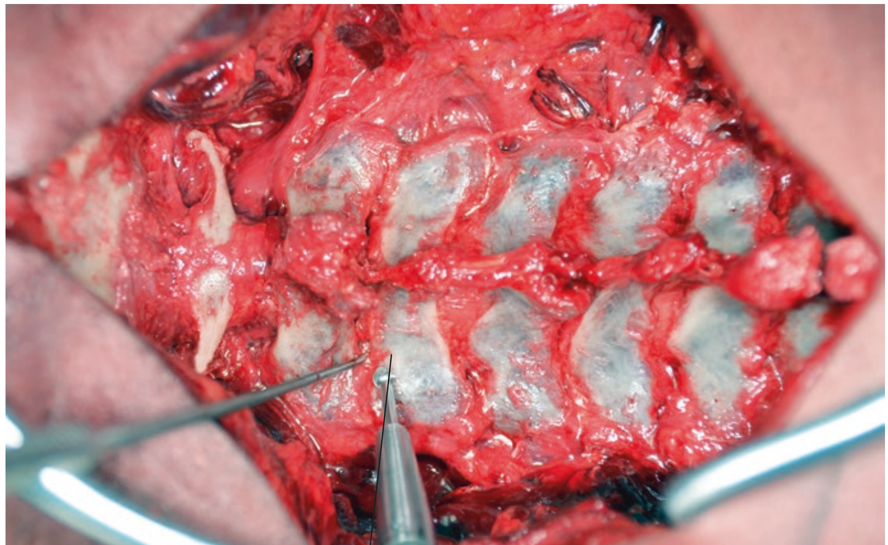

Fig. 2.39 Identify the medial border of the lateral mass by a nerve hook to locate the hinge site and opening site

Deep cervical artery: usually arises from the costocervical trunk, and ascends to the C2 level between the semispinalis capitis muscle and the semispinalis cervicis. The deep cervical artery supplies the surrounding muscles, and converges with the deep branch of the descending branch of occipital artery and the branches of vertebral artery. It also gives off a spinal twig which enters into the spinal canal between the C7 and T1 level. Therefore, surgeons should avoid injuring the deep cervical artery during the operation (Fig. 2.40).

Deep cervical vein: accompanies the deep cervical arterys. It arises from the suboccipital region and the venous plexus around the spinous processes of the cervical spine, and terminates in the inferior part of the vertebral vein (Fig. 2.40).

Semispinalis cervicis muscle: a relatively thick muscle that arises by a series tendinous fibers from the transverse processes of the upper T5–T6 spine, and proceeds upwards to the transverse processes of the C2–C5 spine. The semispinalis cervicis muscle is an important kinetic stabilizer that maintains cervical spine stability and normal sagittal alignment. The loss of cervical lordosis post-laminoplasty is associated with the functional loss of the semispinalis cervicis muscle caused by stripping the muscle from its attachment site on C2. Thus, surgeons should avoid damaging the attachment site of the semispinalis cervicis muscle on C2 spinous process (Fig. 2.40).

Dorsal rami of cervical nerve: the dorsal rami of the spinal nerve are smaller than the ventral ones, and are distributed segmentally. Besides the 1st cervical nerve, all of the branches are divided into internal and external branches, which innervate the skin and muscle of the neck (Fig. 2.40).

Ligamentum flavum: connects to adjacent vertebral laminas in the spinal canal. Its attachment sites arise from the facet joint capsule to the spinous processes of the vertebral laminas. The ligamentum flavum starts from both sides of the spine and converges at the midline. The communicating branches of the internal vertebral venous plexus and intervertebral lamina venous plexus perforate the midline of the ligamentum flavum. The ligamentum flavum appears as a yellow elastic fibrous tissue in a living body. Its fibers are arranged in an almost vertical fashion, which run from the lower anterior margin of the vertebral lamina downward to the upper posterior margin of the superior vertebral lamina. The front of ligament is covered by a continuous, thin and smooth layer of demarcation membrane. The ligamentum flavum is thinner, wider and longer in the cervical region (Fig. 2.41).

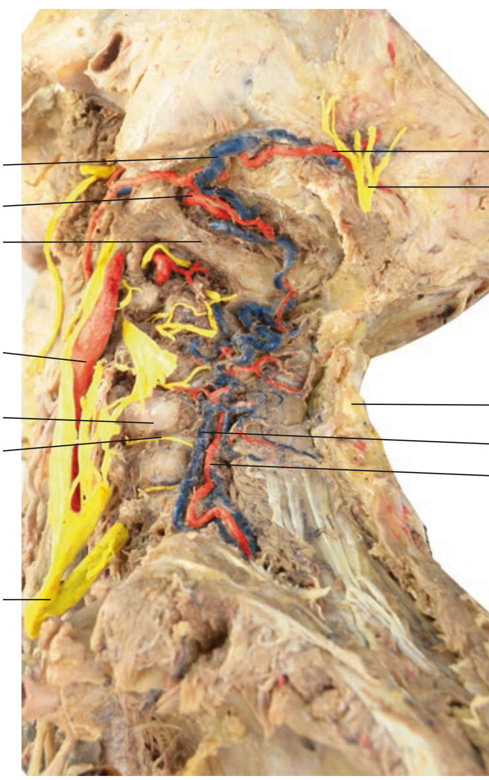

Fig. 2.40 Deep artery and vein of the posterior neck

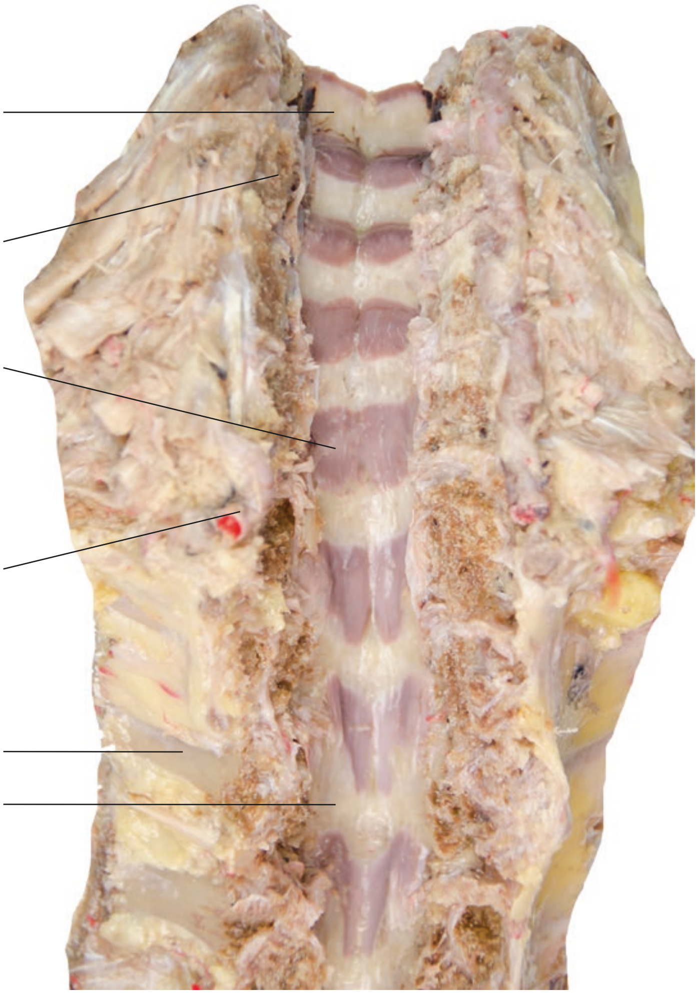

Fig. 2.41 Ligamentum flavum cervcal and cervicothoracic (formalin fixed and paraffin embedded ligamentum flavum appear as purple)

The external vertebral lamina and cancellous bone are removed with a high-speed cutting burr from the boundary of the lateral mass. Subsequently, a smaller burr is used to thinning the inner bony cortex on the hinge side (Fig. 2.42).

If the inner bony cortex on the hinge side are accidentally fractured, the opposite side of the plate can be used as the hinge site.

The opening and hinge sites are located between the vertebral lamina and the facet joint capsule. This opening width is wider than the spinal cord and can achieve full decompression, at the same time prevents damage to the neural structure (Figs. 2.43, 2.44, 2.45, 2.46, and 2.47).

After the same procedures are conducted at the opposite side, the thickness of the inner cortical bone and the medial border of the lateral mass are identified with a nerve hook (Fig. 2.48).

The inner bony cortex and ligamentum flavum along the opening site are removed with a Kerrison rongeur (Fig. 2.49).

Bipolar electrocautery or gelatin sponge can be used to achieve hemostasis, when epidural bleeding is encountered.

Push the spinous process of the surgical section to the hinge side, and open the door carefully with the help of a periosteal detacher.

Fix one end of the Arch titanium plate to the lateral mass, and the other end at the root of the spinous process with 2.0 mm-diameter self-tapping screws of proper length. Screws are inserted vertically into the vertebral lamina and the lateral mass. Avoid penetrating the contralateral cortical bone to prevent damages to the spinal cord, nerve root and vertebral artery (Figs. 2.50, 2.51 and 2.52).

Bone grafting is not needed if the door hinge closes naturally. If there is a large gap in the hinge site, small pieces of bone can be grafted into the gap. Avoid bone grafting between the vertebral laminas to prevent the fusion of the cervical spine.

The direction and position of the Arch titanium plate and screws are confirmed by intraoperative fluoroscopy

Fig. 2.42 Removal of the external vertebral plate with a high-speed cutting burr

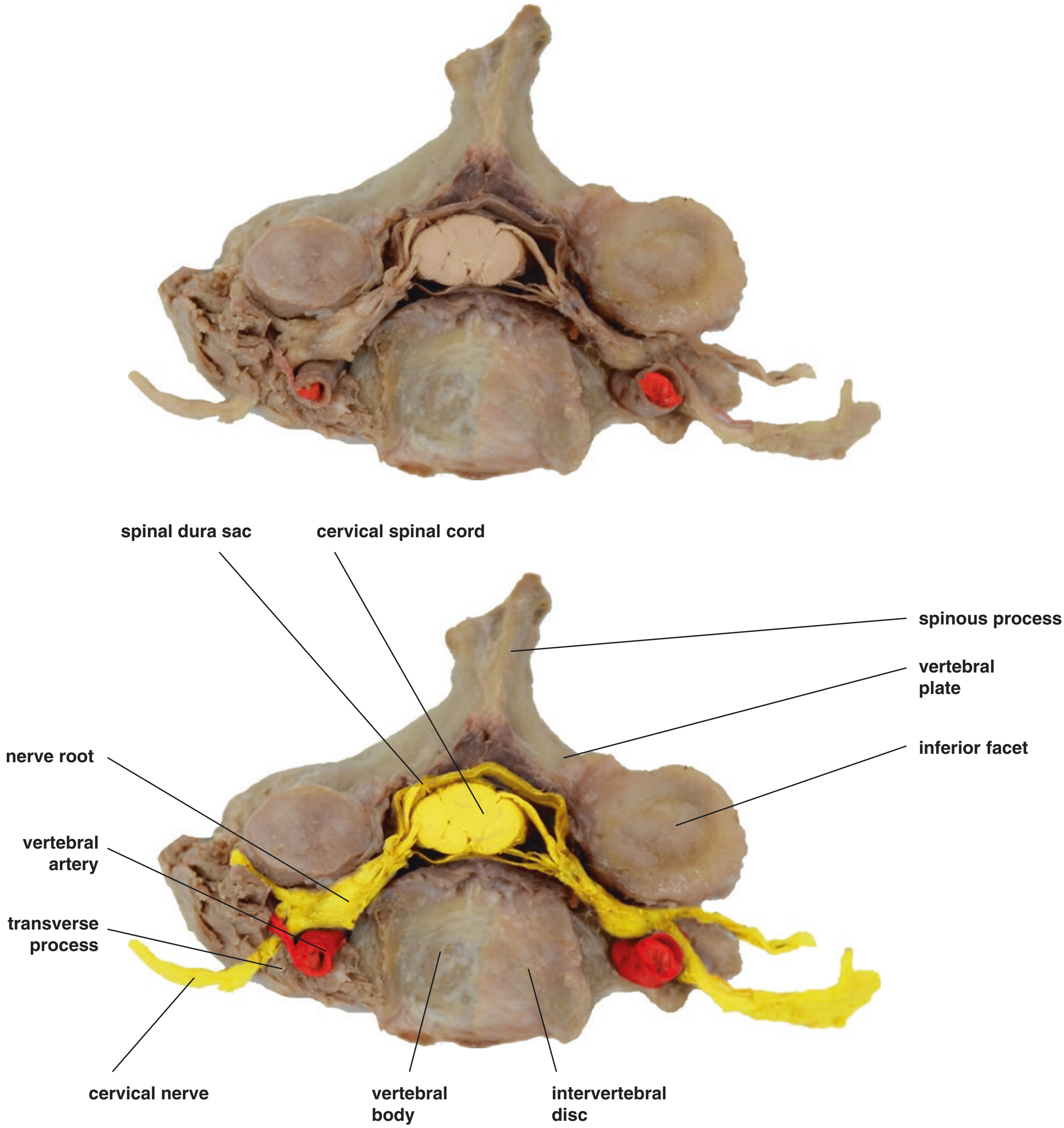

Fig. 2.43 Top view of the third cervical spine

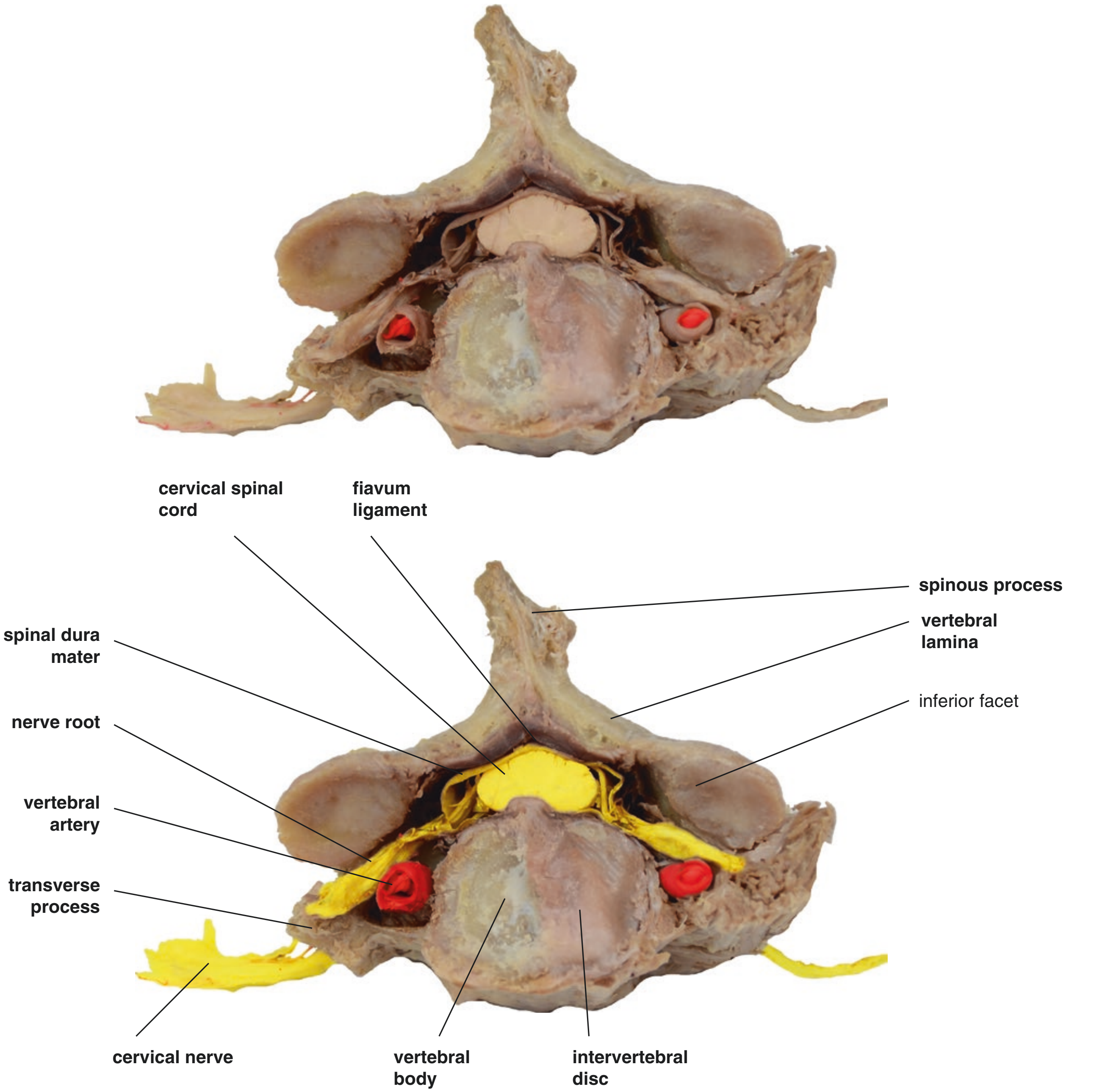

Fig. 2.44 Bottom view of the third cervical spine

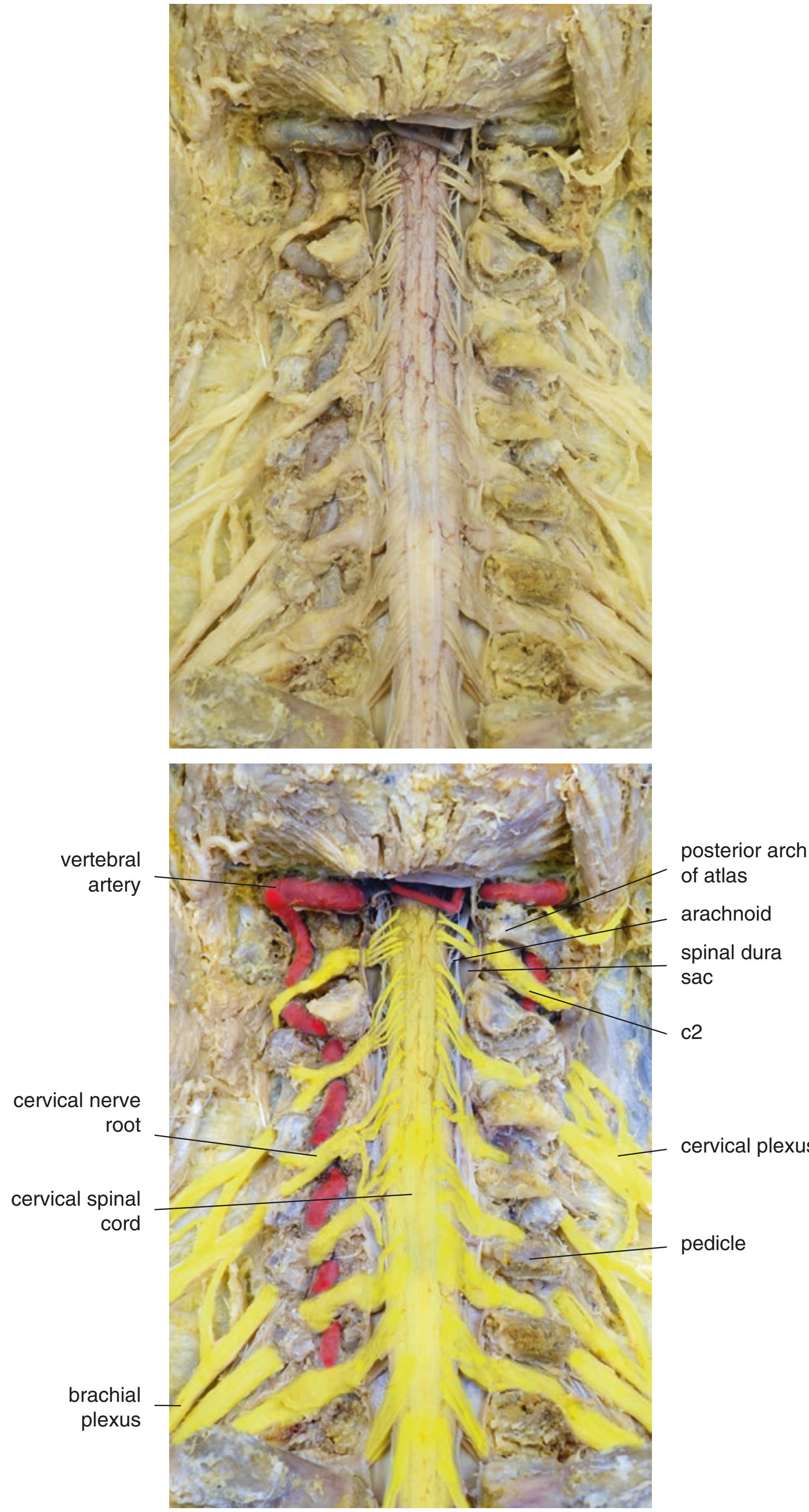

Fig. 2.45 Posterior lateral view of the cervical spine (posterior bony structures and dural sac removed)

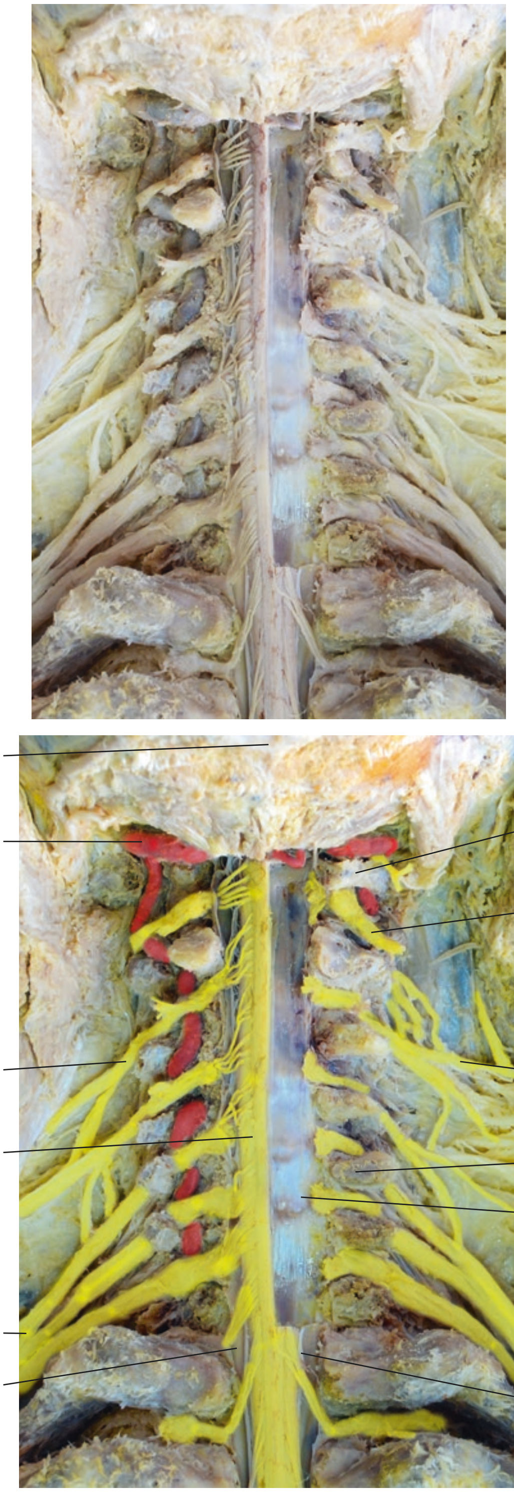

Fig. 2.46 Posterior lateral view of the cervical spine (right side of the spinal cord partially resected)

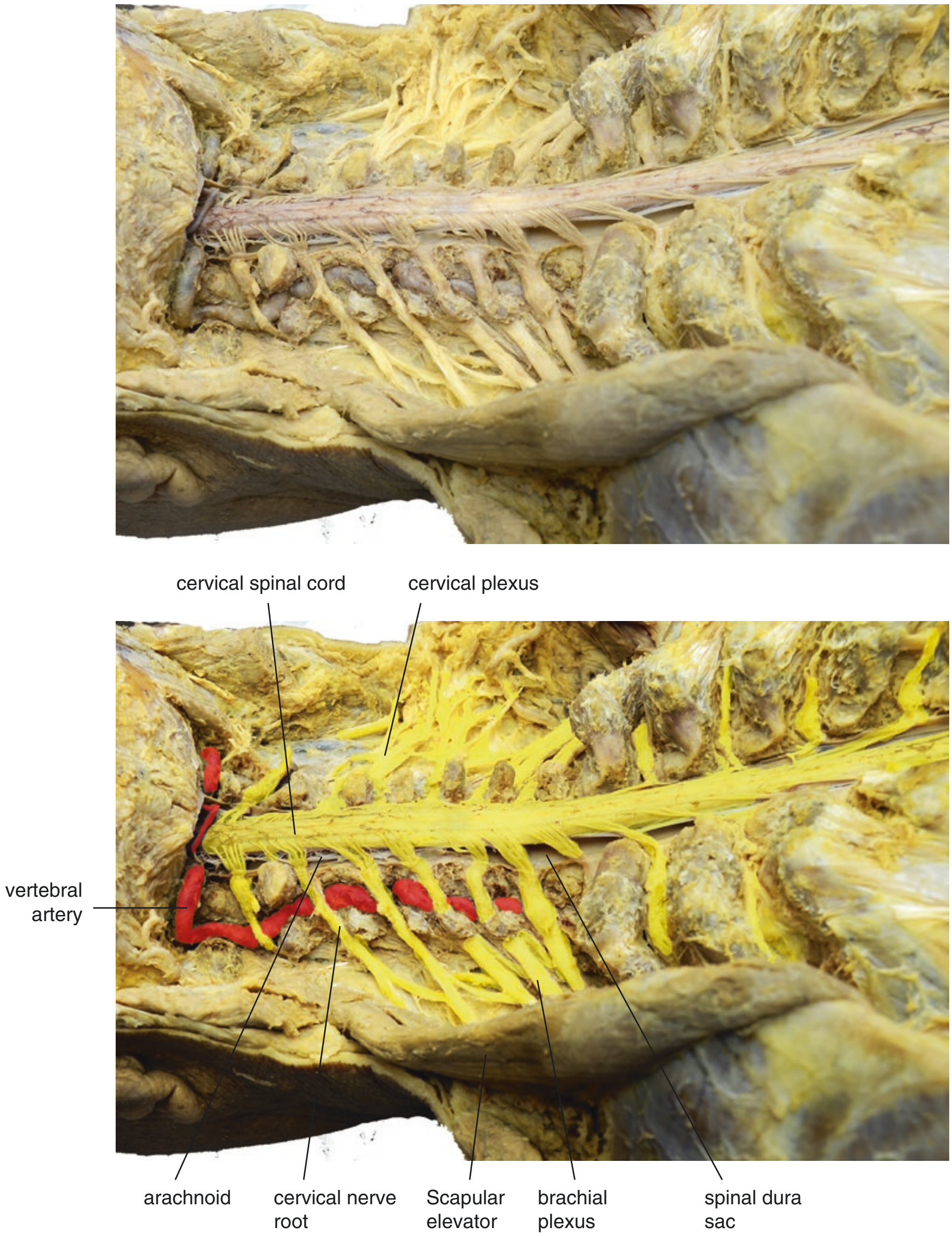

Fig. 2.47 Posterior lateral view of the cervical spine (posterior bony structures and dural sac removed)

Fig. 2.48 Identification of the thickness of the inner cortical bone and the medial border of the lateral mass with a nerve hook

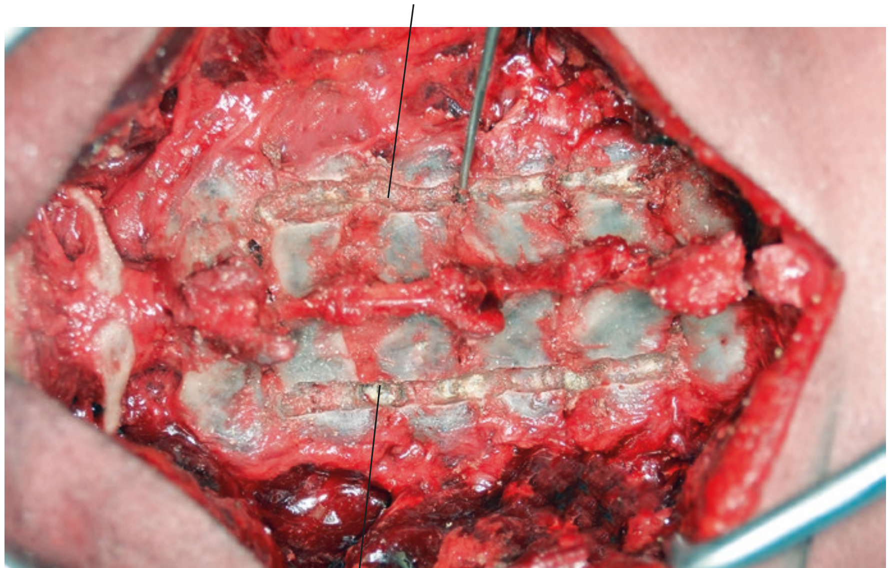

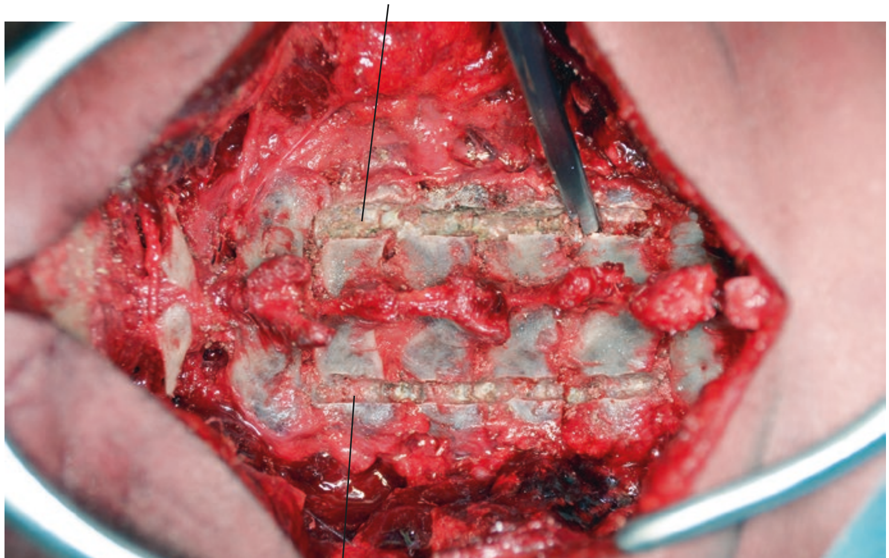

Fig. 2.49 Removal of the inner bony cortex and ligamentum flavum along the opening site

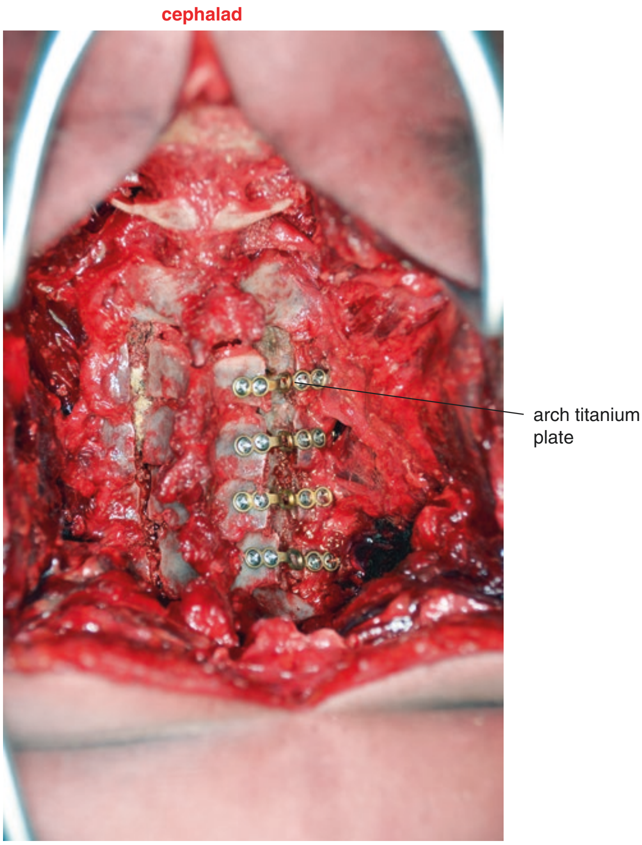

Fig. 2.50 Placement of the Arch titanium plate after opening the vertebral lamina to a suitable angle

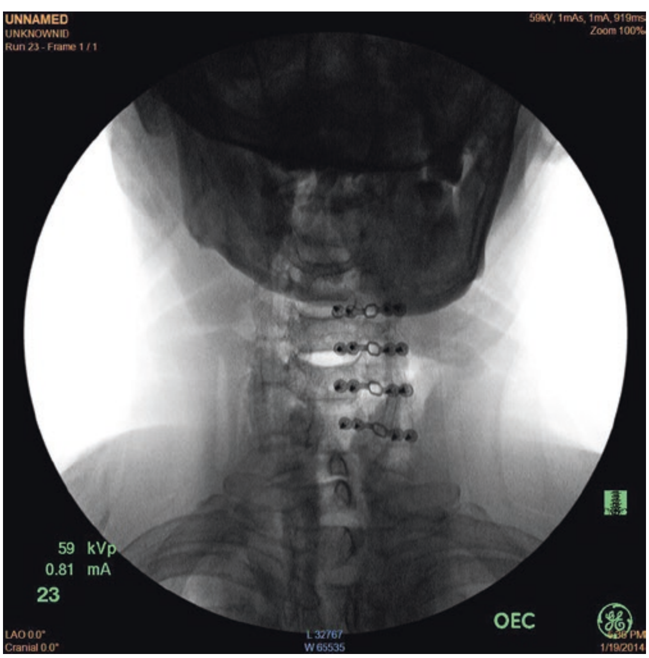

Fig. 2.51 Position of the Arch titanium plate and screw by intraoperative anteroposterior fluoroscopy

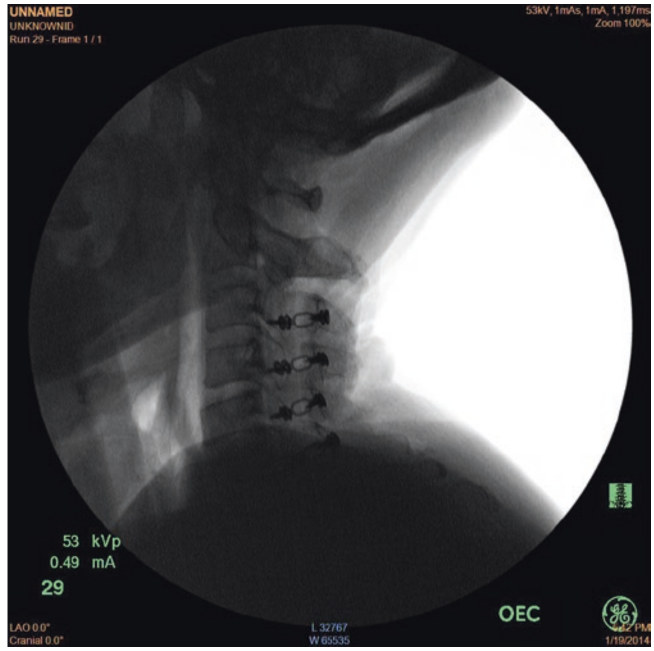

Fig. 2.52 Position of the Arch titanium plate and screw by intraoperative lateral fluoroscopy

3 Exposure of the Lateral Vertebral Artery and Intervertebral Foramen of the Subaxial Cervical Spine

3.1 Overview

Surgical approach for the exposure of vertebral artery and intervertebral foramen of the subaxial cervical spine is a technique that was first reported by Hodgson in 1965 for treating lesions that occur on the spinal transverse process or cervical nerves. This approach is performed in the lateral avascular area of the carotid sheath and the sternocleidomastoid muscle. The intervertebral foramen, vertebral artery, and anterior and posterior tubercles of the transverse process can be fully exposed by the lateral cervical approach. The advantage of this approach is that it avoids exposure of the trachea and esophagus, and allows easy anesthetic management.

3.2 Position

The supine position is generally preferred. The lateral position is only used when the exposure of the posterior facet joint is also required (Fig. 2.53).

Surgical exposure or intraoperative fluoroscopy may be obstructed by the shoulder. In this case, the shoulder can be retracted caudally with a pair of wide bandages to facilitate intraoperative fluoroscopy.

Fig. 2.53 Position and incision of the exposure of lateral vertebral artery and nerve root in the subaxial cervical spine

3.3 Exposure

Based on the segment of exposure, the skin is incised along the posterior margin of the sternocleidomastoid muscle (Fig. 2.53). If the exposure area needs to be extended, additional transverse incisions can be made above and below to form a incision of zigzag fasion.

The skin, subcutaneous soft tissues and platysma are incised along the posterior margin of the sternocleidomastoid muscle (Figs. 2.54 and 2.55).

Expose the posterior margin of the sternocleidomastoid muscle. The deep fascia is dissected to expose the cervical plexus, transverse cervical nerve and great auricular nerve in the center of the muscle's posterior margin.

The spinal accessory nerve can be found at about 2–3 cm above the cervical plexus at the posterior margin of the sternocleidomastoid muscle. Caution should be taken to protect the accessory nerve during operation.

Great auricular nerve: largest ascending branch of the cervical plexus. It arises from the ventral rami of the second and third cervical nerves, winds around the posterior border of the sternocleidomastoid muscle, after perforating the deep cervical fascia, ascends beneath the platysma to the parotid gland, where it divides into an anterior and a posterior branch. The anterior branch is distributed to the skin of the face over the parotid gland, while the posterior branch innervates the skin over the mastoid process and on the back of the auricula (Fig. 2.56)

Supraclavicular nerves: their main trunk arises from the ventral rami of the third and fourth cervical nerves. They emerge beneath the posterior border of the sternocleidomastoid muscle, and spread over the pectoralis major above the second rib, the skin covers the deltoid muscle, and the upper posterior skin of the shoulders (Fig. 2.56).

External jugular vein: receives the greater part of the blood from the scalp and face, and descends diagonally from the angle of mandible to the middle of the clavicle. It perforates the deep fascia from the lateral

Fig. 2.54 Incision of the skin and platysma

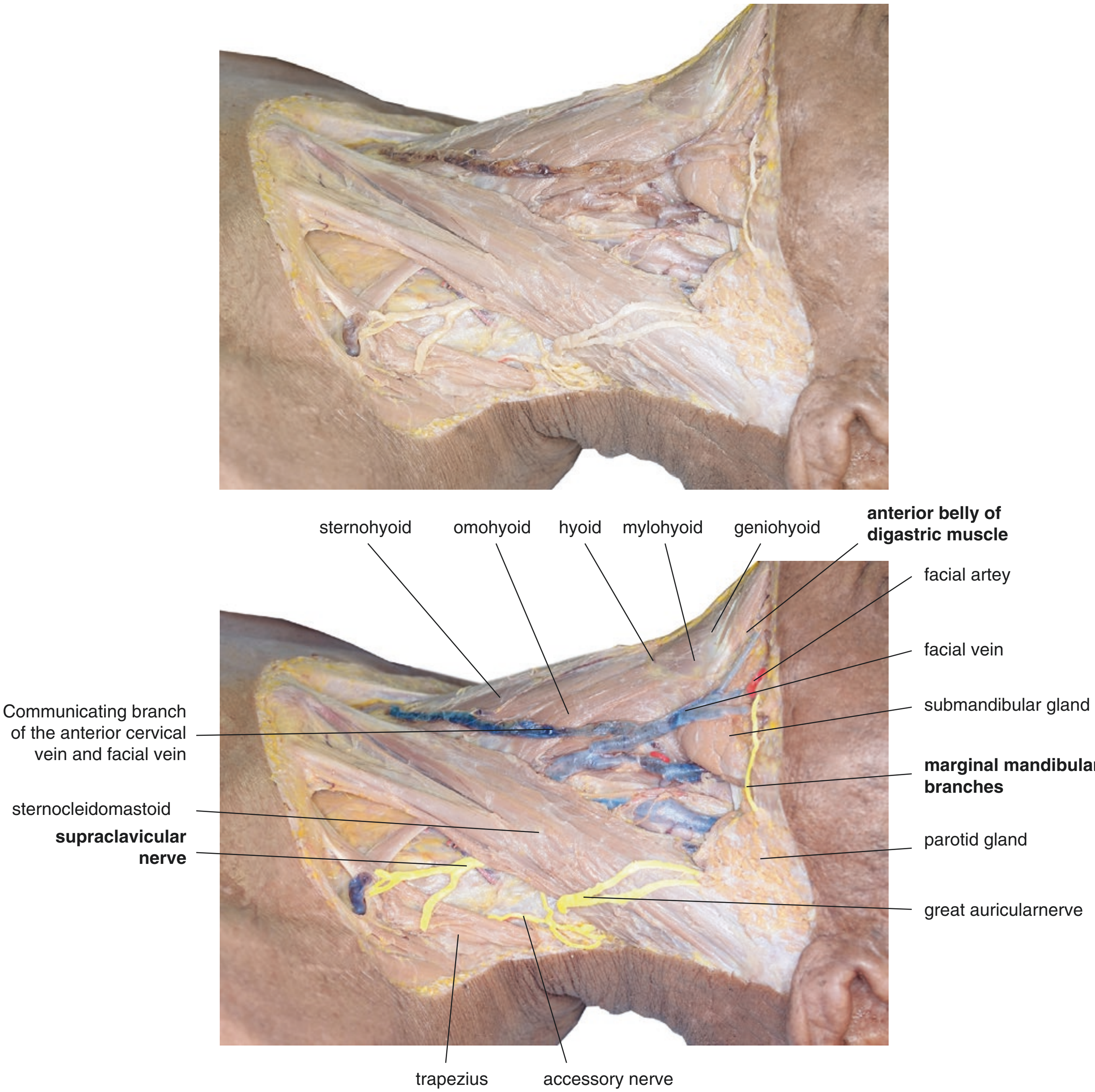

Fig. 2.55 Left view of the structures within the deep cervical fascia

side or the front of anterior scalene muscle and ends in the subclavion vein. The external jugular vein crosses the transverse cervical nerve and runs parallel with the great auricular nerve (Fig. 2.56).

The posterior margin of the sternocleidomastoid muscle is retracted medially for the separation of the loose connective tissue underneath (Fig. 2.57).

The position of the carotid sheath is identified by palpation.

The sternocleidomastoid muscle and the carotid sheath are retracted anteromedially, to expose the anterior scalene muscle and longuscolli muscle. The anterior scalene muscle begins from the anterior and posterior tubercles of the transverse process. When dissecting the anterior scalene muscle, the surgeon should make sure to protect the phrenic nerve and the accessory phrenic nerve that run downward in front of the muscle.

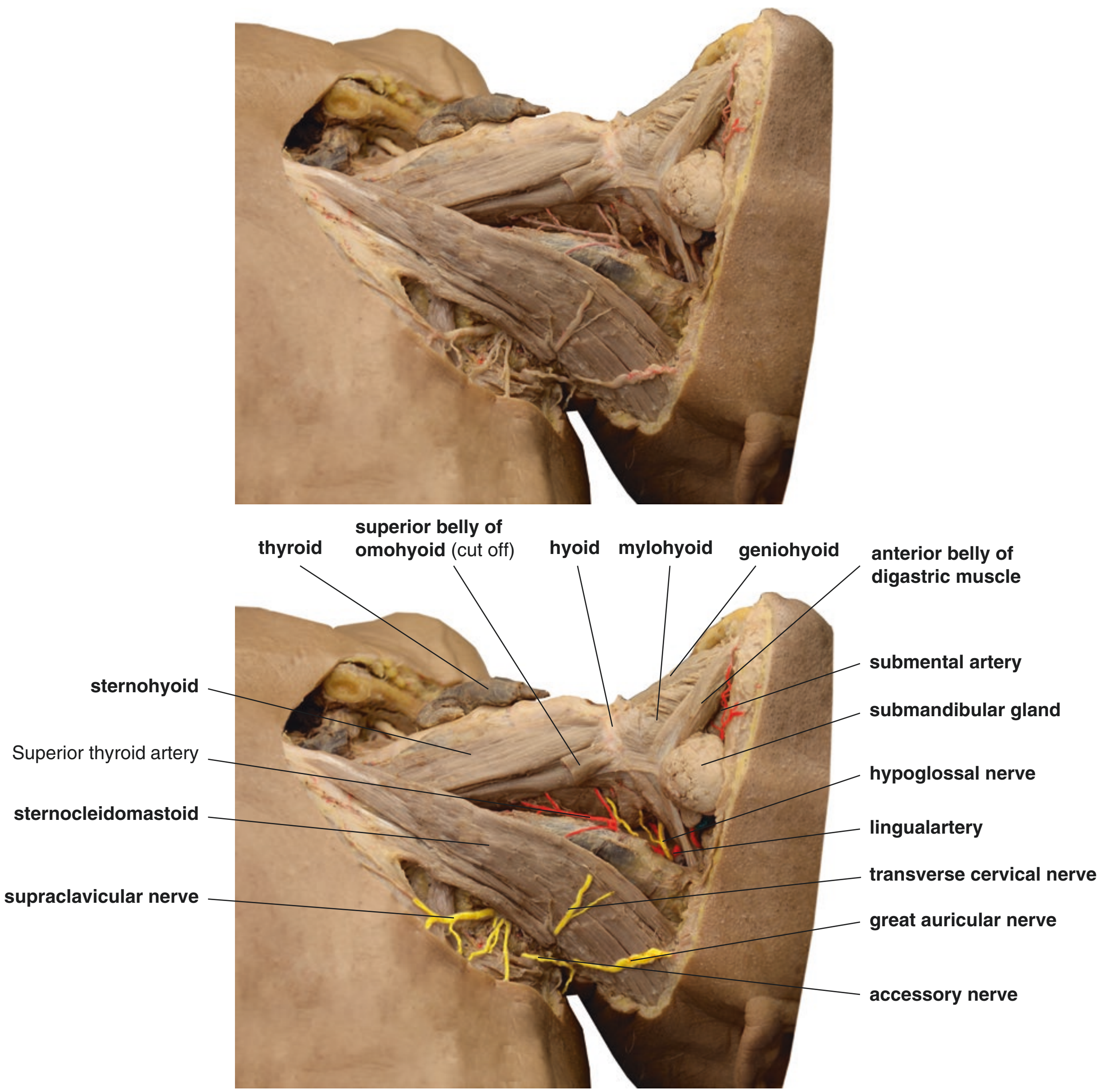

Fig. 2.56 Left view of the structures within the deep cervical fascia (omohyoid muscle resected)

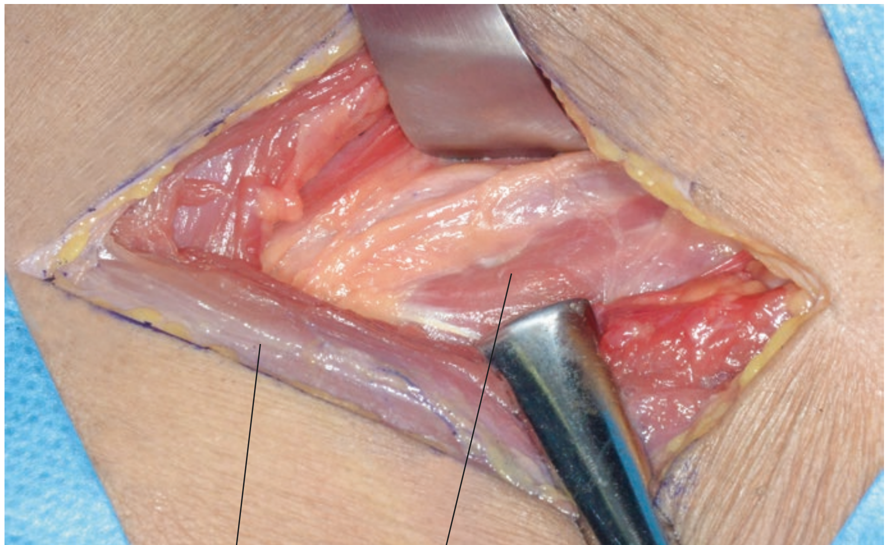

Fig. 2.57 Exposure of the phrenic nerve by retracted the sternocleidomastoid muscle medially

Phrenic nerve: originates mainly from the ventral ramus of the fourth cervical nerve and includes the fibers of the third and fifth cervical nerves. The phrenic nerve is formed at the outer border of the anterior scalene muscle, and crosses the muscle beneath the prevertebral fascia. It descends vertically before the anterior scalene muscle, and enters the thoracic cavity after crossing the internal thoracic artery (Figs. 2.58 and 2.59).

Accessory nerve: perforates above the center of the posterior border of the sternocleidomastoid muscle, about 2 cm above the emergence of the great auricular nerve and 4–6 cm away from the mastoid tip. It runs to the anterior border of the trapezius muscle at 3–5 cm above the clavicle, and enters into the trapezius muscle. In the neck, the accessory nerve runs along a single path, which begins from the lower front of the tragus to the tip of the transverse process of atlas, then crosses the sternocleidomastoid muscle and posterior triangle of the neck, to the 3–5 cm above the clavicle at the anterior border of the trapezius muscle (Figs. 2.58 and 2.59).

Cervical plexus: composed of the ventral rami of the upper four cervical nerves, and innervates the cervical muscles, diaphragm and skin of the head, neck and chest. Besides the ventral ramus of the 1st cervical nerve, the ventral rami of the other three cervical nerves are divided into the ascending and descending branches which intertwine and form into loops. Some of these branches include deep branches that innervate the muscles, and superficial branches that innervate the skin. The superficial branches are divided into the ascending branch (lesser occipital nerve, great auricular nerve and transverse cervical nerve) and descending branch (supraclavicular nerve) (Figs. 2.58 and 2.59).

Brachial plexus: a network of nerves formed by the ventral rami of the lower four cervical nerves and first thoracic nerve, which innervate the muscles, joints and skin of the upper limbs. It originates from the posterior triangle of the neck, which is the region formed between the clavicle and the lower posterior border of the sternocleidomastoid muscle, and perforates between the anterior and middle scalene muscles (Figs. 2.58 and 2.59).

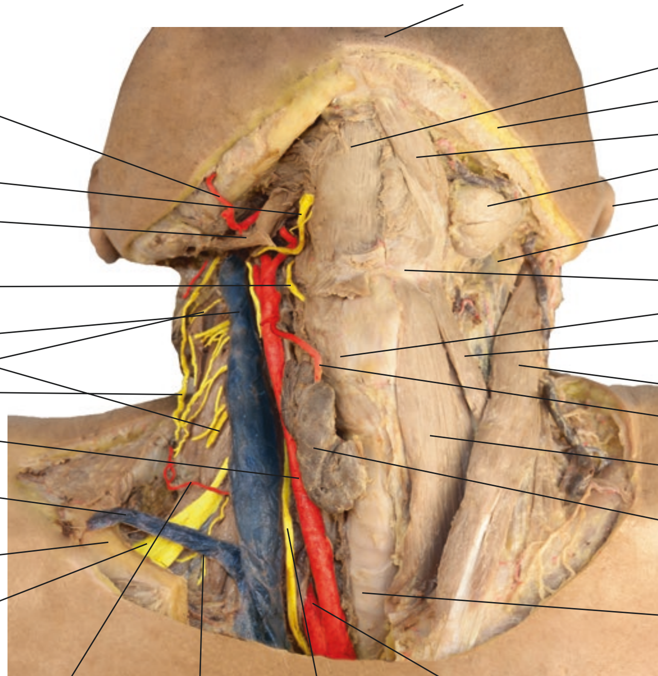

Fig. 2.58 Structures beneath the right sternocleidomastoid muscle (carotid sheath opened)

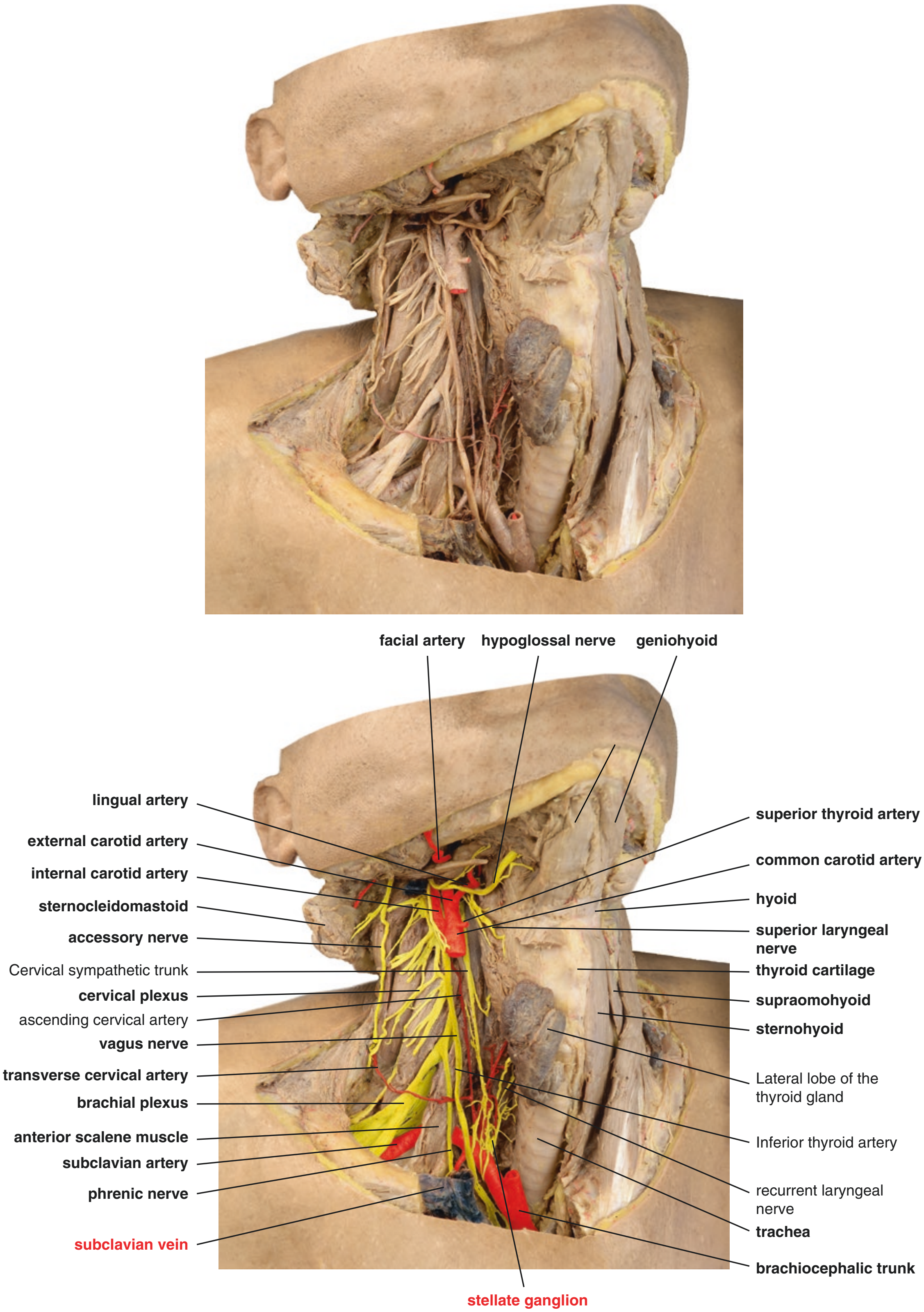

Fig. 2.59 Structures beneath the right sternocleidomastoid muscle (common carotid artery andinternal jugular vein resected)

Palpate the anterior tubercle of the cervical transverse process and vertebral body. The longuscolli muscle and sympathetic trunk are retracted medially to expose the anterior tubercle.

Dissect the attachment points of the anterior and middle scalene muscles to expose the anterior tubercle of the transverse process (Fig. 2.60).

The nerve roots run in the intertubercular grooves of the transverse process, and the vertebral artery is to the anterior to the nerve roots.

Separate the soft tissue carefully between the anterior tubercle of the transverse process and the luschka joint. Hemostasis is achieved by bipolar cautery when bleeding from the vertebral vein is encountered, the vertebral artery is then exposed.

The vertebral artery enters the transverse foramina from the transverse process of the sixth cervical spine, but can sometimes enter from the fourth, fifth or seventh cervical spine. Therefore, the path of the vertebral artery should be confirmed by preoperative imaging (Fig. 2.60).

The cupula of pleura is adjacent to the superior border of the C8 nerve root. During the operation, the C8 nerve root can be used as a landmark to avoid injuring the cupula.

Since the thoracic duct drains into the venous angle on the left side, the thoracic duct can be identified by firstly locating the venous angle. This method can prevent injury to the thoracic duct. However, if the duct is injured, it should be ligated immediately.

Vertebral artery: originates from the subclavian artery, and merges through all of the transverse foraminas except the seventh vertebra. It bends medially around the atlanto-occipital joint at the upper posterior border of the atlantal lateral mass and finally enters the cranial cavity through the foramen magnum. The vertebral artery is crossed by the thoracic duct on the left, and the right lymphatic duct on the right. The inferior cervical ganglion and the ventral rami of the seventh and eighth cervical nerves are in the posterior region of the initial segment of the vertebral artery. The second section of the vertebral artery runs upward through the foramina in the transverse processes of the upper six cervical spine, proceeds in front of the anterior branch of the cervical nerves, ascends in an almost vertical course up to the transverse foramen of the and finally bends laterally into the atlantal transverse foramina. The third section of the vertebral artery curves posteriorly to the medial and posterior region of the atlantal

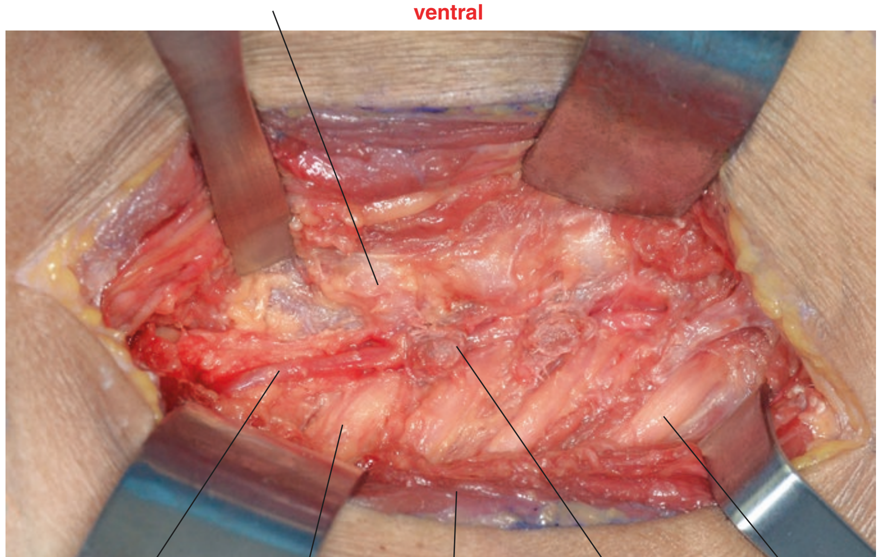

Fig. 2.60 Exposure of the vertebral artery and cervical plexus after excision of the anterior scalene muscle attachment points on the anterior tubercle of transverse process

lateral mass, just lateral to the anterior branch of the first cervical nerve. It then passes into the vertebral artery groove on the upper surface of the posterior arch of the atlas, and enters the spinal canal by passing beneath the inferior border of the posterior atlantooccipital membrane (Fig. 2.61).

Vertebral vein: originates from the internal vertebral venuous plexus, and unites with small veins from the deep muscles of the suboccipital triangle after exiting the spinal canal up through the posterior arch of the atlas. It then enters the foramen in the transverse process of the atlas, bends around the vertebral artery forming a plexus, and descends through consecutive foramen, finally emerging from the foramina of the transverse process of the 6th cervical spine as the vertebral vein. The vertebral vein first begins at the anterior of the vertebral artery, then descends anterolaterally along the vertebral artery, and finally converges with the upper posterior region of the brachiocephalic vein (Fig. 2.62).

Ascending cervical artery: arises from the inferior thyroid artery and ascends anterior to the transverse process between the anterior scalene muscle and the longus capitis muscle. The artery suppliesthe adjacent muscles, and sends one or two spinal branches into the spinal canal through the intervertebral foramina to supply the spinal cord, dural sac and the vertebral body (Fig. 2.62).

Anterior scalene muscle: lies deeply at the side of the neck, within the posteromedial region of the sternocleidomastoid muscle. It is innervated by the branches of the ventral rami of the fourth to sixth cervical nerves. When the upper extremity of the muscle is fixed, anterior scalene muscle contraction can make the cervical spine bend forward and to the side, and the neck rotate to the opposite side. When the superior extremity of the muscle is fixed, muscle contraction can help lift the first rib. The anterior scalene muscle is an important landmark at the root of the neck. The phrenic nerve run across the front of the anterior scalene muscle, and the subclavian artery and brachial plexus are located inferior and lateral to the muscle, respectively (Fig. 2.62).

Middle scalene muscle: the longest and the largest of the three scalene muscles and is innervated by the branches of the ventral rami of the third to eighth cervical nerves. When the inferior extremity of the muscle is fixed, middle scalene contraction can make the cervical spine bend to the same side. When the superior extremity is fixed, its contraction can help lift the first rib (Fig. 2.62).

Ansa cervicalis: The superior root of the ansa cervicalis originates from the hypoglossal nerve, which descends within or superficially to the carotid sheath. The inferior root of the ansa cervicalis, formed by the branches of the ventral rami of the second and third cervical nerves, descends laterally to the internal jugular vein, and forms the ansa cervicalis after converging with the superior root just anterior to the common carotid artery. The two roots develop into the ansa cervicalis, which is also known the ansa nervi hypoglossi. The branches sent out by the ansa cervicalis innervate the sternohyoid muscle, sternothyroid muscle and the inferior belly of the omohyoid muscle. Some branches descend into the thoracic cavity and converge with the cardiac and phrenic nerve (Fig. 2.63).

Stellate ganglion: stellate ganglion is located at the level of C7, anterior to the transverse process of C7 and the neck of the first rib, superior to the cervical pleura and just below the subclavian artery. The stellate ganglion is a sympathetic ganglion formed by the fusion of the inferior cervical ganglion and the first thoracic ganglion. Symptoms associated with injury of stellate ganglion include Horner's syndrome, difficulty swallowing, and vocal cord paralysis.

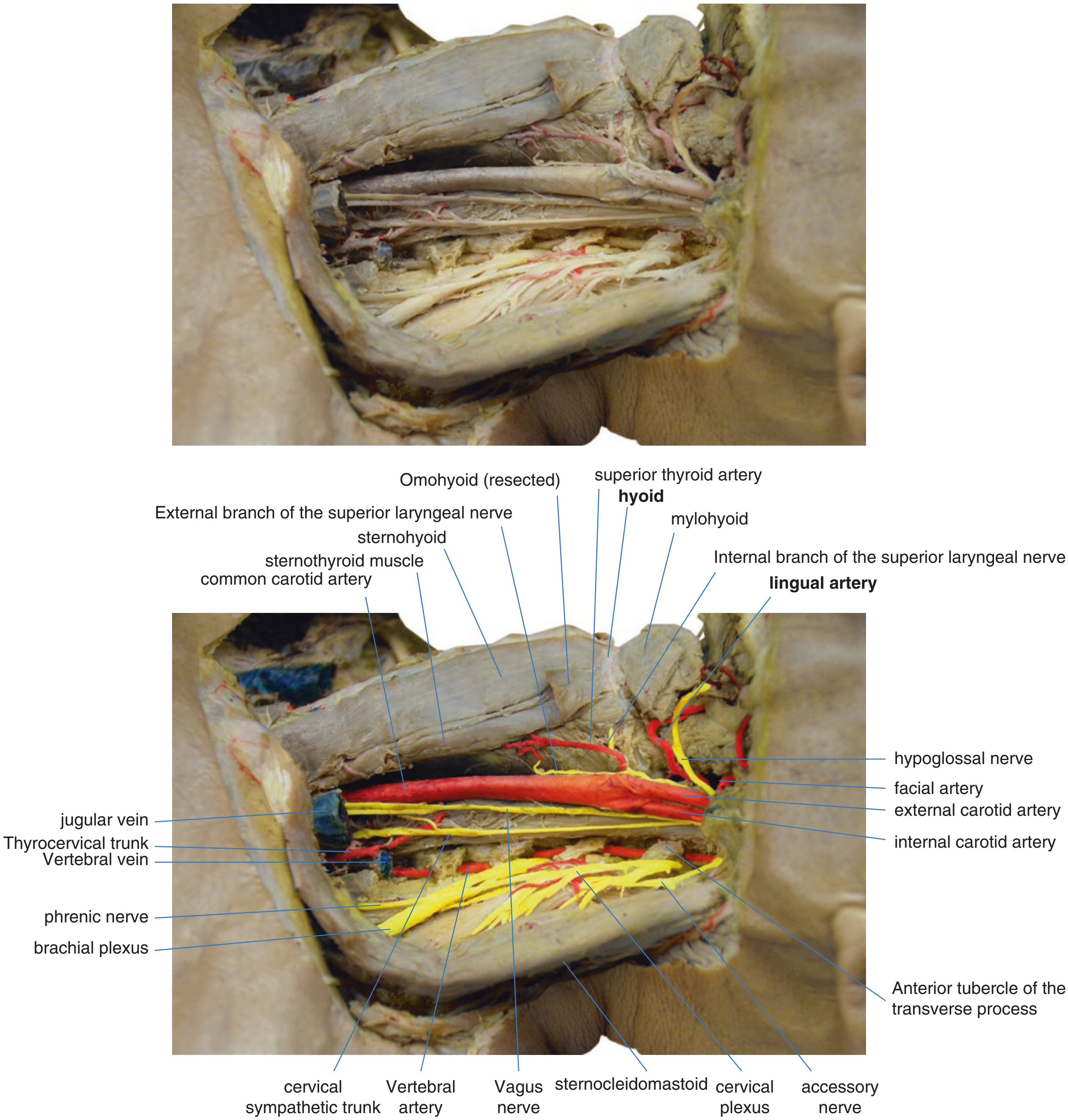

Fig. 2.61 Anatomy of the vertebral artery on the left side

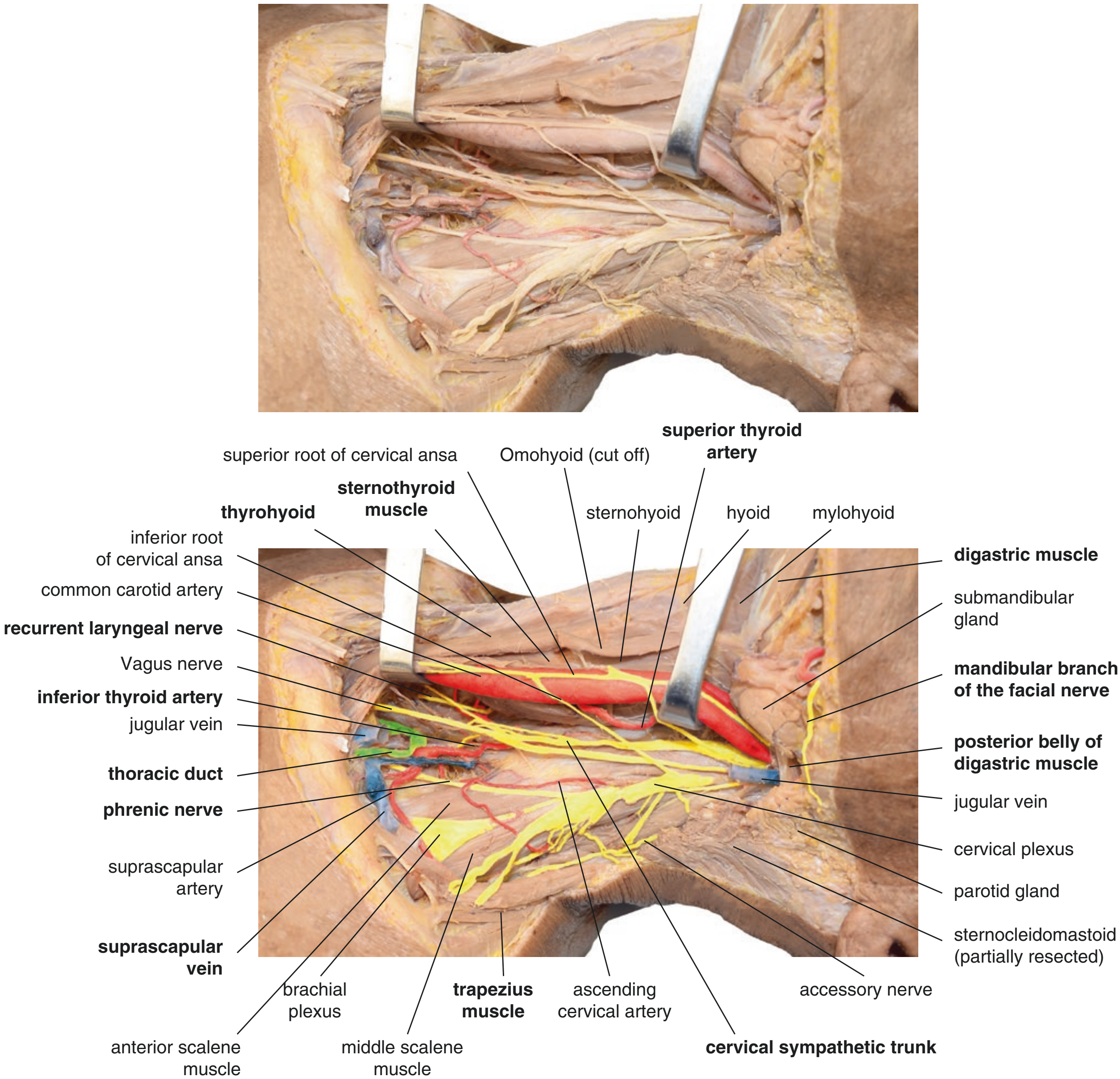

Fig. 2.62 Deep structures around the common carotid artery on the left side

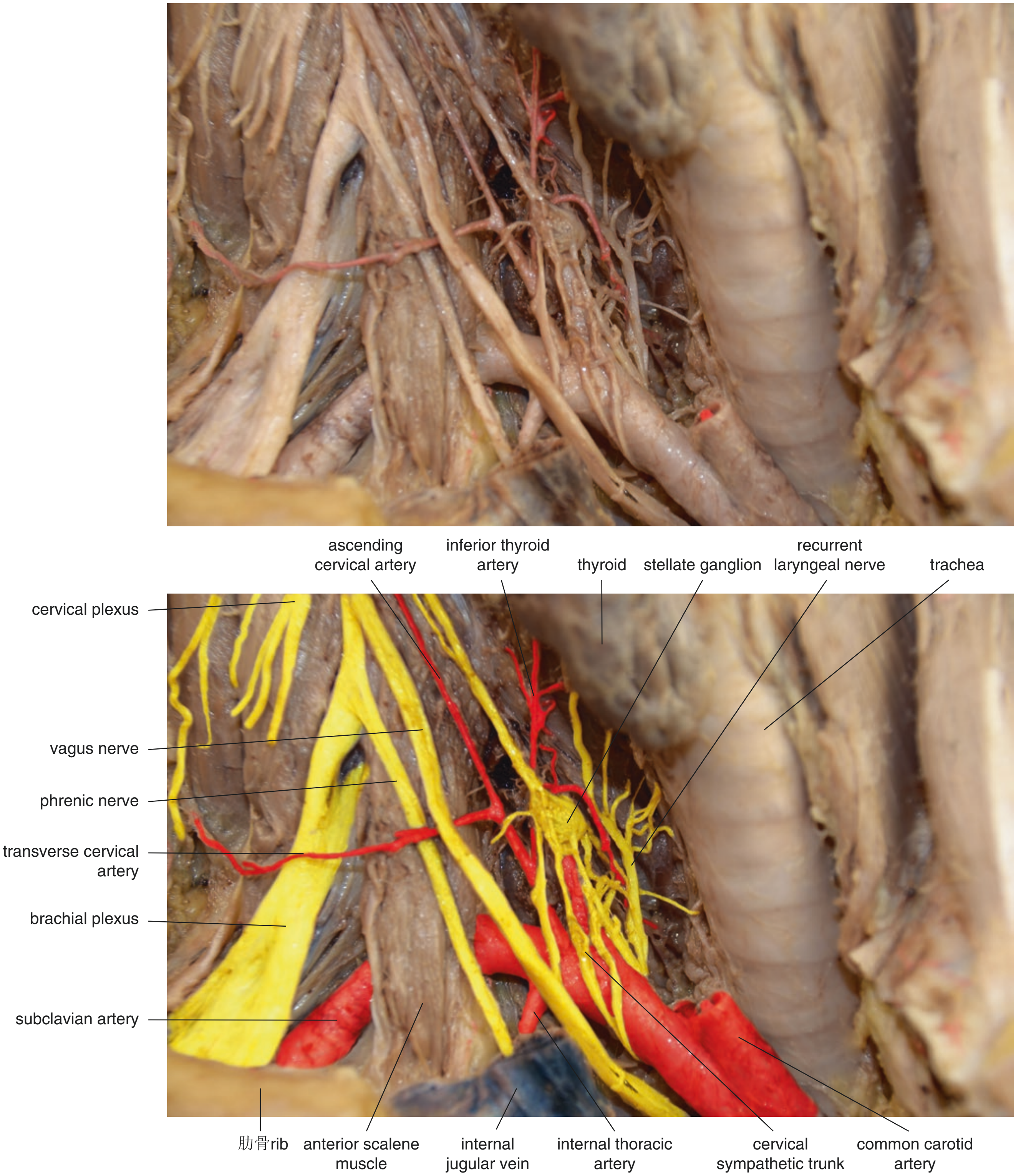

Fig. 2.63 Stellate ganglion

4 Anterior Transsternal Approach, Cervicothoracic Junction Spinal Corpectomy and Fusion

4.1 Overview

Cauchoix et al. were the first orthopedic surgeon to apply the sternotomy approach to treat thoracic tuberculosis. However, the approach was accompanied by frequent postoperative complications with high mortality. In the 80s, Sundaresan et al. and Yasui et al. have made improvements to the approach respectively. The former expanded the field of exposure by incising the manubrium sterni and one third of the left clavicle. Although this approach results in greater trauma, it is suitable for tumor resection of the vertebral body. On the other hand, Yasui developed a combined cervicothoracic approach to expose the cervicothoracic spine to treat the ossification of the posterior longitudinal ligament. This approach only requires the incision of the manubrium sterni, and can still expose the C5–T4 spine with less trauma.

This section will introduce the "U" resection of the manubrium sterni for exposing the T3–T4 thoracic spine and the intervertebral space. Indications of this approach include cases with anterior spinal decompression, vertebral column instability, kyphotic deformity, vertebral or vertebral disc infections combined with abscesses or spinal compression, tumor with or without spinal compression, and vertebral fracture with or without paraplegia in the C5–T4 level.

In the 1960s, Bailey-Badaley proposed a corpectomy and bone graft fusion technique to treat cervical fracture. In 1976, Sakau et al. applied this technique to treat cervical spondylotic myelopathy, ossification of the posterior longitudinal ligament, and stenosis noted at the vertebral body levels. As for cervical myelopathy that involves multiple vertebral bodies and intervertebral spaces, this technique can achieve a more complete decompression compared with anterior cervical discectomy and fusion, and posterior cervical laminectomy. Vertebral stability is reconstructed using mesh and plate after corpectomy, which can reduce the loss of height and complications such as the development of pseudoarthrosis due to bone grafting alone.

4.2 Position

Patient is placed in a supine position, and both scapulae are padded with folded towels.

Soft pads are placed around the neck to stabilize the head, and to slightly extend the neck backward (Fig. 2.64).

Fig. 2.64 Position and incision of cervicothoracic spine exposure using the anterior transsternal approach

4.3 Exposure

The incision is made from the anterior border of the sternocleidomastoid muscle to the sternum, then along the midline to the level of the third ribs (Fig. 2.65)

Separate the subcutaneous tissue and the platysma to expose the sternocleidomastoid muscle and its clavicle head (Fig. 2.66).

If the superficial cervical vein is encountered, it can be isolated and ligated.

Remove the fat and loose connective tissues from the suprasternal notch.

The pectoralis major attached on the sternum is subperiosteal dissected until the sternocostal joint and the bilateral borders of the manubrium can be clearly exposed (Fig. 2.67).

The deep cervical fascia above the manubrium is bluntly dissected by hemostatic forceps.

Insert a finger beneath the manubrium and slowly separate the sternohyoid muscle, sternothyroid muscle and thymus (adipose tissue) from the manubrium. Electrocautery is used to deal with the encountered bleeding of the muscles.

The range of incision should not exceed 80% of the width and the height of the manubrium (Fig. 2.68).

The vertebral body can be fully exposed when both sternoclavicular joints are retained. This also prevents injury to the internal thoracic artery and vein.

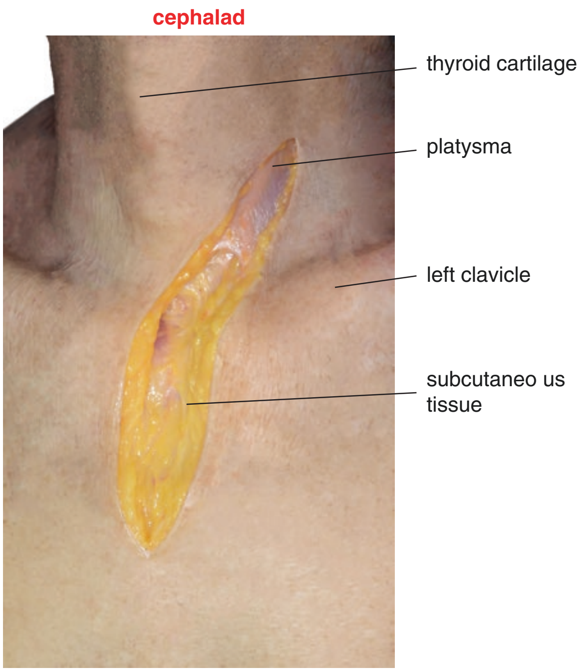

Fig. 2.65 Incision of the skin and subcutaneous tissue

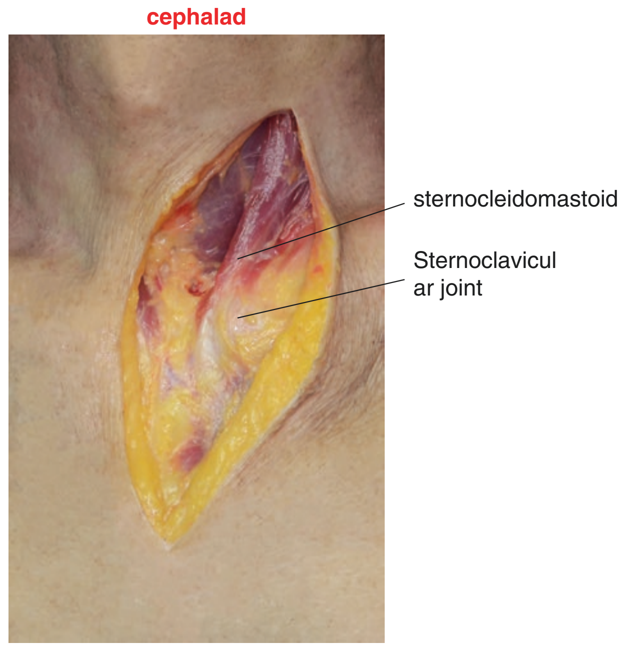

Fig. 2.66 Separation of the subcutaneous tissue to expose the clavicle head of the sternocleidomastoid muscle

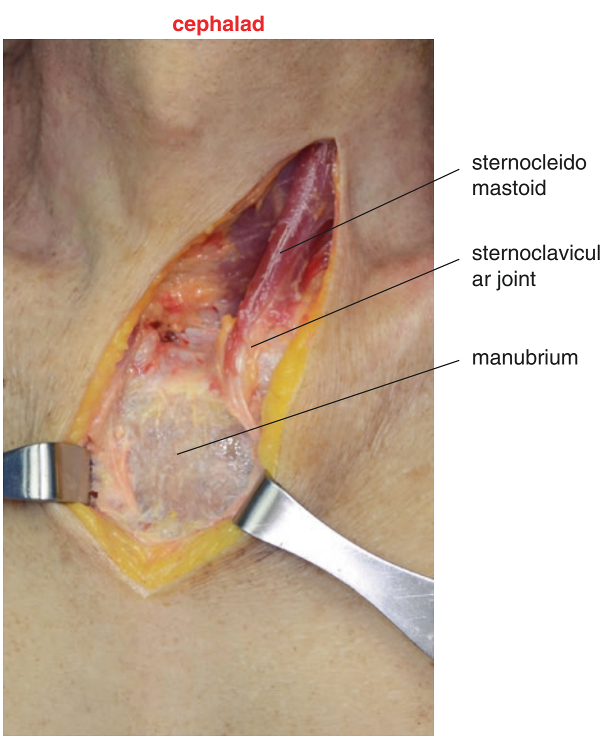

Fig. 2.67 Subperiosteal dissection and exposure of the manubrium

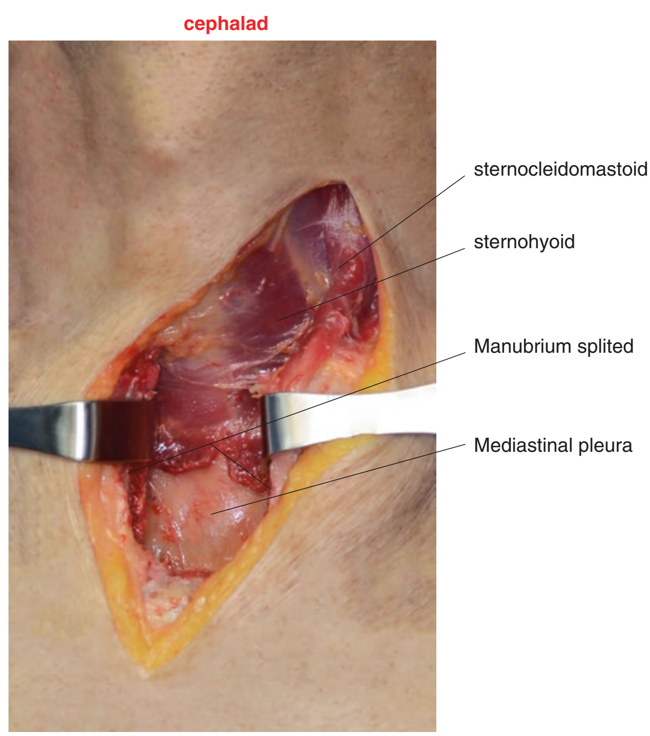

Fig. 2.68 Removal of the manubrium to expose the mediastinum

Internal thoracic artery: arises from the subclavian artery and descends along the posterior of the subclavion vein. It enters the thoracic cavity through the superior thoracic aperture and proceeds downward at 1–2 cm lateral to the outer border of the sternum. The artery runs beneath the costal cartilage and superficial to the transverse thoracic muscle (Fig. 2.69).

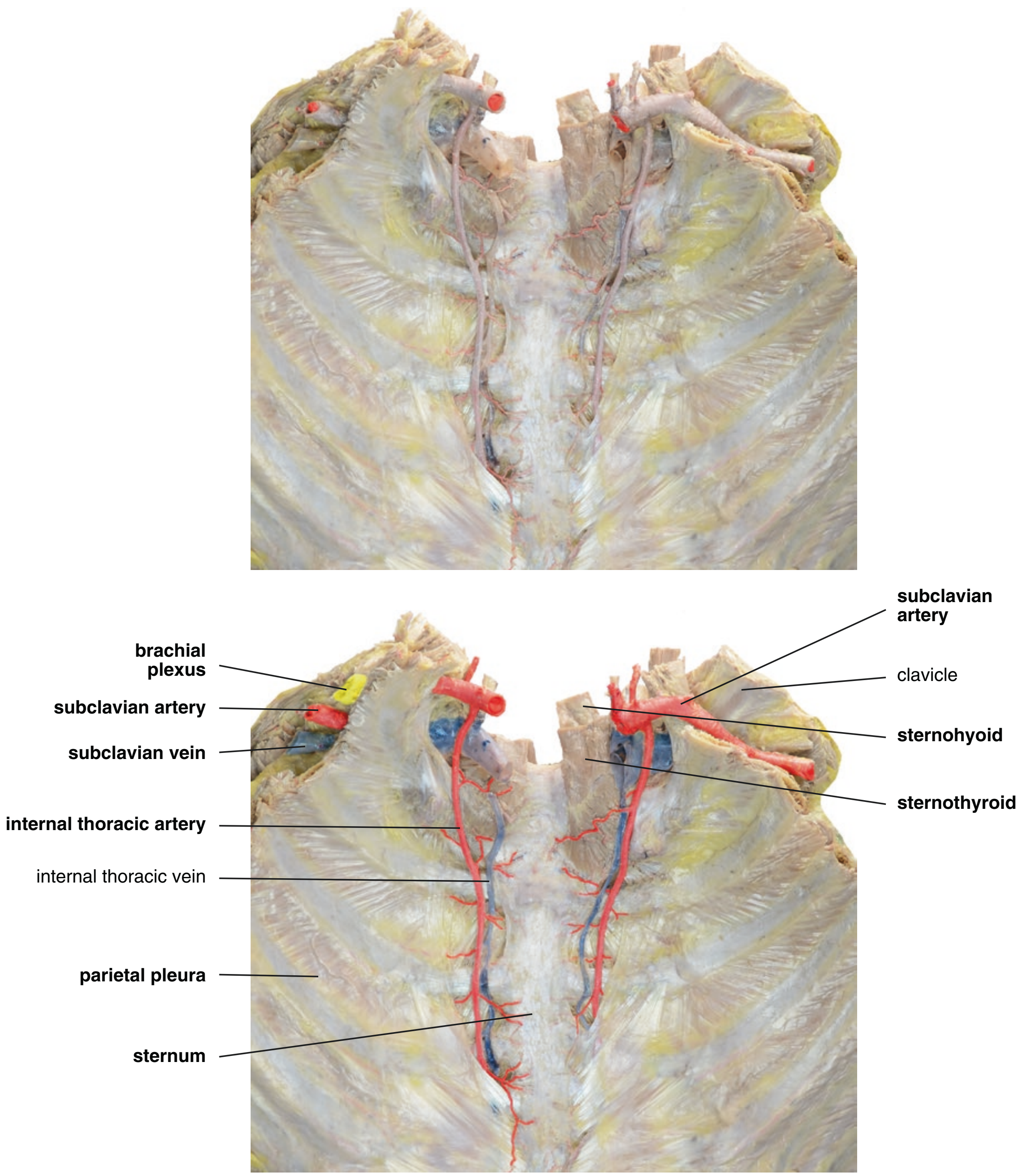

Fig. 2.69 Intrathoracic anatomy

The split manubrium is gently distracted using an automatic distractor to expose the superior mediastinum.

The thymus and adipose tissues is bluntly dissected with a hemostatic forcep. Identify and separate the brachiocephalic trunk and the left common carotid artery by palpation and bluntly dissection.

The left common carotid artery and innominate vein are protected with a retractor above the aortic arch, and the trachea and esophagus are retracted to the right to expose the prevertebral fascia (Fig. 2.70).

The prevertebral fascia is incised and dissected apart to expose the T2–3 intervertebral disc and T3 spine (Figs. 2.71, 2.72 and 2.73).

Structures adjacent to the cervical trachea (from superficial to deep) include: skin, superficial fascia, investing layer of cervical fascia, suprasternal space, jugular venous arch, infrahyoid muscles and anterior tracheal fascia. The esophagus is situated behind the trachea and flanked by the lateral lobes of the thyroid gland. The recurrent laryngeal nerve is located in the tracheoesophageal groove, and the carotid sheath and cervical sympathetic trunk are in the posterolateral region of the trachea and esophagus.

Cervical trachea: It includes 6–8 tracheal cartilages. The upper region is at the level of the inferior edge of the sixth cervical spine, which is contiguous to the inferior border of the cricoid cartilage, and the lower anterior region parallels to the jugular notch, while the lower posterior region parallels to the inferior margin of the seventh cervical spine and turns into the thoracic trachea. The average transverse diameter of the adult cervical trachea is about 1.94 cm, and the sagittal diameter is about 1.87 cm. When the head is turned to one side, the trachea also turns to the same side while the esophagus turns to the other side.

Cupula of pleura: protrudes into the root of the neck with the apex of the lung. Its surface is 2.5 cm above the clavicle. It is medially adjacent to the thyrocervical trunk, vertebral artery, sympathetic trunk and the lateral wall of the vertebral body, and laterally adjacent to the brachial plexus, and middle and posterior scalene muscles. The anterior region of the cupula of pleura is adjacent to the subclavian artery and vein, internal thoracic artery, phrenic nerve and anterior scalene muscle, the latter of which covers the anterolateral region of the cupula of pleura.

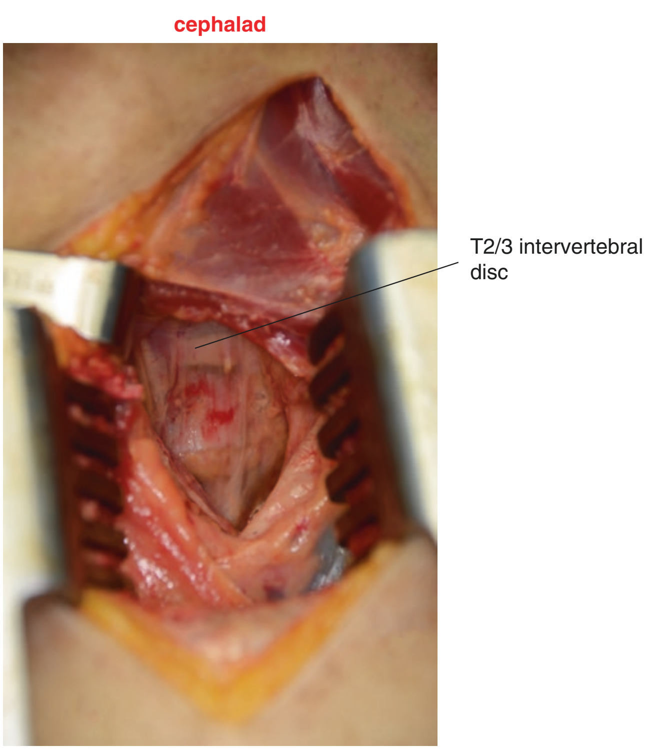

Fig. 2.70 Exposure of the prevertebral fascia

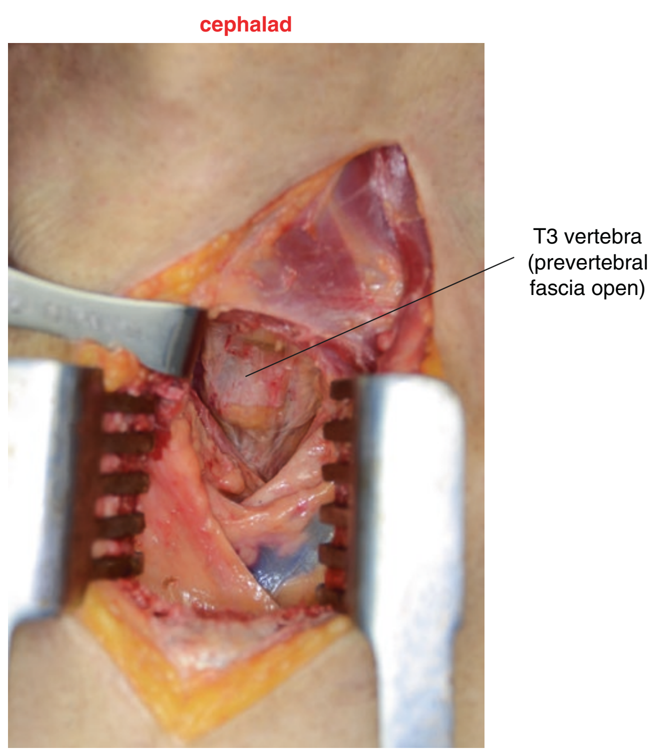

Fig. 2.71 Exposure of the vertebral body and intervertebral disc

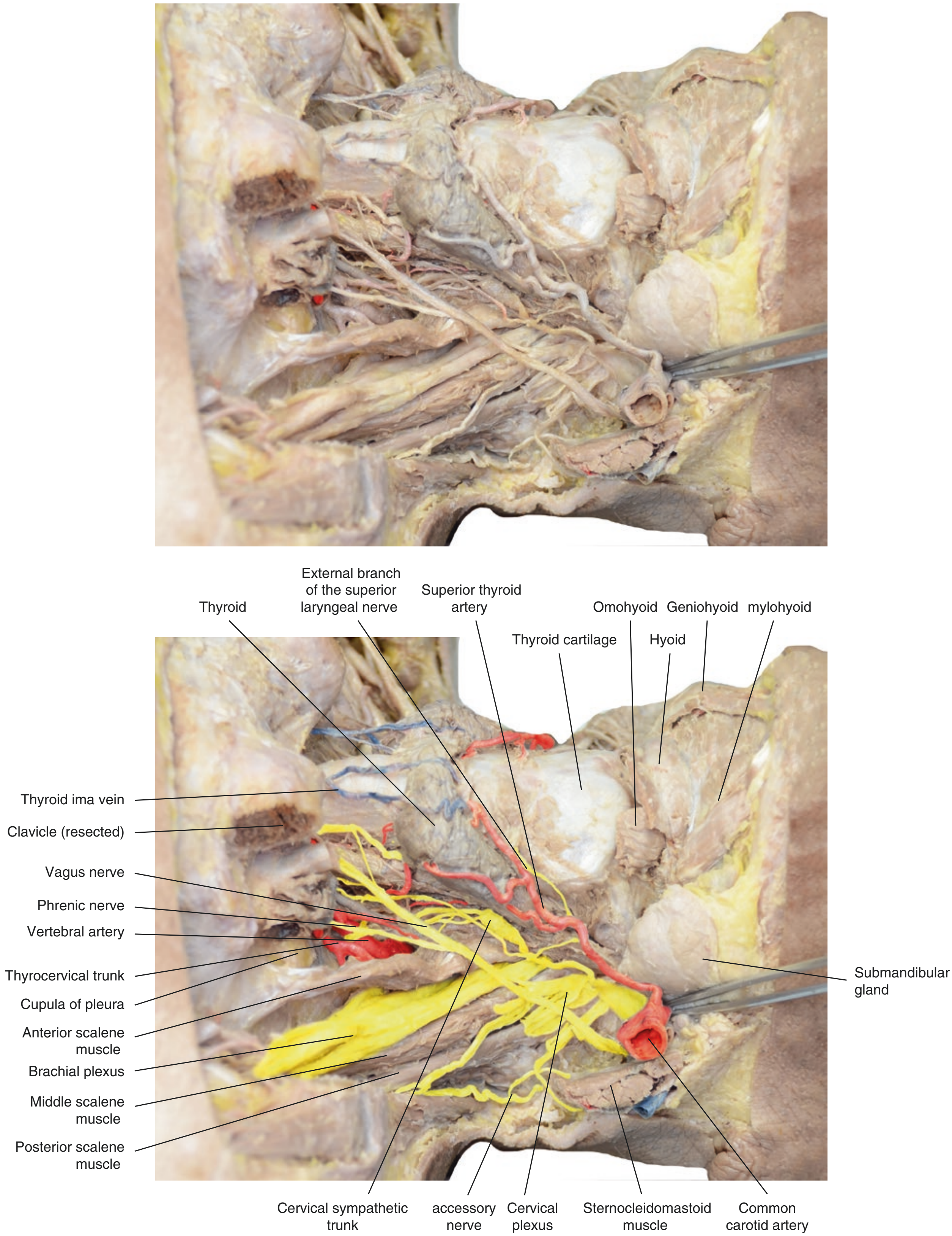

Fig. 2.72 Anatomy of the left cervical root

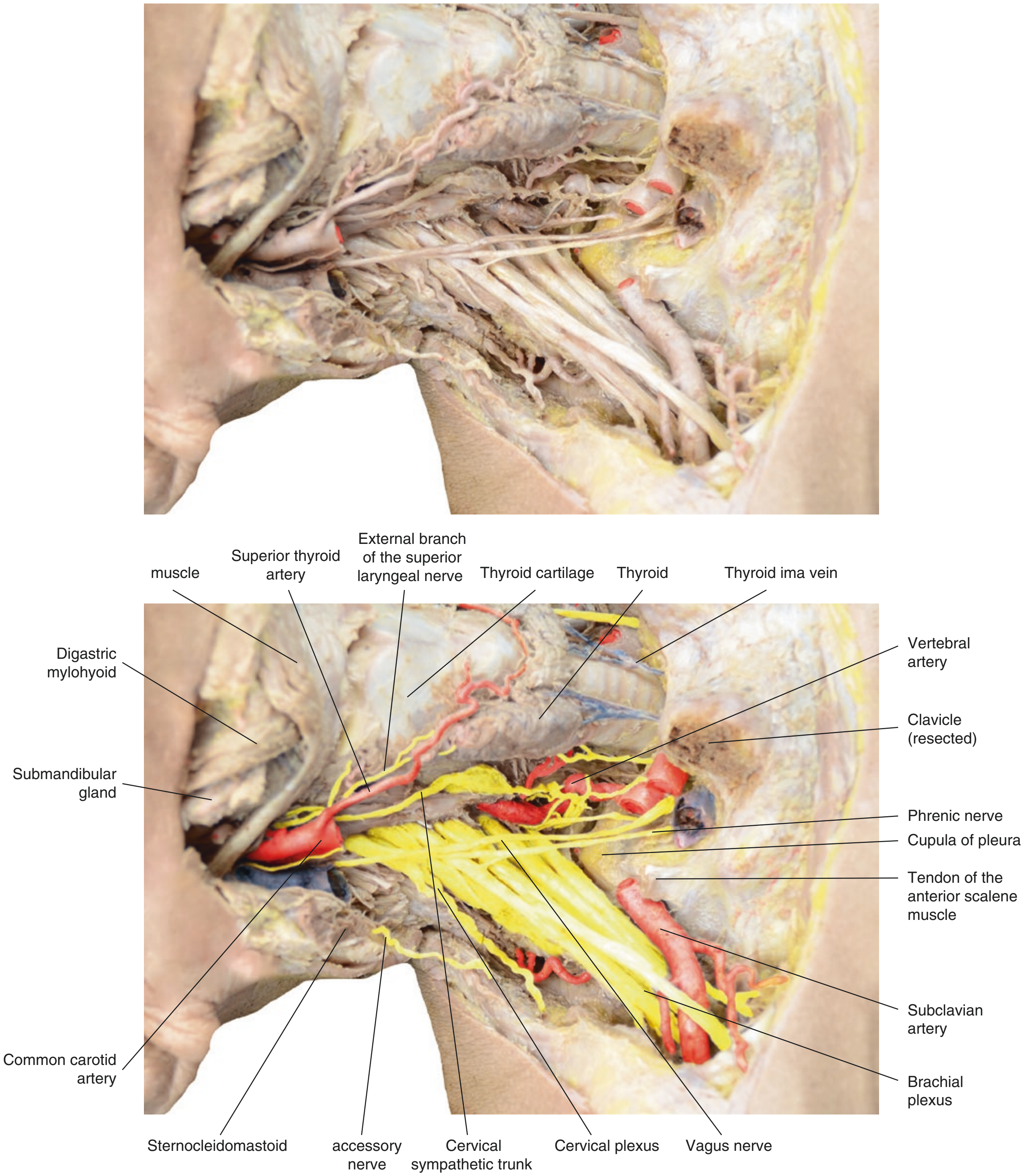

Fig. 2.73 Anatomy of the right cervical root

Manubrium: is at the level of the third and fourth thoracic spine. Its upper border is broad, with the jugular notch, or known as the suprasternal notch. The manubrium is located between the two clavicular notches. The pectoralis major and the sternal end of the sternocleidomastoid muscle are attached to the anterior side of the manubrium, while the sternothyroid is attached to the posterior side of the manubrium at the level of first costal cartilage. Moreover, the most medial fibers of the sternohyoid muscle is attached to the upper border of the manubrium. The sternocostal joint capsules and sternal fibers of the pectoralis major are attached to the anterior side of the sternum body, and the transversus thoracis muscles are attached to the posterior side of the sternum body.

Aortic arch: begins at the level of the upper border of the second sternocostal articulation of the right side, and runs at first upward, backward, and to the left in front of the trachea; then travels backward on the left side of the trachea and finally passes downward on the left side of the body of the fourth thoracic spine. The superior border of the arch is at the same level as the middle or slightly above the center of the manubrium, and the inferior border parallels to the sternal angle. The position of the aortic arch in children is higher.

Phrenic nerve: starts from the medial margin of the anterior scalene muscle at the root of the neck, and exits through the superior thoracic aperture. The phrenic nerve is located between the anterior scalene muscle and the second portion of the subclavian artery, and crosses the anterior of the internal thoracic artery. It then descends medially from the apex of the lung to the anterior of the 1st portion of the subclavian artery, and continues to proceed anteromedially until it crosses over the fibrous pericardial surface and descends to the front of the hilum of lung (Figs. 2.74 and 2.75).

Subclavian vein: a continuation of the axillary vein, and extends from the outer margin of the first rib to the medial border of the anterior scalene muscle, where it joins the internal jugular vein to form the brachiocephalic vein. The subclavian vein and subclavian artery are separated by the anterior scalene muscle and phrenic nerve. As a result, the clavicles and subclavian vein lies anterior to the anterior scalene while the subclavian artery lies posterior above the anterior scalene. Near the conjunction with the internal jugular vein, the thoracic duct drains into the left subclavian vein, and the right lymphatic duct drains into the right subclavian vein.

After exposure of the anterior cervical spine, Caspar distractor pin is inserted into the surgical section and the location is confirmed by intraoperative fluoroscopy (Fig. 2.76).

When exposing the lower cervical spine, attention is paid to avoid damaging the cupula of pleura, stellate ganglion, recurrent laryngeal nerve, vertebral artery and thoracic duct.

Gradually distract the intervertebral space after placement of the Caspar distractor (Fig. 2.77).

The dissection of the longuscolli muscle should be limited within the bilateral uncovertebral joints. The vertebral artery runs anterolaterally to the C7 vertebral body. Excessive separation of the longuscolli muscle may damage the vertebral artery.

Osteophytes on the anterior vertebral body is removed by a Leksell rongeur.

The anterior longitudinal ligament and annulus fibrosus of the adjacent intervertebral discs of the target vertebra are removed (Figs. 2.78 and 2.79).

The remaining intervertebral disc tissues in the intervertebral space is removed by Kerrison rongeurs.

The depth and width of the decompression can be determined by the posterior border of the intervertebral disc and the uncovertebral joint.

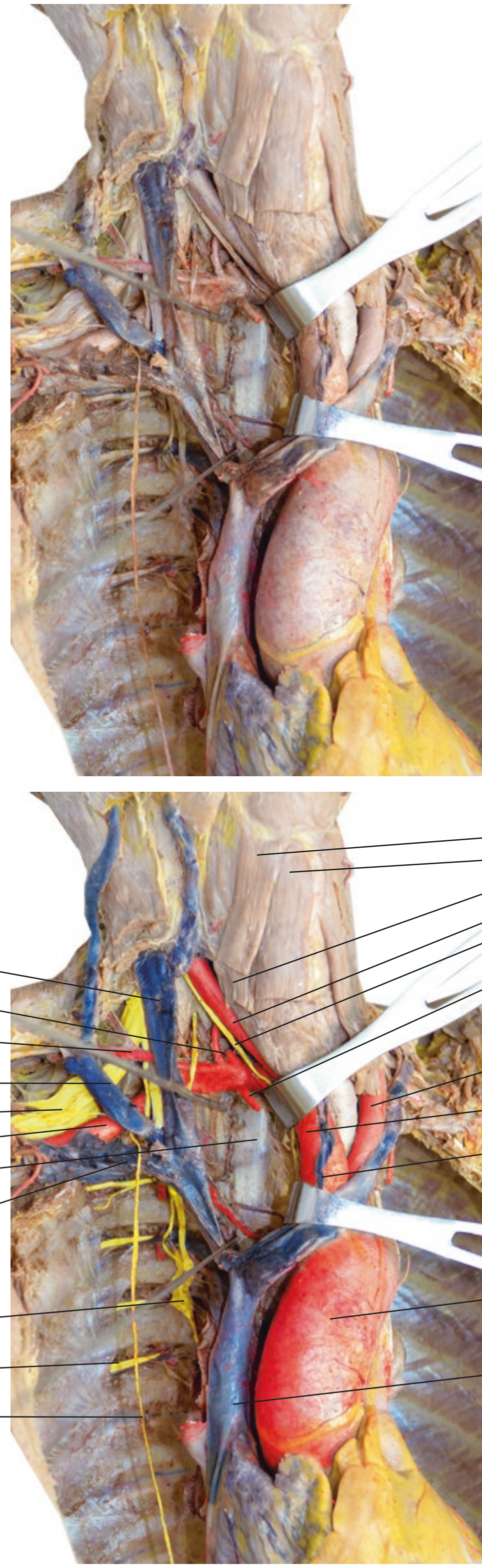

Fig. 2.74 Anatomy of the superior mediastinum (right sided approach)

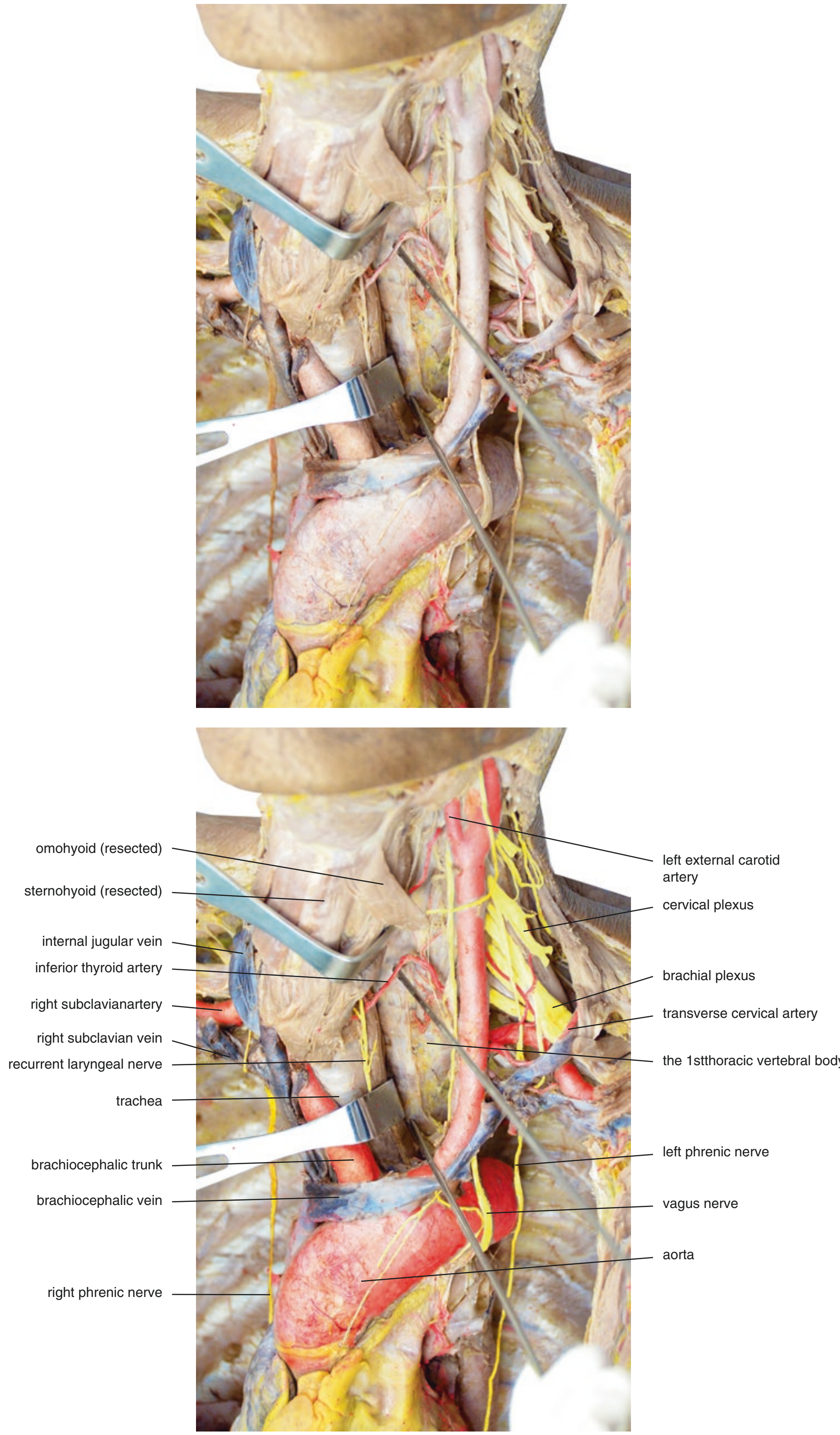

Fig. 2.75 Anatomy of the superior mediastinum (left-sided approach)

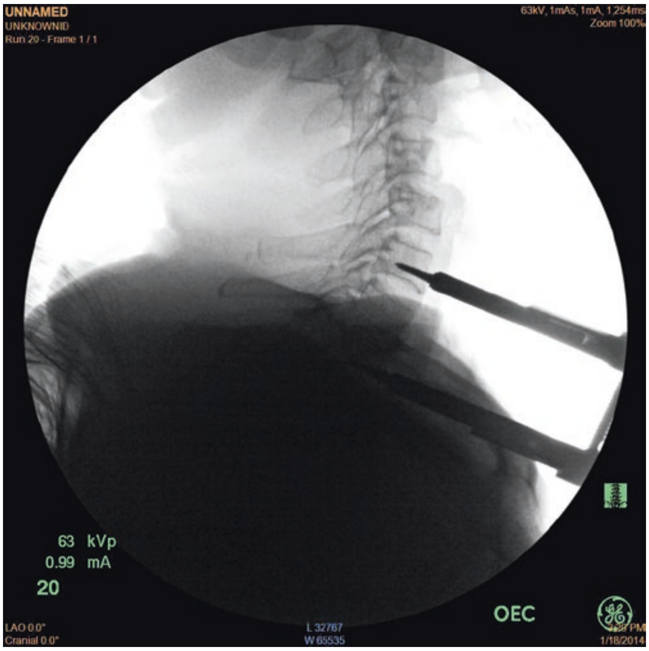

Fig. 2.76 Placement and location of Caspar distractor pin

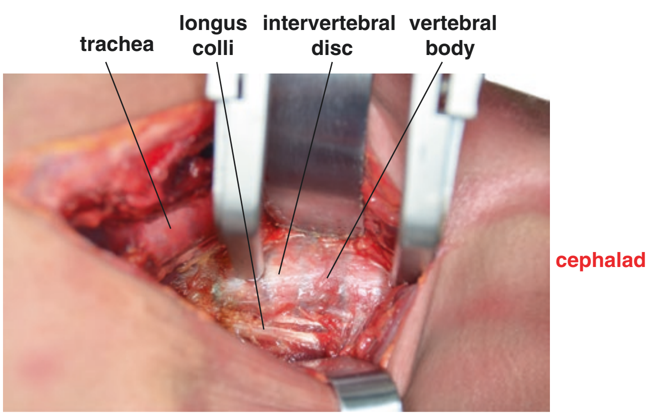

Fig. 2.77 Placement of the Caspar distractor and exposure of the cervical spine

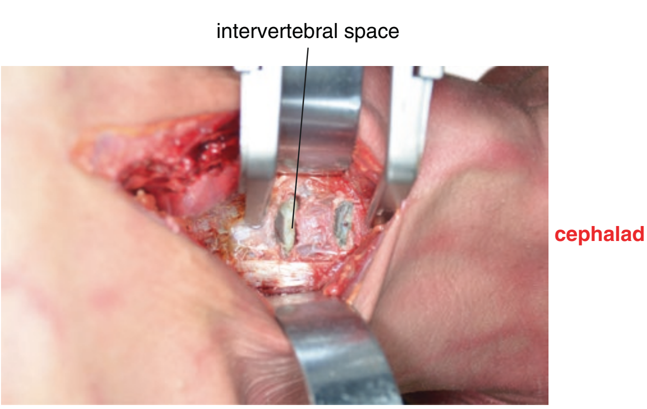

Fig. 2.78 Removal of the anterior annulus fibrosus

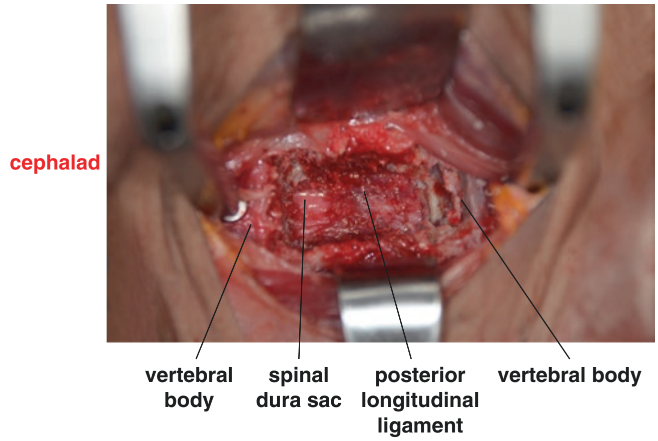

Fig. 2.79 Corpectomy

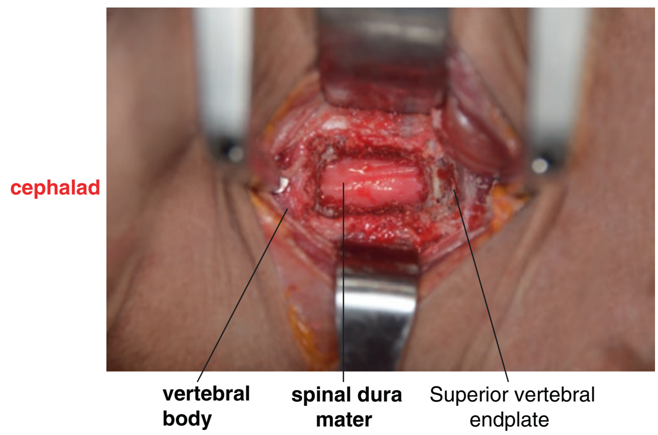

Fig. 2.80 Exposure of the dural sac

4.4 Corpectomy

A bone groove connecting the adjacent intervertebral space is made in the center of the vertebral body by a Leksell rongeur or a high-speed bur. The resection width should be no less than 1.5 cm, but within the bilateral uncovertebral joints.

The Cancellous bone of the target vertebral body is removed by high-speed bur until the posterior border of the vertebra is reached.

A small curette may be used to make a small opening. The opening can be gradually expanded using Kerrison rongeurs to expose the posterior longitudinal ligament.

A nerve hook is used to separate the posterior longitudinal ligament from the spinal dural sac, and then the posterior longitudinal ligament is incised by scalpel along the nerve hook. Kerrison rongeurs are used to remove the posterior longitudinal ligament and remaining vertebral posterior wall to expose of the dural sac (Fig. 2.80).

A small nerve hook can be inserted into the foramen to determine the adequacy of the decompression.

Posterior longitudinal ligament: the ligament is divided into two layers. The superficial layer travels vertically downward from the skull base and extends laterally to the intervertebral foramen. The deep layer is dented and consists some of the fibers that make up the uncovertebral joint capsule (Fig. 2.81).

Uncinate process: protuberance on the lateral edges of the vertebral body and constitutes the uncovertebral joint with the inferior border of the upper vertebra. The uncinate process is a very important anatomical landmark. The uncinated process is an important anatomical landmark for anterior cervical operation. The transverse foramen is located laterally to the uncinate process, through which the vertebral artery, the vein and sympathetic nerve plexus run. The outer posterior region of the process forms the anterior wall of the intervertebral foramen, through which the cervical nerve root and radicular artery run (Figs. 2.82, 2.83, and 2.84). The uncovertebral joint helps stabilize the

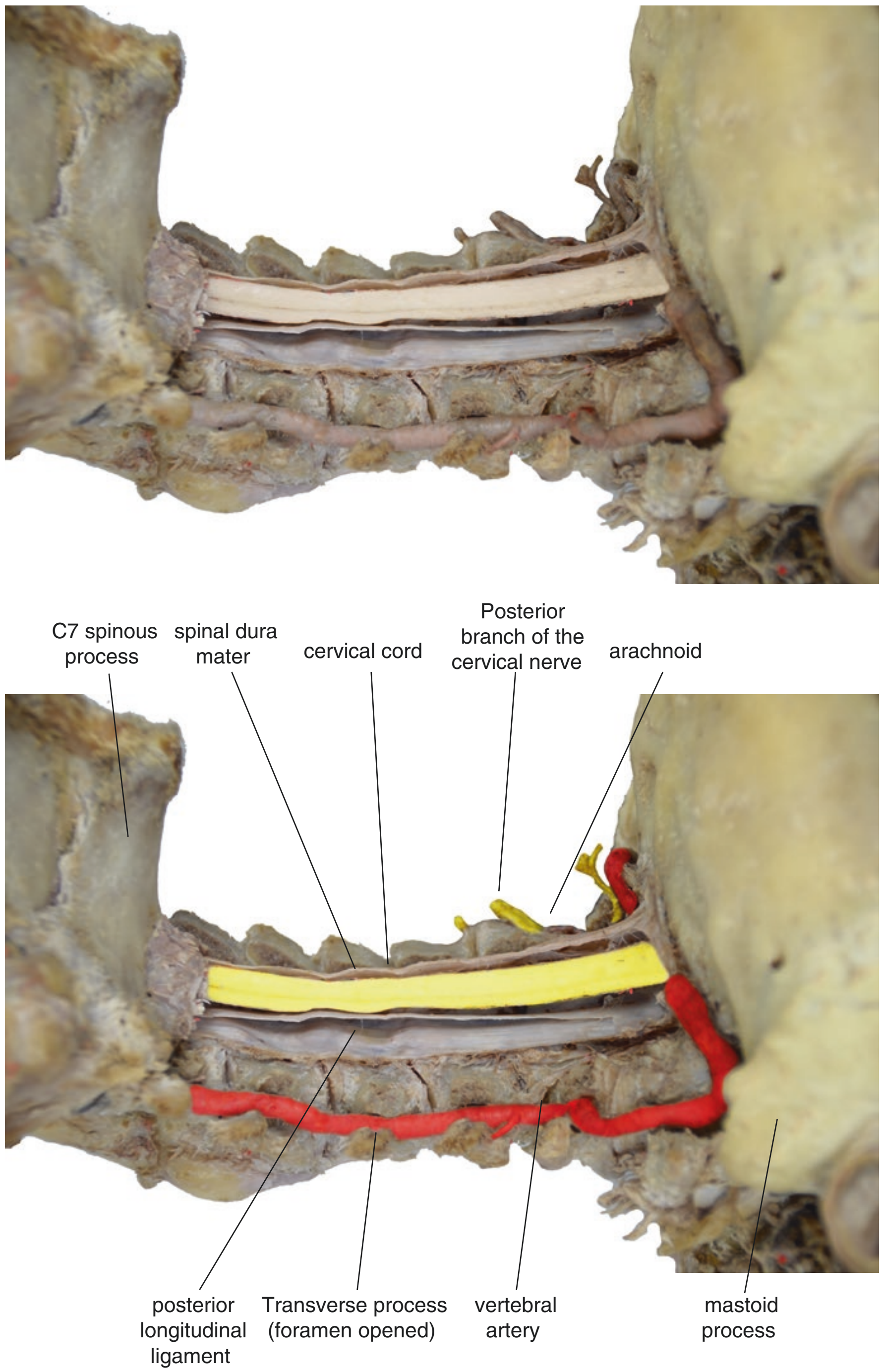

Fig. 2.81 Removal of the vertebral lamina and the right lateral mass by the lateral approach (right side of the spinal cord removed)

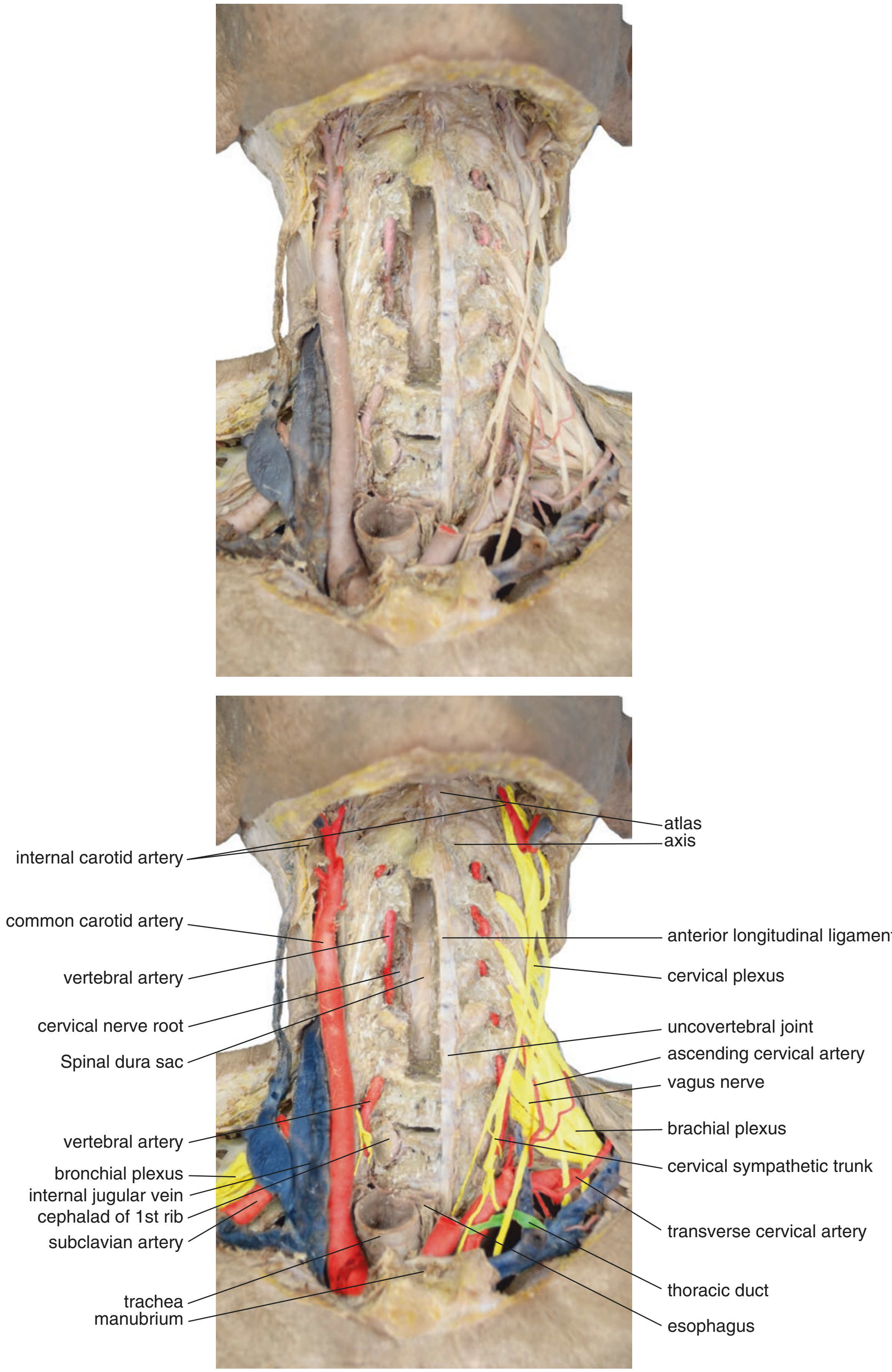

Fig. 2.82 Anterior view of cervical neurovascular structures (vertebral body partially resected on the right)

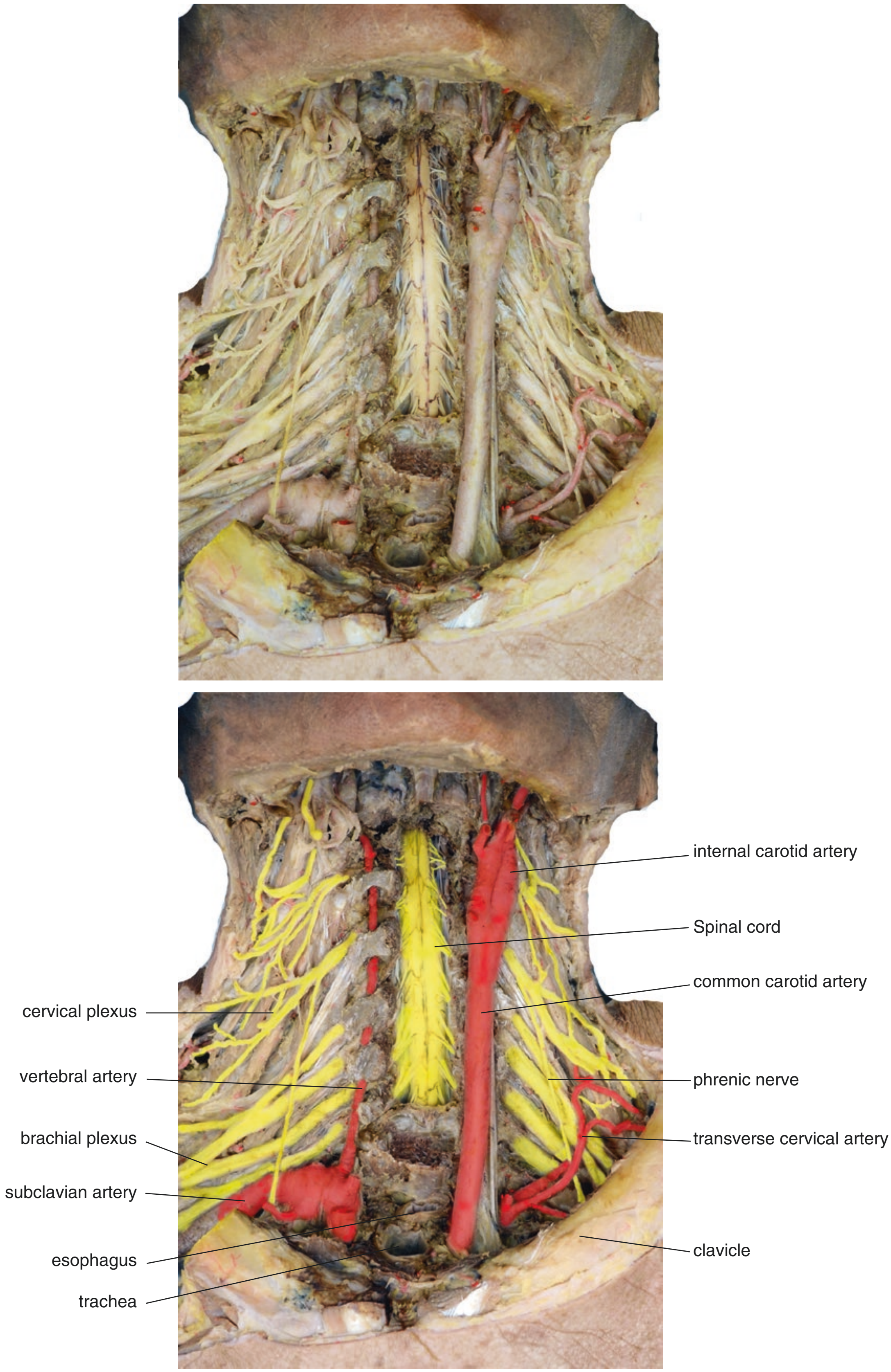

Fig. 2.83 Anterior view of cervical neurovascular structures (vertebral body partially resected)

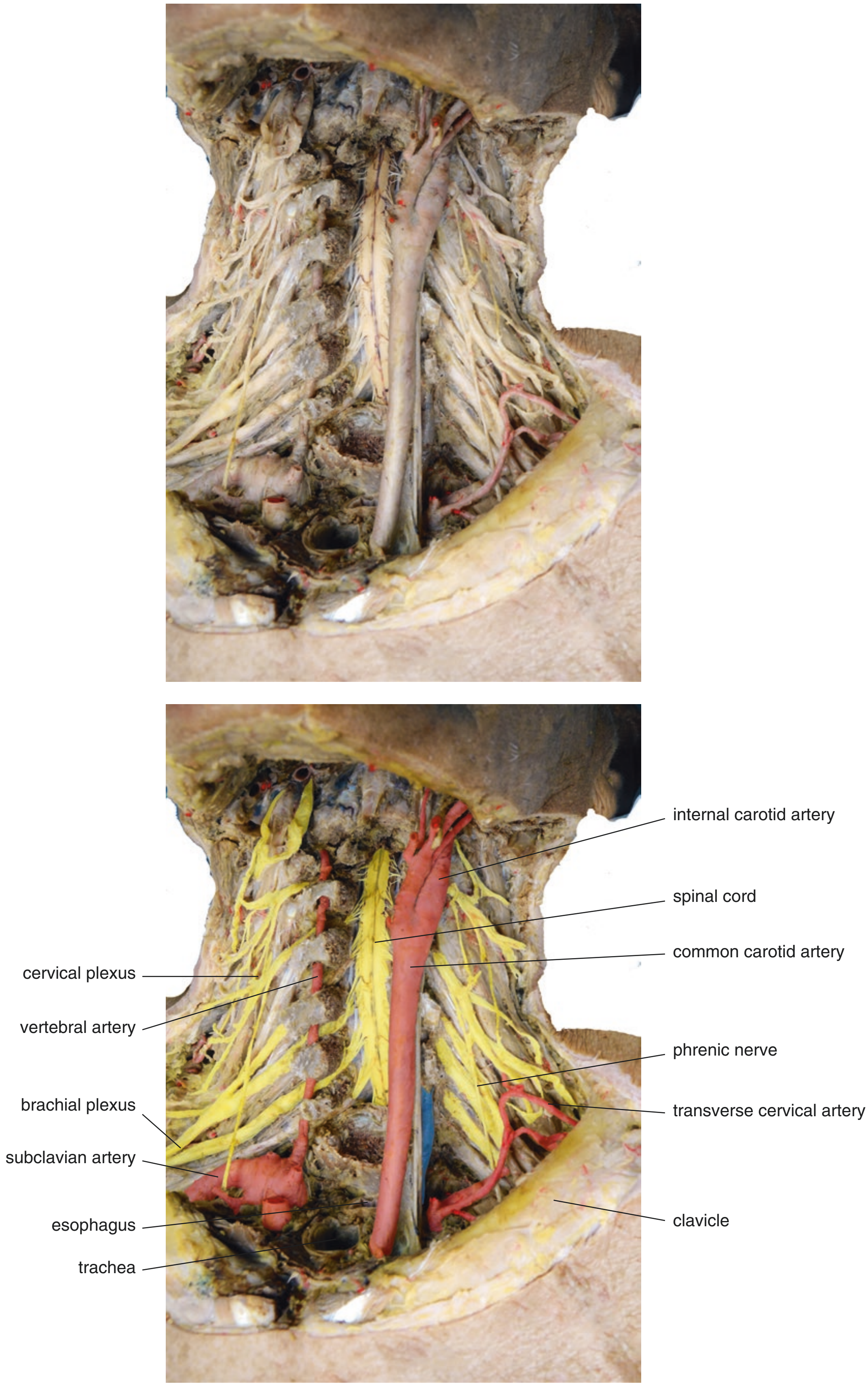

Fig. 2.84 Anterior lateral view of cervical neurovascular structures (vertebral body partially resected)

lateral movement of vertebral body, and hyperplasia and degeneration of the uncovertebral joint may cause stenosis of the invertebral foramen and cause compression to the vertebral artery and cervical nerve root.

4.5 Fusion and Fixation (Fig. 2.85)

Surgeon should avoid excessive distraction when placing the titanium mesh in case the titanium mesh subsidents into the vertebra and cause postoperative axial pain.

The superior endplates of the C6 and C7 spine are not parallel with the endplate above. Therefore, the inferior surface of the titanium mesh can be trimmed into a slanted surface (longer in the front and shorter in the back) to better fit with the shape of the endplates.

The superior and inferior vertebral endplates and the shape of the titanium mesh cage can both be trimmed to ensure tight fitting.

Place the anterior cervical titanium plate onto the mesh cage. Pay attention to the pre-bend angle of the plate that is used for correcting the cervical lordosis in multisegments involved cases (Fig. 2.86).

Identify the position of the longuscolli muscles when placing the plate to avoid misalignment or angulation between the long axis of the titanium plate and cervical spine.

Adjust the screw after fluoroscopy to avoid insertion into the adjacent intervertebral disc or the interface between the vertebrae and titanium cage.

Anteroposterior and lateral intraoperative fluoroscopy show that the anterior cervical titanium plate, screw and mesh cage are all in good position (Figs. 2.87 and 2.88).

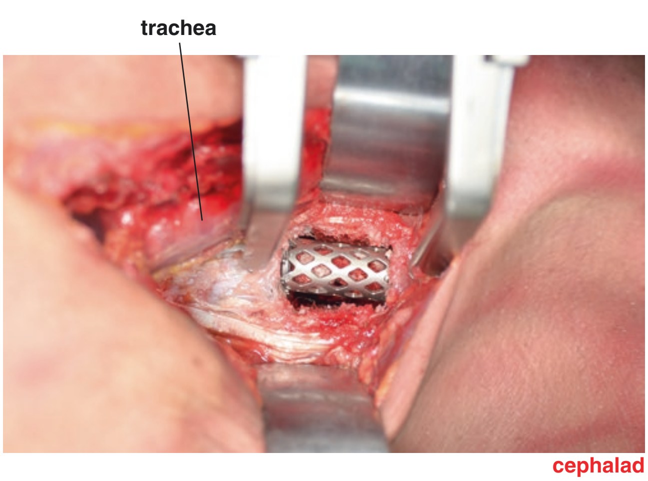

Fig. 2.85 Placement of titanium mesh cage

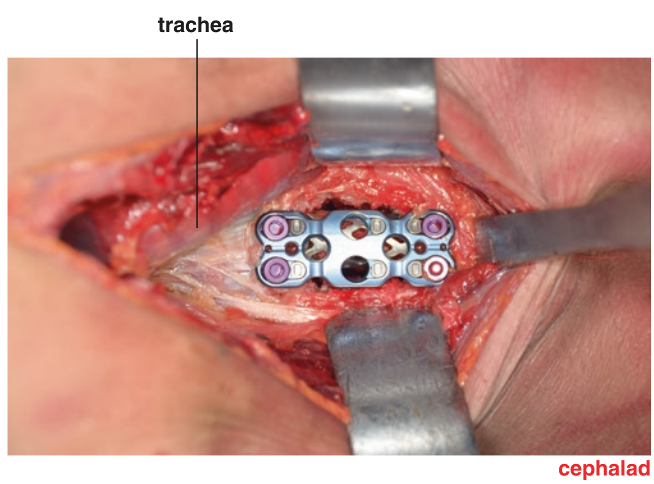

Fig. 2.86 Placement of the plate

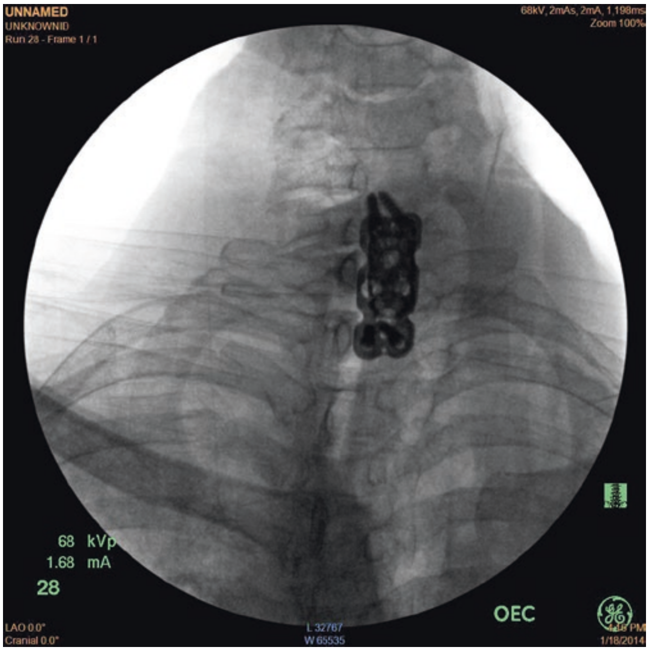

Fig. 2.87 Anteroposterior intraoperative fluoroscopy of the cervical implant

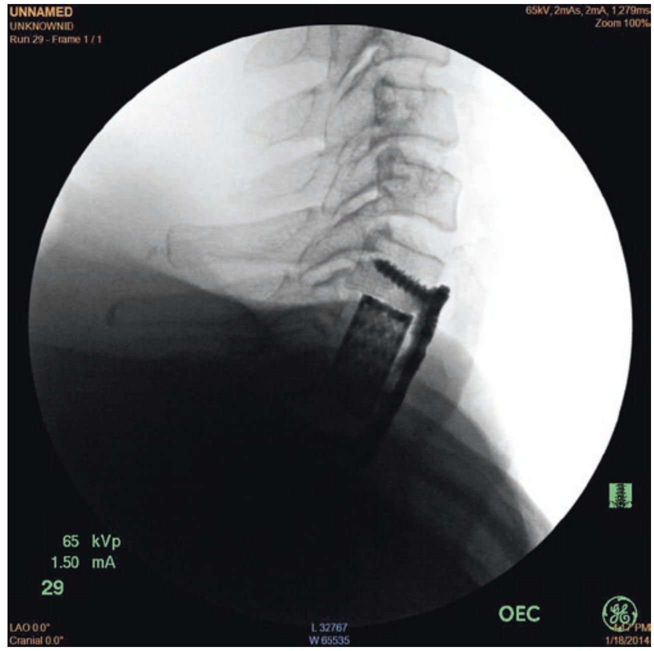

Fig. 2.88 Lateral intraoperative fluoroscopy of the cervical implant

5 Subaxial Cervical Pedicle Screw and Lateral Mass Screw Fixation

5.1 Overview

Cervical pedicle screw internal fixation was firstly reported by Abumi et al. in 1994. Cervical fixation by cervical pedicle screw and rod system provides biomechanical stability that is ideal for cervical kyphosis correction, spinal fixation and fusion, and spinal fracture and dislocation treatment. Since the subaxial cervical pedicle is very small and is located within the narrow space between the vertebral artery, spinal cord, and superior and inferior nerve roots, screw placement into the pedicle is somewhat difficult and risky.

In 1970, Roy-Camille et al. first introduced a lateral mass internal fixation technique using plates and screws to treat cervical fracture and dislocation, and observed satisfactory outcomes. Lateral mass screw fixation is less technically demanding in comparison to pedicle screw fixation and have been universally accepted. As the cervical lateral mass is adjacent to neurovascular structures (the spinal cord is anterolateral to the lateral mass, and the vertebral artery and cervical nerve root are anterior to the lateral mass), the placement of the screws is dangerous to some extent. Thorough knowledge of local anatomy and the application of established surgical techniques are essential for subaxial cervical pedicle screw and lateral mass screw fixation.

5.2 Implantaion of the Subaxial Cervical Pedicle Screw

The pedicle screw entry points for the C3–7 are slightly lateral to the center of the articular mass and close to the inferior margin of the inferior articular process of the supeior vertebra.

The trajectory of screws are with angle of 45° to the sagittal plane for the pedicle for C3–5, 25° to the sagittal plane for C6–C7.

After confirming the target segments, expose the lateral mass within the target segments to allow accurate intraoperative identification of the screw entry point (Fig. 2.89).

The boundaries around the lateral mass must be accurately determined before the entry point can be accurately identified. Presence of articular process hyperplasia and the degeneration may increase the difficulty in determining the screw entry point.

The superior border of the lateral mass should be determined by the surface of the superior articular process instead of the inferior border of the inferior articular process of the superior vertebra. If necessary, the lateral mass joint capsule can be incised to allow better identification.

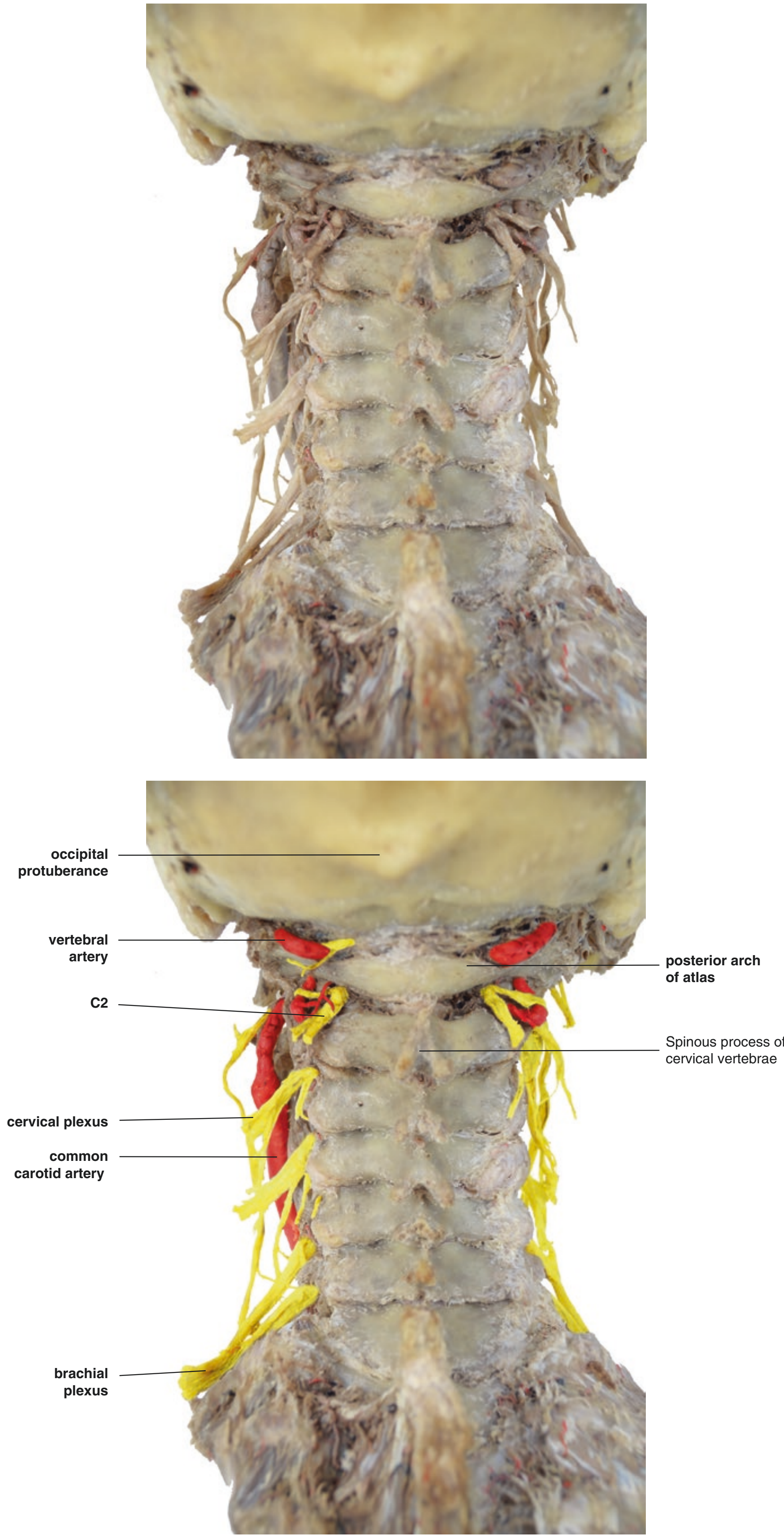

Fig. 2.89 Posterior bony structure of cervical spine

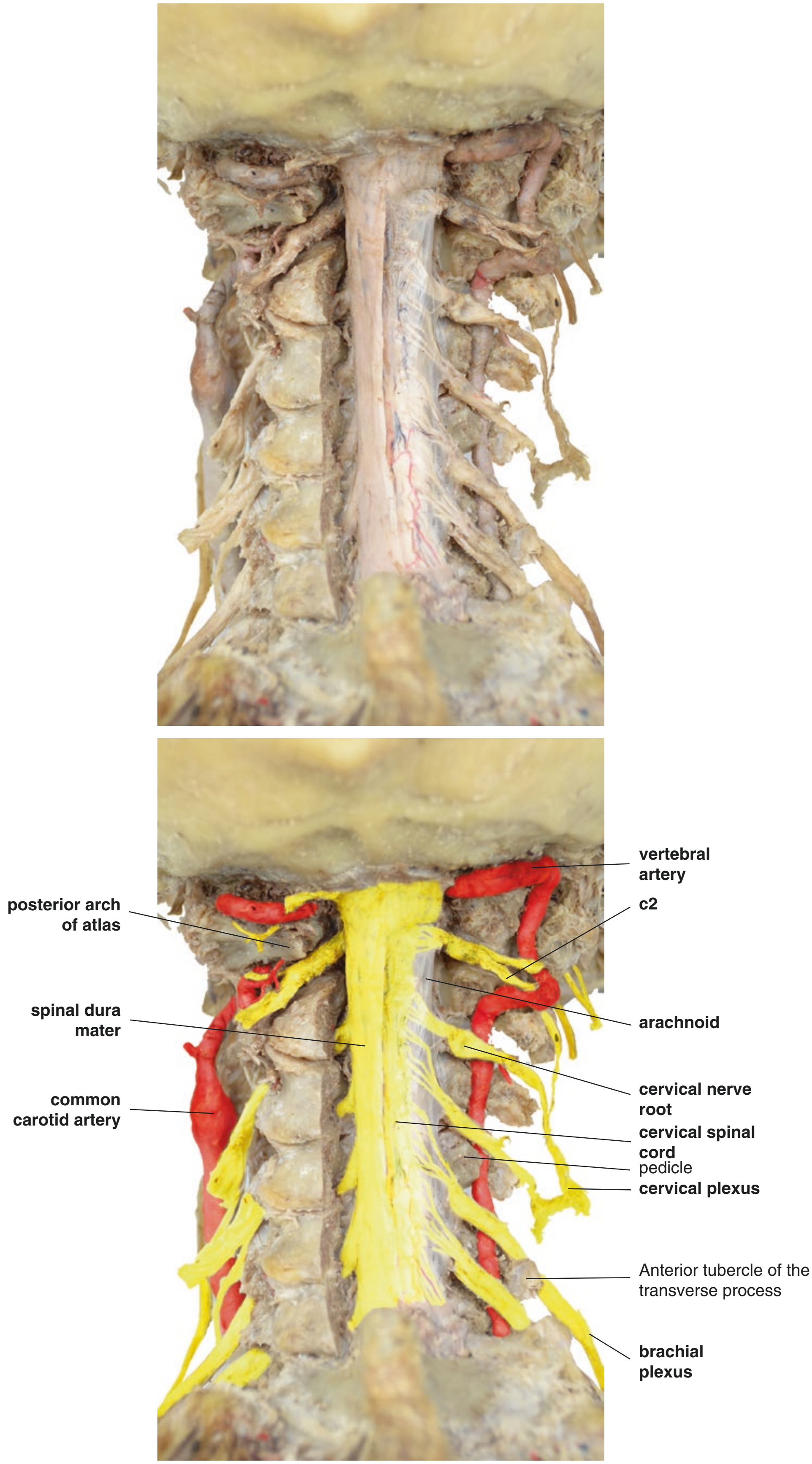

Fig. 2.90 Relations of the nerve root and the vertebral Artery, pedicle and spinal cord (dural sac half-opened)

Pierce vertically through the bone cortex at the entry point with a pointed taper, and then drill into the bone slowly in the direction previously determined.

The hand drill should proceed forward with even resistance.

If a large resistance is felt by the hand drill, stop drilling immediately. If the resistance disappears suddenly or a sense of loss or breakthrough is felt by the drill, these indicate that the hand drill is not running in the pedicle.

From the perspective of anatomy, the lateral wall of the pedicle is very thin and can be easily pierced. Therefore, the medial pedicle cortex should be used as a safe guide to insert the drill or taper through the pedicle.

As the vertebral artery is restricted within by the osseous intervertebral foramen, its freedom of movement is limited and is thereby vulnerable. On the other hand, the spinal cord is safer due to the buffering effects of the epidural fat and dural sac (Fig. 2.90). Therefore, insertion path near the medial side of the pedicle is a safer choice.

The lower nerve root runs tightly along the inferior border of the pedicle, while there is a distance between the upper nerve root and the superior border of the pedicle (Fig. 2.90). Therefore, insertion path near the superior side of the pedicle is a safer choice.

When the drill reaches a depth of about 20–24 mm, use the pedicle sounder to examine the bottom and surrounding walls of the screw path to determine whether they are intact.

If the screw path has already pierced through the bone within 18 mm, it indicates that the trajectory is not correct.

Use C-arm fluroscopy to observe whether the screw path has perforated the cervical pedicle, and whether it is parallel to the endplate and has entered the intervertebral space.

Fig. 2.91 Pedicle screw placement

Angiography of the vertebral artery should be performed if injury of the vertebral artery is suspected. If injury is confirmed, occlusion should be applied.

The screw (3.5 or 4.0 mm) with a length of 20–24 mm should be selected for placement. Tapping is required before screw implantation, otherwise it may be difficult to place the screw into the premade screw path successfully (Fig. 2.91).

Anteroposterior and lateral intraoperative fluoroscopy are conducted to determine the location of the pedicle screws (Figs. 2.92 and 2.93).

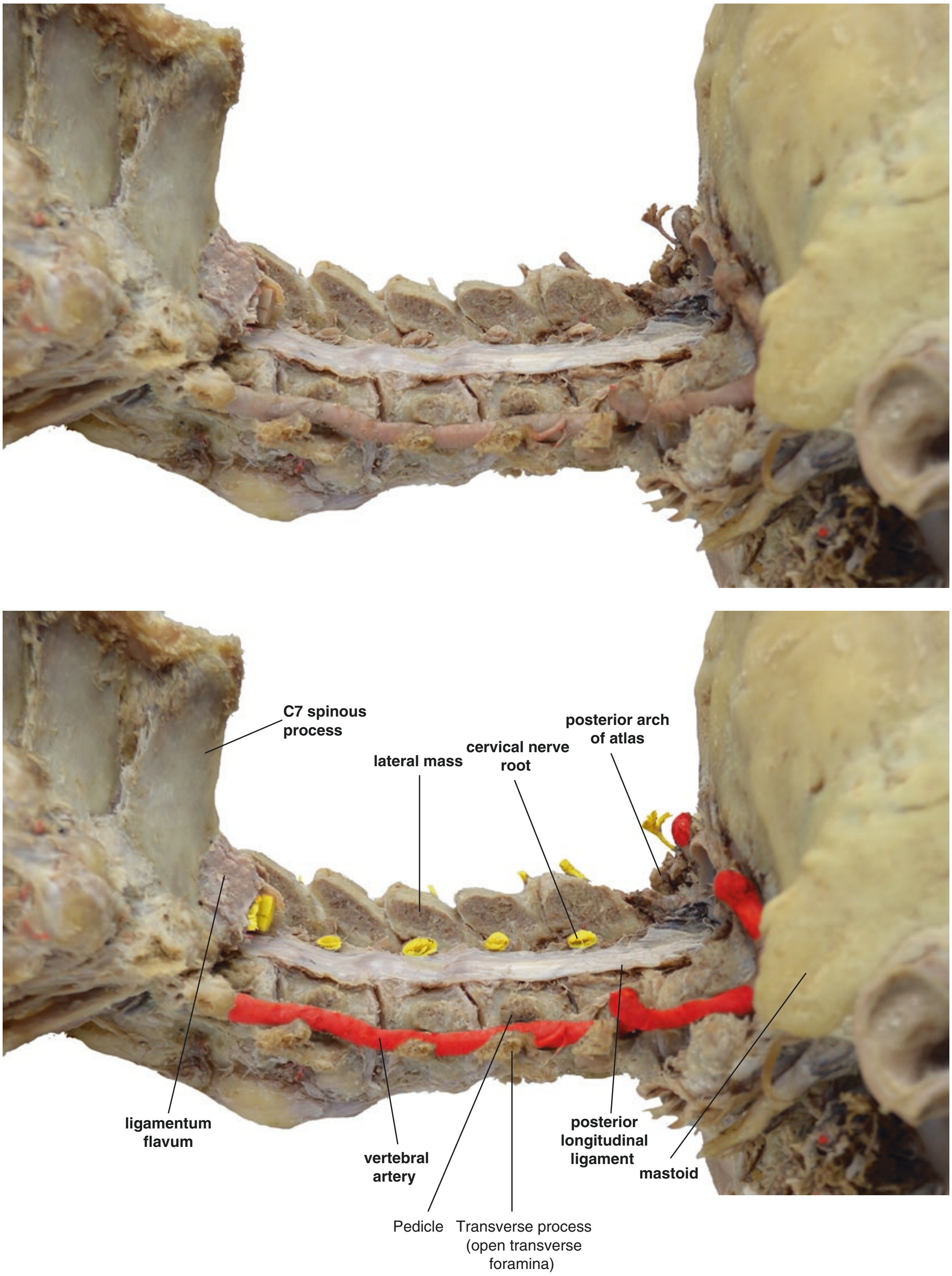

Fig. 2.92 Anteroposterior intraoperative fluoroscopy of the pedicle crews

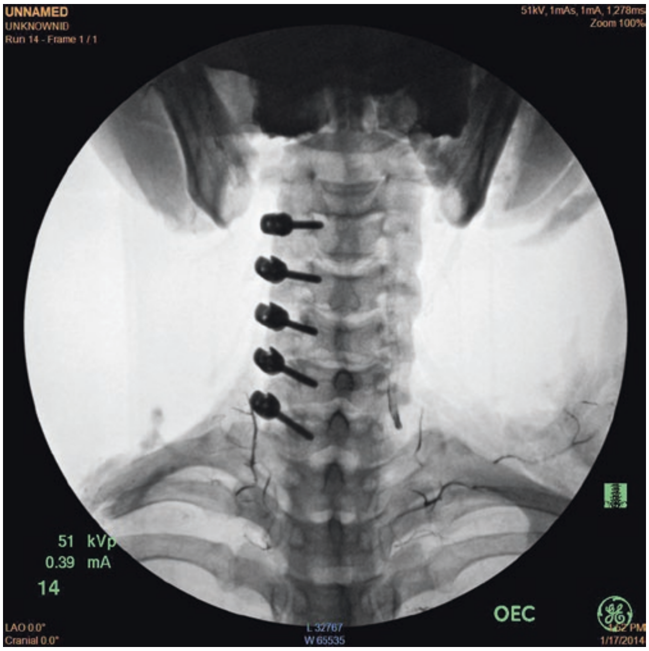

Fig. 2.93 Lateral intraoperative fluoroscopy of the pedicle screws

Fig. 2.94 Sectional morphology of lateral mass and trajectory of lateral mass

5.3 Technique of Subaxial Cervical Lateral Mass Screw Implantation

The entry point and trajectory of the mess screw are vary among different techniques.

The entrance point for the Magerl technique was 1 mm medial and cranial from the center of the posterior surface, and the screw was directed 25° lateral and parallel to facet joint, which is approximately 45° cranial to the posterior surface of the lateral mass.

The entrance point for the Roy-Camille technique was at the center of the posterior surface and the screw was directed 10° lateral and perpendicular to the posterior surface of the lateral mass.

Anderson technique: The entrance point is located 1 mm medial from midpoint of lateral mass, sagittal plane shall decline to head direction, and the enter length is 16–18 mm.

A penfield dissector can be inserted into the lateral mass joint to determine the trajectory (Figs. 2.94 and 2.95).

Screw path is made with the 2.5 mm drill until it drills through the cortical bone in front of the articular process.

Tap to the 2/3 length of the crew path and then place in the screw.

The tapping direction and depth shall be defined before putting the screw to ensure that the screw can be placed successfully. The path will be expanded if the screw is replaced more than once.

Anteroposterior and lateral intraoperative fluoroscopy is conducted to determine the location of lateral mass screw (Figs. 2.96, 2.97 and 2.98).

The entry point of pedicle screw is on the left and the entry point of lateral mass screw is on the right (Figs. 2.99 and 2.100).

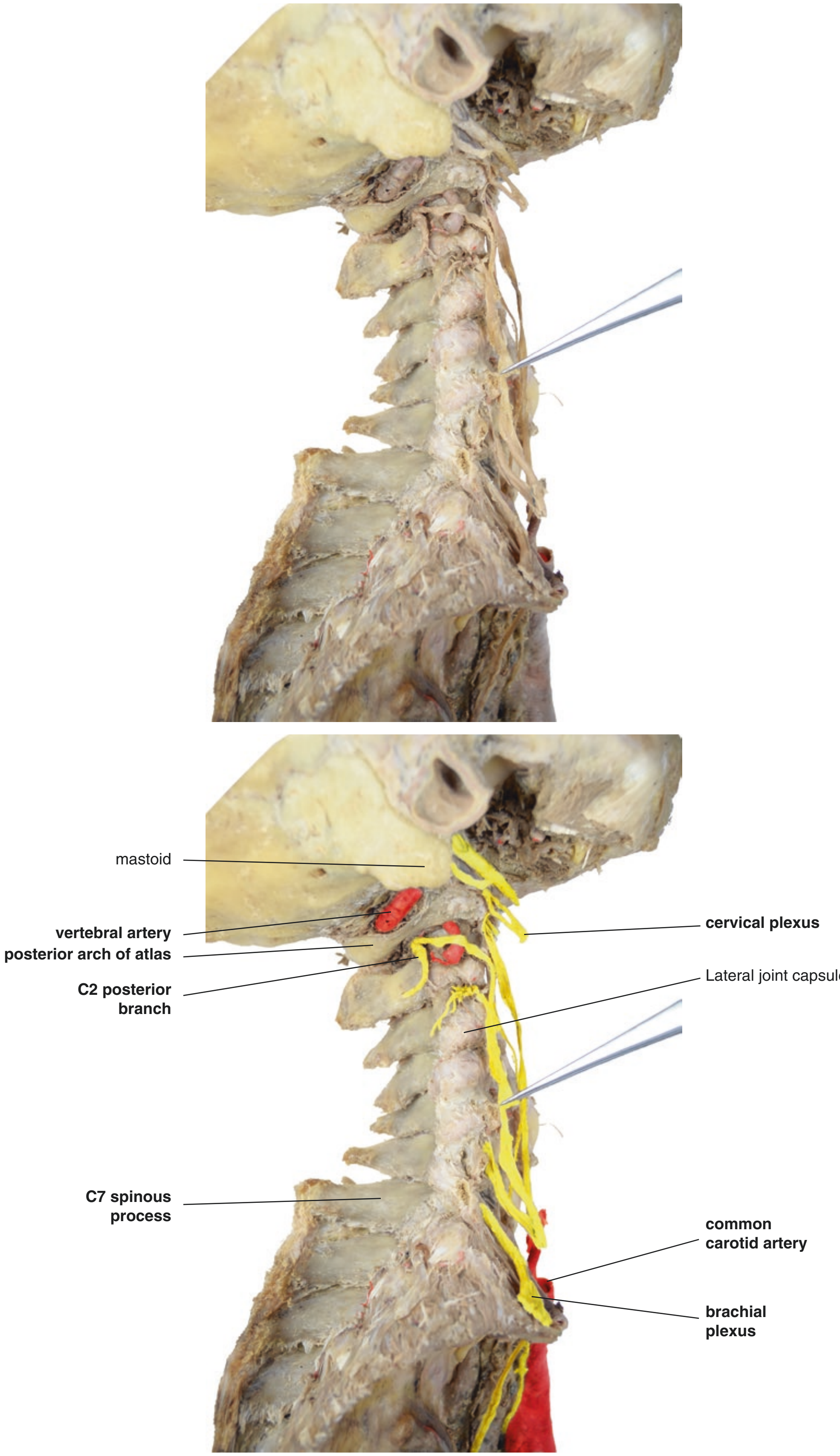

Fig. 2.95 Lateral mass joint with capsule

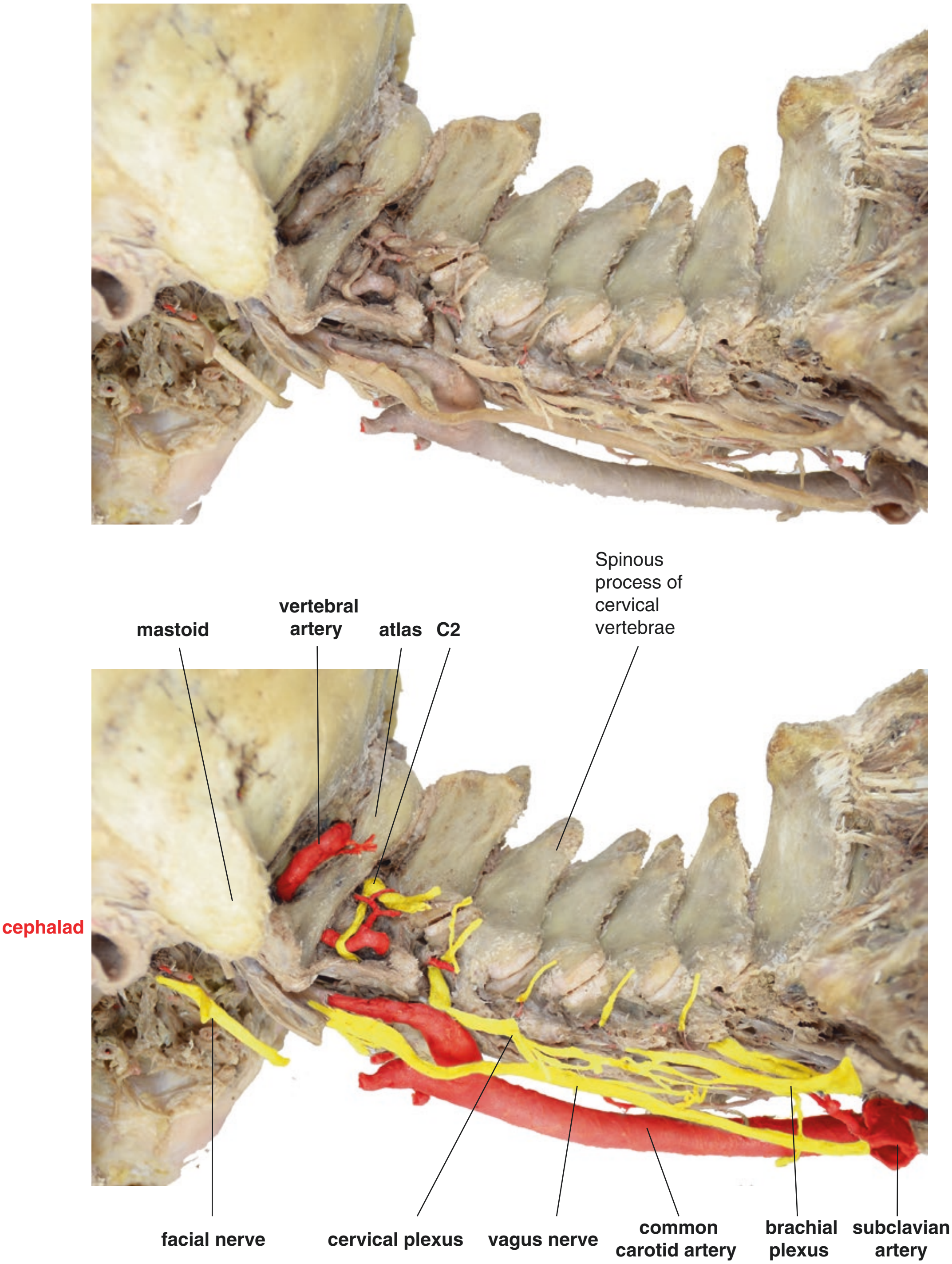

Fig. 2.96 Relations of bony structures of lateral cervical spine and neurovascular structures

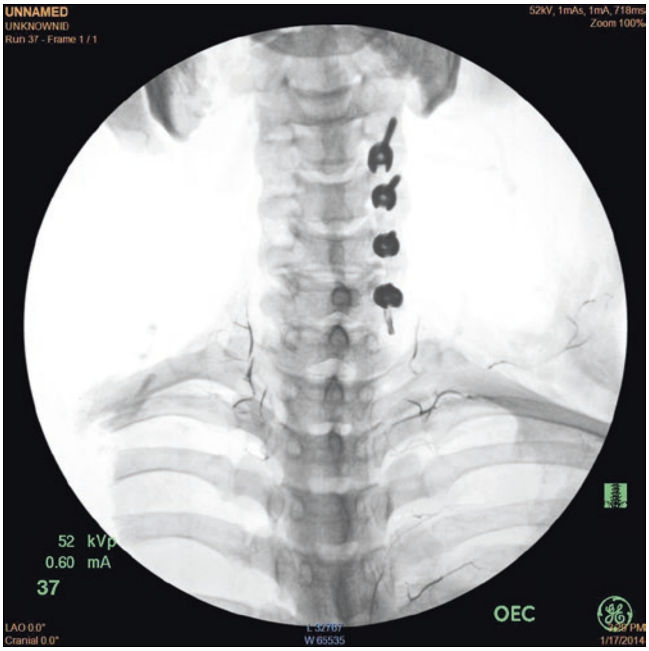

Fig. 2.97 Anteroposterior intraoperative fluoroscopy of the lateral mass screw

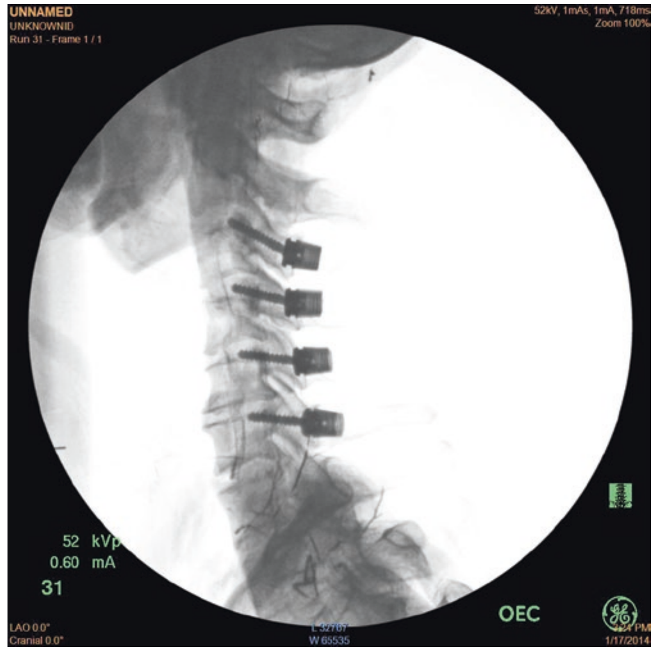

Fig. 2.98 Lateral intraoperative fluoroscopy of the lateral mass screw

Fig. 2.99 Entry points of pedicle screw and lateral mass screw

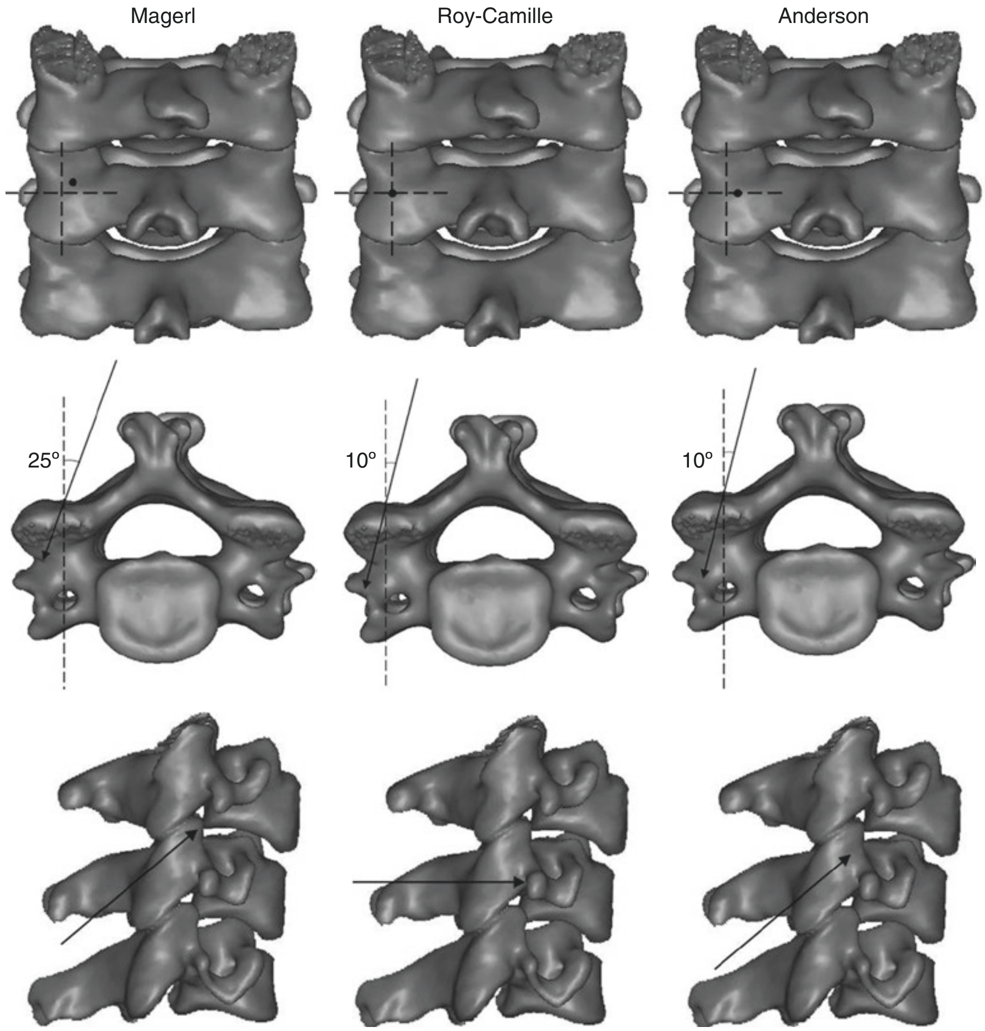

Fig. 2.100 Entrance point and trajectory of three commonly used lateral mass screw placement technique

Bibliography

1. Cauchoix J, Binet JP. Anterior surgical approaches to the spine. Ann R Coll Surg Engl. 1957;21(4):234.
2. Kurz LT, Pursel SE, Herkowitz HN. Modified anterior approach to the cervicothoracic junction. Spine. 1995;20(13):1519–21.
3. Melamed H, Harris MB, Awasthi D. Anatomic considerations of superior laryngeal nerve during anterior cervical spine procedures. Spine. 2002;27(4):83–6.
4. Beutler WJ, Sweeney CA, Connolly PJ. Recurrent laryngeal nerve injury with anterior cervical spine surgery risk with laterality of surgical approach. Spine. 2001;26(12):1337–42.
5. Oh SH, Perin NI, Cooper PR. Quantitative three-dimensional anatomy of the subaxial cervical spine: implication for anterior spinal surgery. Neurosurgery. 1996;38(6):1139–44.
6. Frykholm R. Lower cervical vertebrae and intervertebral discs; surgical anatomy and pathology. Acta Chir Scand. 1951;101(5):345.
7. Russell SM, Benjamin V. The anterior surgical approach to the cervical spine for intervertebral disc disease. Neurosurgery. 2004;54(5):1144–9. discussion 1149
8. Baker ADL. The treatment of certain cervical- spine disorders by anterior removal of the intervertebral disc and interbody fusion. In: Classic papers in orthopaedics. London: Springer; 2014. p. 607–24.
9. Wang Z, Jiang W, Li X, et al. The application of zero-profile anchored spacer in anterior cervical discectomy and fusion. Eur Spine J. 2015;24(1):148–54.
10. Chiba K, Ogawa Y, Matsumoto M, et al. Expansive open-door laminoplasty for ossification of the posterior longitudinal ligament of the cervical spine: surgical indications, technique, and outcomes. In: OPLL. Japan: Springer; 2006. p. 193–9.
11. Hirabayashi K, Watanabe K, Wakano K, et al. Expansive open-door laminoplasty for cervical spinal stenotic myelopathy. Spine. 2001;8(7):693.
12. Yin HF. The complications of posterior approach for cervical spondylitis and its prevention and treatment. Chin J Spine Spinal Cord. 1992;2:134–139.
13. Banovetz JM, Sharp R, Probe RA, et al. Titanium plate fixation: a review of implant failures. J Orthop Trauma. 1996;10(6):389–94.
14. Zhang J, Tsuzuki N, Hirabayashi S, et al. Surgical anatomy of the nerves and muscles in the posterior cervical spine: a guide for avoiding inadvertent nerve injuries during the posterior approach. Spine. 2003;28(13):1379–84.
15. Verbiest H. Anterolateral operations for fractures and dislocations in the middle and lower parts of the cervical spine. J Bone Joint Surg Am. 1969;51(8):1489.
16. Verbiest H. A lateral approach to the cervical spine: technique and indications. J Neurosurg. 1968;28(3):191.

17. Gilsbach JM. Extreme lateral approach to intradural lesions of the cervical spine and foramen magnum. Neurosurgery. 1990;27(2):197–204.
18. Kratimenos GP, Crockard HA. The far lateral approach for ventrally placed foramen magnum and upper cervical spine tumours. Br J Neurosurg. 1993;7(2):129–40.
19. Whitesides TE Jr, Kelly RP. Lateral approach to the upper cervical spine for anterior fusion. South Med J. 1966;59(8):879.
20. Hodgson AR. An approach to the cervical spine (C-3 TO C-7). Clin Orthop Relat Res. 1965;39(4):129.
21. Xu R, Grabow R, Ebraheim NA, et al. Anatomic considerations of a modified anterior approach to the cervicothoracic junction. Am J Orthop. 2000;29(1):37–40.
22. Mousa WF, Shimizu K, Ido K, et al. A modified transsternal approach to the cervicothoracic junction. Neuro-Orthopedics. 1998;24(1):21–31.
23. Maciejczak A, Radek A, Kowalewski J, et al. Anterior transsternal approach to the upper thoracic spine. Acta Chir Hung. 1999;38(1):83.
24. Lesoin F, Autricque A, Villette L, et al. A transsternalbiclavicular approach to the upper anterior thoracic spine. Surg Neurol. 1986;26(3):253.
25. Ikenaga M, Shikata J, Tanaka C. Anterior corpectomy and fusion with fibular strut grafts for multilevel cervical myelopathy. J Neurosurg Spine. 2005;3(3):79–85.
26. Eleraky MA, Llanos C, Sonntag VK. Cervical corpectomy: report of 185 cases and review of the literature. J Neurosurg. 1999;90(90):35–41.
27. Macdonald RL, Fehlings MG, Tator CH, Lozano A, Fleming JR, Gentili F, Bernstein M, Wallace MC, Tasker RR. Multilevel anterior cervical corpectomy and fibular allograft fusion for cervical myelopathy. J Neurosurg. 1997;86(6):990–7.
28. Sundaresan N, Shah J, Feghali JG. A transsternal approach to the upper thoracic vertebrae. Am J Surg. 1984;148(4):473–7.
29. Schulte K, Clark CR, Goel VK. Kinematics of the cervical spine following discectomy and stabilization. Spine. 1989;14(10):1116–21.
30. Böhler J, Gaudernak T. Anterior plate stabilization for fracture-dislocations of the lower cervical spine. J Trauma. 1980;20(3):203–5.
31. Aebi M, Zuber K, Marchesi D. Treatment of cervical spine injuries with anterior plating. Indications, techniques, and results. Spine. 1991;16(3 Suppl):38–45.
32. Kim HS, Suk KS, Moon SH, et al. Safety evaluation of freehand lateral mass screw fixation in the subaxial cervical spine: evaluation of 1256 screws. Spine. 2015;40(1):2–5.
33. Park JH, Jeon SR, Roh SW, et al. The safety and accuracy of freehand pedicle screw placement in the subaxial cervical spine: a series of 45 consecutive patients. Spine. 2014;39(4):280–5.
34. Tofuku K, Koga H, Komiya S. Cervical pedicle screw insertion using a gutter entry point at the transitional area between the lateral mass and lamina. Eur Spine J. 2012;21(2):353–8.
35. Li Y, Liu J, Liu Y, et al. Cervical pedicle screw fixation at C6 and C7: a cadaveric study. Indian J Orthop. 2015;49(4):465–70.
36. Zheng X, Chaudhari R, Wu C, et al. Subaxial cervical pedicle screw insertion with newly defined entry point and trajectory: accuracy evaluation in cadavers. Eur Spine J. 2010;19(1):105–12.
37. Stemper BD, Marawar SV, Yoganandan N, et al. Quantitative anatomy of subaxial cervical lateral mass: an analysis of safe screw lengths for Roy-Camille and magerl techniques. Spine. 2008;33(8):893–7.
38. Ebraheim NA, Klausner T, Xu R, et al. Safe lateral-mass screw lengths in the Roy-Camille and Magerl techniques. An anatomic study. Spine. 1998;23(16):1739–42.
39. Barrey C, Mertens P, Jund J, et al. Quantitative anatomic evaluation of cervical lateral mass fixation with a comparison of the Roy-Camille and the Magerl screw techniques. Spine. 2005;30(6):140–7.

3 Surgical Anatomy of the Thoracic Spine

Jian-gang Shi, Wen Yuan, and Jing-chuan Sun

1 Lateral Retropleural Thoracic Approach and Corpectomy for Spinal Decompression and Fusion

1.1 Overview

The transthoracic approach was first proposed by Robinson in 1917 for pulmonary lobectomy. In 1956, Hodgson and Stock first used the transthoracic approach to perform anterior lesion resection and bone graft of the thoracic spine and, henceforth, have popularized the technique spinal surgery. However, this approach requires the opening of the pleura and can result in various postoperative complications. As a result, this led to the development of the anterolateral retropleural approach. This approach is minimally invasive and does not require the opening of the chest cavity and thereby reduces the risk of surgery. The indications of this technique include anterolateral thoracic spinal decompression, thoracolumbar lesion resection or biopsy, anterior thoracic spinal fusion and internal fixation, and orthopedics of thoracic deformity.

1.2 Position

Patient is placed in a lateral position with the lower side cushioned to avoid compression of the axillary artery and vein. Palpate the radial artery to confirm the absence of compression (Fig. 3.1).

A double-lumen endotracheal tube is placed for selective one-lung ventilation.

Fig. 3.1 Position and incision of lateral retropleural thoracic approach

1.3 Exposure

The incision starts at two finger widths below the inferior angle of the scapula, usually the seventh or eighth rib. Make an arc-shaped incision anteriorly toward the inframammary fold, and extend posterosuperiorly in the direction of the thoracic spine. Incise the skin and subcutaneous tissue as shown in the Fig. 3.2 to reveal the latissimus dorsi muscle (Fig. 3.2).

J.-g. Shi (✉) • W. Yuan • J.-c. Sun
Department of Orthopedics, Changzheng Hospital,
Shanghai, China
e-mail: shijiangang616@163.com; yuanwenspine@163.com;
sjchxc@foxmail.com

J.-g. Shi et al. (eds.), *Anatomy Atlas and Interpretation of Spine Surgery*, https://doi.org/10.1007/978-981-10-5906-3_3

Fig. 3.2 Incision of the skin and subcutaneous tissues in the superficial layer to expose the deep fascia

Serratus anterior muscle: originates from the first to eighth or ninth rib at the side of the chest and ends at medial margin and inferior angle of the scapula. It is mainly supplied by the thoracodorsal artery and innervated by the long thoracic nerve (Fig. 3.3).

Long thoracic nerve: generally composed of the fifth to seventh cervical nerve roots. It runs between the anterior and middle scalene muscles and descends along the lateral side of the middle scalene muscle until the lateral margin of the serratus anterior muscle.

Lateral thoracic artery: originates from the second portion of the axillary artery. It runs along the lateral side of the pectoralis minor muscle to the fifth intercostal space through the deep surface of the pectoralis major muscle. It supplies the serratus anterior muscle, pectoral muscle, axillary lymph node, and subscapularis muscle.

Latissimus dorsi muscle: the large, flat, dorsolateral muscle at the lower part of the thoracic dorsal region and superficial layer of the lumbar region. It starts from the spinous processes of the lower sixth thoracic spine and the posterior layer of the thoracolumbar fascia and attaches to the waist, spinous process of the sacral spine, supraspinous ligament, and the posterior region of the iliac crest. The latissimus dorsi muscle is innervated by the thoracodorsal nerve, which is formed from the anterior branches of the fifth to seventh cervical nerves (Fig. 3.4).

Teres major muscle: a thick and flattened muscle that arises from one-third below the laterodorsal side of the inferior angle of the scapula and ends at the inner lip of the bicipital groove through a flat tendon. The teres major muscle is supplied by the subscapular artery and the thoracic dorsal branch of the latissimus dorsi muscle and posterior humeral circumflex artery. It is innervated by the subscapular nerve (Fig. 3.5).

Teres minor muscle: a narrow, elongated muscle of the rotator cuff that arises from two-thirds above the lateral border and adjacent posterior surface of the scapula. It ascends laterally and ends above the greater tubercle of the humerus and the starting point of the triceps muscles. It is supplied by the circumflex scapular artery and posterior circumflex scapular artery and innervated by the axillary nerve.

Fig. 3.3 Dissection of lateral thorax wall muscle superficial layer

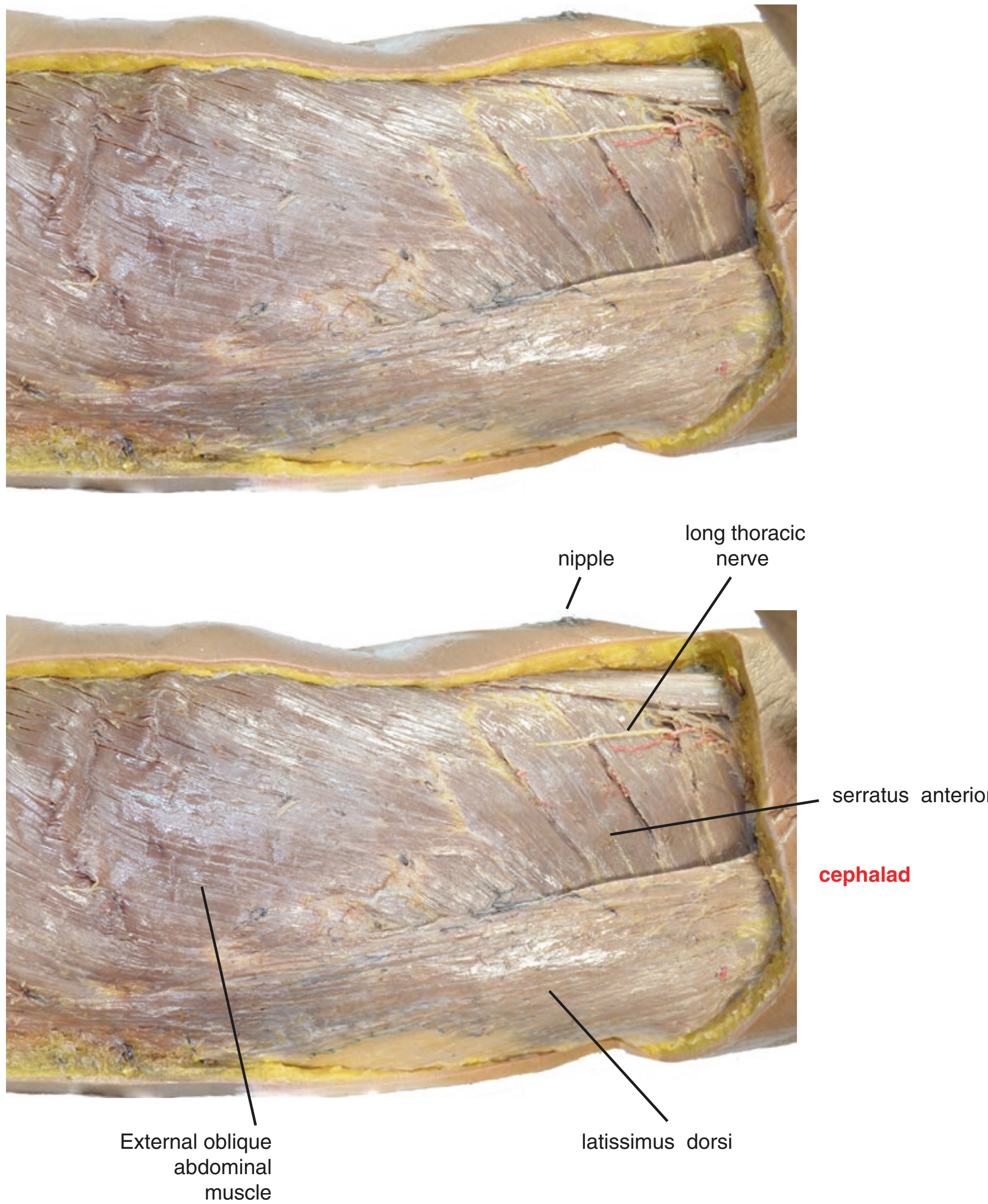

Fig. 3.4 Latissimus dorsi muscle

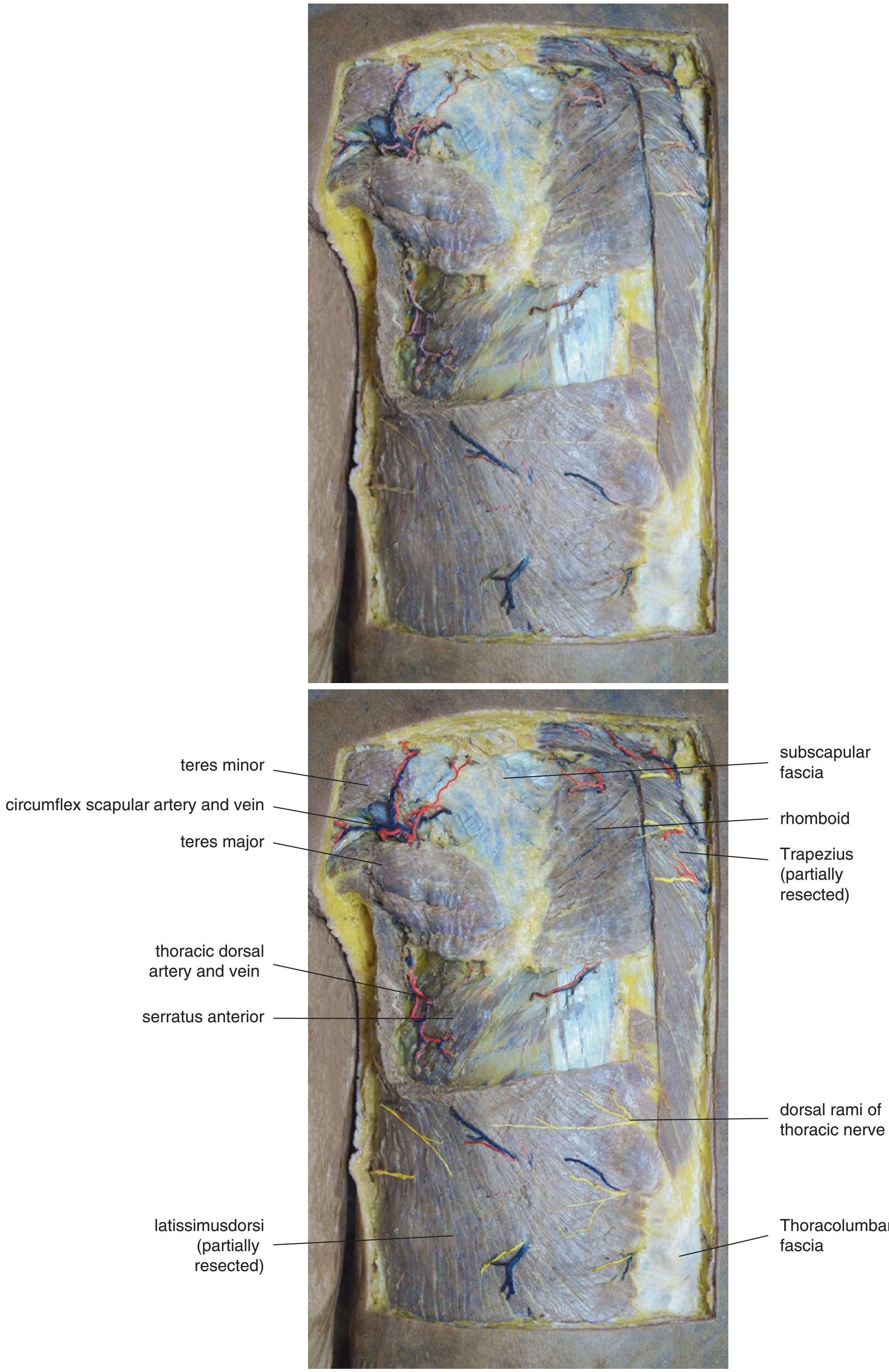

Fig. 3.5 Anatomy of the blood vessels and nerves in the scapular region (latissimus dorsi and trapezius muscles resected)

The trapezius muscle and latissimus dorsi muscle are dissected at the rib near the spine. Retain the muscle attachment point at the inferior angle of scapula for postoperative repair (Fig. 3.6).

The serratus anterior muscle is splitted along the incision to reveal the ribs and external intercostal muscles (Fig. 3.7). The scapularis is lifted to further split the muscle. The rhomboid muscle can also be dissected.

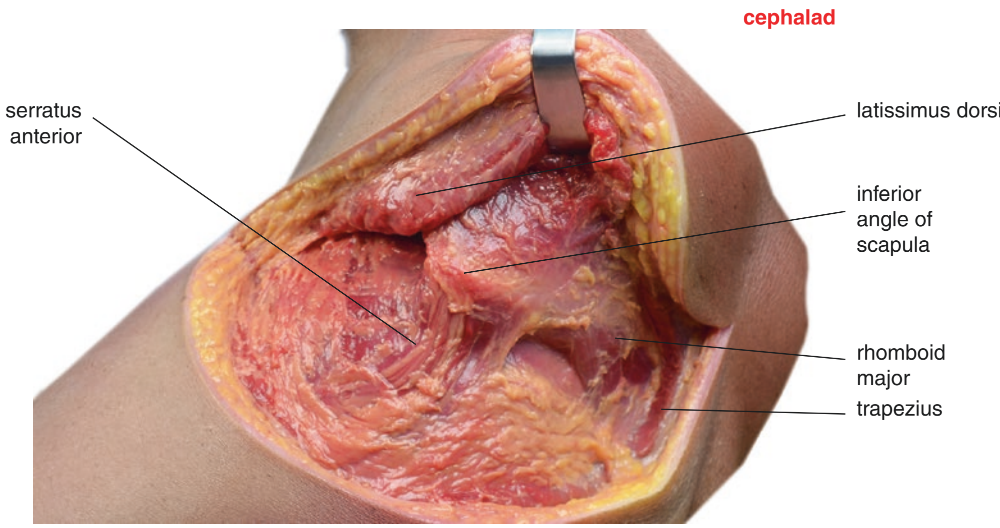

Fig. 3.6 Incision of the trapezius muscle and latissimus dorsi muscle to expose the inferior angle of the scapula

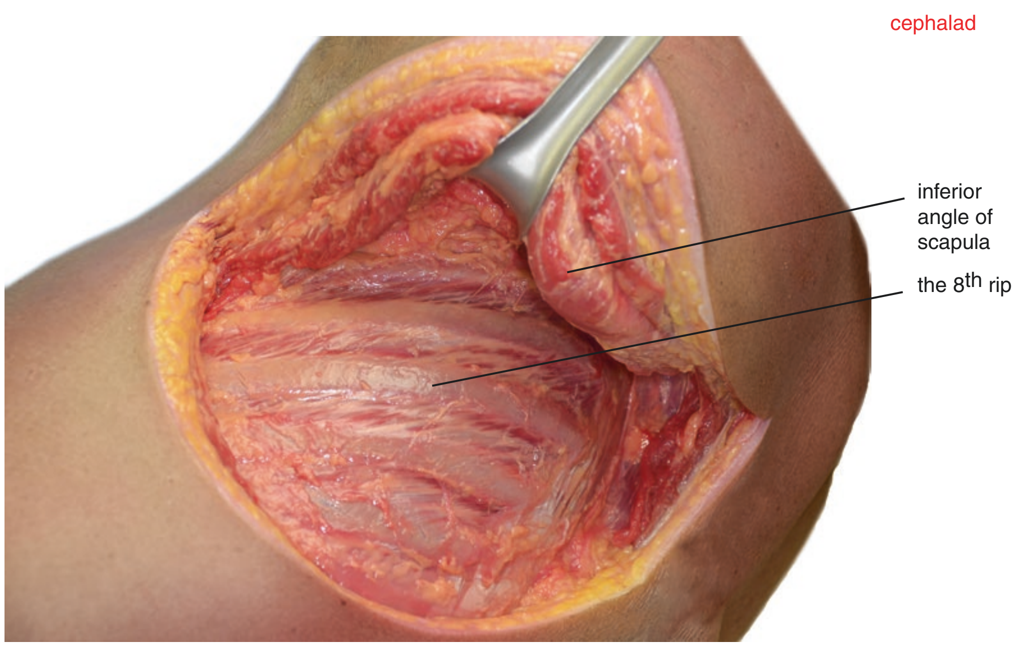

Fig. 3.7 The serratus anterior muscle is splitted to expose the ribs

External intercostal muscles: the muscle fibers start from the inferior border of the upper rib and ends at the superior border of the lower rib. The external intercostal muscles are thicker than the internal intercostal muscles, and they run obliquely downward in an anteromedial direction. It is innervated by the intercostal nerve and functions to lift the rib and assist with breathing (Fig. 3.8).

Spinal erector muscles: a bundle of long muscles at the rear vertebral column, starting from the dorsal surface of the sacrum to the posterior of the occipital bone within the groove between the spinous process and costal angle. It is divided into three parts, namely, the iliocostalis on the lateral side, longissimus in the middle, and spinalis on the medial side (Fig. 3.9).

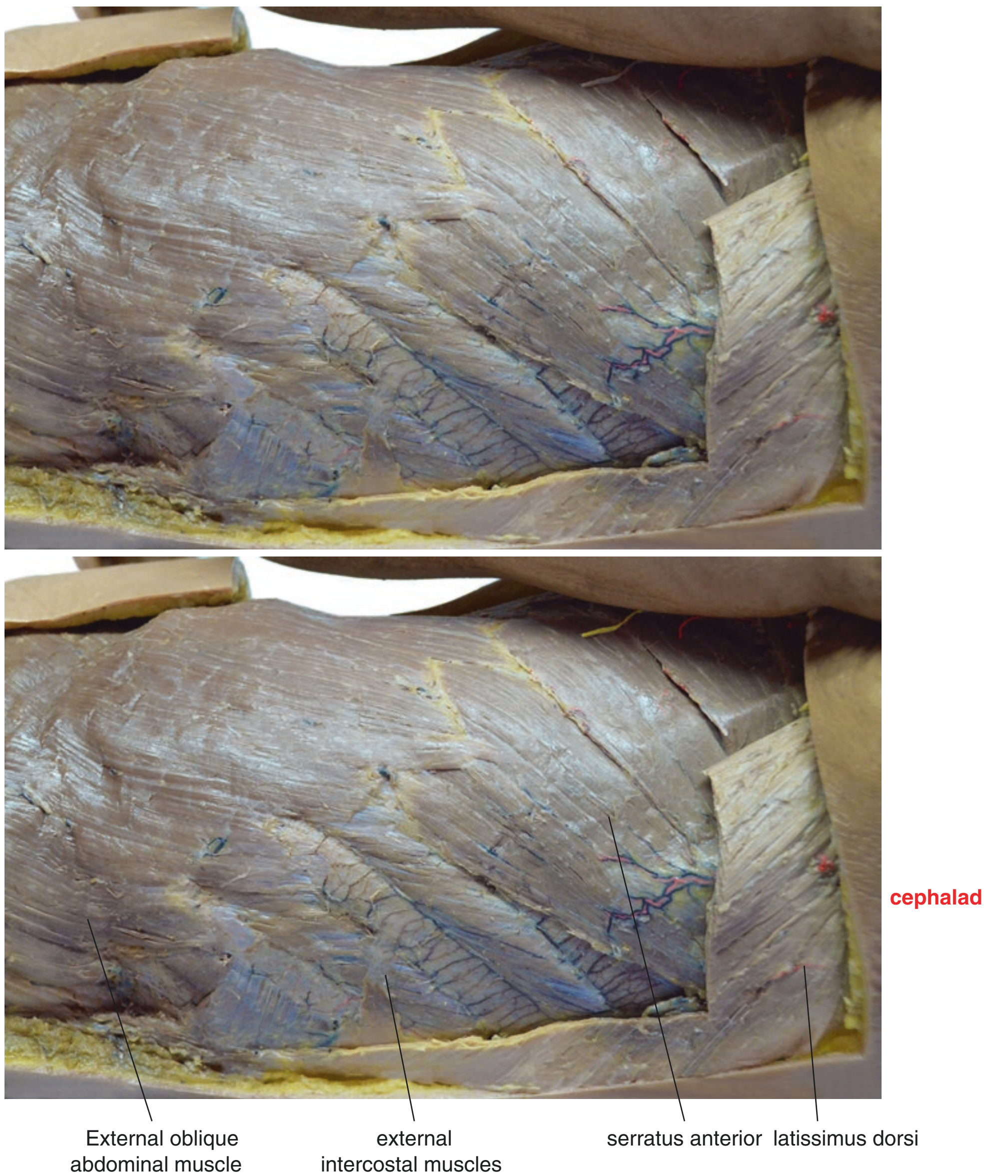

Fig. 3.8 Anatomy of muscles on lateral thorax wall

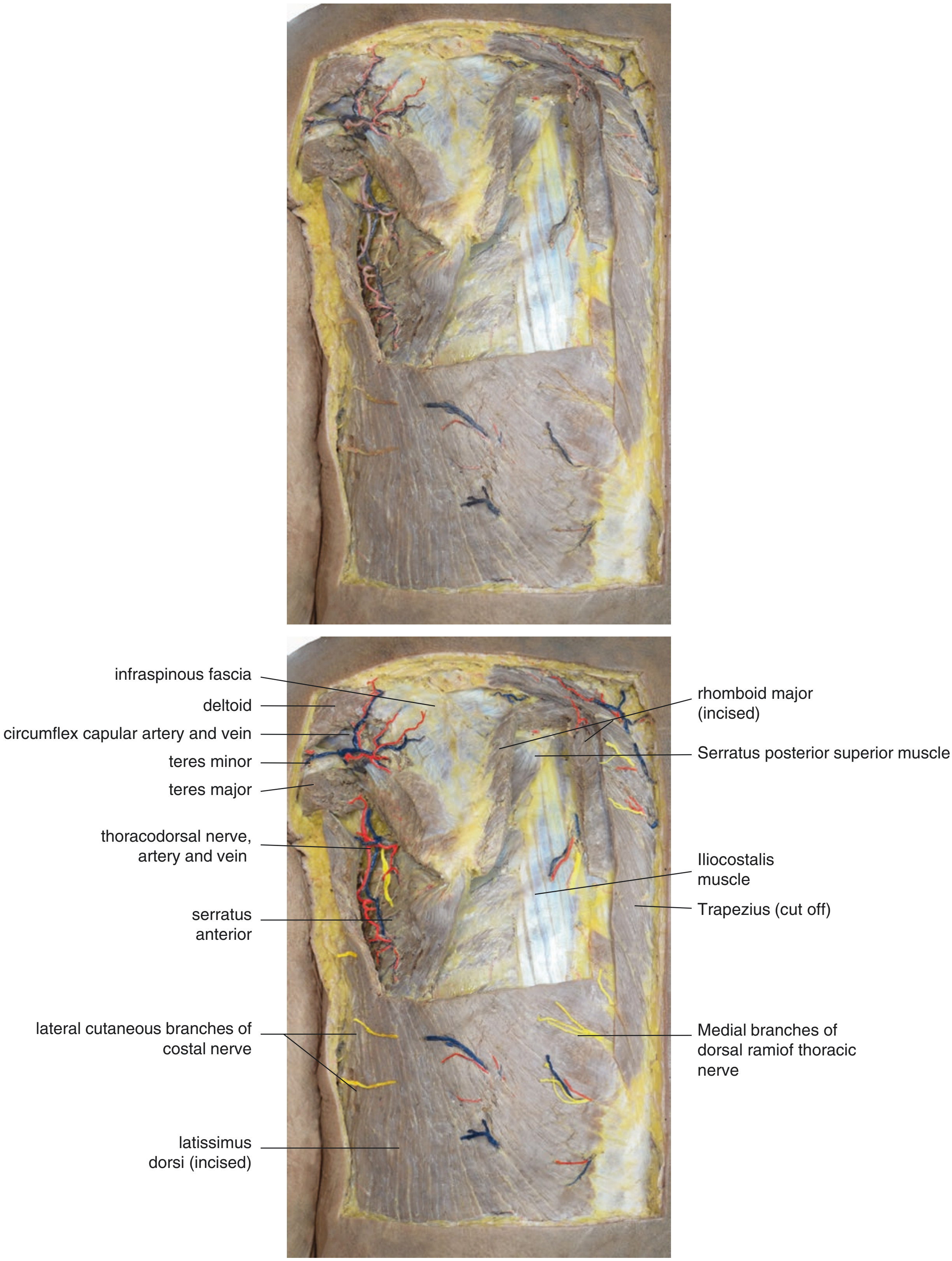

Fig. 3.9 Anatomy of the deep neurovasculature and muscles in the scapular region

Blunt dissection of the intercostal muscle from the ribs is done with a rib detacher. Avoid damaging the blood vessel and nerve below the ribs.

Blunt dissection of the muscle should be done in a posterior to anterior direction from the superior border of the rib and in an anterior to posterior direction from the inferior border of the rib (Fig. 3.10).

Internal intercostal muscles: 11 pairs of muscles that commence anteriorly at the sternum and extend backward to the angles of the ribs. Each muscle arises from the ridge on the inner surface of the rib, as well as from the corresponding costal cartilage, and is inserted into the superior border of the rib below. Their fibers run obliquely, almost perpendicular to the external intercostal muscles. The muscles are innervated by the adjacent intercostal nerves and function to lower the rib and assist with breathing (Fig. 3.11).

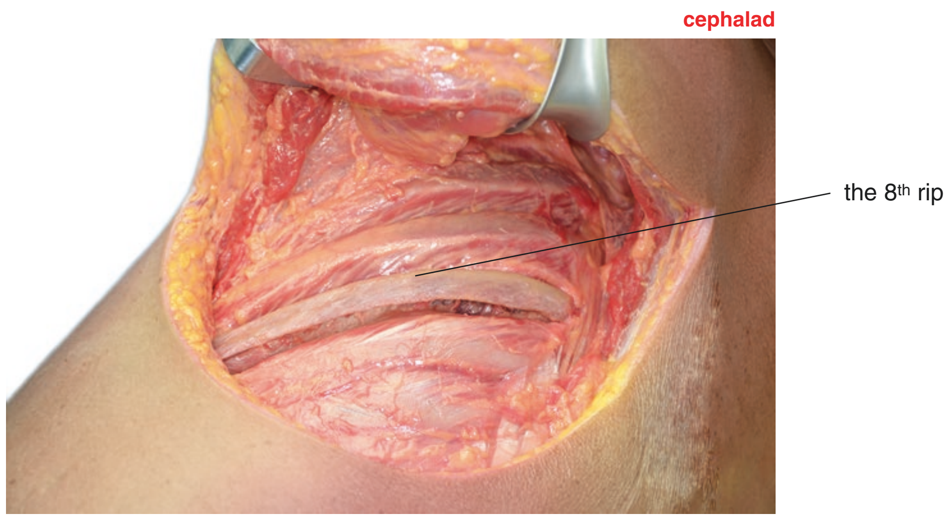

Fig. 3.10 Subperiosteal dissection of the rib

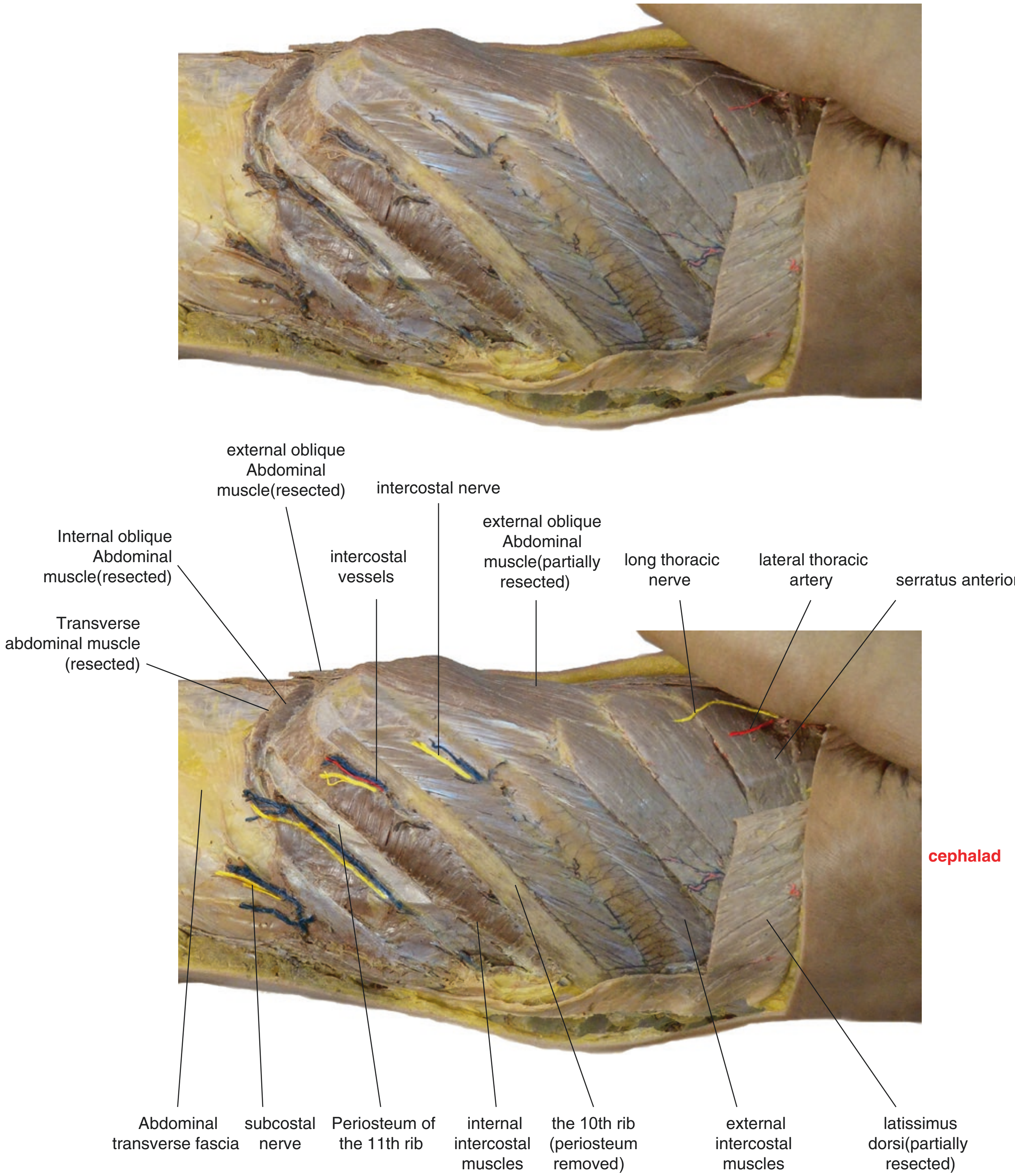

Fig. 3.11 Anatomy of the intercostal muscles (periosteum of the tenth rib removed)

The rib is cut at about 2 cm near the costotransverse joint at the proximal end and at the costal cartilage joint at the distal end. At this time, the anesthetist should change from bilateral ventilation to unilateral pulmonary ventilation to collapse the lung at the operative side.

The periosteum on the rib is carefully resected. The parietal pleura is dissociated from the chest wall as a result of the negative pressure in the chest cavity.

Under the protection of a thin pad, distract the incision of the chest wall with a chest wall retractor, and dissociate the parietal pleura from the chest wall (Fig. 3.12).

The lung and pleura are retracted anteriorly to reveal the posterior wall of the thoracic cavity and gradually expose the head of ribs and lateral thoracic spine along the chest wall (Fig. 3.13).

The target segment is confirmed by C-arm fluoroscopy (Fig. 3.14).

Ligate the segmental vessels at the target segment. Electrocautery is not recommended. The vessels should be dissected at the center part of the lateral vertebral body; otherwise, religation will not be possible after the vessels have retracted.

The posterior two-thirds of the target vertebrae together with the intervertebral discs above and below were removed with curettes and rongeurs. The posterior annulus fibrosis and longitudinal ligament must be removed to achieve thorough decompression of the spinal canal (Fig. 3.15).

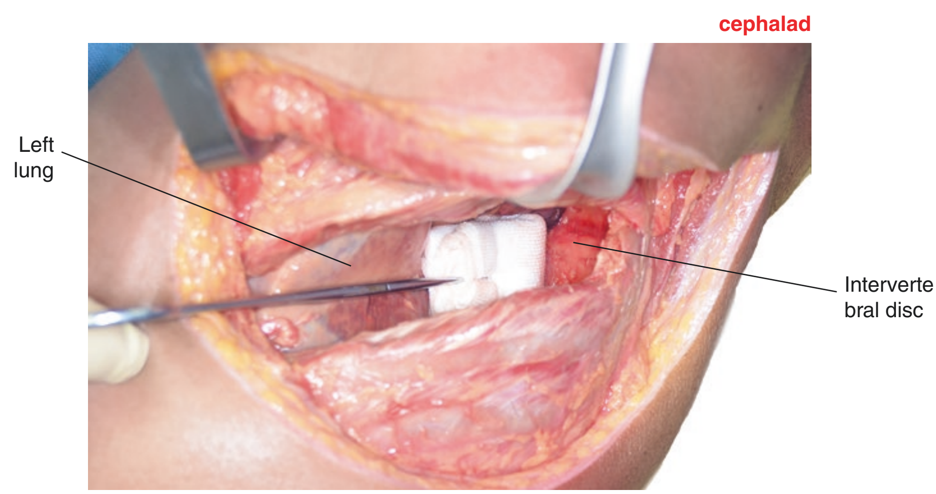

Fig. 3.12 Resected the rib to separate the pleura parietalis

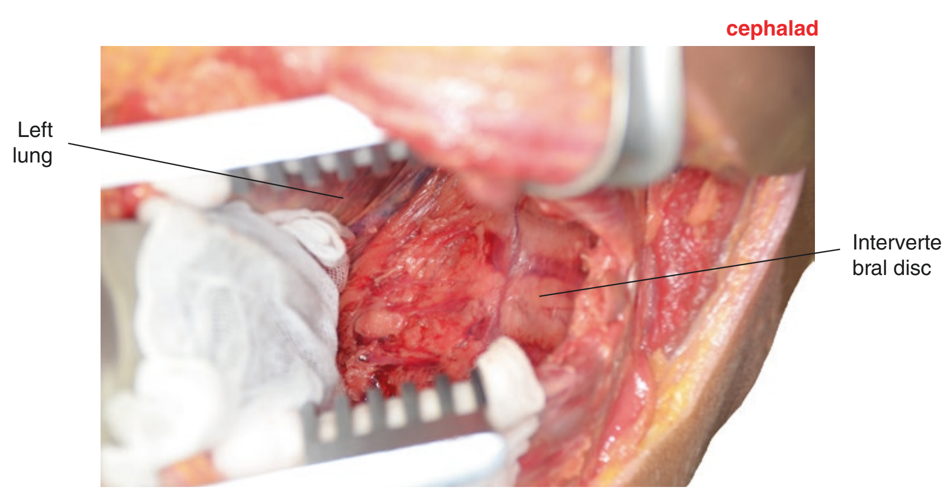

Fig. 3.13 Exposure of the head of ribs and lateral thoracic spine along the chest wall

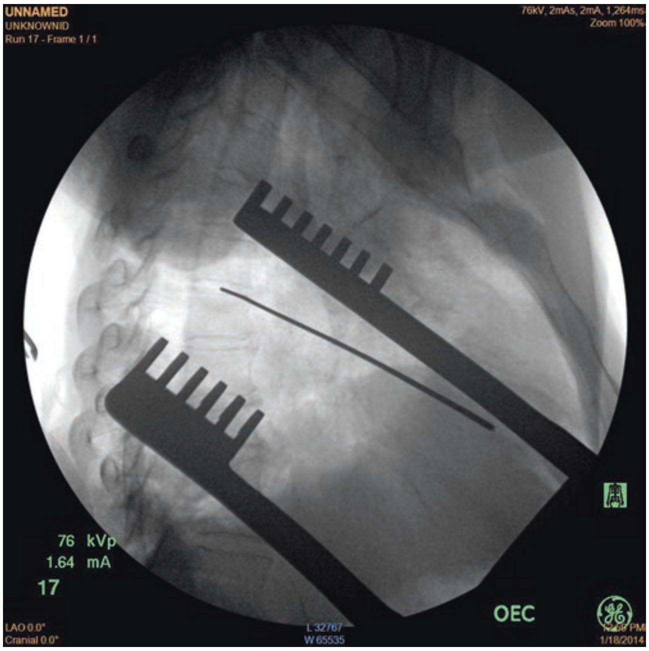

Fig. 3.14 Location of the target segment is confirmed by intraoperative fluoroscopy

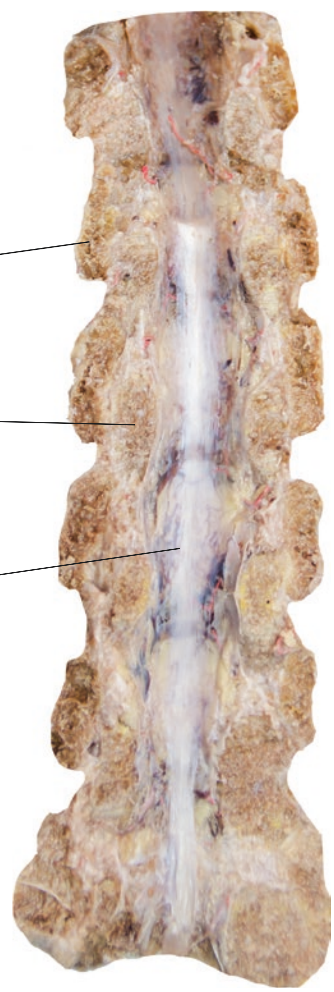

Fig. 3.15 Posterior longitudinal ligament of the thoracic spine

Azygos vein: generally arises from the inferior vena cava below the level of the renal vein. It can arch over or pass through the right crus of diaphragm posteriorly or pass the aortic hiatus at the right side of cisterna chyli. The right greater splanchnic nerve, right lung, and pleura are located at its right side. The thoracic duct and thoracic aorta are located on its left side for most of its course, and the esophagus, trachea, and vagus nerve are on its left while it arches anteriorly. Below the chest, the anterior of the azygos vein is covered by the right pleura capsule fossae and esophagus. It ascends through the posterior of the right lung hilum after leaving the rear of the esophagus (Fig. 3.16).

Thoracic duct: the thoracic duct passes through the aortic hiatus near the inferior border of the twelfth thoracic vertebra and ascends within the posterior mediastinum between the thoracic aorta and azygos vein. The diaphragm and esophagus are located in front of the duct. The thoracic duct runs obliquely to the left and enters the superior mediastinum at the T5 vertebral level and then ascends to the superior thoracic aperture along the left margin of the esophagus. When the thoracic duct enters the neck, it arches outward at the level of the transverse process of the seventh cervical spine, and the arch is 3–4 cm above the clavicle. It then descends along the anterior of the left subclavian artery and ends at the junction of the left subclavian vein and internal jugular vein (Fig. 3.17).

Descending thoracic aorta, hemiazygos vein, left sympathetic trunk, and greater splanchnic nerve are observed when using the left-sided approach (Fig. 3.18).

Thoracic aorta: a continuation of the aortic arch which begins at the inferior border of the fourth thoracic vertebra and descends along the left side of the vertebral column. Starting from below the seventh thoracic vertebra, the thoracic aorta gradually moves toward the midline and runs anterior to the vertebral column, until it perforates through the aortic hiatus at the twelfth thoracic vertebra and becomes the abdominal aorta (Fig. 3.18).

Hemiazygos vein: arises from the left side of the vertebral column and runs upward to the level of the eighth thoracic vertebra along the anterior of the vertebral column. It then crosses the vertebral column behind the aorta, esophagus, and thoracic duct and stops at the azygos vein. Its branches include three posterior intercostal veins, left lumbar ascending vein, and the venous branches of the esophagus and mediastinum (Fig. 3.18).

Accessory hemiazygos vein: ascends along the left side of the vertebral column and receives the posterior intercostal veins from the fourth (or fifth) to eighth intercostal space, as well as the left bronchial vein. It crosses the seventh thoracic vertebra and joins the azygos vein. Sometimes, it can also end in the hemiazygos vein, with its trunk arising from the azygos vein.

Greater splanchnic nerve: about 95% of the nerve is composed of preganglionic fibers that run inwardly from the T5 to T9 sympathetic ganglia. The greater splanchnic nerve runs downward along both sides of the thoracic aorta, and about 75% of the nerve enters the abdominal cavity through the middle crus and medial crus of the diaphragm and stops at the lateral superior region of the celiac ganglia. The left greater splanchnic nerve is located about 3 mm to the left border of the aorta (Fig. 3.18).

There is one thoracic sympathetic trunk on the left and right sides of the vertebral column. They are located anteriorly to the head of ribs, bilaterally to the thoracic vertebrae, and posterolaterally to the azygos, hemiazygos, and accessory hemiazygos veins. There are 10–12 thoracic ganglions along the thoracic sympathetic trunk on each side of the vertebrae, wherein the cervical thoracic ganglion is usually formed by the first thoracic ganglion and inferior cervical ganglion (Fig. 3.18).

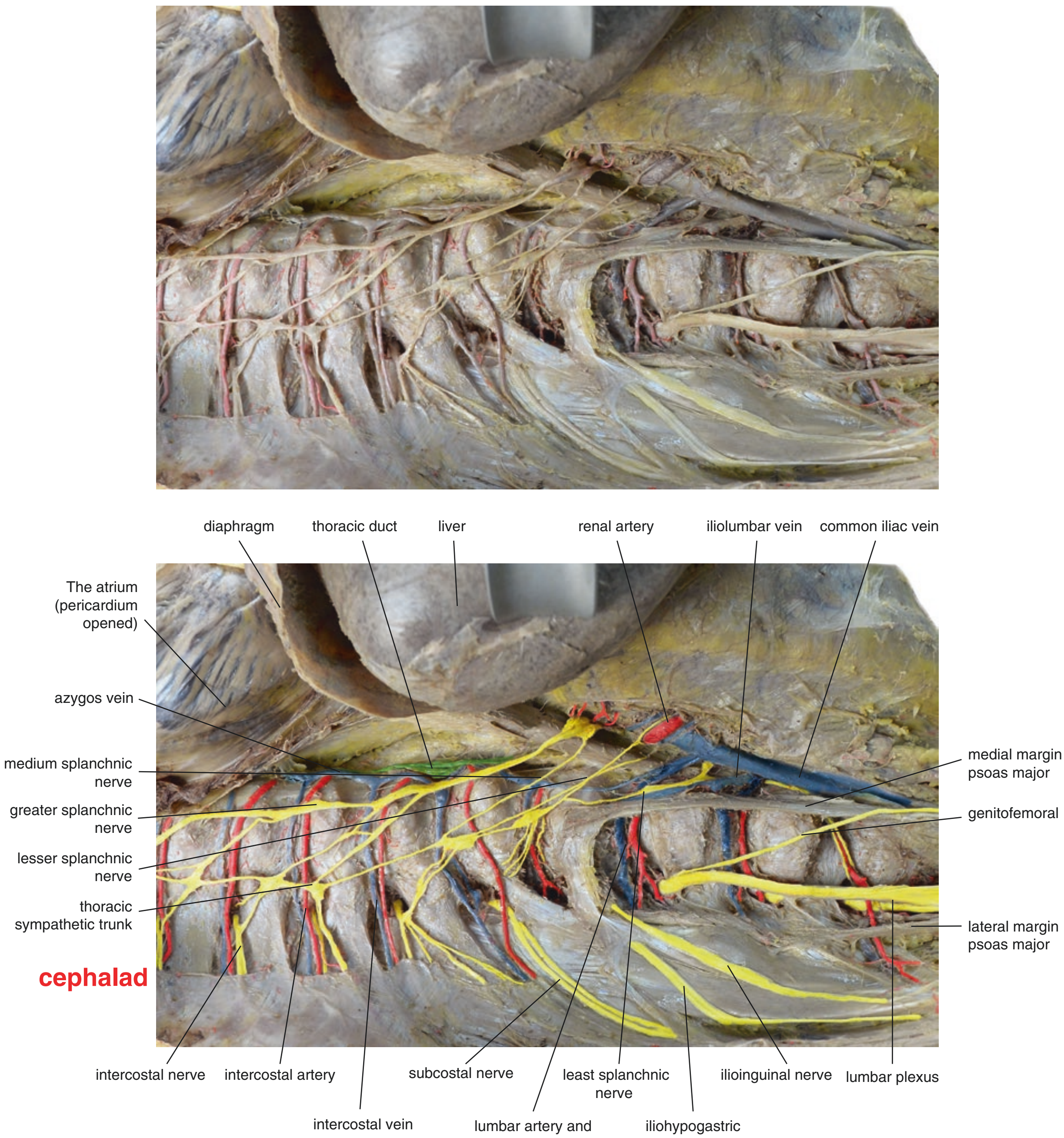

Fig. 3.16 Lateral structures of the thoracolumbar vertebrae on the right

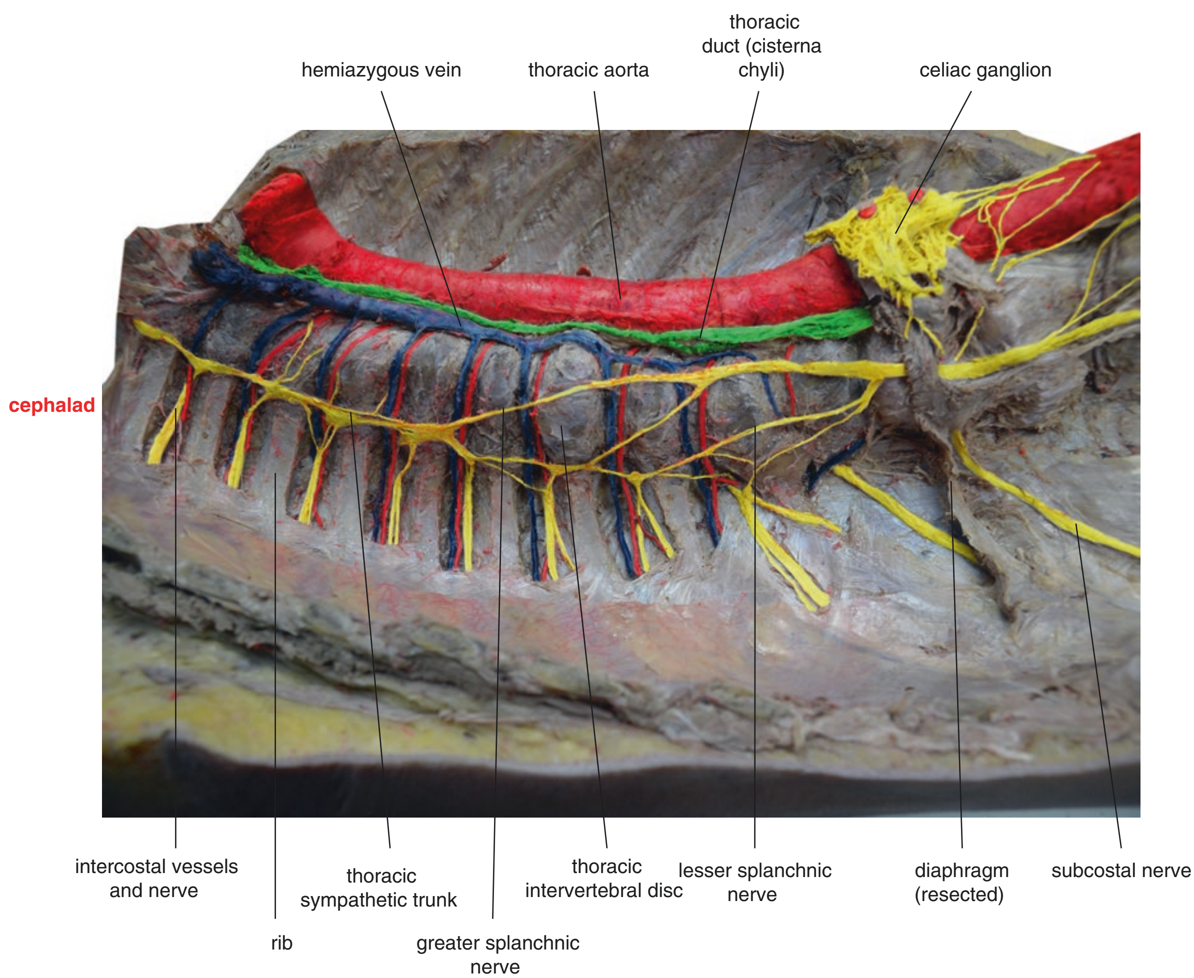

Fig. 3.17 Neurovascular structures on the right of the thoracic spine

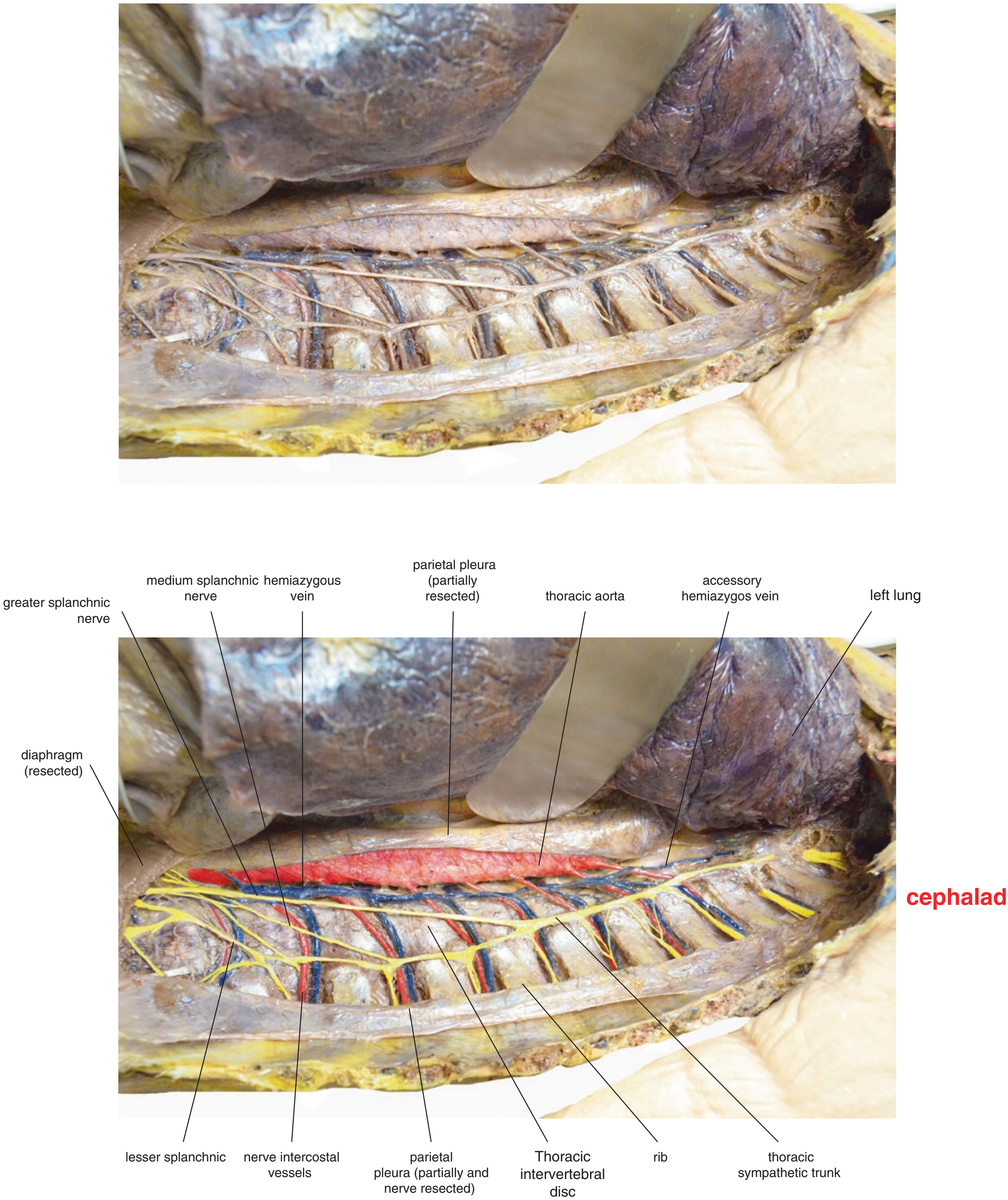

Fig. 3.18 Neurovascular structures on the left of the thoracic spine

The titanium mesh prefilled with bone fragments is knocked into the vertebral defect after endplates are prepared.

The screw with the proper length should be placed into the adjacent vertebral body. Compression and fixation of the rod are subsequently performed.

The titanium mesh, screw, and rod are in good position as seen in intraoperative lateral and anteroposterior fluoroscopy (Figs. 3.19 and 3.20).

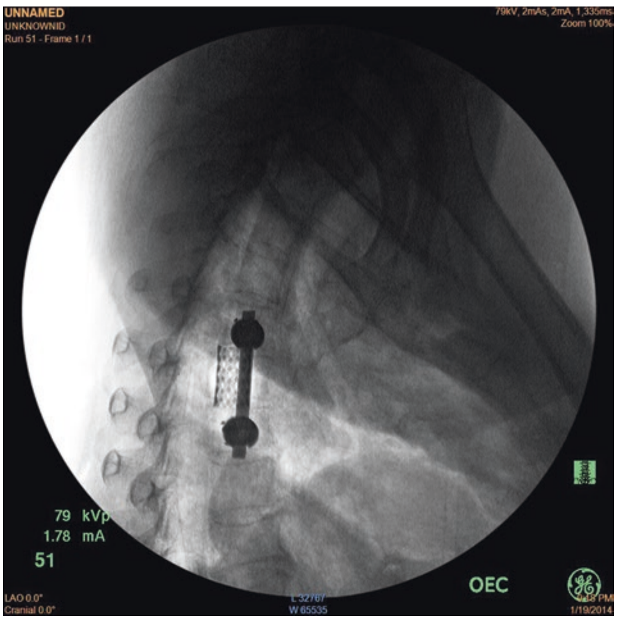

Fig. 3.19 Titanium mesh, screw, and rod are in good position as seen by intraoperative lateral fluoroscopy

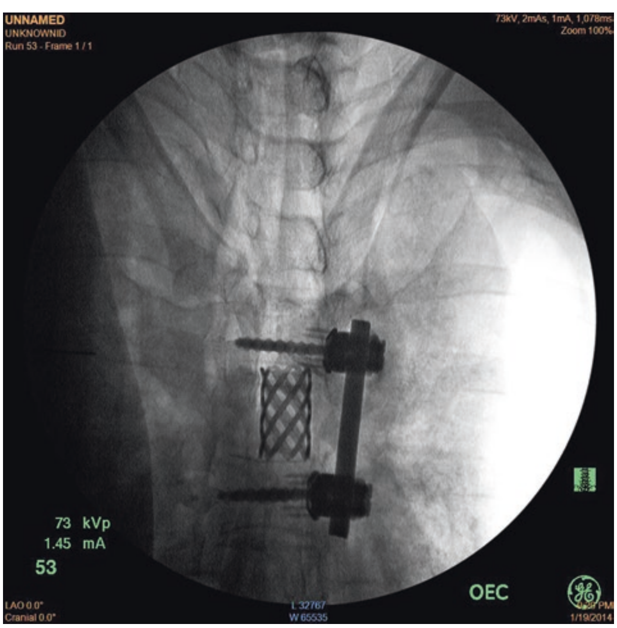

Fig. 3.20 Titanium mesh, screw, and rod are in good position as seen by intraoperative anteroposterior fluoroscopy

2 Posterolateral Thoracic Spine Exposure

2.1 Overview

Exposure of the upper thoracic spine is difficult with the transthoracic approach. The transthoracic approach not only has a high risk, but it also results in a high incidence of complications. Although the posterior approach is relatively safer and simpler, the field of vision and operational space is limited and insufficient for exposing the anterior spinal cord and vertebral body. The posterolateral approach is more suitable for treating lesions on the lateral side of the thoracic spine, especially for abscess drainage, vertebral biopsy, partial corpectomy, limited anterior spinal fusion, anterolateral spinal decompression, and tumor resection.

2.2 Position

Patient is placed in a prone position, with both arms placed on both sides of the head.

The thorax and iliac bone are padded to prevent respiratory obstruction and to promote venous drainage (Fig. 3.21).

2.3 Exposure

An arc-shaped incision is made on the lesion side along with the midline. The incision should cover 1–2 segments above and below the target segment (Fig. 3.22).

The subcutaneous tissue and deep fascia are dissected and retracted to expose the trapezius muscle. The trapezius muscle is retracted toward the spinous process.

The rhomboid muscle is retracted cephaladly or dissected along the skin incision.

Blunt dissection is done between the longissimus dorsi and spinalis thoracis muscles with a hemostatic forceps to expose the transverse process. Retract the spinalis thoracis medially and the longissimus dorsi and iliocostalis laterally to expose the tendon of the longissimus dorsi muscle, which is attached to the transverse process (Fig. 3.23).

Fig. 3.21 Position and incision of posterolateral thoracic spine approach

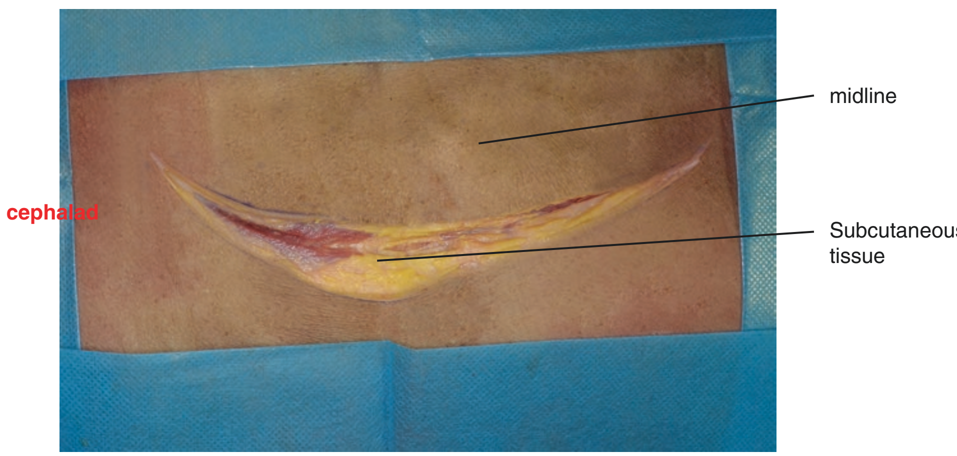

Fig. 3.22 Incision of the skin and subcutaneous tissue and exposure of the trapezius muscle

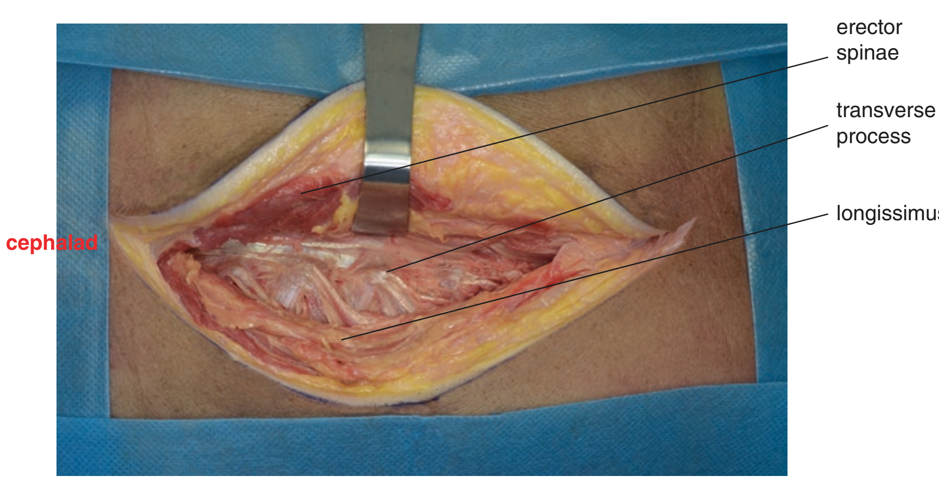

Fig. 3.23 Dissection of the muscles

Trapezius muscle: superficial muscle at the upper and middle back and is divided into the superior, intermediate, and inferior regions based on the direction of the muscle fibers. Contraction of the superior and inferior muscle bundles can lift and depress the scapulae, respectively, and contraction of the entire muscle can retract the scapulae toward the spine. The trapezius muscle arises from the external occipital protuberance, superior nuchal line, nuchal ligament, and the spinous processes from C7 to T12 vertebrae. The upper fibers end at lateral one-third of the clavicle and acromial process, while the middle and lower fibers end at the superior lip and apex of the spine of the scapula, respectively. The superior and intermediate regions of the trapezius muscle are mainly supplied by the superficial branch of the transverse cervical artery, while the intermediate and inferior regions are mainly supplied by the deep branch of the same artery. The trapezius muscle is innervated by the accessory nerve and the ventral rami of the third and fourth cervical nerves.

Rhomboid muscles: rhombus-shaped muscles located at the deep surface of the trapezius muscle which arise from the spinous process of the sixth cervical vertebra to the fourth thoracic vertebra and stop at the spinal border of the scapulae. The muscles are innervated by the dorsal scapular nerve, and their contraction retracts the scapulae toward the spine (Figs. 3.24, 3.25, and 3.26).

Serratus posterior superior muscle: a quadrilateral muscle situated at the lateral side of the upper back part of the thorax, superficial to the thoracolumbar fascia and deep to the rhomboid muscles. It arises from the lower part of the nuchal ligament, the spinous processes of the sixth and seventh cervical vertebrae and the first and second thoracic vertebrae. The muscle fibers incline downward and lateralward and end at the lateral surface of the second to fifth angle of rib. Its main function is to elevate the rib to assist breathing, and it is innervated by the second to fifth intercostal nerves.

Subperiosteal dissection of muscles attached to the ribs with a periosteal elevator to expose the transverse processes and ribs (Fig. 3.27).

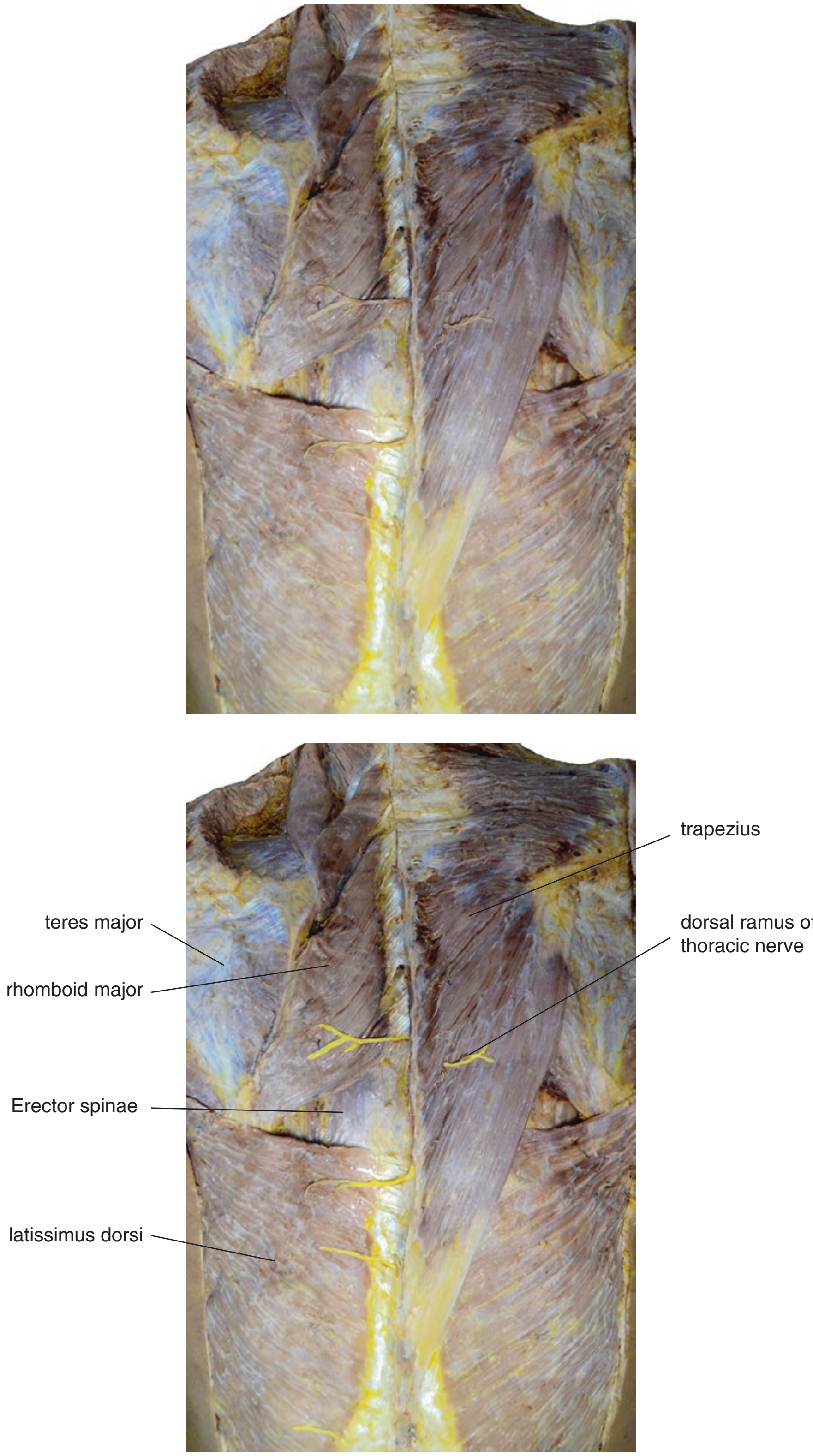

Fig. 3.24 Posterior superficial muscles of the thoracic spine

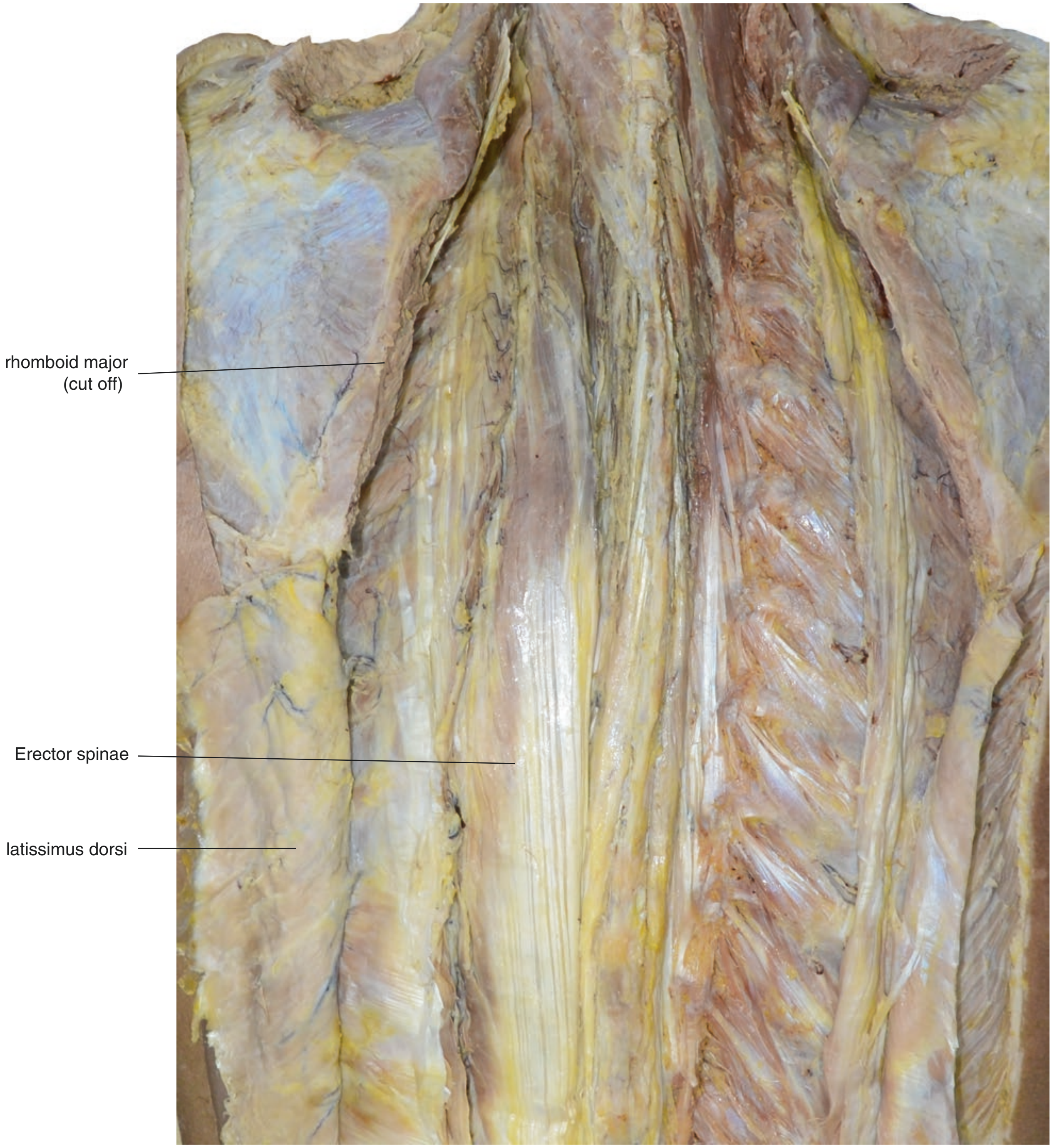

Fig. 3.25 Posterior deep muscles of the thoracic spine

Fig. 3.26 Anatomy of the interscapular muscles

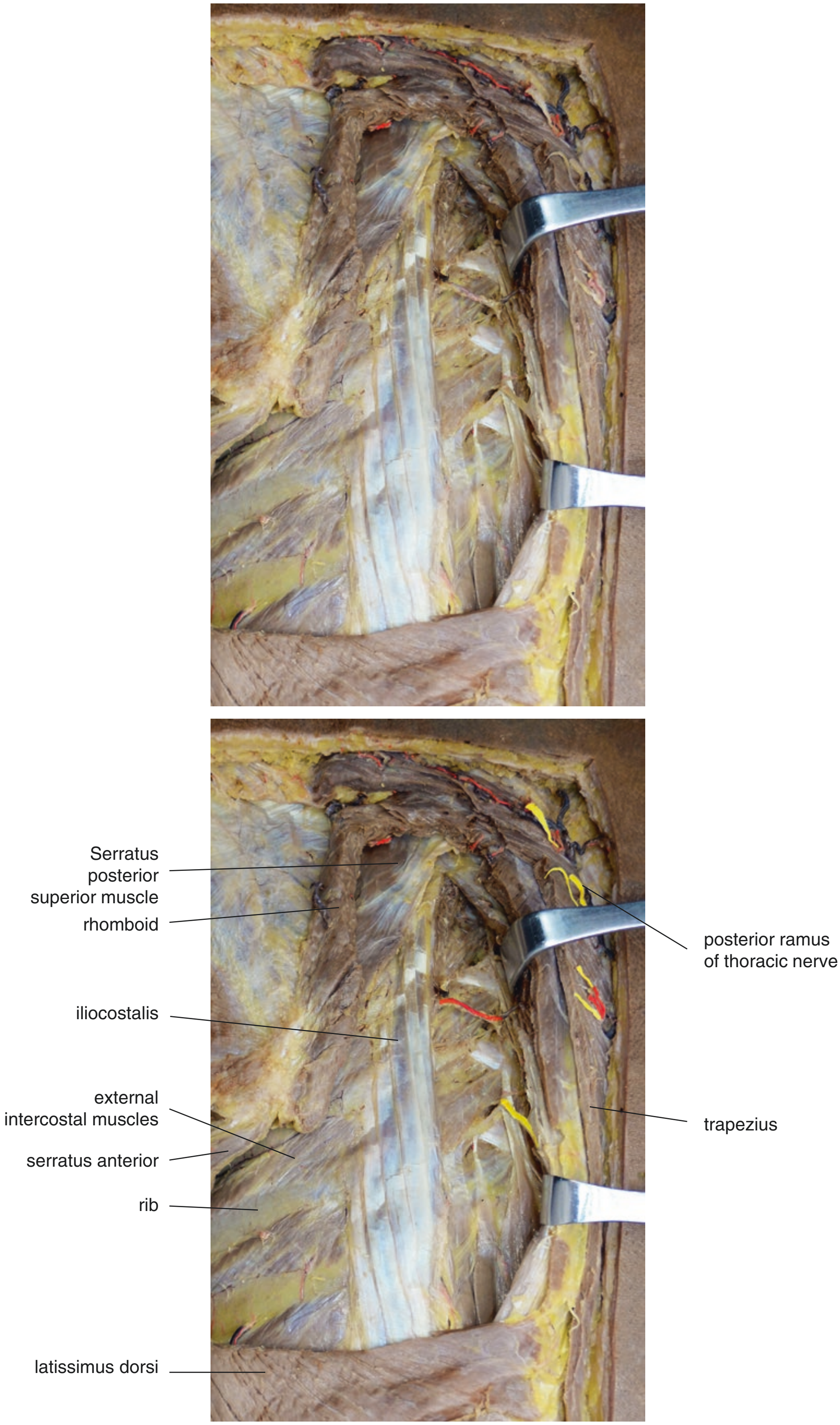

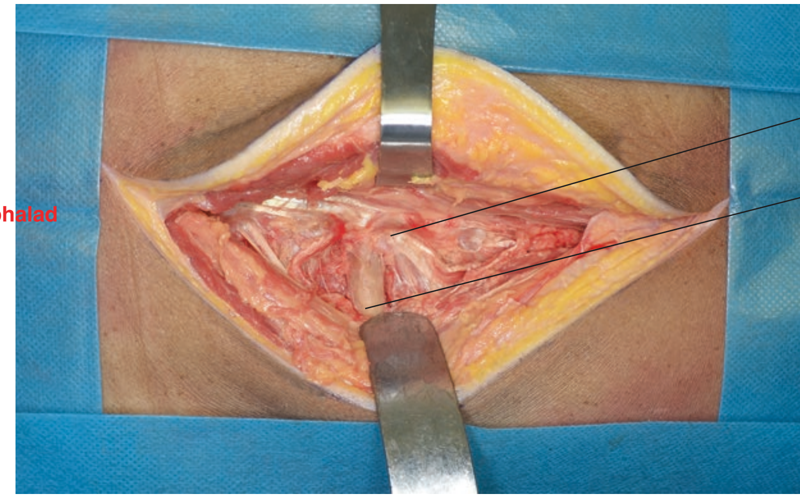

Fig. 3.27 Exposure of the transverse processes and ribs

Thoracic nerves: dorsal rami of the thoracic nerve roots run from the dorsolateral region of the body to the back and divide into medial and lateral branches. They proceed to the deep muscles on the back and innervate the adjacent muscles and skin within the region between the posterior midline and scapular line.

Posterior intercostal arteries: arise from the thoracic aorta and run between the endothoracic fascia and internal intercostal membrane of the third to eleventh intercostal spaces. Inferior branches of the arteries are emitted from the costal angle and run forward along the superior border of the lower rib. This trunk is also called as the superior branch and runs forward along the costal groove between the internal and innermost intercostal muscles (Fig. 3.28).

Muscles with tendons attached to the transverse process include head and neck muscles, semispinalis thoracis muscle, multifidus muscle, rotator muscles, and intertransversarii muscles.

Blunt dissection of the pleura from the excised rib and vertebral body by fingers.

The rib is resected at 6–8 cm from the midline. Lift the proximal end and strip further the periosteum and muscle around the rib to the costotransverse joint (Fig. 3.29).

Detach and remove the rib with a periosteal elevator, rotate the medial portion of the rib to complete the removal of the rib, and expose the lateral aspect of the thoracic spine (Fig. 3.29).

The transverse process is removed from the base with a Leksell Rongeur.

Subperiosteal dissection is performed on the lateral side of the spine from dorsal to ventral side to expose the vertebral bodies and discs (Fig. 3.30). Attention is paid to avoid injury to the vertical sympathetic trunk during this process.

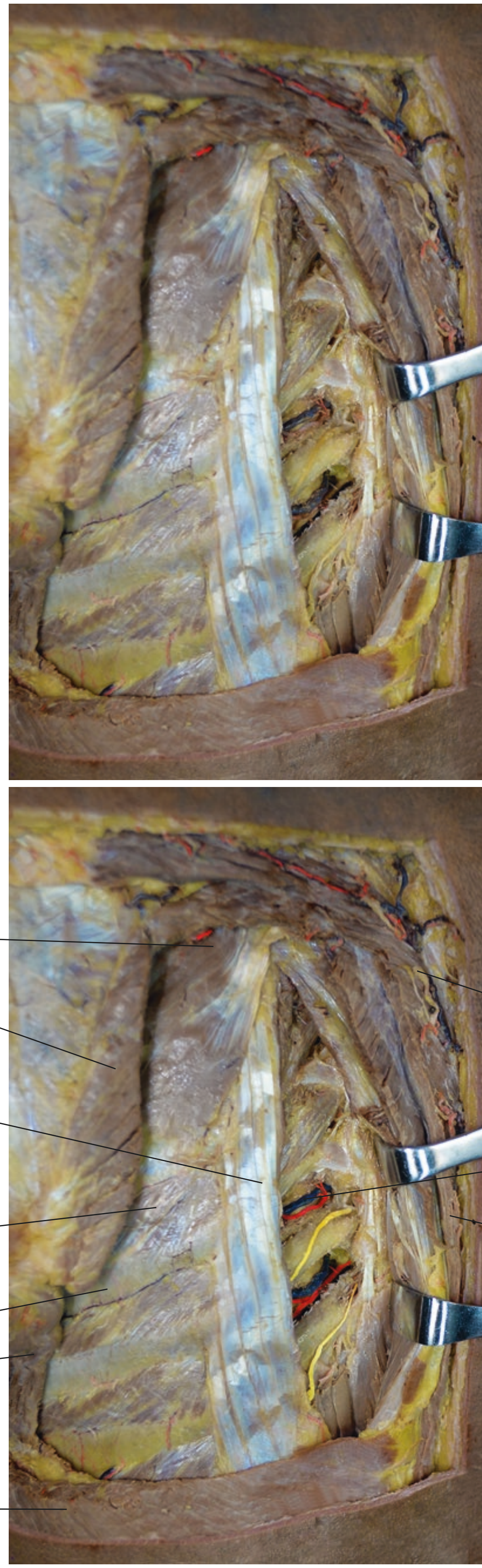

Fig. 3.28 Intercostal vessels and nerves

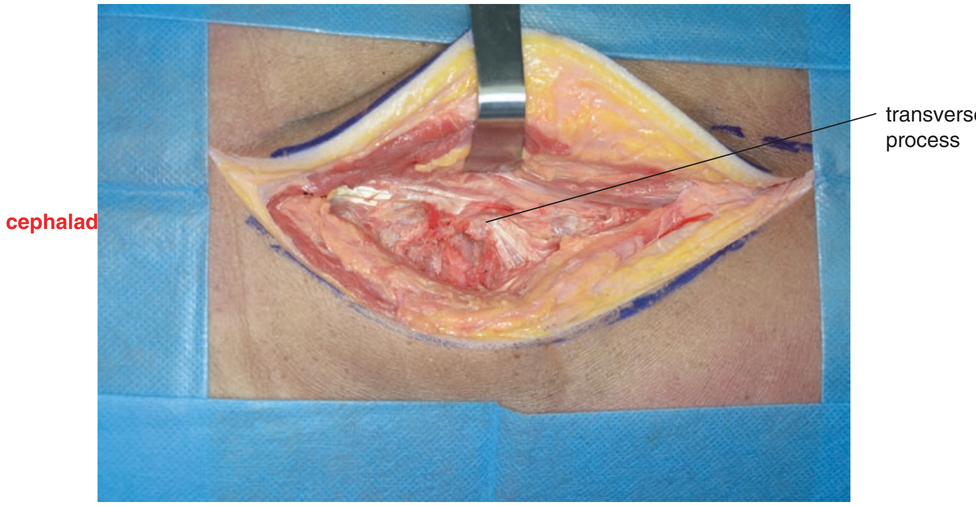

Fig. 3.29 Removal of the rib head

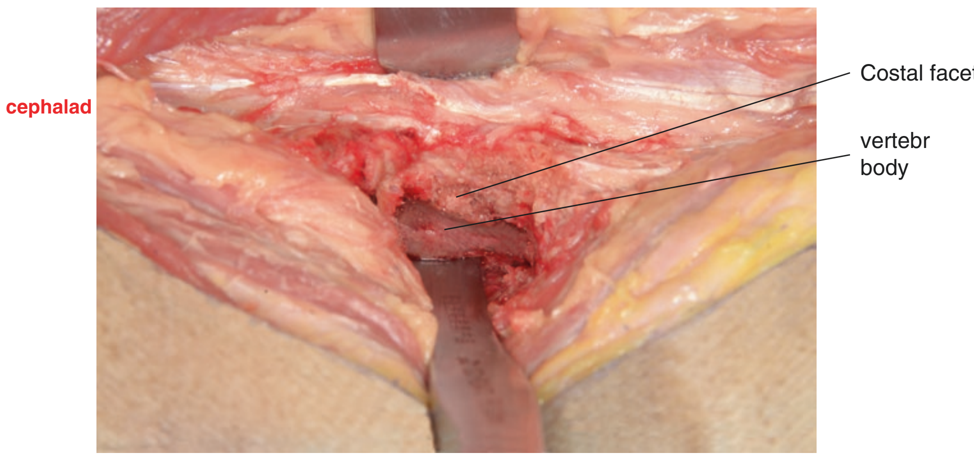

Fig. 3.30 Exposure of the vertebral bodies and discs

Thoracic sympathetic trunk: located in front of the rib head, on both sides of the thoracic spine, and at the posterolateral region of the azygos, hemiazygos, and accessory hemiazygos veins. The thoracic sympathetic trunk and intercostal nerves are connected by gray and white communicating branches (Fig. 3.31).

Intercostal nerves: run within the intercostal spaces between the endothoracic fascia and internal intercostal membrane and proceed forward along the costal groove between the internal and innermost intercostal muscles. Inferior branches are emitted near the costal angle, which proceed forward along the superior border of the lower rib. The intercostal nerves are also called the superior branches, which emerge superficially at about 1 cm lateral to the sternum.

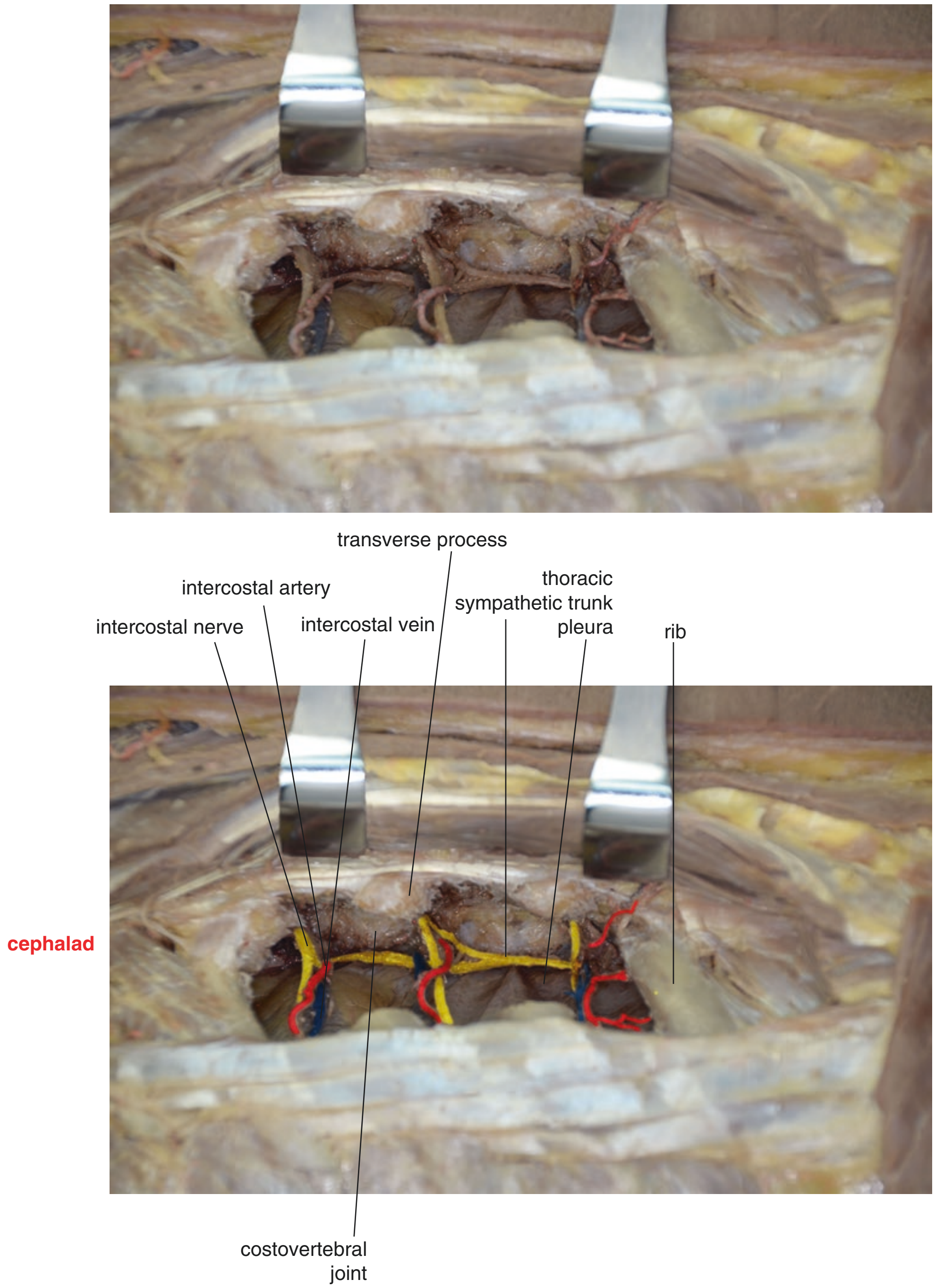

Fig. 3.31 Anatomical adjacency of the intercostal vessels and thoracic sympathetic trunk

3 Total En Bloc Spondylectomy of the Thoracic Spine

3.1 Overview

The total en bloc spondylectomy of the thoracic spine is mainly used for spinal tumor arising in thoracic spine. Posterior thoracic en bloc resection and reconstruction procedure has been demonstrated as an effective treatment for thoracic spinal tumors. The problems with traditional spinal piecemeal resection are the incomplete removal of tumors and high local tumor recurrence rate due to severe dissemination within the surgical area, and cases of recurrent spinal tumors are not candidate for surgical intervention. The Japanese scholars Tomita et al. were the first to propose total en bloc spondylectomy (TES), which involves dividing the spinal column into the anterior and posterior sections for complete excision. TES can not only achieve the complete resection of spinal tumors, but it also maximally enhances the survival rate.

The total en bloc spondylectomy includes resection of the involved vertebrae in two major blocs, rather than in a piecemeal pattern (Fig. 3.32), which effectively reduces the chance of tumor dissemination.
Patient is placed in a prone position under general anesthesia. The chest and iliac crest are padded to elevate the chest and abdomen in order to prevent obstruction of respiration and to promote venous drainage (Fig. 3.33).
The skin incision is done by the posterior midline approach to expose the posterior bone surface of the thoracic spine. The length of the incision should sufficiently expose the target segment as well as two segments above and below (Fig. 3.34).

The muscles are retracted laterally with automatic retractors to expose to the bilateral costotransverse joints.

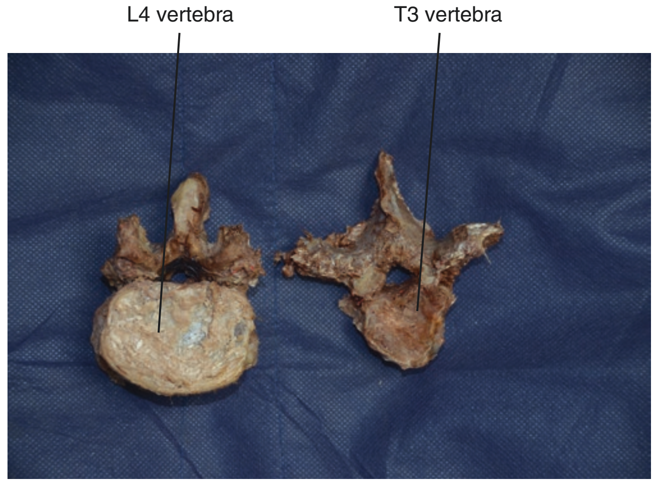

Fig. 3.32 Complete resection of the target segment

Fig. 3.33 Position and incision of posterior approach of thoracic vertebra

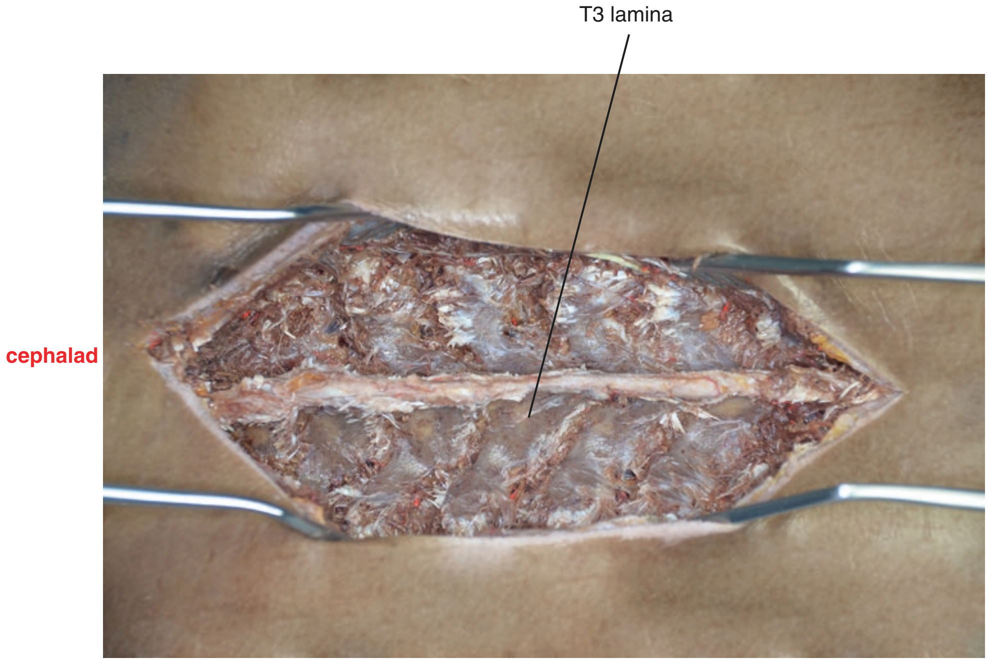

Fig. 3.34 Incision of the skin and subperiosteal dissection of paravertebral muscles to expose the posterior bone surface of the thoracic spine

3.2 Total En Bloc Spondylectomy

Place the pedicle screws at two segments above and below the target vertebra.

Pedicle screws are defined to be in the good position by intraoperative anteroposterior and lateral fluoroscopy (Fig. 3.35, 3.36, and 3.37).

Avoid damaging the pleura when subperiosteally dissecting the proximal ribs on each side of the target vertebra.

The ribs are resected at 3 cm lateral to the costotransverse joint and remove the rib head completely from the costotransverse joint (Fig. 3.38).

The supraspinous ligament and interspinous ligaments between the superior and inferior spinous processes adjacent to the target vertebra are removed.

The inferior facet of the superior vertebra is resected with an osteotome or Kerrison Rongeurs. The ligamentum flavum and part of the vertebral lamina of the superior vertebra are removed with Kerrison Rongeurs (Figs. 3.39 and 3.40).

A T-saw or threadwire is used to cut the pedicle (Fig. 3.41). Alternatively, osteotomes can be used to cut the pedicle.

Insert the osteotomes between the vertebral laminae, and cut the pedicle in a caudal to cranial direction (Fig. 3.42).

The spinal cord and nerve root are under proper protection during the removal of the posterior bone structures of the target vertebra (Fig. 3.43).

The thoracic vertebral foramen is small and round. The thoracic spinal cord is smaller but rounder than the cervical spine. The superior and inferior thoracic vertebral laminae are short, thick, and broad, and they overlap one another.

The pedicle screws on one side are fixed with a connecting rod to avoid spinal cord damage due to spinal instability during the excision of the anterior and middle spinal columns.

The soft tissues on each side of the target vertebra are stripped and pushed toward the front with a Crego elevator (Fig. 3.44).

The lateral and the front sides of the spine are padded with gauze to achieve the isolation of the anterior vertebral tissues and hemostasis.

Ligature of the segmental arteries, which arise from the aorta and run along each side of the spine, can significantly reduce intraoperative bleeding.

Alternatively, a curved elastic retractor can be inserted to the front of the spine to protect the aorta and superior vena cava (Figs. 3.45, 3.46, and 3.47).

A T-saw or threadwire is used to cut intervertebral discs adjacent to the target vertebra. The posterior longitudinal ligament is resected under direct view, and the target vertebra body is dissociated completely.

The resected vertebra is removed by rotating around the spinal cord from anterior position to the posterior (Fig. 3.48).

The intercostal nerve on one side of the spine can be ligated and incised to allow enough space for the removal of the resected vertebra if necessary.

Clean the bony endplates of the upper and lower vertebrae to gain a slightly bleeding graft surface. An appropriate mesh cage filled with autologous iliac bone or allograft bone is placed into the space for the reconstruction of the anterior and middle spinal columns.

The rod on the opposite side is placed with compression. Release the temporary fixed rods and refix them with compression to ensure the titanium mesh is secure within the spine so that the sagittal balance and stability of the spine can be reconstructed (Fig. 3.49).

The mesh cage and pedicle screws are confirmed to be in good position by intraoperative anteroposterior and lateral fluoroscopy.

Fig. 3.35 Placement of pedicle screws

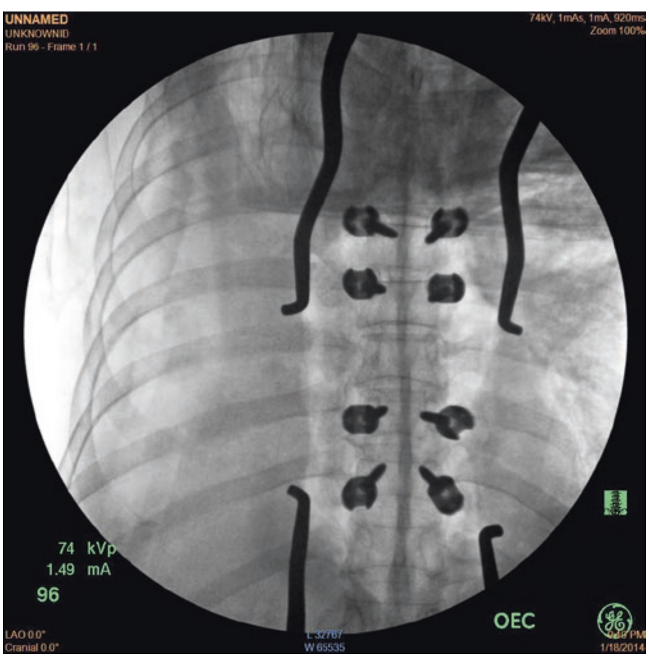

Fig. 3.36 Location of the pedicle screw is defined by intraoperative lateral fluoroscopy

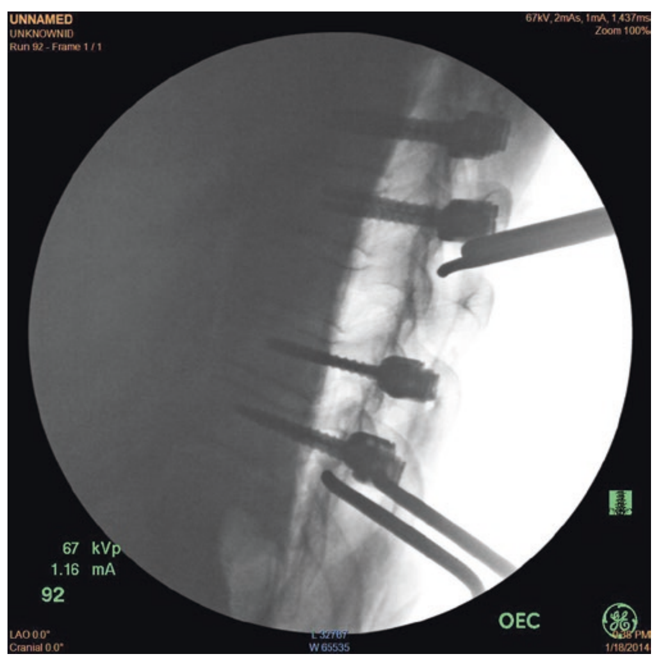

Fig. 3.37 Location of the pedicle screw is defined by intraoperative anteroposterior fluoroscopy

Fig. 3.38 Removal of the bilateral rib heads and proximal ribs of the target segment

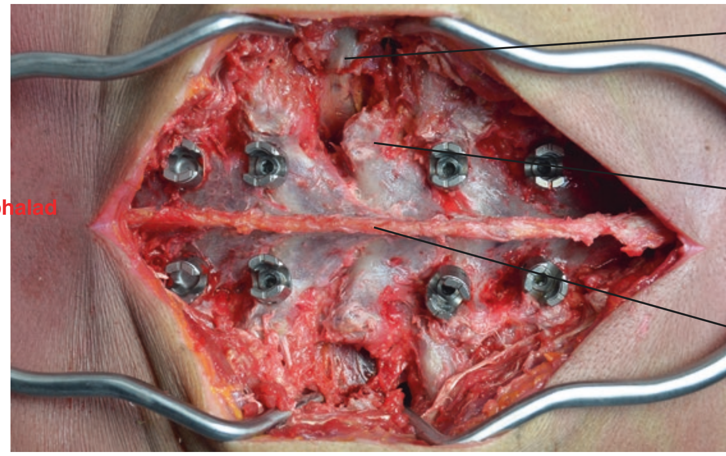

Fig. 3.39 Removal of the inferior facet and ligamentum flavum from the vertebra above the target vertebra with a Kerrison Rongeur

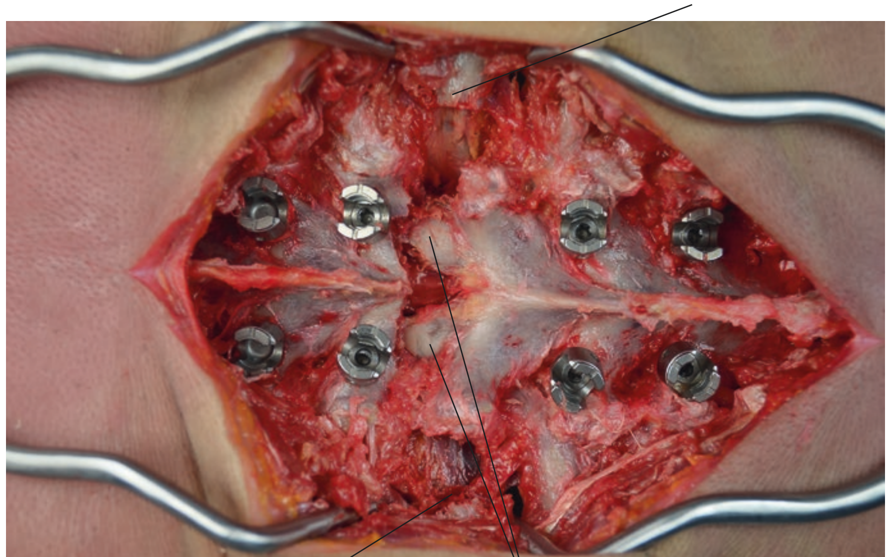

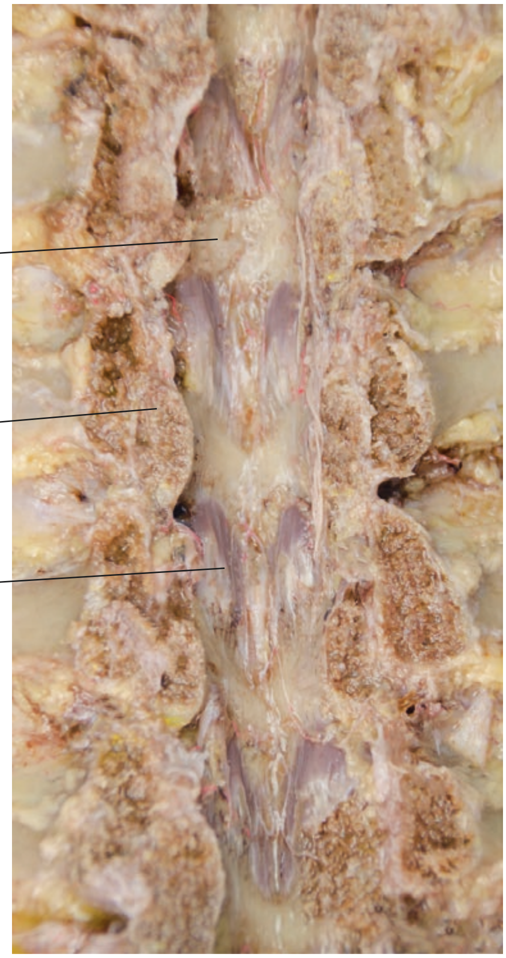

Fig. 3.40 Ligamentum flavum

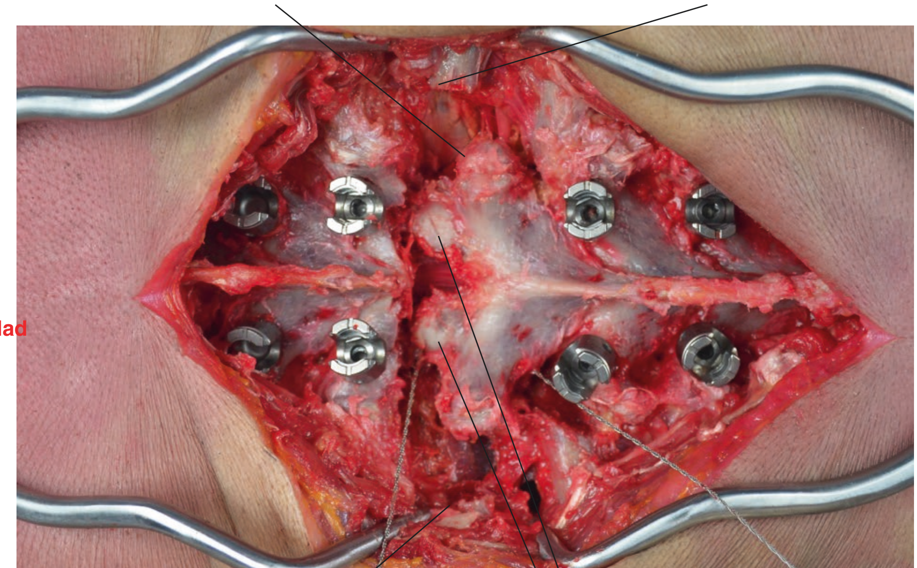

Fig. 3.41 A T-saw or threadwire is used to cut the pedicle

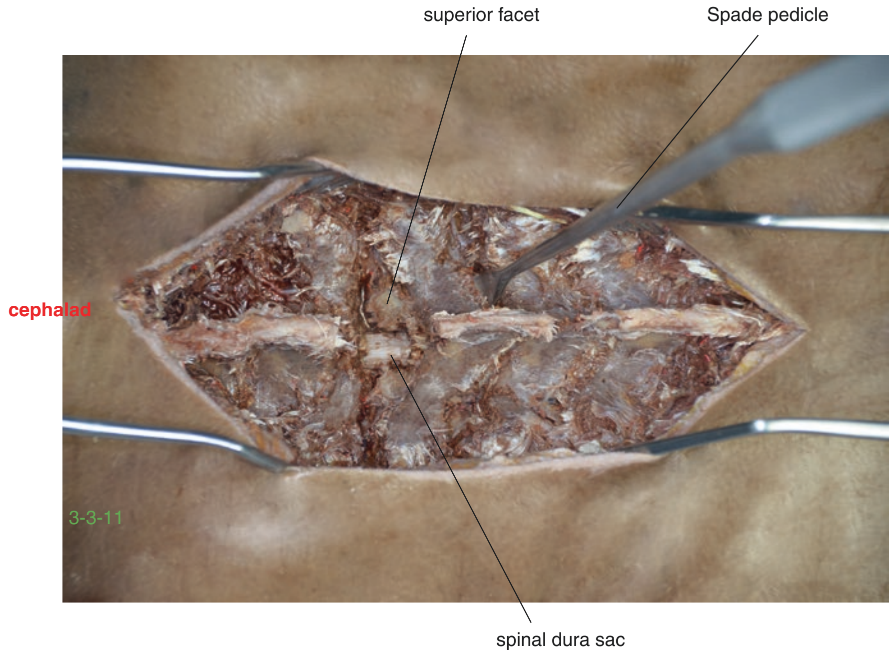

Fig. 3.42 Cut the pedicle with osteotomes

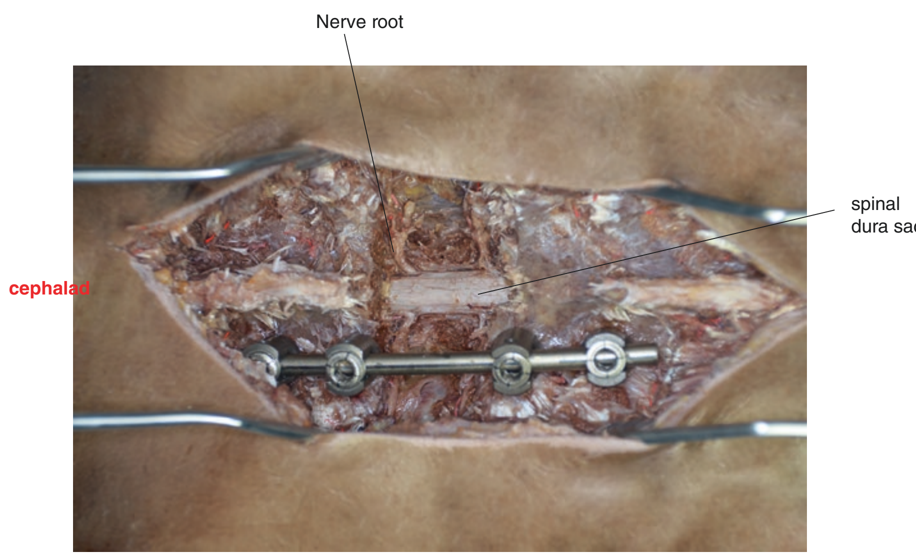

Fig. 3.43 Complete removal of the posterior vertebral bone structures

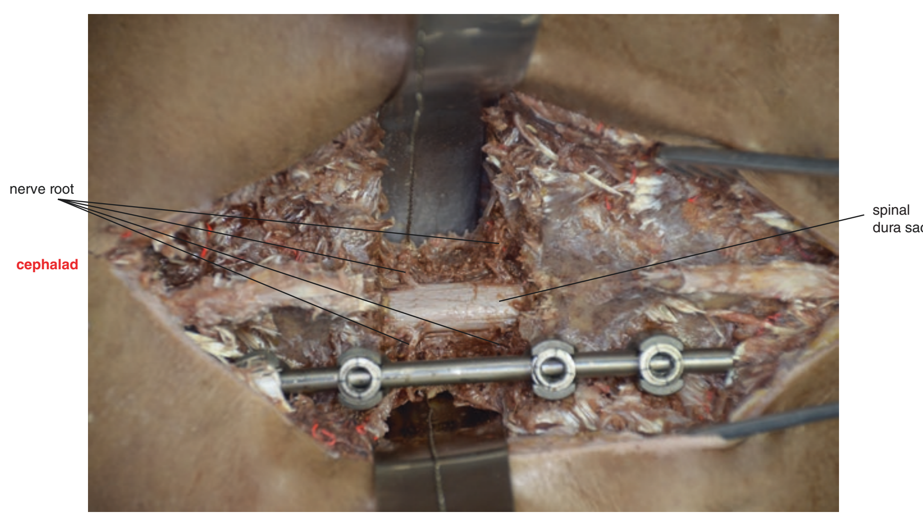

Fig. 3.44 Dissection and distraction of the anterior vertebral body

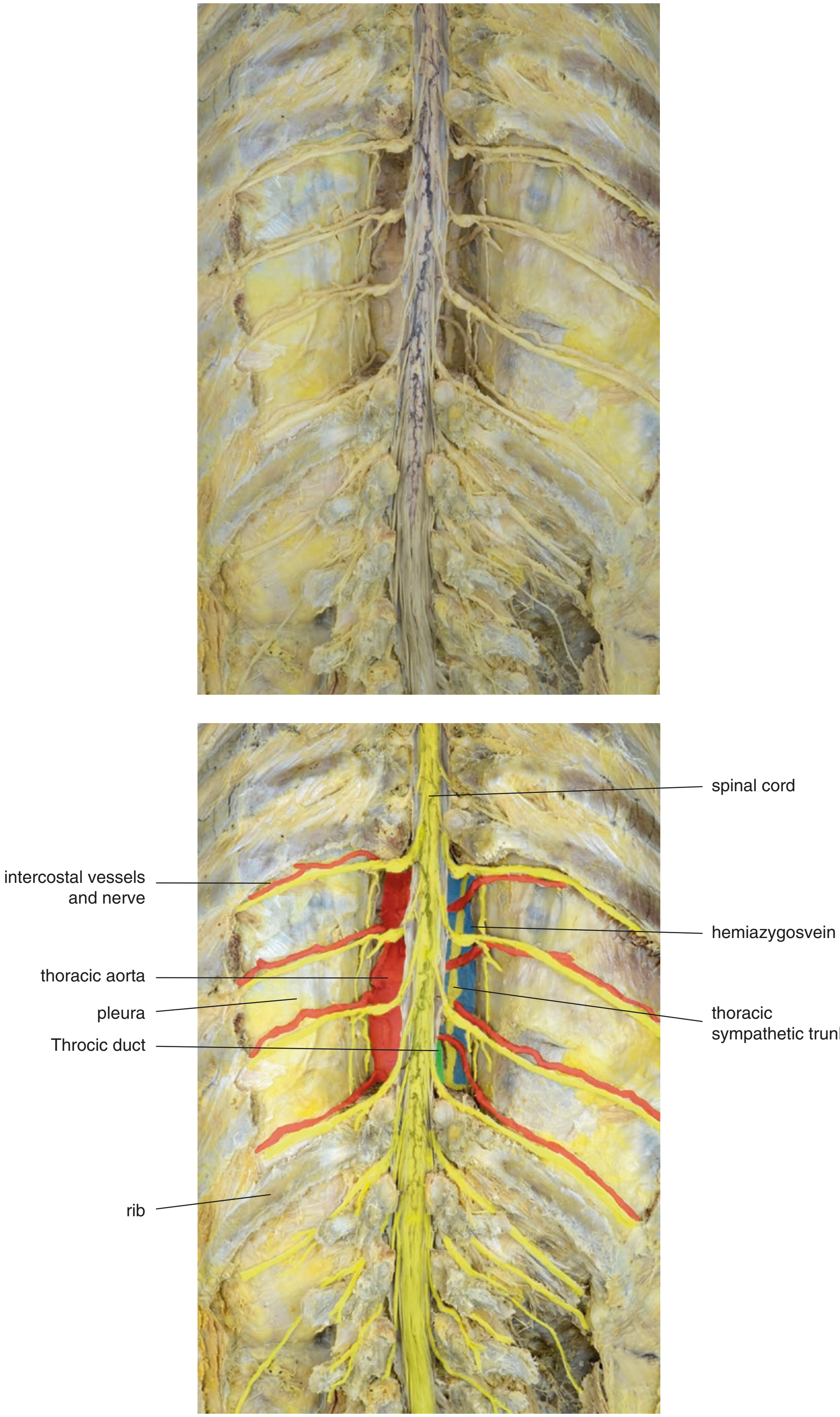

Fig. 3.45 Neurovascular structures anterior to the thoracic spine (T10 and T11 vertebral body resected)

Fig. 3.46 Neurovascular structures anterior to the thoracic spine

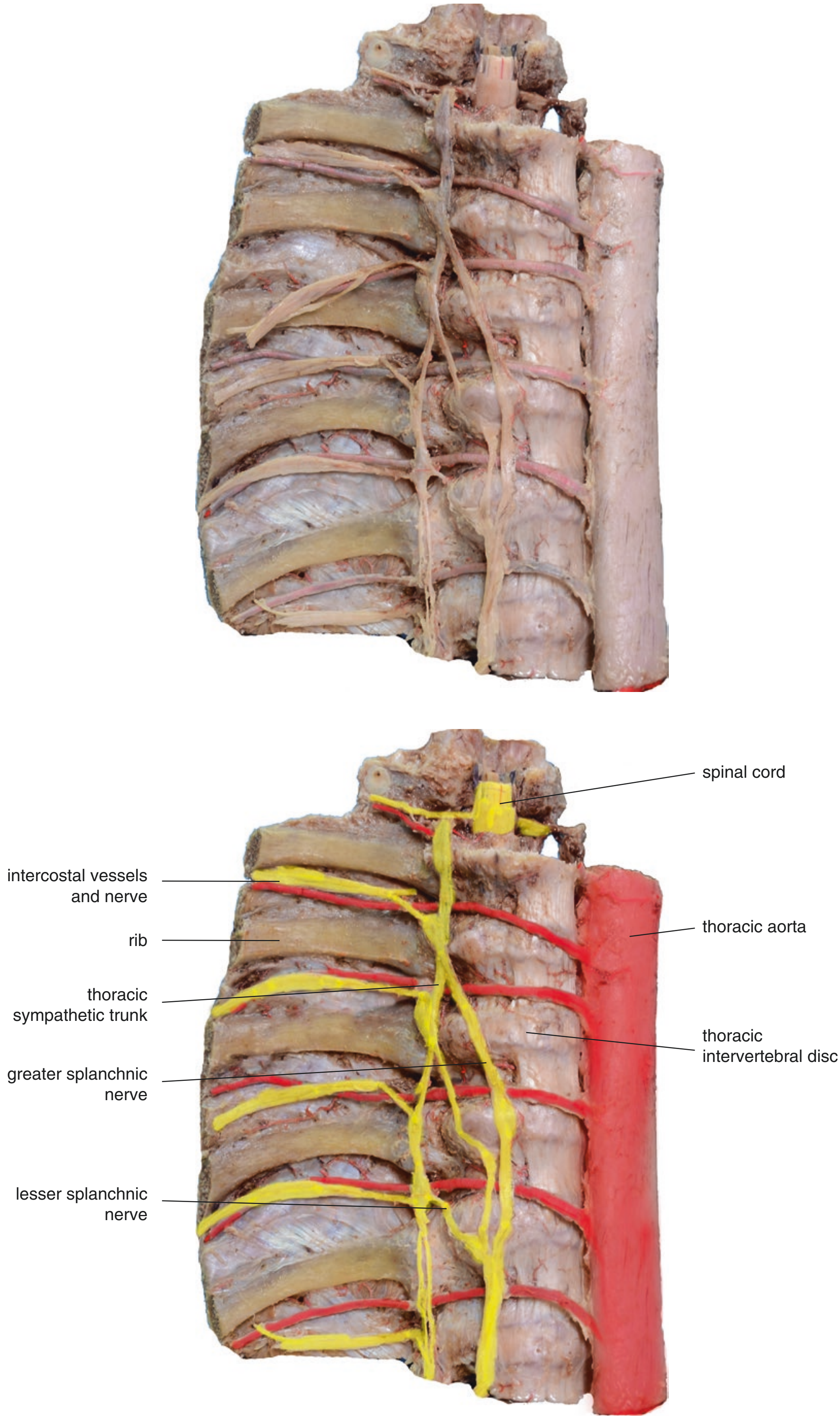

Fig. 3.47 Neurovascular structures anterior to the thoracic spine (sixth to tenth ribs)

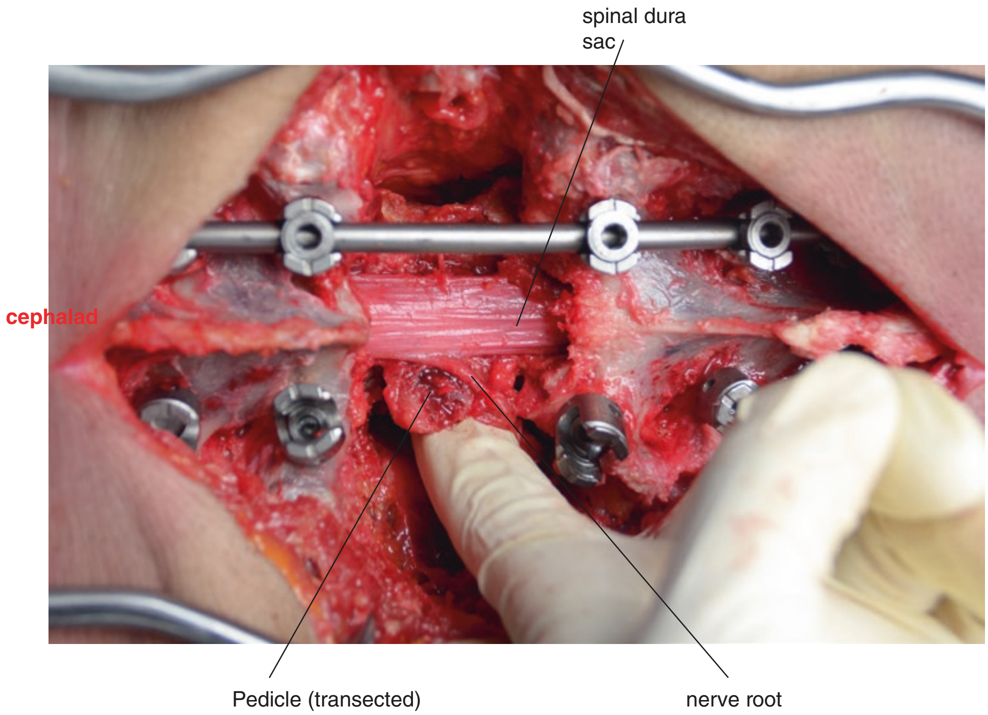

Fig. 3.48 Removal of vertebra from the spinal column

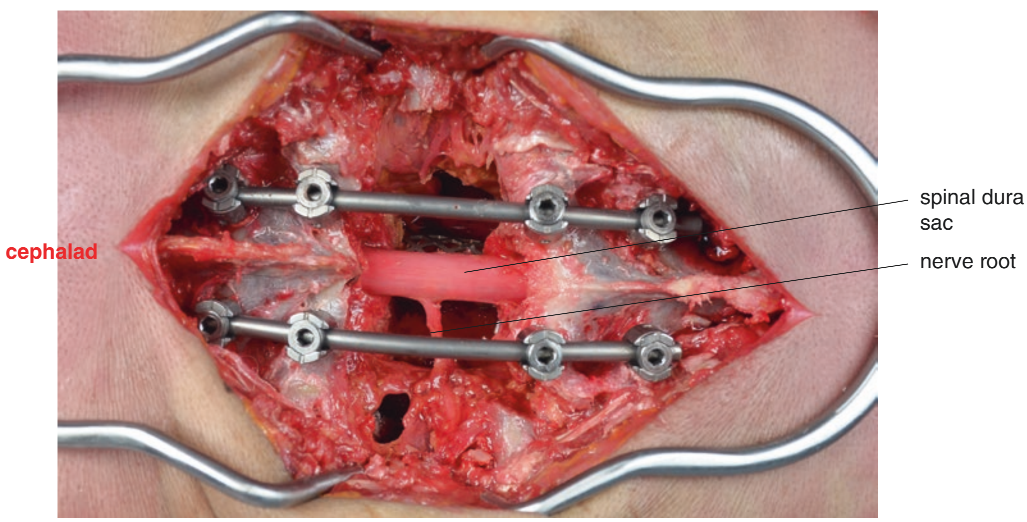

Fig. 3.49 Placement of the mesh cage and fixation of the rod

4 Placement of Thoracic Pedicle Screws

4.1 Overview

In 1949, Michele and Krueger had described the anatomy of the spinal pedicle and inserted screws into the spine through the pedicle using the posterior approach. Doctors in France and Switzerland started using pedicle screws in clinical therapy in 1970, and then Cotrel, Dubousset, Dick, Roy-Camille, and Louis subsequently reported several successful cases of its use. In 1996, the North America Spine Society formally approved the clinical use of pedicle screws.

The thoracic pedicle internal fixation system has a good three-column fixation effect and biomechanical property and has shown significant advantage in restoring spinal stability. It is suitable for treating diseases that cause thoracic spinal instability, such as trauma, tumor, and deformity. Moreover, this technique has shown satisfactory clinical efficacy in spinal deformity correction and reconstruction in recent years.

Thoracic pedicle screw fixation is a procedure with high technical requirements for surgeons. There are two methods of thoracic pedicle screw placement, including intrapedicular and extrapedicular screw placement, where the latter is considered to be easier and safer (Figs. 3.50 and 3.51).

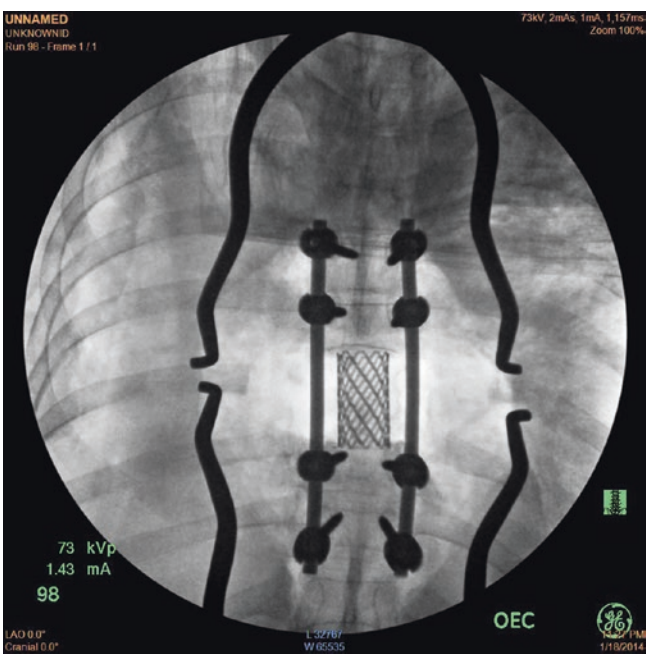

Fig. 3.50 Positions of the mesh cage and pedicle screw shown by intraoperative anteroposterior fluoroscopy

4.2 Position

Patient is placed in a prone position with the chest and iliac crest padded to prevent obstruction of venous drainage and respiration (Figs. 3.52 and 3.53).

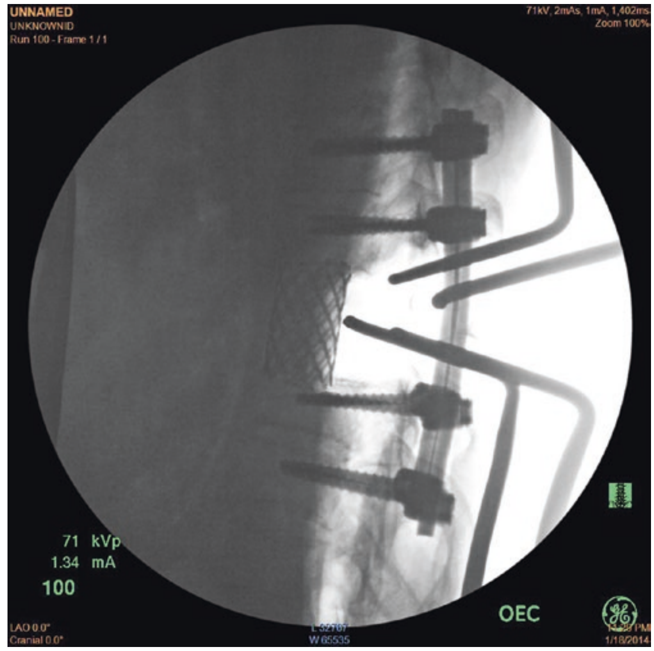

Fig. 3.51 Positions of the titanium mesh and pedicle screw shown by intraoperative lateral fluoroscopy

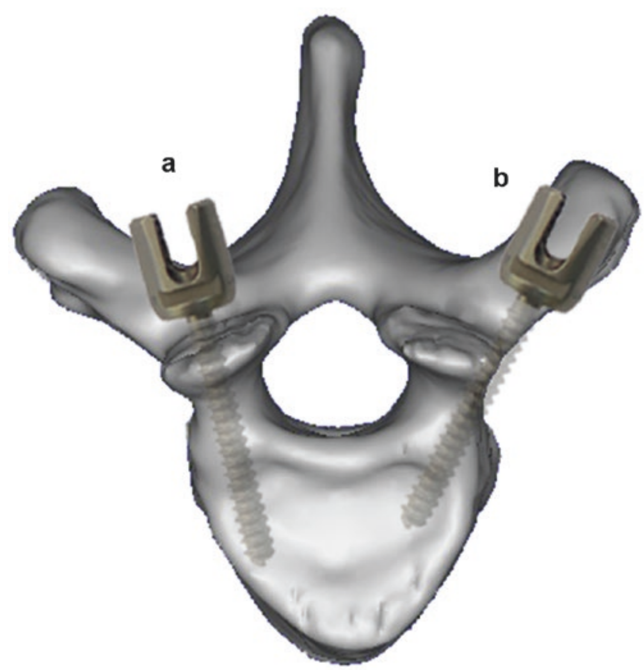

Fig. 3.52 Diagram of intrapedicular and extrapedicular screw replacement. (**a**) Intrapedicular screw placement. (**b**) Extrapedicular screw placement

Fig. 3.53 Position and incision of posterior approach of thoracic spine

4.3 Exposure

The range of the incision should at least include the upper and lower adjacent segment. Medial incision is used for patients without scoliosis (Figs. 3.54 and 3.55).
For patients with scoliosis, the incision can be made along the line drawn between the C7 spinous process and the gluteal cleft.

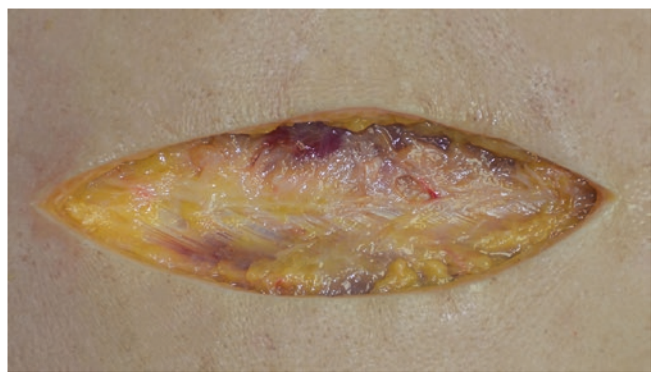

Fig. 3.54 Incision of the skin and subcutaneous tissue to expose

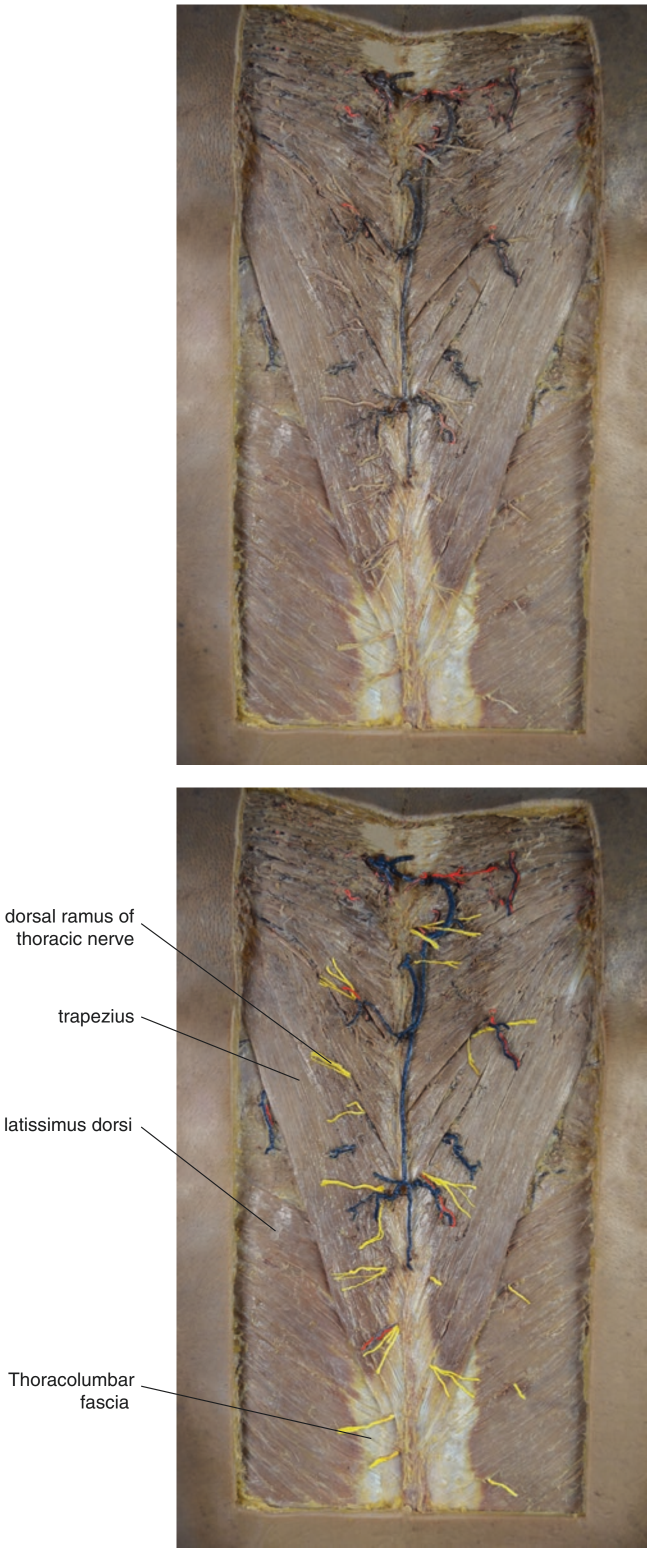

Fig. 3.55 Anatomy of the superficial thoracic muscles, vessels, and nerves

Dorsal rami of the thoracic nerves: run posteriorly from near the facet and divide into the medial and lateral branches. The medial branches are distributed to facet joints and between the medial border of the superior ligament of the costotransverse process and intertransversarii muscles. The lateral branches first proceed between the muscles and the ligaments and then run obliquely from the medial side of the levatores costarum muscles to the back.
Iliocostalis: the iliocostalis thoracis muscle is connected to the superior border of the angle of the six lower ribs. It is also connected to the transverse process of the seventh cervical vertebra and the superior border of the angle of the sixth upper ribs.

Longissimus muscles: the longissimus thoracis is the largest continuation of the erector spinae. In the thoracic region, it is inserted into the tips of the transverse processes of all thoracic vertebrae by rounded tendons.

Spinalis muscles: the spinalis thoracis is the medial continuation of the erector spinae. It is situated at the medial side of the longissimus thoracis. The muscle is connected to the spinous processes of T11–L2 by three to four tendons (Fig. 3.56).

Thoracodorsal artery: a terminal branch of the subscapular artery, which runs posteriorly between the latissimus dorsi and serratus anterior muscles along the lateral border of the scapulae and runs into the latissimus dorsi muscle with the thoracodorsal nerve.

Serratus posterior inferior muscle: a thin and quadrilateral muscle. It arises from the spinous processes of the T11–L3 vertebrae and runs upward and lateralward. It inserts four digitations into the lateral region of the four lower costal angles and is innervated by the ventral rami of the ninth to twelfth thoracic nerve roots.

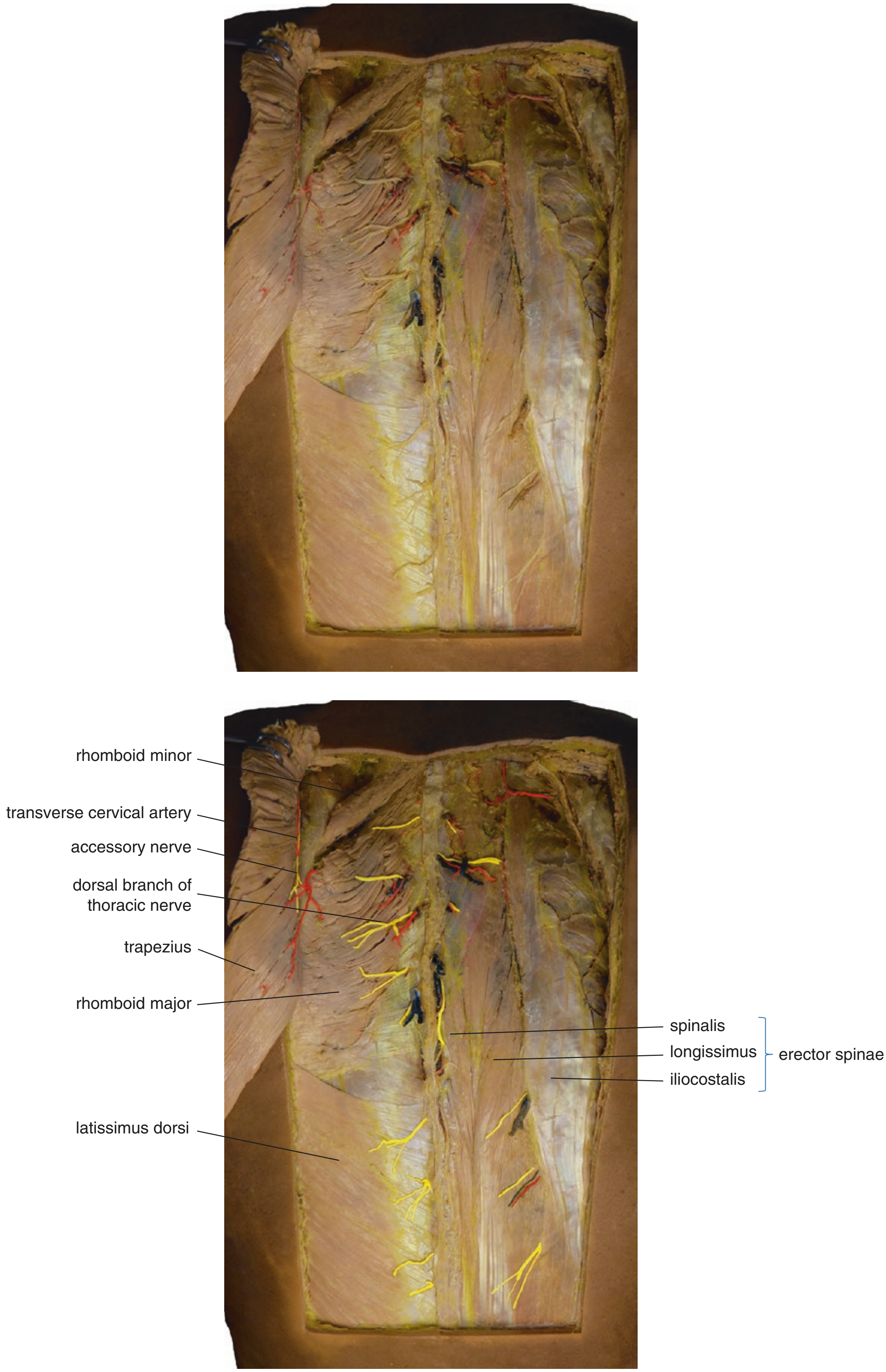

Fig. 3.56 Anatomy of the paravertebral muscles

Subperiosteal dissection of the paravertebral muscles is done to expose the transverse process. This procedure can easily injure the medial and lateral branches of the dorsal rami of the thoracic nerve, especially the medial branch, as well as the accompanying dorsal branch of the posterior intercostal artery (Fig. 3.57).

The electrocautery or hemostatic agents are used to deal with excessive bleeding encountered from the interlaminar vessels when subperiosteally dissecting muscles from the vertebral lamina (Fig. 3.58).

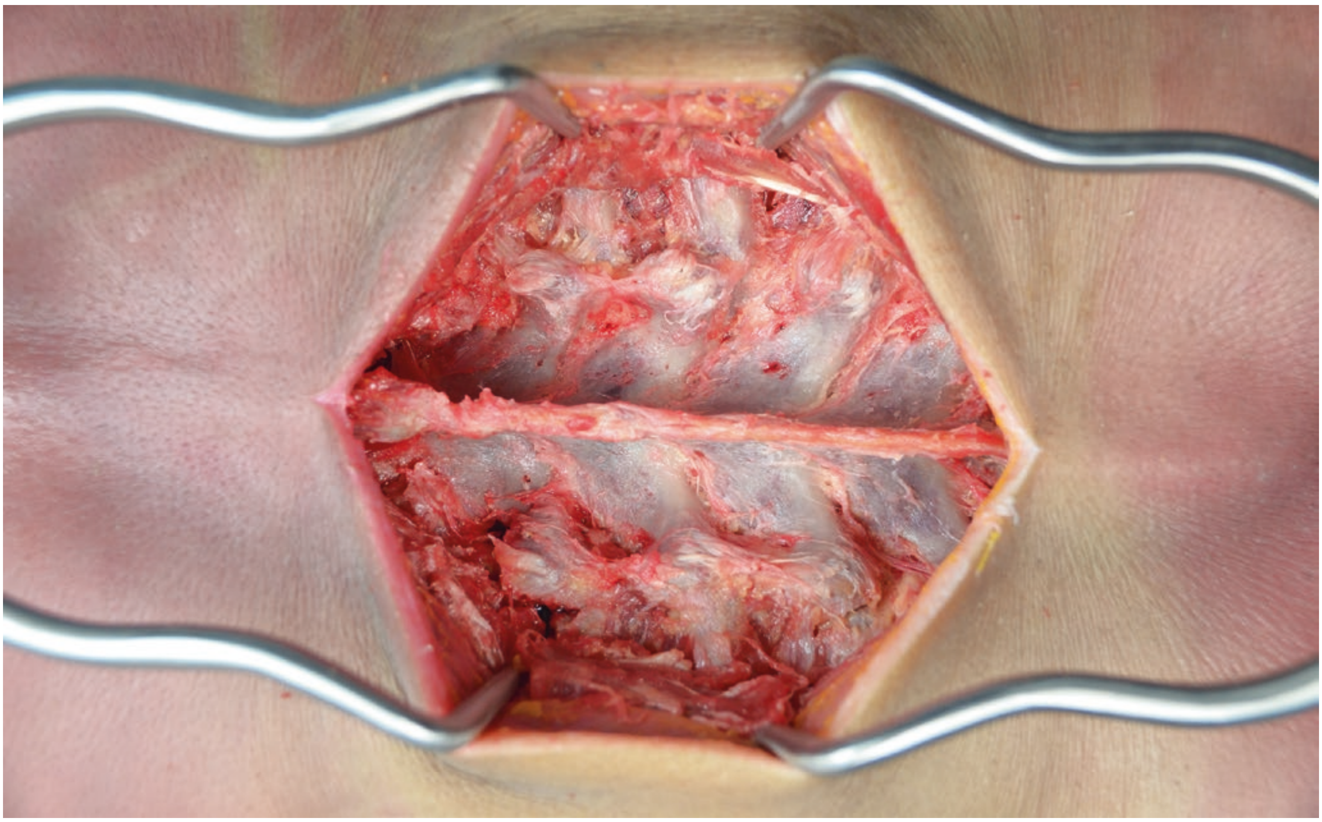

Fig. 3.57 Subperiosteal dissection of the paravertebral muscles to expose the bone surface

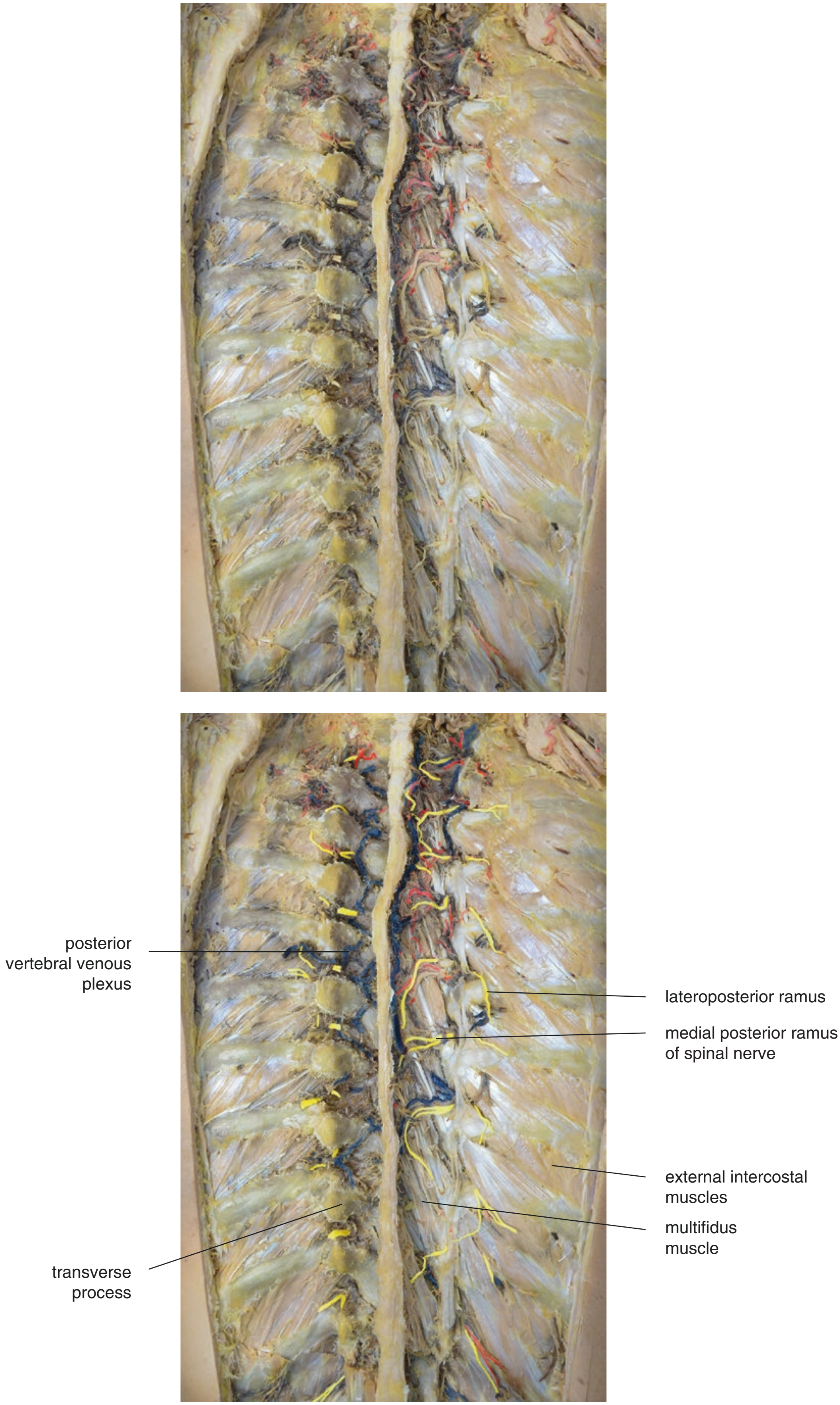

Fig. 3.58 Anatomy of the interlaminar vessels and the dorsal rami of the thoracic nerve

Medial cutaneous branch of the dorsal rami of thoracic nerve descends close to the spinous process for some distance before it innervates the skin. The lateral branch runs downward for some distance, about the width of four ribs, before it becomes the cutaneous branch. An example of this is the dorsal branch of the twelfth thoracic nerve, which runs to the skin in the upper region of the iliac crest (Fig. 3.59).

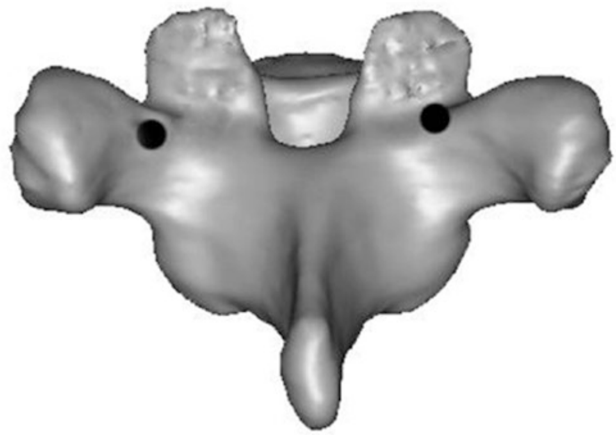

Fig. 3.59 Diagram of the thoracic pedicle screw entry point; Fennell technique on the left and Chung technique on the right

4.4 Entry Point and Trajectory of the Thoracic Pedicle Screw

Fennell technique: the entry point is 3 mm caudal to the junction of the transverse process and the lateral margin of the superior facet. Medial-lateral trajectory is approximately 30° at T1 and T2 and 20° from T3 to T12. Cranial-caudal trajectory is always orthogonal to the dorsal curvature of the spine at corresponding level.

Chung technique: the entry point of the thoracic pedicle is at the base of the superior facet at the junction of the lateral and middle thirds after observing the whole facet joint margin.

Changzheng technique: the entry point is at 3 mm caudal and 3 mm medial at the junction of the lateral margin of the superior facet and the transverse process. Medial-lateral trajectory is approximately 20° from T1 to T3 and 10° from T4 to T12. Cranial-caudal trajectory is always parallel to the superior endplate at corresponding level.

The entry point of the extrapedicular placement needs to be more lateral with a greater medial-lateral trajectory (Fig. 3.60).

Fig. 3.60 Diagram of intrapedicular (*left*) and extrapedicular (*right*) screw

After identifying the lateral margin of the superior facet, remove the cortical bone at 3 mm caudal and 3 mm medial at the junction of the lateral margin of the superior facet and the transverse process (Fig. 3.61).

Steel balls are placed at the entry points of the pedicle screws as shown by anteroposterior fluoroscopy. The figure shows the relative location of pedicles and screw entry points of T1–T4 by anteroposterior fluoroscopy (Fig. 3.62).

The figure shows the trajectory of the T1–T4 pedicle screws (Fig. 3.63).

The figure shows the entry points of the T4–T7 pedicle screws (Fig. 3.64).

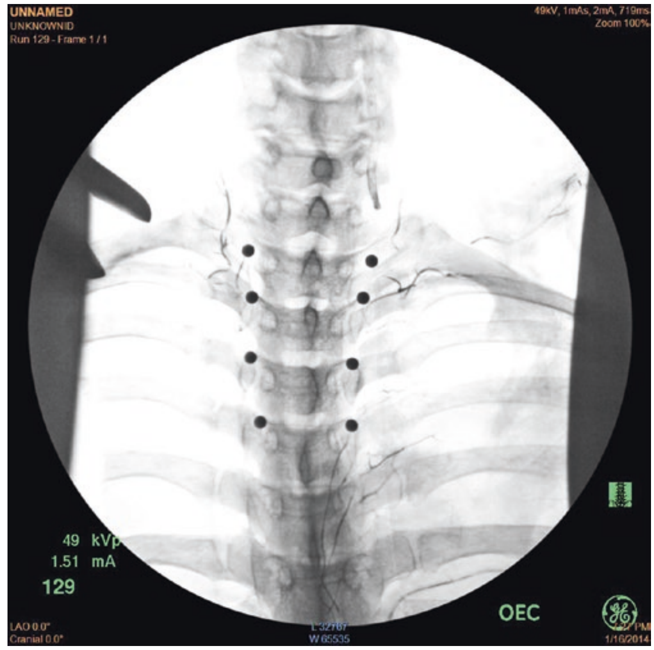

Fig. 3.62 Screw entry points shown by anteroposterior fluoroscopy

Fig. 3.61 Placement of steel balls indicates the entry points of the pedicle screws of T1–T4

Fig. 3.63 Placement of markers indicates the trajectory of the pedicle screws of T1–T4

Steel balls are placed at the entry points of the pedicle screws as shown by anteroposterior fluoroscopy. The figure shows the relative location of pedicles and screw entry points of T4–T7 by anteroposterior fluoroscopy (Fig. 3.65).

The figure shows the trajectory of the T4–T7 pedicle screws (Fig. 3.66).

Fig. 3.64 Placement of steel balls indicates the entry points of the pedicle screws of T4–T7

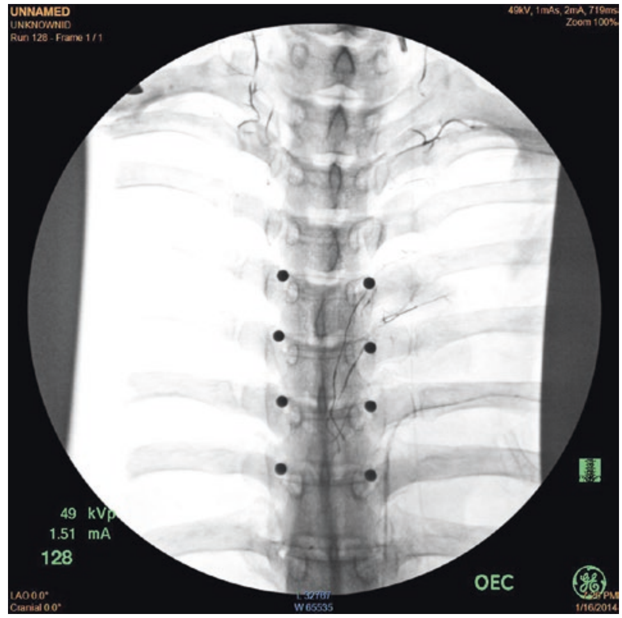

Fig. 3.65 Entry points of the pedicle screws of T4–T7 shown by anteroposterior fluoroscopy

Fig. 3.66 Placement of markers indicates the trajectory of the pedicle screws of T4–T7

Placement of steel balls indicates the entry points of the T9–T12 pedicle screws (Fig. 3.67).

The figure shows the relative location of pedicles and screw entry points of T9–T12 by anteroposterior fluoroscopy (Fig. 3.68).
The figure shows the trajectory of the T9–T12 pedicle screws (Fig. 3.69).
Pedicle screws are confirmed to be in good position by intraoperative lateral fluoroscopy (Fig. 3.70, 3.71, 3.72, 3.73, 3.74, and 3.75).

Fig. 3.67 Entry points of the T9–T12 pedicle screws

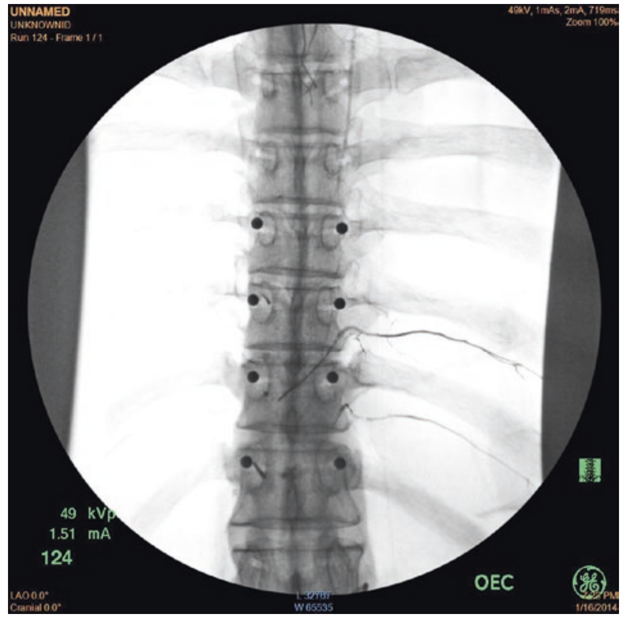

Fig. 3.68 Entry points of the pedicle screws of T9–T12 shown by anteroposterior fluoroscopy

Fig. 3.69 Placement of markers indicates the trajectory of the pedicle screws of T9–T12

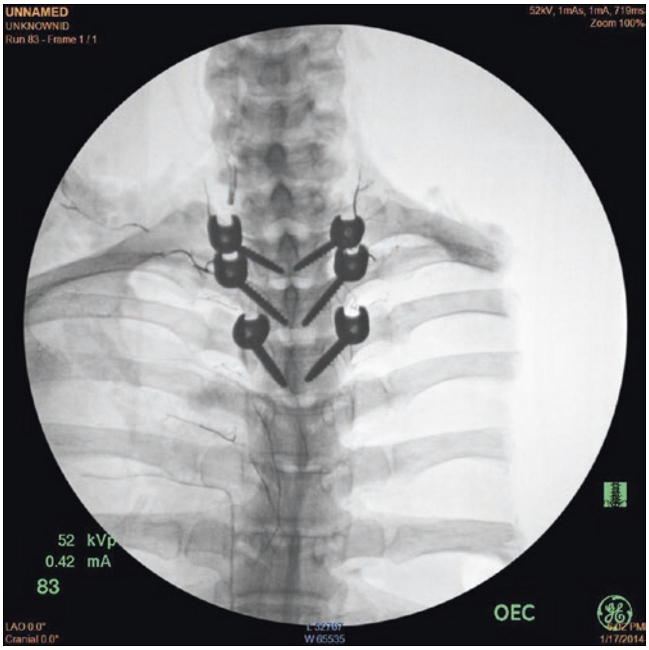

Fig. 3.70 Positions of the T1–T3 pedicle screws shown by anteroposterior fluoroscopy

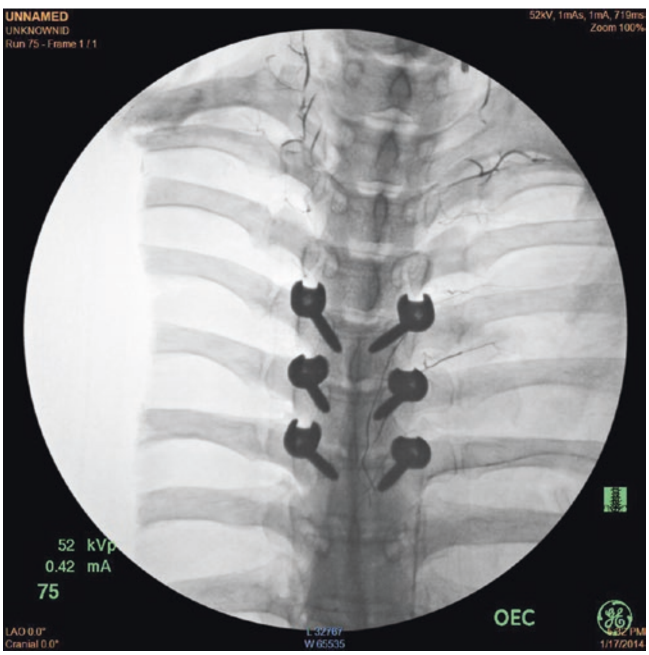

Fig. 3.71 Positions of the T4–T6 pedicle screws shown by anteroposterior fluoroscopy

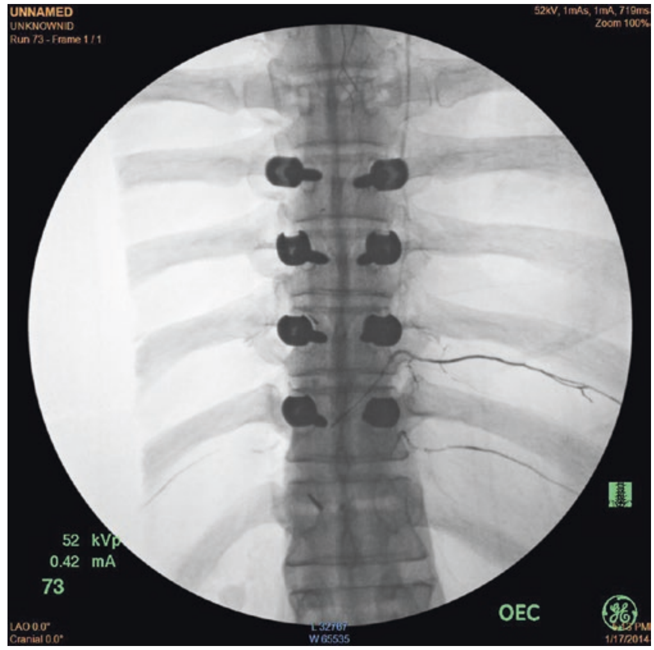

Fig. 3.72 Positions of the T7–T11 pedicle screws shown by anteroposterior fluoroscopy

Fig. 3.73 Positions of the T1–T3 pedicle screws shown by lateral fluoroscopy

Fig. 3.74 Positions of the T4–T6 pedicle screws shown by lateral fluoroscopy

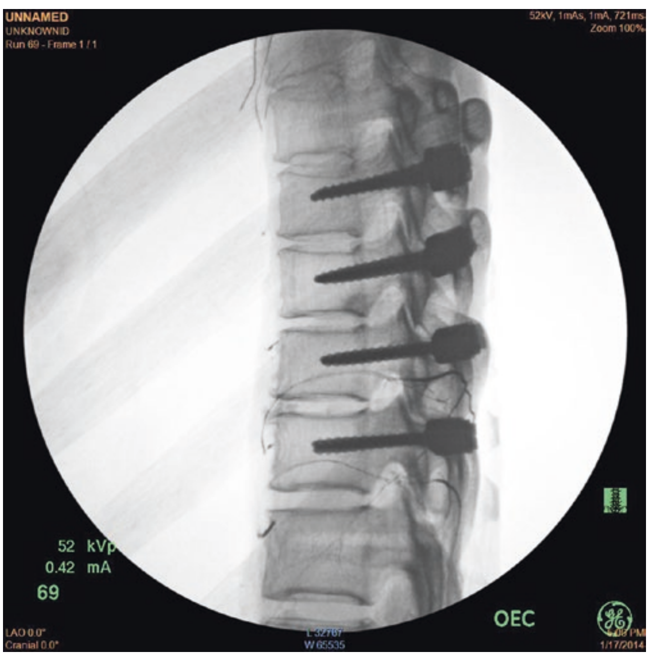

Fig. 3.75 Positions of the T7–T11 pedicle screws shown by lateral fluoroscopy

5 Lateral Thoracolumbar Spine Exposure

5.1 Overview

The lateral approach to the thoracolumbar spine is rarely used due to its high invasiveness. As for thoracolumbar burst fracture, compression of the spinal cord by the intervertebral disc and deformity correction (sagittal or coronal) can be indications for an anterior thoracolumbar approach.

The advantages of this approach include (1) full exposure to facilitate better surgical field, (2) thorough lesion resection under direct vision and better stability reconstruction of the anterior and middle column, and (3) rich bone graft and strong fixation. The disadvantages include opening of the chest cavity, being highly invasive, and greater postoperative complications.

With the wide use of posterior-only approaches, surgeons are becoming less experienced in anterior approaches. However, it is important that the spine surgeon understands the approach, indications, and complications for preoperative planning and intraoperative decision-making.

5.2 Position

Patient is placed in a lateral position (Fig. 3.76).

The skin incision is done along the tenth rib from the paravertebral muscles to costal cartilage, curving gently toward the umbilicus.

The dissection is carried through the deep fascia and the abdominal external oblique muscle along the incision to expose the periosteum of the tenth rib. Make sure the intercostal vessels and nerves are well protected.

Serratus anterior muscle: begins from the rib and ends at the scapulae. The muscle proceeds intimately along the thoracic cavity to the medial border of the scapulae along the ventral surface of the latter. It is supplied by the superior thoracic artery, lateral thoracic artery, and the branches of the thoracodorsal artery anterior to the latissimus dorsi muscle. It is innervated by the long thoracic nerves which descend along the lateral side of the muscle (Figs. 3.77, 3.78, and 3.79).

Fig. 3.76 Position of the combined lateral thoracolumbar approach and incision

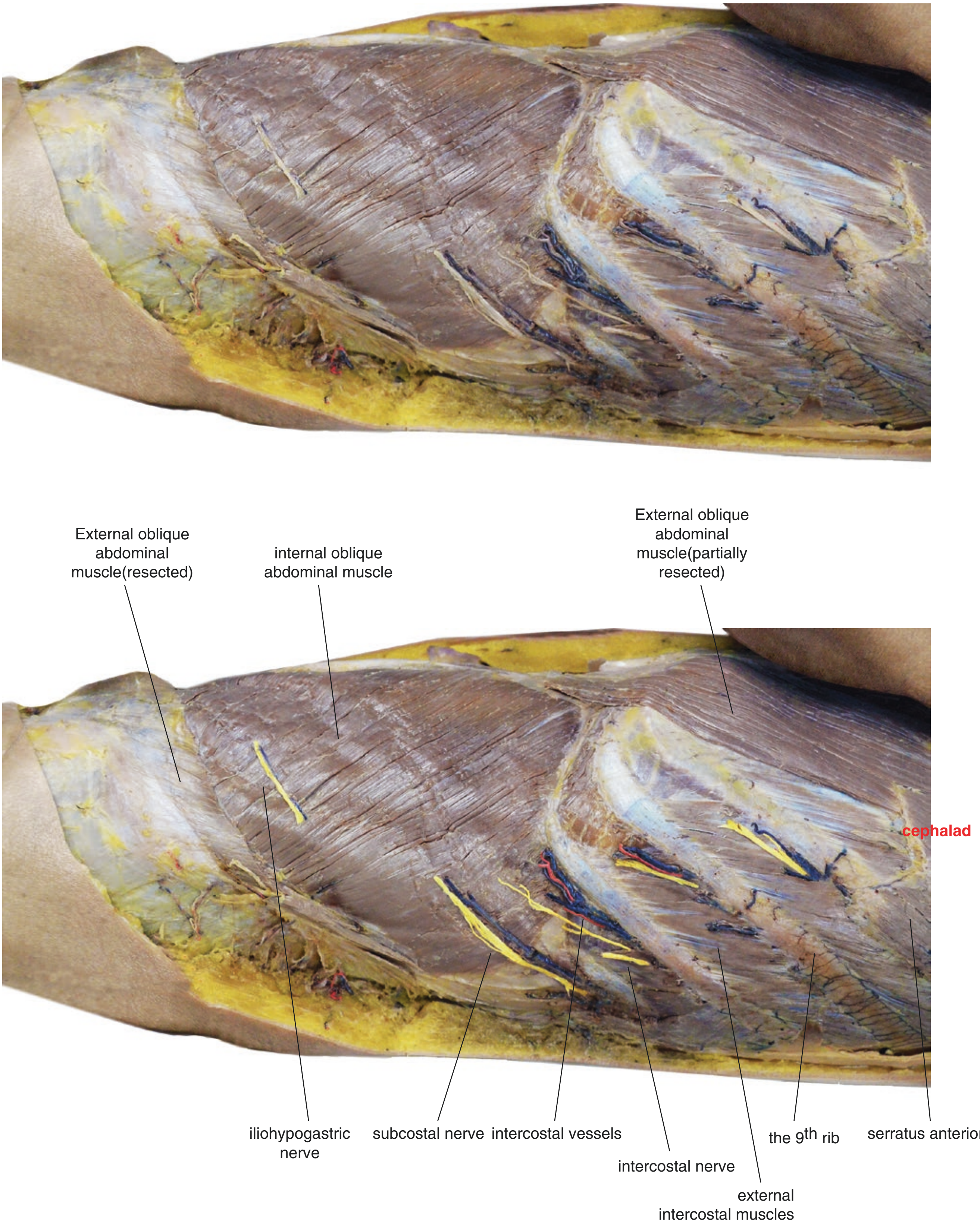

Fig. 3.77 Superficial anatomy of the lateral thoracolumbar wall

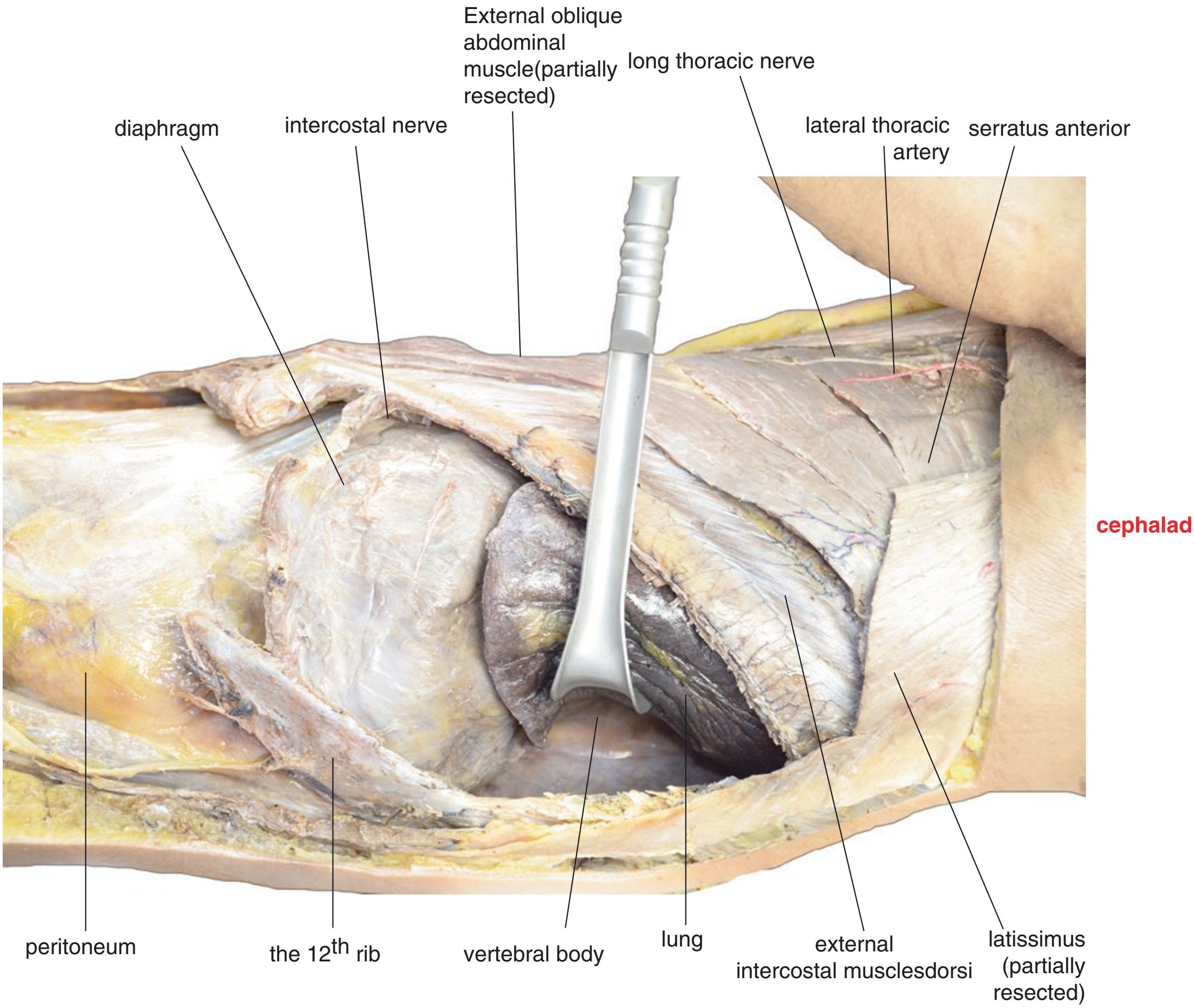

Fig. 3.78 Anatomy of the exposed thoracic cavity

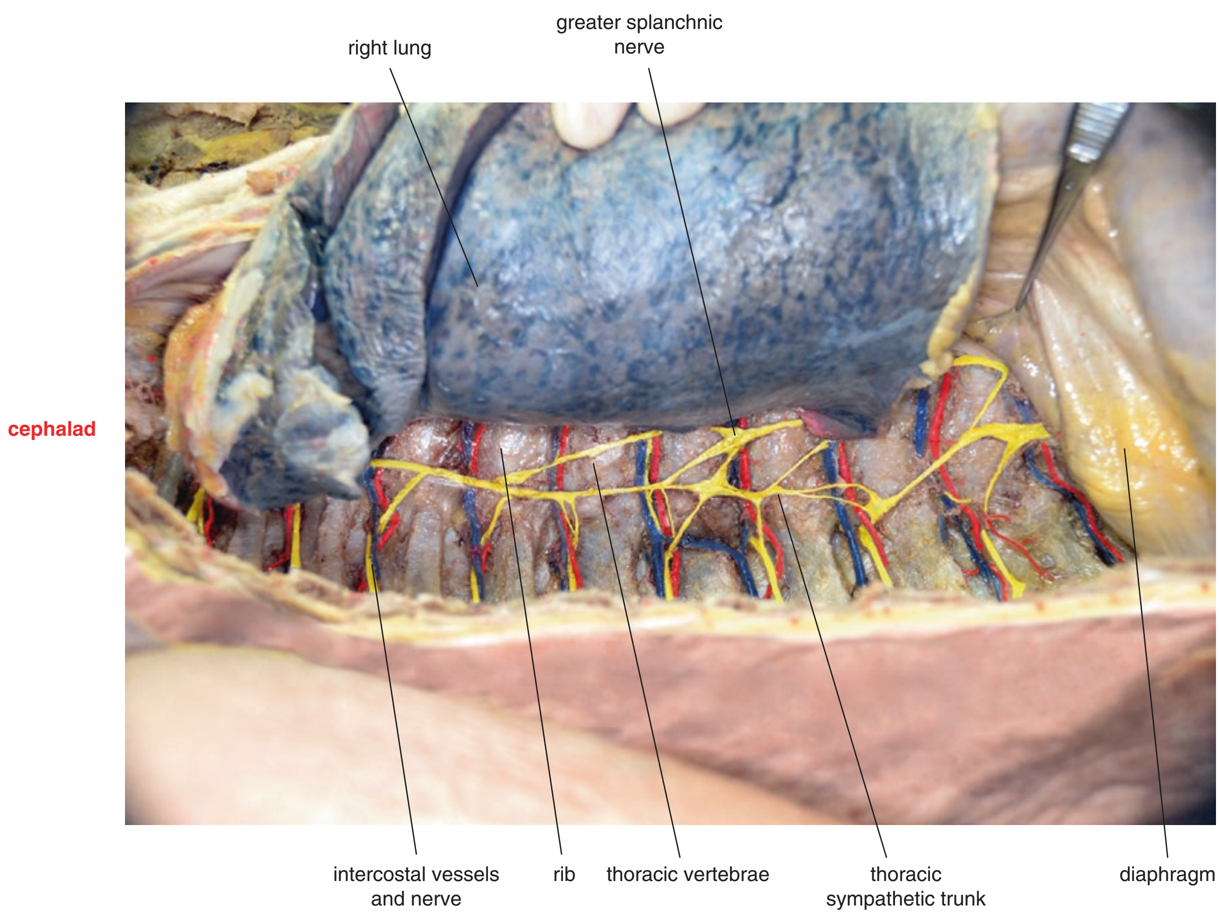

Fig. 3.79 Adjacent structures of the thoracic spine

Incise and detach the periosteum of the tenth rib with a periosteal elevator.

The tenth rib is removed with the distal chondral aspect intact.

The distal chondral aspect is then bisected and tagged as the key anatomic landmark.

The retroperitoneal space is exposed immediately underneath the distal chondral aspect of the tenth rib. Open the costal periosteum with scissors to enter into the pleural cavity and collapse the lung.

Incise the diaphragm from the lateral side of the chest cavity, where the diaphragm should be about 2.5 cm from the peripheral insertion, leaving a cuff of tissue for suturing, yet staying peripheral enough avoiding denervation.

Attachment point of diaphragm: the diaphragmatic fiber begins from the highly oblique outlet of the thorax, and the posterior and bilateral attachment points are lower, while the anterior is high. According to the surrounding attachment area, the diaphragmatic fiber can be divided into three parts: the sternal, the rib, and the lumbar part. The sternum part of two muscle bundles origins from the rear of ensisternum, and this part may be absent occasionally. Rib part origins from the inner face of sixth costal cartilage and adjacent rib in both sides; it interlaces with transverse muscle of the abdomen. The lumbar part origins from two aponeuroses, which are the medial and lateral of arcuate ligament (also known as lumbocostal arch), and it origins from lumbar vertebra by two crura of diaphragm (Fig. 3.80).

Subcostal nerve: ventral ramus of the twelfth thoracic nerve. It descends from the inferior border of the twelfth rib with the subcostal artery. It passes the tendon at the beginning of the transverse abdominal muscle and enters in between the transverse abdominal muscle and internal oblique muscle. Muscular branch: innervates the transverse abdominal muscle, internal oblique muscle, rectus abdominis muscle, quadratus lumborum muscle, and pyramidalis muscle (Fig. 3.81).

Costal cartilage: noncalcified anterior portion of the cartilage template. It is a flat rod-shaped hyaline cartilage that extends from the anterior end of the rib and provides great mobility and elasticity to the chest cavity. The seven upper costal cartilages are attached to the sternum. The eighth to tenth costal cartilages are attached to the inferior borders of the above ribs. The last two costal cartilages have free pointed extremities that end in the abdominal wall.

Anatomy of abdominal wall from superficial to deep: abdominal external oblique muscle, abdominal internal oblique muscle, transverse abdominal muscle, and transverse fascia (Fig. 3.82).

Abdominal external oblique muscle: arises from the external surfaces of the inferior eight ribs, which intersect with the serratus anterior and latissimus dorsi muscles. The muscle fibers are arranged in an oblique direction, which run superolaterally to inferomedially, and become the aponeurosis of the external oblique muscle near the junction of the anterior superior iliac spine and the umbilicus. It forms the anterior lamina of the rectus sheath and ends at the linea alba on the midline.

Abdominal internal oblique muscle: lies in the deep layer of the external oblique muscle. Its fibers arise from the lateral one-half or two-thirds of the inguinal ligament, iliac crest, and thoracolumbar fascia and run superomedially. The posterior fibers terminate at the three inferior ribs, and the other fibers end at the lateral border of the rectus abdominis muscle and become the aponeurosis, which is divided into anterior and posterior layer. These fibers form the anterior and posterior laminae of the rectus sheath that surrounds the rectus abdominis muscle and terminate at the linea alba.

Transverse abdominal muscle: lies in the deep layer of the internal oblique muscle. This muscle is relatively thin and weak, and it arises from the inner surfaces of the lower six costal cartilages and the lateral one-third of the thoracolumbar fascia, iliac crest, and inguinal ligament. The muscle fibers run transversely from the back to the front and become the aponeurosis at the lateral border of the rectus abdominis. They join the posterior lamina of the aponeurosis of the internal oblique muscle and proceed along the back with the rectus abdominis until the linea alba, where they form the posterior lamina of the rectus sheath. The muscle fibers below the arcuate line join the posterior lamina of the aponeurosis of the internal oblique muscle and proceed to the front with the rectus abdominis until the linea alba, where they form the anterior lamina of the rectus sheath.

Lower boundary of pleura: reflection line of the costal pleura and diaphragmatic pleura. Its left side arises from the midpoint of the sixth costal cartilage, and the right side arises from the back of the sixth sternocostal joint. Both sides descend laterally and intersect with the eighth rib at the midclavicular line, with the tenth rib at the midaxillary line, with the eleventh rib in the scapular line, and at the height of the T12 spinous process near the posterior midline (Fig. 3.83).

The greater splanchnic nerve, lesser splanchnic nerve, sympathetic trunk, and ascending lumbar artery all pass through the lumbar region of the diaphragm, while the phrenic nerve crosses the muscles, central tendon, or vena caval foramen of the diaphragm.

Greater splanchnic nerves: about 95% of greater splanchnic nerves are composed of preganglionic fibers that run medially from the T5 to T9 sympathetic ganglions, and they proceed downward along both sides of the thoracic aorta. About 75% of the greater splanchnic nerves enter the abdominal cavity through the middle crus and inner crus of the diaphragm and end at the anterolateral region of the external celiac ganglia at the back. The left greater splanchnic nerve is located at about 3 mm left to the aorta. The right greater splanchnic nerve is located at the aortic hiatus, about 11 mm right to the aorta (Fig. 3.84).

Azygos vein: receives drainage from the right ascending lumbar vein and right subcostal vein at the posterior abdominal wall. It enters the posterior mediastinum of the thoracic cavity through the right crus of the diaphragm and ascends behind the esophagus and along the right side of the thoracic duct and thoracic aorta to the level of the fourth thoracic vertebra, where it arches over the upper back of the right lung root and joins the superior vena cava (Fig. 3.85).

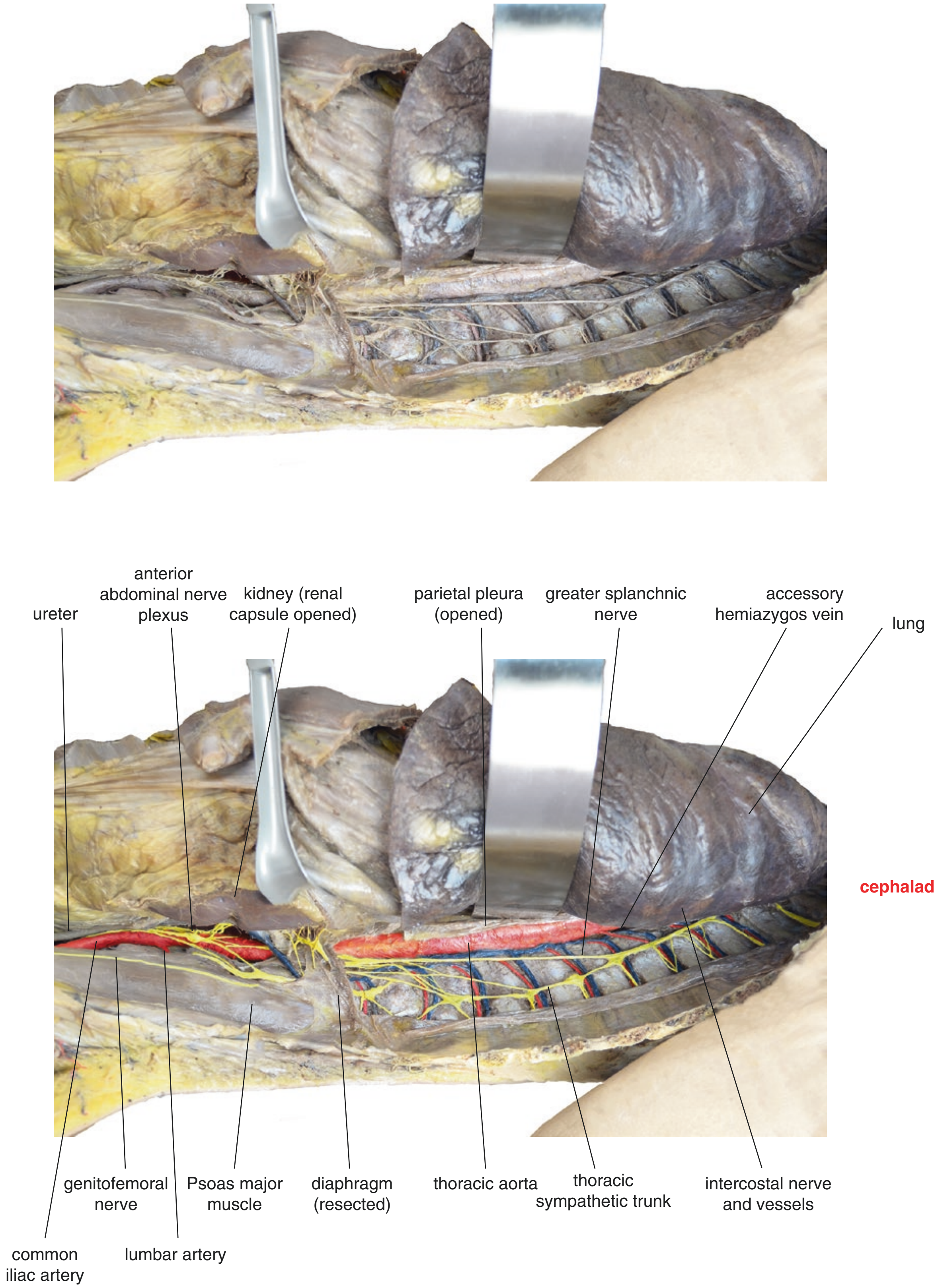

Fig. 3.80 Adjacent structures of the thoracolumbar spine

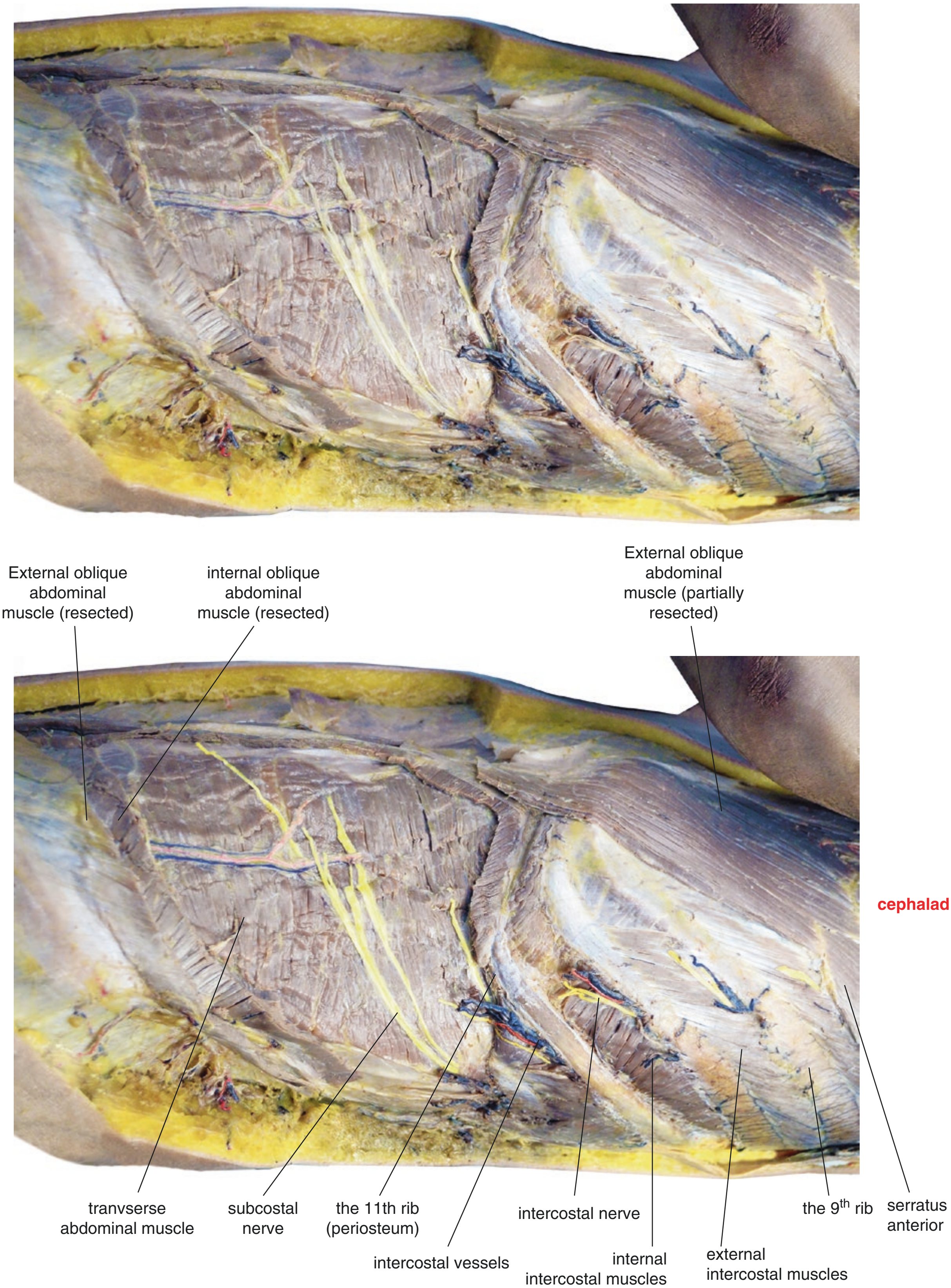

Fig. 3.81 Anatomy of the neurovasculature of the lateral abdominal wall

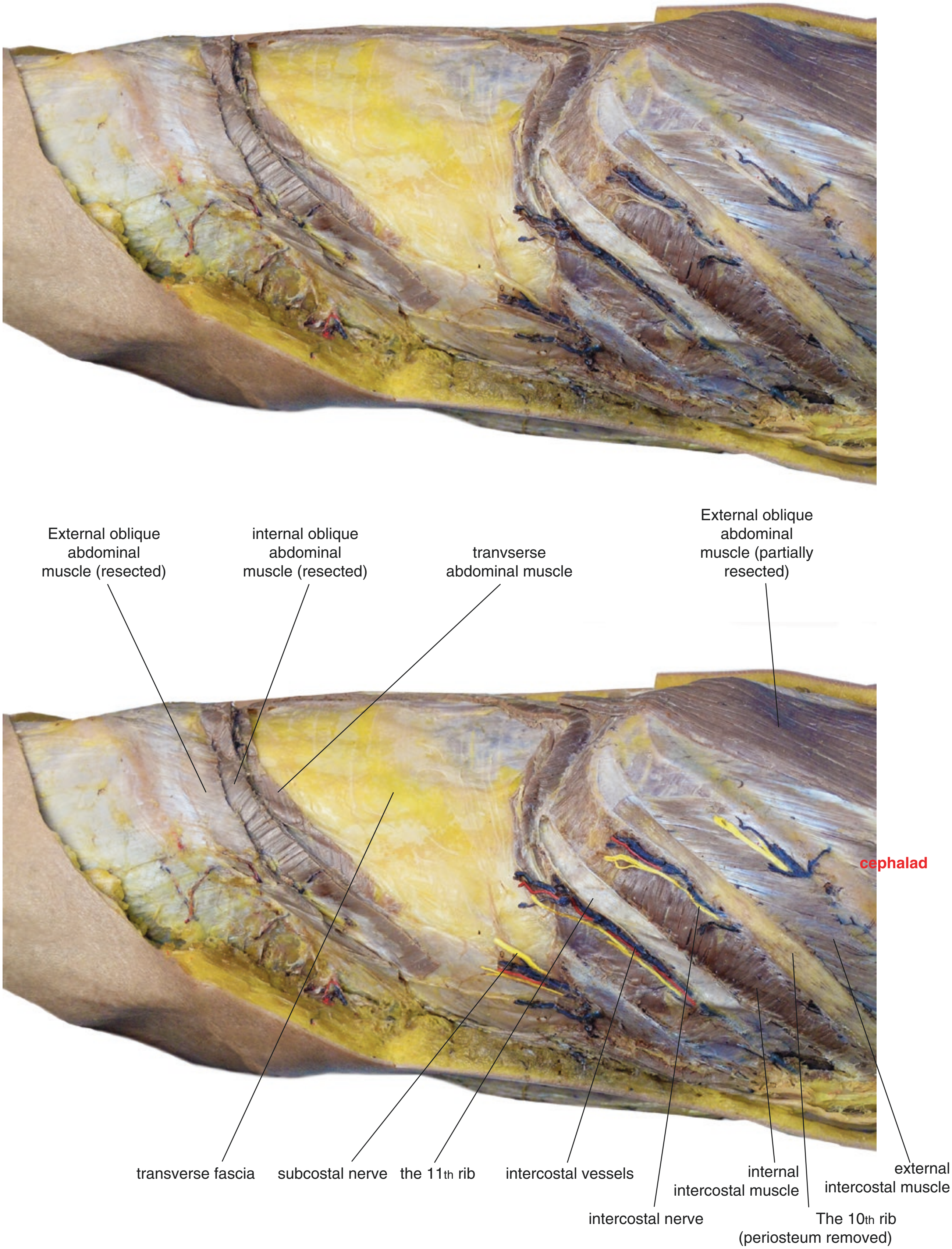

Fig. 3.82 Stratified anatomy of the thoracic and abdominal wall

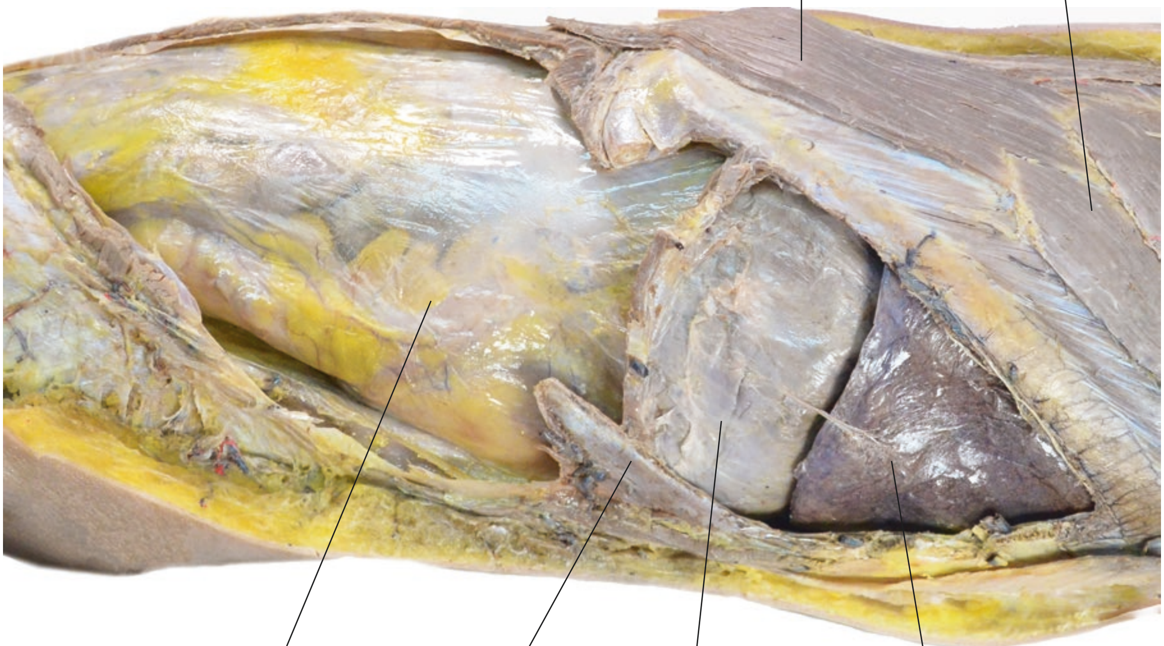

Fig. 3.83 Relationship of the diaphragm, peritoneum, and lung

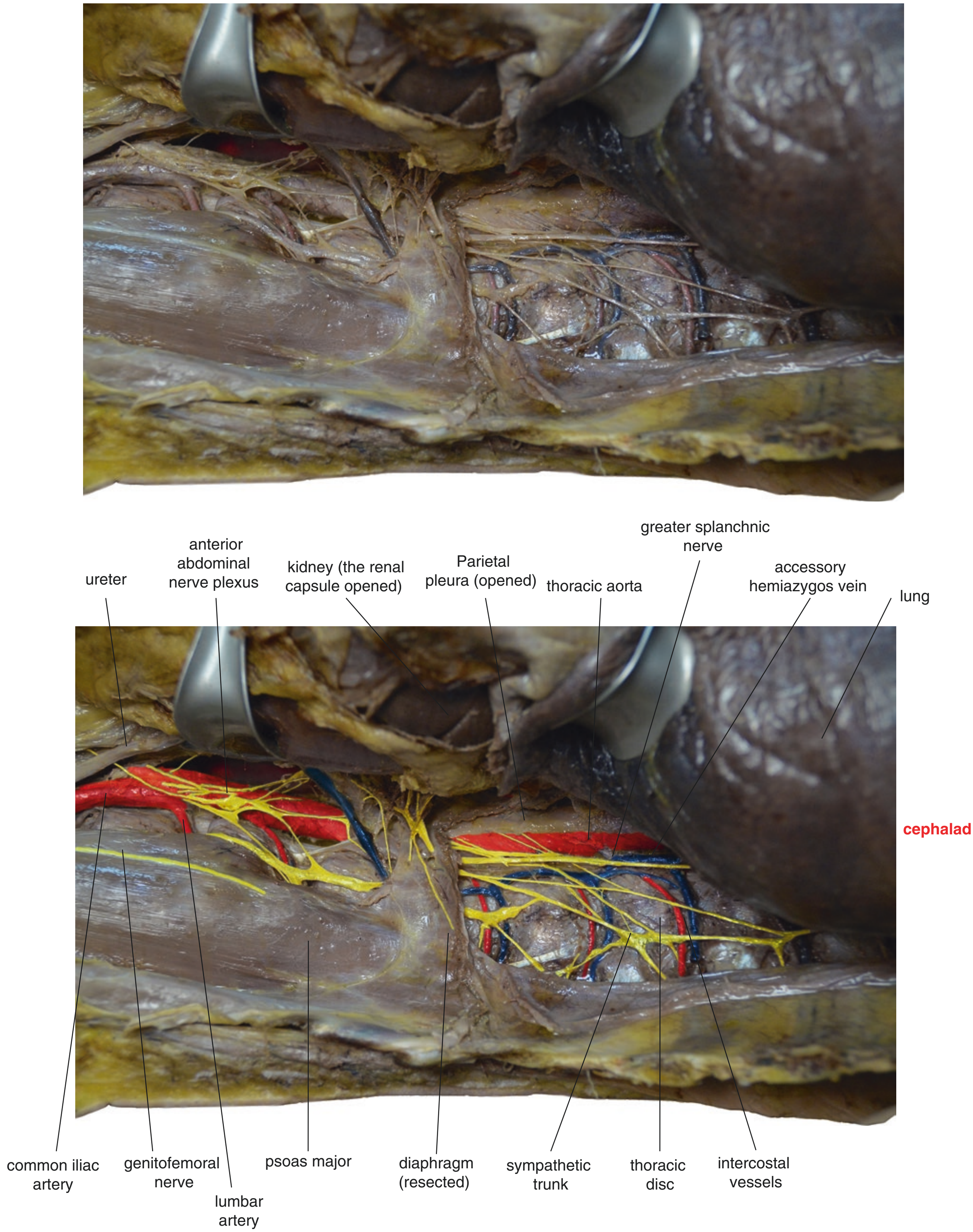

Fig. 3.84 Anatomical adjacency of the diaphragmatic attachments

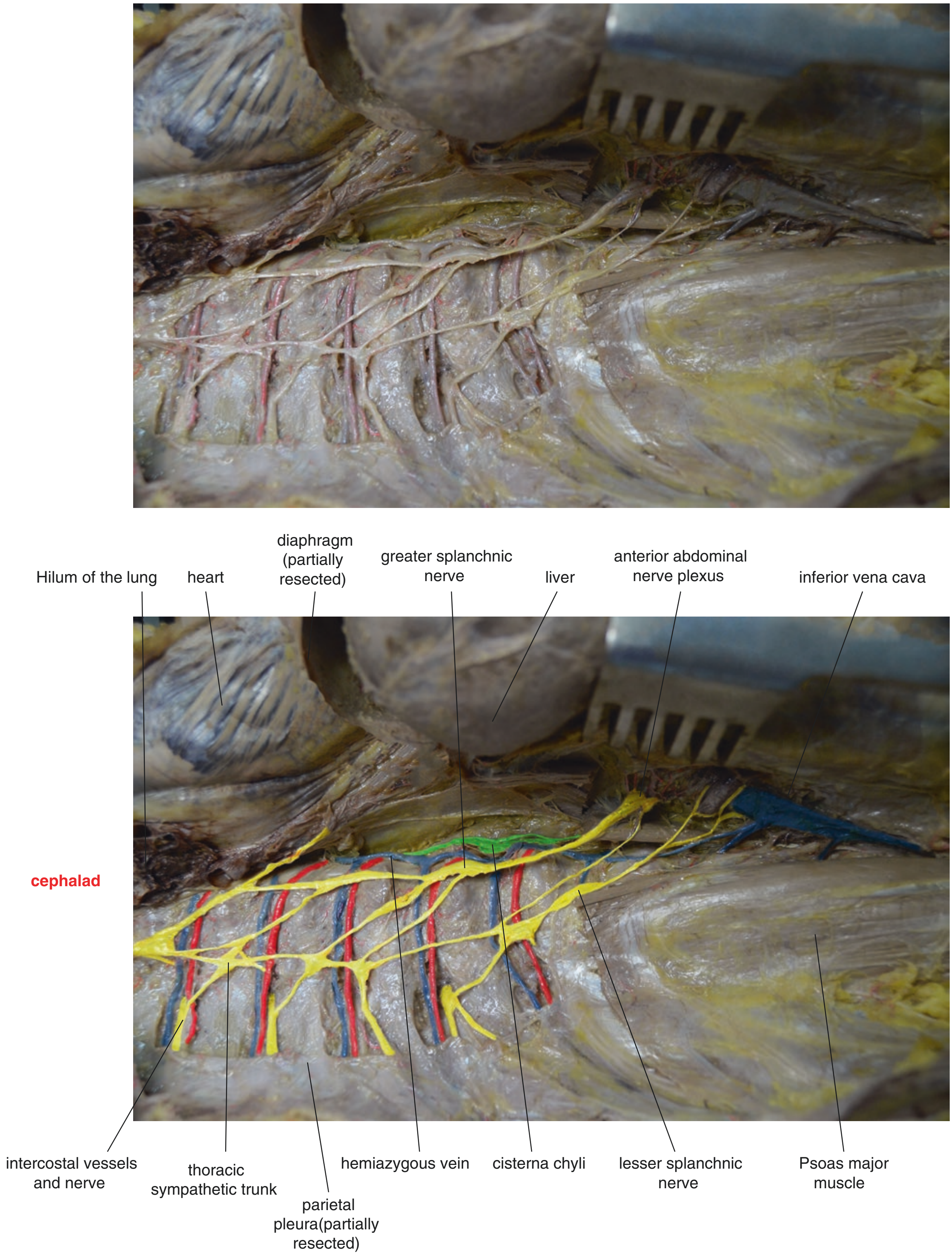

Fig. 3.85 Anatomical adjacency of the diaphragmatic attachments (*right*)

In the lumbar region, dissection of the psoas major muscle and crura of the diaphragm is done from the lumbar spine, and make sure to protect the genitofemoral nerve which perforates through the psoas major muscle.

In the thoracic region, the parietal pleura is opened using standard thoracotomy techniques, and the segmental vessels are ligated, along with the thoracic duct when necessary.

The sympathetic chain should be protected along the anterolateral aspect of the vertebral body.

The lateral thoracolumbar spine approach allows the exposure of the T6–L4 vertebrae.

References

1. Nacar OA, Ulu MO, Pekmezci M, et al. Surgical treatment of thoracic disc disease via minimally invasive lateral transthoracic trans/retropleural approach: analysis of 33 patients. Neurosurg Rev. 2013;36(3):455–65.
2. Ogden AT, Eichholz K, O'Toole J, et al. Cadaveric evaluation of minimally invasive posterolateral thoracic corpectomy: a comparison of 3 approaches. J Spinal Disord Tech. 2009;22(7):524–9.
3. Resnick DK, Benzel EC. Lateral extracavitary approach for thoracic and thoracolumbar spine trauma: operative complications. Neurosurgery. 1998;43(4):802–3.
4. Larson SJ, Holst RA, Hemmy DC, et al. Lateral extracavitary approach to traumatic lesions of the thoracic and lumbar spine. J Neurosurg. 1976;45(6):628.
5. Garrido E. Modified costotransversectomy: a surgical approach to ventrally placed lesions in the thoracic spinal canal. Surg Neurol. 1980;13(2):109–13.
6. Ahlgren BD, Herkowitz HN. A modified posterolateral approach to the thoracic spine. J Spinal Disord. 1995;8(1):69.
7. Hamburger C. Modification of costotransversectomy to approach ventrally located intraspinal lesions. Preliminary report. Acta Neurochir. 1995;136(1–2):12–5.
8. Grunenwald D, Mazel C, Baldeyrou P, et al. En bloc resection of lung cancer invading the spine. Ann Thorac Surg. 1996;61(6):1878–9.
9. Komagata M, Nishiyama M, Imakiire A, et al. Total spondylectomy for en bloc resection of lung cancer invading the chest wall and thoracic spine. Case report. J Neurosurg. 2004;100(4 Suppl Spine):353–7.
10. Schirren J, Dönges T, Melzer M, et al. En bloc resection of non-small-cell lung cancer invading the spine. Eur J Cardiothorac Surg. 2011;40(3):647–54.
11. Fadel E, Missenard G, Chapelier A, et al. En bloc resection of non-small cell lung cancer invading the thoracic inlet and intervertebral foramina. J Thorac Cardiovasc Surg. 2002;123(4):676–85.
12. Nishida K, Doita M, Kawahara N, et al. Total en bloc spondylectomy in the treatment of aggressive osteoblastoma of the thoracic spine. Orthopedics. 2008;31(4):403.
13. Shetty AS, Avadhani R, Mahesha B, et al. Anatomy of the thoracic pedicle in relation to the pedicle screw fixation -a cadaveric study. Biomedicine. 2013;33(1):468–72.
14. Bunmaprasert T, Roobsoong A, Pongmanee S, et al. Safety entry point, size and direction for placement of thoracic pedicle screw--a cadaveric study. J Med Assoc Thai. 2014;97(12):1344–51.
15. Yingsakmonkol W, Karaikovic E, Gaines RW. The accuracy of pedicle screw placement in the thoracic spine using the "Funnel Technique": part 1. A cadaveric study. J Spinal Disord Tech. 2002;15(6):445.
16. Seung-Jae H, Kim YJ, Gene C, et al. Free hand pedicle screw placement in the thoracic spine without any radiographic guidance: technical note, a cadaveric study. J Korean Neurosurg Soc. 2012;51(1):66–70.
17. Mcafee PC. Complications of anterior approaches to the thoracolumbar spine. Emphasis on Kaneda instrumentation. Clin Orthop Relat Res. 1994;306(306):110–9.
18. Birch BD, Desai RD, Mccormick PC. Surgical approaches to the thoracolumbar spine. Neurosurg Clin N Am. 1997;8(4):471.
19. Unruh KP, Camp CL, Zietlow SP. Anatomical variations of the iliolumbar vein with application to the anterior retroperitoneal approach to the lumbar spine: a cadaver study. Clin Anat. 2008;21(7):666–73.

Surgical Anatomy of the Lumbar Spine

4

Jian-gang Shi, Wen Yuan, and Jing-chuan Sun

1 Lateral Retroperitoneal Approach to the Lumbar Spine

1.1 Overview

Lateral retroperitoneal approach is mainly used to expose the vertebral bodies and anterolateral aspects of intervertebral discs at L1–L5 for lumbosacral surgery. Its indications include total or partial resection of a single lumbar vertebral body which is performed with bone grafting, anterior lumbar fusion, drainage of abscess in the psoas major muscle, dissection of an infectious lesion (especially tuberculosis) in a lumbar vertebral body, and resection of lumbar sympathetic ganglions. This approach can expose vertebral bodies and the lateral sides of intervertebral discs and avoid injury to the peritoneum and organs in the abdominal cavity at the same time.

1.2 Position

After general anesthesia, the patient is placed in the lateral position or recumbent position. The armpit and hip joint are cushioned by pillows (Fig. 4.1).

Soft pillows are used to cushion the left upper extremity and lumbar region (or elevate the jackknife of the operating table) so as to increase the distance between the subcostal margin and the iliac crest and thereby facilitate operation (Fig. 4.2).

1.3 Incision

Make an anterior-inferior incision from the point where the subcostal margin intersects with the posterior axillary line, i.e., at the distal end of the 12th rib, to the outer border of the rectus abdominis.

Attention should be paid to the protection of nerves in the abdominal wall during the incision of the skin and subcutaneous tissue. Injuries of the nerves often cause postoperative sensory disturbance or pain of the skin (Fig. 4.3).

Superficial layer of the abdominal wall (Fig. 4.4): the muscular portion of the external oblique muscle of the abdomen blends with the extending muscle fibers of the serratus anterior muscle, and some aponeuroses form the anterior layer of the sheath of the rectus abdominis.

Subcostal nerve: the anterior ramus of the spinal nerve T12, which travels together with subcostal vessels; it runs along the lateral arcuate ligament on the lower border of the 12th rib and the posterior portion of the kidneys, then travels in front of the upper portion of the quadratus lumborum muscle, next passes through the transverse fascia, and finally travels in the

J.-g. Shi (✉) • W. Yuan • J.-c. Sun
Department of Orthopedics, Changzheng Hospital, Shanghai, China
e-mail: shijiangang616@163.com; yuanwenspine@163.com; sjchxc@foxmail.com

J.-g. Shi et al. (eds.), *Anatomy Atlas and Interpretation of Spine Surgery*, https://doi.org/10.1007/978-981-10-5906-3_4

deep aspect of the internal oblique muscle of the abdomen; it is distributed in the skin in the anterior superior iliac spine region and hips, and it can run downward to the greater trochanter of the femur.

Iliohypogastric nerve: one of the branches of the anterior ramus of the first lumbar spinal nerve, which is located between the internal oblique muscle of the abdomen and the transverse abdominal muscle; it passes through the aponeurosis of the external oblique muscle of the abdomen at a point approximately 2.5 cm above the superficial inguinal ring; its anterior cutaneous branch innervates the abdominal skin above the pubic area.

Ilioinguinal nerve: one of the branches of the anterior ramus of the first lumbar spinal nerve, which is located approximately one finger below the iliohypogastric nerve and runs parallel with it; it runs across the inguinal canal with the spermatic cord, then emerges from the superficial inguinal ring, and distributes in the anterior scrotal skin. The genital branch of the genitofemoral nerve runs downward along the medial side of spermatic cord, then emerges from the superficial inguinal ring, and distributes in the cremaster muscle, inner thighs, and scrotums or the labia majora and mons pubis.

The vessels of the anterolateral abdominal wall include superior epigastric vessels of the internal thoracic vessel, branches of musculophrenic vessels, vessels of the inferior epigastric external ilium, deep circumflex iliac vessels, the arteria cruralis, superficial inferior epigastric and iliac circumflex vessels of the great saphenous vein, and the anterior branches of subcostal posterior intercostal vessels located in the 11th intercostal space.

Fig. 4.1 Position for lateral retroperitoneal approach

Fig. 4.2 The distance between the subcostal margin and the iliac crest

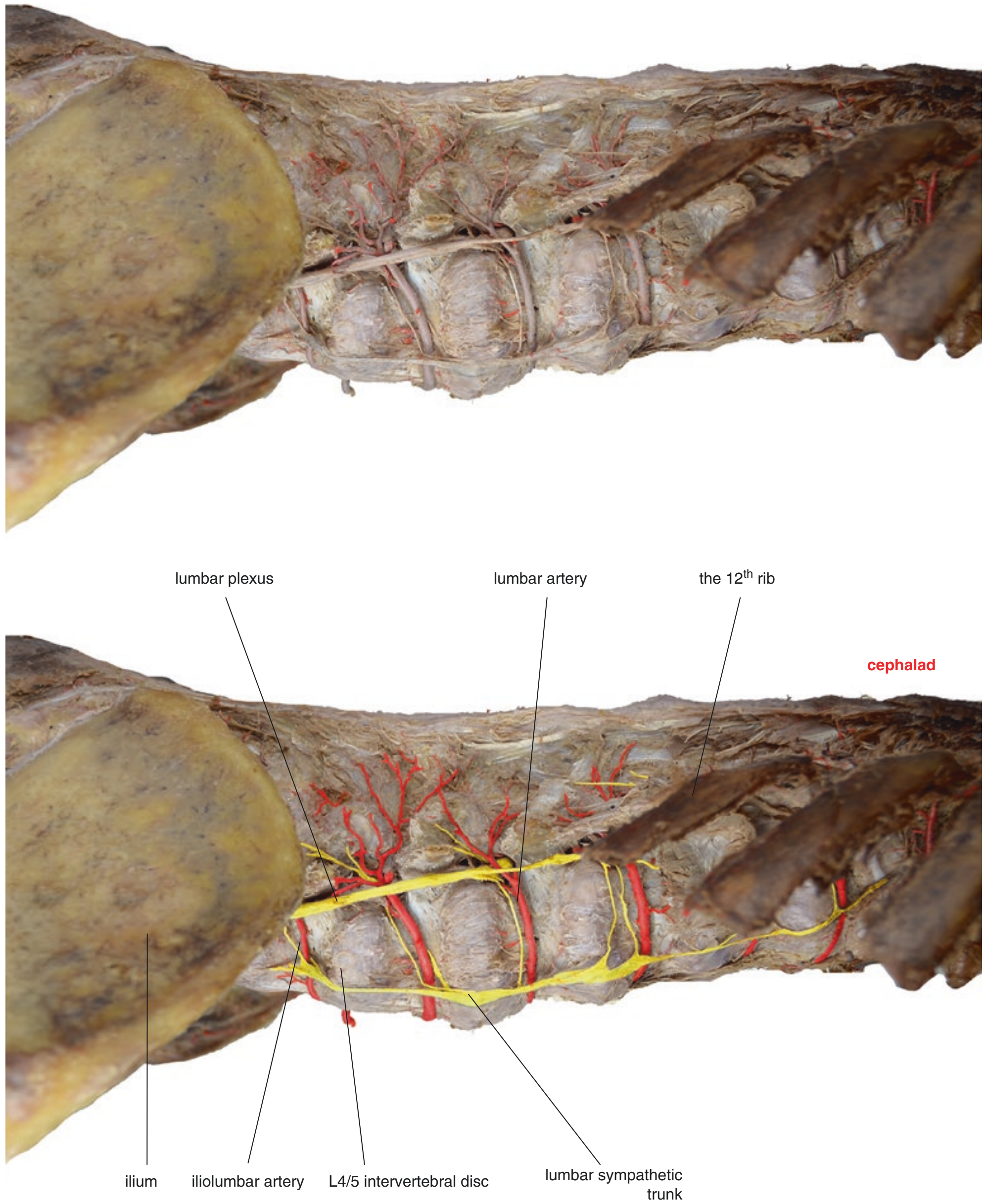

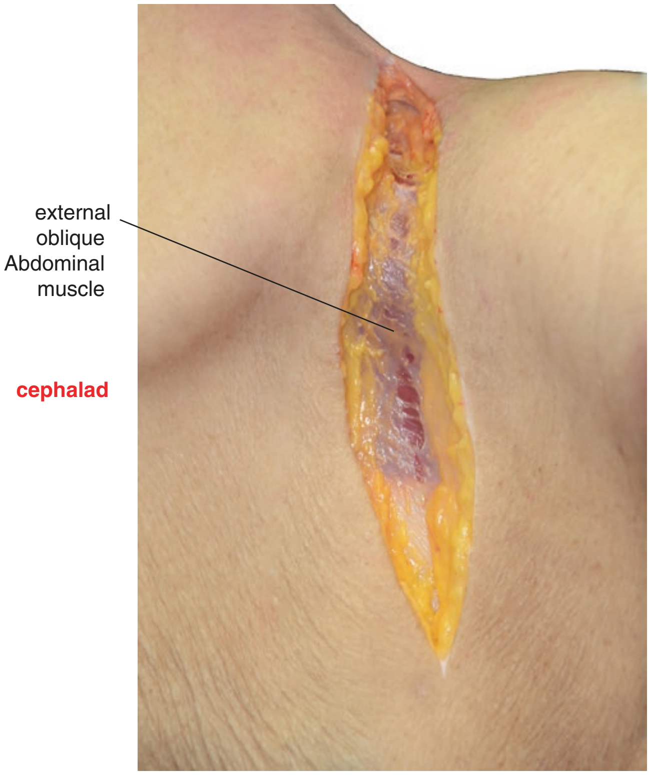

Fig. 4.3 Incision of lateral retroperitoneal approach

Incise the deep fascia and the muscle fiber of the external oblique muscle of the abdomen along the incision (Fig. 4.5) to expose the internal oblique muscle.

Dissect the internal oblique muscle of the abdomen vertically to the muscle fiber (parallel to the skin incision) (Fig. 4.6).

The transverse abdominal muscle and transverse fascia are dissected to expose retroperitoneal fat (Fig. 4.7). The transverse fascia is very thin; attention should be paid to avoid injury of the peritoneum.

The retroperitoneal fat and psoas major fascia are bluntly dissected, and the peritoneum and its contents are retracted toward the anteromedial side (Fig. 4.8).

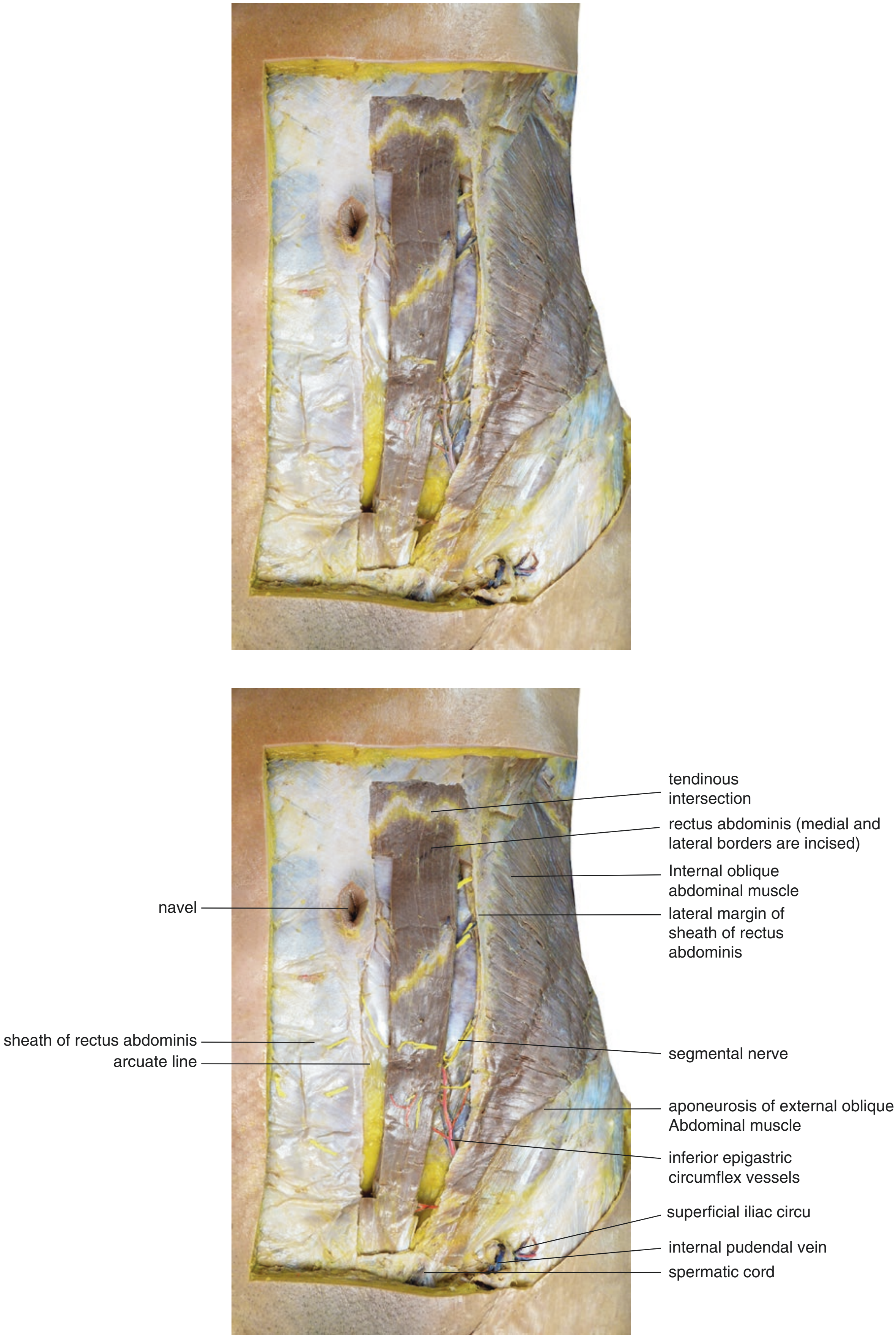

Fig. 4.4 Anatomy related to the abdominal wall

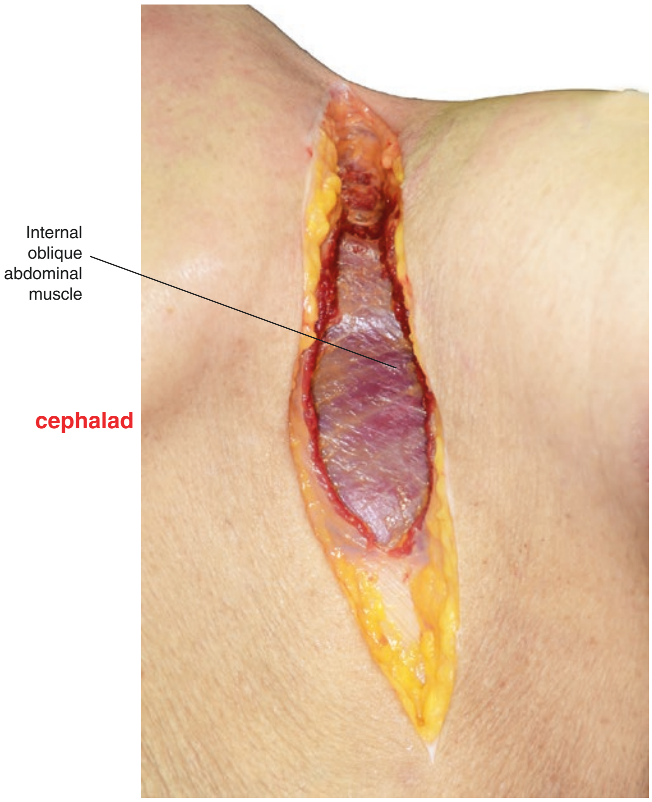

Fig. 4.5 Incision of the external oblique muscle of the abdomen

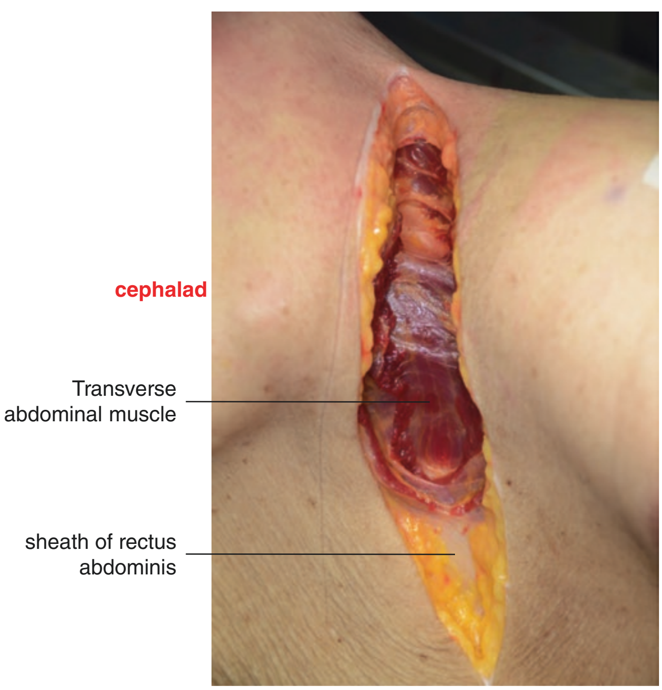

Fig. 4.6 Incision of the internal oblique muscle of the abdomen

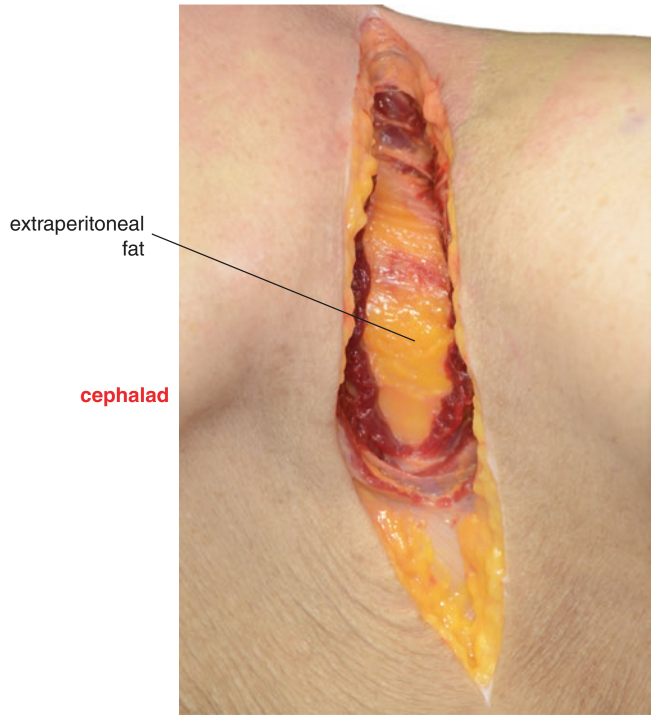

Fig. 4.7 Incision of the transverse abdominal muscle

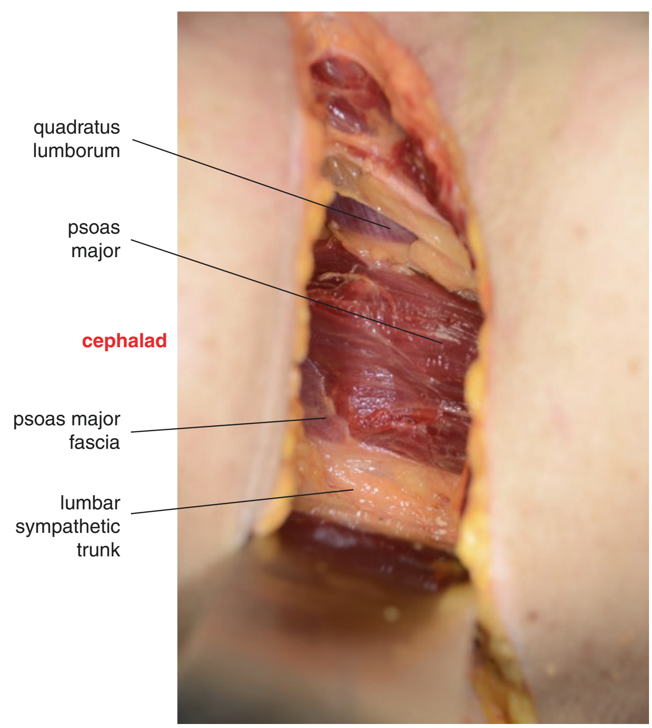

Fig. 4.8 Exposure of the psoas major muscle

External oblique muscle of the abdomen: the external oblique muscle of the abdomen starts from the lateral and inferior border of the 8th rib, and the bottom muscle bundle starts from the tip cartilage of the 12th rib, then runs in the lateral and anterior abdomen, with muscle fiber obliquing from anterolateral to inferior internal. Obliquus externus abdominis aponeurosis is distributed between the anterior superior iliac spine and the pubic tubercle, and its free margin forms the inguinal ligament. The muscle is innervated by terminal branches of the 8th to 12th intercostal nerves and the subcostal nerve and supplied by anterolateral abdominal wall vessels and the posterior lumbar artery. Its main function is to increase intra-abdominal pressure, resist gravity, and bend the trunk laterally (Fig. 4.9).

Internal oblique muscle of the abdomen: the internal oblique muscle of the abdomen has fiber mostly located in the deep layer of the external oblique muscle of the abdomen and is thinner than the external oblique muscle of the abdomen. It starts from the external two thirds of superior border of the inguinal ligament, and the internal oblique muscle of the abdomen starts from the superior iliac crest to the external and ends at the third or fourth rib inferior border and cartilago costalis. The obliquus internus abdominis is similar to the external oblique muscle of the abdomen in terms of innervation and blood supply. Its main function is to increase intra-abdominal pressure and resist gravity with lateral bending (Fig. 4.10).

Transverse abdominal muscle: the transverse abdominal muscle starts at the thoracolumbar fascia, iliac crest, and the external one third of the inguinal ligament and translates to the aponeurosis at the lateral border of the rectus abdominis. The transverse abdominal muscle is similar to the external oblique muscle in terms of innervation and blood supply. Its main function is to increase intra-abdominal pressure (Fig. 4.11).

Transverse fascia: it is close to the deep transverse abdominal muscle layer, and its anterior part connects inferior fascia of the diaphragm, while its inferior part continues to the fascia iliaca and pelvic fascia. Transverse fascia connects loosely to the transverse abdominal muscle but closely to the posterior sheath of the rectus abdominis layer (Fig. 4.12).

Parietal peritoneum: it is the innermost layer of the anterolateral abdominal wall, goes up toward the inferior peritoneum of the diaphragm, and continues down the peritoneum of the pelvic cavity (Fig. Fig. 4.13).

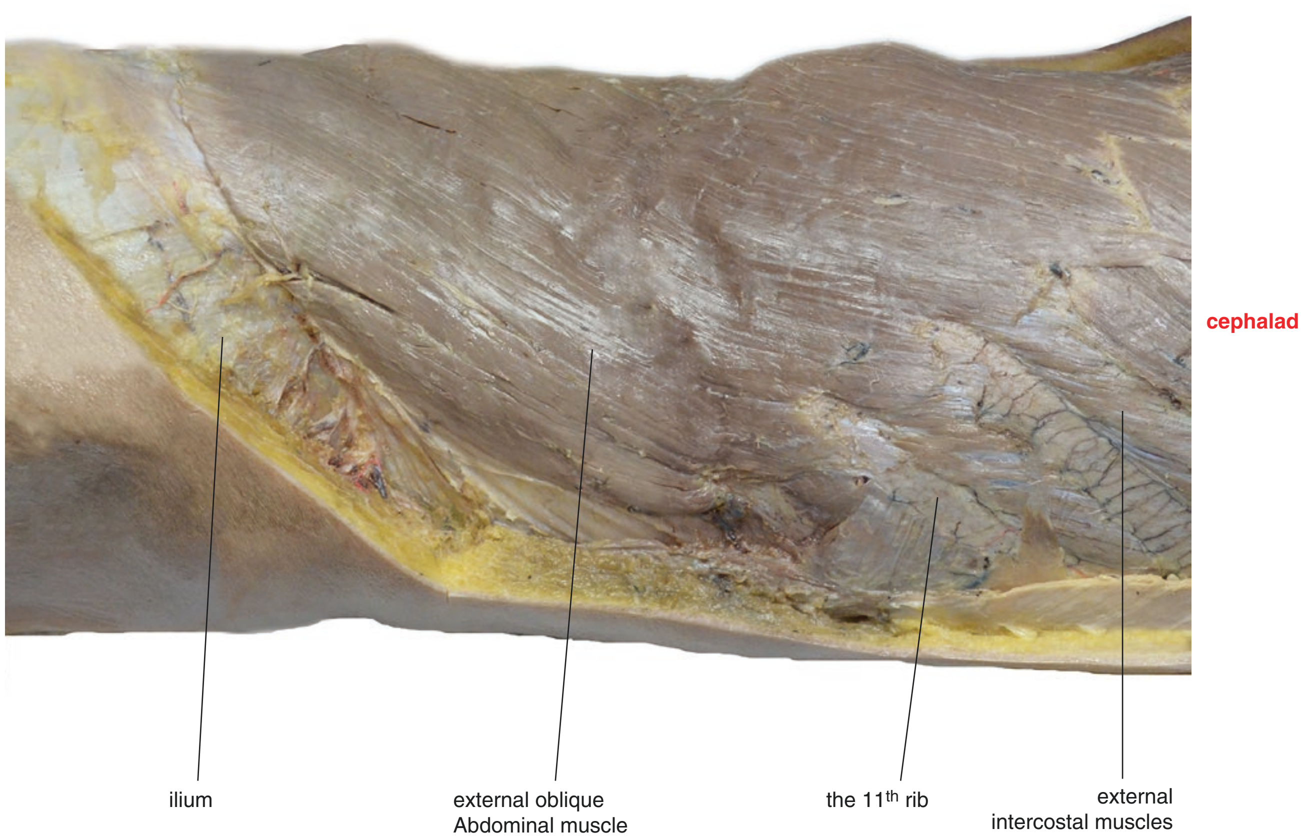

Fig. 4.9 Anatomy related to the lateral abdominal wall (external oblique muscle of the abdomen)

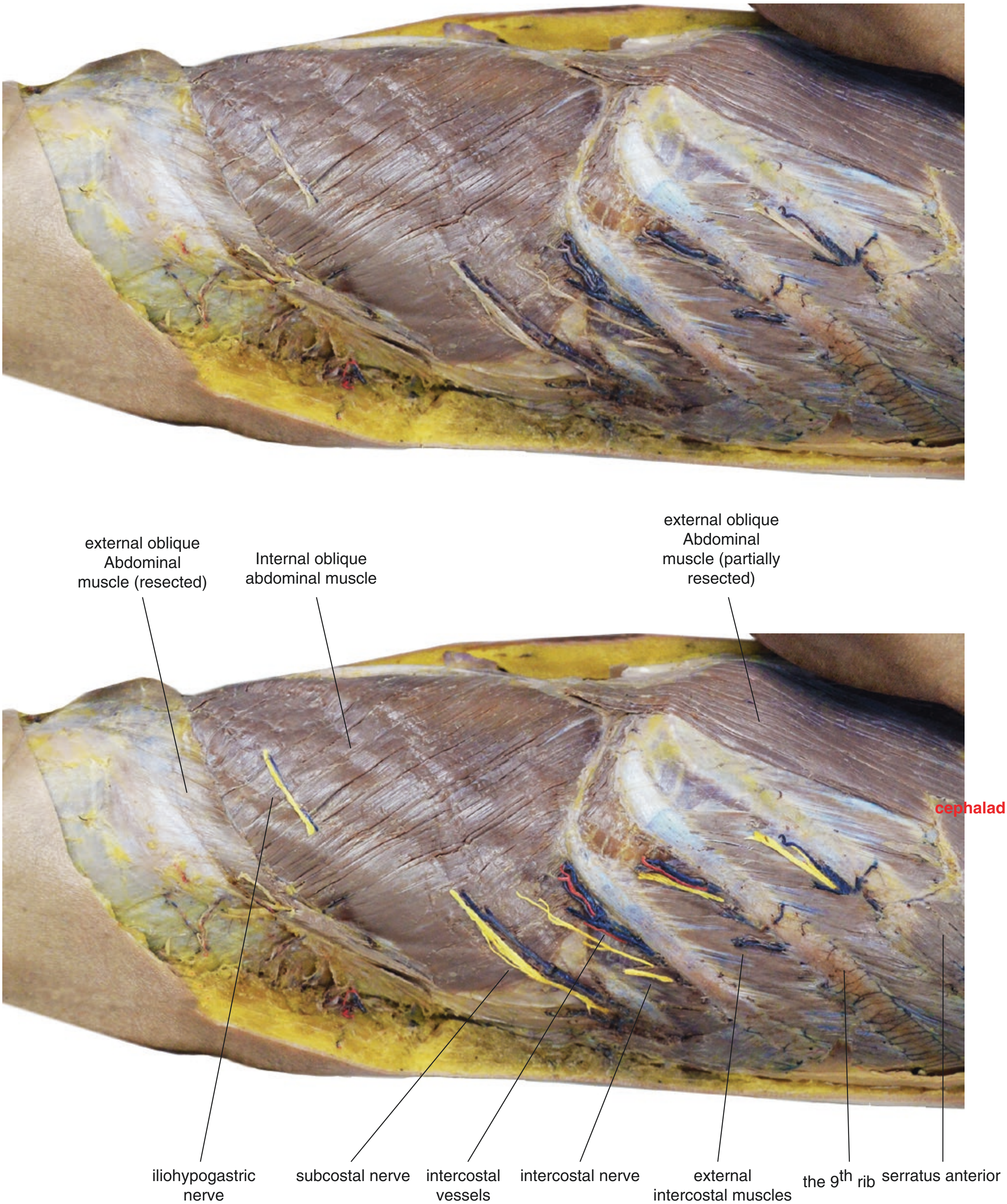

Fig. 4.10 Anatomy of the internal oblique muscle of the abdomen (the external oblique muscle of the abdomen has been removed)

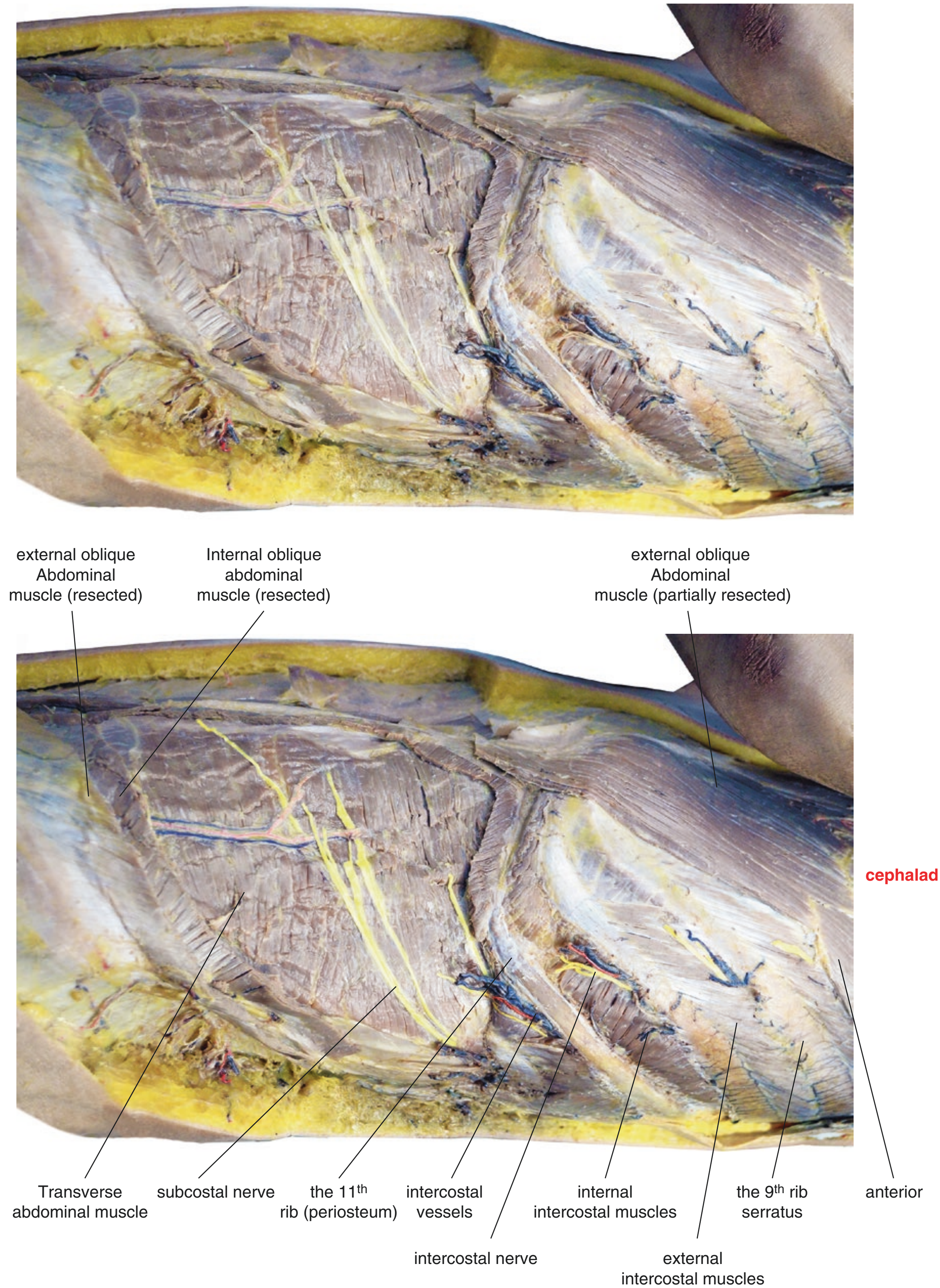

Fig. 4.11 Anatomy of the transverse abdominal muscle (the external oblique muscle of the abdomen and the internal oblique muscle of the abdomen have been removed)

Fig. 4.12 Anatomy of the transverse fascia (the external oblique muscle of the abdomen and the internal oblique muscle of the abdomen have been removed)

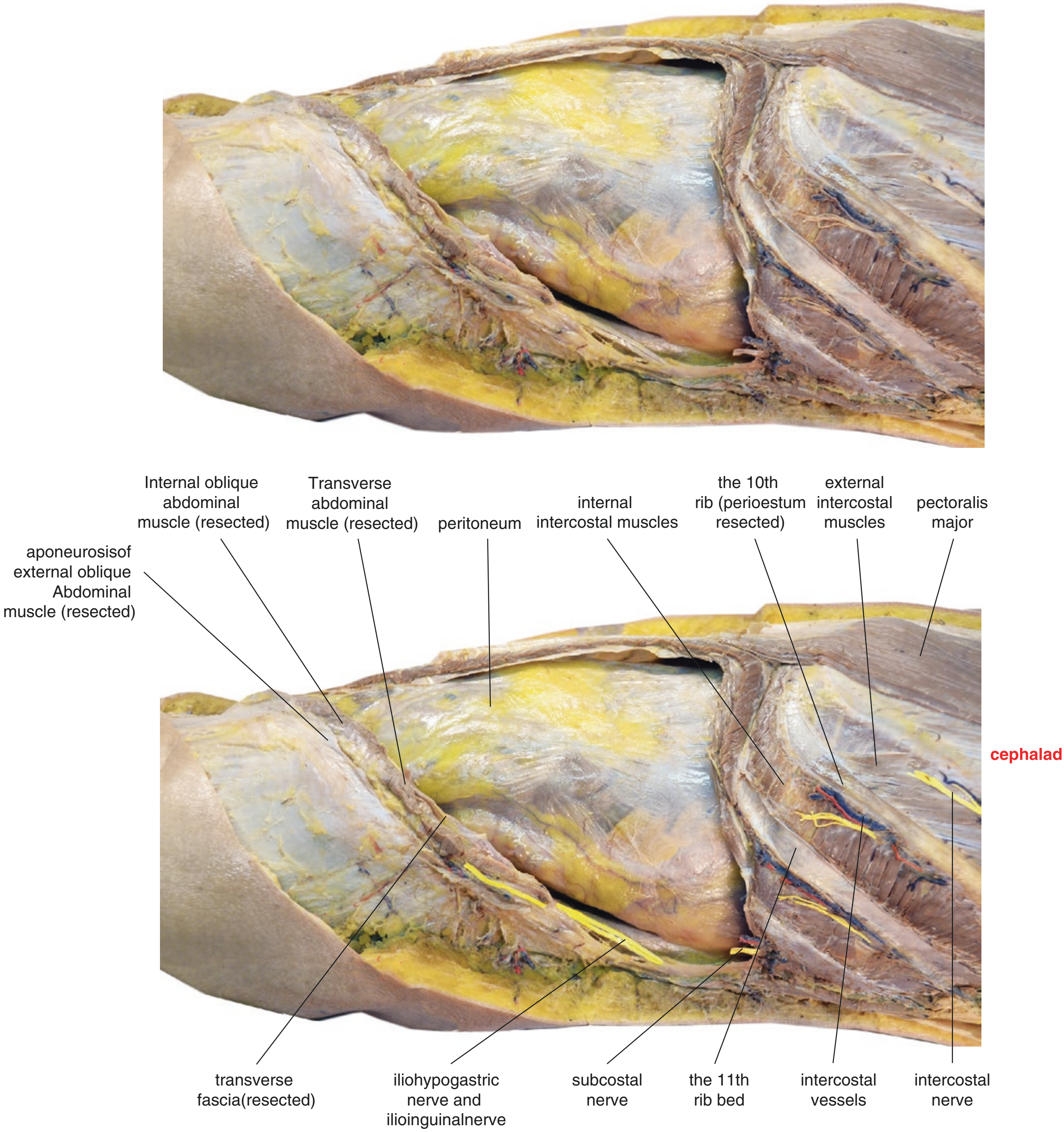

Fig. 4.13 Anatomy related to the lateral abdominal wall (parietal peritoneum)

1.4 Exposure

The psoas major muscle is exposed by retracting the peritoneum and visceral organ to the midline. The ureters which are located on the medial surface of the psoas major can be retracted medially to avoid injury.

The abdominal aorta and inferior vena cava should be protected with wet gauze pads, which are located above the superior L4 body.

The lateral vertebral body to lateral intervertebral disc can be exposed by dissecting the iliopsoas to the dorsal side. The lumbar artery and lumbar vein on the lateral vertebral body surface can be seen at the middle part of the lumbar vertebral body (Fig. 4.14).

If the L5 vertebral body and L4–L5 intervertebral disc need to be exposed, left iliac blood vessels are retracted to the opposite side (Fig. 4.16).

The lumbar artery and lumbar vein on the target vertebral body are ligated. The connective tissue of the vertebral body and intervertebral disc surface should be carefully identified, separated, and then incised to avoid bleeding.

The duration of compression on the iliac artery and iliac vein should not be too long to avoid formation and rupture of thrombus.

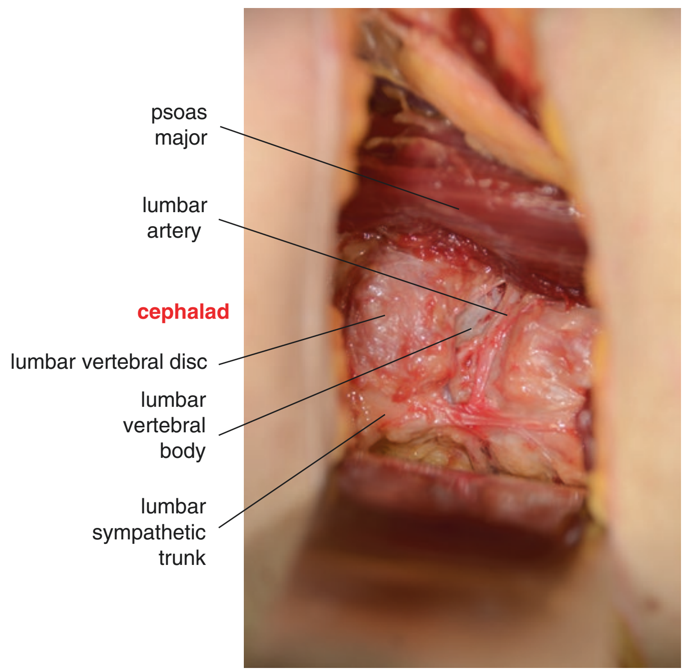

Fig. 4.14 Exposure of vertebral bodies

Retroperitoneal space: it is located between the retroperitoneal peritoneum and the intra-abdominal fascia, and it ranges up from the diaphragm and down the superior pelvic aperture. The space connects to mediastinal tissues through the retroperitoneal fascia on each side and upward to the lumbocostal triangle and down communicates with the retroperitoneal space of the pelvic cavity. So the space infection is easily spread; aseptic condition should be strictly kept during the surgery to avoid the infection in the retroperitoneal space. The contents of retroperitoneal space include the kidneys, adrenal glands, abdominal portion of the ureters, great vessels (such as the abdominal aorta, inferior vena cava, and its branches), nerve, and lymph node duct (Fig. 4.15).

Ureter: with a total length of 25–30 cm and a diameter of 4–7 mm, it is located in the medial aspect of the psoas major fascia surface. The adjacent structures around the abdominal portion of ureters are different on each side. Flexura duodenojejunalis is to the left front, crossed by the left colic artery, left testicular vessel (ovarian vessel for female), and sigmoid mesocolon. The descending portion of the duodenum, right colon, ileocolic vessel, radix of mesentery, and right testicular vessel cross in front of the right ureter from top to bottom. The blood of the abdominal portion of the ureter is supplied by the renal artery, testicular (or ovarian) artery, abdominal aorta, and iliac artery, and these vessels are mostly located in the medial aspect of the ureter (Fig. 4.15).

Lumbar sympathetic trunk (Fig. 4.16): it is composed of 3–5 ganglions, located between the vertebral column and psoas major muscle and covered by the prevertebral fascia. It is adjacent to the abdominal aorta on the left side and covered by the inferior vena cava on the right side. The number of ganglions is variable, and the location of ganglions at L2 and L4 is more stable because they are covered by the medial arcuate ligament and common iliac artery, respectively, and they serve as anatomic landmarks in clinical practice. Transverse ramus communicant is connected to the left and right sympathetic trunks. Injury to the sympathetic trunks may cause retrograde ejaculation or sexual dysfunction, so they should be identified and protected during surgery.

Lumbar artery (Fig. 4.16): lumbar arteries are branches of the abdominal aorta. The four pairs of branches symmetrically arise from each side of the posterior abdominal aorta and cross over lateral aspects of the lumbar vertebral body along with the lumbar vein toward the intervertebral foramen and then divide into the dorsal branch and ventral branch at the medial psoas major border. Dorsal branch is distributed in the muscle and skin of the back. Ventral branch is distributed in the abdominal wall and connects with other arteries in the anterolateral abdominal wall.

Abdominal aorta: it is located in the left front of T12–L4 and arises from the diaphragmatic aortic hiatus, connecting the thoracic aorta above and dividing into left and right common iliac arteries at L4 level. The abdominal aorta is 14–15 cm in length and about 3 cm in diameter. In front of it, there is the pancreas, a horizontal portion of the duodenum and radix mesenterii; L1–L4 vertebral bodies and intervertebral discs are on the posterior side of it; the inferior vena cava is on the right side of it; the left lumbar sympathetic trunk is on the left side of it (Fig. 4.17).

Inferior vena cava: it is located at the L4–L5 level and receives drainage from the convergence of left and right common iliac veins. It runs upward along the right side of the abdominal aorta in front of the vertebral column, crosses the vena caval foramen of the diaphragm, then enters the thoracic cavity. In front of the inferior vena cava, there are the liver, caput pancreas, horizontal portion of the duodenum, right testicular (or ovary) artery, and (small) radix mesenterii. Behind the inferior vena cava, there are the lumbar vertebral body, the right crura of the diaphragm, and the right lumbar sympathetic trunk. The abdominal aorta is to its left, and the right psoas major muscle, right ureter, right kidney, and right adrenal gland are to the right of the inferior vena cava.

Celiac plexus: it is the biggest plexus of the visceral nerve. It is located in front of the left and right crura of the diaphragm and the upper portion of the abdominal aorta, between both sides of the adrenal gland. It surrounds the coeliac trunk and the root of the superior mesenteric artery.

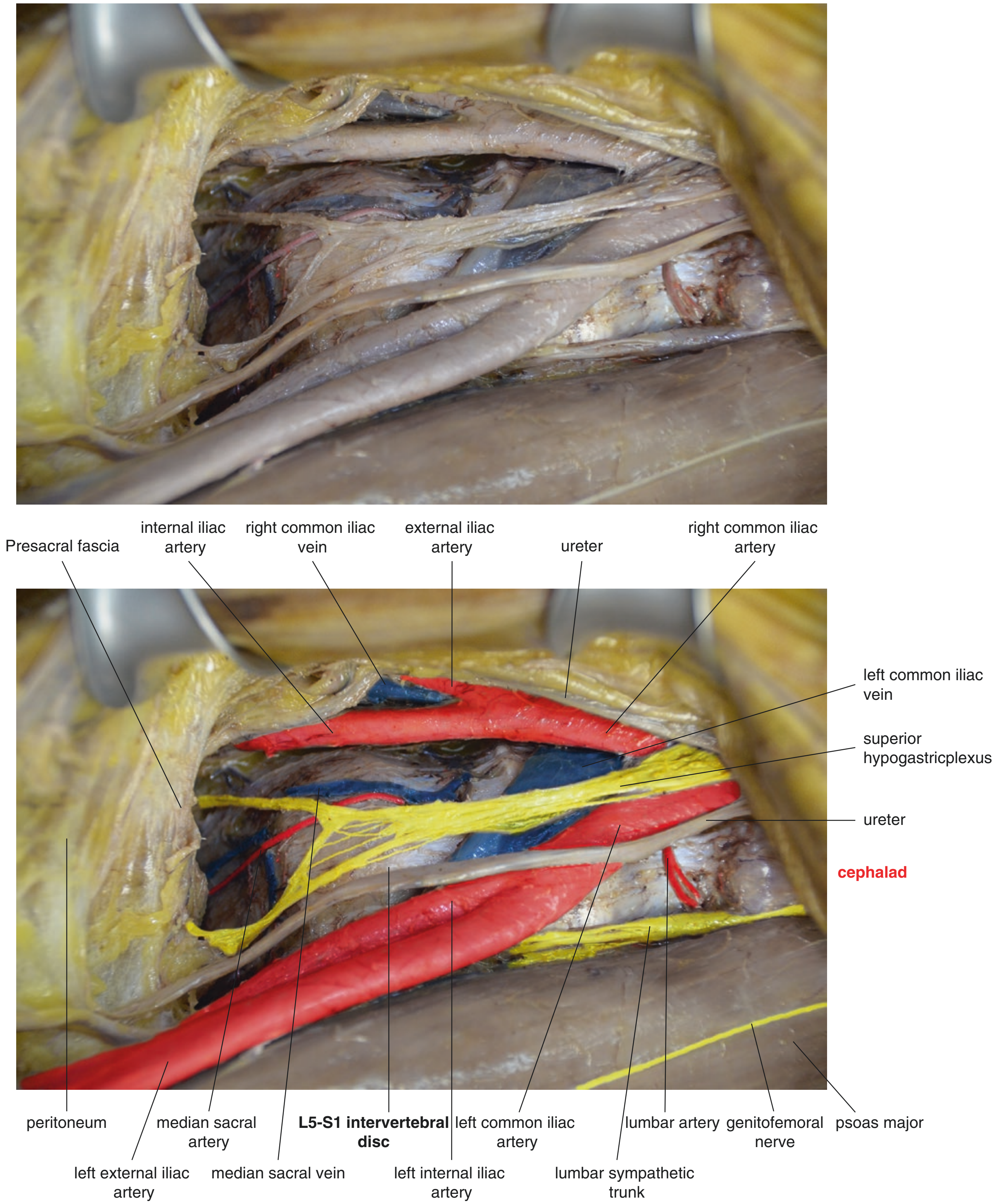

Fig. 4.15 Anatomy related to the retroperitoneum

Fig. 4.16 Lumbar sympathetic trunks

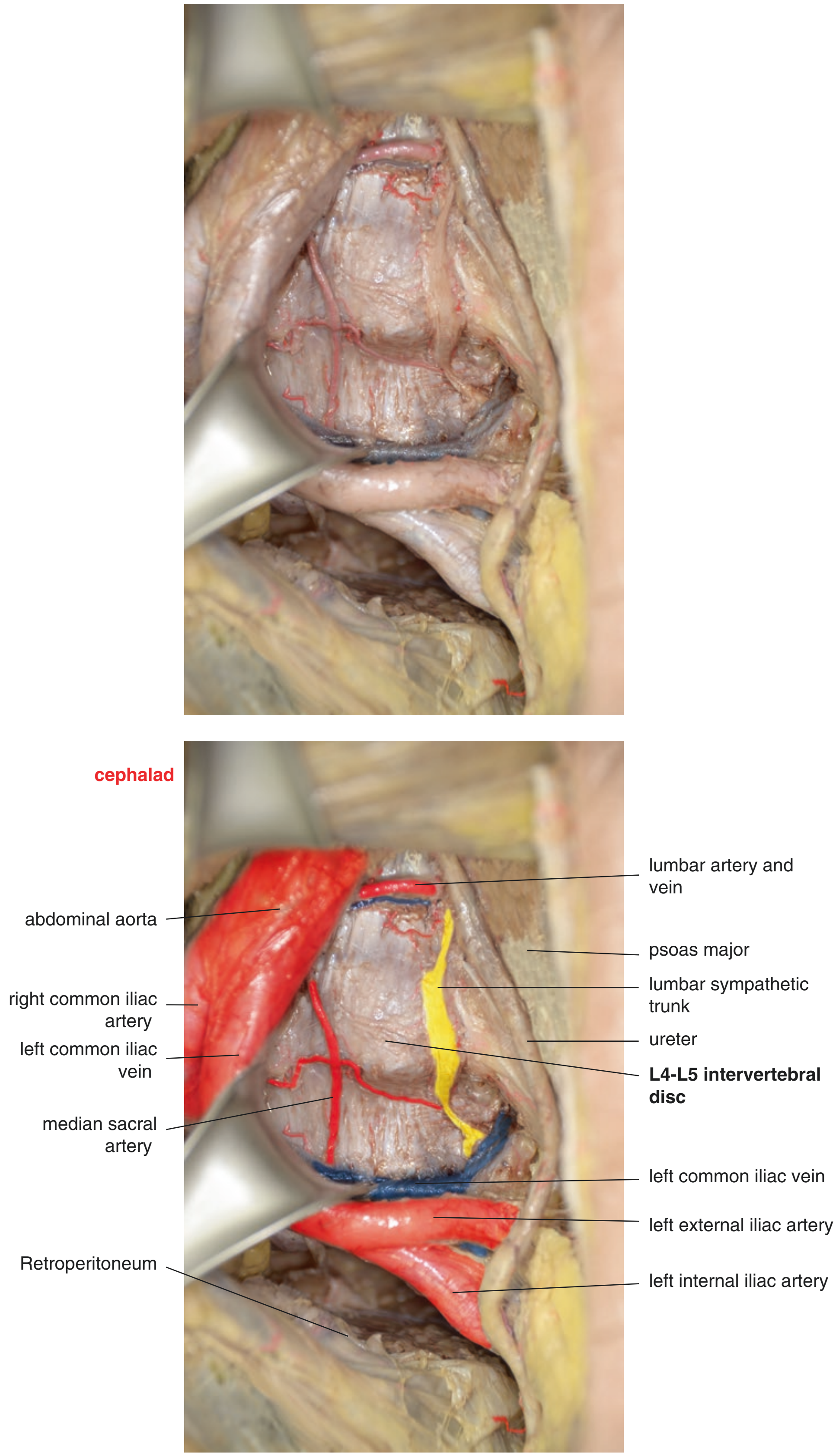

Fig. 4.17 Neurovascular structures in retroperitoneal space

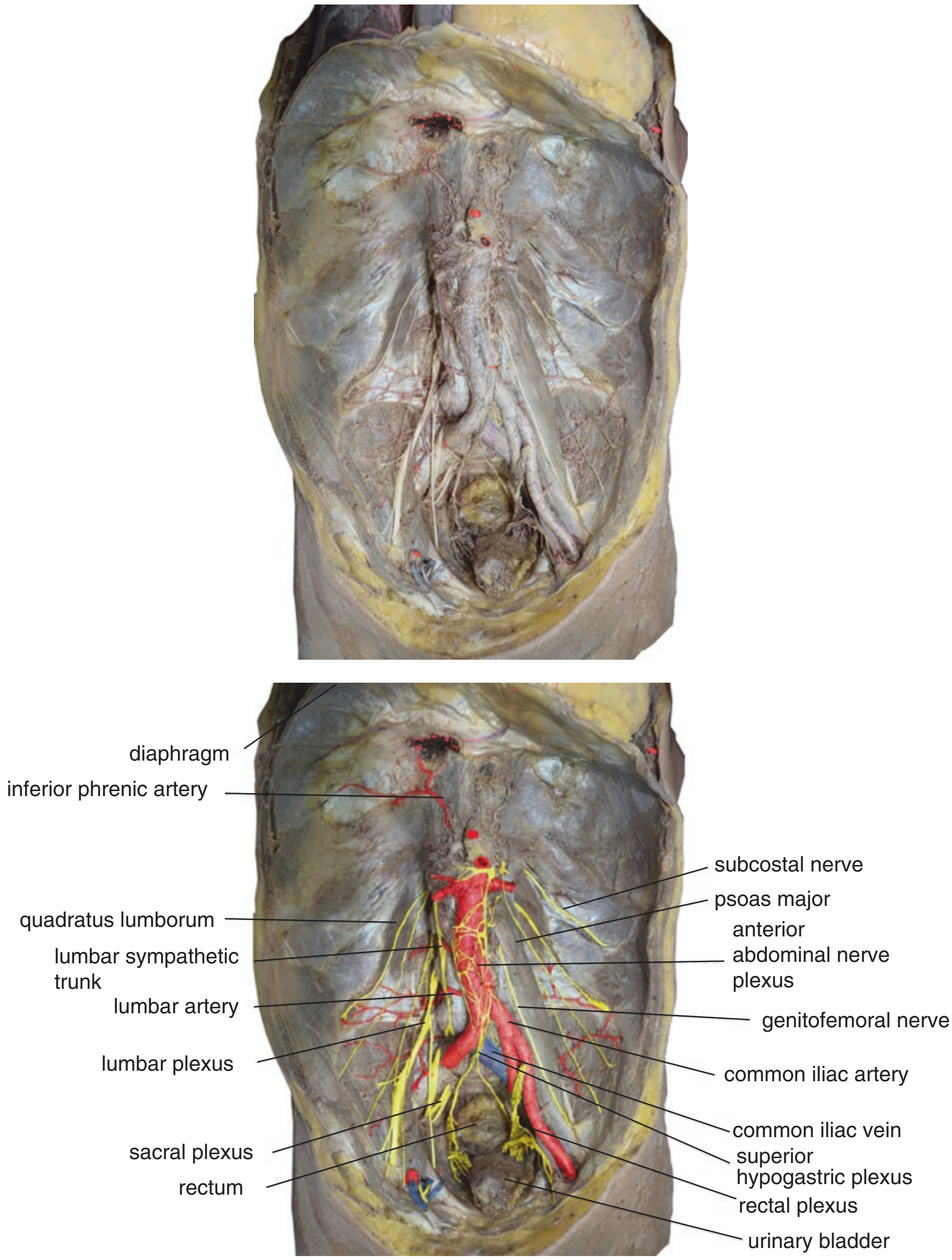

2 Posterior Lumbar Spinal Exposure and Transforaminal Lumbar Interbody Fusion

2.1 Overview

Posterior approaches to the lumbar spine are mainly used for posterior column lesions such as lesions of the vertebral pedicle, transverse process, facet joint and spinous process, and spinal canal as well as central column lesions such as lesions of the intervertebral disc, posterior longitudinal ligament, and posterior vertebral body. The Wiltse approach (a paraspinal intermuscular approach) has advantages involving simple surgical route, minor soft tissue injury, short duration of surgery, less blood loss, and fast recovery.

In 1982, Harms et al. proposed transforaminal lumbar interbody fusion (TLIF). TLIF is an approach mainly via Kambin's triangle to expose the intervertebral space, which can make the dural sac or nerve roots suffer the minimum retraction during interbody fusion and which only weakens the unilateral structures of the posterior lumbar spine. But traditionally, TLIF has relatively narrow indications, because it does not allow complete decompression on the dural sac and nerve root. It is mainly indicated for lumbar degenerative disease without or with unilateral radiolopathy. Hence, modified TLIF was then developed, in which the operating area is shifted more medially than that in traditional TLIF; unilateral facet joints and vertebral plates are partially resected; and thorough decompression is performed around the traversing nerve root and preserving posterior ligamentous complex between spinous processes.

2.2 Position

Patients are usually placed in the prone position after general anesthesia (Fig. 4.18). Keep enough abdominal space to avoid impacts on respiration and meanwhile help decrease compression on venous drainage to reduce intraoperative bleeding.

2.3 Exposure

Make a posterior midline incision along the spinous processes according to the involved levels (Fig. 4.19).

Incision on the skin and subcutaneous tissue is made to expose the lumbodorsal fascia.

Incise the lumbodorsal fascia (Fig. 4.21) to expose the dorsal muscle.

Fig. 4.18 Position for posterior lumbar spinal exposure

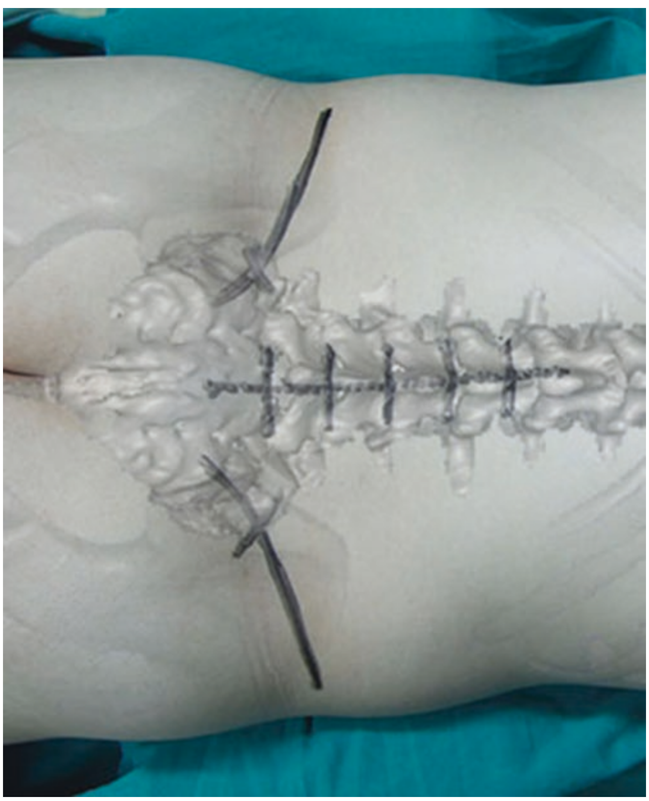

Fig. 4.19 Incision for posterior lumbar spinal exposure

Lumbodorsal fascia, also known as thoracolumbar fascia (Fig. 4.20): the main function of the thoracolumbar fascia is to support and wrap erector spinae muscles. The lumbodorsal fascia originates from the thorax and ends at the sacrum. The lumbodorsal fascia becomes thicker around the lumbar transverse process. In the L4–S1 segments, its transverse fiber is closely connected to the midline structures.

Supraspinous ligament: the supraspinous ligament originates from the C7 spinous process and ends at the median sacral crest. The supraspinous ligament and interspinous ligament are innervated by the terminal of the dorsal rami of the spinal nerves (Figs. 4.21 and 4.22).

Interspinous ligament: it is located between adjacent spinous processes, with the anterior border connected to the ligamentum flavum and the posterior border continuous with the supraspinous ligament. Injury to the interspinous ligament can cause chronical low back pain (Fig. 4.22).

The innervation of the facet joint of a lumbar spine: each lumbar facet joint is innervated by medial branches of the dorsal ramus. The medial branches course caudally under the base of the superior articular process after they split off of the dorsal ramus. They continue in a groove between the superior articular process and transverse process underneath the mamillo-accessory ligament. The medial branches then give off two branches to the adjacent facet joints, the ascending and descending articular branches. The lumbar facet joints have dual innervation from the medial branch of each respective level and the level above (Fig. 4.23).

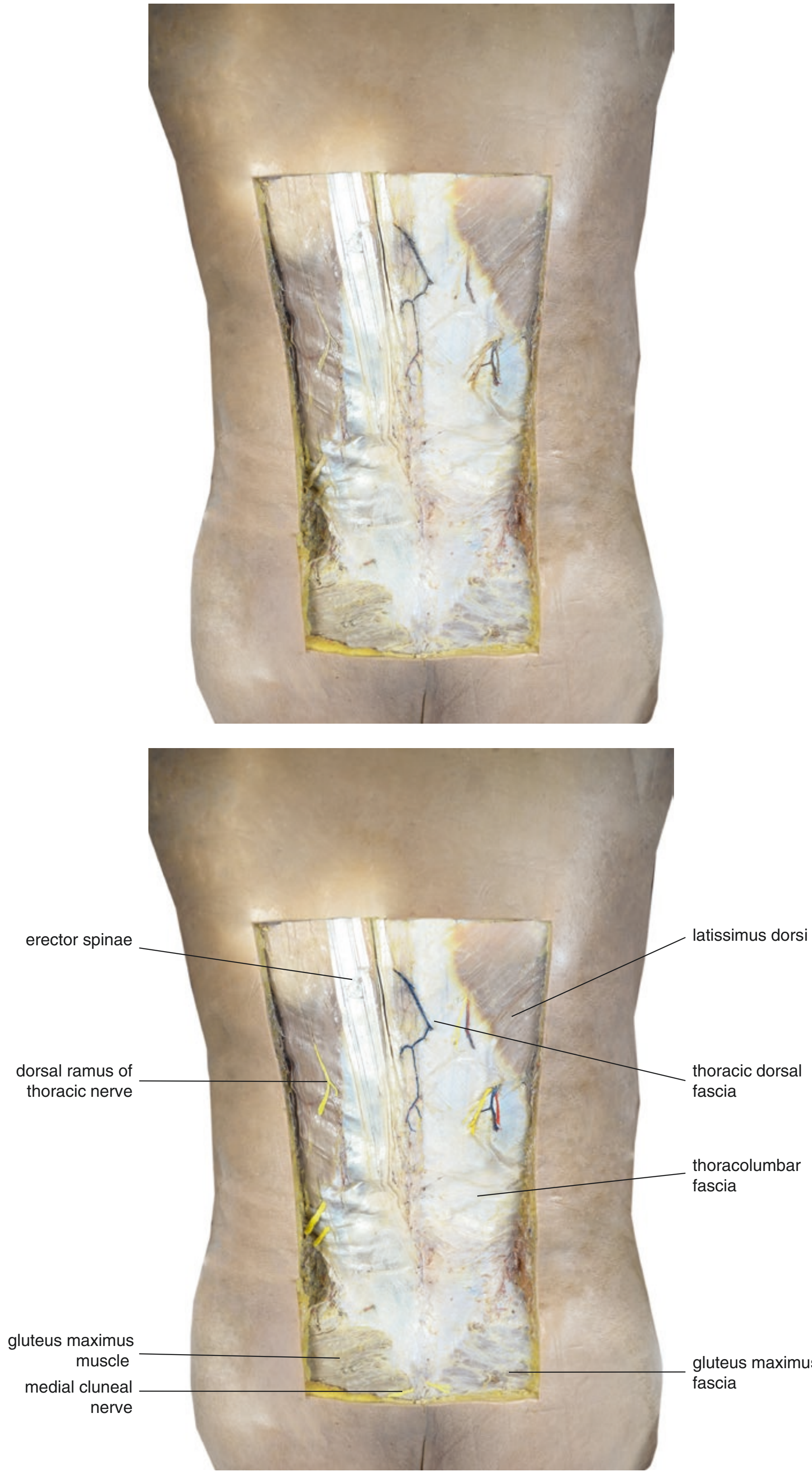

Fig. 4.20 Anatomy related to the posterior approach to the lumbar spine

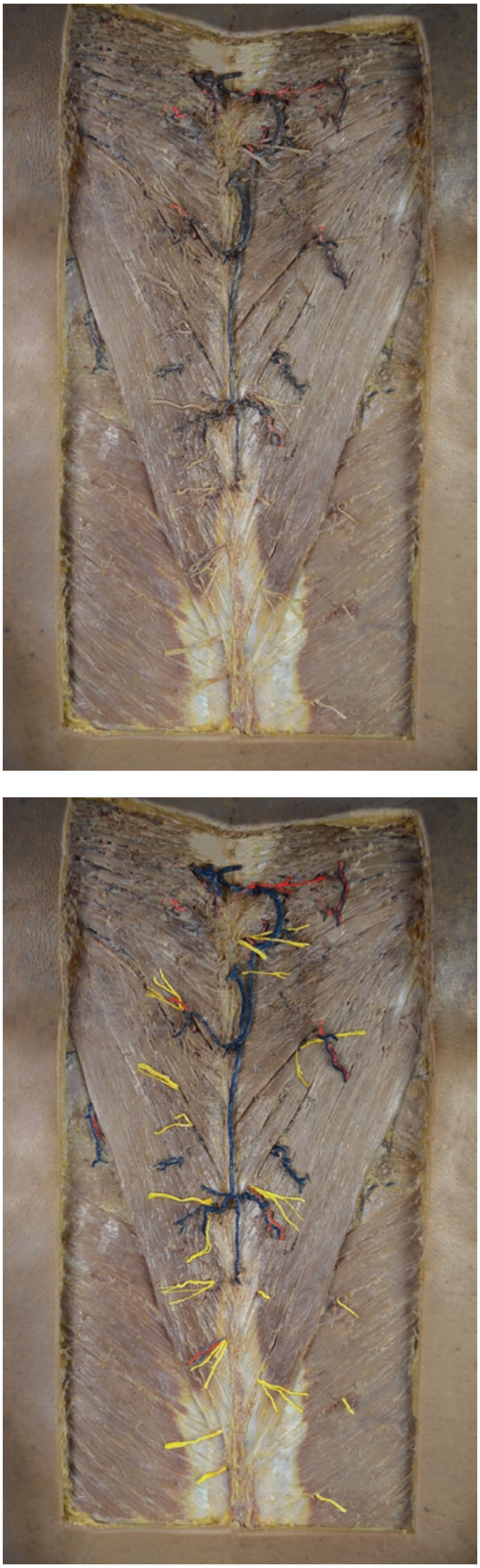

Fig. 4.21 Anatomy related to the posterior approach to the lumbar spine

Subperiosteal dissection is performed along each side of the spinous processes. Attention should be paid to preserving the supraspinous ligaments and interspinous ligaments.

Expose the facet joints on both sides and then use an automatic retractor to expose the posterior structure of the lumbar spine (Fig. 4.24).

Connecting rods are installed on the contralateral screws to the fusion side to help temporarily fix the spine and spread out the intervertebral spaces of the target segments (Figs. 4.25 and 4.26).

The inferior facet of the superior vertebra is removed with an osteotome.

The superior facet and ligamentum flavum are removed with Kerrison rongeur to expose the lateral recess and intervertebral disc (Fig. 4.27).

Expose the lateral spinal canal, dural sac, intervertebral foramen, and traversing nerve root. Superior nerve root exists from the intervertebral foramen beneath the superior vertebral pedicle.

Protect the existing nerve root and traversing nerve root with nerve root retractor.

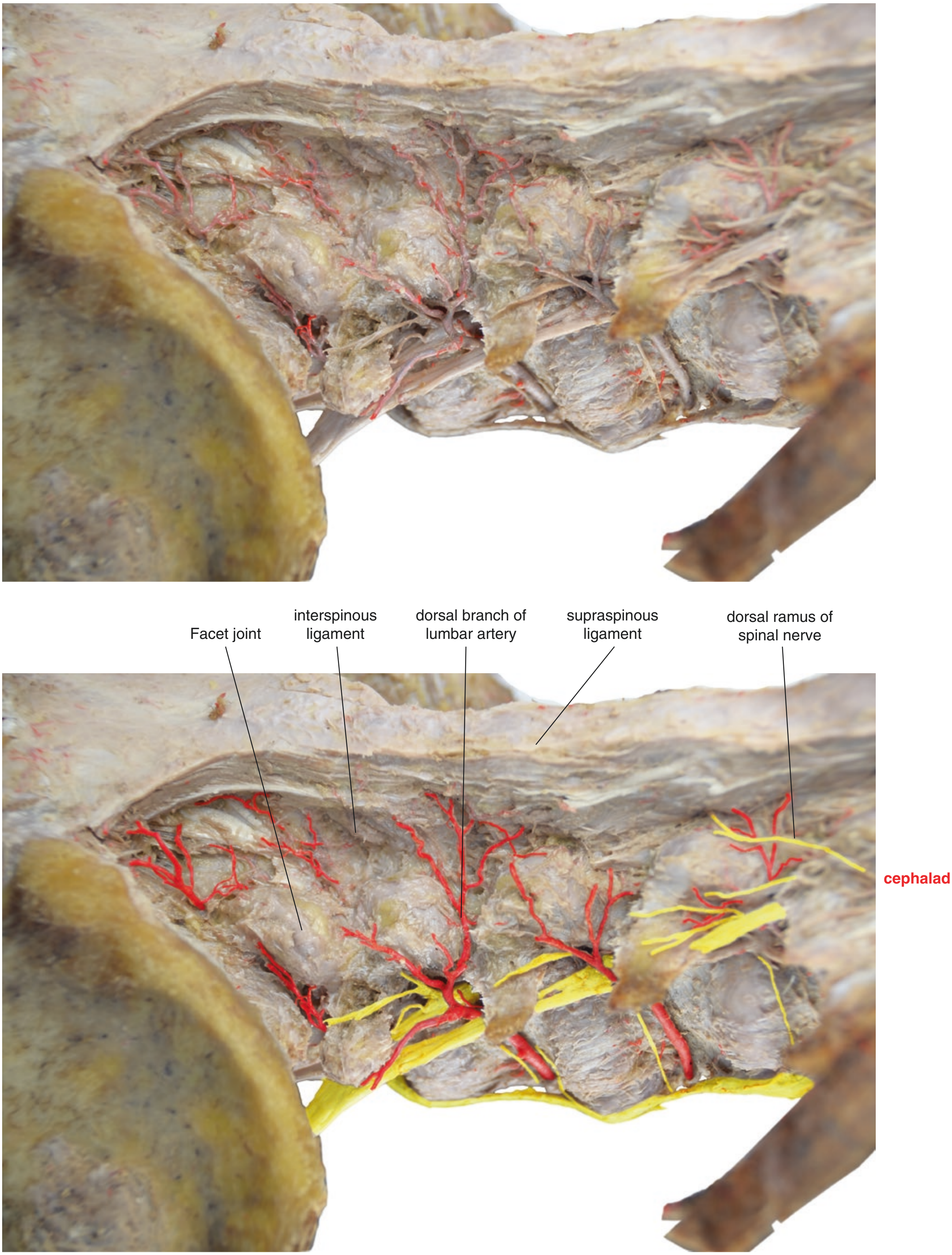

Fig. 4.22 Posterior lumbar ligaments, vessels, and nerves

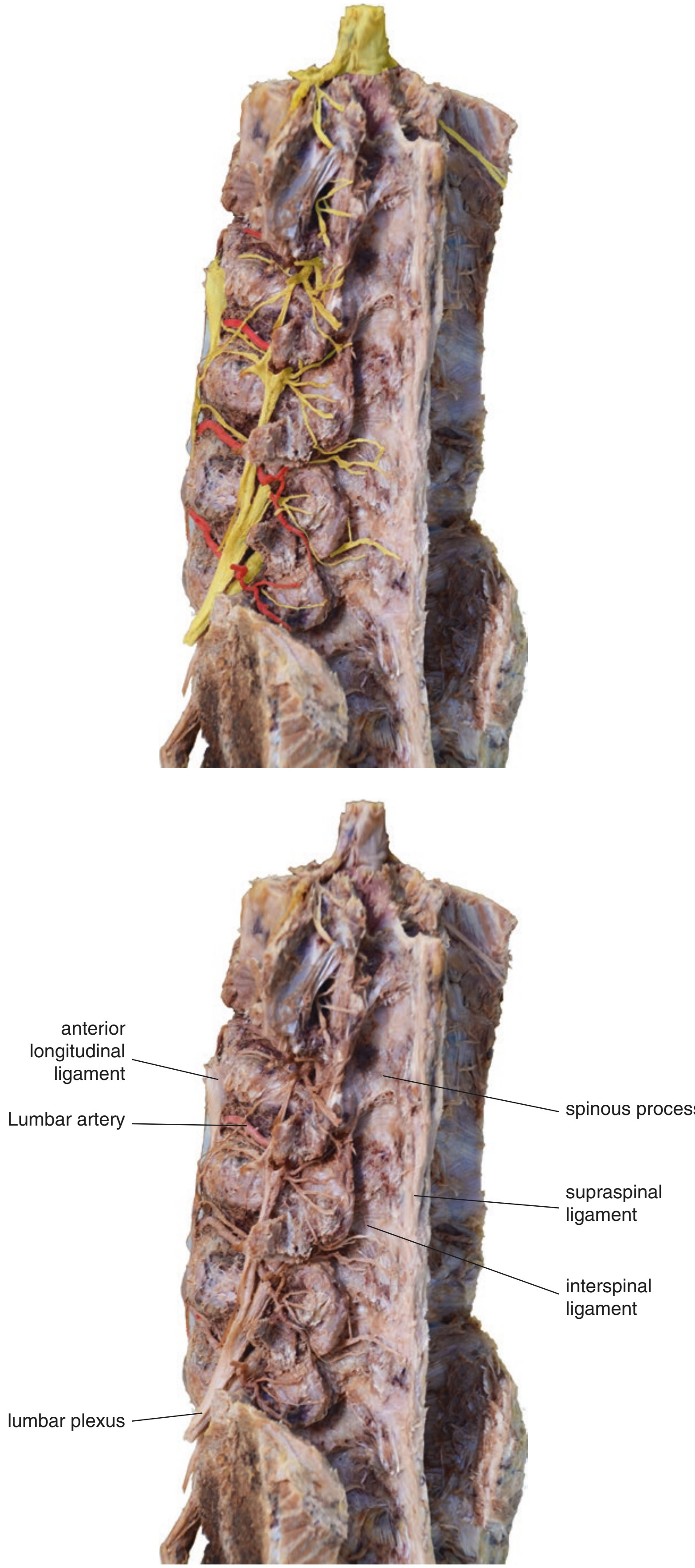

Fig. 4.23 The innervation of the facet joint of a lumbar spine

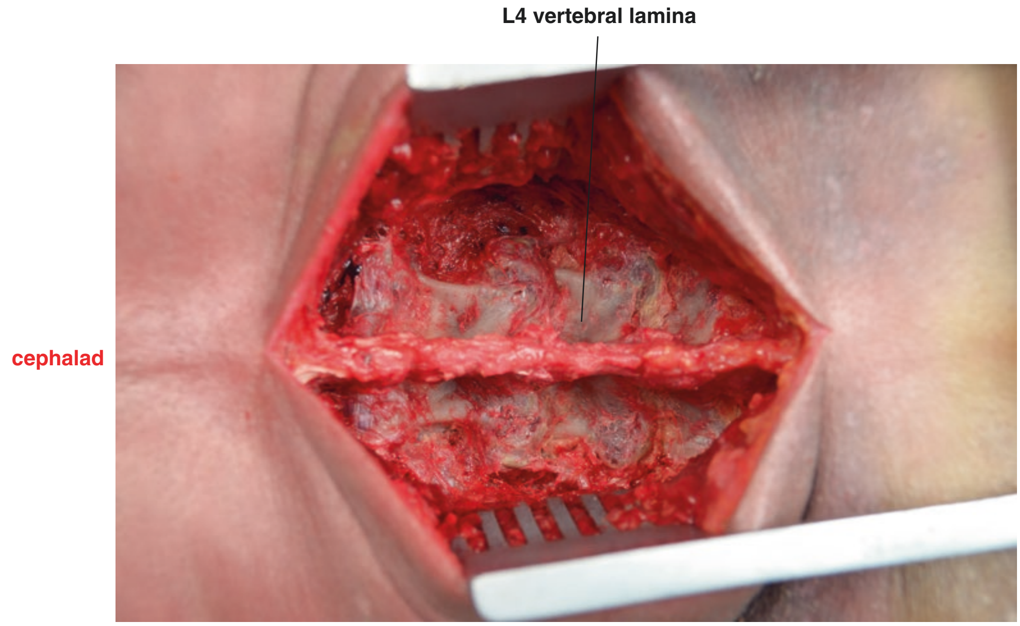

Fig. 4.24 Exposure of the posterior structure of the lumbar spine

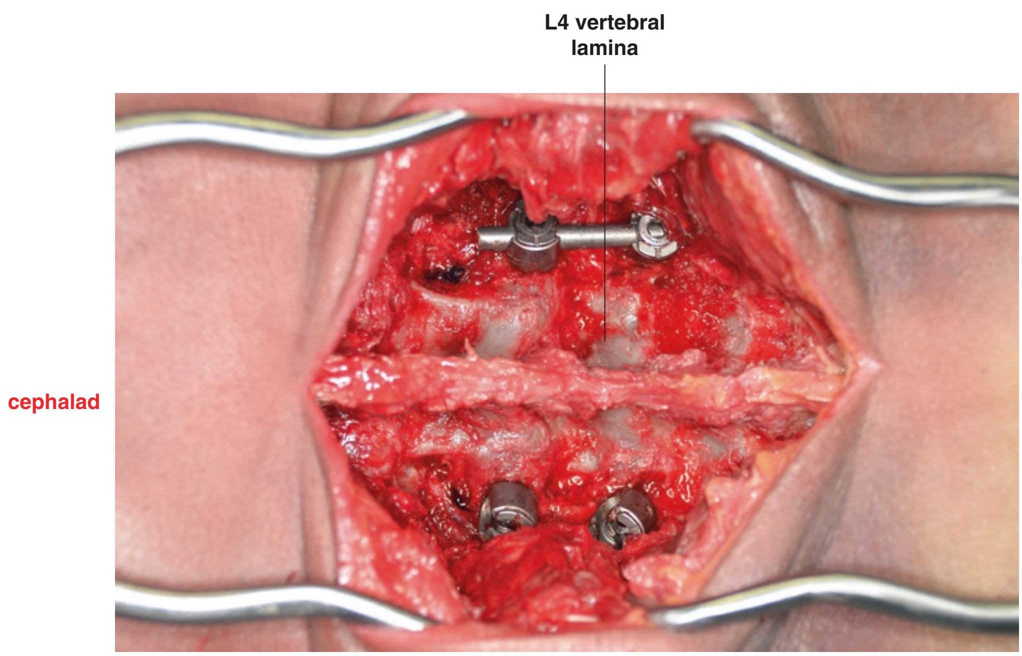

Fig. 4.25 Temporarily stabilizing the involved segments by installing connecting rod

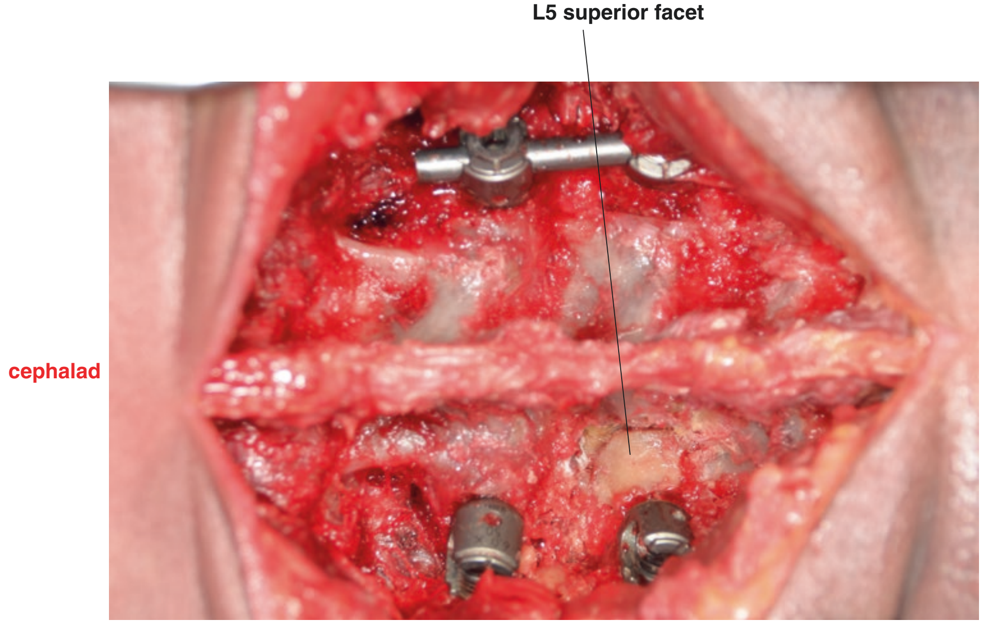

Fig. 4.26 The inferior facet of the superior vertebra is resected with an osteotome

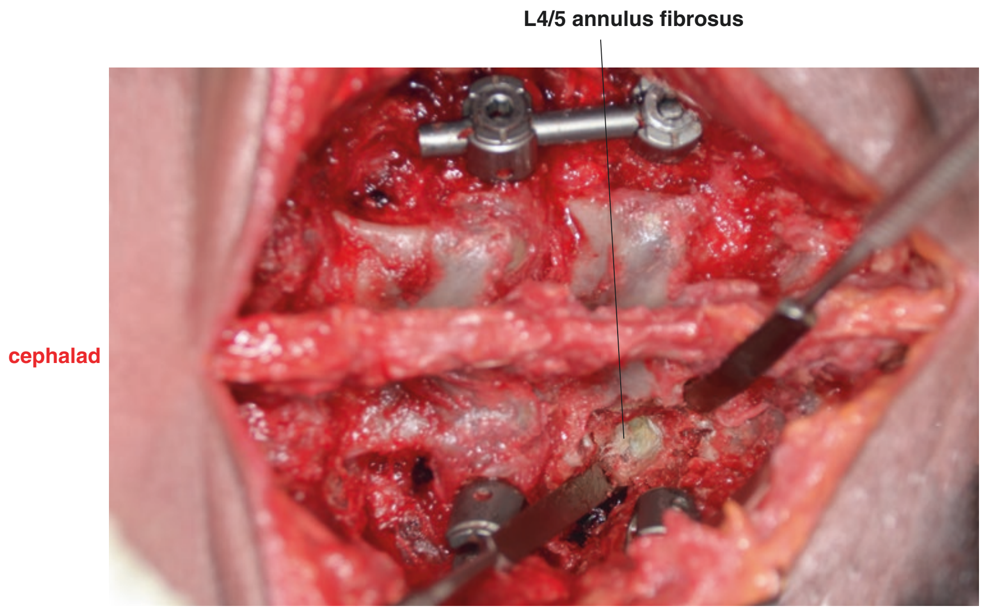

Fig. 4.27 Exposure of the lateral recess and intervertebral disc

Internal vertebral venous plexus: the internal vertebral venous plexus is located in the spinal canal, distributed between the vertebral periosteum and the dural sac. The greatest venous density of internal vertebral venous plexus is the posterior to the vertebral bodies and intervertebral discs, which form two longitudinal veins on both sides of the posterior longitudinal ligament. The posterior plexus is located in the vertebral arch and the deep layer of the ligamentum flavum. The internal vertebral venous plexus receives drainage from the vertebral bodies and communicates superiorly with the dural venous sinuses and through the intervertebral foramina by way of the intervertebral veins at all levels (Fig. 4.28).

Fig. 4.28 Anatomy of the posterior aspect of spinal column

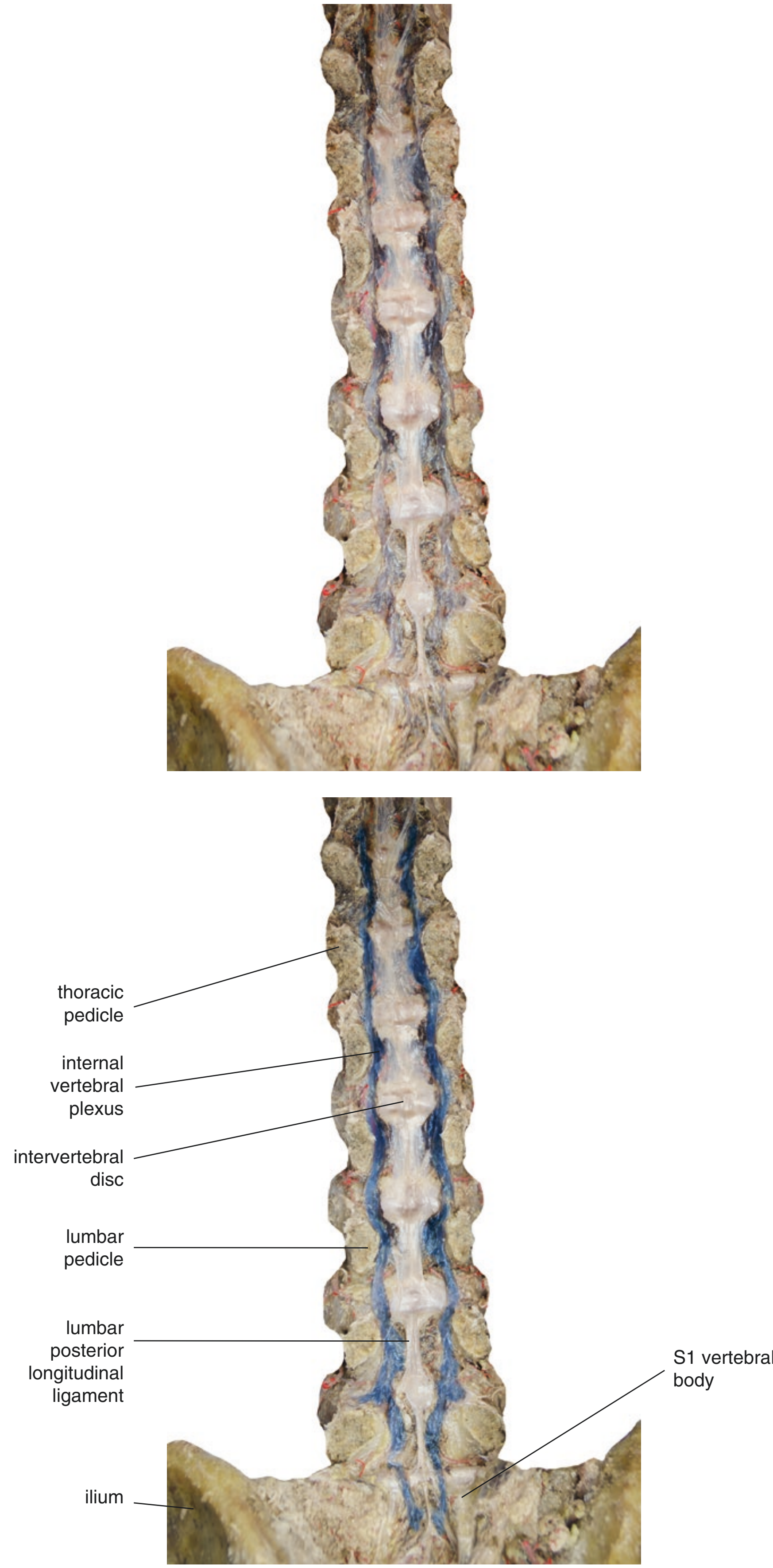

Decompression: perform decompression of the inferior nerve root and dural sac by removing the inferior and superior facets, ligamentum flavum, and intervertebral disc.

Prior to intervertebral fusion, explore the nerve root canal to make sure there are no obstruction and compression (Fig. 4.29).

The triangle space formed by the inferior vertebral pedicle, dural sac, and exiting nerve root is termed as a "safety triangle" or "Kambin's triangle" (Figs. 4.30, 4.31, 4.32, 4.33, 4.34, and 4.35).

The dural sac is retracted medially with a nerve root retractor. The annulus fibrosus is incised with a scalpel. Remove the nucleus pulposus and nucleus of the intervertebral disc with pituitary rongeurs, curettes, and shavers, respectively (Fig. 4.36).

Care must be taken to avoid damage to the subchondral bone of the end plates during disc space preparation.

In intervertebral fusion cage, a suitable size is placed into the anterior central portion of the intervertebral space, and the location is verified by intraoperative fluoroscopy (Fig. 4.37).

The C-arm fluoroscopy shows the pedicle screw and intervertebral fusion cage are located well (Figs. 4.38 and 4.39).

Place the connecting rod on the fusion side and compress the intervertebral space. Compression on the intervertebral space not only promotes intervertebral fusion and restoration of lumbar lordosis (Fig. 4.40).

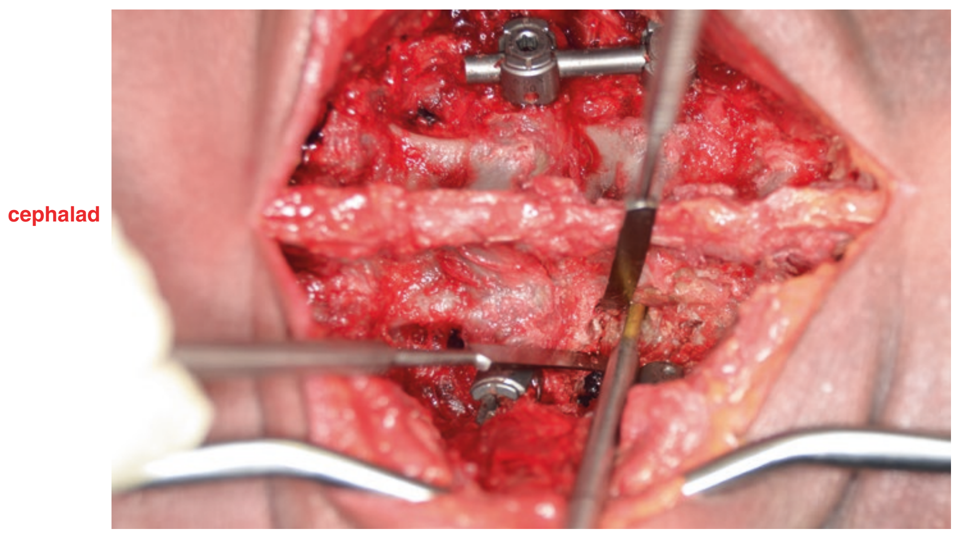

Fig. 4.29 Treatment of the intervertebral space

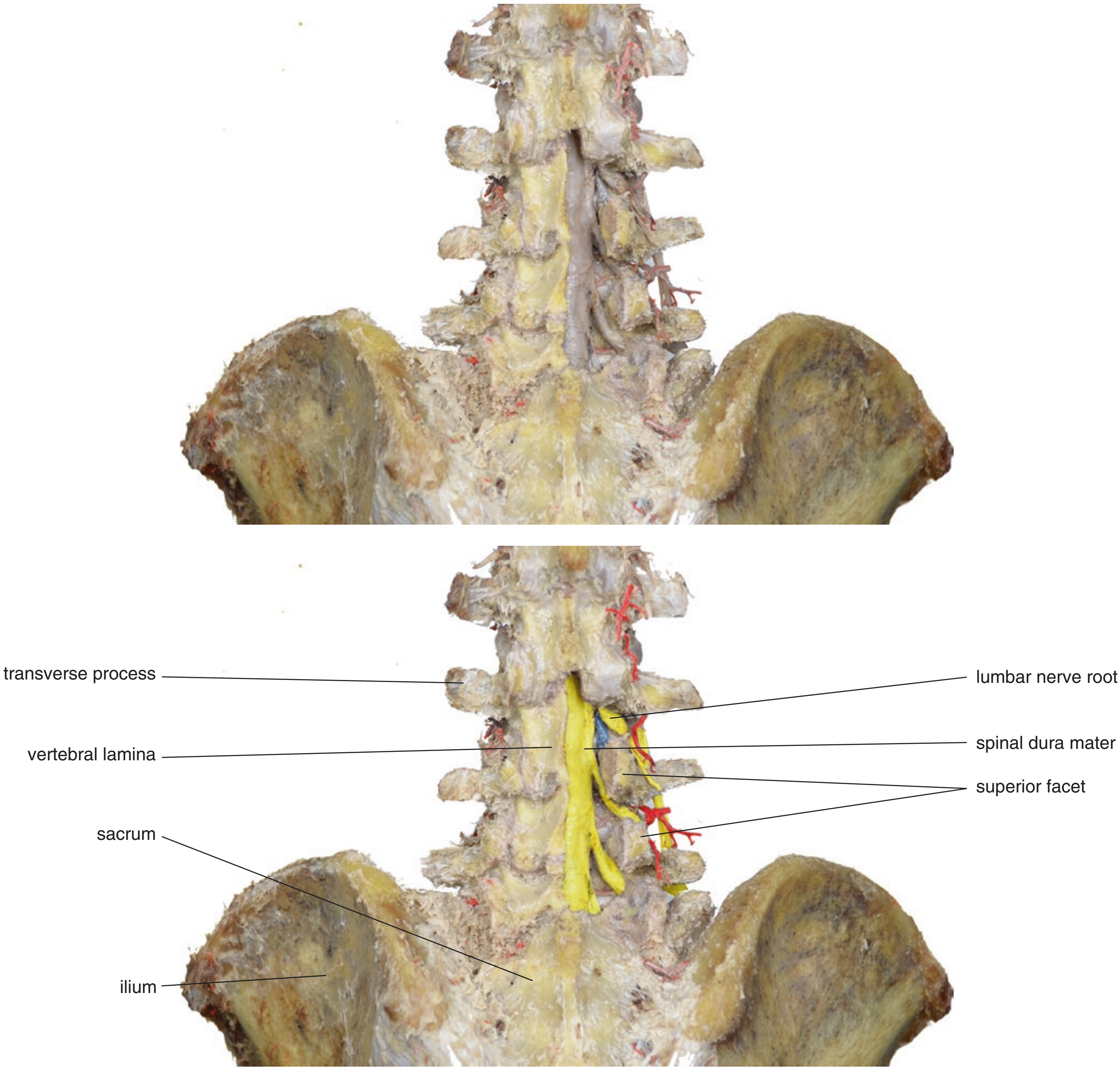

Fig. 4.30 Posterior view of relationship among the lumbar nerve root, intervertebral disc, and bony structure (posterior bony elements partially removed)

Fig. 4.31 Posterior view of relationship among the lumbar nerve roots, intervertebral discs, and bony structure (posterior bony elements partially removed)

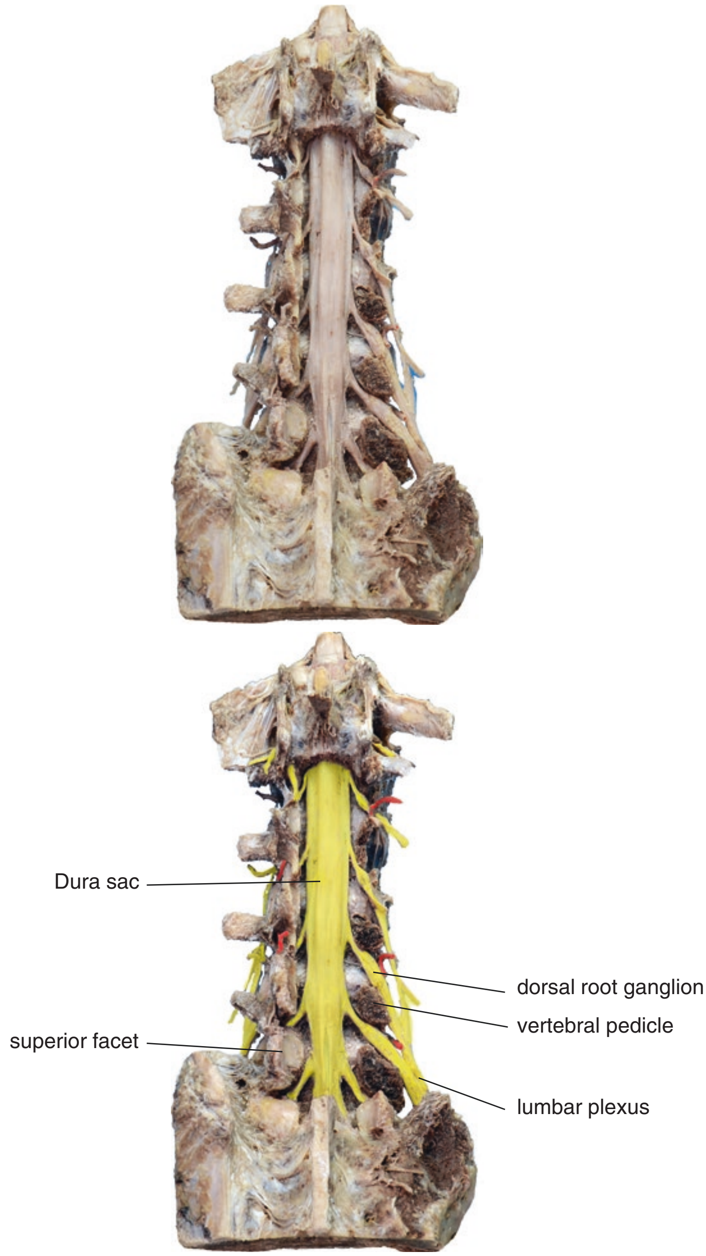

Fig. 4.32 Posterior view of relationship among the lumbar nerve roots, intervertebral discs, and bony structure (posterior bony elements partially removed)

Fig. 4.33 Posterior view of relationship among the lumbar nerve roots, intervertebral discs, and bony structure (posterior bony elements and dural sac removed)

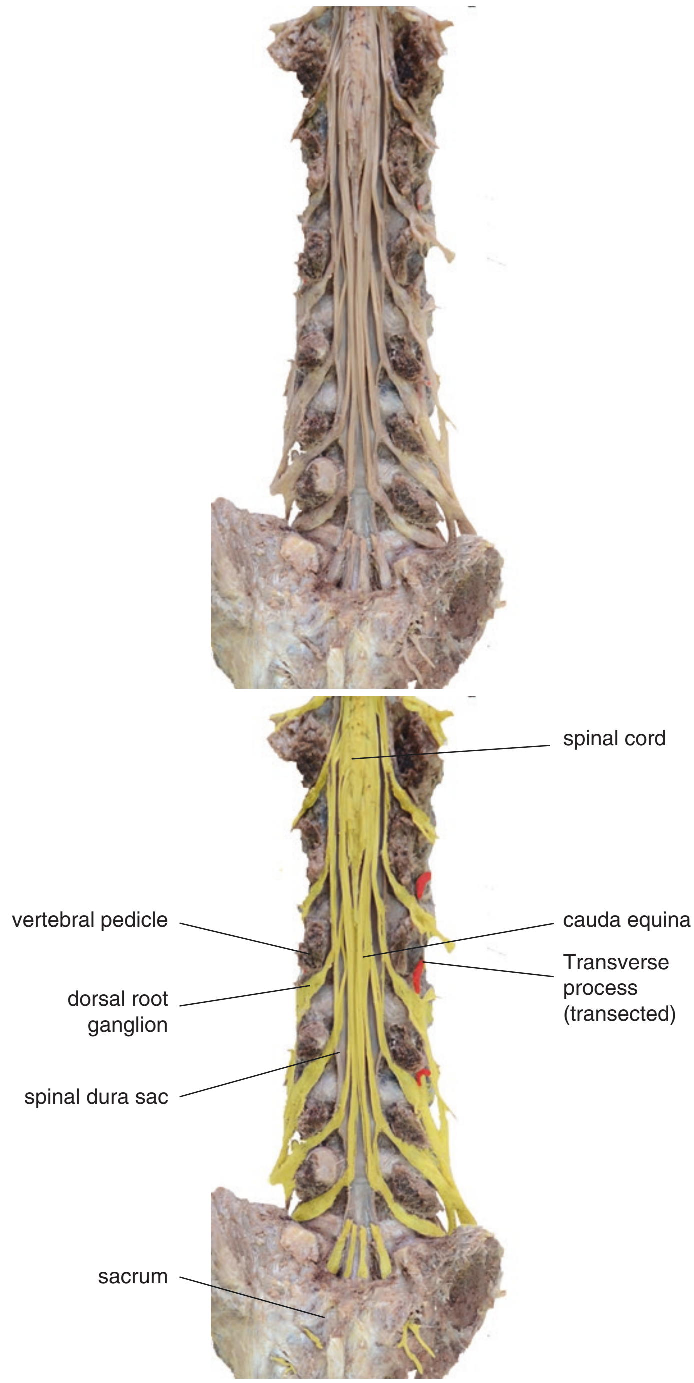

Fig. 4.34 Anterior view of relationship among the lumbar nerve roots, ligamentum flavum, and bony structure (spinal column removed)

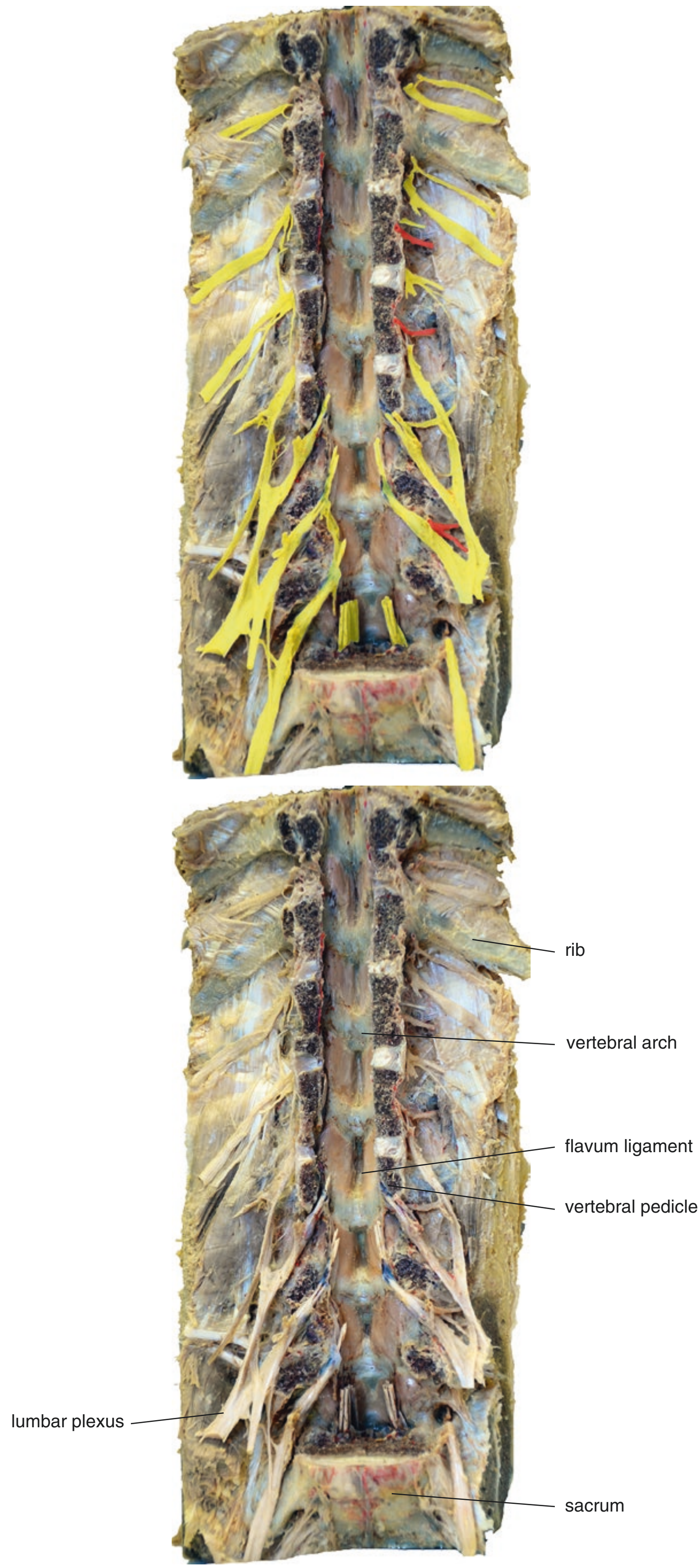

Fig. 4.35 Kambin's triangle

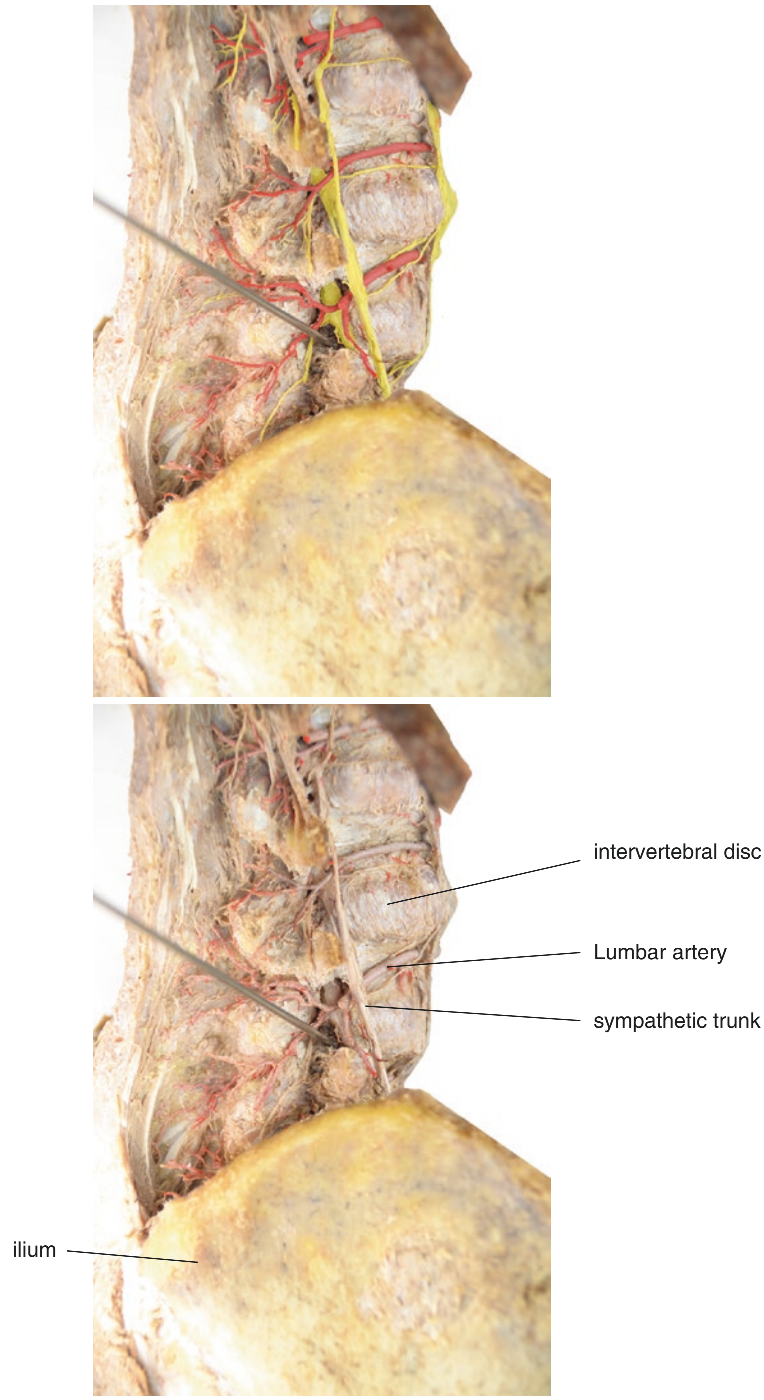

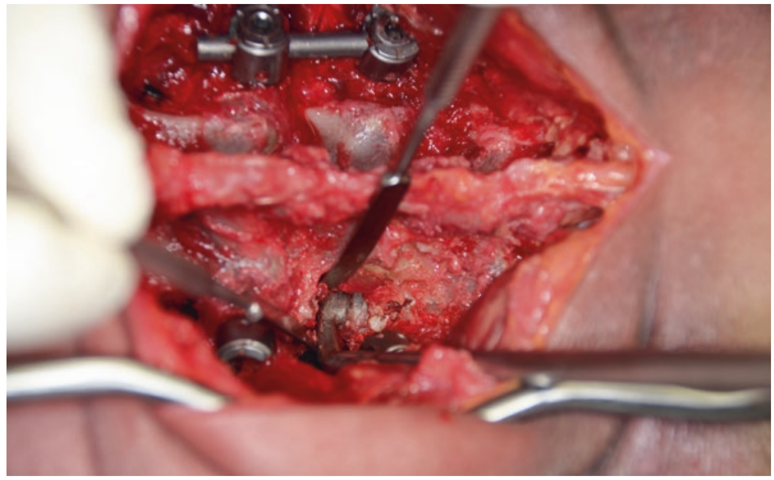

Fig. 4.36 Graft bed preparation

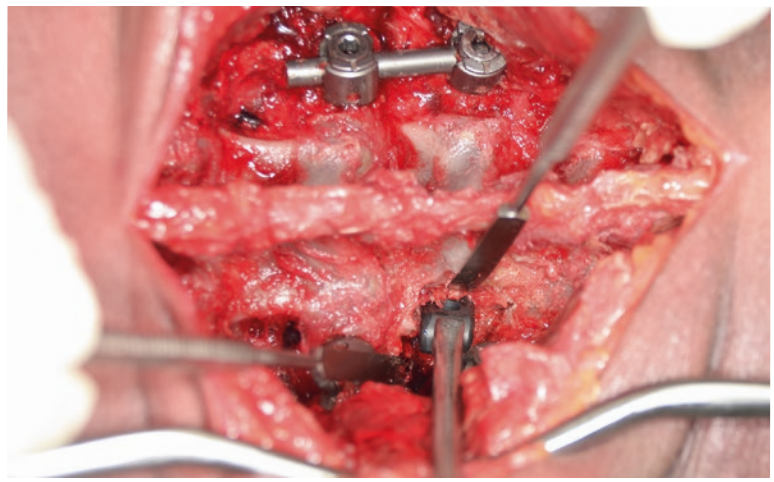

Fig. 4.37 Placement of an intervertebral fusion cage

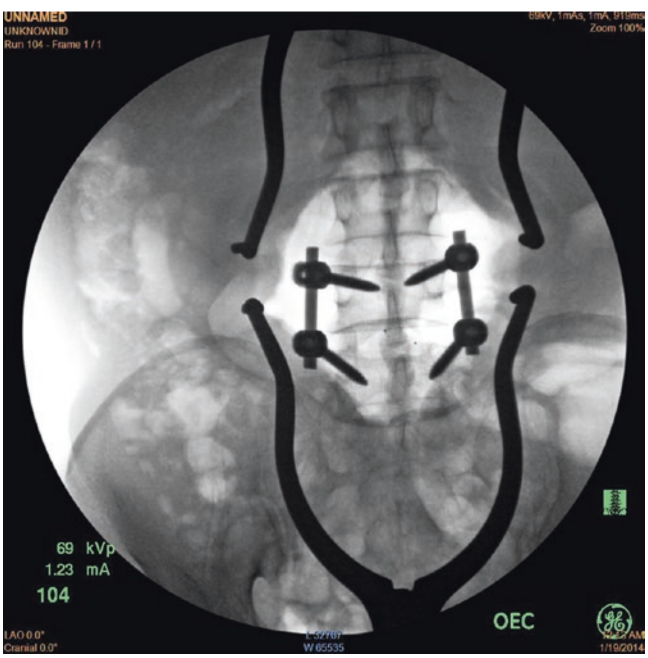

Fig. 4.38 Placement of an intervertebral fusion cage (anteroposterior C-arm fluoroscopy)

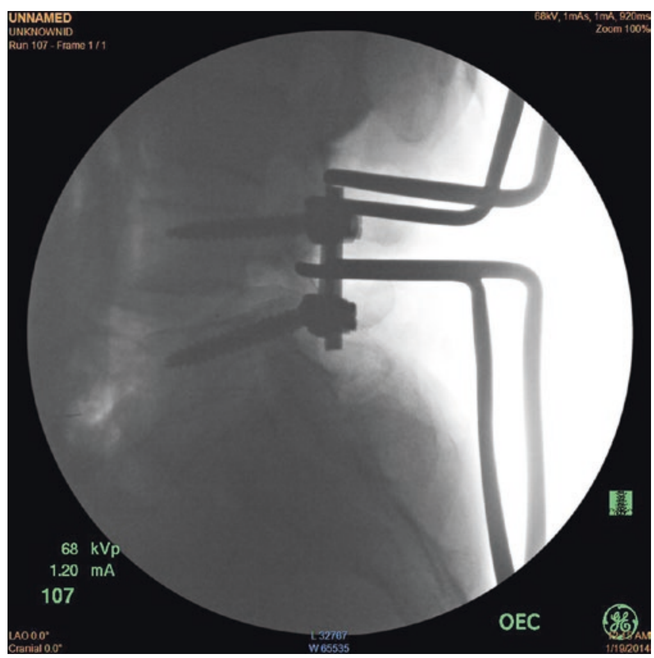

Fig. 4.39 Placement of an intervertebral fusion cage (lateral C-arm fluoroscopy)

Fig. 4.40 Place the connecting rod on the fusion side and compress the intervertebral space

cephalad

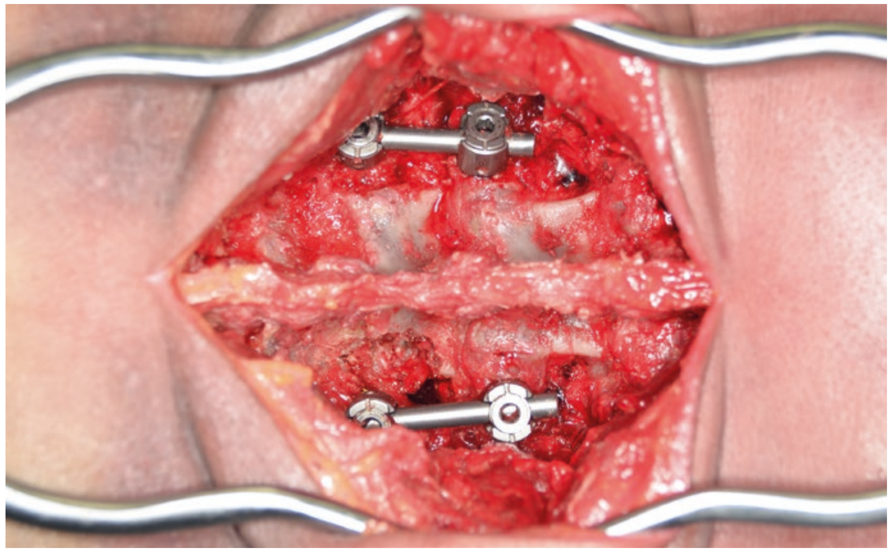

2.4 Minimally Invasive TLIF

Incision for minimally invasive TLIF (Fig. 4.41).

Wiltse approach or subperiosteal dissection is used to expose the facet joint of the target level.

Pedicle screws are placed via the Wiltse approach or percutaneously on the opposite side.

The skin, subcutaneous tissue, and superficial fascia are incised to expose the lumbodorsal fascia. Palpate the facet joint to identify the intermuscular space (Fig. 4.42).

Longitudinally incise the lumbodorsal fascia. Blunt dissection is performed along the intermuscular space of the longissimus and multifidus muscles to expose the facet joint and the transverse process (Fig. 4.43).

Screws are placed in the pedicles in the superior and inferior vertebra of the involved disc (Fig. 4.44).

The anteroposterior C-arm fluoroscopy shows the pedicle screw is located well (Fig. 4.45).

The lateral C-arm fluoroscopy shows pedicle screw is located well (Fig. 4.46).

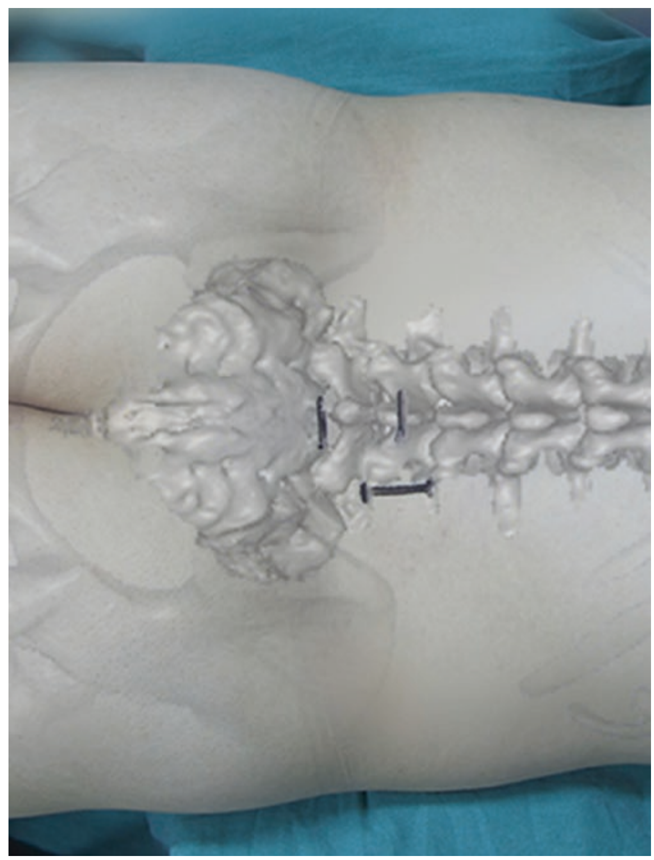

Fig. 4.41 Incision for minimally invasive TLIF

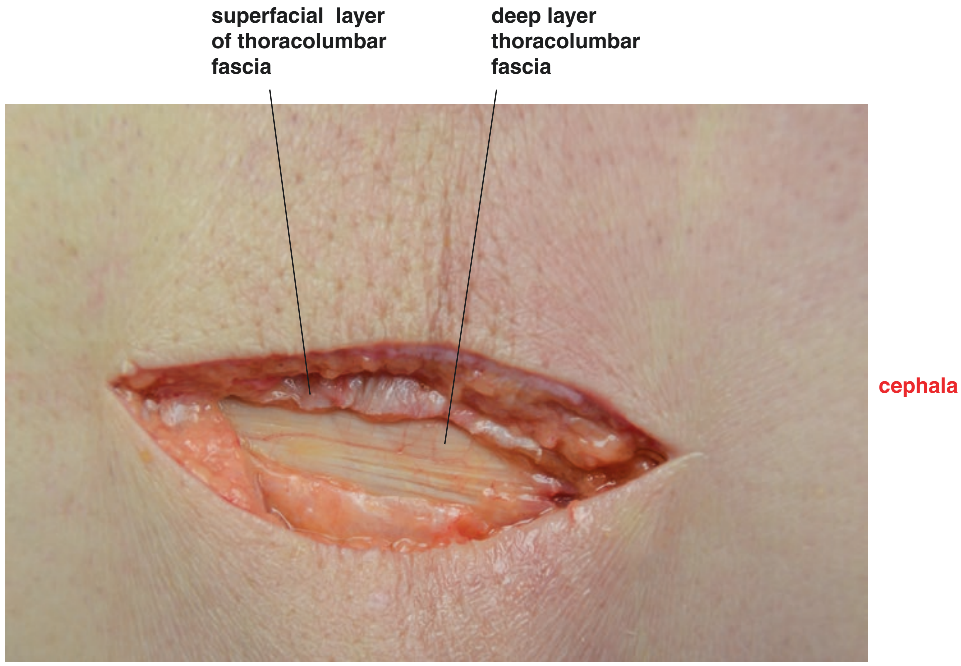

Fig. 4.42 Incision for minimally invasive TLIF

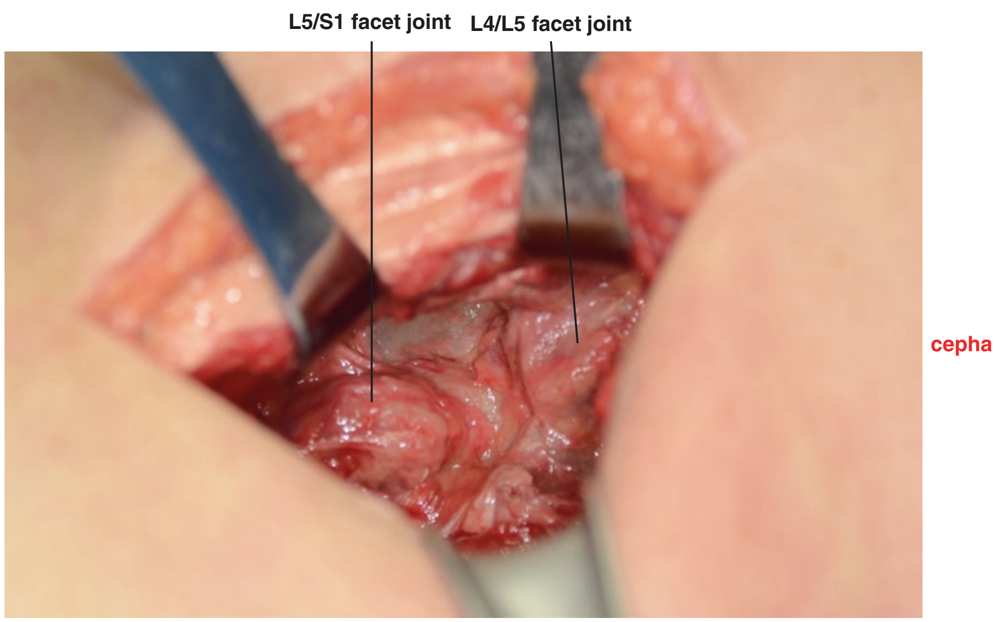

Fig. 4.43 Minimally invasive TLIF exposure

Fig. 4.44 Relationship among the transverse processes, multifidus muscle, and facets

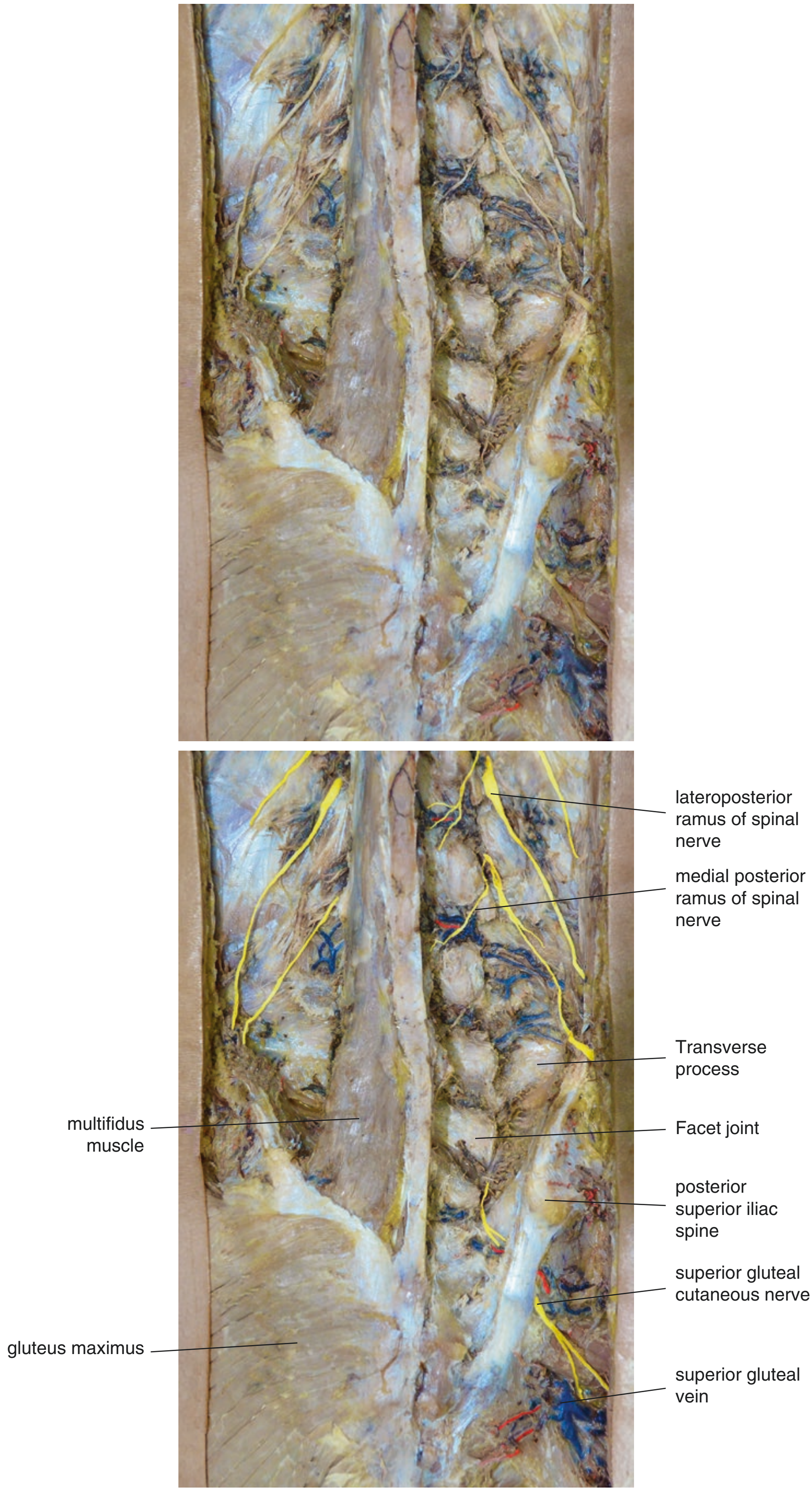

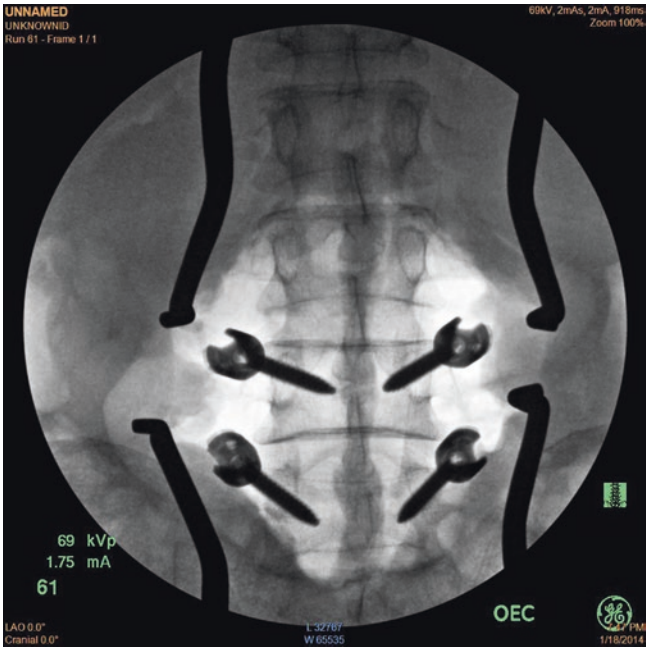

Fig. 4.45 Placement of the pedicle screws (anteroposterior C-arm fluoroscopy)

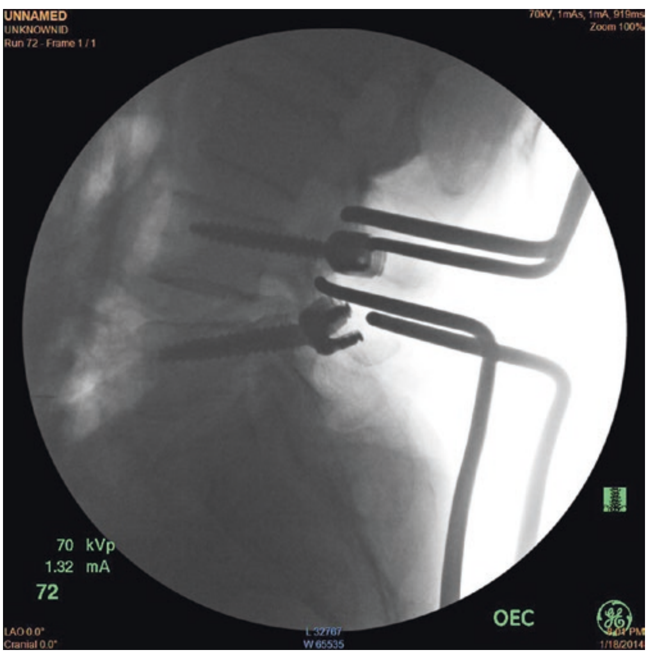

Fig. 4.46 Placement of the pedicle screws (lateral C-arm fluoroscopy)

3 Pedicle Subtraction Osteotomy

3.1 Overview

In 1985, Thomasen put forward pedicle subtraction osteotomy (PSO) to treat kyphosis in ankylosing spondylitis. PSO is mainly applied to correct spinal deformity in the sagittal plane. Such technique is a closing wedge osteotomy, in which the vertebral plate and the pedicle in the posterior spine are resected; then the anterior vertebral body undergoes wedge-shaped resection; next, posterior elements of the spine are closed to achieve bony contact between the anterior column and the middle column; finally, the C7 plumb line is allowed to fall to the posterior part or the posterior-superior border of the S1 vertebral body so as to achieve the goal of balancing the spine in the sagittal plane. And meanwhile, the technique, to some extent, also can correct the imbalance of the coronal plane through the adjustment of osteotomy in the coronal plane. But if osteotomy is performed in the upper lumbar region and the posterior column is excessively shortened, it will cause spinal cord kinking or folds and then result in serious neural complications. Therefore, it is generally believed that PSO is mainly indicated for those with serious kyphotic deformity, a Cobb angle of more than 40° rigid deformity in thoracolumbar joints and ligaments, who experience failure in nonsurgical treatment.

3.2 Position

After general anesthesia, patients are placed in a prone position (Figs. 4.47 and 4.48) on a jackknife table with appropriate padding.

During surgery, the jackknife table can be elevated to extend the lower extremities and chest to close the osteotomy.

Fig. 4.47 Position for PSO

Fig. 4.48 Jackknife table can be elevated to extend the lower extremities and chest to close the osteotomy

3.3 Exposure

A posterior midline incision is utilized (Fig. 4.49).

Subperiosteal dissection of the paraspinal muscles from the involved spine to the lateral margin of the transverse process.

Pedicle screws are placed in one segment above and two segments below (or two segments, respectively, above and below) the osteotomy segment (Figs. 4.50 and 4.51).

For cases in which there is difficulty in identifying bony landmarks, screw placement can be completed under the observation of a CT navigation system.

Pedicle screws and temporary rod are placed on one side (Fig. 4.52) so as to facilitate temporary stability and follow up closure of the bone surface when osteotomy is performed.

The range of osteotomy covers the inferior pole of the cephalad pedicles to the superior pole of the caudad pedicles (Fig. 4.53).

An asymmetric wedge resection can be carried out when a two-plane sagittal/coronal correction is acquired (Fig. 4.54).

The posterior lamina of the osteotomy segment, lower part of the spinous process, and vertebral plate of the superior segment are resected by a rongeur (Fig. 4.55).

An osteotome is used to remove the inferior facet of the superior segment. The inferior vertebral plate of the superior segment is removed with a Kerrison rongeur (Fig. 4.56).

A Kerrison rongeur is used to resect the vertebral plate, inferior facet, and ligamentum flavum in the osteotomy segment (Fig. 4.57).

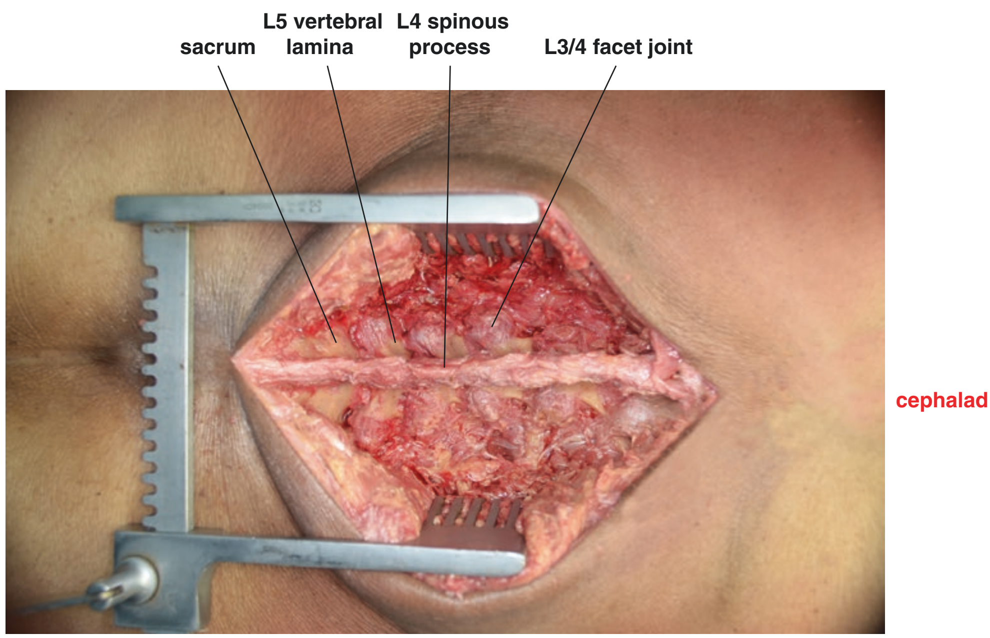

Fig. 4.49 Exposure of the involved spine for PSO

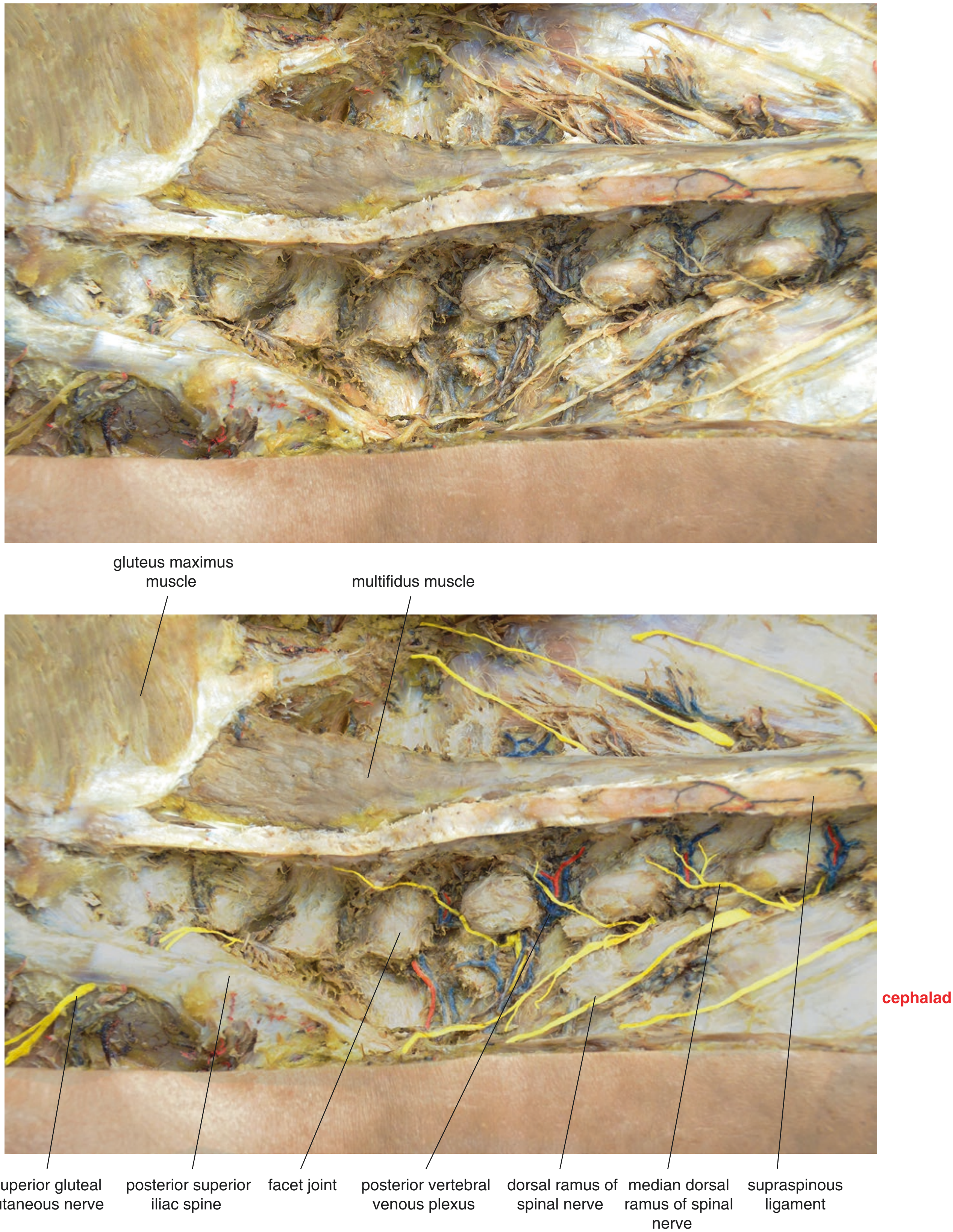

Fig. 4.50 Anatomy of the posterior lumbar spine

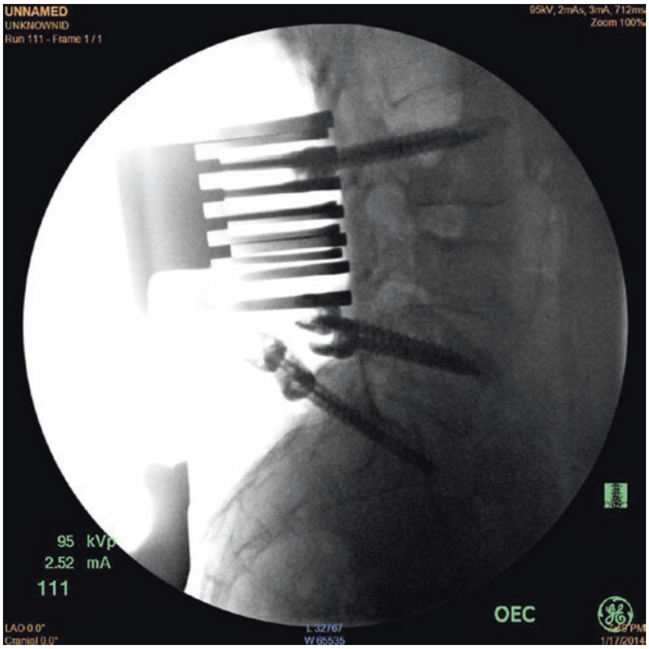

Fig. 4.51 Pedicle screw placement

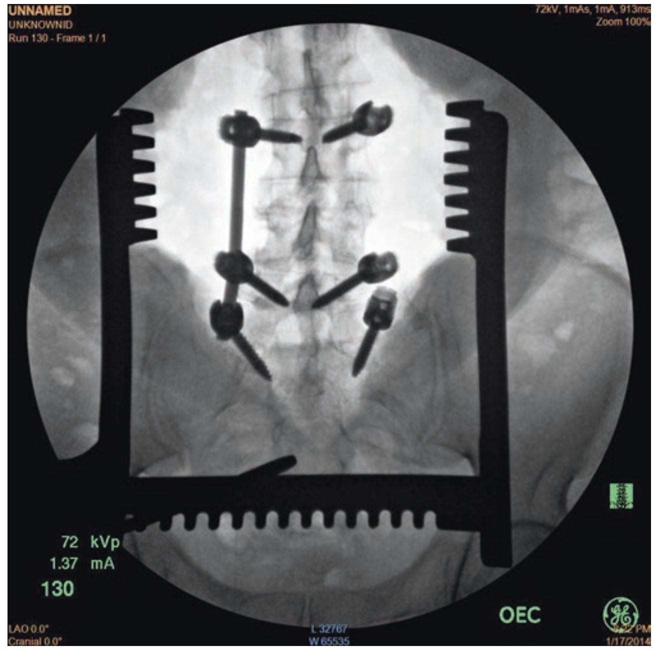

Fig. 4.53 Intraoperative anteroposterior fluoroscopy of temporary fixation of a titanium rod on one side

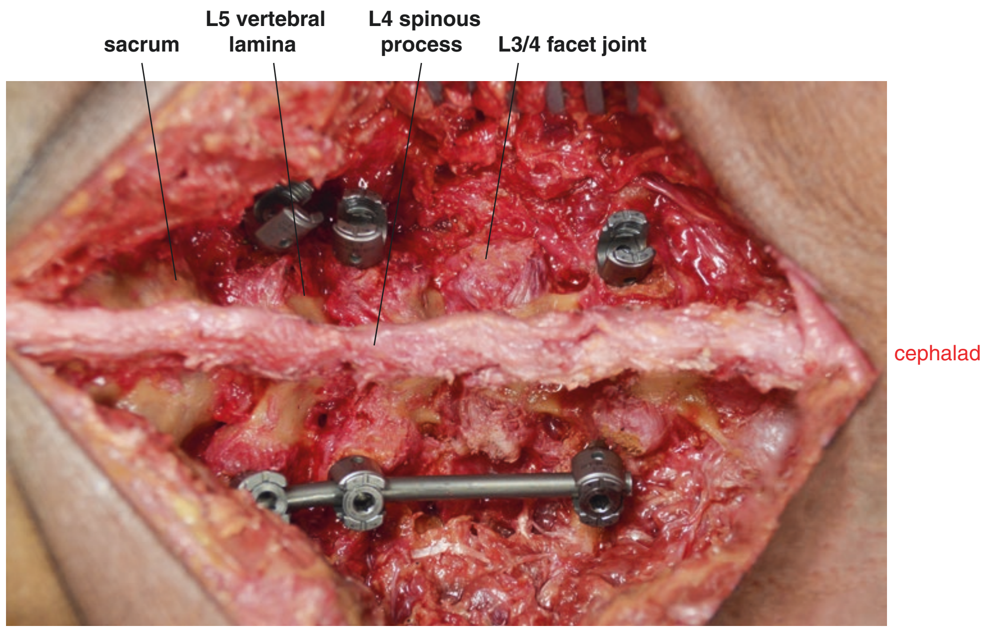

Fig. 4.52 Rod fixation on one side

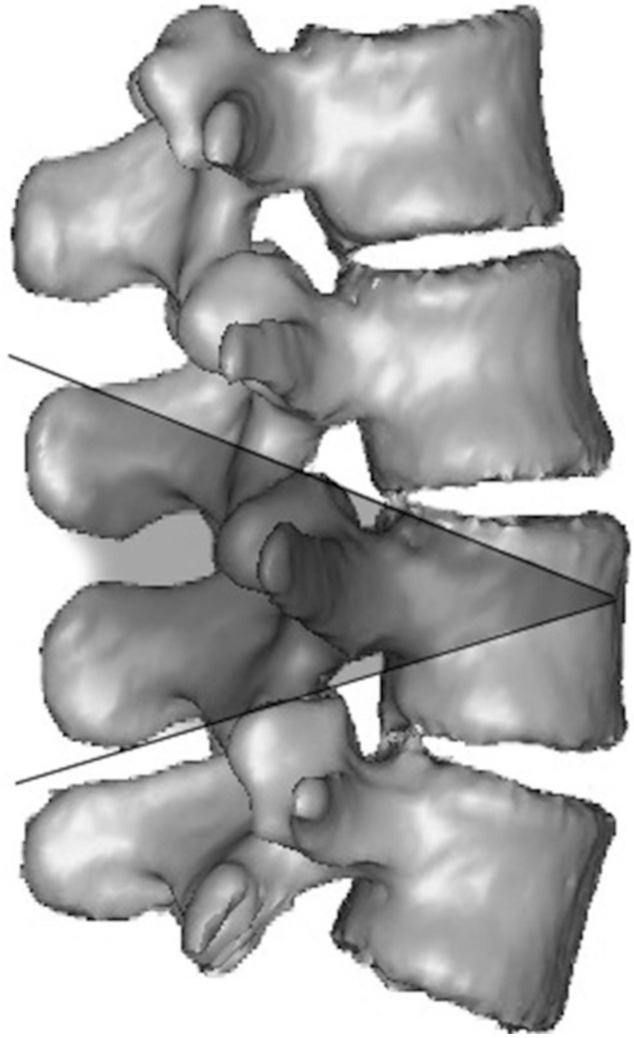

Fig. 4.54 Wedge-shaped fashion of PSO

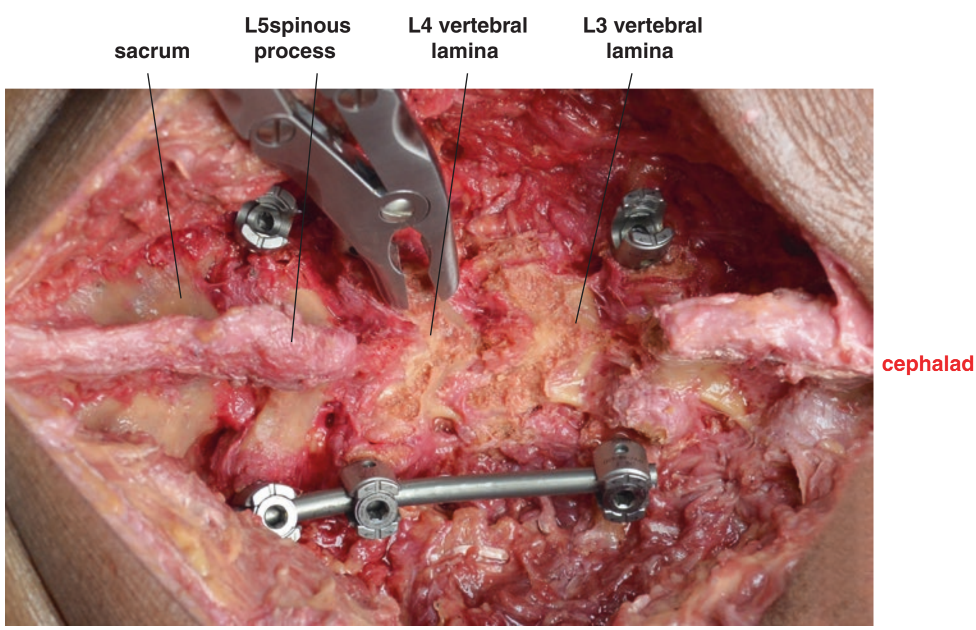

Fig. 4.55 Removal of the posterior lamina of the osteotomy segment, lower part of the spinous process, and vertebral plate of the superior segment

Fig. 4.56 Resection of the inferior facet of the superior segment

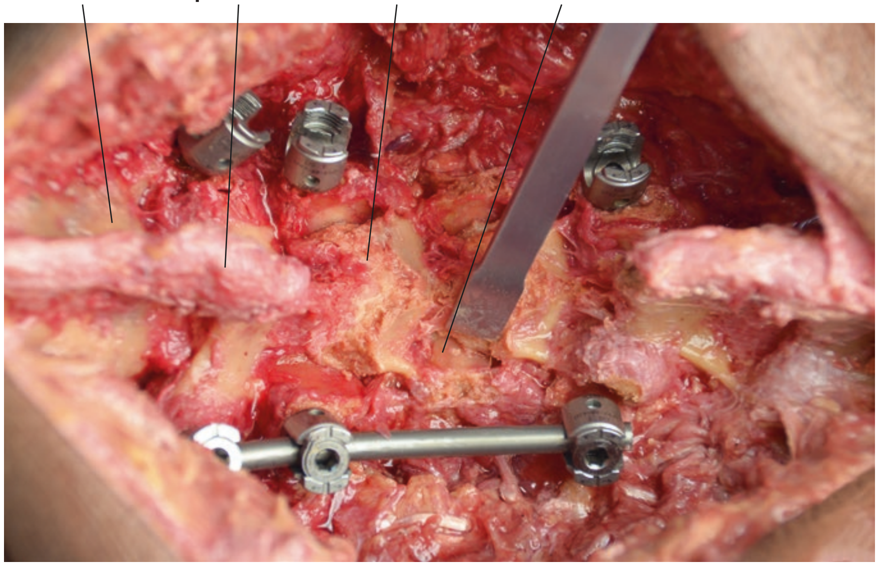

Fig. 4.57 Resection of the vertebral plate and ligamentum flavum in the osteotomy segment

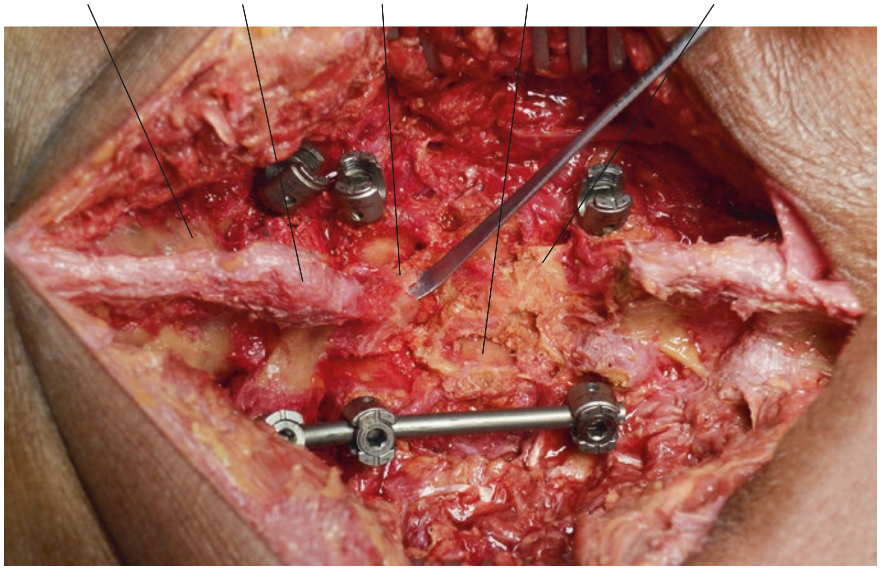

Ligamentum flavum (Fig. 4.58) is connected to the lamina of adjacent vertebrae within the spinal canal. The ligamentum flavum is mainly composed of yellow elastic fibrous tissue, which is distributed vertically and goes downward from the anterior-inferior margin of the superior vertebral plate to reach the posterior-superior margin of the inferior vertebral plate. The ligamentum flavum in the lumbar spine is the thickest. It serves as an important landmark in the posterior approach for lumbar surgery.

Fig. 4.58 The lumbar ligamentum flavum

The ligamentum flavum is removed (Fig. 4.59) to expose the dural sac. In the procedure, the attention should be paid to avoid injury to the dural sac, which will cause cerebrospinal fluid leakage.

Use a nerve probe to detect the nerve root canals above and below the osteotomy pedicle and the exiting nerve roots, to avoid compression on the nerve roots during osteotomy and closure of the osteotomy (Fig. 4.60).

Remove the superior facet in the osteotomy segment with an osteotome and rongeurs to expose the pedicle.

Use the nerve root retractor to separate the dural sac and nerve roots from the intravertebral fat and venous plexus (Figs. 4.61 and 4.62).

The cancellous bone within the osteotomy level pedicle is removed with different size of curettes (Fig. 4.63).

The epidural bleeding encountered is dealt with bipolar electrocautery, hemostatic agents, and cottonoids sponges.

Under the protection of the nerve retractors, the residual pedicle cortical bone is dissected by Kerrison rongeurs (Fig. 4.64).

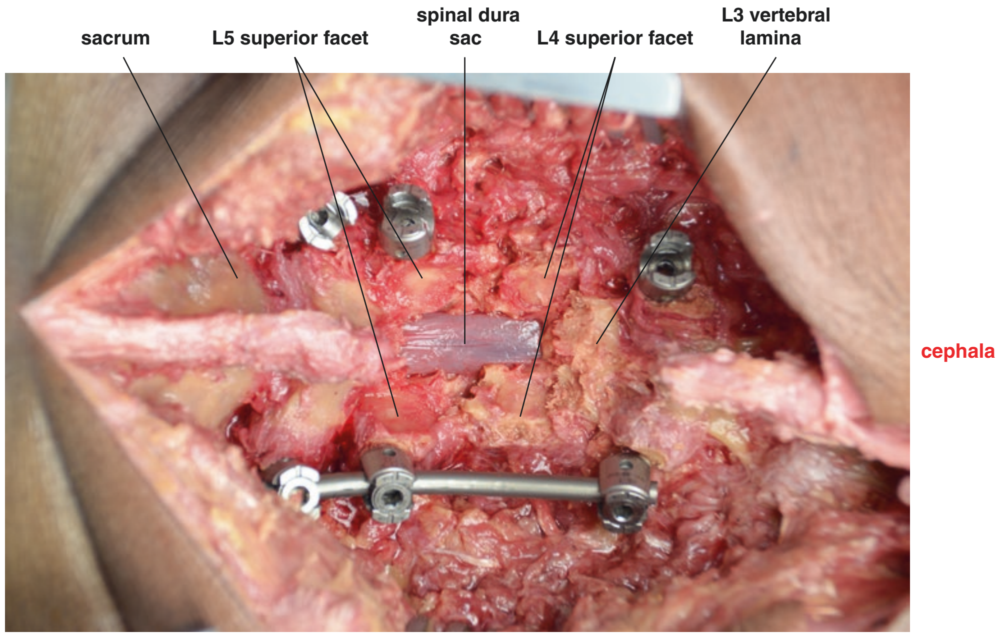

Fig. 4.59 Removal of the ligamentum flavum

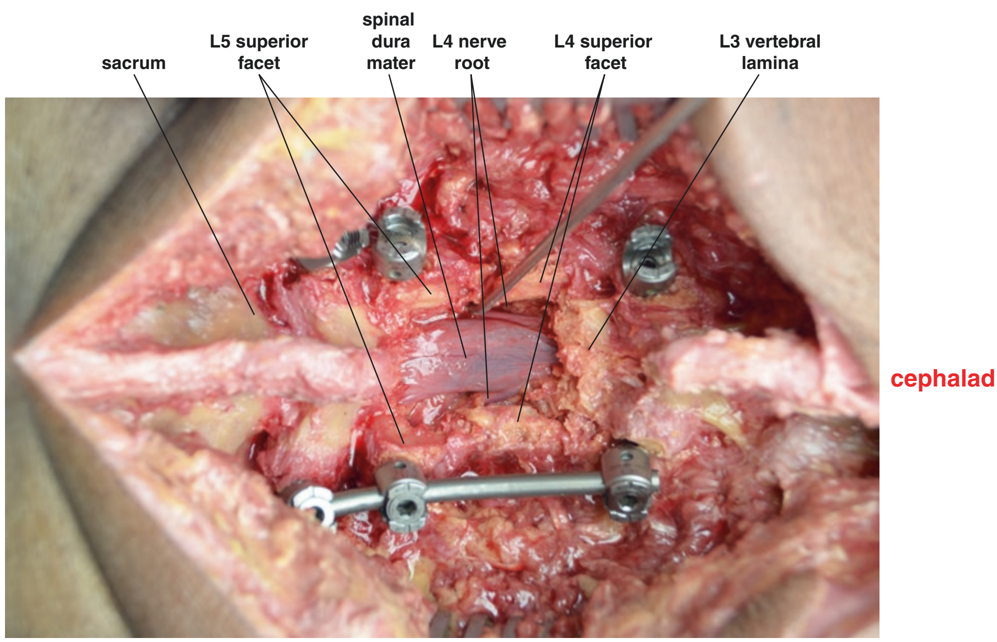

Fig. 4.60 Decompression of the nerve root in the osteotomy segment

Fig. 4.61 Pedicles, traversing nerve roots, and the exiting nerve roots

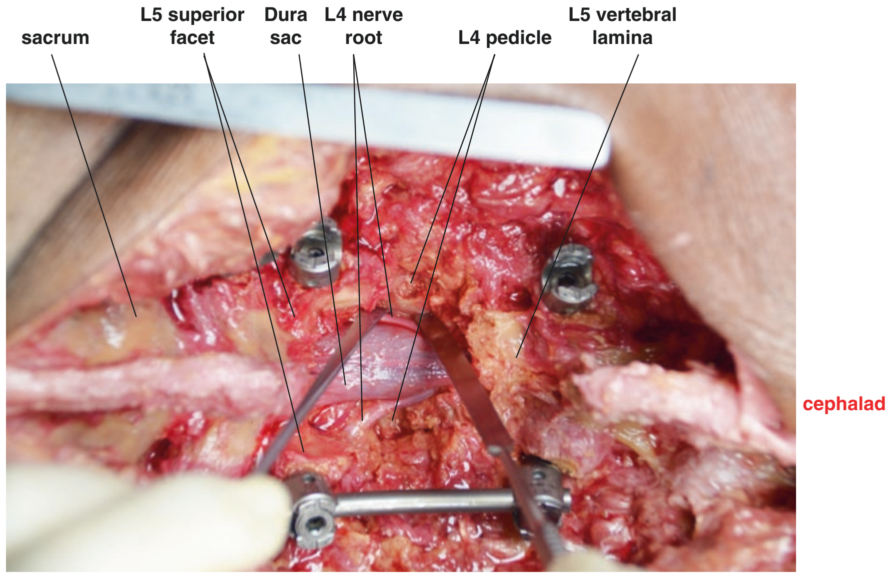

Fig. 4.62 The nerve root beside the osteotomy level pedicle is retracted and protected

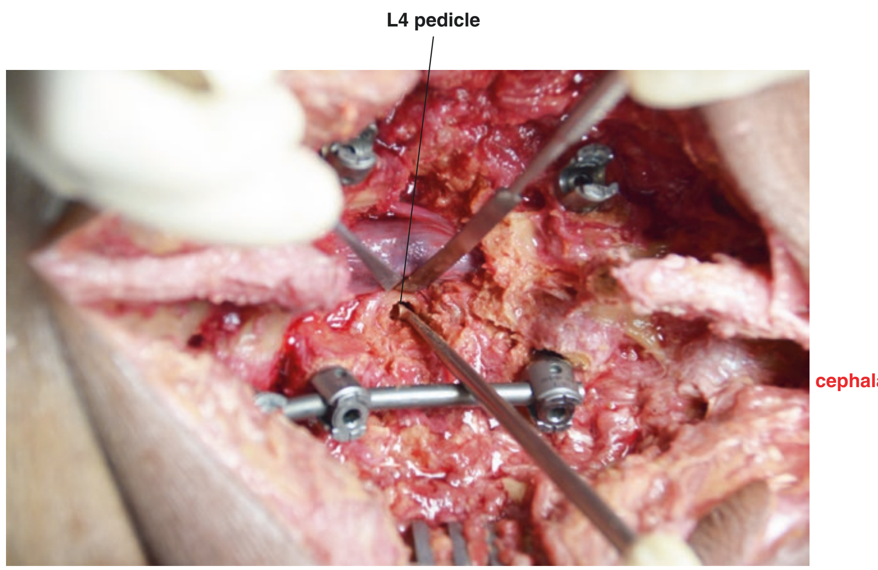

Fig. 4.63 Remove the cancellous bone within the pedicle with curettes

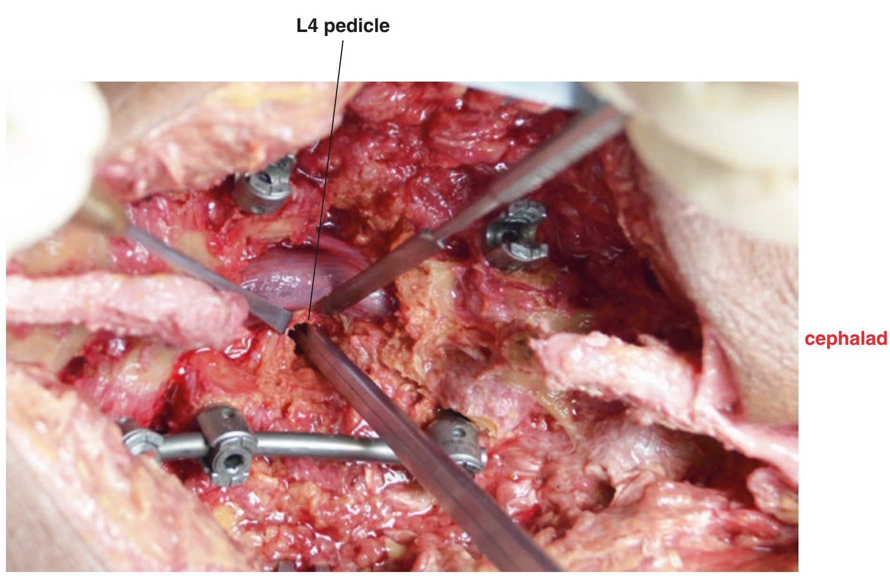

Fig. 4.64 Osteotomy of the pedicle

Intervertebral foramen of the lumbar spine: it is the area where the lumbar nerve root exits out of the spinal canal, and it has a "light bulb" appearance. The intervertebral foramen is a route connecting the vertebral canal and the retroperitoneal space for segmental vessels and nerves. The anterior wall of the intervertebral foramen is formed by the lower aspect of the body of the upper vertebra above, by the intervertebral disc in the middle and lower part, and by the small upper portion of the back of the body of the lower vertebra at the lowest level. The posterior wall, on the other hand, is formed by the lower portion of the pars interarticularis of the lamina of the higher vertebra superiorly and the superior articular process of the lower vertebra inferiorly. Most nerve roots exiting out of the intervertebral foramen are within the superior one fourth of the foramen (Fig. 4.65).

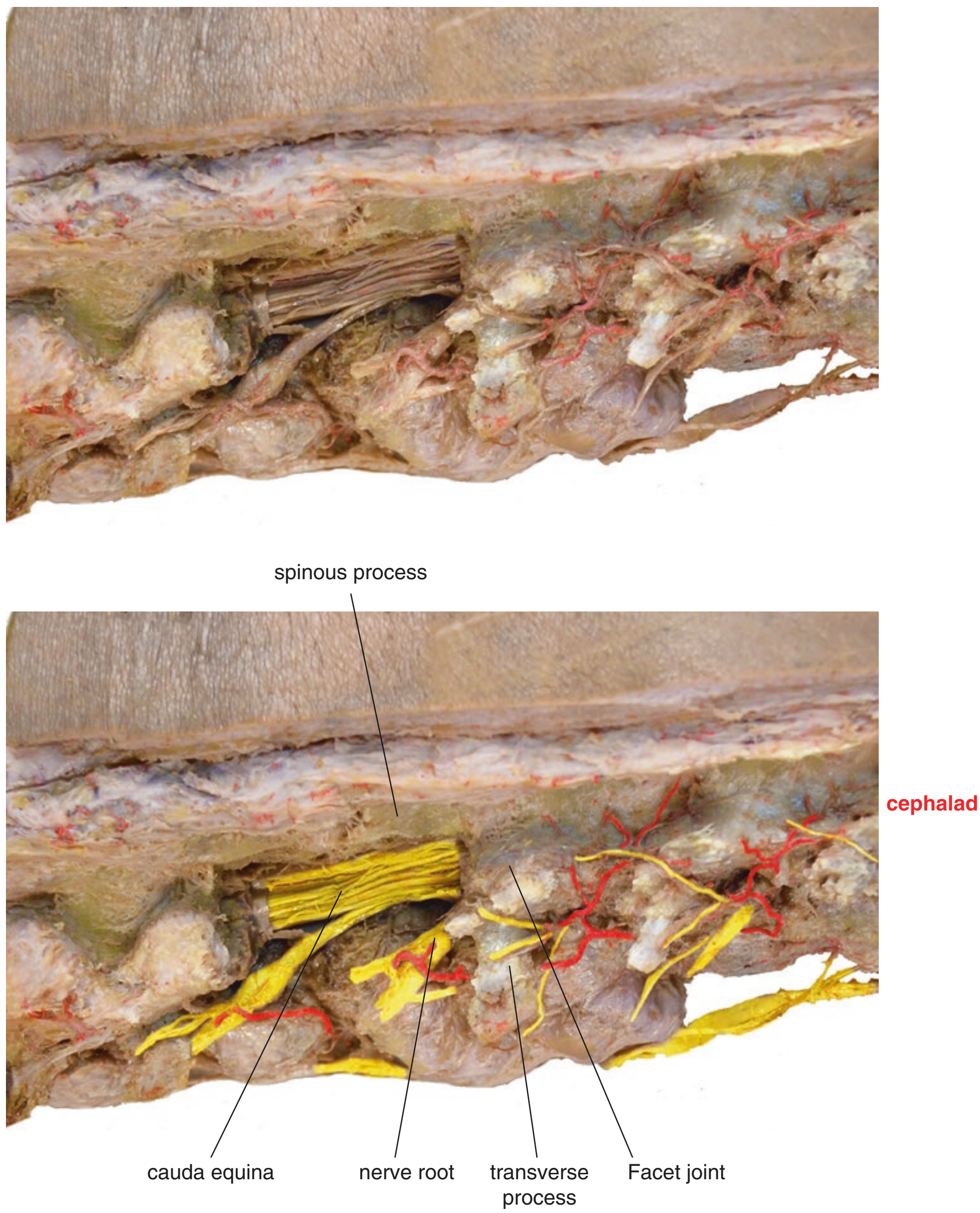

Fig. 4.65 Relationship among the nerve root, cauda equina, and bony structure (the posterior bony structures are removed on the right side of the target level for PSO)

The same osteotomy is done to the opposite side (Fig. 4.66).

Medial retraction of the dural sac and nerve root should be limited not further than midline.

The figure shows the relationships among the vertebral body, nerve roots, sympathetic trunk, and segmental vessels (Fig. 4.67).

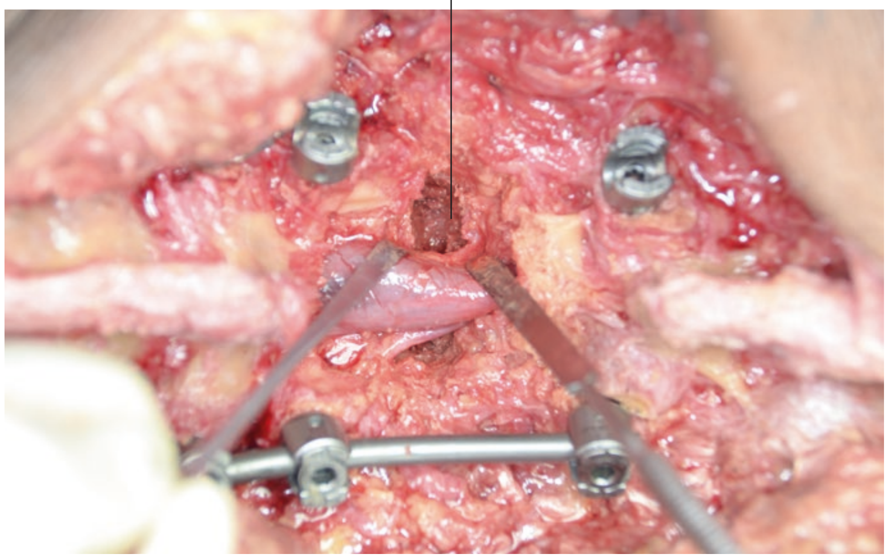

Fig. 4.66 Osteotomy of the vertebral body

Fig. 4.67 Neurovascular structures around the lumbar spine

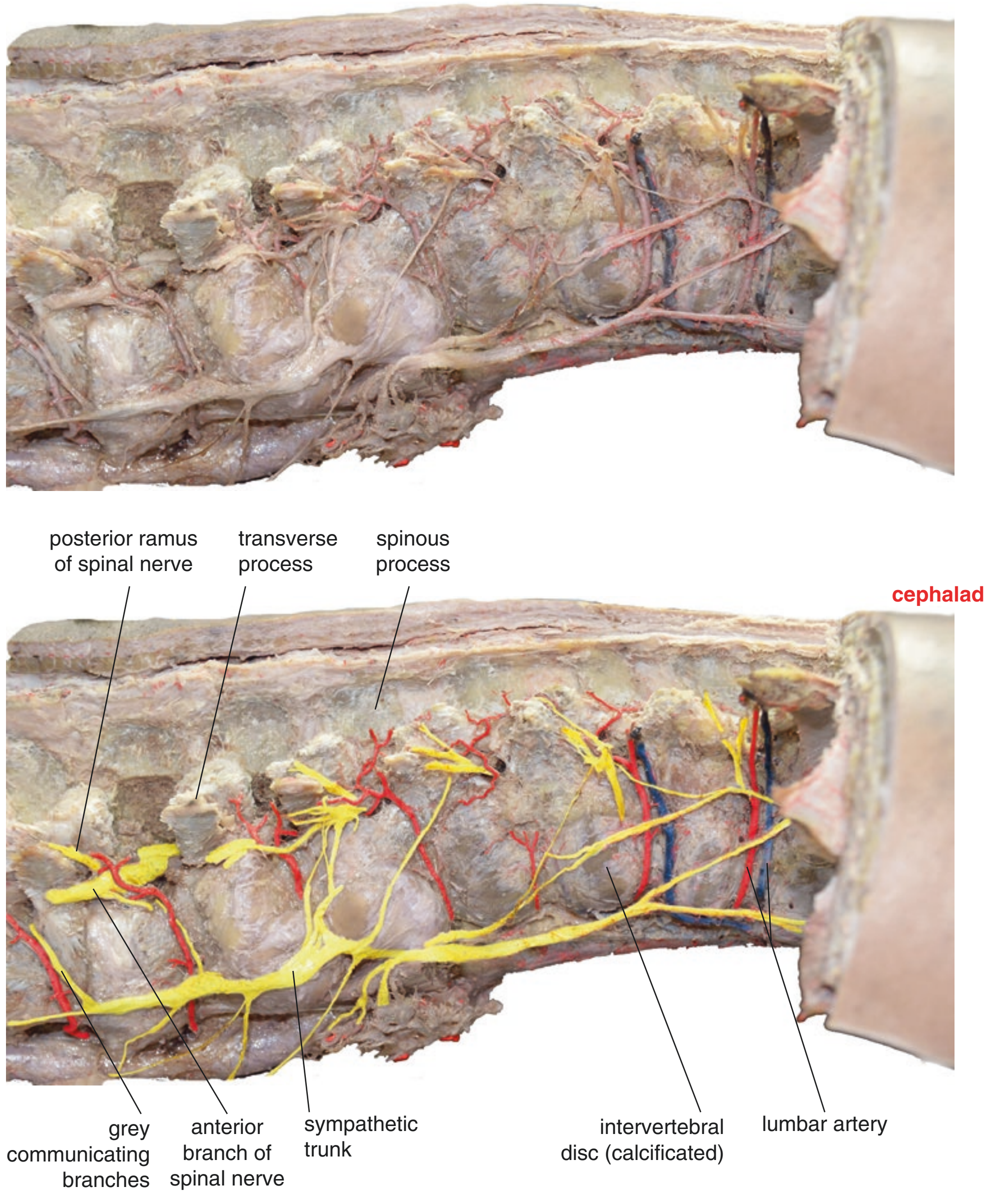

Place a foot-shaped posterior wall impactor into the ventral part of the dural sac, and then impact the posterior vertebral wall down into the vertebral body defect (Figs. 4.68 and 4.69).

Use a rongeur to remove the partial bone in the posterior wall of the vertebral body of osteotomy edge in both ends to avoid compression on the dural sac.

An osteotome is used to perform wedge-shape resection of the lateral vertebral body. A curette is used to remove cancellous bone in the vertebral body to make the osteotomy in a wedge-shaped fashion.

Determine whether the resection depth and area in the anterior part of the vertebral body meet the requirements by observing the C-arm fluoroscopy image (Figs. 4.70 and 4.71).

A compressor is used to apply force to the pedicle screws bilaterally in the osteotomy segment and close the osteotomy (Fig. 4.72).

A jackknife bed that can break in the middle can also be used to facilitate the closure of the osteotomy. The lumbar of the patient can be hyperextended by placing the table into V shape during the correction procedure.

In the process of closing the osteotomy, it should be rechecked that there is no compression on the neural elements of the osteotomy segment (Fig. 4.73).

Use the nerve root probe to inspect the intervertebral foramen (Fig. 4.74), and remove the excessive bone or soft tissue that will cause compression on the nerve root or dural sac.

Fluoroscopy shows the osteotomy is closed and the implants are in good position (Figs. 4.75 and 4.76).

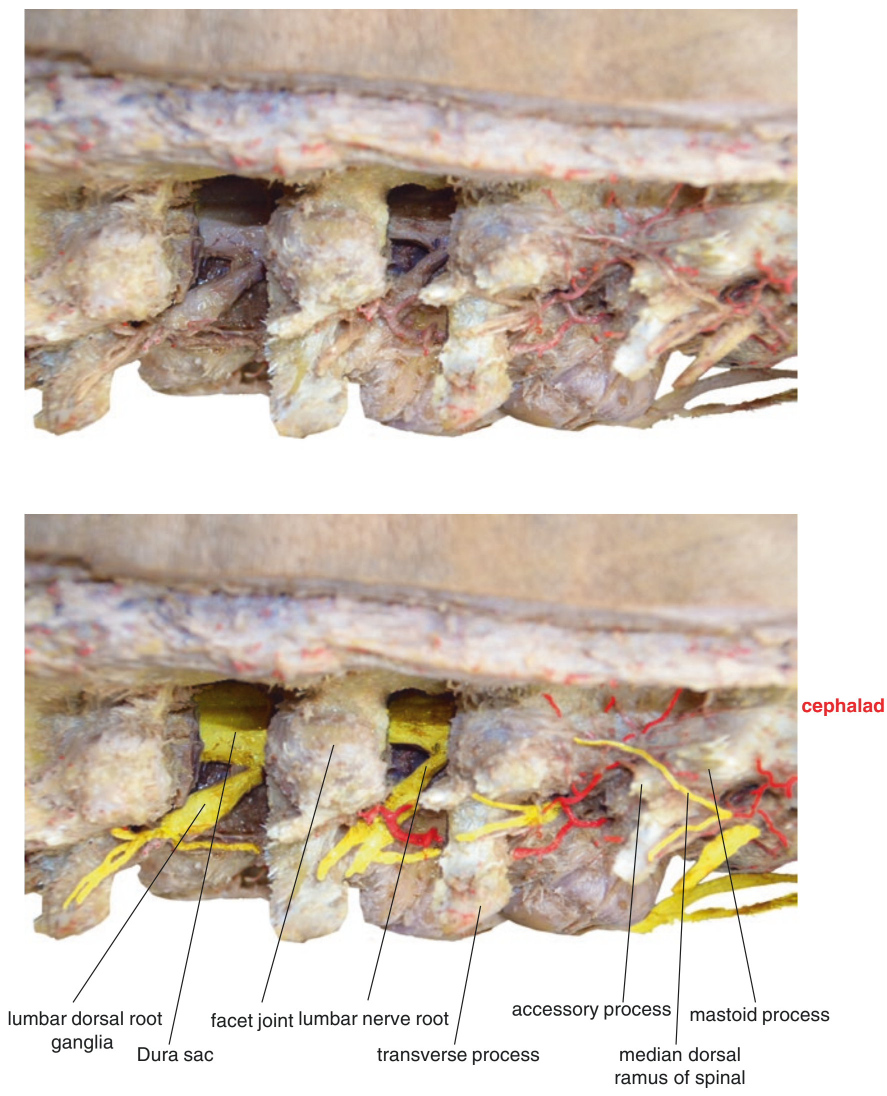

Fig. 4.68 Relationships among the dural sac, nerve roots, and vertebral body (vertebral plates are partially resected)

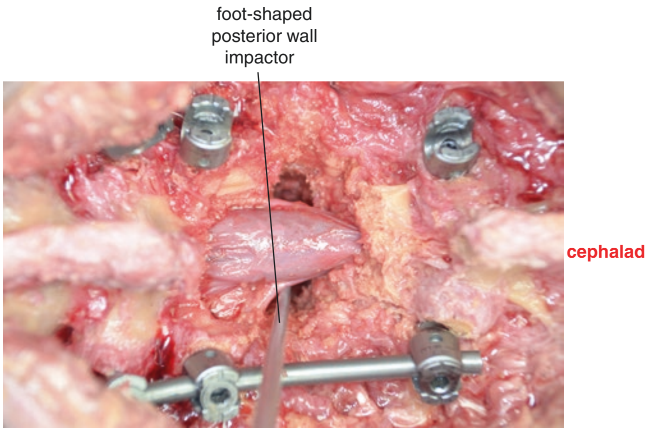

Fig. 4.69 Vertebral osteotomy

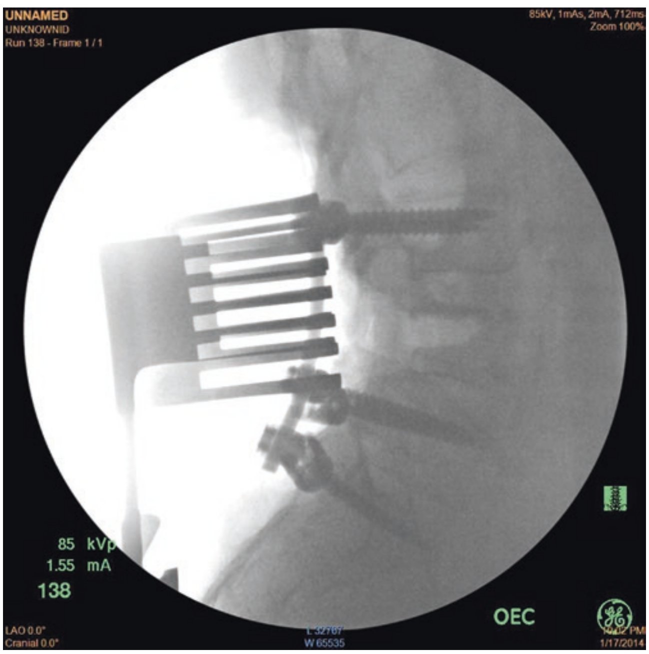

Fig. 4.70 Lateral C-arm fluoroscopy of PSO

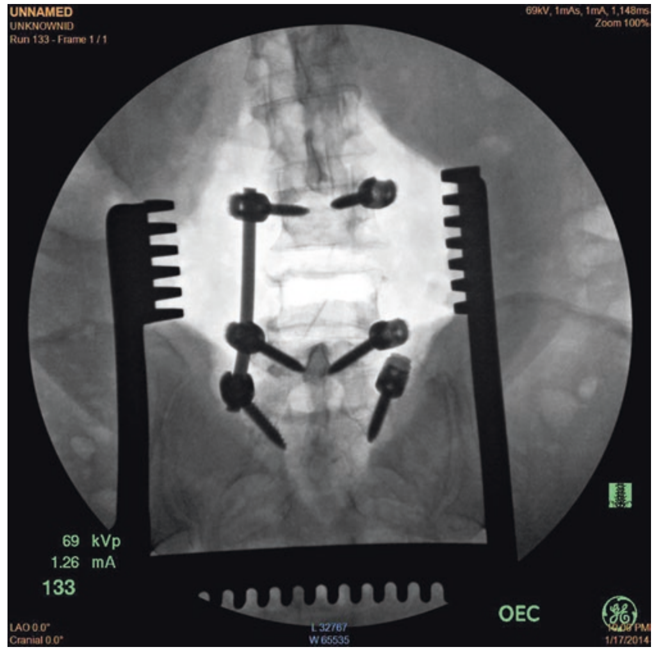

Fig. 4.71 Anteroposterior C-arm fluoroscopy of PSO

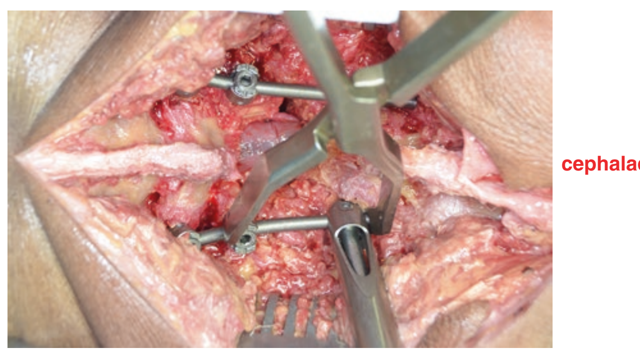

Fig. 4.72 A compressor is used to apply force to the pedicle screws to facilitate the closure of the osteotomy

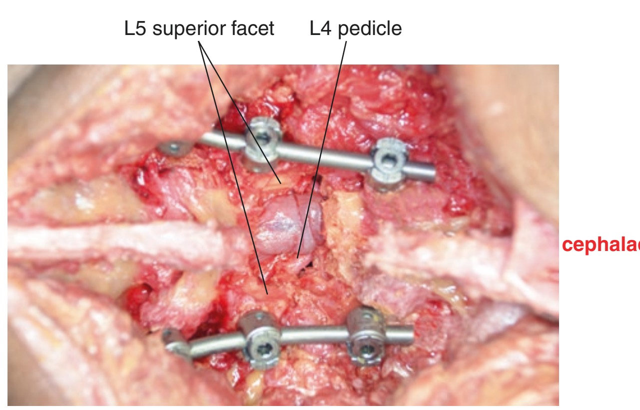

Fig. 4.73 The osteotomy is closed

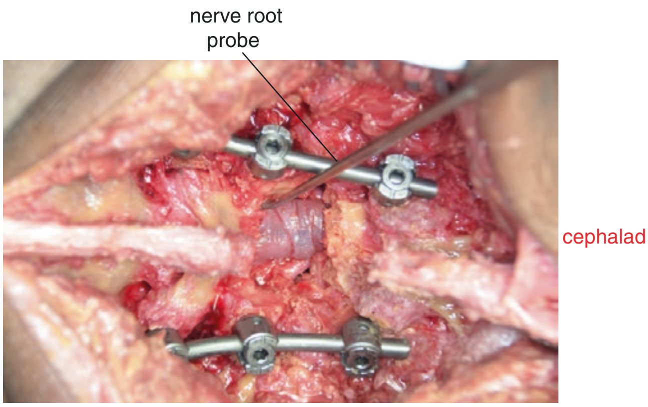

Fig. 4.74 Inspect the intervertebral foramen to check if compression exists on the nerve root

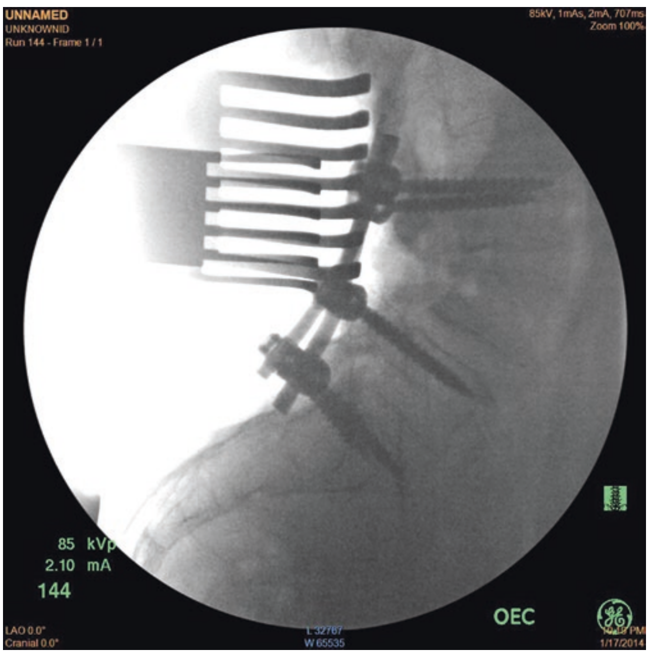

Fig. 4.75 Lateral fluoroscopy of the closed osteotomy

4 Extreme Lateral Interbody Fusion (XLIF)

4.1 Overview

Extreme lateral interbody fusion (XLIF), firstly reported by Neilwright in 2003, is a new minimally invasive technique for intervertebral fusion reaching the lumbar spine through

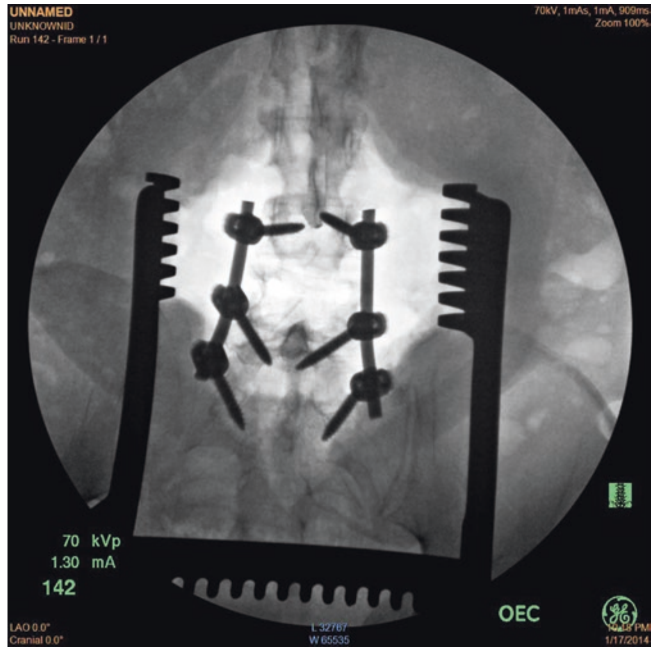

Fig. 4.76 Anteroposterior fluoroscopy of the closed osteotomy

the retroperitoneal space and psoas major muscle. As a novel lateral retroperitoneal approach for the lumbar spine, XLIF has its special advantages over PLIF and TLIF. This approach can remain the integrity of anterior and posterior longitudinal ligaments and allow implanting a bigger interbody fusion cage with a larger fusion area, which could have better biomechanical stability and fusion rate.

The principle of XLIF lies in indirect decompression, which is achieved by restoring the height of the intervertebral space, and thus achieves the following results: (1) increasing the area of the intervertebral foramen, (2) extending the thickened ligamentum flavum and posterior longitudinal ligament that protrude into the spinal canal, and (3) correcting the alignment of the vertebral column. The successful establishment of the operation route passing through the retroperitoneum and psoas major muscle is the key to the success of the procedure. Surgical indications of XLIF are as follows: discogenic low back pain or intervertebral disc degenerative disease with lumbar instability and recurrent intervertebral disc herniation; grade 1–2 spondylolisthesis; mild degenerative lumbar vertebra scoliosis; replacement and repair for artificial lumbar intervertebral discs; and revision surgery for previous posterior lumbar interbody fusion which includes pseudarthrosis and adjacent segment degeneration.

4.2 Position

The patient is placed in the lateral decubitus position (Figs. 4.77 and 4.78) after intubation. The kidney rest is elevated to gain maximum opening of the space between the ribs and the iliac crest to facilitate the access to the target disc.

The bolsters and generous padding are used to position the patient. Tapes are used to secure the patient in position.

To avoid damage to the liver or inferior vena cava, the right lateral position and left-sided approach are usually adopted.

In cases with degenerative scoliosis with a right-sided lumbar curve, the left lateral position and right approach can facilitate exposure to the intervertebral space of the wedging variable and close side.

Both hip joints are placed in inflection position to relax the psoas major muscle.

The attachment point of midaxillary line of diaphragm muscle lied between the inferior edge of the 10th rib and the superior edge of the 12th rib. The attachments on both sides of the vertebral column are mainly located between the upper edge of T12 vertebra and L1–L2 disc (Figs. 4.79 and 4.80).

Fig. 4.77 Position of lumbar XLIF

Fig. 4.78 Position of lumbar XLIF

Fig. 4.79 The attachment point of the diaphragm muscle on the left side

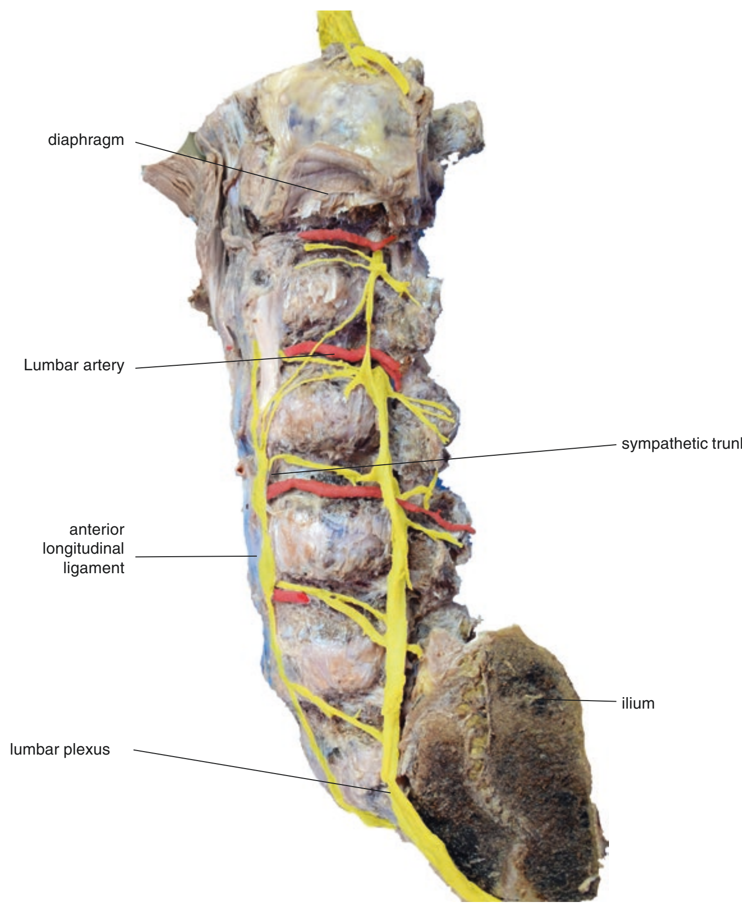

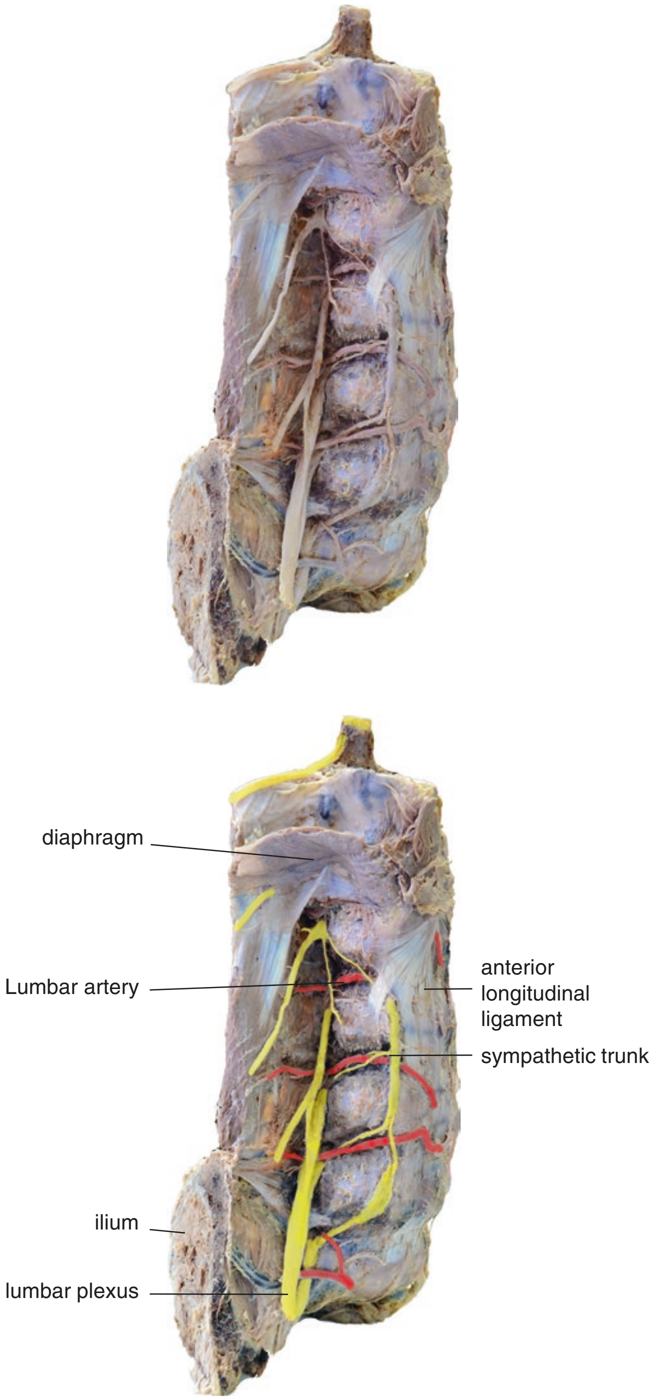

Fig. 4.80 The attachment point of the diaphragm muscle on the right side

A transthoracic approach should be considered when the target level was above T12 vertebrae, whereas a retroperitoneal approach should be chosen when target level was below L1–L2 disc. If the target level is located between T12 and L1–L2 disc, whether via transthoracic, retropleural, or retroperitoneal approach should be determined according to the conditions of patients and the skill and experience of the surgeon.

Incision should be made above the 10th rib for the transthoracic approach and below the 12th rib for the retroperitoneal approach.

True lateral image is performed and the table is tilted to adjust the position and obtain a true lateral view of the target disc. A true lateral view of the target disc is critical in XLIF procedure, for it allows a safe trajectory directly perpendicular to the floor and a better sense for the surgeon of the intraoperative spinal anatomy (Figs. 4.81 and 4.82).

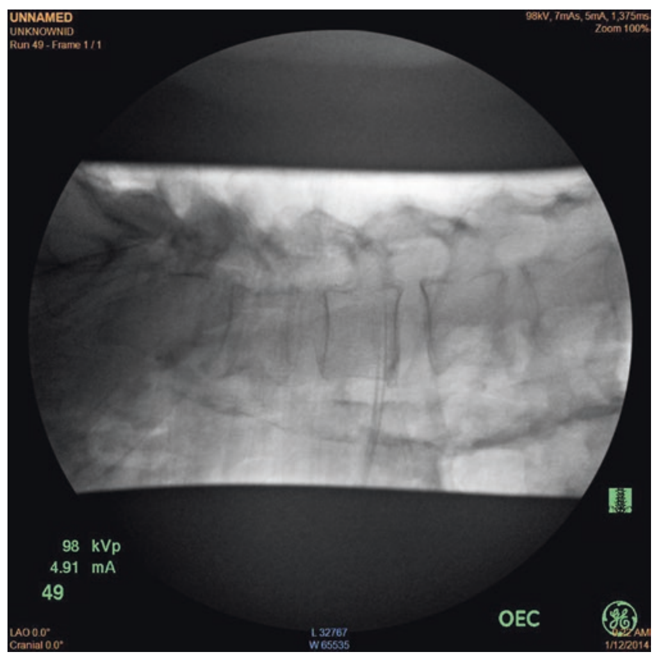

Fig. 4.81 True lateral image is performed during the placement of the patient to gain a true lateral view of the target disc

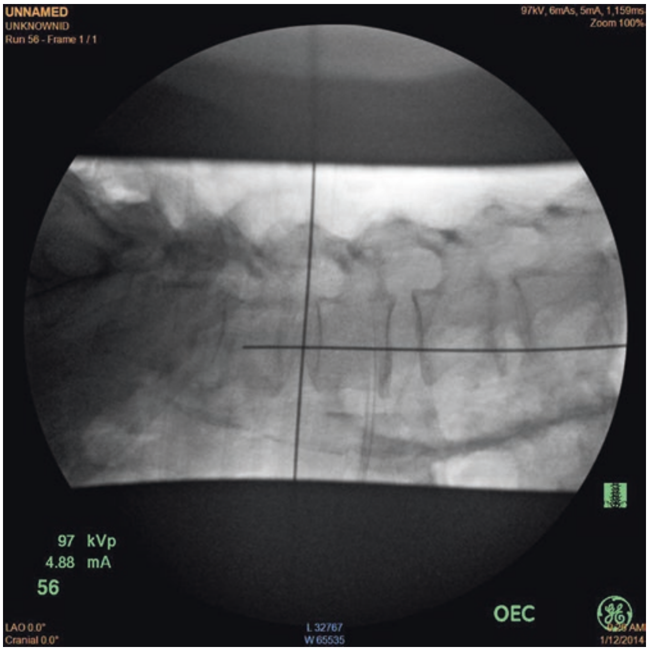

Fig. 4.82 Locate the target disc under fluoroscopy

4.3 Exposure

Longitudinally, incision is made on the skin, and the obliquus externus abdominis, obliquus internus abdominis, and musculus transversus abdominis are bluntly dissected.

Make sure there is no peritoneum underneath the abdominal transverse fascia before incising the transverse fascia.

The surgeon uses his or her finger to perform blunt dissection and create a retroperitoneal space. Then a guide wire is placed along the finger into position directly over the psoas muscle.

The psoas major fiber is bluntly dissected till the intervertebral disc with initial dilatator. The blunt dissection proceeds from the anterior part of the vertebral body to avoid injury to the lumbar plexus and nerve roots.

Psoas major muscle: the psoas major muscle is a long fusiform muscle located on the side of the lumbar region of the vertebral column. The psoas major is divided into two parts. The deep part originates from the transverse processes of L1–L5. The superficial part originates from the lateral surfaces and neighboring intervertebral discs of the T12–L4. The lumbar plexus lies between the two layers. The psoas major serves as an important anatomic landmark in XLIF (Fig. 4.83).

Genitofemoral nerve: a nerve originating from the ventral rami of the L1–L2 nerve roots. It penetrates the surface of the psoas major muscle at the L3–L4 level and runs downwardly on the surface of the psoas major muscle. It diverges into the ramus genitalis and ramus femoralis above the inguinal ligament, of which the former enters the inguinal canal deep ring and is distributed in the cremaster and scrotum and the latter runs across the crural sheath and femoral fascia and is distributed in the skin of femoral triangle. During the approach of XLIF, entry point of the initial dilator should avoid the genitofemoral nerve (Fig. 4.83).

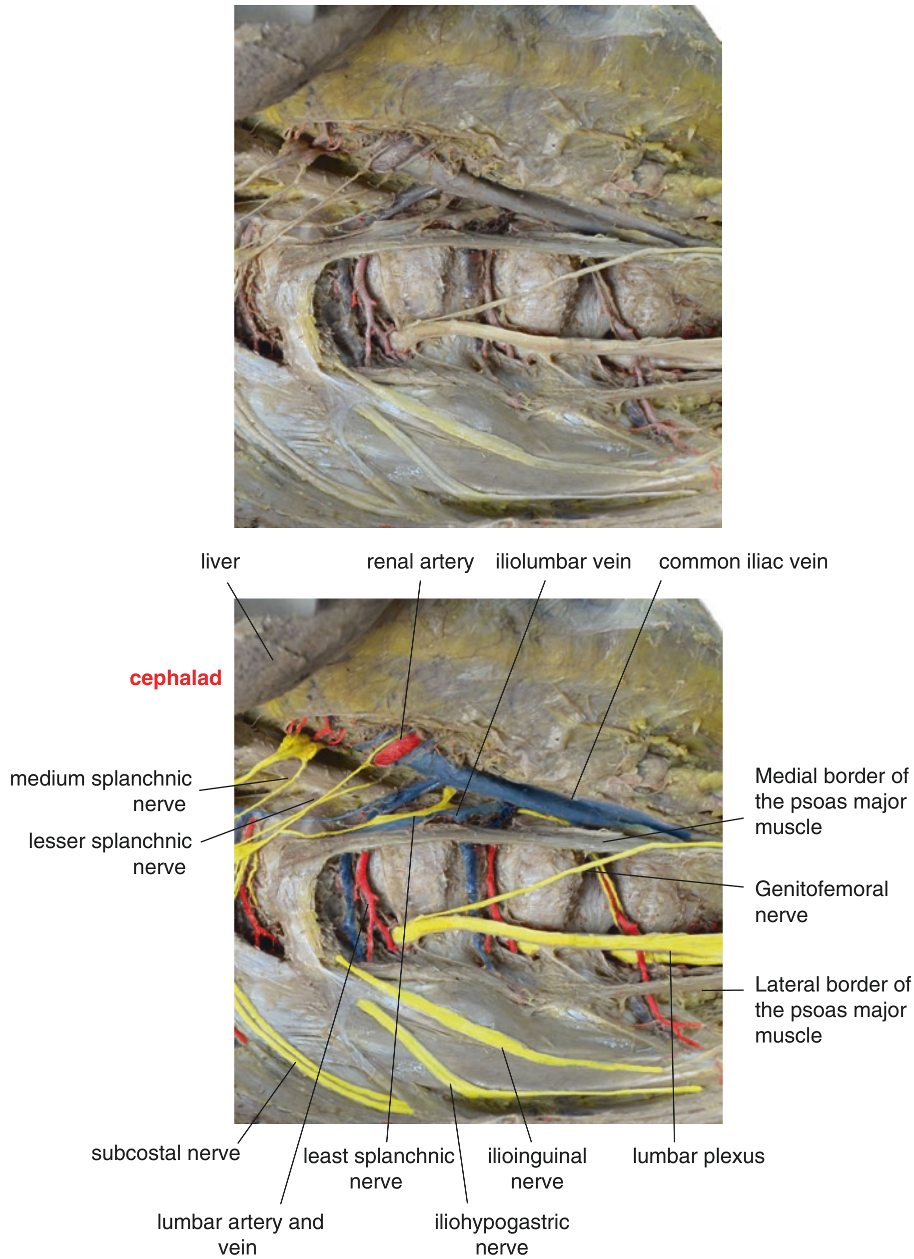

Fig. 4.83 Structures related to psoas major (psoas major resected with the boundary retained)

Make sure that the dilator is placed slightly anterior to the center of the target intervertebral space under fluoroscopy (Figs. 4.84 and 4.85).

A guide wire is gently introduced through the initial dilator into the intervertebral space, and then the location is confirmed by fluoroscopy (Fig. 4.86).

Dilators are then introduced sequentially through the psoas muscle with lateral fluoroscopic image confirming the position and depth (Figs. 4.87 and 4.88).

The retractors are placed along the dilators (Fig. 4.89).

The surgical field is exposed after opening the retractor blades, the tissue over the disc space is cleaned with a penfield dissector, and the nerve within the field can be swept dorsally and placed behind the retractor blade (Figs. 4.90 and 4.91).

The retractors are then adjusted into the proper place and locked to the bed with a retractor articulating arm (Figs. 4.92 and 4.93).

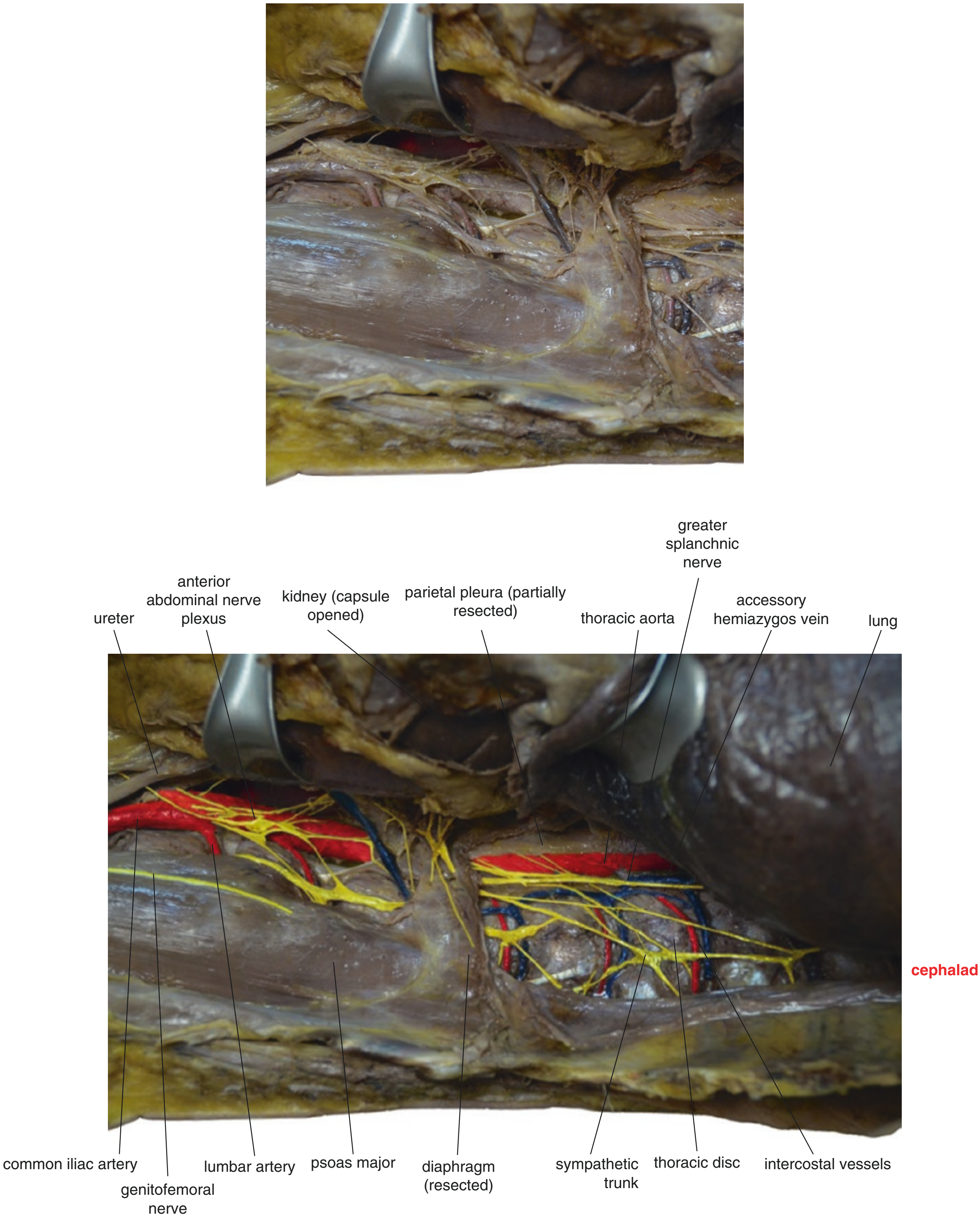

Fig. 4.84 Anatomy related to the psoas major muscle

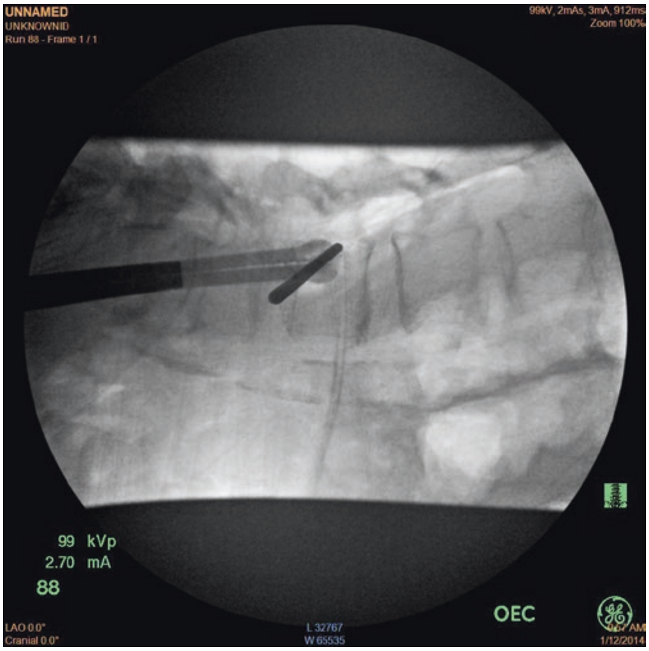

Fig. 4.85 Location of the L3–L4 intervertebral space

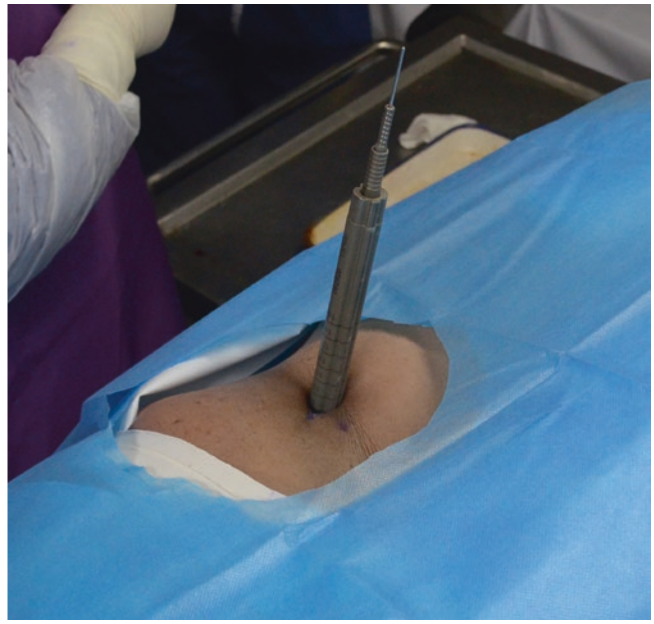

Fig. 4.87 Dilators are introduced sequentially through the psoas muscle

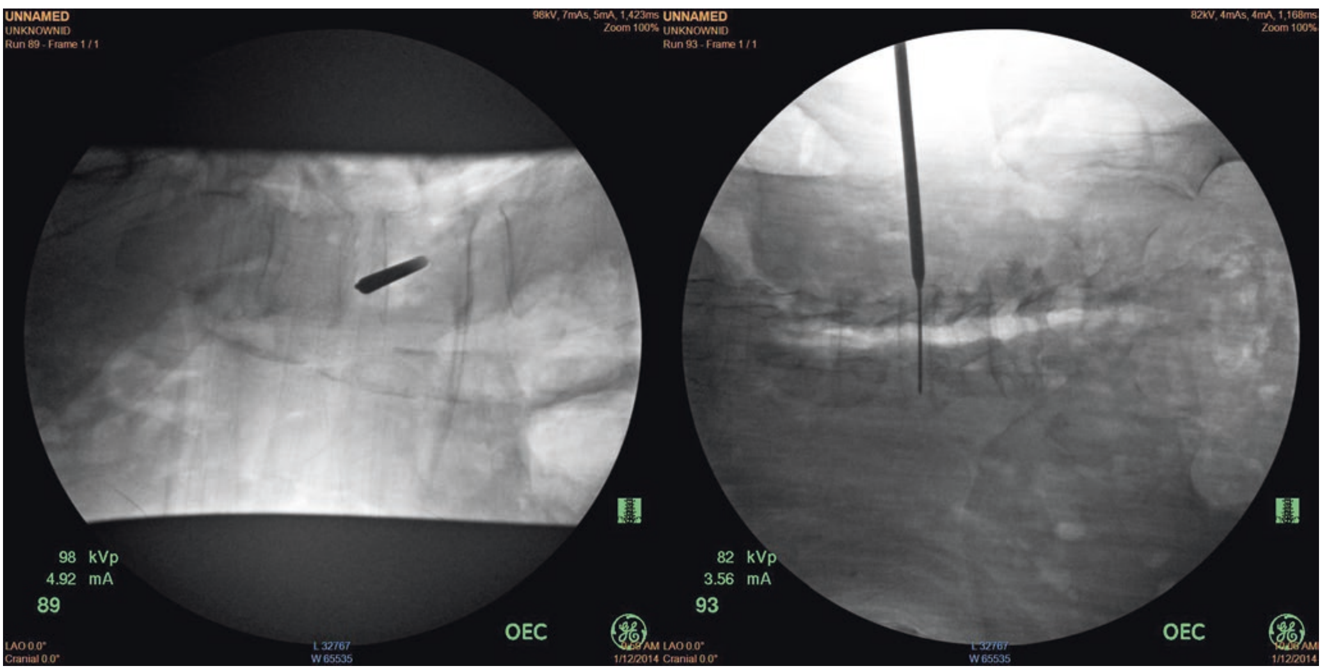

Fig. 4.86 The position and depth of guide wire are confirmed by fluoroscopy

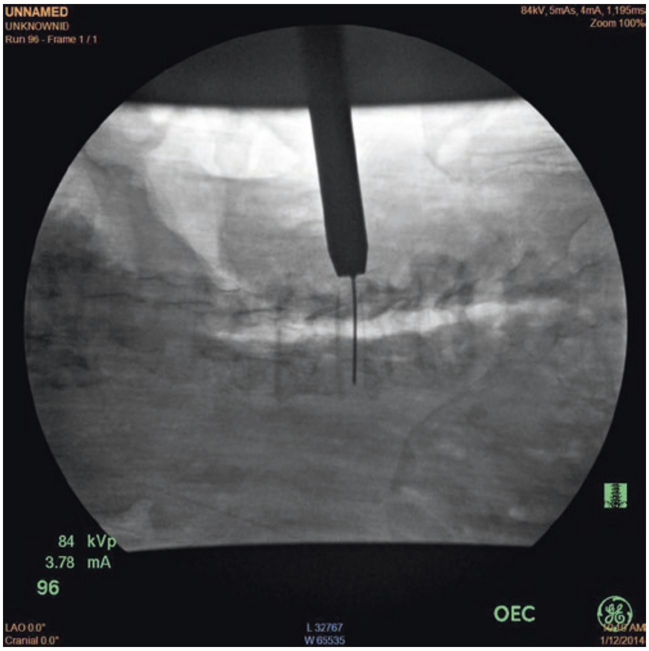

Fig. 4.88 Lateral fluoroscopic image showing dilators expanding the psoas major muscle to the intervertebral disc surface

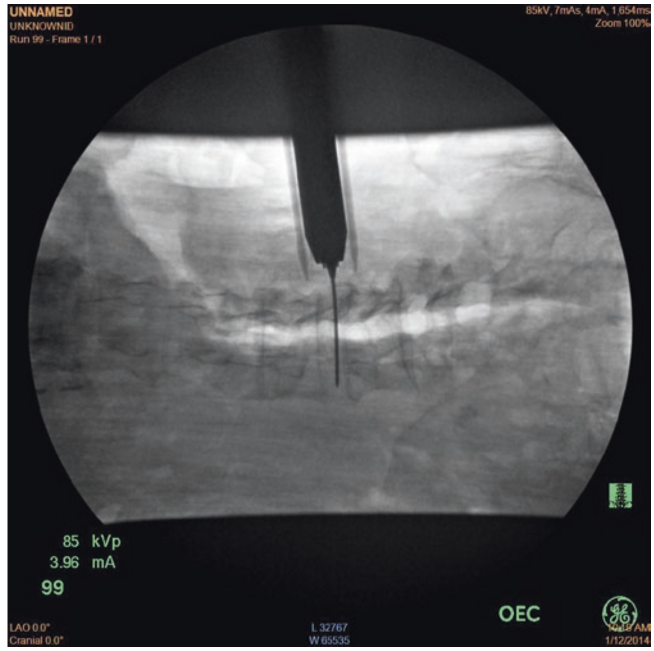

Fig. 4.90 The retractor blades are confirmed in location on lateral fluoroscopy; pins can be placed into the vertebral body to fix the retractor blades in place

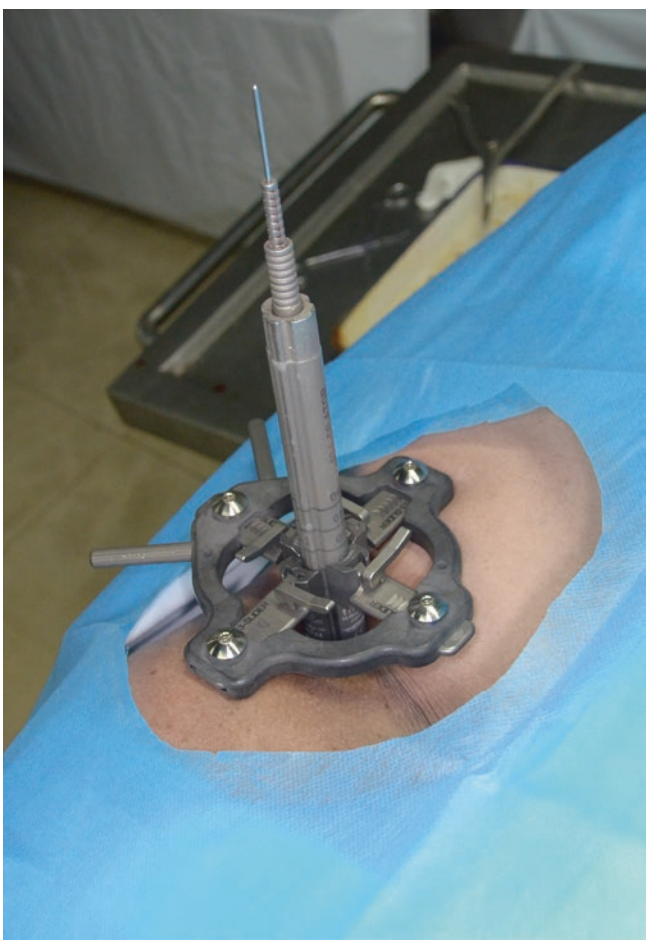

Fig. 4.89 Placement of the retractors

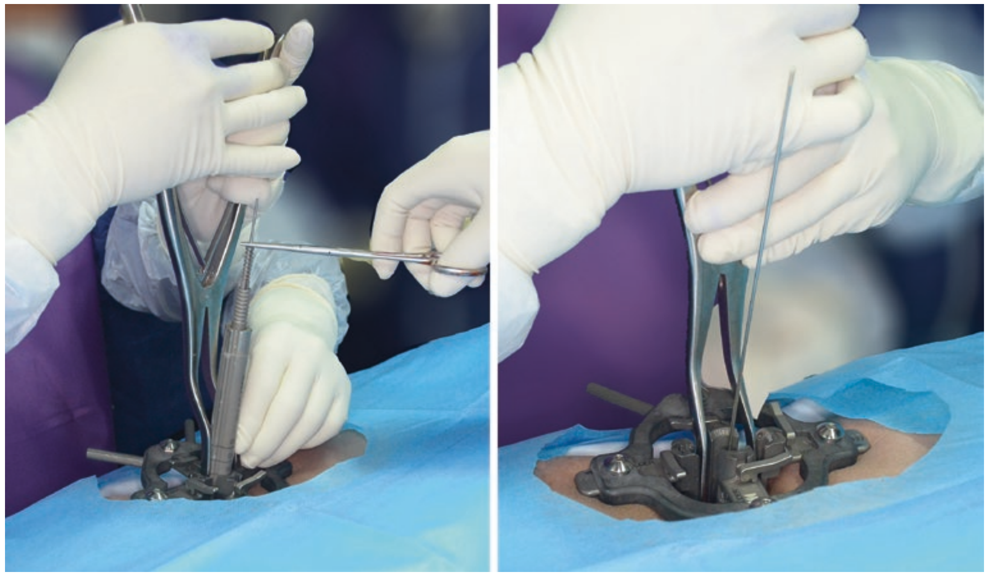

Fig. 4.91 Open the retractor blades with a dilator to expose the surgical field

Fig. 4.92 Fix the retractor on the bed

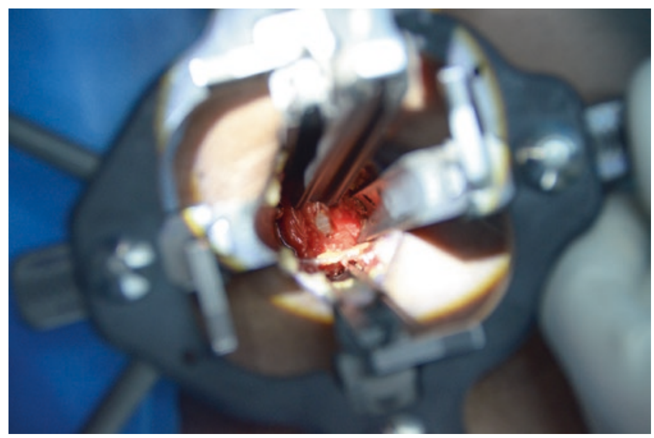

Fig. 4.93 Direct view of the intervertebral disc through the retractor

4.4 Discectomy

A blade is used to incise the anterior two thirds of the disc space. Pituitary rongeurs are used to remove nucleus pulposus.

The disc spaces and end plates are prepared with curettes, reamers, shavers, and rasps.

During surgery, keep the position of the patient unchanged to avoid trajectory bias and an increase in the risk of injury to the major vessels or the lumbosacral plexus (Fig. 4.94).

The intervertebral reamer is used to release the annulus on the contralateral side and cross just beyond the disc space under fluoroscopy (Fig. 4.95).

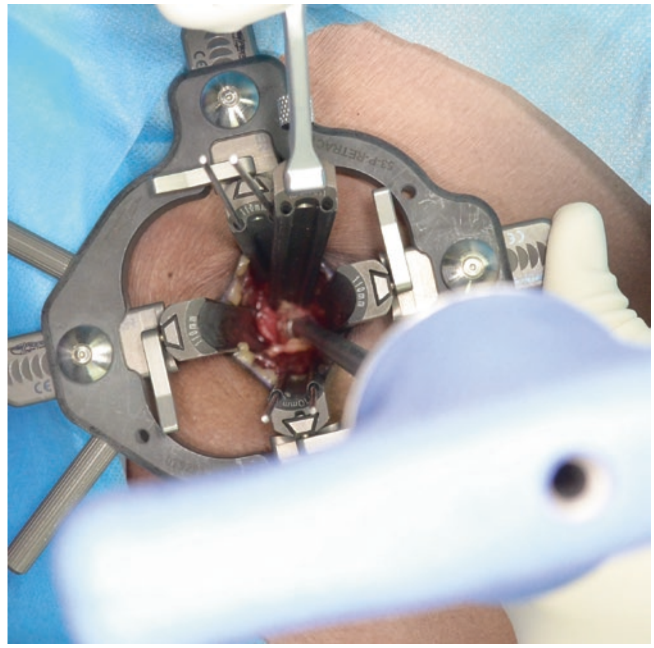

Fig. 4.94 Discectomy

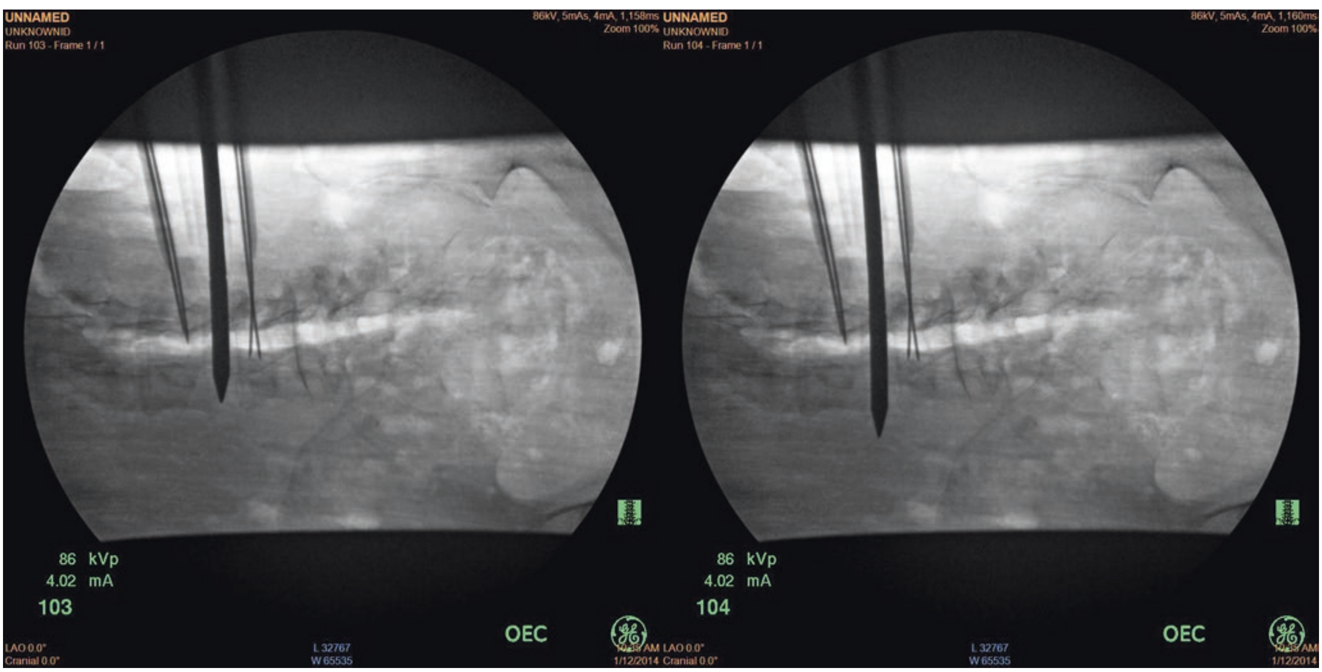

Fig. 4.95 Anteroposterior radiographic image shows intervertebral reamer to the contralateral side

The lumbar plexus (Figs. 4.96 and 4.97) is located posterior to the psoas major muscle and anterior to the lumbar transverse process, consisting of the ventral rami of L1–L3 nerve roots and most fiber of the ventral rami of L4 nerve root. To help avoid damage to the lumbar plexus in the approach of XLIF, the psoas muscle can be divided into four zones based on the distance between the anterior (zone I) and posterior (zone IV) borders of the vertebral bodies. At the level above L3, the lumbar plexus and nerve roots were found posterior to zone III. The nerves were in zone III at L4–L5 (Figs. 4.97 and 4.98).

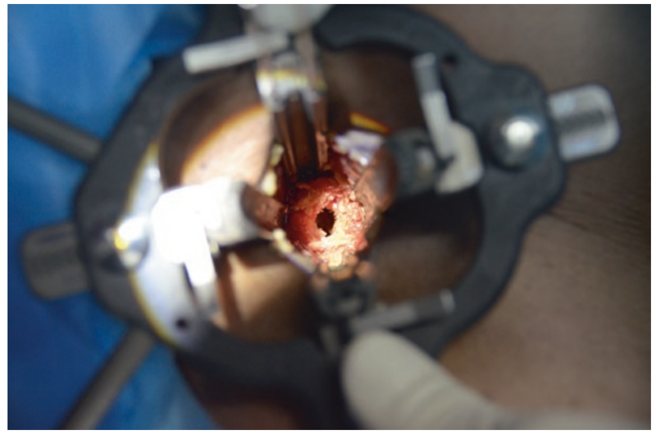

Fig. 4.96 Postdiscectomy

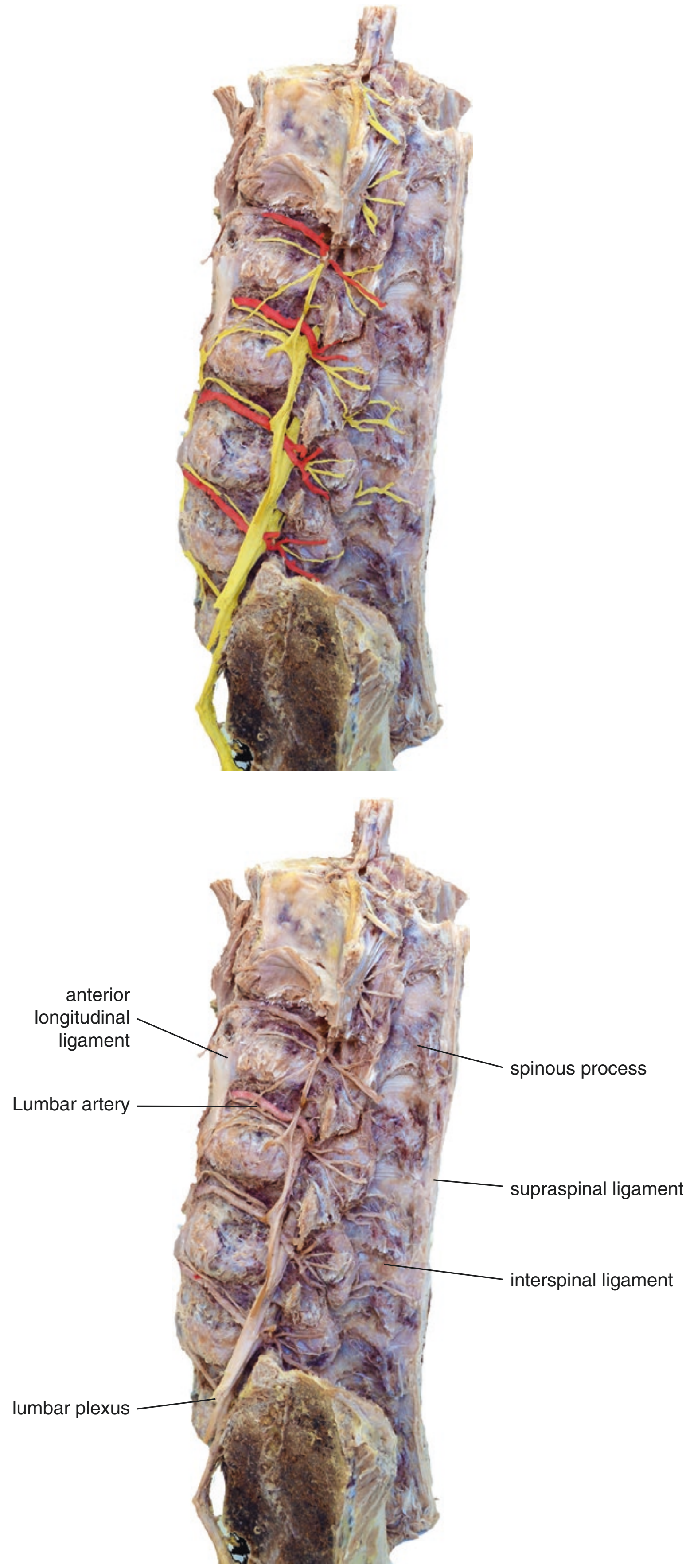

Fig. 4.97 Relationship among the vessel, nerve, and foramen intervertebrale

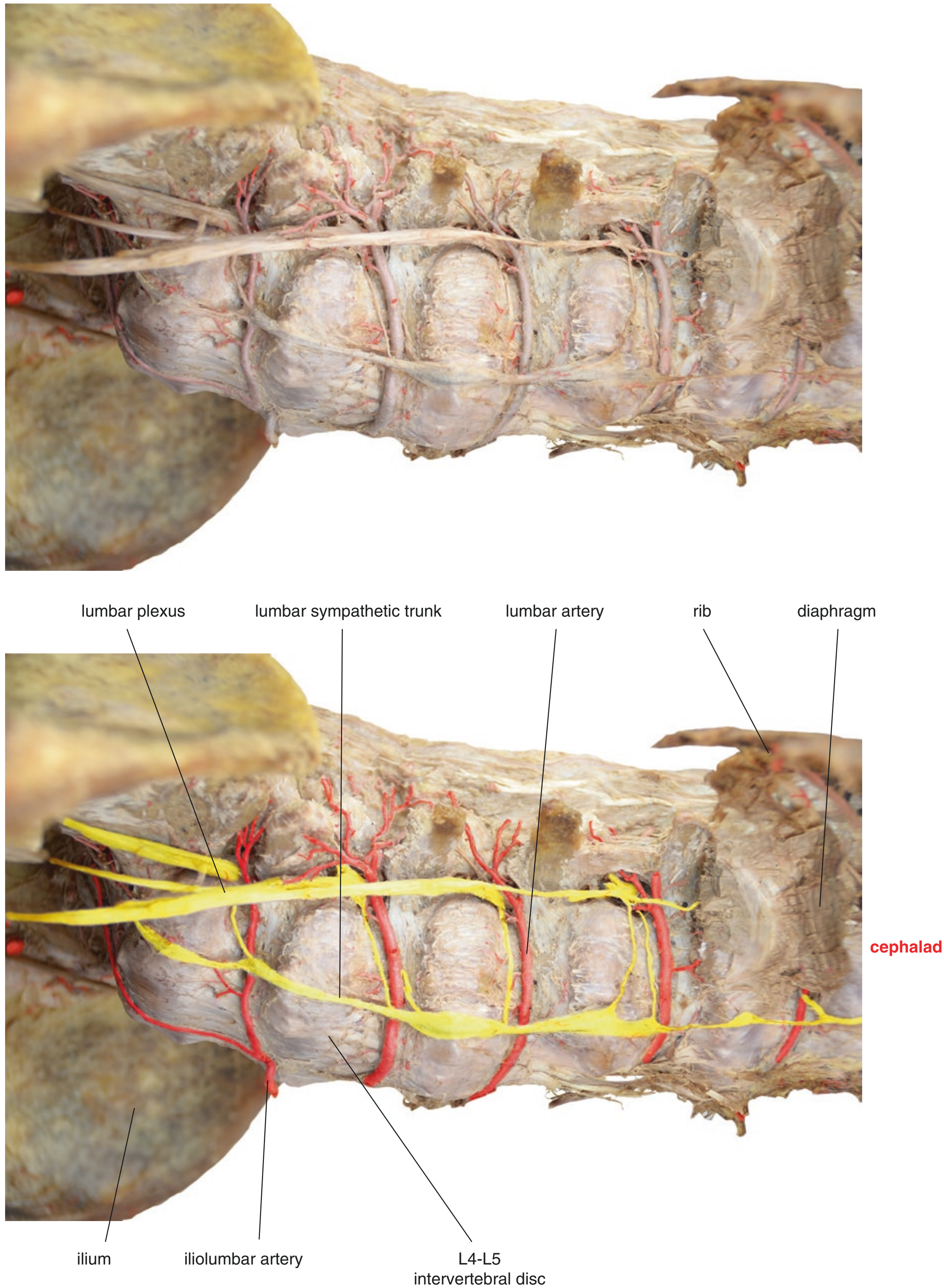

Fig. 4.98 Relationship among the vessel, nerve, and foramen intervertebrale

Trial spacers are used to determine the size and length of the implant (Fig. 4.99).

Place the intervertebral fusion cage filled with an autogenous bone or artificial bones into the intervertebral space (Fig. 4.100).

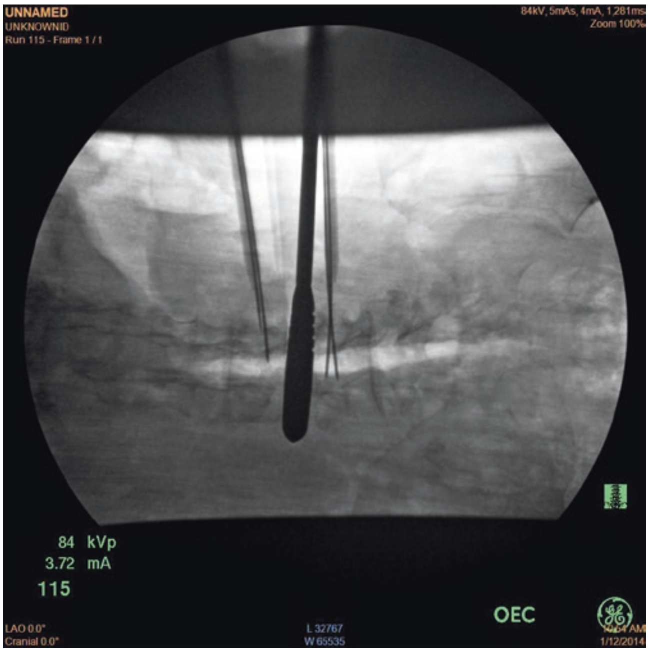

Fig. 4.99 Anteroposterior fluoroscopy shows a trial spacer to the contralateral side

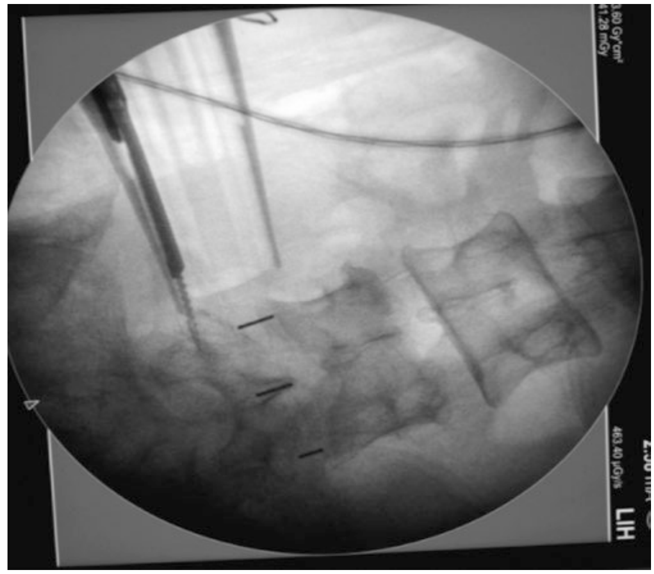

Fig. 4.100 Intraoperative fluoroscopy confirms that the intervertebral fusion cage is well located

5 Anterior Transperitoneal Approach to the Lumbar Spine

5.1 Overview

The anterior approach to the lumbosacral junction is used for the exposure of L4–S1 vertebral bodies and anterior intervertebral discs. It is indicated for surgery in this region, such as resection of infectious lesions (including tuberculosis) on the anterior of lumbar spine, excision of tumors of vertebral bodies, severe lumbar spondylolisthesis that indicates fusion via the anterior approach, and artificial intervertebral disc replacement. Intestinal paralysis can occur after surgery, so a stomach tube is placed before surgery to facilitate postoperative parenteral nutrition. Another complication of this approach is venous thrombus especially when exposure of L4–L5 intervertebral spaces is needed. Though the incision can be extended caudally to the ensisternum and intervertebral spaces above L4 can be exposed in this approach, it's easier to reach spaces above L4 via retroperitoneum approach. Thus, this approach isn't recommended for exposure above L4.

5.2 Position

Patients are placed in the supine position after general anesthesia (Fig. 4.101).

A towel is placed under the iliac crests to hyperextend the lumbar spine.

Generally, the L5/S1 disc is at the same level as the midpoint between the symphysis pubis and the umbilicus.

The L4/L5 disc space is located at the same level as the lower border of the umbilicus.

A transverse or midline vertical incision can be made for anterior transperitoneal approach to the lumbar spine.

The transverse incision is more cosmetic; however, it is mostly used for one level exposure.

The linea alba is incised in the midline to avoid opening the rectus sheath.

The rectus abdominis muscle (Figs. 4.102 and 4.103) is located on both sides of the linea alba with the sheath of the rectus abdominis muscle wrapping its superior and deep surfaces, and its bottom originates from the pubic symphysis to the crista pubica and ends at the 5th–7th costal cartilage. The rectus abdominis muscle is innervated by the inferior intercostal nerves and the subcostal nerve. The blood supply is from the superior epigastric artery and inferior epigastric artery.
The figure shows resection of a part of the rectus abdominis muscle and exposure of the inferior abdominal vessels, and dissection close to the linea alba can prevent injury to the vessels and segmental nerve (Fig. 4.104).

Inferior epigastric artery: originates from the external iliac artery posterior to the inguinal ligament. Along its course, it is accompanied by a similarly named vein, the inferior epigastric vein. Inferior epigastric artery curves forward in the subperitoneal tissue, ascends along the medial margin of the abdominal inguinal ring, then pierces the transversalis fascia, passes in front of the linea semicircularis, and ascends between the rectus abdominis and the posterior lamella of its sheath.

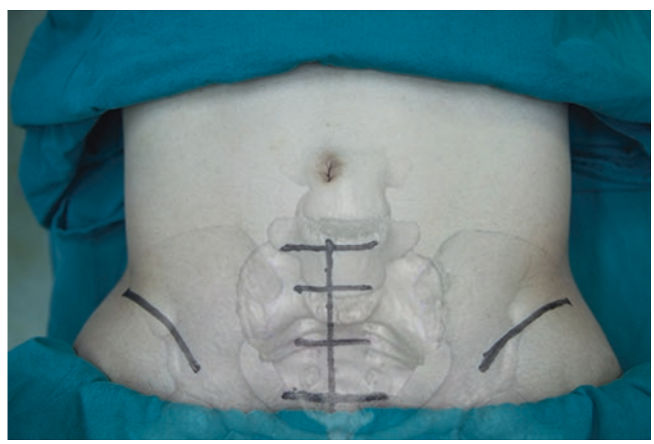

Fig. 4.101 Position and incision for anterior transperitoneal approach to the lumbar spine

Fig. 4.102 Anatomy of the superficial layer of the abdominal wall

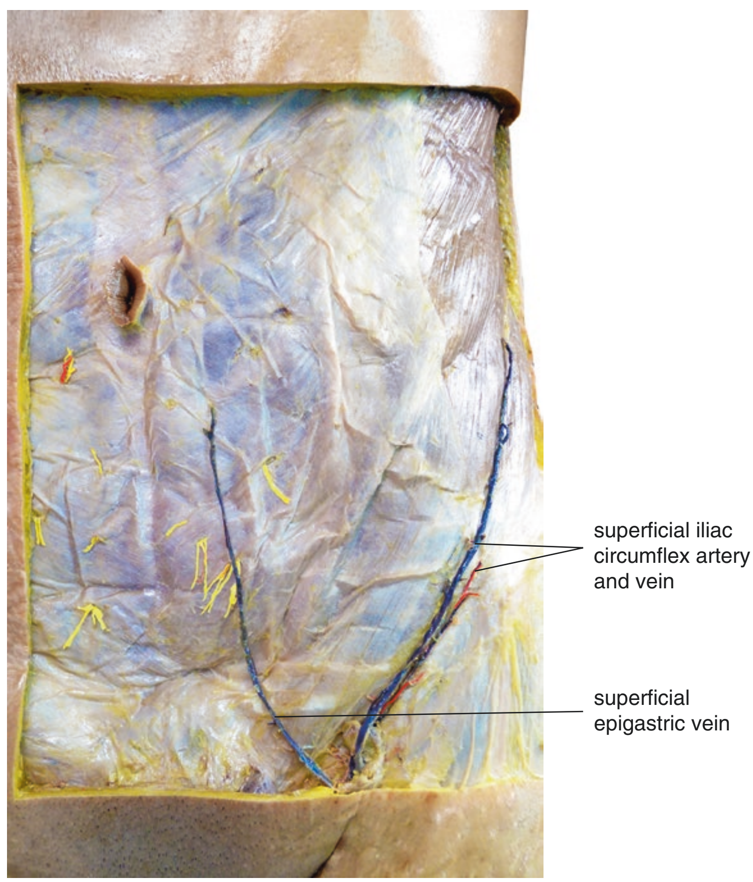

Fig. 4.103 Anatomy of the rectus abdominis muscle

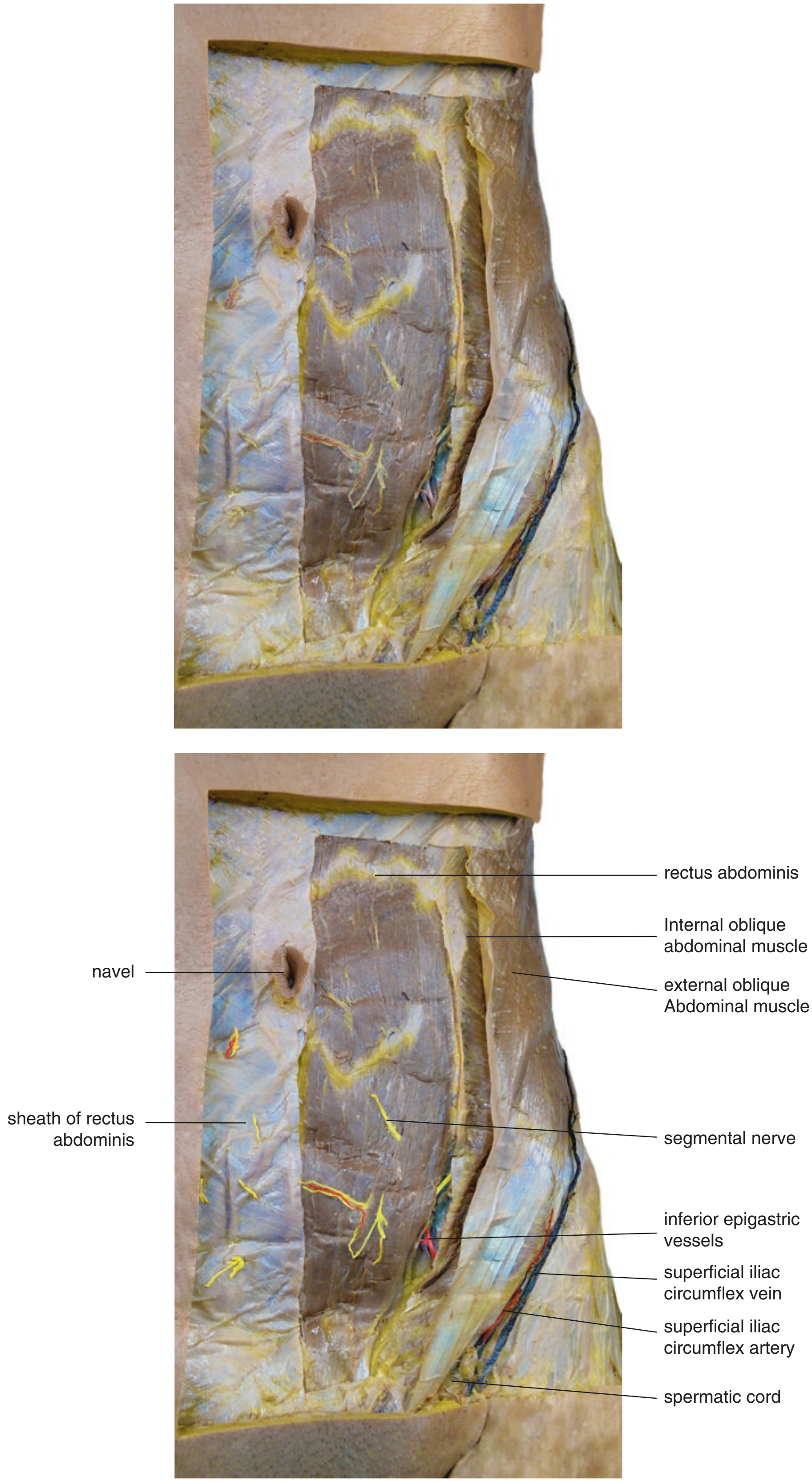

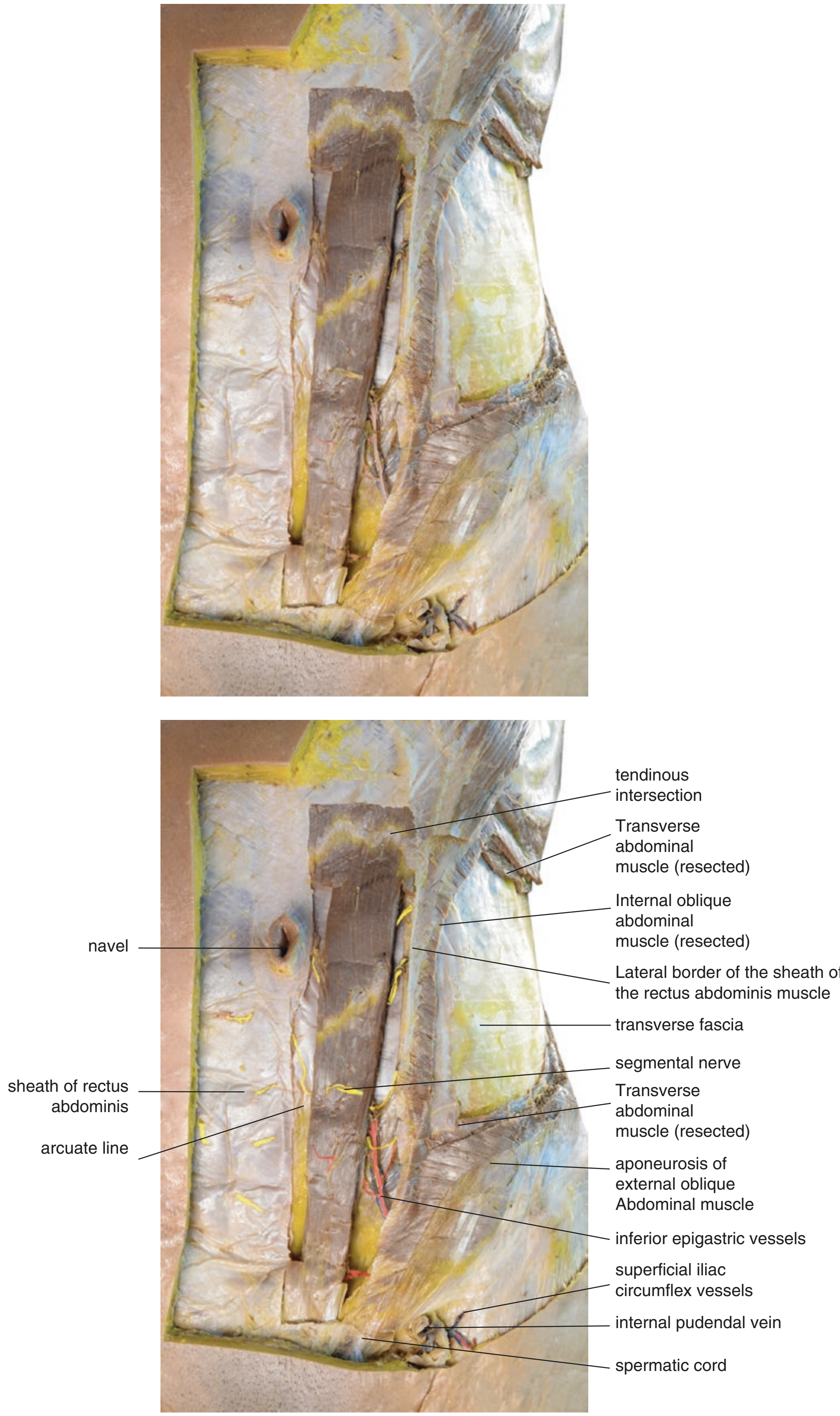

Fig. 4.104 Anatomy of the inferior epigastric artery

5.3 Open Abdominal Cavity

The peritoneum under the linea alba is elevated with a pair of forceps on both sides of the midline.

A scalpel is used to open the peritoneum between the forceps with care to avoid damage to the abdominal contents (Fig. 4.105).

A finger is inserted underneath the peritoneum to separate the peritoneum from the visceral organs. A scissors is then used to extend the incision cranially and caudally.

The small bowel is gently retracted to the right and the sigmoid colon to the left.

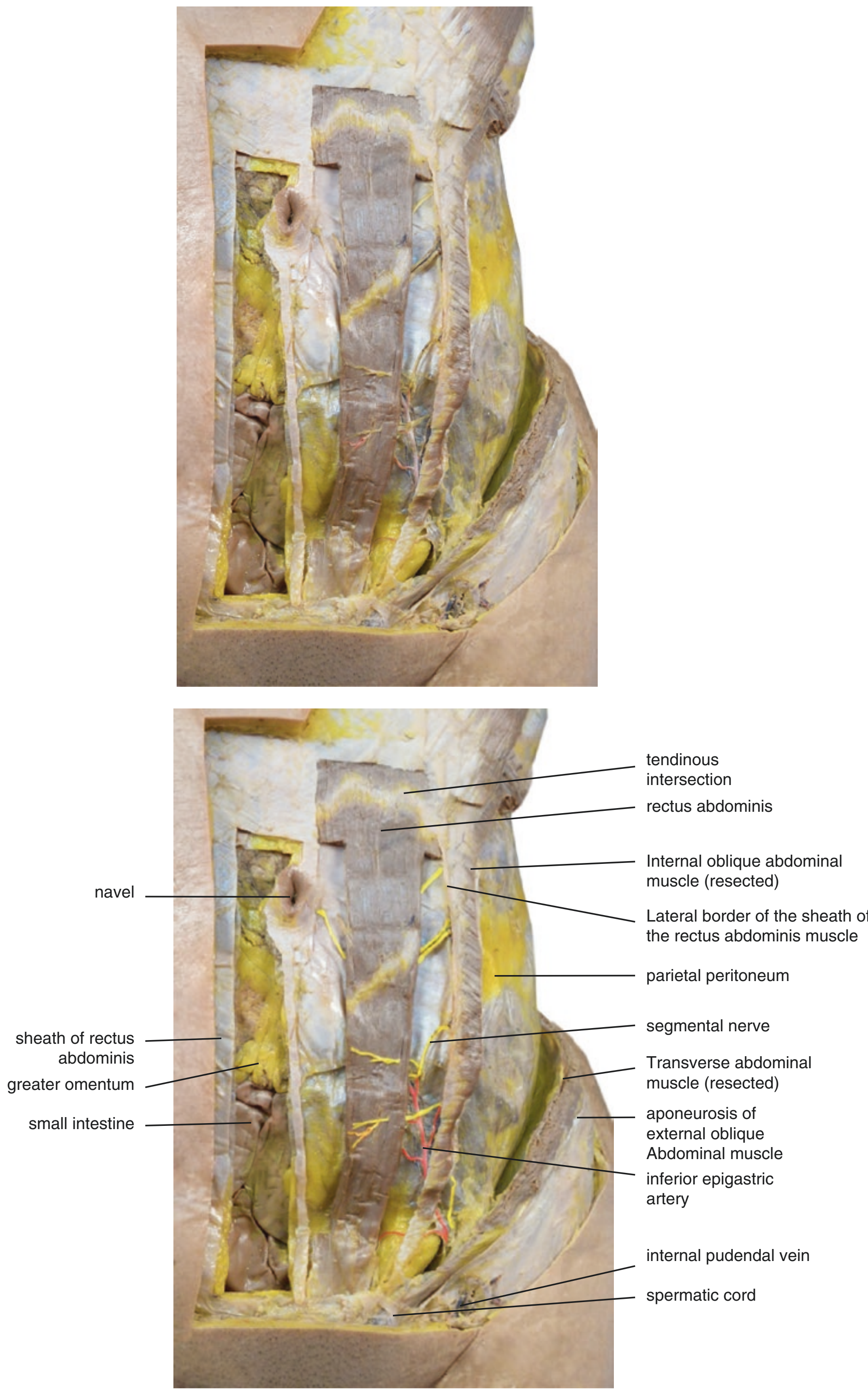

Fig. 4.105 Structures around the sheath of the rectus abdominis muscle

Retroperitoneal space (Fig. 4.106): is the anatomical space in the abdominal cavity behind the peritoneum. Except for the excessively thin individuals, the retroperitoneal space is usually filled with adipose tissue.

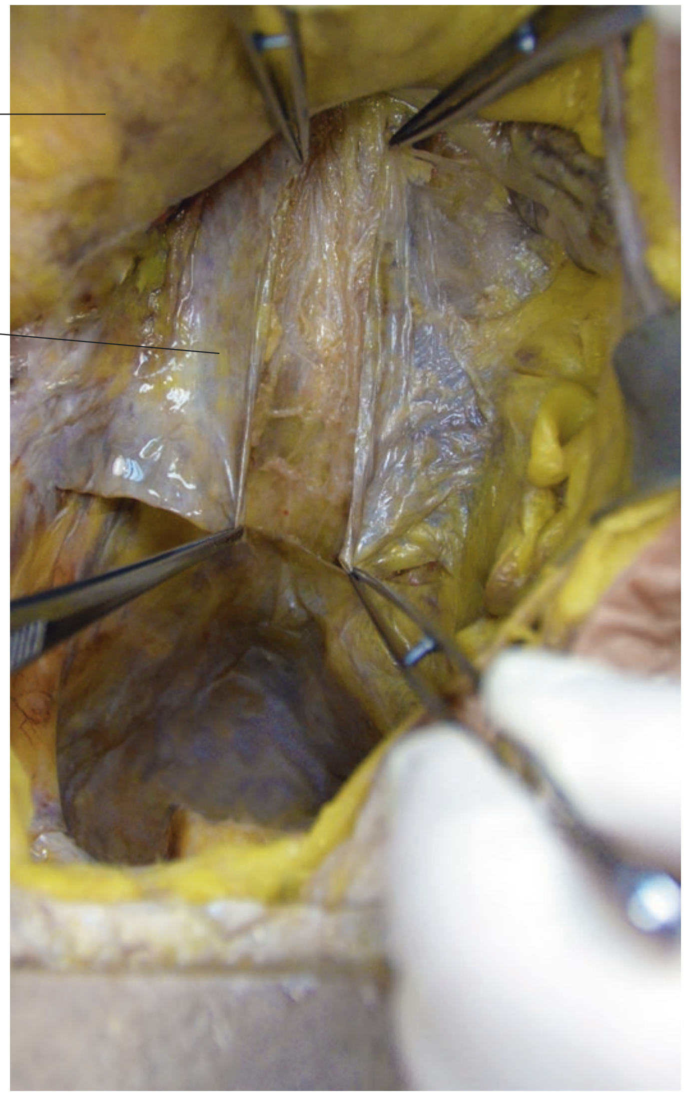

Fig. 4.106 The posterior peritoneum (incised)

5.4 Exposure of Vertebral Bodies

The sacral promontory, aorta, and iliac vessels are palpated.

Infiltrate presacral soft tissue with a little normal saline to identify and separate contents within the retroperitoneal space.

The retroperitoneum is elevated and the incision extended cranially and caudally with care taken to avoid the underlying great vessels and autonomic nerves (Fig. 4.107).

Presacral fascia: the presacral fascia is located between the lumbosacral vertebrae and the posterior peritoneum, with the superior hypogastric plexus running in front of it and the sacral vessel and lumbosacral sympathetic nerve running posterior to it (Fig. 4.108).

Superior hypogastric plexus: it is formed by the abdominal aorta plexus with the lumbar splanchnic nerves branched from L3 to L4 ganglions. It is flat and strip shaped, running along the abdominal aorta branches in the left midline down to the anterior of L5 vertebra, extending down to the nerve plexus, and then dividing into left and the right hypogastric plexus further connecting with the inferior hypogastric plexus.

Make an incision on one side of the superior hypogastric plexus; carefully retract the superior hypogastric plexus along with the presacral fascia to the opposite side. Injection of normal saline in presacral soft tissue can facilitate the identification and protection of the superior hypogastric plexus.

Incise the presacral fascia to one side to expose the L5–S1 intervertebral space, and bluntly peel the remaining tissue from the midline of the other side of the intervertebral space (Figs. 4.109 and 4.110).

During operation in the L4–L5 intervertebral space, more extensive exposure is needed, and the great vessel usually needs to be separated and moved.

The ureter is located in the lateral side of the operative field, which should not be retracted excessively to prevent postoperative ischemic stenosis.

Median sacral artery runs down along the anterior sacrum, and it should be ligatured during surgery.

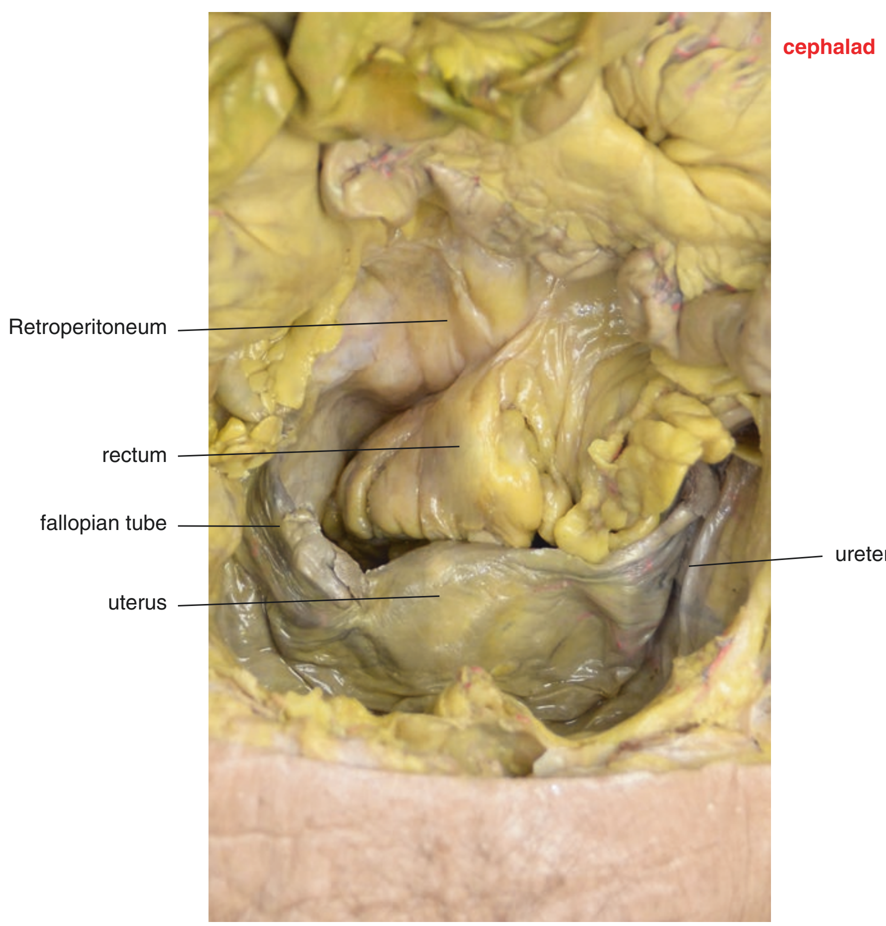

Fig. 4.107 Contents in the pelvic cavity (female)

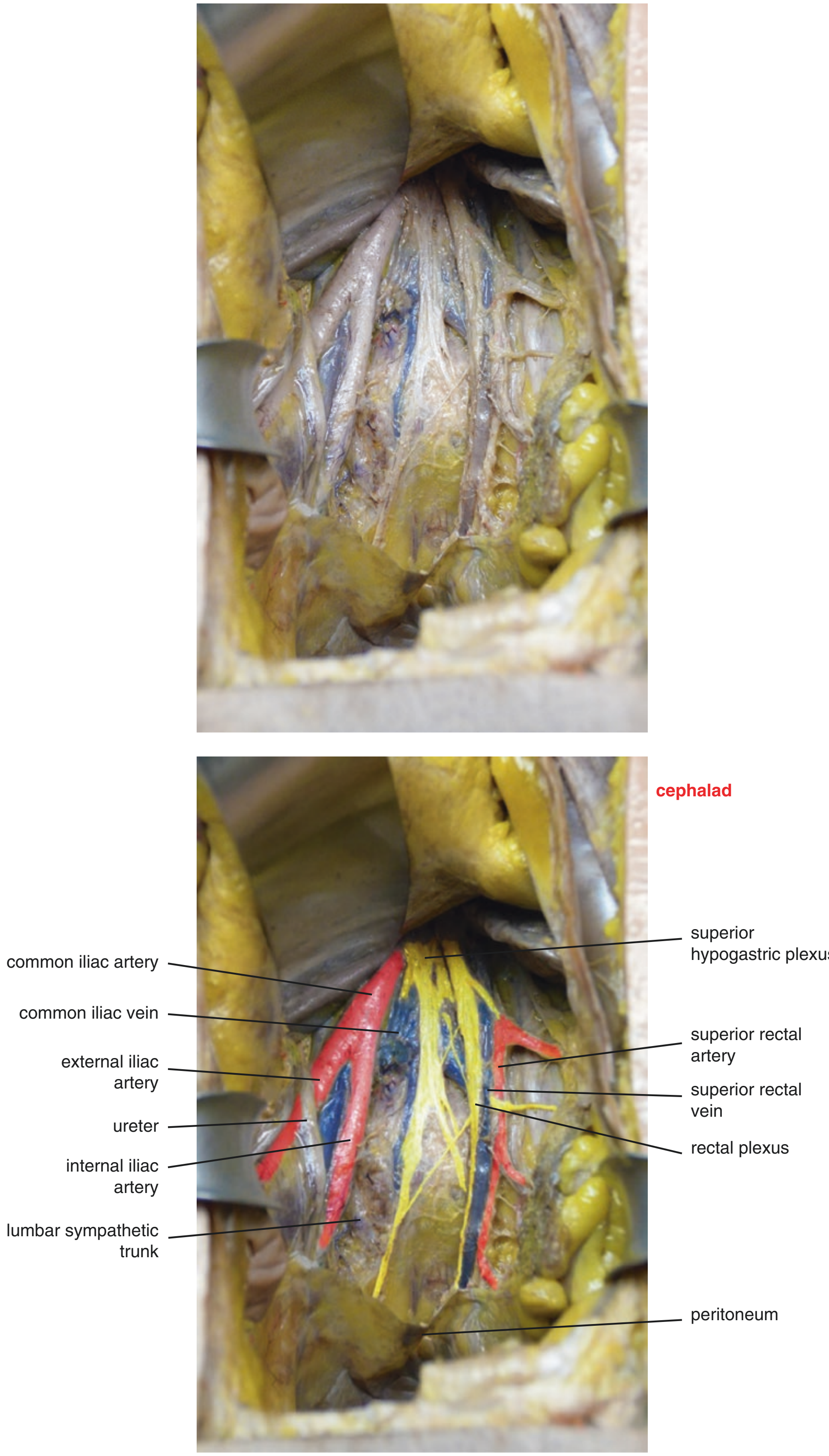

Fig. 4.108 Retroperitoneal nerves and vessels

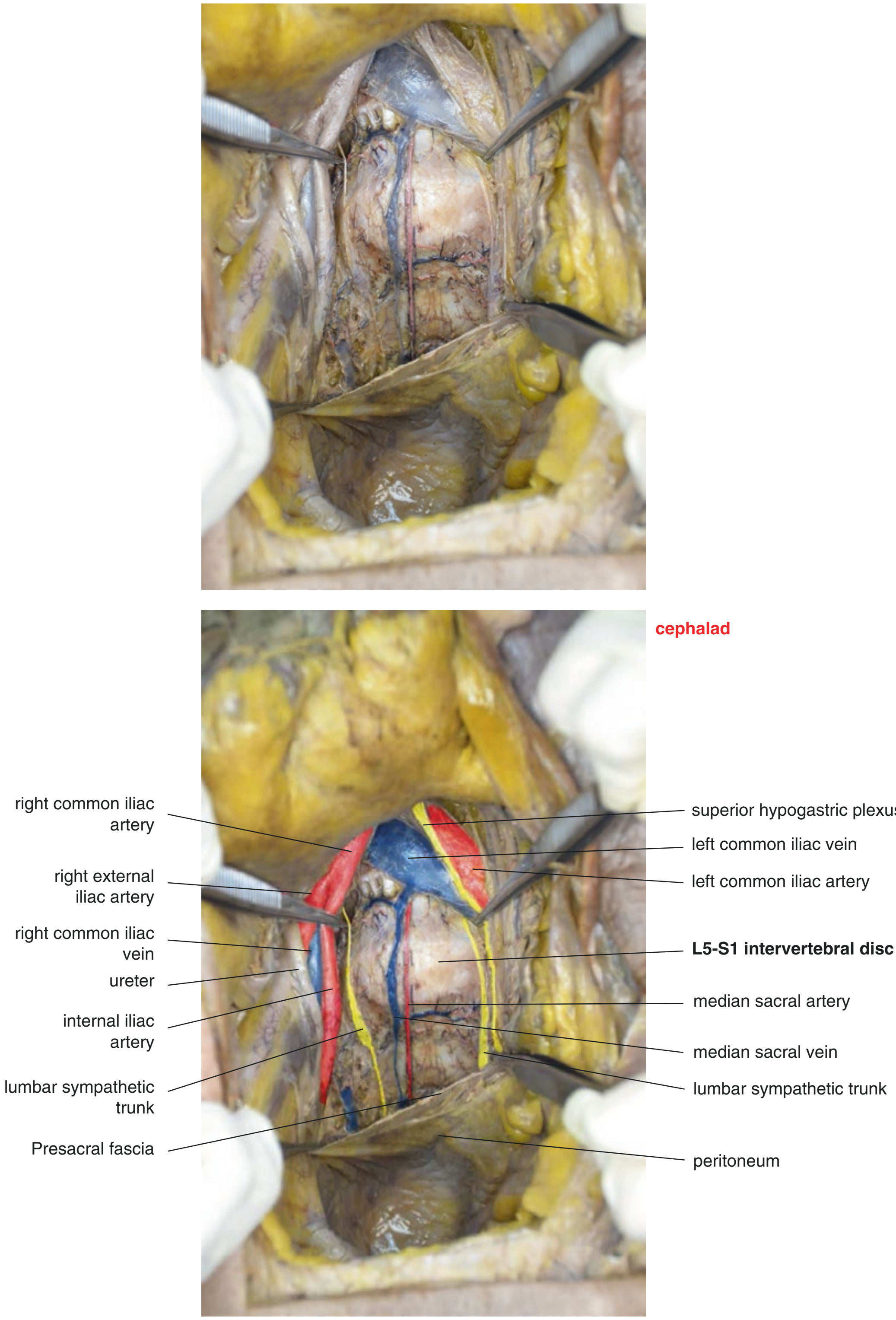

Fig. 4.109 Exposure of the intervertebral space at L5–S1

Fig. 4.110 Anatomy of the anterior sacrum

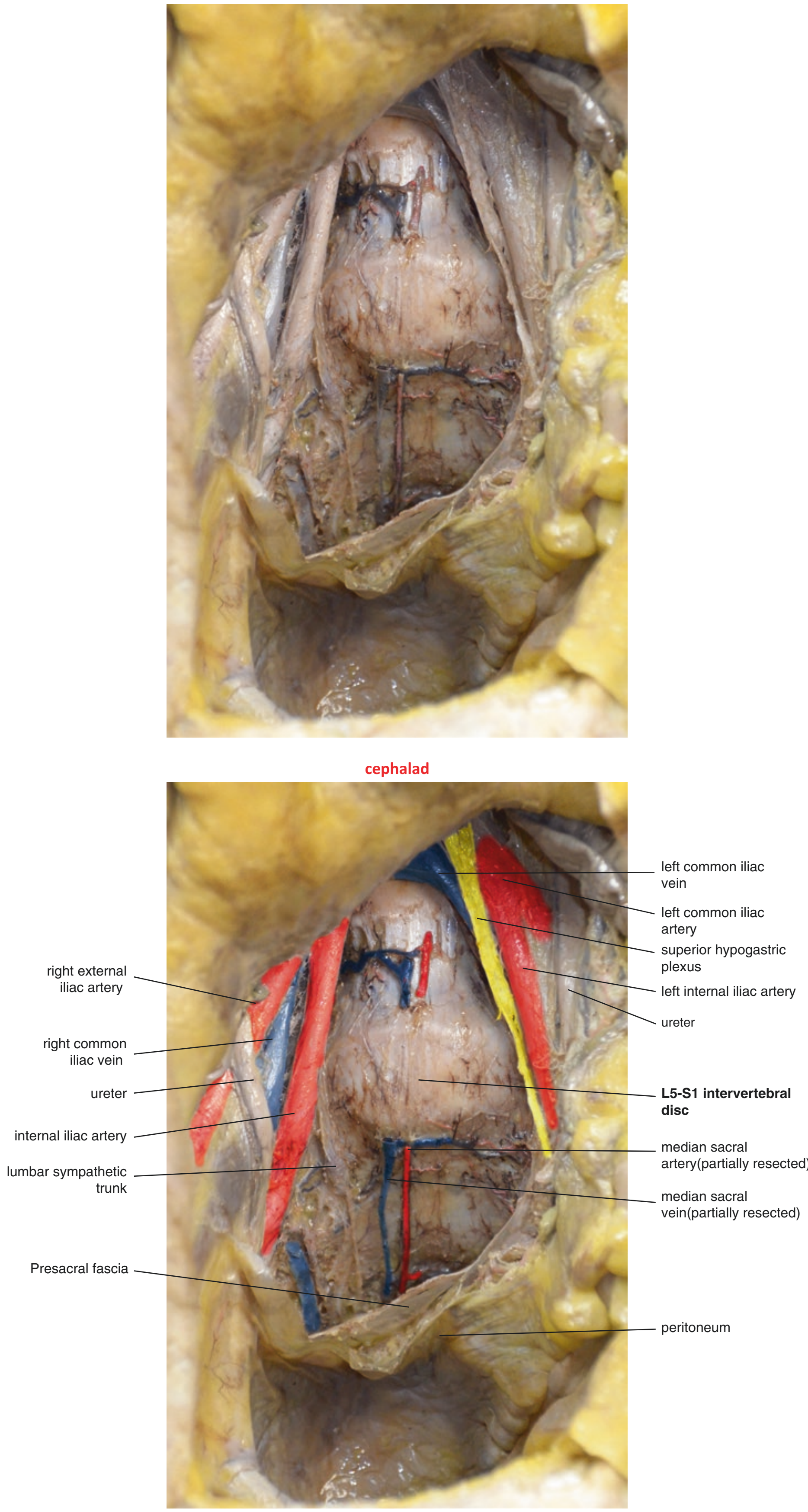

6 Paramedian Retroperitoneal Approach and Anterior Lumbar Interbody Fusion

6.1 Overview

The paramedian retroperitoneal approach can expose the distal lumbar and anterior sacral spine (L3–S1). The main indications of anterior lumbar interbody fusion (ALIF) include lumbar intervertebral disc protrusion (including recurrent lumbar disc herniation), lumbar instability, lumbar degeneration and lumbar isthmic spondylolisthesis, tumors (primary or metastatic) on the distal lumbar or sacral spine, lumbar or sacral inflammation (tuberculous or purulent), and lumbar spinal trauma. Preoperative CT or MRI examination is necessary to determine the anatomy among the abdominal aorta, vena cava, and iliac vessels in the segments requiring surgery.

6.2 Position

Patients are placed in the supine position after general anesthesia (Fig. 4.111).

The C-arm fluoroscopy is performed to determine the level for surgery.

A transverse skin incision can be made from the midline to the lateral border of the rectus abdominis for exposure of one or two levels.

A slightly curved longitudinal incision centered over the lateral border of the rectus abdominis is used for the exposure of one to two or more levels.

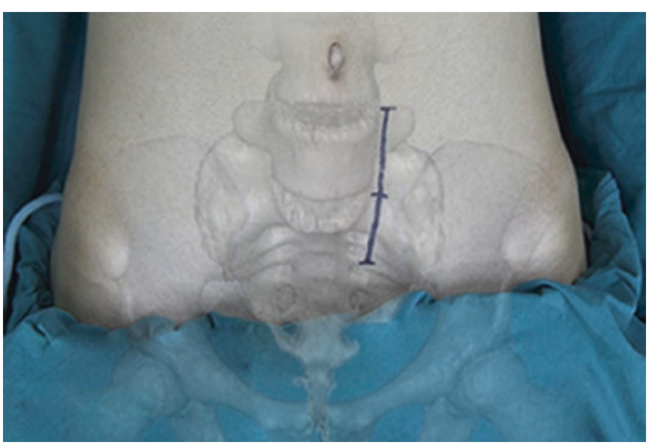

Fig. 4.111 Position and incision for exposure of the lumbar spine via the paramedian retroperitoneal approach

6.3 Exposure

The lateral border of the rectus abdominis is palpated, and the anterior rectus fascia is incised along this border (Figs. 4.112 and 4.113).

The rectus muscles are then retracted medially to expose the posterior rectus fascia and transversalis fascia.

The inferior epigastric vessel encountered can be ligated or protected by a moistened drape and then retracted laterally.

The transversalis fascia is incised to expose the preperitoneal fat and peritoneum (Fig. 4.114).

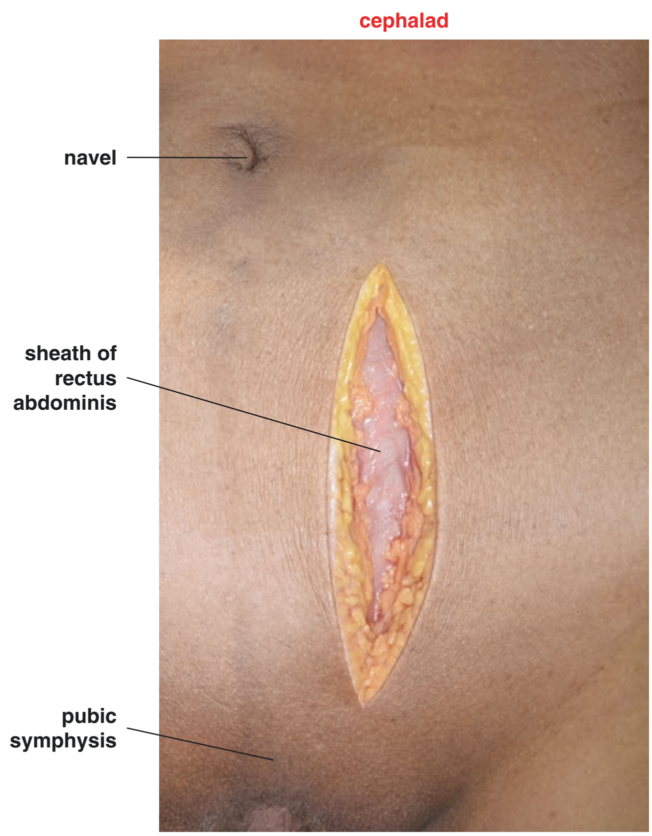

Fig. 4.112 Exposure of the anterior rectus fascia

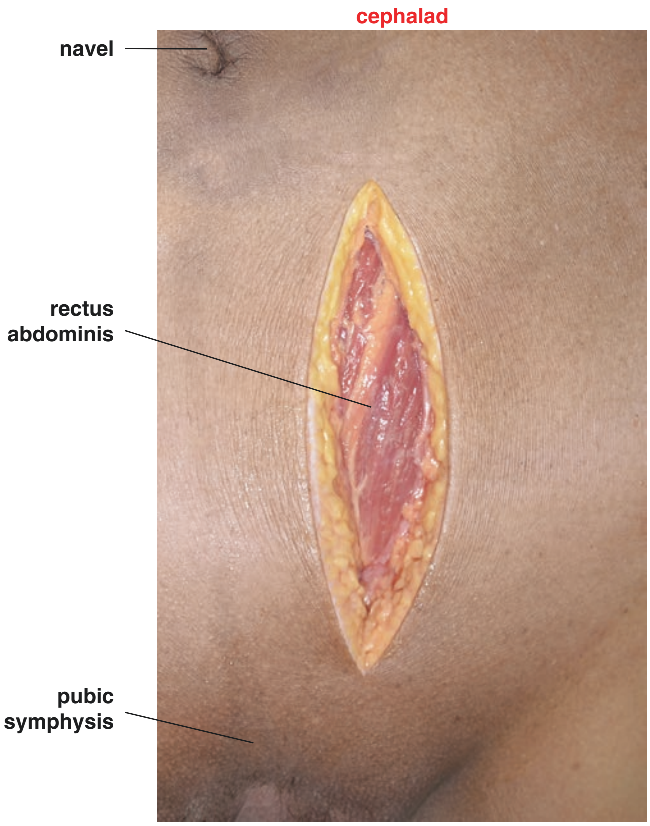

Fig. 4.113 Exposure of the rectus abdominis muscle

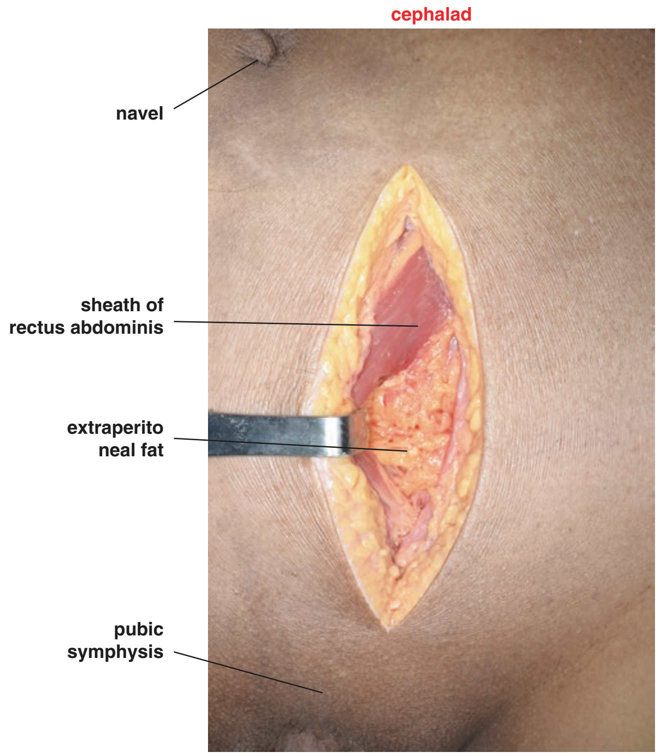

Fig. 4.114 Exposure of the preperitoneal fat

The anterior sheath of the rectus abdominis muscle, the rectus abdominis muscle, the posterior sheath of the rectus abdominis muscle, and the peritoneum (Fig. 4.115). The incision should not be lower than the inferior epigastric vessel. Moreover, protect the innervation and blood supply of the rectus abdominis muscle. The spermatic cord and the testicular vein are located at the distal end of the incision. The proximal end of the arcuate line is the posterior sheath of rectus abdominis, while the distal end is the transverse fascia.

Fig. 4.115 Anatomy of the abdominal wall

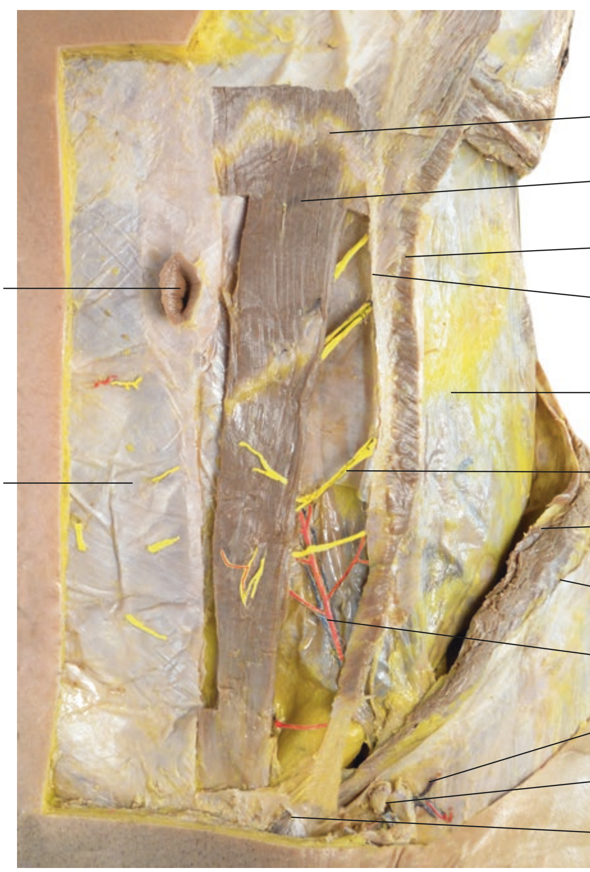

Bluntly separate the retroperitoneal space until it reaches the anterior vertebrae, and retract the peritoneum and the abdominal viscera to the medial side.

The segmental vessels should be ligated and cut close to the vena cava and aorta.

If the L4/L5 disc space is to be exposed, all the branches of the left common iliac vein must be ligated and cut to enable the movement of the common iliac vein. If the exposure is to L5/S1, there is no need to mobilize the iliac vessels; however, ligation and transection of the middle sacral artery and vein are needed (Fig. 4.116).

During surgery, don't use an electrotome under the aortic bifurcation to prevent the superior hypogastric plexus from being injured.

The superior hypogastric plexus is bluntly dissected to either side of the vertebral body.

Common iliac arteries: they originate from the abdominal aorta at the level of the L4 vertebral body or L4–L5 intervertebral disc and end in front of the sacroiliac joint, and each bifurcates into the external and internal iliac arteries. The angle between the common iliac arteries is about 60° in male, while the angle in female is about 40°. They run in the deep surface of the parietal peritoneum, and there are ureters and the genital gland vessels run in front of them (Figs. 4.117 and 4.118).

The lumbar sympathetic trunk (Fig. 4.119) is composed of three or four ganglions and interganglionic branches. It is located between the vertebral column and the psoas major muscle and covered by the prevertebral fascia. Its superior portion is connected with the thoracic sympathetic trunk, and its inferior portion is connected to the sacral sympathetic trunk. The left lumbar sympathetic trunk is adjacent to the left margin of the abdominal aorta, and the distance between them is about 0.5–2 cm (mostly about 1 cm). The anterior area of the right lumbar sympathetic trunk is covered by the inferior vena cava and sometimes passed through by one or two lumbar veins. The inferior sympathetic trunk is located behind the right common iliac vein. The left and right sympathetic trunks travel together with the genitofemoral nerve on the lateral lumbar sides.

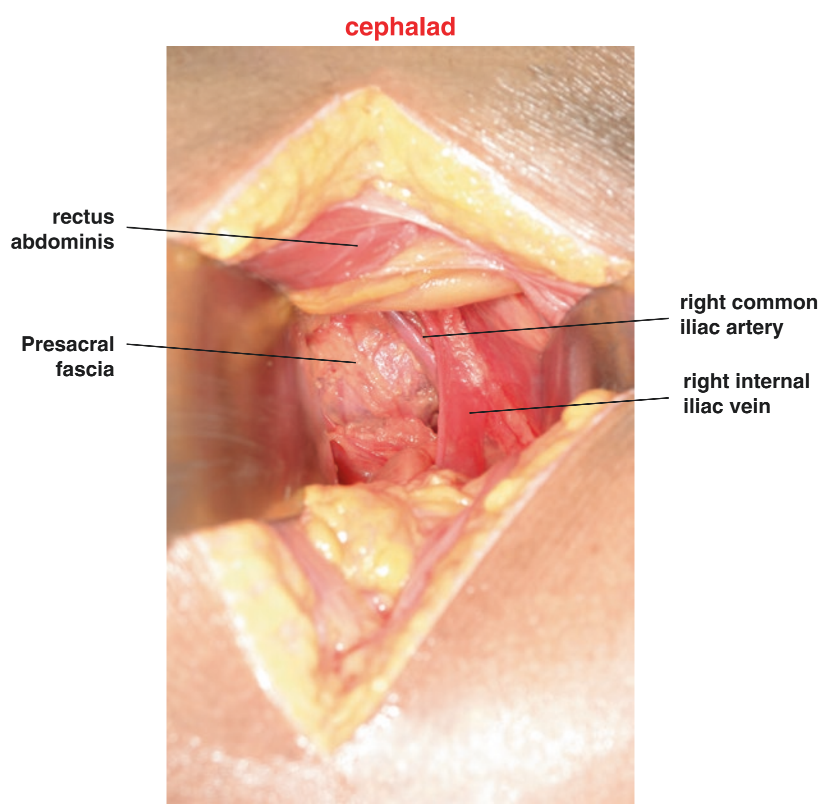

Fig. 4.116 Exposure of the anatomic structure of the anterior vertebral body

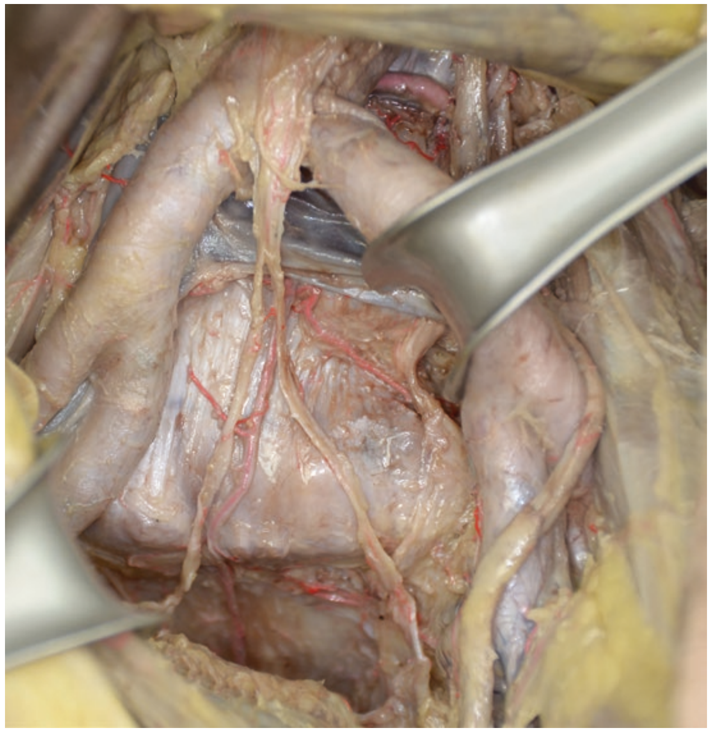

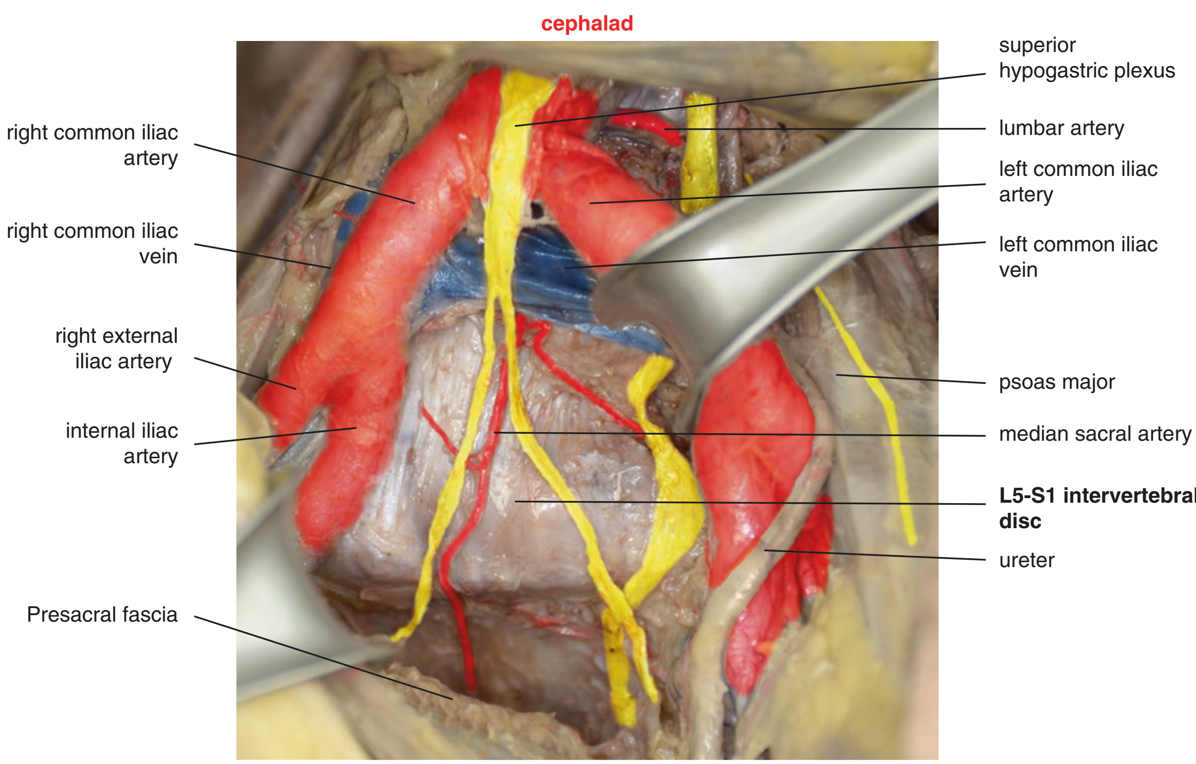

Fig. 4.117 Retroperitoneal space of the lumbosacral level

Fig. 4.118 Neurovascular structures within the pelvic cavity

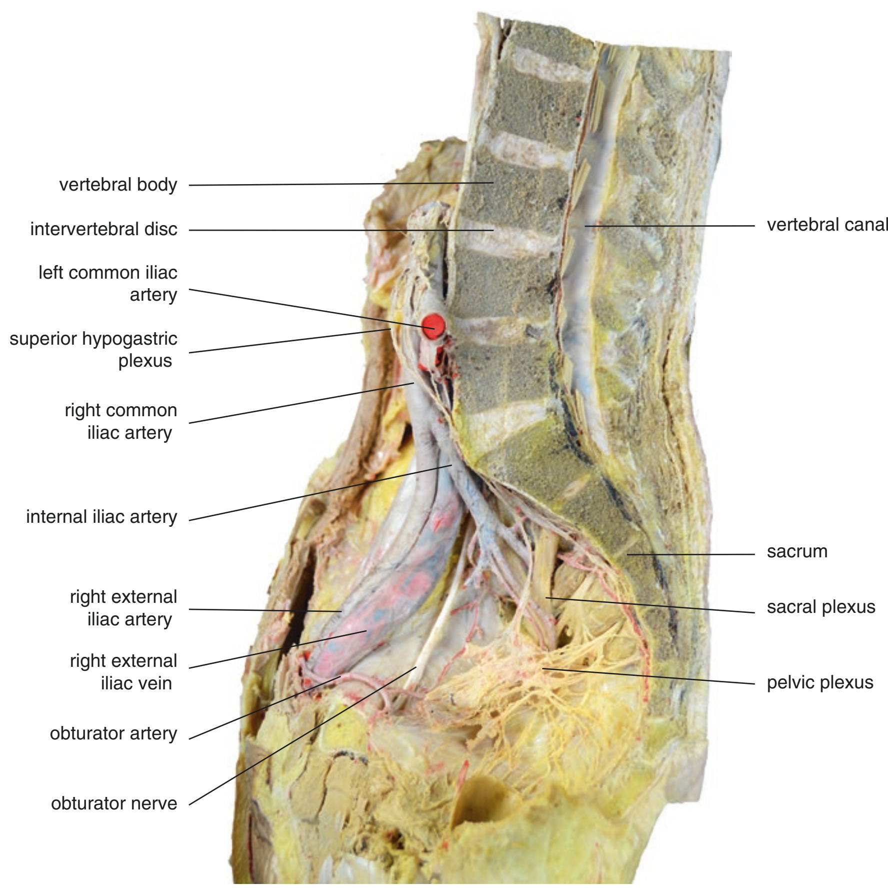

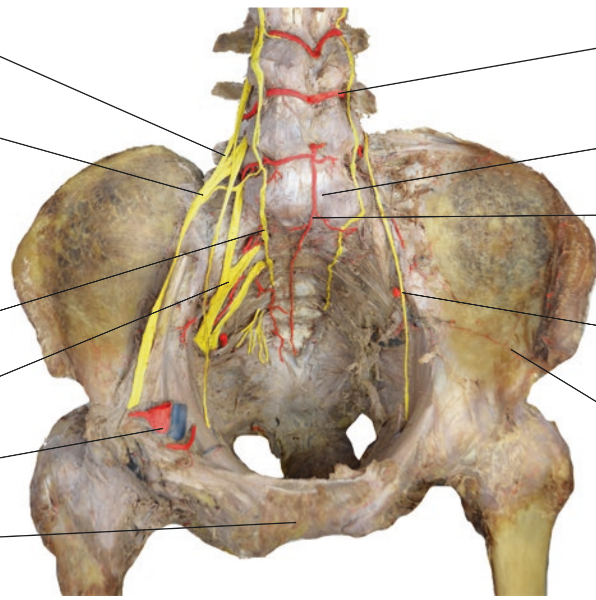

Fig. 4.119 Anatomy of the anterior vertebral body

6.4 Discectomy

A long handle blade is used to incise the anterior annulus fibrosus. Rongeurs and curettes are used to remove the disc contents (Fig. 4.120).

Use a shaver to prepare the end plate to gain a mild bleeding end plate for bone graft and fusion.

The intervertebral fusion cage with a proper size and graft bones is placed into the intervertebral disc.

The anteroposterior fluoroscopy and lateral fluoroscopy show the anterior intervertebral fusion cage is located well (Figs. 4.121 and 4.122).

Fig. 4.120 Exposure of the L5–S1 intervertebral disc

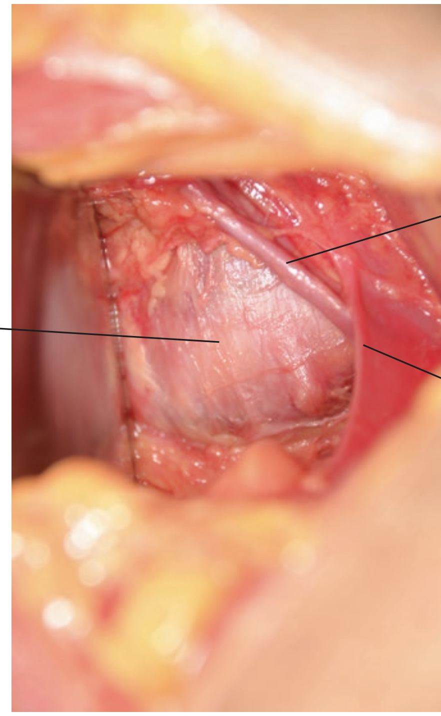

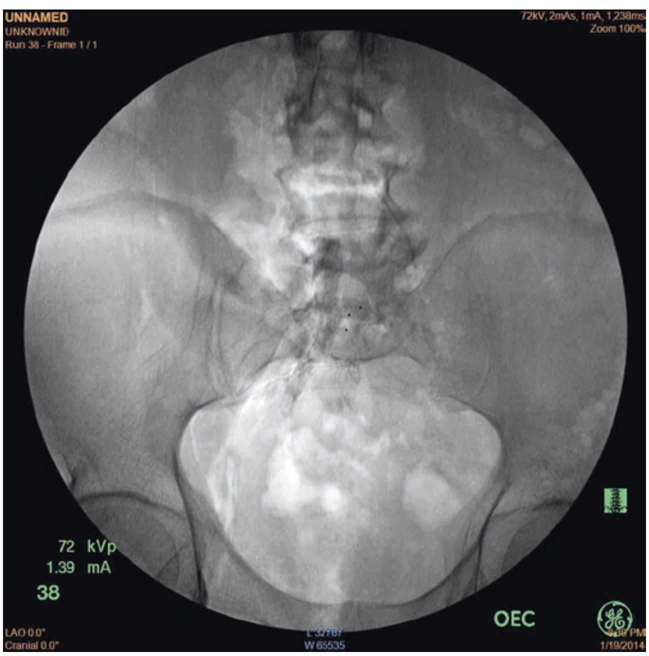

Fig. 4.121 Placement of an intervertebral fusion cage (anteroposterior fluoroscopy)

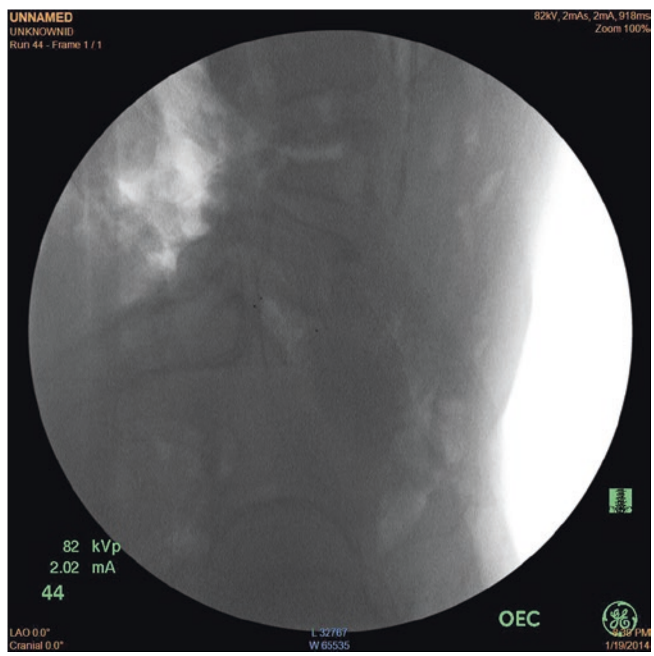

Fig. 4.122 Placement of an intervertebral fusion cage (lateral fluoroscopy)

7 Placement of Lumbar Pedicle Screws

7.1 Overview

After years of clinical use, lumbar pedicle screws have proved to be a safe and effective technique for intervertebral stabilization. Indications of lumbar pedicle screw placement include excision of lumbar nucleus pulposus, laminectomy for decompression, lumbar fusion, tumor resection, lumbar spine spondylolisthesis, fractures, and restoration and internal fixation after dislocation. The entry point, entry angle, and entry depth should be determined based on the individual anatomical characteristics after fully referring to various existing methods.

7.2 Entry Point and Trajectory

The entry points are at the junction of the lateral margin of the superior facet and the horizontal line of the center of the transverse processes (Fig. 4.123).

For L1–3 and L4–5, the angles between the drilling pathbreaker and the sagittal plane are 5–10° and 10–15°, respectively, and the sagittal trajectory should be parallel with the end plates of vertebral bodies.

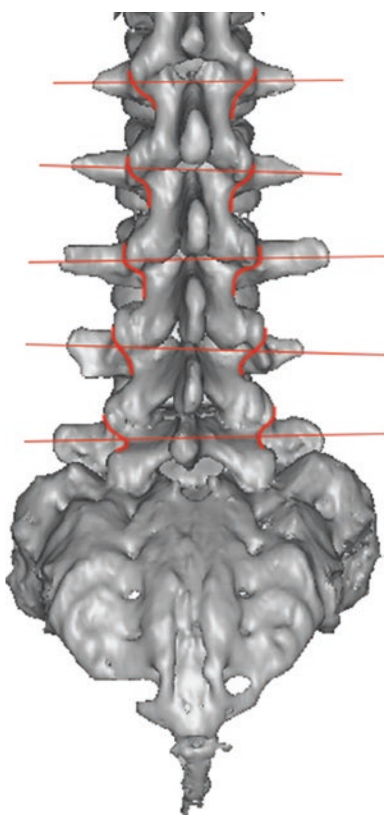

Fig. 4.123 Roy-Camille technique

7.3 Screw Placement

The cortical bone over the entry points is removed by a high-speed burr or rongeur.

Place a hand drill into entry points and slowly drill into the pedicles at an appropriate angle.

Strictly maintain the trajectory for screw placement. Small transverse plane trajectories may cause penetration through the lateral cortical bone of the pedicle and injury of adjacent organs. Too much transverse plane trajectories can result in violation into the spinal canal and injure the spinal nerve roots or cauda equina.

Markers are placed into the screw path to facilitate further intraoperative fluoroscopy to determine whether the screw path needs to be adjusted (Figs. Fig. 4.124, 4.125, and Fig. 4.126).

A pedicle sounder is used to detect the walls of screw path and depths.

In general, the entry depths are 40–50 mm (40–45 mm at L1 and 45–50 mm at L5).

Perform a lateral fluoroscopy to ensure that the entry depths do not exceed 80% of the anteroposterior length of the vertebral bodies.

Pedicle screws are placed after tapping and sounding of the screw path (Fig. 4.127).

Pedicle screws should be parallel to end plates or slightly incline upward to be placed in high-density end plates (Figs. 4.128 and 4.129).

Fig. 4.124 Steel balls are placed into the entry points in each segments to show the entry point on the fluoroscopy

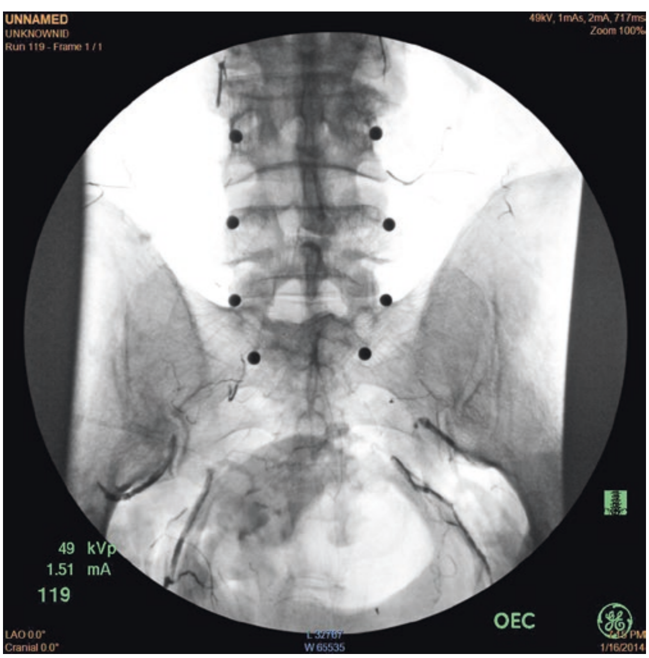

Fig. 4.125 Fluoroscopy shows the relationship between the entry points marked by steel balls and pedicles

Fig. 4.126 Markers are placed into the screw paths

Fig. 4.127 Pedicle screws are placed into the target segments

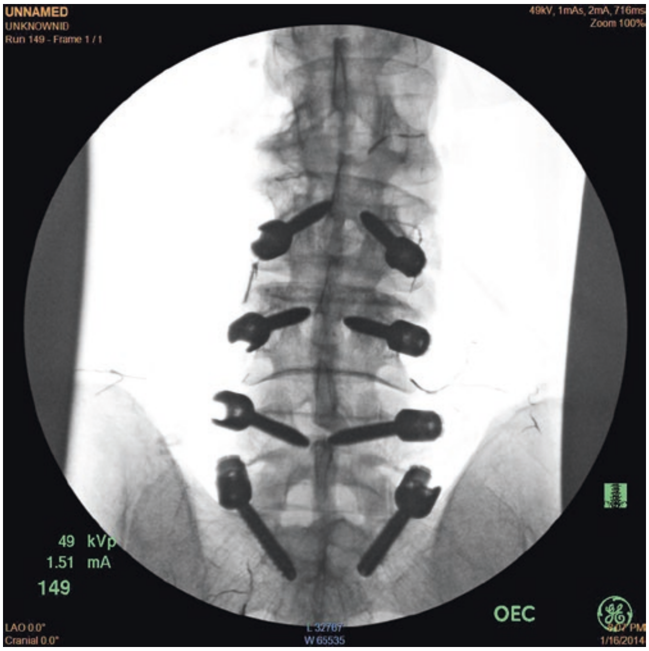

Fig. 4.128 Perform a fluoroscopy after screws are placed into vertebral bodies (anteroposterior view), and it shows pedicle screws are located well

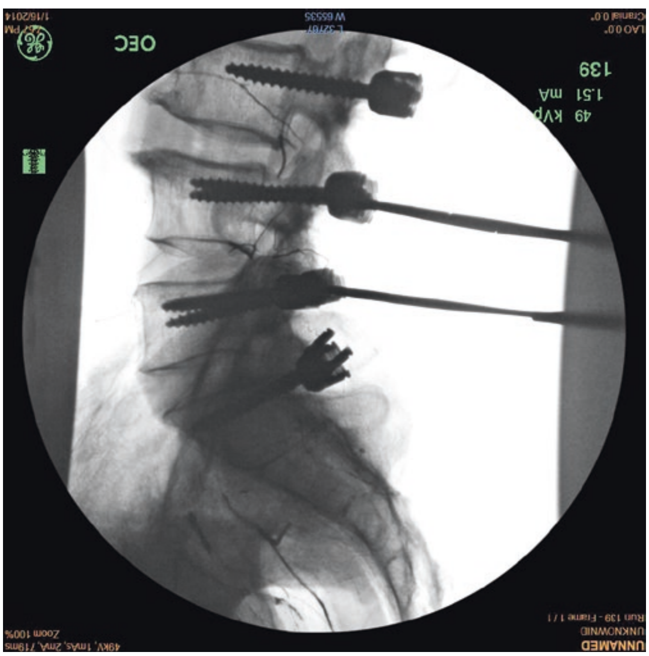

Fig. 4.129 Perform a fluoroscopy after inserting screws into vertebral bodies (lateral view)

References

1. Shepard M, Safain M, Burke SM, et al. Lateral retroperitoneal transpsoas approach to the lumbar spine for the treatment of spondylodiscitis. Minim Invasive Ther Allied Technol. 2014;23(5):ii.
2. Ghobrial GM, Alsaiegh F, Franco D, et al. Lateral lumbar retroperitoneal transpsoas approach in the setting of spondylodiscitis: a technical note. J Clin Neurosci. 2017;39:193–8.
3. Marsicano J, Mirovsky Y, Remer S, et al. Thrombotic occlusion of the left common iliac artery after an anterior retroperitoneal approach to the lumbar spine. Spine. 1994;19(3):357–9.
4. Rajaraman V, Vingan R, Roth P, et al. Visceral and vascular complications resulting from anterior lumbar interbody fusion. J Neurosurg. 1999;91(1 Suppl):60.
5. Mobbs RJ, Phan K, Daly D, et al. Approach-related complications of anterior lumbar Interbody fusion: results of a combined spine and vascular surgical team. Global Spine J. 2016;6(2):147–54.
6. Kettler A, Schmoelz W, Kast E, et al. In vitro stabilizing effect of a transforaminal compared with two posterior lumbar interbody fusion cages. Spine. 2005;30(22):665–70.
7. Rosenberg WS, Mummaneni PV. Transforaminal lumbar interbody fusion: technique, complications, and early results. Neurosurgery. 2001;48(3):569.
8. Harris BM, Hilibrand AS, Savas PE, et al. Transforaminal lumbar interbody fusion: the effect of various instrumentation techniques on the flexibility of the lumbar spine. Spine. 2004;29(4):E65.
9. Osman SG, Nibu K, Panjabi MM, et al. Transforaminal and posterior decompressions of the lumbar spine. A comparative study of stability and intervertebral foramen area. Spine. 1997;22(15):1690.
10. Golub BS, Silverman B. Transforaminal ligaments of the lumbar spine. J Bone Joint Surg (Am Vol). 1969;51(5):947.
11. Park HK, Rudrappa S, Dujovny M, et al. Intervertebral foraminal ligaments of the lumbar spine: anatomy and biomechanics. Childs Nerv Syst. 2001;17(4):275–82.
12. Hasegawa T, An HS, Haughton VM, et al. Lumbar foraminal stenosis: critical heights of the intervertebral discs and foramina. A cryomicrotome study in cadavera. J Bone Joint Surg Am. 1995;77(1):32–8.
13. Inufusa A, An HS, Lim TH, et al. Anatomic changes of the spinal canal and intervertebral foramen associated with flexion-extension movement. Spine. 1996;21(21):2412–20.
14. Bridwell KH, Lewis SJ, Rinella A, et al. Pedicle subtraction osteotomy for the treatment of fixed sagittal imbalance. Surgical technique. J Bone Joint Surg Am. 2004;86-A(Suppl 1):3–44.
15. Cho KJ, Bridwell KH, Lenke LG, et al. Comparison of Smith-Petersen versus pedicle subtraction osteotomy for the correction of fixed sagittal imbalance. Spine. 2005;30(18):2030.
16. Bridwell KH, Lewis SJ, Edwards C, et al. Complications and outcomes of pedicle subtraction osteotomies for fixed sagittal imbalance. Spine. 2003;28(18):2093–101.
17. Hyun SJ, Rhim SC. Clinical outcomes and complications after pedicle subtraction osteotomy for fixed sagittal imbalance patients: a long-term follow-up data. J Korean Neurosurg Soc. 2010;47(2):95–101.
18. Debarge R, Demey G, Roussouly P. Sagittal balance analysis after pedicle subtraction osteotomy in ankylosing spondylitis. Eur Spine J. 2011;20(5):619–25.

19. Kepler CK, Bogner EA, Herzog RJ, et al. Anatomy of the psoas muscle and lumbar plexus with respect to the surgical approach for lateral transpsoas interbody fusion. Eur Spine J. 2011;20(4):550.
20. Davis TT, Bae HW, Mok JM, et al. Lumbar plexus anatomy within the psoas muscle: implications for the transpsoas lateral approach to the L4-L5 disc. Jbjs. 2011;93(16):1482.
21. Paulino C, Patel A, Carrer A. Anatomical considerations for the extreme lateral (XLIF) approach. Curr Orthop Pract. 2010;21(21):368–74.
22. Sun JC, Wang JR, Luo T, et al. Surgical incision and approach in thoracolumbar extreme lateral interbody fusion surgery: an anatomic study of the diaphragmatic attachments. Spine. 2016;41(4):E186.
23. Baaj AA, Papadimitriou K, Amin AG, et al. Surgical anatomy of the diaphragm in the anterolateral approach to the spine: a cadaveric study. J Spinal Disord Tech. 2014;27(4):220–3.
24. Sembrano JN, Yson SC, Horazdovsky RD, et al. Radiographic comparison of lateral lumbar interbody fusion versus traditional fusion approaches: analysis of sagittal contour change. Int J Spine Surg. 2015;9:16.
25. Tubbs RS, Salter EG, Rd WJ, et al. Anatomical landmarks for the lumbar plexus on the posterior abdominal wall. J Neurosurg Spine. 2005;2(3):335–8.
26. Sasso RC, Kenneth BJ, Lehuec JC. Retrograde ejaculation after anterior lumbar interbody fusion: transperitoneal versus retroperitoneal exposure. Spine. 2003;28(10):1023.
27. Lieberman IH, Willsher PC, Litwin DE, et al. Transperitoneal laparoscopic exposure for lumbar interbody fusion. Spine. 2000;25(4):509.
28. Wimmer C, Krismer M, Gluch H, et al. Anterior interbody fusion of the lumbar spine. Orthopade. 1997;26(6):563–7.
29. Kim DH. Surgical anatomy & techniques to the spine. Philadelphia: Saunders Elsevier; 2006.
30. Lane JD Jr, Moore ES Jr. Transperitoneal approach to the intervertebral disc in the lumbar area. Ann Surg. 1948;127(3):537–51.
31. Unruh KP, Camp CL, Zietlow SP. Anatomical variations of the iliolumbar vein with application to the anterior retroperitoneal approach to the lumbar spine: a cadaver study. Clin Anat. 2008;21(7):666–73.
32. Lazennec JY, Pouzet B, Ramare S, et al. Anatomic basis of minimal anterior extraperitoneal approach to the lumbar spine. Surg Radiol Anat. 1999;21(1):7–15.
33. Taheri SA, Gawronski S, Smith D. Paramedian retroperitoneal approach to the abdominal aorta. J Cardiovasc Surg. 1983;24(5):529–31.
34. Crofts KM, Wong DA, Murr PC. Anterior paramedian retroperitoneal surgical approach to the lumbar spine. Orthopedics. 1994;17(8):699.
35. Gumbs AA, Shah RV, Yue JJ, et al. The open anterior paramedian retroperitoneal approach for spine procedures. Arch Surg. 2005;140(4):339–43.
36. Shetty AS, Avadhani R, Mahesha B, et al. Anatomy of the thoracic pedicle in relation to the pedicle screw fixation -a cadaveric study. Biomedicine. 2013;33(1):468–72.
37. Yang H, Xing WP, Shang XW. A clinical analysis of manual placement of 277 lumbar pedicle screws. Chongqing Med. 2010.
38. Smith HE, Welsch MD, Sasso RC, et al. Comparison of radiation exposure in lumbar pedicle screw placement with fluoroscopy vs computer-assisted image guidance with intraoperative three-dimensional imaging. J Spinal Cord Med. 2008;31(5):532–7.
39. Gertzbein SD, Robbins SE. Accuracy of pedicular screw placement in vivo. Spine. 1990;15(1):11–4.
40. Gelalis ID, Paschos NK, Pakos EE, et al. Accuracy of pedicle screw placement: a systematic review of prospective in vivo studies comparing free hand, fluoroscopy guidance and navigation techniques. Eur Spine J. 2012;21(2):247–55.
41. Beresford ZM, Kendall RW, Willick SE. Lumbar facet syndromes. Curr Sports Med Rep. 2010;9(1):50.

Surgical Anatomy of the Sacral Spine

5

Jian-gang Shi, Wen Yuan, and Jing-chuan Sun

1 Posterior Exposure of the Sacrum and the Internal Fixation Technique of Pedicle Screws and Iliac Screws

1.1 Overview

Posterior approach and fixation technique of the lumbosacral spine are commonly used for the treatment of severe spinal diseases. To provide a rigid construct, it's often required to perform internal fixation in the sacrum and ilium in the treatment of severe scoliosis, lumbar vertebral slippage, tumor metastasis, infections, degeneration, or traumas. Pedicle screw fixation of S1 is the most commonly used technique, and internal fixation with iliac screws should also be taken into consideration when necessary. Mastering the anatomical and morphological knowledge about the sacrum is a key precondition for a successful operation.

1.2 Position

Patients are placed in the prone position (Fig. 5.1).

Fig. 5.1 Position for posterior exposure of the lumbosacral region

J.-g. Shi (✉) • W. Yuan • J.-c. Sun
Department of Orthopedics, Changzheng Hospital,
Shanghai, China
e-mail: shijiangang616@163.com; yuanwenspine@163.com; sjchxc@foxmail.com

J.-g. Shi et al. (eds.), *Anatomy Atlas and Interpretation of Spine Surgery*, https://doi.org/10.1007/978-981-10-5906-3_5

1.3 Exposure

Make a midline incision through a posterior approach of the lumbar spine and extend it to the involved sacral segments (Fig. 5.2).

There are some palpable structures that can aid in the range division of incision. Generally, the posterior superior iliac spine is at L5/S1 disc; the top of the iliac crests is at L4/L5 disc.

Bilaterally, dissection of the subcutaneous tissue is done through the posterior midline approach until the lumbodorsal fascia is exposed. Then the lumbodorsal fascias are incised until the spinous processes of the lumbosacral spine are exposed (Fig. 5.3).

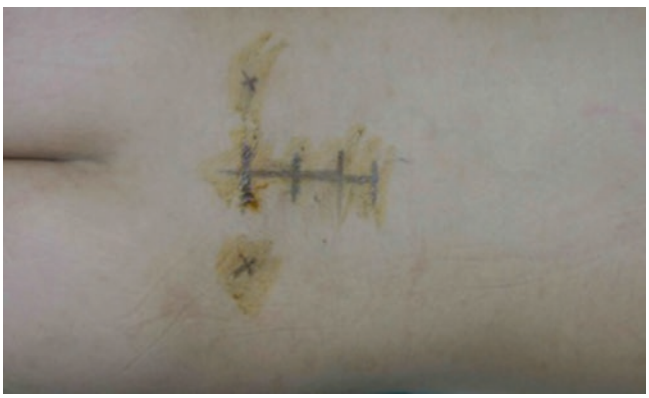

Fig. 5.2 An incision extending to the involved sacral segments

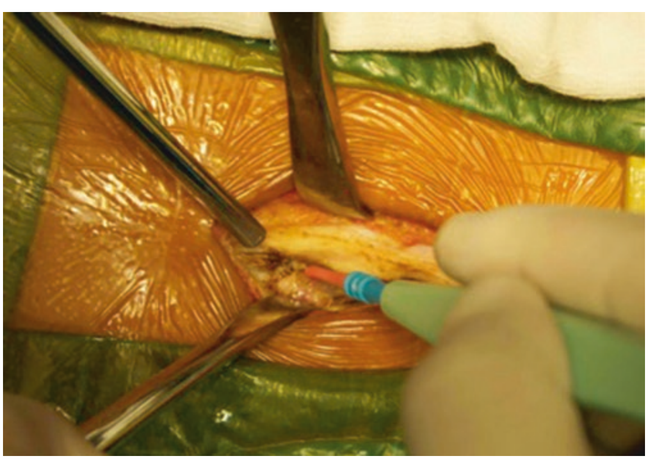

Fig. 5.3 Exposure of the deep fascia

The paravertebral muscles are subperiosteally dissected from the spinous processes on both sides until the vertebral laminae, facet joints, L5 transverse process, and iliac alae on both sides are exposed (Figs. 5.4, 5.5, 5.6, and 5.7).

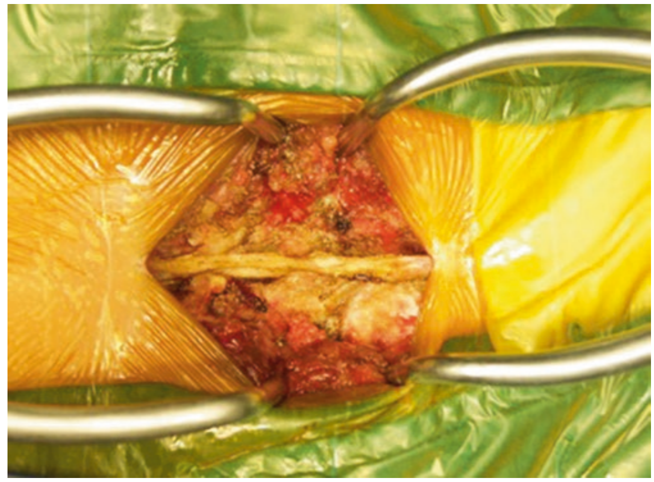

Fig. 5.4 Subperiosteal dissection of paravertebral muscles on both sides

Fig. 5.5 A gross sample of the lumbosacral spine

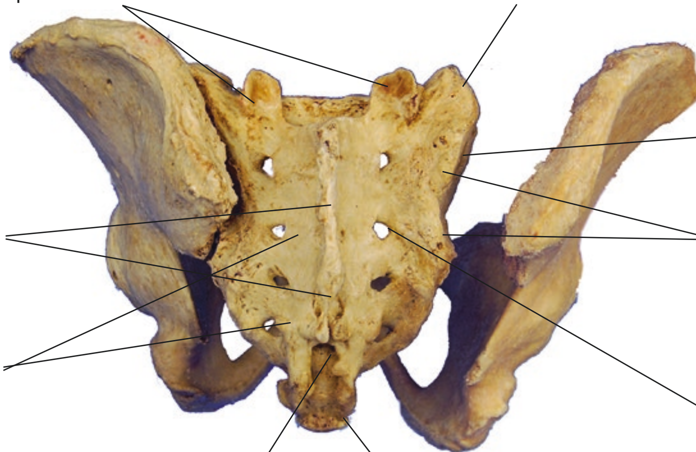

Fig. 5.6 Posterior view of the pelvis

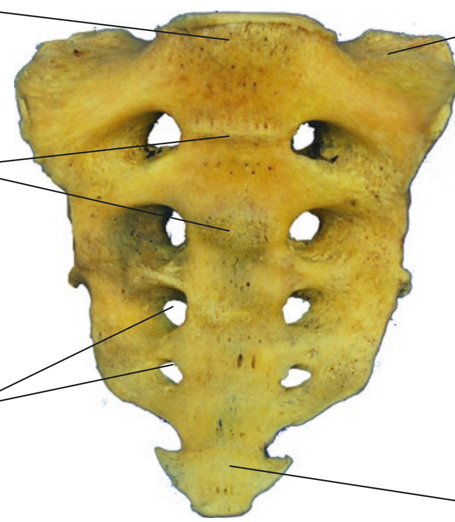

Fig. 5.7 Anterior view of the sacrum

Sacrum: a bone formed by the developmental fusion of five sacral vertebrae with a unique anatomical structure.

An appropriate coronary trajectory for S1 pedicle screws is a guarantee of avoiding neurovascular injury. Generally, the screws are directed medially at an approximately 20° in the coronary trajectory.

1.4 Screw Placement

Select entry points for pedicle screw placement in the lumbosacral spine according to the anatomic landmarks. The entry points for S1 pedicle screws are located in the caudal and lateral borders of the S1 facet joint (Fig. 5.8).

The sagittal trajectory for S1 pedicle screws is directed at a slight angle toward the sacropromontory so as to enable screws to lie beneath the superior end plate of S1 and thereby to provide stronger bite (Figs. 5.9 and 5.10).

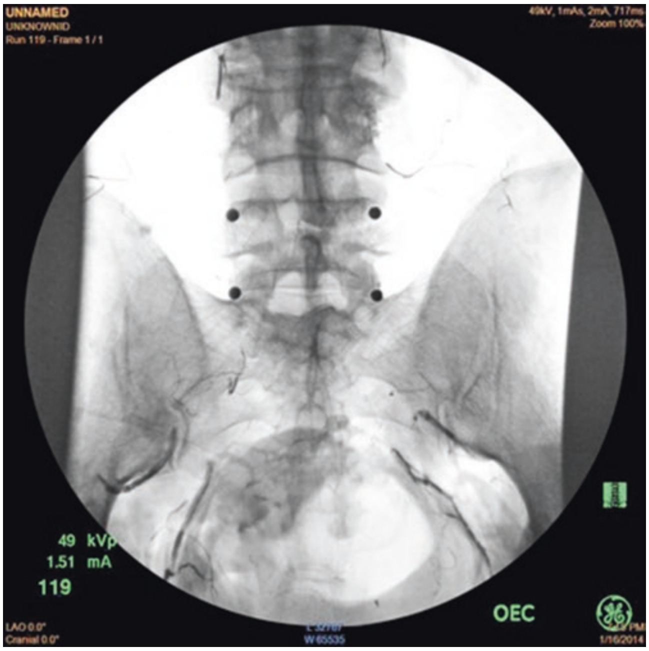

Fig. 5.8 Intraoperative fluoroscopy of the entry points for L5 and S1 pedicle screws (marked with steel balls)

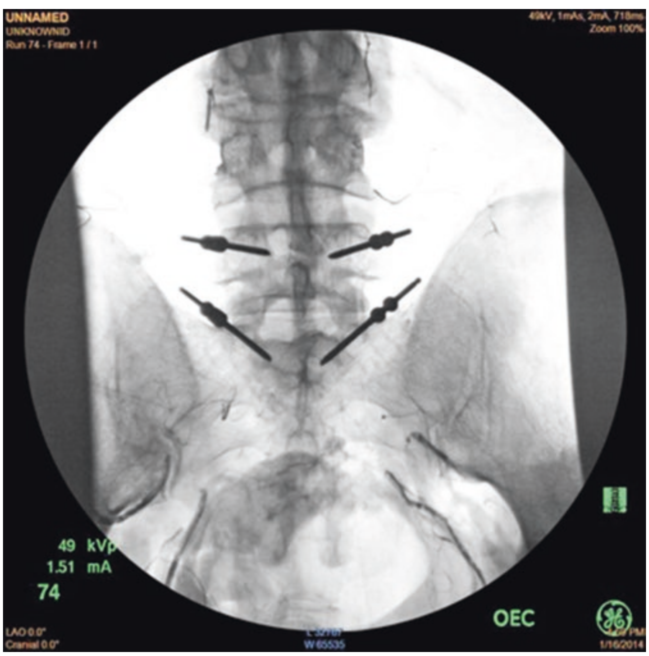

Fig. 5.9 Intraoperative fluoroscopy of the trajectory for L5 and S1 pedicle screws

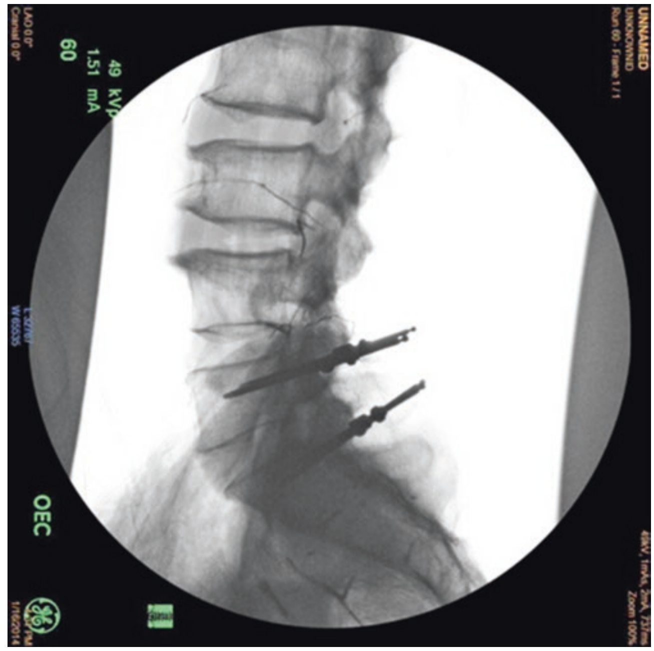

Fig. 5.10 Intraoperative fluoroscopy demonstrates the sagittal trajectory of the L5 and S1 pedicle screws

Pedicle screws are placed after fluoroscopy shows that markers are placed correctly (Fig. 5.11).

Fig. 5.11 A gross sample of L3–S1 where pedicle screws are placed

Iliac screw placement: appropriately resect the posterior cortex of the posterior superior iliac spine to facilitate further connection of lumbosacral screws. The entry points are located 5 mm laterally from the sacroiliac joint, and the paths for screw placement lie between the two cortices of iliac alae. The screws are directed outward at an approximately 20–40° angle in the horizontal plane and toward the anterior superior iliac spine in the sagittal plane.

Case: severe slippage at L5/S1 in an 8-year-old female. An anteroposterior X-ray picture (Fig. 5.12) and a lateral X-ray picture (Fig. 5.13) are taken after the placement of L5 screws (5 mm × 35 mm), S1 screws (5 mm × 30 mm), and iliac screws (6 mm × 50 mm).

Fig. 5.12 Anteroposterior fluoroscopy picture taken after the placement of L5/S1 pedicle screws and iliac screws

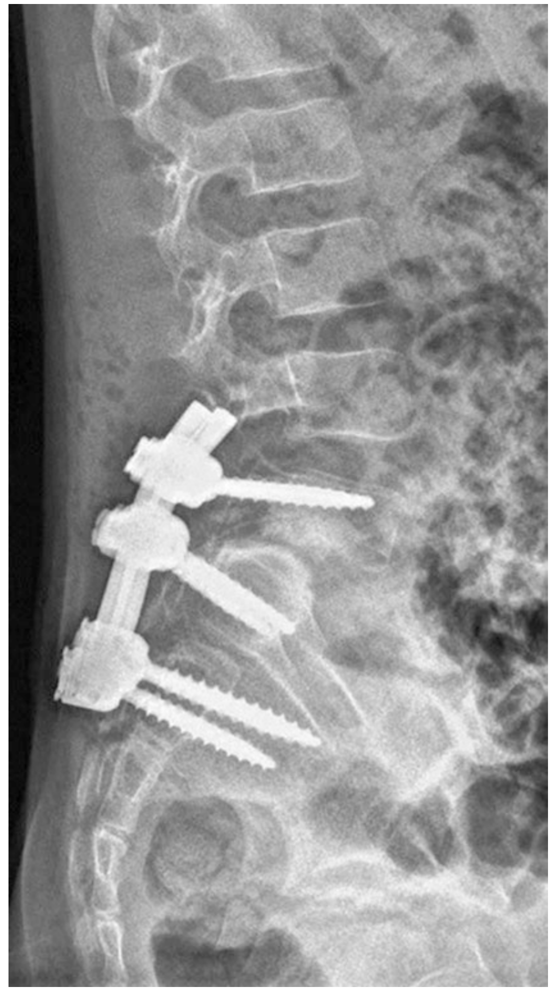

Fig. 5.13 Lateral fluoroscopy taken after the placement of L5/S1 pedicle screws and iliac screws

2 Anterior Approach for the Sacral Spine

2.1 Overview

Exposure of the sacrum via an anterior approach is mostly used for the surgical resection of sacral tumors. Anterior approach is indicated for the treatment of primary soft tissue tumors in the pelvic cavity, which invade only the surface of the anterior margin of the sacrum and can be thoroughly resected via an anterior approach. Combined anteroposterior approaches are indicated for large sacral tumors above S2, which originate in the pelvic cavity and seriously invade the sacrum.

The structure of the pelvic cavity in front of the sacrum is very complicated with important organs, blood vessels, and nerves. Hence, it is very difficult and highly risky to resect anterior sacral tumors exposed via an anterior approach. But if the anterior approach is used proficiently, it can effectively reduce the risk of injury to important organs and tissues in front of the sacrum, which is the common complication of the posterior approach to tumor resection.

2.2 Position

Patients are placed in the supine position or lithotomy position to facilitate the operation in the deep pelvic cavity (Fig. 5.14).

2.3 Incision

Make a midline incision downward from 2 to 3 cm below the umbilicus to the pubic symphysis. Then the subcutaneous tissue is incised to expose the linea alba (Fig. 5.15).

Fig. 5.14 Lithotomy position for exposure of the anterior sacrum

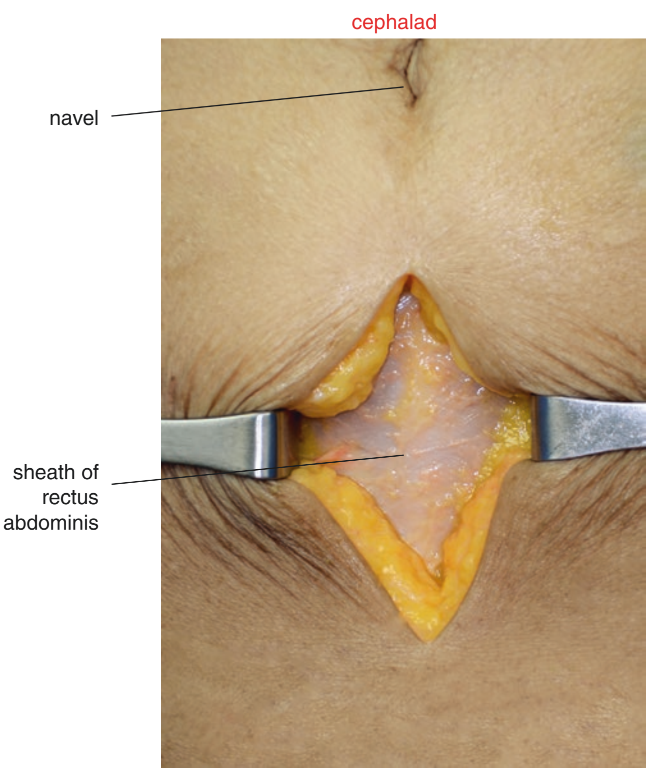

Fig. 5.15 Incision of the skin and subcutaneous tissue to expose the sheath of rectus abdominis

2.4 Exposure

The midline of the sheath of rectus abdominis is the linea alba (Fig. 5.15).

The linea alba is incised in the midline to avoid opening the rectus sheath.

The underlying peritoneum is then elevated gently with forceps on both sides of the midline to avoid damage to the abdominal contents.

The incision in the peritoneum is between the forceps and extended with scissors cranially and caudally under the protection of the other finger (Fig. 5.16).

The small bowel and the sigmoid colon are retracted laterally under the protection of moistened drape to expose the midline posterior parietal peritoneum.

The posterior parietal peritoneum is elevated with forceps on both sides of the midline and vertically incised with a pair of scissors.

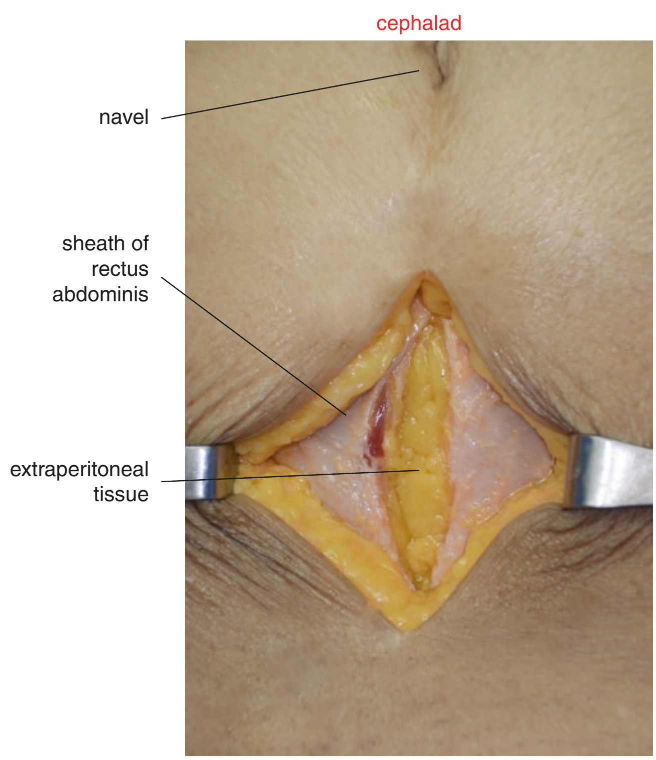

Fig. 5.16 Entering the pelvic cavity

Femoral nerve: the largest branch of the lumbar plexus, which is composed of L2–L4 nerves. It emerges from the lateral border of the psoas major muscle and goes downward between the psoas major muscle and the iliacus muscle; it then passes through the deep surface of the inguinal ligament slightly outside the midpoint of the ligament and the outer side of the femoral artery; and finally, it enters the femoral triangle.

Obturator nerve: a nerve arising from the lumbar plexus, going through the medial border of the psoas major muscle, then going forward along the medial wall of the small pelvis, next traveling together with obturator vessels to pass through the obturator canal, and finally passing out of the small pelvis.

Lumbosacral trunk: a nerve trunk composed of a part of anterior branch of the fourth lumbar nerve and the anterior ramus of the fifth lumbar nerve, which are joined by the sacral plexus.

Sacral plexus: a nerve plexus composed of the lumbosacral trunk (L4, L5) and all sacral nerves and the anterior rami of coccygeal nerves. It is located in the pelvic cavity, in front of the sacrum and piriformis, and in the rear of the internal iliac artery. There is the sigmoid colon in front of the left sacral plexus and an ileal loop in front of the right sacral plexus (Figs. 5.17 and 5.18).

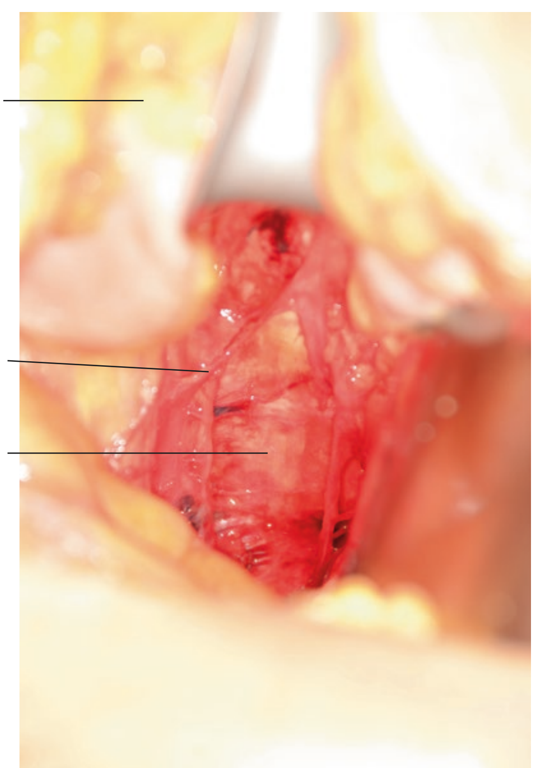

Fig. 5.17 Exposure of the anterior sacrum

Sacral parasympathetic nerve: a pelvic visceral nerve originating from S2–S4 nerves. Its fiber is scattered in the visceral plexus within the pelvic cavity, which surrounds the aortic bifurcation and runs downward along the intervertebral discs of L5/S1, anterior sacrum, and retroperitoneal region and which is easy to be damaged when this region is exposed. This plexus plays a role in maintaining sexual function. Its damage may cause retrograde ejaculation and erectile dysfunction in males but has no impact on females (Fig. 5.19).

Common iliac artery: an artery originating from the abdominal aortic bifurcation, which runs downward along the medial side of the psoas major muscle and then bifurcates into the internal iliac artery and external iliac artery at the sacroiliac joint.

Internal iliac artery: the main artery of the pelvis, which is a short trunk running downward along the lateral wall of the pelvic cavity and then bifurcates into wall branches and visceral branches.

Obturator artery: a wall branch of the internal iliac artery, which runs downward along the lateral wall of the pelvis and crosses the obturator canal and then bifurcates into two branches on the medial side of the thigh, which supply blood to the muscles on the medial side of the thigh and the hip joint.

Superior gluteal artery and inferior gluteal artery: wall branches of the internal iliac artery, which respectively go through the suprapiriform and infrapiriform foramens and then reach the hip to supply the gluteus and hip joint.

Lateral sacral artery: a wall branch of the internal iliac artery, which is distributed in the iliopsoas, posterior pelvic wall, and sacral canal.

Internal pudendal artery: a visceral branch of the internal iliac artery, which goes downward in front of the inferior gluteal artery, passes through the infrapiriform foramen, and then leaves the pelvic cavity.

Uterine artery: an artery which goes downward along the lateral wall of the pelvic cavity wall and then enters the base of the broad ligament of the uterus.

Median sacral artery: a small vessel that arises from the superior portion of the posterior wall of the terminal abdominal aorta and then goes downward along the fifth lumbar vertebra and the anterior sacrum. It usually needs to be ligated and dissected to avoid being damaged before exposure of sacral vertebral bodies.

Visceral organs in front of the sacrum: the ureters, bladder, rectum, and prostate in males and ovaries, oviducts, and uterus in females.

Presacral nerves: the lumbosacral trunk, sacral plexus, and sacral parasympathetic nerves.

Presacral vessels: bilateral common iliac arteries and veins, bilateral internal iliac arteries and veins and their branches, as well as the median sacral artery.

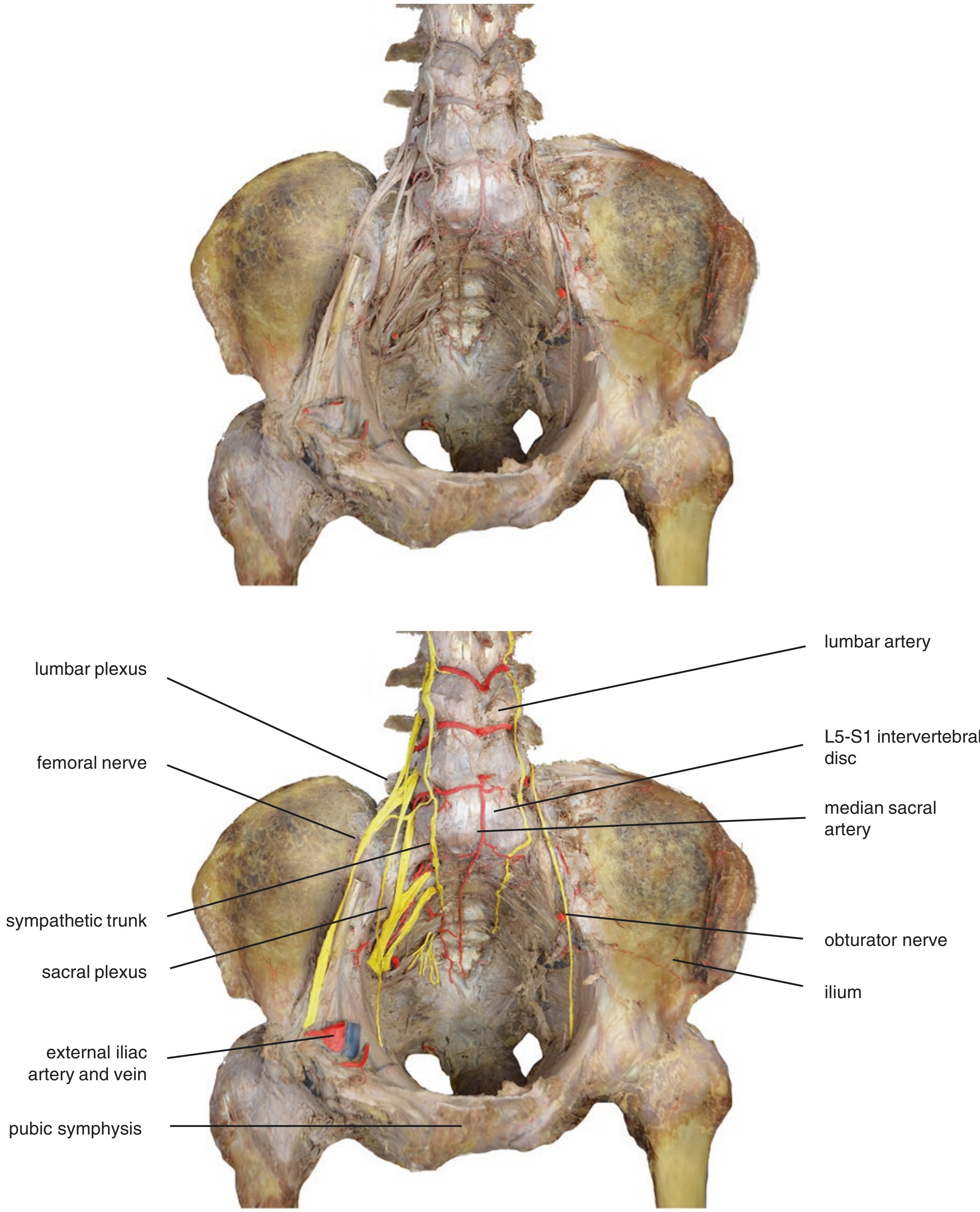

Fig. 5.18 Nerves, blood vessels, and skeletal structures in the lumbosacral region

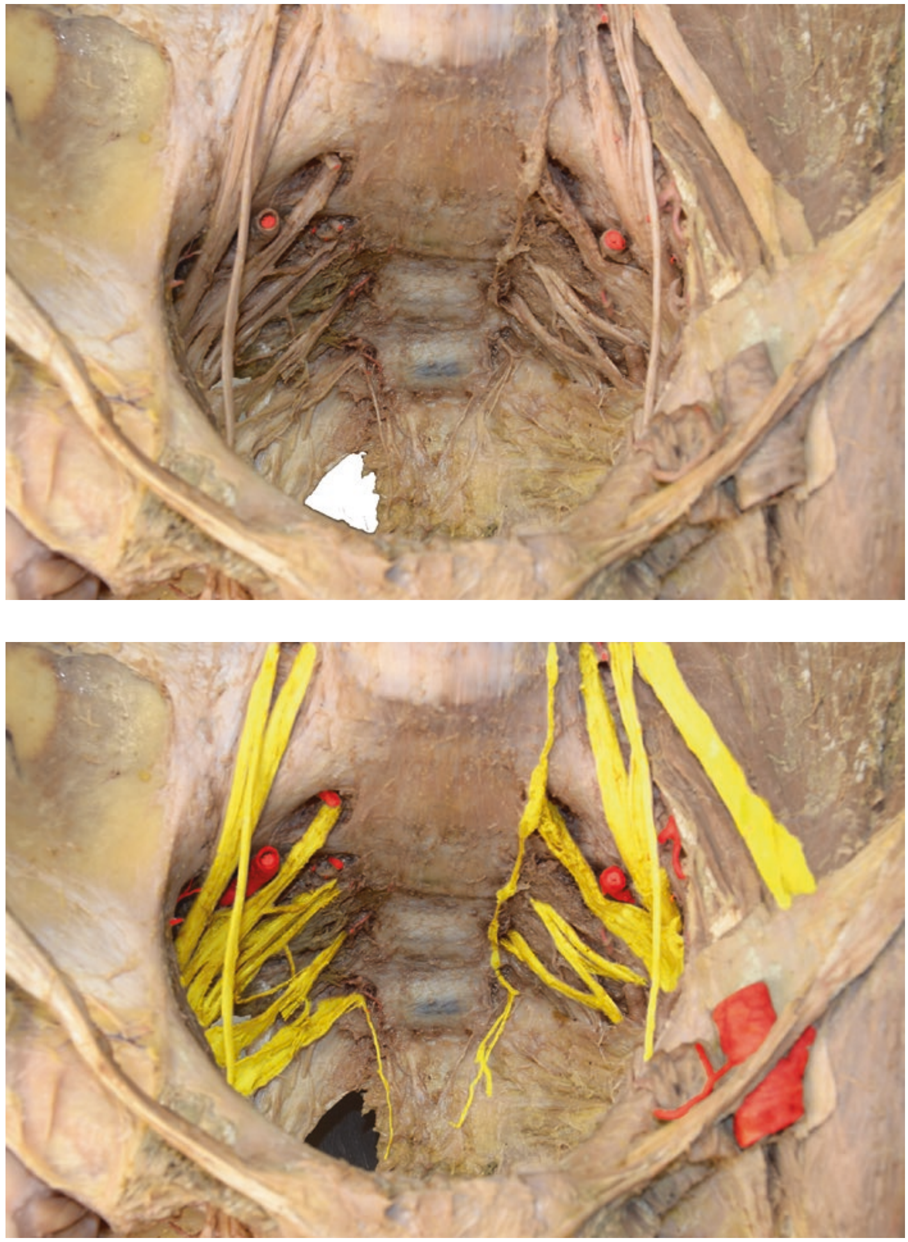

Fig. 5.19 Nerves, blood vessels, and skeletal structures in the pelvic cavity

References

1. Sar C, Kilicoglu O. S1 pediculoiliac screw fixation in instabilities of the sacroiliac complex: biomechanical study and report of two cases. J Orthop Trauma. 2003;17(4):262–70.
2. Varga PP, Szövérfi Z, Lazary A. Surgical treatment of primary malignant tumors of the sacrum. Neurol Res. 2014;36(6):577–87.
3. Bianchi C, Ballard JL, Abou-Zamzam AM, et al. Anterior retroperitoneal lumbosacral spine exposure: operative technique and results. Ann Vasc Surg. 2003;17(2):137–42.
4. Inamasu J, Guiot BH. Vascular injury and complication in neurosurgical spine surgery. Acta Neurochir. 2006;148(4):375–87.